THE

PHYSICAL REVIEW

Volume [illegible] Second Series Number [illegible]

SEPTEMBER 15, 1949

Published for the

AMERICAN PHYSICAL SOCIETY

by the

[illegible]

[illegible]

THE PHYSICAL REVIEW

A journal of experimental and theoretical physics established by E. L. Nichols in 1893

Published by the American Institute of Physics for the

AMERICAN PHYSICAL SOCIETY

Officers

President

F. W. Loomis
University of Illinois
Urbana, Illinois

Vice-President

I. I. Rabi
Columbia University
New York, New York

Secretary

K. K. Darrow
Bell Telephone Laboratories
Office:
Columbia University
New York 27, New York

Treasurer

G. B. Pegram
Columbia University
New York 27, New York

Local Secretary for the Pacific Coast

J. Kaplan
University of California at Los Angeles
Los Angeles, California

Managing Editor

John T. Tate
University of Minnesota
Minneapolis, Minnesota

BOARD OF EDITORS

Editor — John T. Tate

Assistant Editor — J. W. Buchta

Associate Editors

H. A. Bethe — S. A. Goudsmit — W. E. Lamb, Jr.
L. A. Ruhlmann — E. M. Purcell — R. G. Herb
W. H. Zachariasen — V. F. Weisskopf — J. Bardeen

Manuscripts for publication should be submitted to John T. Tate, University of Minnesota, Minneapolis, Minnesota. The authors' institutions are requested to pay a publication charge of $4 per page which, if honored, entitles them to 100 free reprints. Instructions will be sent with galley proofs.

Proof and all correspondence concerning papers in the process of publication should be addressed to the Publication Manager, American Institute of Physics, 57 East 55 Street, New York 22, New York.

Subscription Price

United States and Canada.....$25.00
Members.....$27.00

Back Numbers[1]

Yearly back number rate when complete year is available:
Prior to 1949: $20.00
Thereafter: $27.00
Single copies: $2.50 each, prior to July, 1929;
$1.00 each, July, 1929–December, 1941;
$2.00 each, January, 1942–December, 1946;
$1.00 each, January, 1947–December, 1948.
Current issues: $1.25 each.
Current index, 1893–1930: $4.00.

Subscriptions and orders for back numbers should be addressed to Prince and Lemon Streets, Lancaster, Pennsylvania, or to the American Institute of Physics, 57 East 55 Street, New York 22, New York.

Changes of address in the case of members of the American Physical Society should be addressed to the Treasurer; in the case of other subscribers to the Business Manager, American Institute of Physics.

[1] Write Radio Library of Physics Department, Cornell University, Ithaca, New York.

The Physical Review is published bimonthly at Prince and Lemon Streets, Lancaster, Pennsylvania.

Entered as second-class matter March 6, 1918, at the Post Office at Lancaster, Pennsylvania, under the Act of March 3, 1879.

Acceptance for mailing at special rate of postage provided for in paragraph 4, section 538, P. L. & R., authorized January 27, 1925.

THE
PHYSICAL REVIEW

A journal of experimental and theoretical physics established by E. L. Nichols in 1893

SECOND SERIES, VOL. 76, NO. 6 SEPTEMBER 15, 1949

A Precision Measurement of the Ratio of the Nuclear g Values of Li^7 and Li^6

P. KUSCH AND A. K. MANN*
Columbia University, New York, New York
(Received June 15, 1949)

The molecular beam magnetic resonance method has been used to make a precision measurement of the ratio of the nuclear g factors of Li^7 and Li^6. The central maximum of the Li^7 line and the center of the Li^6 line in the spectra of LiI and LiBr give the ratio g_7/g_6 to a precision limited only by experimental factors. The mean of eight independent determinations, under various experimental conditions, is 2.64094 ± 0.00005. This value of the ratio is compared with that calculated by use of the Fermi formula from the known ratio $\Delta\nu_7/\Delta\nu_6$. The cube of the ratio of the reduced masses of the $2s$ electrons in Li^6 and Li^7 is included as a factor in the calculation by analogy with the corresponding case of the hydrogens. The observed value of g_7/g_6 is greater than the value calculated by (0.012 ± 0.003) percent.

INTRODUCTION

IT is the purpose of this paper to describe a precision measurement of the ratio of the nuclear g factor of Li^7 and that of Li^6 by the molecular beam magnetic resonance method. In the work of Nafe and Nelson,[1] the h.f.s. separations of the ground states of H and D were measured, and the observed ratio $\Delta\nu_H/\Delta\nu_D$ compared with that calculated from the accurately known[2,3] ratio of the magnetic moments, μ_H/μ_D. It was found that the experimental value was lower by 0.017 percent than the calculated value. This discrepancy was explained by Bohr[4] in terms of the compound structure of the deuteron. In that portion of the electron orbit which is close to the nucleus, the electron velocity is much greater than that of the nucleons. Consequently, the electron orbit is centered about the slowly moving proton rather than about the center of mass of the nucleus. When the electron is within the nucleus, the neutron appears as a shell within which a magnetic interaction occurs only between proton and electron. From an analysis of this process, Bohr has shown that the apparent ratio of the nuclear moments, μ_H/μ_D as determined from the h.f.s. must be increased by 0.018 percent. Nelson and Nafe[5] have also measured the h.f.s. separation of the ground state of tritium. Using the ratio of the magnetic moments of the proton and triton, obtained by Bloch, Graves, Packard, and Spence,[6] and the measured value of $\Delta\nu_H$, the tritium h.f.s. can be calculated. The calculated and measured values of $\Delta\nu_T$ agree within 1 part in 10^5. Avery and Sachs[7] have estimated that the fractional reduction of $\Delta\nu_T$ from that calculated from $\Delta\nu_H$ and the ratio μ_H/μ_T would be roughly 5 percent of that which occurs for the deuteron.

In the present paper, the measured ratio g_7/g_6 is compared with that calculated from the known ratio $\Delta\nu_7/\Delta\nu_6$. The $\Delta\nu$'s of Li^6 and Li^7 were originally measured by Kusch, Millman, and Rabi,[8] who obtained $\Delta\nu_7/\Delta\nu_6=3.52090\pm0.00025$. Recently, Kusch and Taub[9] have remeasured these $\Delta\nu$'s with much greater precisionl Their value for the ratio is 3.52096 ± 0.00006. It shoud, be noted that the uncertainty in this value is less than that obtained from the published values of the $\Delta\nu$'s since uncertainties in the frequency of the crystal. against which all frequency measurements were made, have no effect on the ratio of the $\Delta\nu$'s.

METHOD

The resonance line, observed in the spectrum of a diatomic molecule and which arises from a reorientation

* Now at the University of Pennsylvania, Philadelphia, Pennsylvania.

[1] J. E. Nafe and E. B. Nelson, Phys. Rev. **73**, 718 (1948).
[2] Bloch, Levinthal, and Packard, Phys. Rev. **72**, 1125 (1947).
[3] A. Roberts, Phys. Rev. **72**, 979 (1947).
[4] A. Bohr, Phys. Rev. **73**, 1109 (1948).
[5] E. B. Nelson and J. E. Nafe, Phys. Rev. **75**, 1194 (1949).
[6] Bloch, Graves, Packard, and Spence, Phys. Rev. **71**, 551 (1947).
[7] R. Avery and R. G. Sachs, Phys. Rev. **74**, 1320 (1948).
[8] Kusch, Millman, and Rabi, Phys. Rev. **57**, 765 (1940).
[9] P. Kusch and H. Taub, Phys. Rev. **75**, 1477 (1949).

of the nuclear spin with respect to the magnetic field, is the envelope of a large number of unresolved lines which result from the transition $\Delta m_I = \pm 1$ in the various rotational states, J, m_J. The structure of these lines has been discussed by Feld and Lamb[10] and by Nierenberg and Ramsey.[11] The principal interactions which give rise to the line structure are the interaction of the nuclear electric quadrupole moment with the gradient of the electric field at the nucleus, and the interaction of the nuclear magnetic dipole moment with the magnetic field produced at the nucleus by the molecular rotation. When $I=\frac{3}{2}$, as for Li^7, the envelope of the unresolved lines exhibits three maxima. At sufficiently high magnetic fields, the whole structure is symmetrical about the frequency $f_0=\mu_0 g_I H/h$ and the central maximum is, itself, symmetrical about this frequency. However, at intermediate fields, considerable departures from symmetry may occur. The frequencies of the components of the central maximum ($m_I=\frac{1}{2}\leftrightarrow m_I=-\frac{1}{2}$) are, to the second order, given[11] by:

$$f=-g_I\mu_0 H/h-m_J c/h + [3(b/h)^2(1-z^2)(9z^2-1)]/(4g_I\mu_0 H/h) - [(c/h)^2 J^2(1-z^2)]/(2g_I\mu_0 H/h), \quad (1)$$

where $z=m_J/J$, $b=e^2qQ/4$ and is the energy separation of each of the satellite maxima from the central peak, and c is the energy of interaction of the nuclear magnetic moment with the magnetic field produced by unit molecular rotation.

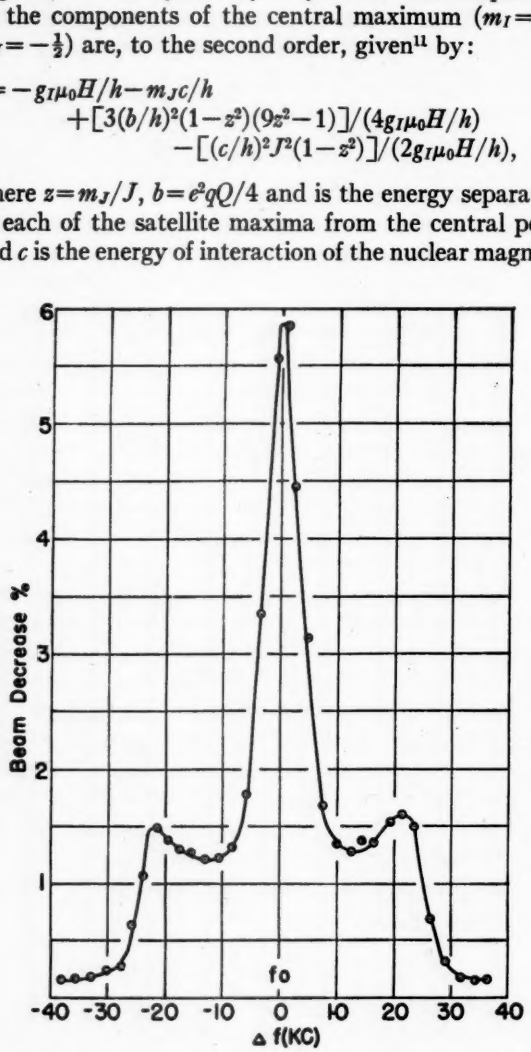

FIG. 1. Nuclear resonance spectrum of Li^7 in LiI.

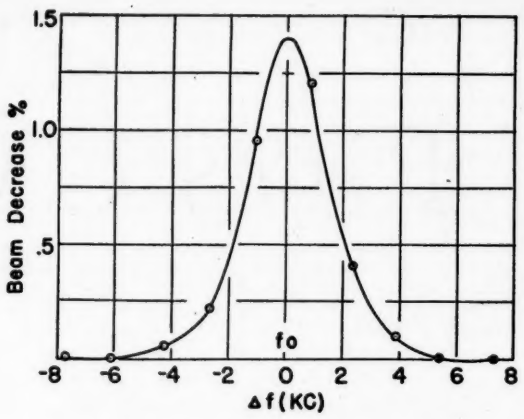

FIG. 2. Nuclear resonance spectrum of Li^6 in LiI.

The first term gives a line whose width is determined by the resolution of the apparatus and which is symmetrical about the frequency f_0. The second term broadens this line symmetrically, since positive and negative m_J are equally probable. The contribution of this term to the width of the line at half-intensity is:

$$\Delta f = 0.954ac/h, \quad (2)$$

where

$$a^2 = h^2/8\pi^2 AkT.$$

To find the effect of the last term in (1), it is necessary to evaluate the term $(c/h)^2J^2$. For small a, the most probable value of $J \simeq 0.707/a$. For this value of J, $(c/h)^2J^2 = 0.55(\Delta f)^2$. In the case of Li^7 in LiI, $\Delta f \leqslant 8.5 \times 10^3$ sec.$^{-1}$. If we consider the limiting value of $z=0$, at a frequency of observation $f_0 = 16\times 10^6$ sec.$^{-1}$ ($H=10^4$ gauss), the value of the last term becomes about 1.3 sec.$^{-1}$. The effect is entirely negligible and becomes even smaller for Li^6. The third term in the expression for the frequency has a maximum value at $z^2=5/9$. For Li^7 in LiI, $b/h = 21.5\times 10^3$ sec.$^{-1}$. For $f_0 = 16\times 10^6$ sec.$^{-1}$, and $z^2=5/9$, the third term becomes about 40 sec.$^{-1}$. This represents the maximum shift of any one of the components of the line from its position at infinite field. The over-all effect on the envelope of all the lines is less than this and is, therefore, negligible to within 1 part in 500,000. The effect of the quadrupole term on the position of the resonance line of Li^6 is even smaller. The case of LiBr is almost identical to that of LiI.

The central maximum of the Li^7 line and the center of the Li^6 line may thus serve to determine the ratio of the two nuclear g values to a precision limited only by experimental factors.

APPARATUS AND PROCEDURE

The apparatus used in this experiment is the same as that used in the work on the nuclear electric quadrupole

[10] B. T. Feld and W. E. Lamb, Jr., Phys. Rev. **67**, 15 (1945).
[11] W. A. Nierenberg and N. F. Ramsey, Phys. Rev. **72**, 1075 (1947).

moment of Li^6,[12] and in the determination of the proton moment.[13] A beam of LiI molecules was obtained by heating LiI in a gold-plated iron oven. The gold-plating was found very useful in preventing free iodine, presumably produced by thermal dissociation, from reacting with the iron. The LiBr beam was produced directly from an iron oven. The resolution half-width of the apparatus, for a perfectly homogeneous magnetic field, is about 1.2 kc/sec. for LiI and about 1.5 kc/sec. for LiBr. The observed half-widths are, for Li^6 in LiI and LiBr, 2.85 and 4.4 kc/sec., respectively, and, for the central maximum of Li^7 in LiI and LiBr, 8.5 and 12.3 kc/sec., respectively. Figures 1 and 2 show the nuclear resonance lines of Li^7 and Li^6 in LiI. The line structure has been observed to be entirely independent of magnetic field. The spectra for LiBr are essentially similar.

The data of this experiment are the frequencies of the Li^6 and Li^7 lines measured in the same constant magnetic field. Since the magnetic field does, in fact, vary with time during the period of observation, it is necessary to correct for this variation by observing the current in the magnet winding at each frequency reading. The method of making this correction has been described in detail previously,[13] and no further discussion will be given here. It should be mentioned that the direction of the magnetic field was reversed between successive runs as in the experiment[13] on the determination of the g value of the proton. The frequency of a line was determined by observations of the frequencies of two points on the resonance curve at which equal reduction of beam intensity was observed. The resonance curve was alternately traversed in opposite directions, and the fractional reduction of intensity at the points of observation was varied in order to reduce the possibility of systematic errors. The frequencies were measured with a General Radio heterodyne frequency meter, Type 620A. In the course of the experiment, two different meters were used with an identical result. The limitation on the precision of this experiment was imposed primarily by fluctuations in the magnetic field, not readily correlated to fluctuations in magnet current.

A careful study was made of the perturbing effects of power supplies on the magnetic field, the effect of the magnitudes of r-f current within a reasonable range, and the effect of different r-f generators coupled separately to the molecular beam apparatus. The maximum observed variation in the frequency of the Li^7 line under widely varying experimental conditions was too small to be meaningful.

[12] P. Kusch, Phys. Rev. **75**, 887 (1949).
[13] H. Taub and P. Kusch, Phys. Rev. **75**, 1481 (1949).

TABLE I. Results of individual determinations of g_7/g_6.

Run	Field direction	$H\times10^{-3}$ gauss	g_7/g_6	Molecule
1	N	14	2.64099	LiI
2	R	10	2.64088	
3	R	10	2.64088	
4	N	10	2.64091	
5	R	10	2.64091	
6	N	10	2.64105	
7	N	10	2.64095	LiBr
8	R	10	2.64091	

RESULTS AND CONCLUSIONS

The results of this experiment are given in Table I. At least five separate determinations of the ratio g_7/g_6 were made in each run. Each determination involved a minimum of two measurements of the resonant frequencies of both Li^6 and Li^7. The mean of these values is 2.64094 ± 0.00005, where the error is the average deviation.

It is possible to calculate the ratio g_7/g_6 from the known value of the ratio of the $\Delta\nu$'s by means of the Fermi[14] formula, in which the compound structure of the nucleus is not considered. This gives:

$$g_7/g_6=[(2I+1)_6/(2I+1)_7](m_{r6}/m_{r7})^3\Delta\nu_7/\Delta\nu_6 = 2.64061\pm0.00005, \quad (3)$$

where $m_{r6,r7}$ are the reduced masses of the $2s$ electrons in Li^6 and Li^7, and the stated error is the error only in the ratio $\Delta\nu_7/\Delta\nu_6$. The inclusion of the factor $(m_{r6}/m_{r7})^3$ is made by analogy with the corresponding case of the hydrogens, since in each case the problem is one involving a single s electron. No rigorous justification of the inclusion of this factor has been made. The neglect of this factor increases the ratio g_7/g_6 obtained from the $\Delta\nu$'s to 2.64072 ± 0.00005. The discrepancy between the observed value of g_7/g_6 and that calculated from (3) is then 0.00033 ± 0.00007. It seems probable that this discrepancy can be explained in a manner similar to that used in the treatment of H and D. This awaits a more detailed calculation of the effect of the nuclear structure of Li on the h.f.s.

[14] E. Fermi, Zeits. f. Physik **60**, 320 (1930).

Interaction of 14-Mev Neutrons with Deuterons*

J. H. Coon and R. F. Taschek
Los Alamos Scientific Laboratory, Los Alamos, New Mexico
(Received May 24, 1949)

By coincidence counting of recoil deuterons in a proportional counter telescope the angular distribution for $n-d$ scattering has been measured using monoergic neutrons of 14-Mev energy. The measurements covered the angular range corresponding to neutrons being scattered at angles between 180° and 70° in the center of mass system, and by extrapolation an approximate curve was obtained over all angles. Upper limits can be placed on the probability of the n-$2n$ disintegration process for ejection of protons in the angular range from 0° to 120° in the center of mass system.

INTRODUCTION

THERE have been numerous investigations, both experimental and theoretical, on the interaction of fast neutrons with deuterons. The difficulty in the development of adequate theory for this three particle system has more or less paralleled the difficulty of experimenters in the determination of reliable data. Recent[1] and forthcoming data in the region of 100 Mev has encouraged more theoretical investigation.[2,3] Extensive calculations in the energy region below 14 Mev have been made by Massey and Buckingham,[4,5] who have compared the results of their calculations with experimental data on angular distributions for scattering[6] at 2.5 Mev and with data on total $n-d$ cross sections[7] at several energies up to 13.5 Mev. Recent cloud chamber data of Darby and Swan[8] at 2.5 Mev agrees in character, but disagrees quantitatively, with ion chamber data of Coon and Barschall.[6]

Angular distribution data have not, to our knowledge, been published for neutron energies greater than 2.5 Mev.[9] For neutron energies above the threshold ($\frac{3}{2}\times 2.2$ Mev) for the disintegration of the deuteron, any experimental search should seek to isolate the scattering process from the $n-2n$ process. Ageno *et al.*[7] give uncertain experimental evidence for the existence of the $n-2n$ process at 14 Mev and compare their results with those of other experimenters and with theory, though the information is extremely meager.

The experiments of Ageno *et al.* were made difficult by their not having an intense source of monoergic neutrons. The recent development[10,11] of sources in this laboratory using the reaction $T(d,n)\mathrm{He}^4$ makes available an intense monoergic neutron source in the energy region from 12 to 18 Mev and simplifies the techniques required for measuring angular distributions and for differentiating between the scattering and $n-2n$ processes. In the present measurements, by using this source at a single neutron energy of 14 Mev, we have measured the angular distribution for scattering, and have been able to set upper limits for the $n-2n$ reaction over the angular region, for proton emission, from 0° to 80° in the laboratory system.

APPARATUS

The triple coincidence counting telescope and associated equipment used by Barschall and Taschek[12] for measuring $n-p$ scattering has been used, with methods similar to theirs, to investigate $n-d$ scattering. For most of the details regarding the neutron source, the proportional counter telescope, and the electronic counting circuits, reference may be made to the section on "Apparatus" in their report. Suitable variations in procedures were used in the present work to search for the possible presence of protons arising from the disintegration of the deuteron.

The 14-Mev neutrons from the $T(d,n)\mathrm{He}^4$ reaction were incident on a deuterium target located within the envelope of the counter telescope. The deuterium target was in the form of a thin layer of heavy paraffin melted in vacuum into a 0.004-inch recess in a 0.050-inch thick flat platinum button and then machined to a uniform thickness. The layer had a total weight of 15.98 mg, surface density 9.82 mg cm^{-2}, diameter about 1.5 cm, and for determination of the number of deuterium target atoms was assumed to have chemical composition $C_{45}D_{92}$. The proton impurity in the heavy paraffin was probably several percent, though there was no reliable analysis of the purity. The radiator was located inside

* This document is based on work performed at Los Alamos Scientific Laboratory of the University of California under Government Contract W-7405-eng-36.

[1] Cook, McMillan, Peterson, and Sewell, Phys. Rev. **72**, 1264 (1947); **75**, 7 (1949).

[2] Ta-You Wu and Julius Ashkin, Phys. Rev. **73**, 986 (1948).

[3] Geoffrey F. Chew, Phys. Rev. **74**, 809 (1948).

[4] H. S. W. Massey and R. A. Buckingham, Phys. Rev. **71**, 558 (1947).

[5] R. A. Buckingham and H. S. W. Massey, Proc. Roy. Soc. **A179**, 123 (1941).

[6] J. H. Coon and H. H. Barschall, Phys. Rev. **70**, 592 (1946).

[7] Ageno, Amaldi, Bocciarelli, and Trabacchi, Phys. Rev. **71**, 20 (1947).

[8] J. F. Darby and J. B. Swan, Nature **161**, 22 (1948); Australian J. Sci. Res. **A1**, 18 (1948).

[9] Gordon L. Griffith has kindly communicated to us from the University of Illinois preliminary cloud-chamber data on the angular distribution using 10 Mev neutrons. Comparison of the two sets of data shows fair agreement.

[10] Taschek, Hemmendinger, and Jarvis, Phys. Rev. **75**, 1464 (1949).

[11] Graves, Rodrigues, Goldblatt, and Meyer, to be published in Rev. Sci. Inst.

[12] H. H. Barschall and R. F. Taschek, Phys. Rev. **75**, 1819 (1949).

the common envelope of the three-counter system at a distance of 18.0 cm from the neutron source.

Limiting apertures with $\frac{3}{4}$-inch diameter holes were located in front of each of the three counters. An ionizing particle ejected from the radiator would cause a double and triple coincidence count simultaneously if it passed near the axis of the counter system through all three of the limiting apertures. The distance r between the radiator and the apertures determined the solid angle for counting and was different for different sets of data as well as for double and triple coincidence. All data were adjusted, by the factor $1/r^2$, to the distance 21.0 cm which was the value applying directly to the best angular distribution data. At the distance of 21.0 cm the maximum angular range for acceptance of particles ejected from the radiator was about ± 7 degrees. To obtain angular distributions the counter assembly was mounted so as to pivot about an axis through the radiator.

PROCEDURE

In order to distinguish between recoil deuterons and disintegration protons, the detector system was operated under a variety of conditions to obtain information about the range of ejected particles. In Fig. 1 range-angle curves are plotted for the various particles which may emerge when 14 Mev neutrons are incident on the heavy paraffin radiator. These are derived from well-known range-energy curves and the energy-momentum considerations of the possible processes. Since the $n-2n$ process leads to three product particles (unless a di-neutron is ejected), the disintegration protons will presumably have a continuous range of energies. Curve c is derived by assuming the case in which two separate neutrons emerge in the same direction and with the same energy. For such a case the energy E_p of the proton is determined by

$$(E_p)^{\frac{1}{2}}=\tfrac{1}{3}(E_n)^{\frac{1}{2}}\cos\theta\pm\tfrac{1}{3}(E_n\cos^2\theta+3E_n-6Q)^{\frac{1}{2}},$$

where E_n is the energy of the incident neutron, Q is the binding energy of the deuteron, and θ is the angle in the laboratory system between the direction of the incident neutron and that of the ejected proton. If the above assumption is correct, curve c gives the upper limit of the range of disintegration protons.

Examination of the curves of Fig. 1 suggests ways of discriminating between the different possible particles, and toward this end three sets of angular distribution data were taken as indicated below. The distance from the radiator to the $\frac{3}{4}$-inch diameter limiting aperture in front of the second or third counter is denoted respectively by "doubles r" which applies to double coincidence counting, and by "triples r" which applies to triple coincidence counting.

(1) 1.8 atmos. argon in counters; doubles $r=22.12$ cm, triples $r=29.23$ cm: With this pressure a particle required 57 cm range to penetrate through the counter telescope and cause a triple coincidence count. Similarly 44 cm range was required for a double coincidence count.

(2) 0.20 atmos. argon pressure; doubles $r=14.09$ cm, triples $r=21.00$ cm: This low pressure allowed particles of relatively small range to penetrate through the counters. A range of only 4.6 cm was required for triples and of 3.2 cm for doubles.

(3) 0.20 atmos. argon pressure; a 0.007-inch platinum absorber between the second and third counters; doubles $r=13.50$ cm, triples $r=20.86$ cm: The platinum absorber thickness was chosen so as barely to stop recoil deuterons at $\theta=0°$ (100 cm range). Thus a range greater than about 110 cm was necessary for triples, whereas, as in case (2), a range of only 3.2 cm was necessary for doubles.

One further set of data was taken at 0.20 atmos. pressure after reducing the size of the collimating apertures in the counter telescope from $\frac{3}{4}$-inch diameter to $\frac{3}{8}$-inch diameter. This reduced the over-all angular spread from about $\pm 7°$ to $\pm 4°$ and was done in an attempt to determine whether the angular resolution had large effect on the shape of the angular distribution curve.

As described in reference 12, many pulses induced by neutrons and by gamma-rays in the individual counters were larger than pulses originating from the small amount of ionization of the high energy protons or deuterons. On this account considerable care had to be taken in setting the bias level on the three pulse height discriminators which eliminated small pulses. Allowing too many small pulses to pass through to the coincidence circuit would cause a high background of accidental coincidence counts. For our 1.8 atmos. data the biases were set in the same manner as described in reference 12, using plutonium 239 alpha-particles inside the counters as a reproducible calibrating standard. In the case of our 0.20 atmos. data, a proton of energy 14 Mev lost only about 35 kev by ionization in one counter. For reliable setting of biases at this low level it was found more desirable to use, as a reproducible standard of pulse height, the small

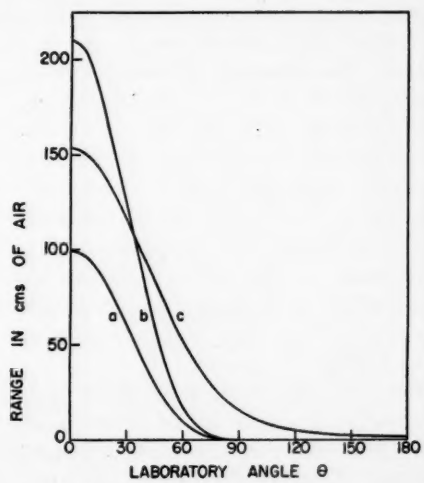

FIG. 1. Range *versus* angle for particles ejected from the heavy paraffin radiator by 14-Mev neutrons. Curve *a* is for recoil deuterons, curve *b* for recoil protons, and curve *c* for maximum-energy disintegration protons from $d(n,2n)p$.

TABLE I. Triple and double coincidence counts. The "Total count, rad. in" and "Total count, rad. out" correspond to the same number of monitor counts.

Recoil angle in lab system $=\theta$ Neutron angle in cm system $=\phi$	0 180	10 160	15 150	20 140	25 130	27.5 125	30 120	35 110	40 100	50 80	55 70	62.5 55	70 40	80 20
1.8 atmos. argon pressure														
Triples ($r=29.23$ cm)														
Total count, rad. in	701	200	56	52	84	37	36	22	45					
Total count, rad. out	28	6	3	9	26	13	9	9	37					
Net $\times (r_1/r)^2$ per monitor unit	109	94	54	21	14	12	14	6	2					
Standard error in net	±4	±7	±8	±4	±3	±4	±4	±2	±2					
Doubles ($r=22.12$ cm)														
Total count, rad. in	1480	390	112	180	304	128	139	124	404					
Total count, rad. out	207	63	38	72	211	101	84	86	374					
Net $\times (r_1/r)^2$ per monitor unit	118	91	41	30	13	8	15	11	3					
Standard error in net	±4	±6	±7	±5	±3	±4	±4	±4	±3					
0.20 atmos. argon pressure														
Triples ($r=r_1=21.00$ cm)														
Total count, rad. in	1073	934		429			383		325	466	381	189	145	124
Total count, rad. out	255	282		215			235		199	251	194	122	128	121
Net $\times (r_1/r)^2$ per monitor unit	126	82		36			19		21	27	29	17	4	0.7
Standard error in net	±6	±4		±4			±3		±4	±3	±4	±5	±4	±3
Doubles ($r=14.09$ cm)														
Total count, rad. in	6216	5280		3500			4213		3298	4165	3508	1999	1879	1914
Total count, rad. out	3900	3740		3046			3871		3019	3702	3053	1750	1789	1906
Net $\times (r_1/r)^2$ per monitor unit	123	87		34			19		21	26	32	28	10	0.9
Standard error in net	±5	±5		±6			±5		±6	±5	±6	±7	±7	±7
0.20 atmos. 0.007″ Pt absorber														
Triples ($r=20.86$ cm)														
Total count, rad. in	63	18		27										
Total count, rad. out	29	5		11										
Net $\times (r_1/r)^2$ per monitor unit	4.2	3.2		2.7										
Standard error in net	±1.2	±1.4		±1.0										
Doubles ($r=13.50$ cm)														
Total count, rad. in	6742	2901		3920										
Total count, rad. out	4267	1928		3434										
Net $\times (r_1/r)^2$ per monitor unit	128	102		33										
Standard error in net	±5	±7		±6										

gamma-ray-induced pulses from a weak radium source placed in a reproducible geometry outside the counter at the time of bias setting. The method of bias setting was as follows. Bias curves for coincidence counting of recoil deuterons at 0° (where specific ionization is a minimum) were taken, and the end of the bias plateau determined on the arbitrary but linear scale of an artificial pulse generator. To insure that high energy protons also be recorded, the operating bias was then chosen a little less than half the value at the end of the bias plateau curve, since the specific ionization of fast protons is half that of deuterons of the same energy. The counting rate with the radium source in place was then immediately determined at this bias setting and subsequently used for making small corrections in bias setting to account for daily fluctuations in gas multiplication and electronic gain.

Since the neutrons originated from the reaction $T(d,n)\mathrm{He}^4$, the relative number of neutrons incident on the deuterium radiator in any given counting interval was monitored by counting the alpha-particles in known geometry. An alpha-particle count would enable one to determine the absolute neutron yield at any angle if either of the following two conditions existed: if the angular distribution for the $D-T$ reaction were well known, or if the alpha-particles were counted at an angle ϕ_α equal to the neutron angle ϕ_n minus 180° in the center of mass system. As to the first of these conditions, rough measurements in this laboratory indicate that the thick target neutron yield is nearly isotropic in the center of mass system for our deuteron bombarding energy of 200 kev. As to the second condition, in our geometry ϕ_n was 100°, corresponding to which the most desirable angle for counting alphas would be $\phi_\alpha=80°$. Since our alpha-counting was done at $\phi_\alpha=116°$, one would expect an angular anisotropy to have a relatively small effect on our measurement. Combining the above considerations, we estimate that anisotropy will not introduce an error of more than 5 percent in our determination of the absolute number of neutrons incident on the heavy paraffin radiator.

The coincidence counting data was taken in cycles in which a count with the heavy paraffin in place was always followed by a background count taken with the paraffin coated platinum button rotated through 180° so as to expose clean platinum in place of the heavy paraffin. Subtraction of the background count then

gave the coincidence count due only to particles ejected from the heavy paraffin radiator.

RESULTS

Most of the experimental results on the angular dependence of coincidence counts are summarized in Table I. Three sets of data are given as obtained under the three sets of conditions described above. The total number of counts obtained with the radiator in place ("rad. in") and with the radiator rotated out ("rad. out") are listed and determine the statistical accuracy of the data. In analysis of the data the total count per 64,000 counts ("monitor unit") on the alpha-particle monitor is determined, and the result for "rad. out" is subtracted as a background from that for "rad. in" to determine the net coincidence count due to the presence of the radiator. The net count is then adjusted to the solid angle corresponding to the $r=21.0$ cm distance and listed in Table I under "Net $\times (r_1/r)^2$ per monitor unit" along with the statistical error.

In the discussion that follows it will become evident that the net coincidence count must be almost entirely due to recoil deuterons, to the exclusion of disintegration protons or recoil protons. The first evidence for this appears in examination of the data from 0 to 20°. In this angular range the doubles and triples at 1.8 and at 0.20 atmos. all agree within statistical errors. This implies that, within our accuracy of about ± 10 percent, all particles having range greater than 3.2 cm also have range greater than 57 cm; i.e., there are no disintegration protons of energy between about 1.5 Mev and 7 Mev. Since, for the 0.20 atmos. data, there is very little difference in the range required for doubles (3.2 cm) and for triples (4.6 cm), the agreement between these data is good evidence to justify our method of adjusting the data to one solid angle by the appropriate $1/r^2$ factors.

Further evidence for the premise stated above lies in examination of the data at angles greater than 20°. With increasing angle above 20°, the 1.8 atmos. data rapidly fall below the 0.20 atmos. data. This is to be expected if the particles are recoil deuterons, since at 1.8 atmos. recoil deuterons at angles larger than 20° begin failing to have sufficient range to penetrate into the third counter if one includes the effects of radiator thickness (8.6 cm air equivalent) and angular spread. The corresponding angle for recoil contamination protons is 38°, and for maximum-range disintegration protons is 46 degrees. Similar angles applying to the occurrence of double coincidences are about 5° larger. The low value of the 1.8 atmos. datum at 40° sets an upper limit to the number of disintegration protons of energy greater than 7 Mev at this angle.

The 0.20 atmos. data, as shown in Fig. 2, form a smooth curve for angles up to about 55° where there is a fairly sudden drop, slightly more delayed for the doubles data (solid circles) than for the triples data (hollow circles). This drop must be expected for recoil deuterons, which, for angles greater than 50°, begin failing to have range enough to cause triples. The corresponding angle for recoil protons is 56° and for maximum-range disintegration protons is 86°, while the same angles applying to double coincidences are a few degrees larger. The break in the curve is not very sharp because of the effect of radiator thickness and because of lack of angular resolution. The low value of the 0.20 atmos. data in the region of 80° sets an upper limit to the number of disintegration protons near 80° of energy greater than about 1.5 Mev.

The data with the platinum absorbing foil at 0°, 10°, and 20°, also shown in Fig. 2, indicates that at 0° the number of particles of range greater than 110 cm is about 3 percent of the number of particles of range less than 110 cm. Assuming all of this 3 percent count is due to contamination protons, and using the best available values of the $n-p$ and $n-d$ differential scattering cross sections for 0° recoils, we can calculate the proton contamination in the heavy paraffin radiator. The value so obtained is 6 percent, which is not an unexpectedly high value. Thus an upper limit is set on the number of disintegration protons at 0° of range greater than 110 cm.

The above rather detailed and piecemeal evidence against the presence of disintegration protons leads the authors to believe that almost certainly the integrated cross section for the disintegration process over the range from 0° to 80° in the laboratory system and

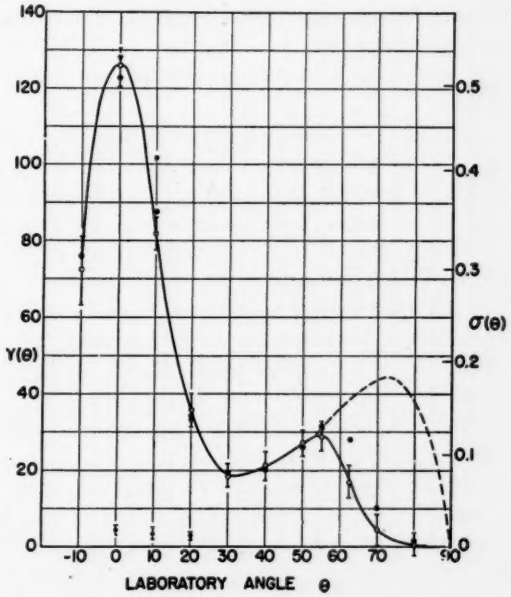

FIG. 2. Coincidence counting data as a function of laboratory angle θ for recoil deuteron. $Y(\theta)$=net number of coincidence counts per 64,000 alpha-monitor counts. $\sigma(\theta)$=cross section per unit solid angle. The dashed curve is an extrapolation drawn to give an area under the curve corresponding to the total scattering cross-section value taken from reference 10.

⧗=triples at 0.20 atmos. pressure in counters.
●=doubles at 0.20 atmos.
⧗=triples with 0.007" Pt absorber, 0.20 atmos.
✱=doubles with 0.007" Pt absorber, 0.20 atmos.

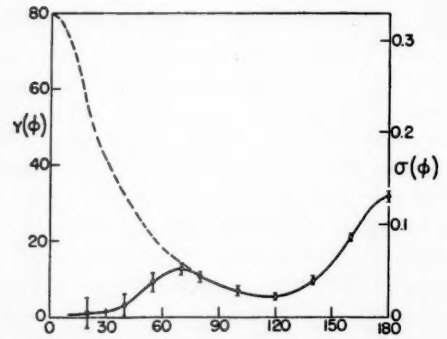

FIG. 3. Angular distribution data plotted in center of mass system. The data plotted are the triple coincidence data with 0.20 atmos. pressure in counters. The dashed curve is an extrapolation drawn to give an area under the curve corresponding to the total scattering cross-section value taken from reference 10. $\sigma(\phi)$ = scattering cross section per unit solid angle in the center of mass system.

yielding protons of energy greater than about 2 Mev is less than about 0.05 barn. It follows that the curve of Fig. 2 is essentially the $n-d$ scattering angular distribution in the range from 0 to 50°. Information about the curve in the remaining region between 50° and 90° may be gotten by extrapolation using the total cross-section values of Ageno *et al.*[7] The method of extrapolation will be described below.

The data taken with the narrow geometry for which the angular resolution was about ±4° are compared with the ±7° resolution data in Table II, which tabulates the ratio of the count with $\theta=0°$ to the count with $\theta=10°$. Within statistical accuracies the change in angular resolution has no effect on these ratios, indicating that the ±7° resolution data are not badly distorted.

Examination of Table I shows abnormally high background coincidence rates for the 0.20 atmos. data as compared to the 1.8 atmos. data. It was shown, by measurements of the time resolution of the detecting and counting system and by recording the individual counts occurring in each of the three counters, that most of this high background was not due to accidental coincidences. It is reasonable to expect that there are many relatively short range background particles from the brass counter walls, steel diaphragms, and filling gas which can cause a high true coincidence background at 0.20 atmos. but not at 1.8 atmos.

By making observations at 0° Ageno *et al.*[7] conclude that possibly the $n-2n$ process has a cross section of the order of 0.05 barn. Our data at 0° sets an upper limit of about 0.05 barn for differential cross section in the laboratory system at 0° unless there are a relatively large number of low energy protons of energy less than 1.5 Mev. The two sets of data are therefore not inconsistent.

Figure 3 shows our angular distribution data plotted in the center of mass system, ϕ being the angle for the scattered neutron. The data plotted are the triple coincidence data at 0.20 atmos. counter pressure, and the dashed curve is the extrapolation referred to above. The extrapolation was made in two ways, and essentially the same result obtained. The first method was to assume our absolute neutron flux measurement by alpha-particle counting was correct, calculate the differential cross section at $\phi=180°$, and draw the extrapolation with a somewhat arbitrary shape but in such a way that $\int_0^\pi \sigma(\phi)\sin\phi d\phi$ was equal to the value 0.86 barn given in reference 7. The second method used the fact that the $n-p$ scattering measurements of Barschall and Taschek had been performed with identical equipment and under directly comparable geometric conditions. The alpha-particle counter was considered not as a neutron flux measuring device but only as a flux monitor. Then the extrapolation of the $n-d$ scattering yield curve was drawn to satisfy the relation

$$\int_0^\pi Y_{nd}(\phi)\sin\phi d\phi=\frac{N_d\sigma_{nd}(\text{total})}{N_p\sigma_{np}(\text{total})}\int^\pi Y_{np}(\phi)\sin\phi d\phi,$$

where the $Y(\phi)$'s are relative yields per monitor count, N is the total number of deuterons or protons in the radiators, and where the $n-p$ scattering is assumed isotropic in the center of mass system. This method thus does not depend on our absolute neutron flux determination and uses the ratio $\sigma_{nd}(\text{total})/\sigma_{np}(\text{total})$ of the total cross-section values rather than either of the individual cross sections given in reference 7. Both methods determine the fraction of the area under the yield curve in the extrapolated region, but the second method does not determine the scale of values for the absolute differential scattering cross section $\sigma(\phi)$. The two methods agree as to the fraction of the area in the extrapolated region, and one therefore has more confidence in the neutron flux measurement which determines the scale of absolute values indicated in Fig. 3. The corresponding scale of values of differential cross section $\sigma(\theta)$ for the recoil deuteron yield in the laboratory system is shown in Fig. 2.

Since the total cross section is obtained by integrating the function $\sigma(\phi)\sin\phi$, our extrapolation gives a poor determination of $\sigma(\phi)$ at $\phi=0°$. However, it is certain that there is a peak for forward scattering of the neutron which is considerably larger than the peak for backward scattering, even though the forward scattering peak is in the extrapolated region. A direct measurement of the forward scattering peak would be very desirable, but may be accessible only to measurements in which the scattered neutrons themselves are detected.

TABLE II. Effect of angular resolution.

		Doubles	Triples
±7° resolution:	$\frac{0°\text{ count}}{10°\text{ count}}=$	1.41±0.12	1.54±0.12
±4° resolution:	$\frac{0°\text{ count}}{10°\text{ count}}=$	1.59±0.11	1.55±0.22

From a comparison of our curve at 14 Mev with the theoretical curves of Buckingham and Massey[5] at 11.5 Mev, one may make the following general statements. The theoretical and the experimental curves agree in features of marked angular asymmetry with a minimum at about 110° and a forward scattering peak larger than the backward scattering peak. However, regardless of how the curves are normalized the experimental curve differs at some angles by factors of several from the various theoretical curves. As is pointed out by Massey and Buckingham,[4] their "exchange force" calculations will probably come into better agreement with experimental *total* cross-section values[7] in the region of 14 Mev when they take into account the contributions of higher than p angular momentum states, which were ignored in their original calculations. Such a refinement in the "exchange force" theory may also bring it into better agreement with our angular distribution data. If such an extension of the theory gives favorable results, the *over-all* evidence will be somewhat more in favor of "exchange forces" than "ordinary forces." However, as Darby and Swan[8] point out, their angular distribution data at 2.5 Mev agrees very closely with the "ordinary force" curve of Buckingham and Massey, whereas the data of Coon and Barschall[6] at this energy fits better with the "exchange force" curve. Obviously more accurate and complete data are necessary.

We wish to thank S. G. Forbes for keeping the detecting equipment in operating condition as well as for much of the data taking, and E. R. Graves for helpful discussions and criticisms.

PHYSICAL REVIEW VOLUME 76, NUMBER 6 SEPTEMBER 15, 1949

Some Properties of Superconductors below 1°K. I. Titanium

J. G. DAUNT AND C. V. HEER*
The Mendenhall Laboratory, The Ohio State University, Columbus, Ohio
(Received June 6, 1949)

Magnetic measurements on titanium metal of purity 99.95 percent have been carried out down to 0.3°K. The titanium was found to be superconductive with a transition temperature of 0.53°K. Measurements of the magnetic threshold curve were made for which the initial slope was found to be 470 gauss per degree.

INTRODUCTION

IN carrying out investigations on techniques required for the observation of nuclear paramagnetism, the properties of some superconductors have been studied below 1°K. Details of the results obtained with high purity titanium are given herewith.

Titanium of stated purity approximately 99.75 percent was found by Meissner[1] in 1930 to become superconductive by observation of the resistance of a single crystal specimen. The transition point in zero magnetic field was found to be 1.13°K. Subsequent resistance measurements by Meissner, Franz, and Westerhoff[2] on other titanium samples showed superconductive transitions at higher temperatures, one being as high as 1.77°K. de Haas and van Alphen[3] using titanium of unstated purity found by resistance measurements a superconductive transition at about 1.72°K, with a broad transition region. Webber and Reynolds[4] in 1948 observed an anomaly in the resistance of a titanium specimen, prepared in a different manner from the above, the resistance showing a marked decrease over a broad temperature range between 3°K and 1°K without, however, showing superconductivity.

Measurements by Shoenberg,[5] on the other hand, on the magnetic properties of titanium of purity 99.9 percent revealed no sign of superconductivity, defined by the establishment of zero magnetic induction throughout the entire specimen, down to temperatures of about 1.0°K. Shoenberg[5] reported, however, the occurrence of a very small diamagnetic anomaly at about 1.5°K and suggested that the previous observations of zero resistance at about this temperature were due to very small regions in the specimen becoming superconductive where chemical or physical impurity might have been concentrated. Such a view is supported by the considerable scatter in the values of transition points observed.[1-3]

The experiments reported in this paper were undertaken in order to clarify the question of the possible occurrence of superconductivity in titanium which in view of Shoenberg's work appeared doubtful. From the position of titanium in the periodic table it would appear that it should become superconductive, since the other metals in the same sub-group are super-

* Frederick Gardner Cottrell Fellow.
[1] W. Meissner, Zeits. f. Physik **60**, 181 (1930).
[2] Meissner, Franz, and Westerhoff, Ann. d. Physik **13**, 555 (1932).
[3] W. J. de Haas and P. M. van Alphen, Proc. Amst. Roy. Akad. Sci. **34**, 70 (1931).
[4] R. T. Webber and J. M. Reynolds, Phys. Rev. **73**, 640 (1948).
[5] D. Shoenberg, Proc. Camb. Phil. Soc. **36**, 84 (1940).

conductors.[6] This view is supported by consideration of its atomic volume.[7] It seemed of interest, therefore, to extend magnetic measurements on a titanium sample of higher purity than previously used to the temperature region below 1°K.

EXPERIMENTAL METHODS AND RESULTS

A special sample of titanium of 99.95 percent purity was kindly furnished us by the Battelle Memorial Institute. The method of preparation by the thermal decomposition of the iodide on a hot wire has been fully described elsewhere.[8]

Cooling to liquid helium temperature was carried out by the use of a Simon-type[9] expansion liquefier having provision for withdrawing the liquid helium into external cryostats.[10] Temperatures below 1°K were obtained by the magnetic methods,[11] using chromium potassium alum as the working substance, the magnetic field being produced by a large permanent magnet giving a field of 8000 gauss in a 2-inch gap.

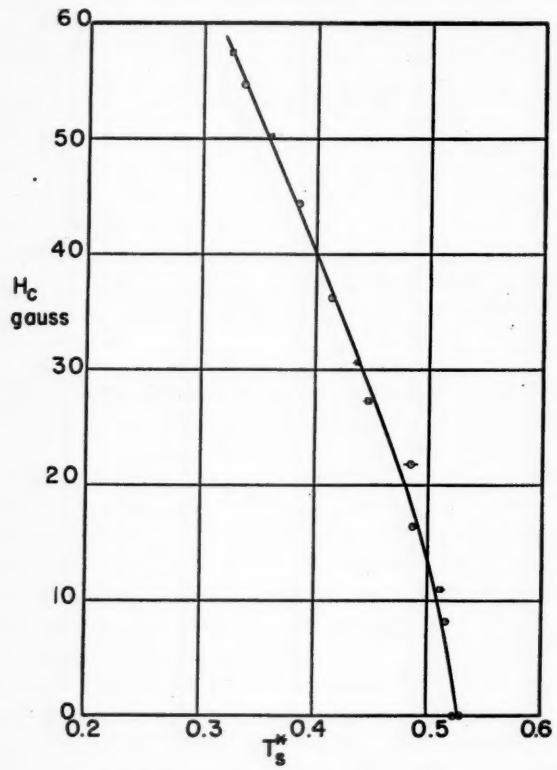

FIG. 1. The measured magnetic threshold as a function of temperature (Curie scale).

Thermal contact between the chromium potassium alum and the titanium metal was achieved mechanically, as previously carried out by Kurti and Simon.[6(b)] The metal was divided into small pieces of linear dimensions approximately 2–3 mm and these pieces were distributed at random in the powdered salt and the mixture compressed under a pressure of 200–300 atmos. into an ellipsoidal pill having major and minor axes of length 27 mm and 13 mm, respectively. This direct method of making thermal contact was found to be satisfactory down to the lowest temperatures used (0.3°K), as previously found by Kurti and Simon.[6(b)]

The filling factor, f, of the specimen, i.e., the ratio of the distributed density of the powder to the crystalline density, was 0.79. Hence, the calculated value of Δ, given by $\Delta = cf(4\pi/3 - N)$, where c is the Curie constant per cc and N the demagnetizing factor of the specimen, was taken to be 0.011 degrees. This value has been taken in calculating T_s^*, i.e., the extrapolated temperature based on Curie's law for a spherical specimen.[12]

The temperature was calculated in the usual manner from observations of the magnetic susceptibility of the sample, the latter being measured by the ballistic mutual inductance method.[13] These susceptibility measurements served also to detect the occurrence of the transition from the superconductive to the normal state of the titanium, such transitions producing sudden changes in the observed total susceptibility of the specimen, due to the perfect diamagnetic properties of the superconductive state.

The measurements were made by allowing the specimen to warm up slowly either in a small externally applied magnetic field (<60 gauss) or in zero field, susceptibility measurements being taken at regular time intervals. Superconductivity, evident by strong diamagnetism of the titanium, was observed at temperatures below 0.53 degrees. Details of the kind of transitions observed will be given in a subsequent publication. From the measurements in zero magnetic field, an assessment could be made of the percentage volume of the titanium which became superconductive. Within experimental error this was 100 percent, indicating that the superconductive effects were not due to impurities. The rate of warm-up was sufficiently slow to ensure satisfactory temperature equilibrium between the salt and the metal, approximately one hour being required for the specimen to warm from 0.3°K to 0.6°K. This warm-up time corresponded to an average heat influx of 350 ergs per minute.

The transition temperature for the titanium was found to be 0.527 ± 0.006, with a slope for the magnetic

[6] (a) W. Meissner, Ergeb. d. exakt. Naturwiss. **11**, 222 (1932); (b) N. Kurti and F. Simon, Proc. Roy. Soc. **A151**, 610 (1935); and (c) D. Shoenberg, *Superconductivity* (Cambridge University Press, London 1938), p. 2.

[7] See, for example, Burton, Grayson-Smith, and Wilhelm, *Phenomena at the Temperature of Liquid Helium* (Reinhold Publishing Corporation, New York, 1940), p. 94.

[8] Campbell, Jaffee, Blocher, Gurland, and Gonser, J. Electrochem. Soc. **93** 271 (1948).

[9] F. Simon, Physik Zeits. **34**, 232 (1933).

[10] R. B. Scott and J. W. Cook, Rev. Sci. Inst. **19**, 889 (1948).

[11] P. Debye, Ann. d, Physik **81**, 1154 (1926); and W. F. Giaque J. Am. Chem. Soc. **49**, 1864 (1927).

[12] See N. Kurti and F. Simon, Phil. Mag. **26**, 849 (1938).

[13] See N. Kurti and F. Simon, Proc. Roy. Soc. **A149**, 152 (1935); and W. J. de Haas and Wiersma, Physica **2**, 335 (1935).

threshold of

$$(dH_c/dT)_{H=0}=470 \text{ gauss/degree.}$$

No traces of minor magnetic anomalies at temperatures between 0.53 and 4.2°K were observed. A plot of the measured magnetic threshold curve is given in Fig. 1, the temperatures being plotted on the Curie scale, T_s^*. The possible error in interpreting the observed results is given by the lines drawn through the points in Fig. 1. Within the temperature range concerned, the deviations of the values of T_s^* from the absolute temperature would be small and not greater than the experimental error of observation.

DISCUSSION

The low value found for the superconducting transition point of titanium (0.53) confirms the work of Shoenberg[5] who found no sign of complete superconductivity down to 1.0°K, and indicates that the results previously obtained by resistance measurements were probably due to physical or chemical impurity effects rather than being characteristic of pure titanium metal. The low transition point also lends some support to the considerations put forward by de Launay and Dolecek.[14]

The high value for the slope of the magnetic threshold curve is comparable with that for the "hard" superconductors, e.g., Ta and Cb.[15] The magnetic threshold curve for Zr, in the same sub-group of the periodic table as Ti, also has a high slope, being approximately 400 gauss per degree.[6(a)] For very pure thorium, however, the only other superconductor in Group IVa for which the magnetic threshold curve has been measured,[5] is as small as 190 gauss per degree, a figure comparable with those for the "soft" superconductors.[15,16] On the other hand, measurements[5] on less pure and on cold-worked thorium showed much higher slopes for the threshold curve, a result which made the subdivision between hard and soft superconductors appear artificial, the high slopes possibly being due to impurity effects or physical strain. This view is supported by the work of Lasarew and Galkin[17] on the effect of strain, and it would consequently be desirable to extend the magnetic measurements on the hard superconductors to include systematically the effects of annealing, etc.** In summation, it is certainly not possible to regard the magnetic threshold curves of the hard superconductors as forming a basis for the calculation of the thermodynamical properties, such as entropy difference, etc., with the same confidence as those for the soft superconductors. In view of this and because of the limited temperature range of our measured curve for titanium, no calculations have been made of thermodynamical properties.

ACKNOWLEDGMENTS

We wish to thank Professor H. H. Nielsen for his support of this low temperature program in the Mendenhall Laboratory, and the Research Corporation for their grant-in-aid of research on nuclear paramagnetism for which this work is preliminary and for their establishment of a fellowship for one of us (C.V.H.).

Our thanks are also due to the Ohio State University Research Foundation and the Ohio State University Development Fund for their aid. The later stages of the work were assisted by a contract between the Office of Naval Research and the Ohio State University Research Foundation.

We also thank Mr. A. A. Silvidi for his assistance during the experiments.

[14] J. de Launay and R. L. Dolecek, Phys. Rev. **72**, 141 (1947).
[15] Daunt, Horseman, and Mendelssohn, Phil. Mag. **27**, 754 (1939).
[16] J. G. Daunt and K. Mendelssohn, Proc. Roy. Soc. **A160**, 127 (1937).
[17] B. Lasarew and A. Galkin, J. Phys. U.S.S.R. **8**, 376 (1944).

** Measurements of the magnetic properties of superconducting tantalum in various physical states have been made by R. T. Webber (Phys. Rev. **72**, 1241 (1947)). However the observed slopes of the threshold curves even for the annealed specimens were not smaller than that previously reported by Daunt and Mendelssohn (see reference 16).

Radiations from Indium (114) and Barium (140)*

C. E. MANDEVILLE AND E. SHAPIRO
Bartol Research Foundation of the Franklin Institute, Swarthmore, Pennsylvania

(Received May 13, 1949)

Indium (114) emits soft conversion electrons (range ~20 mg/cm²) and hard nuclear beta-rays of energy 1.89 Mev. Lead absorption gives quantum energies of 0.15 Mev and 0.70 Mev whereas coincidence absorption yields a maximum quantum energy of 0.90 Mev. The harder quanta are associated with an inner beta-ray group constituting less than 1.5 percent of the total beta-radiation, if with any group at all. A gamma-gamma-coincidence rate of $(0.25\pm0.02)\times10^{-3}$ coincidence per gamma-ray was noted.

Barium (140) emits nuclear beta-rays having a maximum energy of 0.91 Mev and two gamma-rays having quantum energies of 0.14 Mev and 0.6 Mev as indicated by absorption in lead. Beta-gamma-coincidence data, obtained from Ba^{140} in equilibrium with La^{140} and from Ba^{140} freshly separated from its daughter element, show that the beta-ray spectrum is complex and that about twenty percent of the disintegrations proceed by way of the inner beta-ray group which is coincident in time with gamma-radiation.

See note added in proof.

INTRODUCTION

THE radiations of the isomers of In^{114} have been studied intensively by many investigators. Lawson and Cork[1,2] report a maximum beta-ray energy of 1.98 Mev (cloud chamber and magnetic field) for the 72-second In^{114}. The value for the converted gamma-ray of $*In^{114}$ was reported as 0.19 Mev[2]. A more recent classified report,[3] gives spectrometric values of 1.98 Mev and 0.186 Mev for these radiation energies. A recent report by Cork *et al.*[4] gives 190.9 kev as the energy of the highly converted gamma-ray of $*In^{114}$ and 0.81 Mev as the energy of a relatively hard gamma-ray emitted by the two isomers in equilibrium.

No comment is made in their paper regarding the presence of the harder gamma-ray. Its energy value, obtained by lead absorption, is simply quoted in their Table I. The presence of the hard quantum stimulated some interest in the matter on the part of the writers so that some radioactive indium was obtained from the Oak Ridge pile for investigation. Chemical separations were carried out for the removal of Ag, Cu, Fe, Pb, Ca, and Ni as contaminants indicated by spectrographic analysis.

The historic barium (140), parent element of the 40-hour lanthanum (140), is among the products of uranium fission.[5] Among the few papers in the open literature dealing with this activity are an absorption value of 1.2 Mev and a spectrometric measurement giving 1.05 Mev[6] as the maximum energy of the nuclear beta-rays. The gamma-radiation is reported to have an energy of 0.54 Mev. Classified measurements include beta-ray end points at 0.4 Mev and 1.0 Mev and lead absorption measurements, giving a quantum energy of 0.5 Mev.[7] Still other classified measurements give an absorption limit of 1.1 Mev for the beta-rays[8] and a spectrometric value of 0.529 Mev for the hard gamma-ray.[9] Additional classified data[10] give good agreement with the values already quoted.

For this investigation, Ba^{140} was produced in the fission process at the Oak Ridge pile. Measurements of radiation energies and coincidence rates of Ba^{140} were carried out when it was in equilibrium with La^{140} as well as when freshly separated from it.

A complete description of the general methods and techniques used in obtaining the data to follow has been previously given.[11]

In^{114}

A thin source of the chemically purified $*In^{114}-In^{114}$ was placed before a single G-M counter, and the absorption curve of Fig. 1 was obtained. The end point, occurring at 0.87 g/cm² in aluminum, corresponds to a maximum energy of 1.89 kev as calculated by Feather's equation.[12] In the region of small absorber thickness, (< 20 mg/cm²), the conversion electrons of the 48-day metastable state of $*In^{114}$ are clearly evident. The curve closely resembles one previously published by Lawson and Cork.[2] If the portion of the curve relating to the 72-second period is extrapolated to zero absorber thickness, it can be shown that the number of nuclear beta-rays present is about equal to the number of conversion electrons, indicating a conversion coefficient of the order of one hundred percent.

The gamma-radiation of the purified indium source was absorbed in lead as plotted in Fig. 2. It is immedi-

* Assisted by the joint program of ONR and the AEC.

[1] J. L. Lawson and J. M. Cork, Phys. Rev. **56**, 291 (1939).

[2] J. L. Lawson and J. M. Cork, Phys. Rev. **57**, 982 (1940). Other references to measurements carried out prior to 1940 may be found in this paper.

[3] P. W. Levy, Plutonium Proj. Rept. Mon P-250 (February, 1947), p. 26, quoted by Seaborg and Perlman in their recent isotopic table.

[4] Cork, Shreffler, and Fowler, Phys. Rev. **74**, 1657 (1948).

[5] O. Hahn and F. Strassman, Naturwiss. **27**, 11 (1939).

[6] W. Rall and R. G. Wilkinson, Phys. Rev. **71**, 321 (1947).

[7] D. W. Engelkemeier, Plutonium Proj. Rept. CC-1959 (August, 1944), quoted by Seaborg and Perlman.

[8] H. A. Levy and L. G. Stang, Plutonium Proj. Rept. CC-1204, (January, 1944), p. 9, quoted by Seaborg and Perlman.

[9] V. A. Nedzel and M. B. Sampson, Plutonium Proj. Rept. CC-2283 (October, 1944), quoted by Seaborg and Perlman.

[10] Plutonium Proj. Rept., "Nuclei formed in fission," Rev. Mod. Phys. **18**, 513 (1946).

[11] C. E. Mandeville and M. V. Scherb, Nucleonics **3**, 2 (1948).

[12] N. Feather, Proc. Camb. Phil. Soc. **34**, 599 (1938).

ately clear that two gamma-rays are present. Resolution of the curve into its two components gives linear absorption coefficients corresponding to quantum energies of 0.15 Mev and 0.70 Mev. Taking into account the variation with energy of the quantum efficiency of the counter, it is estimated that the soft radiation is about six times as intense as the hard gamma-rays. The harder gamma-ray is undoubtedly that previously noted by Cork *et al.*[4] It cannot be said whether the softer quanta are emitted with the disintegration of the 72-second period or whether they are unconverted gamma-rays emitted at the 48-day level. Because of the inaccuracies of absorption methods, the latter possibility cannot be dismissed.

A source of $^{*}In^{114}-In^{114}$ was placed behind a thick aluminum block so that recoil electrons ejected from the block by the gamma-rays would traverse two G-M counters in coincidence. Aluminum absorbers were placed between the two counters to obtain the coincidence absorption curve of Fig. 3. From a previously published calibration curve,[13] an energy of 0.90 Mev is deduced. The disagreement between the two values of the energy of the harder gamma-ray may be simply a result of the inaccuracies of absorption methods. When a source of radioactive indium was placed between two gamma-ray counters in coincidence, a gamma-gamma-coincidence rate of $(0.25\pm0.02)\times10^{-3}$ coincidence per gamma-ray was measured. Several different geometries were employed, but the gamma-gamma-coincidence rate persisted, attesting the validity of the effect. A search was made for beta-gamma-coincidences, but none were detected. Assuming that a genuine coincidence rate as large as the accidental rate could be detected, knowing the calibration of the gamma-ray counter of the beta-gamma-coincidence counting arrangement, and assuming that the beta-rays of a low intensity inner beta-ray group are followed by about 0.8 Mev of gamma-ray energy, it was concluded that the softer beta-rays have an intensity less than 1.5 percent of the principal group at 1.89 Mev. This conclusion rests upon the assumption that the hard gamma-rays are indeed coupled with a nuclear beta-ray spectrum. Naturally, it cannot be said whether the supposed beta-ray spectrum originates at the 72-second level or at the 48-day level.

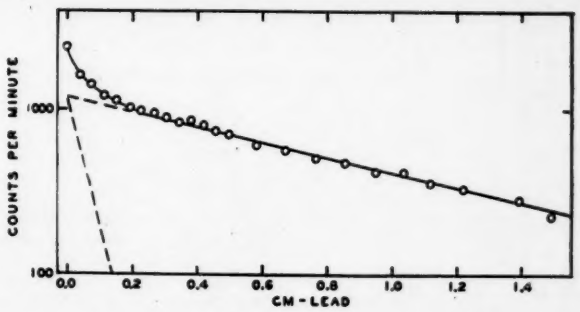

FIG. 2. Absorption in lead of the gamma-rays of indium (114). The linear absorption coefficients taken from the curve correspond to quantum energies of 0.15 Mev and 0.70 Mev.

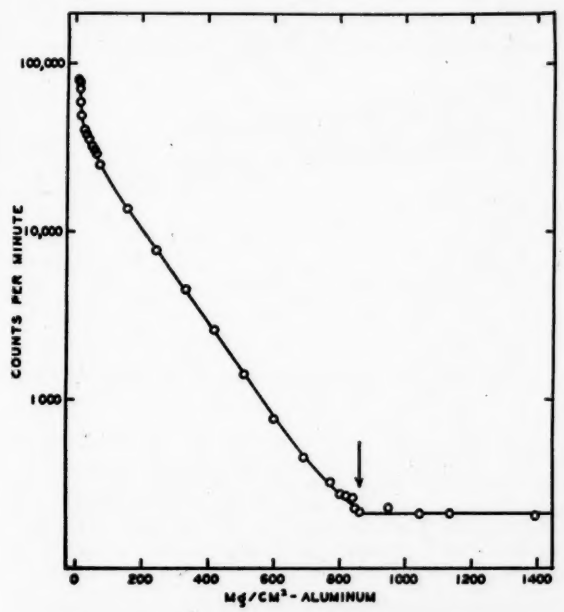

FIG. 1. Absorption in aluminum of the charged particles of $^{*}In^{114}-In^{114}$. Soft conversion electrons and hard nuclear beta-rays are present. The end point corresponds to a maximum beta-ray energy of 1.89 Mev as calculated by Feather's equation.

[13] C. E. Mandeville and M. V. Scherb, Phys. Rev. **73**, 1434 (1948).

Ba^{140}

The aluminum absorption curve of the beta-rays of Ba^{140}, separated from La^{140}, is shown in Fig. 4. The measurements were completed within 40 minutes after the chemical separation. The end point corresponds to a maximum beta-ray energy of 0.91 Mev.

The gamma-rays of Ba^{140} were absorbed in lead as shown in Fig. 5. The starting time of each curve after the initial separation of barium from lanthanum is indicated at the right of the drawing. Each curve was completed in less than twenty minutes after the starting time; that is, the first curve was commenced five minutes after chemical separation and completed within twenty-five minutes after separation. It is evident that the first curve, the five minute curve, is readily analyzed into two components. The linear absorption coefficients taken from the curve correspond to quantum energies of 140 kev and 0.6 Mev, respectively. These values are only approximate since they are subject to the inaccuracies of the absorption method. It appears, however, that the softer gamma-ray has not been previously reported. The curves of Fig. 5 show how the gamma-count increases with time and with the growth of La^{140}, a hard gamma-ray emitter. The curvature in the region of low energy becomes less and less apparent with time and as the activity of the daughter element increases. This shows that the soft radiation, so clearly evident on the curve taken five minutes after

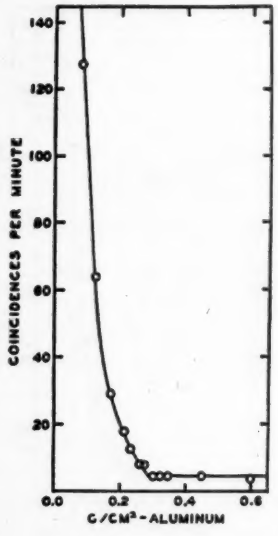

FIG. 3. Coincidence absorption of the recoil electrons of the gamma-rays of In^{114}. The quantum energy calculated from the end point is 0.90 Mev.

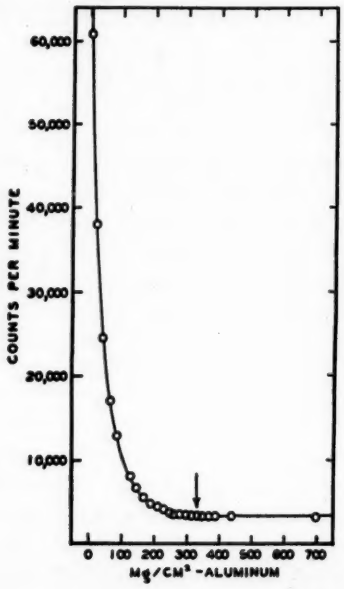

FIG. 4. Absorption in aluminum of the beta-rays of Ba^{140}. The end point corresponds to an energy of 0.91 Mev as calculated by Feather's equation.

chemical separation, is definitely emitted in the disintegration of Ba^{140}.

The beta-gamma-coincidence rate of Ba^{140}, in equilibrium with La^{140}, is shown in curve *A* of Fig. 6. The curve is seen to rise from an extrapolated value of 1.0×10^{-3} coincidence per beta-ray at zero absorber thickness to 1.8×10^{-3} coincidence per beta-ray in the vicinity of 0.34 g/cm². The coincidence rate beyond this absorber thickness is characteristic of La^{140} alone. Below 0.34 g/cm², the coincidence rate of La^{140} is reduced by the presence of the beta-rays of Ba^{140} which are obviously accompanied by much less gamma-ray energy than are those of La^{140}. Were the beta-rays of Ba^{140} accompanied by no gamma-rays whatever, the beta-gamma-coincidence rate at zero absorber thickness would be exactly half as great as it is beyond 0.34 g/cm². From the curve, it is seen that this is not quite the case. This fact alone shows that a small number of beta-gamma-coincidences are present in the disintegration of Ba^{140}.

Curve *B* is a plot of the genuine beta-gamma-coincidence rate of Ba^{140} alone. Barium was chemically separated from lanthanum at each point of the curve. Approximately fifteen minutes were required to prepare and mount the barium source after each separation. Coincidences were observed for about eight minutes at each point so that each measurement was completed in less than twenty-five minutes after the chemical separation. Only brief observations could be made at each point of curve *B* because of the rapid growth of La^{140}. Even very small traces of La^{140} are sufficient to invalidate any Ba^{140} measurements. This results from the fact that La^{140} is characterized by radiation energies and coincidence rates which are very high as compared with those of pure Ba^{140}. The aforementioned brevity of the coincidence measurement at each point of curve *B* made statistical accuracy difficult, and measurements were almost impossible to carry out at appreciable absorber thicknesses. Although the coincidence rate appears to be decreasing with increasing absorber thickness, the statistical accuracy of the points at larger absorber thickness makes it impossible to say that the coincidence rate eventually decreases to zero to indicate a complex spectrum. However, this conclusion can be reached by another rather simple argument.

It has been previously shown[13] in this laboratory that although the beta-ray spectrum of La^{140} is complex, the beta-gamma coincidence rate appears to be constant, independent of the beta-ray energy. It was also concluded that on the average, each beta-ray of La^{140} is followed by 2.3 Mev of gamma-ray energy.* Extra-

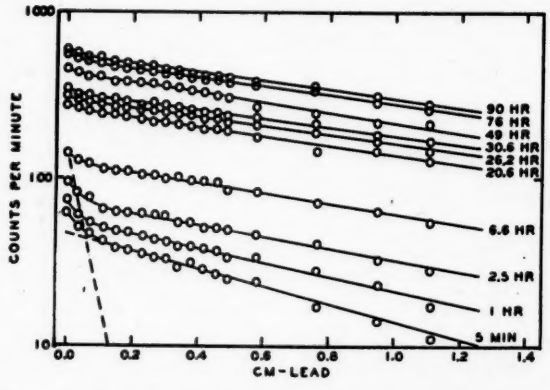

FIG. 5. Absorption in lead of the quantum radiations of Ba^{140}—La^{140}. The time after the initial chemical separation at which each curve was commenced is given at the right of the figure. A time of less than twenty minutes was required to complete each curve. The curve begun five minutes after the separation is analyzed into two components having energies of 140 kev and 0.6 Mev.

* In connection with the gamma-radiation of La^{140}, it should be mentioned that the energy of the hardest gamma-ray was erroneously reported as 2.16 Mev (see reference 13). This estimate was obtained from a preliminary calibration curve for the coincidence counting set which was based upon an unduly low value for the maximum energy of the gamma-rays from Ga^{72}. Taking the energy of the hardest gamma-ray of Ga^{72} to be 2.51 Mev, the maximum energy of the gamma-rays of La^{140} becomes 2.38 Mev.

polation of curve B to zero absorber thickness gives a beta-gamma-coincidence rate of 0.11×10^{-3} coincidence per beta-ray. Since curves A and B were taken with a fixed geometry common to both curves, $1.8/0.11 = 2.3/0.14$.** In other words, at zero absorber thickness, the beta-rays of Ba^{140} are followed on the average by 0.14 Mev of gamma-ray energy. Therefore, the 0.54 Mev gamma-ray cannot be associated with each beta-ray of Ba^{140}. The obvious explanation is that the beta-ray spectrum of Ba^{140} is complex.*** From the coincidence data given herein, it can be concluded that the inner beta-ray group constitutes about twenty percent of the totality of the beta-rays emitted by Ba^{140}. This calculation is based upon the assumption that the harder beta-ray group is associated with a ground state transition in Ba^{140} and hence non-coincident with any gamma-rays. This assumption may be only an approximate truth, because the position of the 140 kev gamma-rays in the disintegration scheme of Ba^{140} is not known. This estimate of relative intensity of the beta-ray spectra is in good agreement with one previously obtained from aluminum absorption and Feather analysis.[7] Returning to Fig. 5 it can be seen that the five minute curve gives 160:480 as the ratio of counts arising from the 0.14 and 0.6 Mev quanta. Assuming that the G-M counter is four times as efficient for the hard radiation as for the soft quanta, the ratio becomes 640:480. Thus, the two quanta are of roughly equal intensity and may be in cascade. Difficulties relating to even minute quantities of La^{140} made it impossible to make reliable gamma-gamma-coincidence measurements in Ba^{140}.

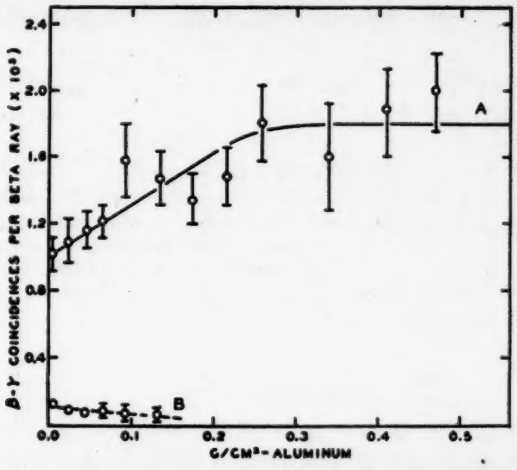

FIG. 6. Curve A is a plot of the beta-gamma-coincidence rate of Ba^{140} in equilibrium with La^{140} as a function of the surface density of aluminum placed before the beta-ray counter. Curve B is the coincidence rate of Ba^{140} alone. A chemical separation of Ba^{140} from La^{140} was made just prior to taking each point of curve B.

APPENDIX I. CHEMICAL PROCEDURE FOR THE PURIFICATION OF INDIUM

Neutron irradiated indium foil plus additional carrier elements silver, copper, iron, lead, calcium, and nickel, known from a spectrographic analysis to be present in the indium as impurities, were dissolved in 6N nitric acid. Potassium chloride was added to the solution, precipitating all of the silver and part of the lead. These chlorides were removed by filtration, and the filtrate was made slightly ammoniacal, precipitating indium, iron, residual lead, copper, and nickel as hydroxides. The filtrate, deep blue in color from the ammonia complexes of copper and nickel, contained no appreciable activity and was therefore discarded. The hydroxides were dissolved in 6N sulfuric acid, and the acid solution was reduced with 30-mesh zinc pellets, precipitating indium, copper, lead, and nickel as metals. Repeated reductions with zinc were necessary to reduce all of the indium. The metals were dissolved in 6N nitric acid and converted to sulfates by adding 1 cc of 18N sulfuric acid and evaporating to SO_3 fumes. The solution was diluted to 10 percent sulfuric acid and filtered to remove the insoluble lead sulfate. The sulfate solution of indium and traces of copper and nickel was made slightly ammoniacal and filtered. The precipitate was dissolved in two cc of 3N hydrochloric acid, and the acid solution was nearly neutralized with ammonia. Five grams of sodium bisulfite was added, and the solution was boiled for 15 minutes, then filtered. The precipitate of basic indium sulfite was washed with cold water, dried at 100°C and used in the experiments.

APPENDIX II. SEPARATION OF BARIUM FROM LANTHANUM

Barium chloride was precipitated from the barium-lanthanum solution with 12N hydrochloric acid. The precipitate was separated from the supernatant liquid by centrifugation, washed with 6N hydrochloric acid, dissolved in hot water, and reprecipitated as barium chloride with 12N hydrochloric acid, centrifuged and counted.

Note added in proof: Since this paper was submitted for publication, the measurements of Boehm and Preiswerk (Helv. Phys. Acta 22, 331 (1949)), have appeared. They report gamma-gamma-coincidences but no beta-gamma-coincidences in In^{114}, in agreement with the findings of the writers. By critical absorption, they have shown that the hard gamma-rays of In^{114} are related to the K-capture process.

** It is here supposed that the energy-quantum efficiency curve of the gamma-ray counter is linear with energy so that the beta-gamma coincidence rate is also proportional to the average amount of gamma-ray energy associated with the beta-rays. This is a good assumption, because the gamma-ray counter is constructed of materials made of the light elements.

*** In making beta-gamma-coincidence measurements on both In^{114} and Ba^{140}, the coincidence resolving time was varied from 0.10 microsecond to 1.0 microsecond. No change in the genuine beta-gamma-coincidence rate of either element was noted. The small beta-gamma-coincidence rate of Ba^{140} and the lack of coincidences in In^{114} therefore cannot be explained by a time delay in this time interval.

Breakdown and Maintenance of Microwave Discharges in Argon

S. KRASIK, D. ALPERT, AND A. O. MCCOUBREY
Westinghouse Research Laboratories, East Pittsburgh, Pennsylvania
(Received May 9, 1949)

The breakdown fields for argon have been measured in a resonant cavity at 3000 megacycles/sec. over a pressure range from 3 to 100 mm Hg. The discharge gap approximates the case of a uniform field between parallel plates. The results are compared with predicted values derived from Holstein's theory; the agreement is quite good, about 5 percent. Measurements taken with the discharge in the cavity permit determination of the voltage-current characteristics of the argon microwave discharge. These are given for a set of pressure values. These characteristics are compared with results on positive column gradients in d.c. discharges.

INTRODUCTION

AN important reason for the study of microwave discharges is their relative simplicity as compared with d.c. or low frequency discharges. There are two reasons for this relative simplicity: first, electrode phenomena need not play a role in the high frequency discharge and second, an electron need not undergo a net drift motion to receive energy from the high frequency field. These differences between the d.c. and high frequency case may be illustrated by a qualitative description of the breakdown process for the two cases.

In the d.c. case[1] a chance electron formed in the gas volume between the two electrodes drifts toward the anode under the influence of the applied field, gaining energy from the field and losing it chiefly through inelastic collisions with gas molecules. Some of these will be ionizing collisions; the resulting electrons also move toward the anode producing still more electrons. Thus the original chance electron produces an exponential increase in electron density with position toward the anode. As Townsend has pointed out, however, this alone cannot result in a self-sustained discharge. For a discharge to occur it is necessary that all the physical phenomena resulting from the passage of the original electron through the gas to the anode shall result in the formation of at least one additional electron in the volume at a potential no greater than that at which the original chance electron started. This regenerative process generally occurs at the cathode through electron emission due to impinging ions, photons and excited atoms. Thus Townsend's d.c. breakdown theory involves two distinct features. These are volume ionization by electrons depending on the gas, gas pressure, and applied field and cathodic emission depending upon all of the above factors plus the nature of the cathode surface.

An electron in a region of high frequency field[2] has an oscillatory motion at the field frequency plus a rectilinear motion whose magnitude and sign depend on the phase of entry of the electron into the field. The maximum energy that can be acquired by a free electron is determined by the field amplitude and frequency. The presence of a gas alters the situation profoundly, however, for now the electrons may make elastic collisions with the gas molecules. In such a collision the electron energy is only slightly reduced because of the disparity in masses, while the electron velocity after collision is more or less randomly directed with respect to the field. As a result of this random orientation of velocity after collision, the electron energy will, on the average, grow with successive collisions until the electron can make excitation and ionizing collisions with gas molecules. Thus the number of electrons will grow with time provided that an electron produces at least one other electron before it is lost. For breakdown considerations the important loss mechanisms are attachment to molecules and diffusion out of the field region. Thus for a non-attaching gas the breakdown criterion is simply this: rate of production of electrons by ionization must exceed rate of loss of electrons by diffusion.

These ideas were developed by Holstein in an unpublished report[3] and formed the basis of his theory of high frequency breakdown in a non-attaching gas.[4] This theory is based on two points the first of which is the breakdown criterion stated above. The second is his observation—in a paper on electron energy distribution functions[5]—that in the pressure region in which the field frequency is less than the frequency of elastic collisions of electrons with the gas and greater than the frequency of inelastic collisions, the electron distribution in energy for the high frequency field is very nearly the same as that in a d.c. field whose value equals the r.m.s. value of the high frequency field. The breakdown case treated by Holstein is that of a uniform field between parallel metal plates; for this geometry the r.m.s. breakdown field E is related to the pressure p and plate separation d by the expression

$$(pd)^2=\frac{\pi^2 kT_e}{e(E/p)(\alpha/p)}, \qquad (1)$$

[1] M. J. Druyvesteyn and F. M. Penning, Rev. Mod. Phys. **12**, 88 (1940).

[2] For these and the following remarks to apply, the drift motion per cycle of an electron in the high frequency field must be small compared to the linear dimensions of the discharge region. At microwave frequencies ($f>10^9$ sec.$^{-1}$) and usual geometries this condition is easily met.

[3] Westinghouse Research Report, R-94411-9A, "The TR switch," Chapter III, *Theory of the TR Switch*, by T. Holstein.

[4] T. Holstein, Phys. Rev. **69**, 50(A) (1946).

[5] T. Holstein, Phys. Rev. **70**, 367 (1946).

where α is Townsend's first coefficient for a d.c. field E and pressure p and T_e is the electron temperature for the same field and pressure. k is Boltzmann's constant and e is the electronic charge.

Some years ago Townsend and Gill[6] summarized certain related remarks as well as pointing out the close similarity between the high frequency discharge and the positive column of a d.c. discharge. Recently microwave breakdown measurements as well as theoretical work have been reported for air with flat plate and cylindrical geometry by Herlin and Brown[7] and for helium with mercury admixture by MacDonald and Brown.[8]

A primary purpose of the work reported here was experimental verification of Eq. (1) above. For this purpose we studied the breakdown field in argon at 3000 megacycles/sec. argon was chosen partly because values of α/p and T_e are known over a suitable range of values of E/p but mainly because the Penning effect[9] with argon is limited to certain chemically active molecules which may be readily removed.

The experiment approximated the idealized case of the theory by providing as the discharge region the space between the ends of two cylindrical reentrant noses in a cylindrical resonant cavity. The input of the cavity was coupled to a generator, the output to a load. Figure 1 illustrates the behavior of the power transmitted by the cavity as the power incident on the cavity is varied.

In the absence of a discharge the power transmitted by the cavity is a linear function of the incident power; this is illustrated by the line OF. The cavity gap field rises as the square root of the incident power, and with a gas at an appropriate pressure in the cavity breakdown may occur. If this occurs at an incident power H, the cavity transmission falls from A to B, and simultaneously a luminous glow appears in the cavity. We use this sudden fall in transmitted power as the breakdown criterion.

The discharge loads the cavity and detunes it, the relative importance of the two depending on the pressure. The net effect of either, however, is to reduce the cavity transmission. The characteristic of the discharge is such that an increase in incident power from H to K causes a fall in transmitted power from B to C. Reducing the incident power toward G, the transmitted power rises, and at G a sudden increase from D to E is observed. This corresponds to extinction of the discharge. Thus the discharge is always present for powers above H, never present for powers below G and may or may not be present for powers between G and H.

Breakdown measurements consist of determining the transmitted power at A. Knowing this power and the electromagnetic properties of the cavity, one may compute the gap voltage at breakdown. Maintenance measurements consist of determining curves such as DBC; with this data plus information on the cavity circuit properties, the discharge conductivity and the voltage-current characteristics of the discharge may be computed.

DESCRIPTION OF APPARATUS

I. Microwave Equipment

The generator used for the experiment was a Sperry 410-R klystron mounted in a water-cooled bath of transformer oil. It was operated as a self-excited oscillator, powered from a regulated supply, with r-f output powers usually around ten watts. The transmission line used was standard $1\frac{1}{2}$ inch$\times$3 inch rectangular brass waveguide (RG-48/U), the various sections being coupled with standard choke-flange points (UG-53/U, UG-54/U).

The high power variable attenuator was especially designed for the experiment and is described in detail elsewhere.[10] It was a variable position tapered vane type, the vane being a hollow Lucite chamber through which an ethelyne glycol and water mixture was circulated. This liquid served as attenuating medium as well as coolant in a closed system using an air cooled heat exchanger. Attenuations from under a db to about 40 db could be obtained with a maximum voltage standing wave ratio of 1.07.

The resonant cavity was specifically designed to satisfy the high frequency requirements of the experiment and to permit bakeout at over 400°C. The cylindrically symmetrical cavity is shown in Fig. 2. The cavity was coupled to the input and output waveguide with identical circular rises 0.562 inch in di-

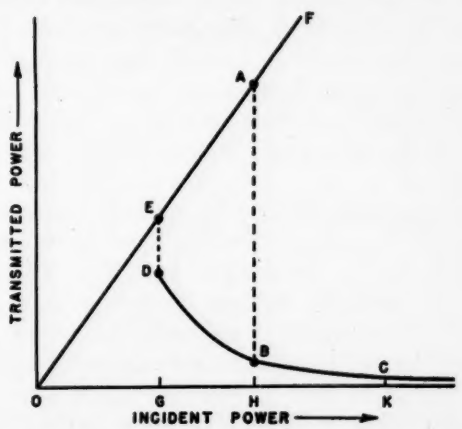

FIG. 1. Diagram illustrating the effect of the discharge on the cavity transmission. OF is the characteristic without a discharge, DBC that with the discharge. AB is the breakdown line, DE the extinction line.

[6] Townsend and Gill, Phil. Mag. **26**, 290 (1938).
[7] M. A. Herlin and S. C. Brown, Phys. Rev. **74**, 291, 910, 1650 (1948).
[8] A. D. MacDonald and S. C. Brown, Phys. Rev. **75**, 411 (1949).
[9] This effect is the ionization of impurity molecules by metastable atoms of the main gas constituent when the energy difference between the ground state and metastable state of the principal gas exceeds the ionization energy of the impurity. Penning, Naturwiss. **15**, 818 (1927).
[10] D. Alpert, Rev. Sci. Inst. (to be published).

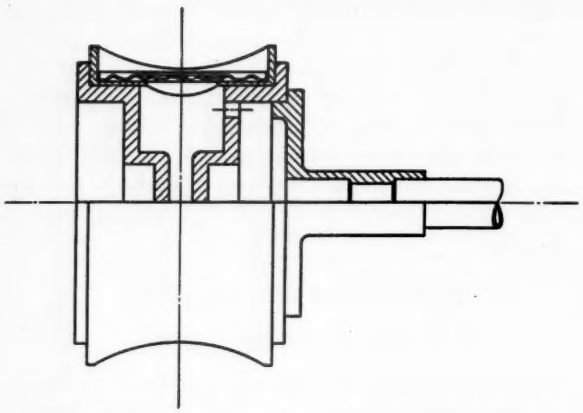

FIG. 2. The resonant cavity used for the experiment.

ameter. The window seals were wide corrugated rings stamped from sheet Kovar to which glass disks were sealed. The noses of the cavity were polished with the edges turned to 0.040 inch radius to eliminate local fields in excess of the central field.[11] The cavity itself was made of OFHC copper. The cavity and seals were assembled by silver brazing in a hydrogen atmosphere. The pumping connection to the interior of the cavity was a series of 8 holes, $\frac{1}{8}$ inch in diameter spaced equally around the bottom of the cavity near the cylinder wall. The technique of making the window seals as well as assembly methods for the cavity have been described in an unpublished report.[12] Figure 3 gives the essential interior dimensions of the cavity.

The cavity mounting was such as to permit the waveguide to be removed during bakeout. The exterior of the cavity was a circular cylinder of height equal to that of the waveguide. The waveguide was bored through to clear the cavity which was rigidly clamped to it by a collar and flange arrangement. Good electrical contact top and bottom was made by using special gaskets of 3-mil copper ribbon, corrugated by rolling between two lengths of gear stock, then bent into a circle in the plane of the ribbon. Electrical measurements indicated an effective and reproducible joint. A vertical slit 0.150 inch wide between the cavity and side walls of the waveguide contributed no significant leakage.

Power was measured by 10 ma Littlefuses used as bolometers in a mount developed at our laboratory during the war by a group under J. E. Hill.[13] These were used with resistance bridges measuring fixed power levels in a conventional manner. The power levels measured by the bolometers were around 1 milliwatt with attenuators used to measure higher powers; for certain maintenance data powers as low as 0.1 milliwatt were measured.

Incident power and higher levels of transmitted power were measured with Bethe hole directional couplers.[14] The two couplers used had attenuations of 15 and 22 db. The low power variable attenuators were of standard design using tapered resistance card vanes.[15]

Figure 4 shows the microwave equipment in block form. The low power attenuator just preceding the discharge cavity was used at very low incident powers. This permitted measurement of a suitable power level in the directional coupler. For lower values of transmitted power the cavity output was connected directly to a low power variable attenuator and bolometer.

All the measuring equipment had voltage standing wave ratios under 1.07 and almost all were better than 1.05. Attenuation of the low power attenuators and directional couplers was known to ± 0.02 db. The directivity of the couplers was better than 20 db. The relative short time error in the bolometers due to temperature drift, bridge sensitivity, etc., was five to ten microwatts at most. Six bolometers of the same design when intercompared gave power measurements within 1 percent. Further, a comparison made during the war between this type of bolometer mount and a M.I.T. Radiation Laboratory thermistor mount gave agreement within 1 percent.

The loaded Q of the cavity was measured by a special sweep frequency technique developed at this laboratory during the war by McCoubrey, Packard, and Krasik for measurements on radar beacon standard frequency cavities. This technique has been described elsewhere.[16] Insertion loss of the cavity was measured by a substitution method using a calibrated attenuator. Cavity measurements were made in the mount used for the discharge experiments either just preceding or immediately following discharge measurements. We estimate the loaded Q of the cavity to have been measured to 3 percent in absolute value and the inser-

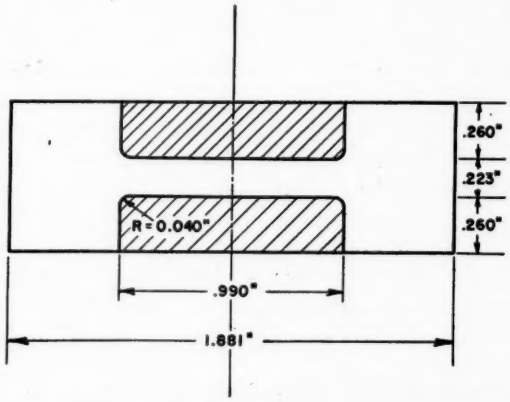

FIG. 3. The interior dimensions of the resonant cavity used for the experiment.

[11] Rogowski and Rengier, Arch. R. Elekt., 16, 73 (1926).
[12] Westinghouse Research Report, R-94411-9A, "The TR switch," Chapter IV, *The 1B24 Design* by D. Alpert.
[13] T. Miller, Proc. I.R.E. 36, 380(A), (1948).
[14] Montgomery, *Technique of Microwave Measurements* (Radiation Laboratory Series), Vol. 11, pp. 858–866.
[15] Reference 14, pages 748–751.
[16] Reference 14, pages 396–403.

tion loss to 0.1 db. These absolute errors are due principally to small residual standing waves; the reproducibility of the measurements was several times better than the estimated errors. Two similar cavities were used in the experiment; the measured values are given in the table below. Most of the breakdown data was taken on cavity No. 1.

	Cavity No. 1	Cavity No. 2
Loaded Q	2780	2890
Insertion loss	8.9 db	8.9 db
Frequency	2950 megacycles/sec.	2950 megacycles/sec.

II. Pumps and Gas Handling Equipment

The pumping and gas handling system is shown schematically in Fig. 5. The discharge cavity, ion gauge and an auxiliary d.c. discharge tube form a central system protected from the oil diffusion pumps and grease stopcocks by liquid air traps. The system is made of Pyrex connected to the cavity through a Kovar-glass seal and a section of annealed copper tubing. The auxiliary discharge tube was used to clean the gas after filling; it had two closely spaced cylindrical electrodes made of magnesium alloyed with some few percent of cerium. The ion gauge was standard with the usual residual air calibration ($1\mu a. = 10^{-5}$ mm Hg).

After the system had been opened to air, the central system and liquid air traps were baked at 425°C for at least 24 hours. Following this the ovens on the traps were removed, and liquid air was placed on the traps while bakeout of the central system proceeded for some hours. After bakeout a shut-off test was made by closing stopcocks S_1 and S_2; an ion gauge current of 10^{-9} amperes was obtained which showed no change in 24 hours.

Pump No. 1 was connected to the central system through a standard type of reentrant liquid air trap. Pump No. 2 was used chiefly for the gas system, which was connected to the central system through two reentrant liquid air traps in series. These traps were of special design and were made in the following way. A sheet of three mil copper foil, six inches wide and about 40 inches long, was corrugated diagonally by rolling it between two lengths of gear stock. The copper sheet was then wrapped around the inner tube of a standard reentrant type liquid air trap so as to fill completely the space between the inner and outer tubes of the trap. The corrugations thus formed a large number of small diameter tubes in parallel spiralling around the inner tube of the trap. This design aimed at a trap which would be effective in removing condensible vapors from gas at fairly high pressures as it entered the central system. A detailed description and performance analysis will be published in a later article by one of the authors (D. A.) in the *Review of Scientific Instruments*.

Pressure was measured with an oil manometer using Octoil S. The manometer read pressures up to 60 mm Hg directly; a stopcock was provided for evacuating the closed side of the manometer or pressurizing it to extend the pressure range. We estimate the error in pressure to be 0.06 mm Hg at most, which is under 1 percent except for the two lowest pressures in the breakdown data.

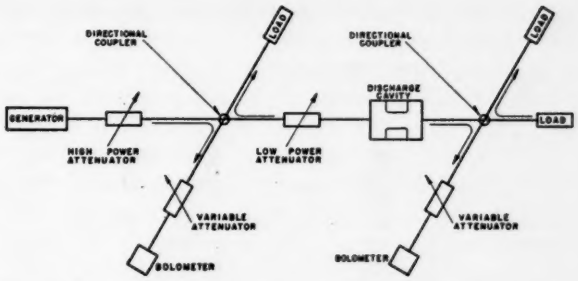

FIG. 4. Line diagram of the microwave equipment used for breakdown and maintenance measurements.

The argon used was of the highest purity obtainable commercially. It was obtained from the two primary suppliers in one liter flasks with break-off tips. Except for possible contamination of the gas itself by the manufacturer, no mercury was present in the system.

Following bakeout gas was admitted to the system to the maximum pressure desired. The auxiliary d.c. discharge was then started and operated continuously during the run and for at least 24 hours preceding any measurements. This discharge operated at about 150 ma and 100 volts from the 60-cycle power line.

BREAKDOWN MEASUREMENTS

For breakdown measurements only the transmitted power at breakdown is required. From this the breakdown voltage may be obtained by a straightforward analysis. The definition of "external" or "transmission" shunt resistance[17] R_2 associated with the output coupling is given by the equation

$$V = (2R_2P_2)^{\frac{1}{2}},$$

where P_2 is the power transmitted to a matched load

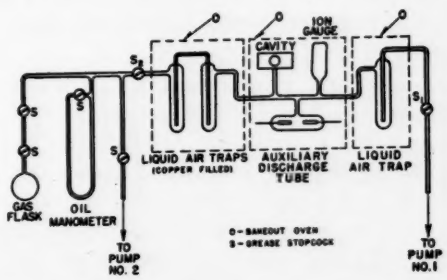

FIG. 5. Diagram of the pumping and gas filling equipment.

[17] The cavity parameter Q is $\omega U/P$ where ω is the circular frequency, U the energy stored in the cavity and P is a power loss. The shunt resistance R is $V^2/2P$ where V is the time peak of the gap voltage. The power P may be the dissipation in the cavity walls, the power transmitted to a coupled circuit or the total power loss of the cavity and associated lines. Corresponding to each power loss a Q and shunt resistance may be defined. Clearly the ratio R/Q is independent of this choice.

TABLE I. Microwave breakdown fields for argon.

Pressure (mm Hg.)	Transmitted power at breakdown (milliwatts)	pd (mm×cm)	E/p (Peak volts/cm×mm)
113.2	266	64.2	10.9
106.0	246	60.1	11.1
103.3	240	58.6	11.3
98.6	224	55.9	11.4
94.5	213	53.6	11.6
89.9	199	51.0	11.8
85.4	186	48.4	12.0
81.0	174	45.9	12.3
76.5	163	43.4	12.6
71.7	152	40.7	13.0
67.7	141	38.4	13.2
63.1	129	35.8	13.6
58.6	117	33.2	13.9
54.4	107	30.9	14.3
49.9	95.3	28.3	14.7
45.3	83.9	25.7	15.3
41.0	74.6	23.3	15.9
36.9	65.6	20.9	16.5
31.0	54.6	17.6	18.0
26.6	46.4	15.1	19.3
22.4	38.4	12.7	20.9
18.1	30.9	10.3	23.2
13.8	23.7	7.83	26.6
9.6	18.1	5.43	33.5
5.45	14.4	3.09	52.4
3.25	14.0	1.84	87.0

and V is the peak gap voltage in the cavity. For a cavity with equal input and output couplings[18,19]

$$Q_2/Q_L=2/(T)^{\frac{1}{2}},$$

where Q_L is the loaded Q of the cavity and T is the fractional transmission of the cavity at resonance. Further since

$$R_2=(R/Q)Q_2, \quad V=2[(R/Q)Q_LP_2]^{\frac{1}{2}}(T)^{-\frac{1}{2}}. \qquad (2)$$

In this expression if P_2 is the power transmitted at breakdown, V is the gap breakdown voltage. The value of R/Q for the cavity was calculated for us by T. Holstein who obtained the value 58.9 ohms. The breakdown voltages may be computed by using this and the measured values of Q_L, T and transmitted power. The circuit analysis used here assumes the cavity has a single resonant mode with loaded $Q\gg1$.

The measurement procedure was as follows: with no discharge in the cavity the incident power level was set somewhat below that causing breakdown. The bridge reading the transmitted power was then balanced and maintained in balance continuously as the incident power level was slowly raised. At breakdown the bridge unbalanced sharply; the power reading at which it had been balanced just previous to breakdown was then noted. This value we call the transmitted power at breakdown. Three successive trials were taken, the agreement in general being better than one percent. Breakdown measurements at various pressures of Argon were obtained by starting with the highest pressure desired and evacuating through pump No. 2.

The results of our breakdown measurements in argon are given in Table I and the solid curve of Fig. 6. The data given are values of breakdown field over pressure *vs.* the product of pressure and gap spacing. The theoretical curve was given by Holstein in an unpublished report.[3] It was obtained using the published data for α given by Kruithof and Penning[20] and the electron temperature data of Townsend and Bailey[21] in Eq. (1). The experimental curve lies from 4 percent to 8 percent below the theoretical curve; we consider such agreement to be satisfactory verification of the breakdown theory over the region of applicability.

From our maximum error estimates of 3 percent for Q_L, 2.5 percent for T, 0.5 percent for P and Holstein's estimate of 1 percent for his value of R/Q we estimate the error limit in breakdown voltage to be about 3 percent. This excludes the question of absolute bolometer calibration; in view of the intercomparisons made, we believe this question to be satisfactorily resolved. Data taken with cavity No. 2 gave agreement to within 1 percent of the solid curve of Fig. 6 over the range of comparison with theory; the departure was as much as 5 percent for lower values of E/p.

Our gap geometry deviates from that of a uniform field between parallel plates assumed in the theory in at least two respects. First, because the gap diameter is an appreciable fraction of a wave-length, the field decreases from the axis of the cylinder to the outer edge. Second, there is a sidewise diffusion of electrons out of the gap region. Both effects should cause the measured breakdown voltage to be higher than that for an ideal gap geometry. Concerning the first point we find that at the outer boundary of the gap the field is down to about 85 percent of its value at the center; hence the average field does not deviate by over 7 percent from the extreme values and is probably better. Concerning the sidewise diffusion loss out of the gap region, Hol-

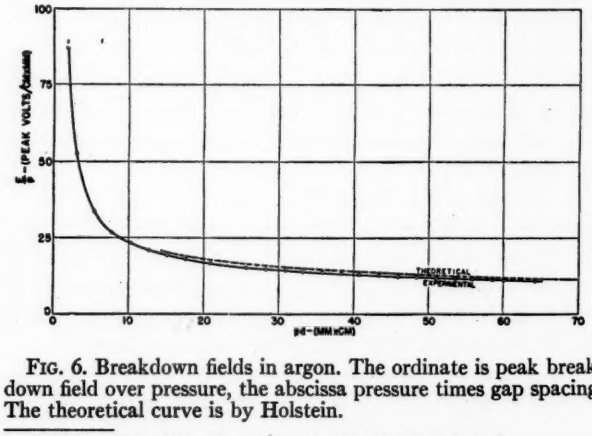

FIG. 6. Breakdown fields in argon. The ordinate is peak breakdown field over pressure, the abscissa pressure times gap spacing. The theoretical curve is by Holstein.

[18] T. Holstein, *Transmission Characteristics of Resonant Cavities in Microwave Systems* (unpublished report, Westinghouse Research Report R-94318-F).

[19] Cf. Smullin and Montgomery, *Microwave Duplexers* (Radiation Laboratory Series), Vol. 14, Chapter II. Also reference 14, 286–293.

[20] Kruithof and Penning, Physica 4, 430 (1937).

[21] Townsend and Bailey, Phil. Mag. 44, 1033 (1922).

stein, in an unpublished calculation, has shown it to be a negligible fraction of the total diffusion loss.

In these measurements a number of argon samples were used. Before cleaning with the auxiliary discharge, two or three of the samples gave essentially identical breakdown *vs.* pressure curves while the remainder of the samples gave curves lying below this common curve by varying amounts. Differences of as much as 20 percent were observed at the higher pressures—above 40 mm Hg. At pressures below 10 mm Hg there seemed to be little difference among samples, however. For a sample giving low breakdown voltage, operation of the cleaning discharge for an hour produced a marked rise in breakdown voltage, and operation for 24 hours brought it into agreement (better than 1 percent) with the common top curve. Further operation of the auxiliary discharge for 24 hours and longer periods had no measurable effect; moreover, the cleaning discharge had no effect on the breakdown voltage of those samples originally giving the common top curve. We conclude that a contaminant removable by a cleaning discharge and measurably affecting the breakdown voltage of argon is present to a varying extent in the gas samples furnished us; apparently our own gas handling system introduced no such contaminant.

To reduce the statistical spread in breakdown voltage measurements we found it necessary to use a radioactive source to provide a sufficient electron density. We used a 100 microcurie ampule of radium which was placed on top of the cavity; the cavity copper thickness in this region was 9/64 inch.

MAINTENANCE MEASUREMENTS

With the discharge present in the cavity we may assume that the cavity is loaded with a gas discharge admittance Y_G at the gap. If the generator frequency is the resonant frequency of the cavity without the discharge, with the discharge the following expression of Holstein's[3] for the ratio of incident power P_i to transmitted power P_2 may be used.

$$P_i/P_2=1/T|1+Y_GR_L|^2. \qquad (3)$$

Here R_L is the loaded shunt resistance of the cavity (without the discharge), and T is defined as before. By measuring the incident and transmitted powers with the discharge present we know all the quantities in Eq. (3) except Y_G. To obtain the magnitude of Y_G from this equation we must know the phase of Y_G or make some reasonable assumption about it. We chose the latter procedure for reasons to be discussed later. Having the magnitude of Y_G and the gap voltage at any transmitted power from Eq. (2), we may obtain the gap current and thus the voltage-current characteristics of the discharge.

The procedure used to obtain incident and transmitted powers was the following: with the cavity filled with argon at the desired pressure, the discharge was started and the incident power increased to the maximum value used, about six watts. The bridges reading incident and transmitted powers were balanced and the values noted; a set of such readings were then taken reducing the incident power in steps. In order to obtain the point at which the discharge was extinguished we proceeded as follows: at an incident power slightly above that at which the discharge was extinguished, the bridge reading transmitted power was balanced and maintained in balance continuously as the incident power was lowered slowly. At extinction the bridge

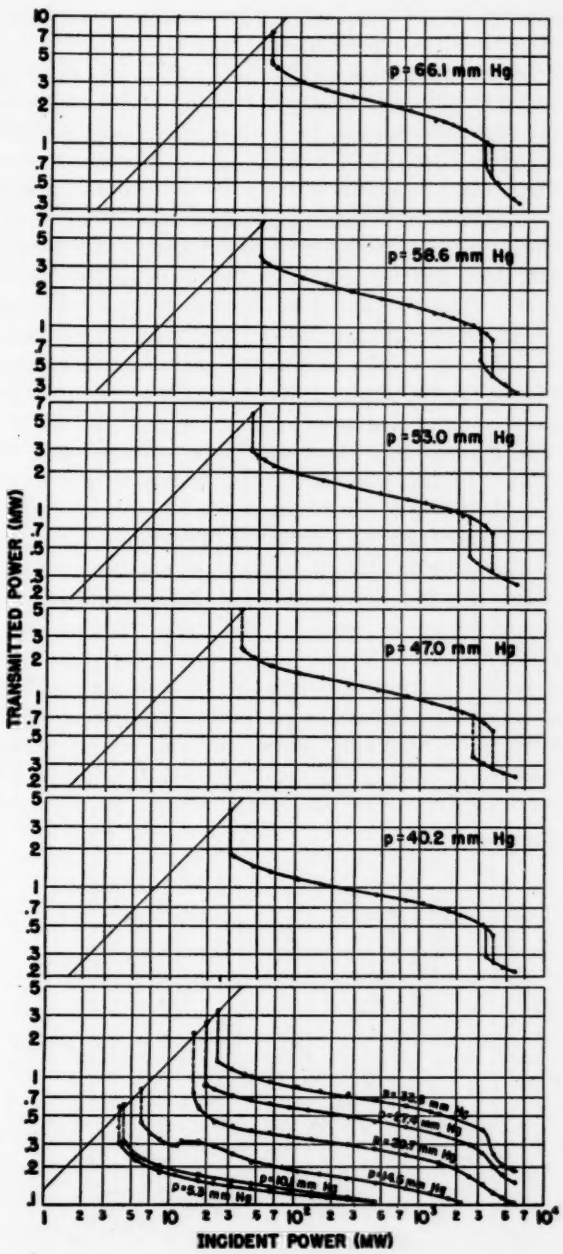

FIG. 7. Maintenance data for the argon discharge; the abscissa is incident power in milliwatts, the ordinate transmitted power in milliwatts. The range of incident powers is from 1 to 10^4 milliwatts. The line at the left with 45° slope is the line of cavity transmission without the discharge.

suddenly unbalanced; the value at which it had just previously been balanced was noted, after which it was rebalanced for the higher value of transmitted power. At the same time the bridge reading incident power was balanced and the value noted. This procedure, similar to that used to obtain the breakdown voltage, was also used to locate the discontinuities in the maintenance characteristics. Following each run, a set of check points was taken which included the extinction point. Reproducibility better than 2 percent was considered satisfactory. Incident powers below 20 milliwatts were measured by inserting the low-power attenuator in the main line as shown in Fig. 4.

In these measurements the generator was carefully tuned to within 0.05 bandwidth of the cavity resonance preceding each run and each set of check points. There was no measurable detuning of the generator with variation in attenuator setting. As with the breakdown measurements the cavity was filled with gas to the highest pressure desired with runs taken at successively lower pressures by exhausting through pump No. 2. Again we found that cleaning of the gas with the auxiliary discharge was necessary for reproducible data; after cleaning, various samples of gas gave maintenance data within the limits of reproducibility of measurements on a given sample.

The maintenance data which we obtained is given in Fig. 7 in the form of curves of transmitted power *vs.* incident power for a series of 11 pressures from 5.3 to 66.1 mm Hg. The curves lie above one another in the order of increasing pressure; because of the discontinuities in the curves for the higher pressures at incident powers between 3 and 4 watts, they are given as separate plots. At pressures below those given here, the curves of transmitted power *vs.* incident power lie above one another as the pressure is reduced since 5.3 mm Hg gives about the minimum value of transmitted power over the range of incident powers examined. At each discontinuity in the data including extinction we have connected initial and final transmitted powers with a vertical dashed line. All measured points in the runs given, including check values, are shown.

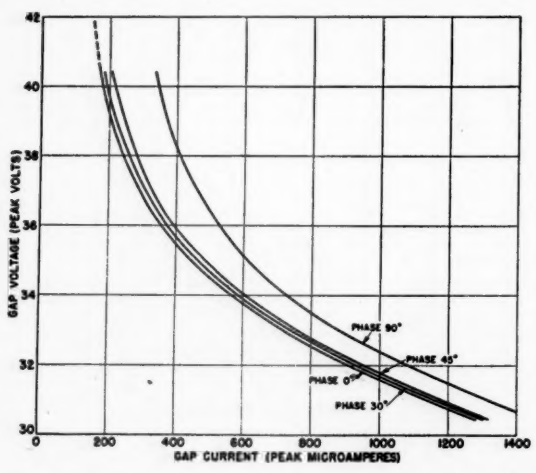

FIG. 8. Voltage-current characteristics of the argon discharge at 27.4 mm Hg assuming phase angles for the discharge admittance of 0, 30, 45 and 90 degrees.

The breaks in the maintenance data curves are reproducible as is the indicated hysteresis effect in changing from one condition to the other. Accompanying the sudden transition, the discharge, which on the higher curve appears to be a more or less uniform luminous region across the entire gap, develops a bright luminous ball at the center of the gap while the remainder of the glow appears reduced in intensity. At the lower pressures, 33.8, 27.4, and 20.7 mm Hg, where the transition is gradual, the development of the luminous ball is likewise gradual. It has been suggested that this phenomenon is similar to "contraction" in the d.c. positive column.[22] The curious bump in the curve for 14.5 mm Hg near extinction is not understood. The effect is definitely connected with the discharge and is independent of the measuring equipment; it is quite reproducible although it occurs only around this pressure.

We have previously remarked that reduction of the power data to discharge characteristics requires some information about the phase of Y_G. Because the particular cavity we used was very loosely coupled to the transmission lines, measurement of the phase of Y_G directly was not easy. By the following considerations, however, we can make a sufficiently good estimate of the phase angle ϕ associated with Y_G. Townsend and Gill[6] have pointed out that the minimum value of discharge field as a function of pressure corresponds to $\omega\tau$ of the order of magnitude unity, ω being the circular frequency of the generator and τ the mean time between collisions. An order of magnitude calculation for the relation between ϕ and τ gives $\tan\phi=\omega\tau$, and if the distribution function does not change very much with pressure, $\tan\phi$ varies as $1/p$.[23] To be conservative let us assume $\tan\phi=2$ at 5 mm Hg;[24] for 20 mm Hg we

[22] Reference 1, page 170.

[23] If we define a high frequency electron mobility K as the average over all the electrons of the ratio to the field of the electron velocity component in the field direction, the phase of this mobility and the phase of the discharge admittance are the same. For electrons of a given speed v this mobility may be calculated by simple mechanics. For a single electron the result is

$$K=(1/i\omega)e/m\{1-\exp[i\omega(t_0-t)]\},$$

e/m being the charge to mass ratio of the electron, t the time considered and t_0 the time previous to t at which the electron suffered its last collision. Next K is averaged over all the electrons of speed v by introducing the probability that the electron has gone for a time $(t-t_0)$ without a collision; this probability may be written in terms of the mean free path $\lambda(v)$ and v. The resulting average K is a real factor times the complex number $(1+i\omega\tau)$, τ being $\lambda(v)/v$. Thus for electrons of velocity v, $\tan\phi=\omega\tau$. For an electron distribution in energy τ must be averaged over the distribution and in general will not be equal to $\lambda/\bar{v}$ where λ and $\bar{v}$ are averaged independently. For helium $\lambda(v)/v$ is essentially independent of v, thus $\tan\phi=\omega\tau$ is true even in the average; for other gases for which the phase varies with electron energy, a factor, presumably of the order of magnitude of unity, is involved. Whatever this factor, if the electron distribution in energy does not vary greatly with pressure, $\omega\tau$ will vary as $1/p$.

[24] We may estimate $\omega\tau$ at 5 mm Hg directly. Suppose we take the average electron energy to be about 1/3 the ionization poten-

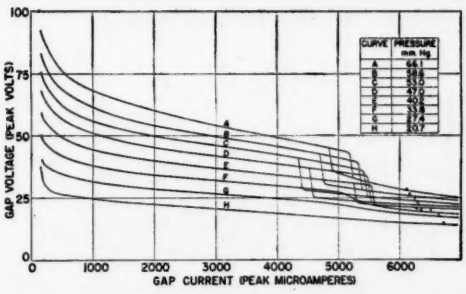

FIG. 9. Voltage-current characteristics of the argon discharge over a range of pressures. We calculated these from the data assuming the gap current to be in phase with the gap voltage.

would thus expect ϕ to be under 30°. The very small effect of such phase angles on the voltage-current curve is illustrated by Fig. 8.

Here we have reduced the data for 27.4 mm Hg assuming phase angles 0, 30, 45, and 90 degrees. The effect of phase angle is clearly greatest at low currents. Around 200 microamperes, which is practically extinction, the difference in voltage between phase angles of zero and 30 degrees is only about 1 percent and between zero and 45 degrees less than 5 percent. At 500 microamperes the difference in voltage from zero phase angle is 0.5 percent for 30 degrees, 1 percent for 45 degrees, and 5 percent for 90 degrees. In view of these results we have computed voltage-current characteristics for our discharge for pressures of 20.7 mm Hg and higher assuming the phase of Y_G to be zero. These are given in Fig. 9.

The operating point of the discharge in a given circuit with a given incident power may be determined graphically in a manner similar to the procedure used with d.c. discharges. The results are quite simple for the case of Y_G real. From Eqs. (2) and (3) we get

$$V=2(2P_i/R_2)^{\frac{1}{2}}(R_L/1+R_LY_G).$$

We can get an equation for I, the peak gap current, by multiplying this by Y_G. These two equations represent a relation between V and I in terms of the parameter R_LY_G. Solving, we obtain

$$V=2R_L(2P_i/R)^{\frac{1}{2}}-IR_L. \qquad (4)$$

This is the equation for a straight line in the $V-I$ plane with a slope $-R_L$ and intercept for $I=0$ equal to the gap voltage without a discharge. This straight line is the locus of all possible gap currents and voltages for the particular cavity with a given incident power. The result is illustrated by Fig. 10. P_{i1}, P_{i2}, P_{i3}, and P_{i4} represent four successively higher values of the incident power. The intersections, A and B, of the discharge characteristic with the line labeled P_{i4} presumably represent two possible operating points of the discharge in the cavity with incident power P_{i4}. However, by the usual stability arguments,[25] only A is a stable operating point. Lowering the incident power to P_{i3} moves the operating point to C; still lower incident powers move the operating point to E, the point of tangency and extinction. Thus at extinction the slope of the discharge characteristic is $-R_L$. The portion of the characteristic above E, EDB, can be explored only with a cavity with higher value of R_L.

In Fig. 11 we have plotted the discharge characteristic for 47.0 mm Hg to illustrate this behavior, the points representing values calculated from our data while the straight lines are drawn with a slope $-R_L$. At both extinction and the transition points the agreement of the slopes is quite good.

The close similarity between the high frequency discharge and the d.c. positive column has been pointed out.[6] In the high frequency discharge between parallel plates the applied high frequency field produces ionization while loss occurs by a diffusion motion to the plates. In a positive column in a cylindrical tube, ionization is produced by the longitudinal gradient due to the applied d.c. field while the loss is by radial diffusion to the tube wall. To compare the high frequency data with positive column data, account must be taken of the relative rates of ionization by the d.c. and high frequency fields and the geometry difference which affects the diffusion rate. Concerning the first point it has already been pointed out[5] that a d.c. field of amplitude E and high frequency field of r.m.s. value E result is essentially the same electron energy distribution over the range of frequency to pressure ratios which we use. The diffusive loss in a plane geometry with plate separation d is equal to that in a cylindrical tube of radius R for[3]

$$\pi/d=2.405/R.$$

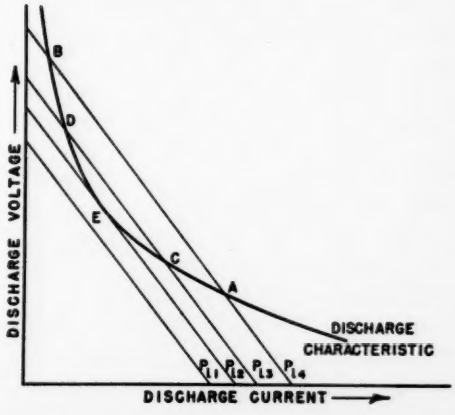

FIG. 10. Diagram illustrating the location of the operating point by the intersection of the circuit characteristic with the discharge characteristic.

tial or 5 volts (see reference 5 page 381). This corresponds to $\bar{v}$ of about 1.4×10^8 cm/sec. We may take as a conservative estimate $\lambda=(1/30p)$ cm in the average (see Kollath, Physik. Zeits. **31**, 997 (1930)), p being the pressure in mm Hg. This gives about 0.9 for $\omega\tau$.

[25] Engel and Steenbeck, *Elektrische Gasentladungen* (J. Springer, Berlin, 1932), II, 170–175.

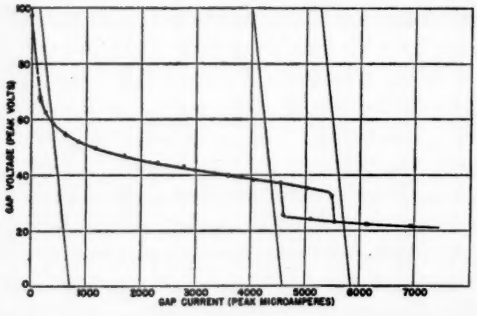

FIG. 11. Voltage-current characteristic of the Argon discharge at 47.0 mm Hg showing the characteristic slope at extinction and at the transitions. The straight lines are drawn with slope $-R_L$.

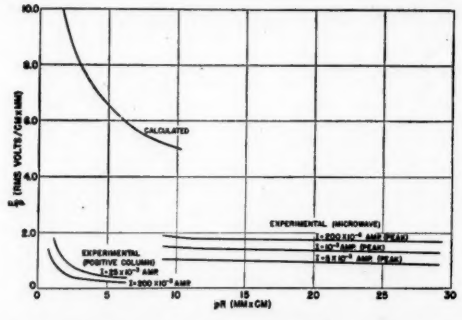

FIG. 12. Comparison of the longitudinal gradient in the d.c. positive column with high frequency maintenance fields. The calculated curve is by Holstein and is based on ambipolar diffusion. The experimental positive column data is from Klarfeld. The ordinate E/p is either longitudinal gradient in the positive column or the r.m.s. maintenance field over the pressure.

In Fig. 12 we compare our maintenance data taken at selected values of current from Fig. 9 with positive column measurements by Klarfeld[26] taken in a tube of radius 1 cm and a calculation by Holstein[3] the calculation being made in a manner very similar to that for breakdown. The maintenance calculation differs from that for breakdown in that the densities are presumed to be sufficiently high so that the electron diffusion is ambipolar rather than free. The electron energy distribution is taken to be the same at all radii and equivalent to the distribution for a d.c. field equal to the r.m.s. value of the high frequency field. Numerical values are obtained using published values of the parameters.

While the range of the abscissas for the various curves do not overlap well, it would seem that the high frequency discharge is more nearly represented by the calculation than is the positive column data. Presumably cumulative ionization processes are extremely important in the positive column; the fact that the high frequency data lies below the calculation suggests that these cumulative processes are also important here.

We may estimate our density by assuming the current uniformly distributed over the area of the gap and further that the mobility in the high frequency field is the same as for a d.c. field of the same magnitude as the r.m.s. value of the high frequency field. Using published values of mobility,[27] we estimate densities of 3×10^8, 2×10^9 and 10^{10} per cc. for peak gap currents of 200, 1000, and 5000 microamperes, respectively. At densities of 10^8 per cc we should expect the diffusion rate of electrons to be greater than the ambipolar rate[28] so that surprisingly enough the difference to be ascribed to cumulative processes is even greater than is indicated by Fig. 12. The other possibility, of course, is that the space charge field does have an appreciable effect on the energy distribution of the electrons.

In conclusion we wish to thank Dr. T. Holstein of this laboratory for proposing this experiment and assisting in interpretation of the results.

[26] Klarfeld, Tech. Phys. U.S.S.R. **5**, 725 (1938).

[27] R. A. Nielsen, Phys. Rev. **50**, 950 (1936).

[28] T. Holstein, Phys. Rev. **75**, 1323A (1949).

Gamma-Ray Measurements with a Magnetic Lens Spectrometer

W. F. HORNYAK, T. LAURITSEN, AND V. K. RASMUSSEN
Kellogg Radiation Laboratory, California Institute of Technology, Pasadena, California
(Received May 16, 1949)

Effects of instrument resolution and converter thickness on photoelectron lines have been investigated experimentally for gamma-radiation from 0.4 to 3 Mev. While determinations based on the high energy extrapolated edge of the lines seem to require no corrections for converter thicknesses, the peak value, which does require corrections, is in some cases more easily located. Peak shifts determined for thorium converters near 0.5 Mev are extrapolated to other energies by use of theoretical arguments. Values based on both types of determinations are quoted for gamma-radiation from the reactions $Li^7(p\,p')Li^{7*}$, $Be^9(d\,n)B^{10*}$, and $Co^{60}(\beta^-)Ni^{60*}$. The corresponding excited level transition energies obtained are Li^{7*}: 476.7±0.9 kev; B^{10*}: 713.8±1.3 kev; Ni^{60*}: 1172.4±1.8 kev and 1330.9±2.1 kev.

THE comparatively large aperture and high resolution of the magnetic lens beta-ray spectrometer have led to its increasing application to the precise determination of gamma-ray energies in the range from a few tens of kilovolts to several Mev. The most common method used consists in observing the spectrum of photoelectrons produced by the gamma-radiation either by internal conversion in the source or by external conversion in a suitable foil. In both cases, essentially monochromatic lines are observed, broadened, and displaced to varying degrees depending on the energy losses in the source or converter and on the resolution of the instrument. We have attempted to make a systematic examination of these effects as they apply to the determination of certain gamma-ray energies in the region from 0.4 to 3 Mev.

APPARATUS

The spectrometer used in this work was patterned after the instrument described by Deutsch, Elliott, and Evans,[1] modified to use the annular focusing discussed by Frankel and others.[2] It comprises a brass tube 10″ in diameter and 48″ long (Fig. 1) in which are placed suitable baffles to limit the electron trajectories and to reduce scattering and direct radiation background. A helical baffle is provided to permit distinction between positive and negative electrons. The focusing magnetic field is produced by four individual water-cooled coils which were in the present experiments grouped together at the middle of the tube. Since the magnetic circuit contains no iron, the field is proportional to the current. As a measure of the current in the spectrometer coils, the millivolt reading on a Type K Leeds and Northrup potentiometer in conjunction with a set of carefully intercalibrated Manganin shunts was used. The unbalanced output of the potentiometer was simultaneously indicated on a sensitive galvanometer and amplified as an a.c. signal after being changed into a square wave at a low signal level by a Western Electric sealed pressure relay. This amplified signal was used to control a ½-K.W. amplidyne in the field circuit of the 60-K.W. generator supplying the spectrometer current. The spectrometer current was held to better than 2 parts in 10,000 on the average.[3]

A vacuum connection to a 1.4-Mev electrostatic accelerator enabled suitable targets at the source position to be bombarded by high energy protons or deuterons for the study of prompt and short-lived radioactive gamma-radiation. Gamma-rays produced at the source position ejected secondary electrons from a heavy element converter immediately adjacent. A schematic diagram of the source assembly is shown in Fig. 2. The source and converter were supported by an 0.02 inch wire and the region around the source was completely free of scattering materials for a minimum of three inches. Particular care was taken to reproduce accurately the centering and axial locations of the sources and, while the diversity in the nature of the gamma-ray sources required some variation in techniques, the geometry of the source assembly was standardized as much as possible.

The internal parts of the spectrometer were centered with respect to the tube at assembly. Further adjustment of the geometrical alignment was made by moving the tube with respect to the axis of the coils in such a way as to maximize the observed intensity of the high energy internal conversion "X" line ($B\rho$=10,000 gauss cm) of ThD. Stray lateral magnetic fields were then compensated, by means of two large, mutually perpendicular coils, to give maximum intensity for the comparatively low energy "F" line from ThC ($B\rho$=1385 gauss cm), the "I" line ($B\rho$=1750 gauss cm) being used as an auxiliary check. It was observed that when the compensation was properly set, the instrument resolution was the same for all of the internal conversion lines. When the compensation was incorrect the first sign of maladjustment was a line broadening and loss in intensity which was progressively worse the lower the line energy. Only after a considerable amount of maladjustment of the compensation were the line shapes

[1] Deutsch, Elliott, and Evans, Rev. Sci. Inst. **15**, 178 (1944).
[2] S. Frankel, Phys. Rev. **73**, 804 (1948); J. M. DuMond, Rev. Sci. Inst. **20**, 160 (1949); Persico, *ibid.*, 191.

[3] We are indebted to Mr. G. W. Downs for much helpful advice on this control system and to Messrs. C. B. Dougherty and W. D. Gibbs for putting it into operation.

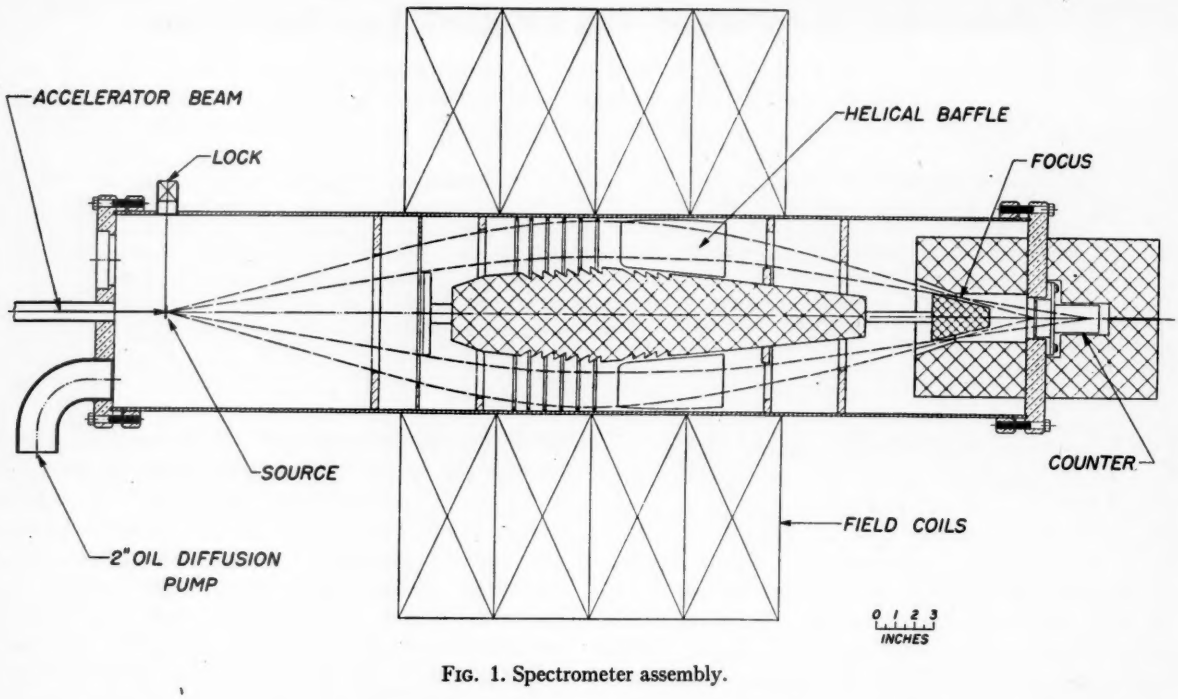

FIG. 1. Spectrometer assembly.

asymmetrical or noticeably shifted. Because the component of stray field parallel to the spectrometer axis was not compensated, a small correction to the observed line position was made. For the arrangement used here, this correction is

$$\delta \text{M.V.}/\text{M.V.} = 22S/B\rho,^{4}$$

where S is the axial component of the stray field in gauss, $B\rho$ the momentum of the line in gauss cm, and M.V. is the millivolt reading on the potentiometer indicating the spectrometer coil current. Since in this experiment a value of $S = 0.3_0 \pm 0.1$ gauss was measured, the correction at 2000 gauss cm, for example, is 0.3_3 percent.

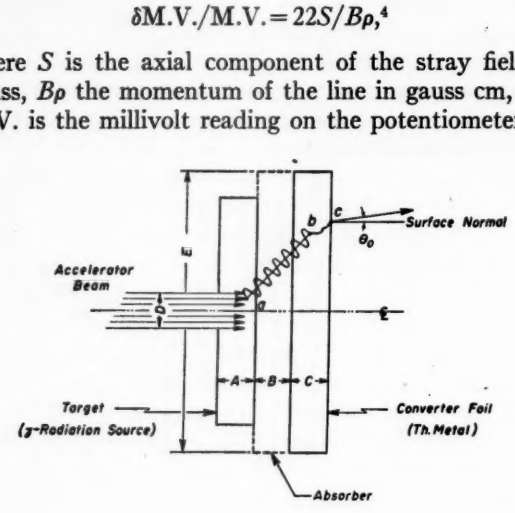

Typical Dimensions	
A	.0001-.010"
B	0 -.030"
C	.00025-.005"
D	.080"
E	.375"
θ_0	13°

FIG. 2. Schematic drawing of source assembly.

In the final configuration, the spectrometer yielded a symmetric curve, with a shape well approximated by a Gaussian function (Fig. 3) of width at half maximum of 1.5_2 percent. In general this width will depend on the instrument aperture arrangement and the source size. An investigation showed that for the range of source sizes used here, the line shapes were comparatively independent of source size. The solid angle is estimated to be 0.5 percent of a sphere.

GAMMA-RAY MEASUREMENTS: INTERNAL CONVERSION

Internal conversion photoelectrons provide a particularly simple indication of the gamma-ray energy, if the available intensity is great enough to permit the use of a source of such thickness that the energy loss of the electrons may be ignored. In such cases, the observed electron distribution is simply the "window" or resolution curve of the instrument and the determination may be made directly in terms of either the peak or the extrapolated edge positions. Comparison with a known line of the same character then provides the calibration. As an example of this technique, and for a calibration required for subsequent work we have made an intercomparison of the internal conversion lines of the gamma-radiation of ThD (X line) and Au^{198} (K and L lines). The former line was measured by Ellis[5] in terms of the I line for which he obtained an absolute value by measurement of the magnetic field.

[4] The dimensional constant 22 is for a configuration: source to counter distance = 114 cm; full width at half maximum of axial component of focusing field = 53 cm; maximum radial electron excursion for median ray = 10 cm; acceptance angle for median ray = 13°.

[5] Ellis, Proc. Roy. Soc. A138, 318 (1932).

Siegbahn[6] measured the absolute values of the I and F lines by comparing the difference with x-ray spectroscopic values and obtained momenta on the average 0.11 percent lower than those given by Ellis. Taking the mean of the two I line determinations and using Ellis' X/I ratio, one obtains a momentum value of 10,000±14 gauss cm, or 2.618±.004 Mev for the gamma-ray energy.[7]

The gamma-radiation of Au^{198} has been measured in a curved crystal spectrometer by DuMond, Lind and Watson[8] who give 411.2±0.1 kev for the energy, yielding values of $B\rho = 2219.7$ gauss cm for the K conversion line and $B\rho = 2502.1$ gauss cm for the L line. The K and L binding energies used here were determined from the critical absorption wave-length table of Compton and Allison.[9] Since the L_I, L_{II}, and L_{III} lines were not resolved, a weighted mean value for the L shell energy was used. Table I gives the pertinent values for the elements used in these experiments.

For the "X" line measurements, sources of ~4 mm diameter of ThB were prepared by electrostatic collection from Tn gas on .0005-inch Al foils. The thin (essentially mono-molecular) deposits so obtained were covered by an additional layer of .0005 inch Al foil to prevent recoil ThC'' nuclei from escaping. The Au^{198} source was plated from solution on a .0005 inch Cu foil and had a thickness of less than 0.1 mg/cm².[10] The total activity of these sources was of the order of 20 μ curies. Typical curves obtained are reproduced in Fig. 3 and Fig. 4, and the resulting peak and edge calibration values in terms of millivolts drop across a standard shunt presented in Table II.[11] The indicated locations of the X_a and X_{a1} lines in Fig. 3 are calculated from Ellis' data. The close agreement of the calibrations attests to the accuracy of the method and provides a relative check on the two independent standards.[12]

Measurements were also made on the ThF and I lines, but the uncertainties in the stray magnetic field corrections limited the precision to about 0.5 percent. The values obtained were in agreement with the ratios quoted by Ellis within this accuracy.

[6] Siegbahn, Arkiv f. Ast. Math. Fys. **30A**, No. 20 (1944).
[7] $B\rho = (10^4/2.99776)[E(E+1.02158)]^{\frac{1}{2}}$; E in Mev (absolute).
[8] DuMond, Lind, and Watson, Phys. Rev. **73**, 1392 (1948).
[9] Compton and Allison, *X-Rays in Theory and Experiment* (Van Nostrand Company, Inc., New York, 1935). p. 794.
[10] We are indebted to the AEC for their cooperation in supplying the Au^{198} and Co^{60} sources and to Mr. J. H. Sullivan for the chemical preparations involved in certain of the applications.
[11] The focusing current for lines having momenta greater than 4500 gauss cm was measured on a shunt having .1330₃ times the resistance of the standard shunt.
[12] If one uses the peak calibration for the Au^{198} to determine the X line value from this experiment, a value of 9998 gauss cm is obtained, corresponding to a gamma-ray energy of 2.618 Mev with a probable error of 4 kev. The corresponding extrapolated edge value, which is in this case considered somewhat less reliable because of the overlapping with the X_a line, yields $B\rho = 9989$ gauss cm or 2.615±.006 Mev. This comparison has been recently repeated with a resolution of 1.0%, resulting in a $B\rho$ value of 9982 gauss cm for the X line peak or an energy of 2.613±.004 Mev.

TABLE I. K and L shell energies.

Element	E_K (kev)	E_{LI} (kev)	E_{LII} (kev)	E_{LIII} (kev)	$\bar{E}_L$ (kev)
Thorium	109.8	20.5	19.7	16.3	20.1
Lead	88.0	15.8	15.2	13.0	15.6
Mercury	83.1	14.8	14.2	12.3	14.5
Nickel	8.3₄	—	—	—	—

EXTERNAL CONVERSION MEASUREMENTS

For gamma-ray sources in which no appreciable internal conversion occurs, photoelectrons may be produced in an external converter of high atomic number, using the arrangement of Fig. 2. Radiation produced in the target as at a in the figure will undergo photoelectric conversion throughout the volume of the converter foil. One such process is schematically illustrated at b; the photoelectron so produced will then emerge from the foil at some point c after having followed a path determined by a comparatively large number of small angle elastic scatterings, resulting principally from the interaction of the photoelectron with the nuclear coulomb fields of the converter atoms. At the same time, the photoelectron suffers ionization loss by interaction with the electrons in the converter, resulting in its emergence at c with a total loss of energy determined by the path length b–c. Because of the effects of scattering and straggling in the foil, the number of electrons emerging in a given energy interval will decrease as the energy loss increases, leading to a spectrum with a maximum value for zero energy loss, tailing off monotonically toward lower energies at a rate determined by the initial photoelectron energy and the converter thickness and atomic number. The observation of such a distribution with an instrument of finite resolution will in general result in a shifting of the peak and extrapolated front edge of the curve by a magnitude depending on the resolution and on the exact shape of the spectrum.

To illustrate the effect of converter thickness on line shape at a comparatively low energy, experimental

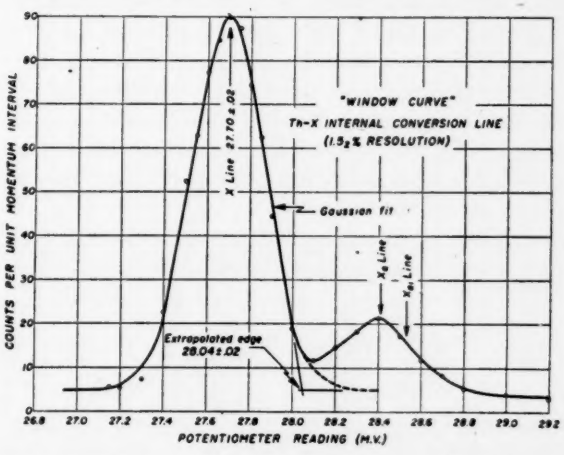

FIG. 3. "Window curve": observed spectrum from internal conversion lines of 2.62 Mev gamma-radiation of ThD.

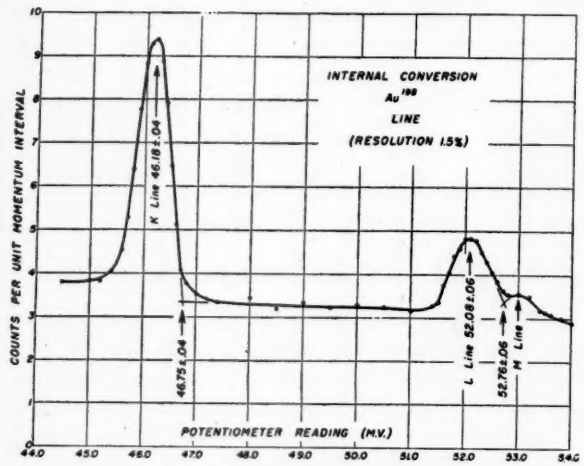

FIG. 4. Internal conversion lines of 411 kev gamma-radiation of Au^{198}.

curves of the K conversion in thorium foils of the 411.2 kev gamma-radiation of Au^{198} are shown in Fig. 5. The source used for this work consisted of a 1 mm square of activated Au foil .001 inch thick placed on the back of a .030 inch copper absorber, to which were attached the thorium foils.[13] The copper absorber was used to suppress the continuous β radiation. The ordinates of the various curves have been adjusted only to the extent that backgrounds of the order of 30 percent, due partly to the tailing of the L and M lines at ≈ 51 M.V. and partly to general radiation, have been subtracted. The intensities plotted are for a constant source strength in all cases.

Perhaps the most significant feature of these curves, from the standpoint of their usefulness in energy determinations, is the observation that the intersection of the extrapolated front edge with the background is apparently independent of converter thickness. A similar set of curves for the 717 kev gamma-radiation from the reaction $Be^9(d\,n)B^{10*}$ is shown in Fig. 6. The curves of Fig. 7 illustrate the two high energy gamma-rays accompanying the decay of Co^{60}, where the background has not been subtracted.[14] In all cases the extrapolated edge values for the K conversion lines were found to be independent of converter thickness to within about 0.2 percent. Reference to Table III shows that the value of the Au^{198} gamma-ray deduced from the extrapolated edge agrees within 0.1 kev with the known value (using extrapolated edges of the internal conversion lines referred to above for calibration).

[13] Throughout this paper the converter thicknesses quoted in inches are nominal thicknesses. By weighing these have been determined to be:

.00025 inches	7 mg/cm²
.0005 inches	16 mg/cm²
.001 inches	25 mg/cm²
.002 inches	57 mg/cm²
.003 inches	78 mg/cm²
.004 inches	113 mg/cm²
.005 inches	150 mg/cm²

[14] The cobalt curves were run with only .001 inch Cu absorber: the abnormal intensity of the L lines is due to the superposition on them of the internal conversion K lines, shifted by the energy loss in the absorber.

The height and location of the peaks and the magnitude of the low energy side of the distributions, on the other hand, are clearly affected by changes in the converter thickness. Between the .00025 inch and the .0005 inch curves in Fig. 5, one observed an increase of intensity and a shift of the maximum toward lower energy. As compared with the expected peak for zero converter thickness, the .00025 inch peak is shifted by 1.7 kev and the .0005 inch by 3.2 kev. For thicknesses greater than .0005 inch one observes no further shift or increase in peak intensity (the intensity actually decreases somewhat because of the absorption of the gamma-radiation) and only the lower energy tail seems to be affected.

In an effort to ascertain the primary distribution of the electrons emerging from the converter, the experimental curves of Fig. 5 have been "unfolded," i.e., the effect of finite resolution removed, by a method of successive approximations assuming a Gaussian window shape. Although such a procedure cannot in general be expected to reveal changes occurring in intervals small compared to the resolution width (7.3 kev), in this case the unfolding was facilitated by the fact that the upper limit of the primary spectrum was known absolutely from the calibration. The curves of Fig. 8, which exhibit the inferred spectra for three converter thicknesses, show that the number of electrons per unit momentum interval emerging from the converter drops very sharply in less than ~ 3 kev and thereafter falls more gradually at a rate depending on converter thickness. The ordinates in these curves are in the same (arbitrary) units as those of Fig. 5, to facilitate comparison. As a check on the reliability of the inferred primary distribution, the .0005 inch converter curve was repeated at a resolution of 0.65 percent, using a smaller source, and introducing several other modifications in the spectrometer. The primary spectrum representing the best fit for the two resolutions is shown in Fig. 9, where the numerically integrated "folds" with gaussians of 0.65 percent and 1.5 percent width are also shown, together with the experimental points. This inferred distribution agrees well with the corresponding one in Fig. 8: the initial decrease in the number of electrons per unit energy interval is again very pronounced. The unfolding of several other curves obtained from 0.7 and 1.1 Mev gamma-rays has yielded similar shapes. While the present experiments appear to indicate that the character of the primary spectrum undergoes an abrupt change in the neighborhood of two to four kev energy loss (for the Au^{198} radiation), it should be pointed out that the unfolding process is necessarily quite sensitive to small experimental errors; an upward shift of the assumed front edge of the primary spectrum of 0.5 kev—about the probable error—yields a satisfactory fit with a distribution function dropping off to half the maximum value in four to six kev and consequently with a considerably less abrupt

TABLE II. Calibration lines.

Line	$E\gamma$ (kev)	E_e (kev)	$B\rho$	Edge† M.V.	Peak† M.V.	($B\rho$/M.V.) edge	($B\rho$/M.V.) peak
ThD K	2618 ±4	2530	10,000	211.1_0*	208.6_4*	47.37_0	47.92_9
Au^{198} decay K	411.2± .1	328.1	2,219.7	46.89	46.32	47.33_8	47.92_1
Au^{198} decay L	411.2± .1	396.7	2,502.1	52.90	52.22	47.29_9	47.91_5
					Calibration**:	47.34_9±.03	47.92_5±.03

† Corrected for axial component of stray field.
* Including 9 gauss cm correction for cover foil; reduced to standard shunt readings.
** ThD values weighted 3×; mean of three runs given in table.

change in slope. More definite information on the exact shape of the primary spectrum in the first few kilovolts must clearly be sought in further experiments employing significantly higher resolution. In any case, it is clear that there exists near the high energy limit of the spectrum a considerable excess of electrons over what might be expected if scattering and straggling effects were neglected and that the common assumption of a rectangular distribution may be quite misleading in this energy region. It is presumably just the existence of this large number of electrons with small energy loss which accounts for the fact that the extrapolated edge of the distribution observed with the resolutions used here is relatively independent of converter thickness. With a considerably broader window curve, one might expect the influence of the back slope to become relatively more important, resulting in a detectable edge shift.

The behavior of the distribution as a function of energy was studied using K photoelectrons produced in a .0005-inch thorium foil by the following gamma-rays:

(a) Au^{198} radiation (411.2 kev)—.030 inch Cu absorber and .0005 inch Th converter.

(b) Li^{7*} radiation (478 kev)—produced by bombardment of a Li target by protons: same absorber and converter.

(c) Annihilation radiation (510.8 kev)—from 10 min N^{13} produced by bombarding a .010 inch thick graphite target with deuterons; same absorber and converter.

(d) B^{10*} (717 kev)—produced in the reaction $Be^9(d\,n)B^{10*}$ by deuteron bombardment of an .004 inch Be target with the .0005 inch Th converter only.

The observed spectra are illustrated in Fig. 10, where the momentum scales have been adjusted by multiplication to bring the front edges into coincidence. The location $B\rho/B\rho_0 = 1.000$ corresponds to the true position of the photoelectron line, determined absolutely for the Au^{198} radiation. In Table III, the gamma-ray energies derived from the observed extrapolated front edges are presented, including the Co^{60} determinations from Fig. 7.

An independent check on the consistency of the data and support for the assumption that the extrapolated front edge does not, within the present uncertainty, require correction for converter thickness is provided by the close agreement of the observed value of the annihilation radiation to the known figure of 510.8 kev.[15] The probable errors indicated include estimates of uncertainties in matching the curves and subtracting background in addition to such systematic errors as appear in current measurement, source location and stray field corrections.

Examination of the curves of Fig. 10 shows that, as the energy is increased, the tail of the distribution becomes less prominent compared to the resolution of the instrument, which is given by a constant width on this plot. The peak locations for the four curves are identical within the experimental error of about 0.1 percent and indicate a displacement downward of 0.66 percent in momentum. That the peaks coincide in this case is to some extent fortuitous; a thinner converter would be expected to give a relatively smaller shift at the higher energy (compare Fig. 11).

PEAK SHIFT CORRECTIONS

It would appear from these experiments that, as long as variations in source diameter sufficient to affect the window curve are avoided, the extrapolated edge determination is to be preferred because of its relative independence of converter thickness. However, in many practical cases, uncertainties in the background and the interference of neighboring lines may make such deter-

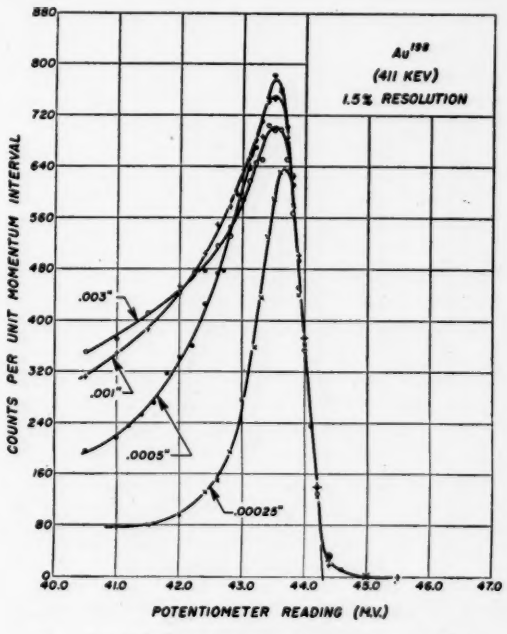

FIG. 5. 411 kev radiation of Au^{198}, converted in various thorium foils.

[15] DuMond and Cohen, Rev. Mod. Phys. **20**, 82 (1948); DuMond, Lind, and Watson, Phys. Rev. **75**, 1226 (1949).

TABLE III. *K*-line extrapolated edge determinations—.0005-inch thorium converter.

γ-Ray source	M.V.† (current)	$B\rho$††† (gauss-cm)	E_e (kev)	E_e+E_k (kev)
Au^{198} decay	44.48	2106.1	301.3	411.1± .6
Li^{7*}	50.42	2387.3	368.5	478.3± .7
e^+ annihilation	53.21	2519.4	401.0	510.8± .7
B^{10*}	70.04	3316.3	606.9	716.7±1.0
Co^{60} decay (a)	104.8_6 ††	4965	$1062._8$	$1172._6$±2.5
Co^{60} decay (b)	116.5_4	5518	$1220._4$	$1330._2$±2.9

† Corrected for axial component of stray field.
†† Values reduced to standard shunt readings.
††† Using as a calibration $B\rho$/M.V. $=47.34_9\pm.03$.

minations more difficult than the location of the peak. As has already been pointed out, if peak values are to be used, allowance must be made for the converter effects. The corrections to be applied may be roughly estimated from consideration of the effect of folding the window curve into the characteristic primary distribution. For "thin" converters, in which the energy loss is small compared to the resolution width, Jensen, Laslett, and Pratt[16] have pointed out that, if straggling is neglected, this distribution can be approximated by a rectangle of width equal to the average energy loss in the foil, and that the resulting peak shift is one-half this width. The straggling in energy loss due to the relatively infrequent close collisions is, however, an appreciable factor, and will have the effect of spreading the electron distribution on the low energy side. Since the "average" energy loss is heavily weighted by the small fraction of electrons which have lost large amounts of energy and which thus will have little influence on the peak location, it would seem reasonable that the effective width of the distribution is better measured by the "most probable" energy loss, which gives more equitable weighting to the majority of the electrons. Values of the most probable energy loss in thorium have been calculated for the thicknesses used in these experiments, by R. F. Christy and E. R. Cohen,[17] and the resulting shift limits are shown in Fig. 11 by the three dashed curves extending horizontally to the right; the upward trend at low energies reflects to some extent the influence of scattering in increasing the effective path length. The importance of straggling effects even in the region from 1 to 3 Mev may be judged from the fact that these shift limits are about a factor of two lower than those corresponding to the average energy loss.

For thicker foils, or lower energies the scattering may reach such proportions that many of the photoelectrons produced will become essentially diffused and will either be lost completely or suffer so large energy degradation as to fail to appear in the observed part of the spectrum. The plural scattering and diffusion of electrons has been treated theoretically by Bothe[18] and by Bethe, Rose, and Smith[19] who find that the number of electrons penetrating a given thickness of material drops off very rapidly for thicknesses of the order of the "transport mean free path," which is defined as the distance in which the root mean square scattering angle becomes of the order of $\pi/4$. By associating a most probable energy loss with the effective path length for electrons originating at various depths in the converter, one obtains a distribution which decreases monotonically from a maximum at zero energy loss to half intensity at a value corresponding roughly to the most probable energy loss in the transport mean free path. The folding of the window curve into such a spectrum leads to a peak shift approximately equal to the half

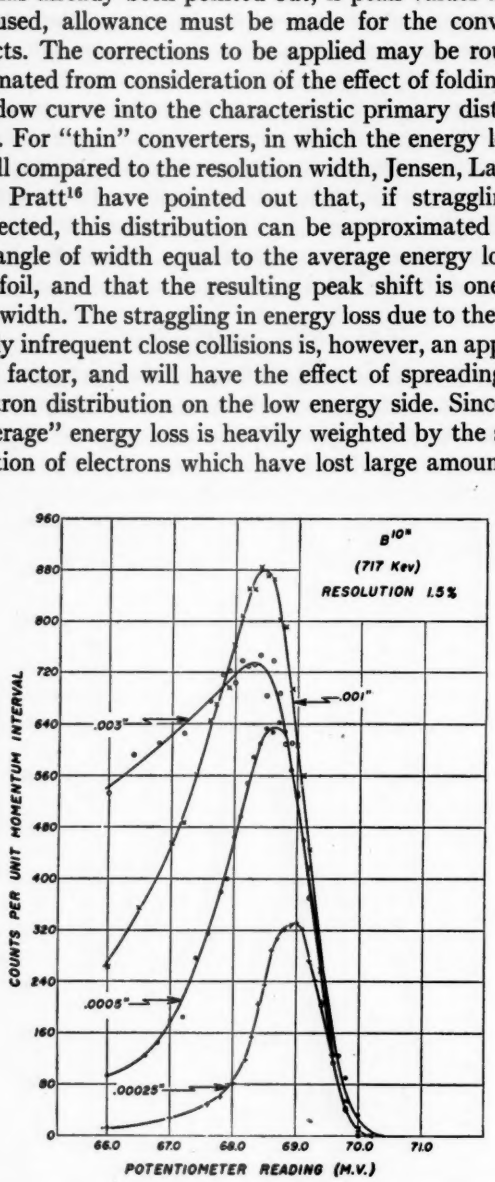

FIG. 6. 717 kev radiation from $Be^9(d\,n)B^{10*}$, converted in various thorium foils.

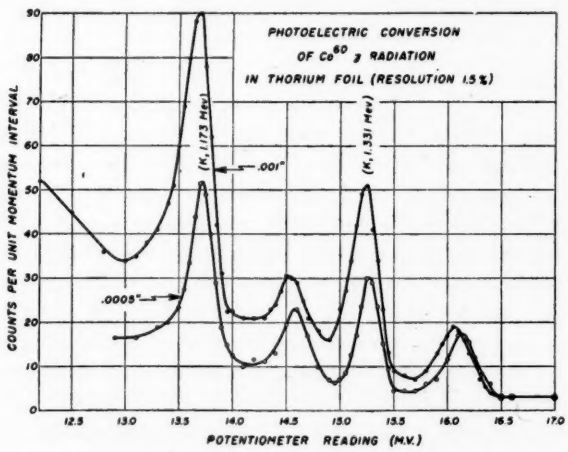

FIG. 7. 1.17 and 1.33 Mev gamma-radiation from Co^{60}, converted in .0005-inch and .001-inch thorium foils.

[16] Jensen, Laslett, and Pratt, Phys. Rev. **75**, 458 (1949).

[17] R. F. Christy and E. R. Cohen (to be published).
[18] W. Bothe, Zeits. f. Physik **54**, 161 (1929).
[19] Bethe, Rose, and Smith, Proc. Am. Phil. Soc. **78**, 573 (1938).

width at $1/e$ of the maximum (0.60 times the full width at half maximum) of the window curve. This limit, indicated by the dashed diagonal line of Fig. 11, is quite insensitive to the detailed shape of the primary distribution and should give a fairly reliable upper limit to the shift in the energy range 0.2 to 1.0 Mev for resolution widths less than about 5 percent. This line represents then the limiting case of an infinitely thick converter which together with the "thin" converter limit accounts for the main feature of the curves of Fig. 11. A somewhat more detailed treatment, assuming an exponential distribution cut off sharply at the most probable energy loss, for intermediate converter thicknesses leads to the solid curves of Fig. 11. The coefficient of the exponential was taken as inversely proportional to the energy loss in a transport mean free path, the constant of proportionality having been adjusted to fit the experimentally determined shifts for Au^{198} and annihilation radiation. The limiting cases of thick and thin converters exhibited in these curves merge reasonably well into the limits indicated by the more general considerations.

The extent to which the above discussed effects are applicable may be seen, at least qualitatively from the distributions of Fig. 5 and Fig. 8. Photoelectrons that are produced at a depth within the converter such that the most probable energy loss suffered in emerging from the foil is less than approximately the resolution of the spectrometer will be the most effective in determining both the location and the intensity of the observed line peak. In the present case this amounts to energy losses

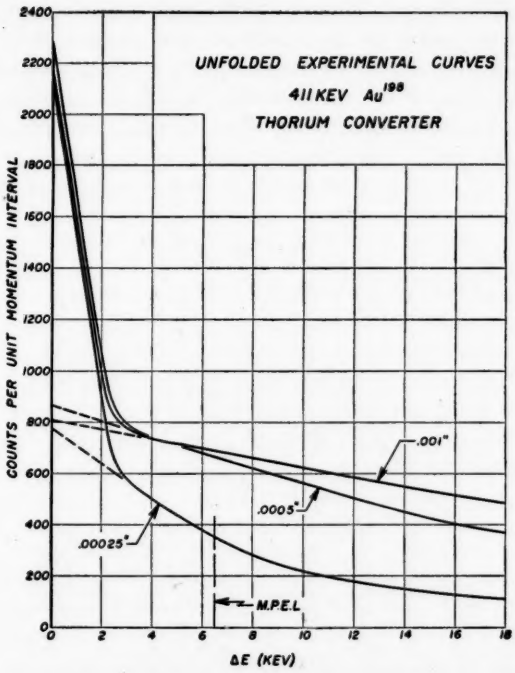

FIG. 8. Inferred "primary" distribution in energy of photoelectrons emerging from thorium converters irradiated by 411 kev Au^{198} gamma-radiation, as would be observed with infinitely high resolution.

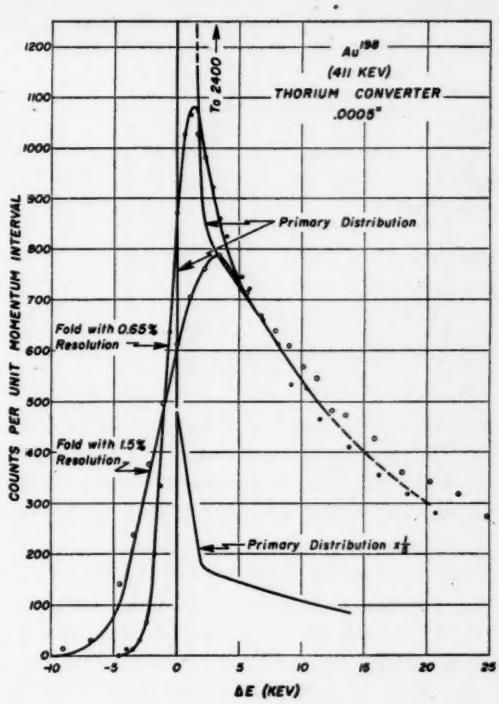

FIG. 9. Inferred primary distribution of photoelectrons produced by 411 kev Au^{198} radiation in .0005-inch thorium foil. The theoretical "folds" with 1.5 percent and 0.65 percent Gaussian window curves are compared with the observed points.

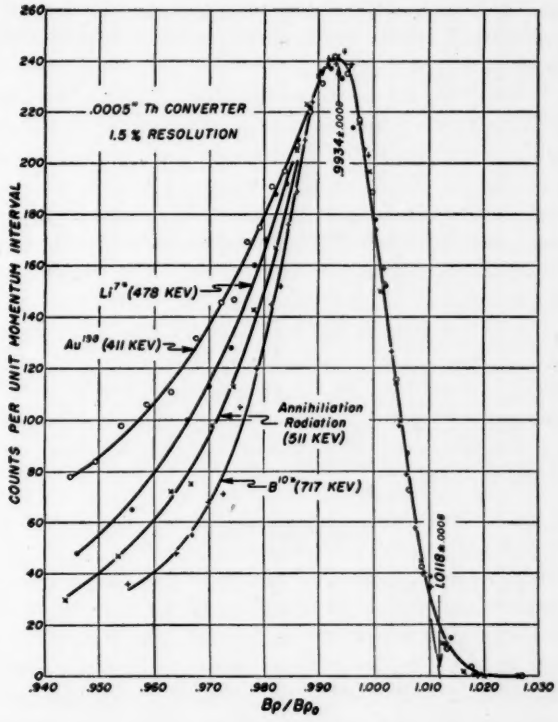

FIG. 10. Observed K photoelectron distributions for several gamma-rays, converted in .0005 inch thorium. The abscissa $B\rho/B\rho_0 = 1.000$ corresponds to the true momentum of the photoelectrons, i.e., the expected peak location for an infinitely thin converter.

TABLE IV. Peak determinations, .0005-inch thorium converter.

γ-Ray source	Line	M.V.† (current)	$B\rho$††† (Gauss-cm)	E_e (kev)	$E_e+E_{K,L}$ (kev)	Shift (kev)	$E\gamma$ (kev)
Au^{198} decay	K	43.67	2092.9	298.2	408.0	3.2	411.2
Li^{7*}	K	49.50	2372.3	364.8	474.6	(3.8)	478.4± .9
Au^{198} decay	L	51.38	2462.4	386.9	407.0	4.2	411.2
e^+ annihilation	K	52.24	2503.6	397.1	506.9	3.9	510.8
B^{10*}	K	68.77	3295.8	601.4	711.2	(4.9)	716.1±1.3
Co^{60} decay (a)	K	103.2_6\††	4949	$1058._2$	$1168._0$	(4.2)	$1172._2$±2.5
Co^{60} decay (b)	K	114.9_6∫	5509	$1217._8$	$1327._6$	(4.0)	$1331._6$±2.9

† Corrected for axial component of stray fields.
†† Values reduced to standard shunt reading.
††† Using as a calibration $B\rho$/M.V. $=47.92_8\pm.03$.

less than 8 kev or a depth less than about .0003 inch of thorium. Thus it is observed that the increase of the peak intensity in going from .00025 inch to .0005 inch is comparatively slight although a shift in the location of the peak to a lower energy is apparent. Increasing the foil thickness beyond the "resolution depth" should however materially increase the prominence of the tail just below the peak until a thickness comparable to the transport mean free path is reached. The transport mean free path is estimated to be .0004 inch for this energy. After a thickness of the order of two or three times this value is reached, very few additional electrons are observed even in the tail. The "cut-off" used in the theory is indicated in Fig. 8 for the .00025-inch foil thickness. The absence of any sharp discontinuity in the .00025-inch curve at this energy loss emphasizes the approximate nature of the theory used in obtaining the curves of Fig. 11.

In Table IV are presented the observed peak locations for the various gamma-rays discussed earlier, together with the estimated shift values (in parentheses) taken from Fig. 11. While no great claim to precision can be made in the arguments on which the corrections are based, a comparison with the values of Table III indicates satisfactory agreement between the two sets of determinations. It may be remarked that in the case of the Li^{7*} radiation, the fact that the line is bracketed between two known values makes the determination almost independent of the corrections adduced above. For the Co^{60}, a direct extrapolation, ignoring the peak shift would lead to values about 6 kev higher than those quoted in Table IV.

DOPPLER SHIFT

In the cases of the Li^{7*} and B^{10*} radiations, an appreciable correction for Doppler effect is involved in the determination of the energy of the excited state because of the center of mass motion. The shift associated with a center of mass velocity along the spectrometer v is, neglecting effects of order v^2/c^2 and assuming isotropic disintegration,

$$\delta=(v/c)E_\gamma\langle\cos\theta\rangle$$

where $\langle\cos\theta\rangle$ is the mean cosine of the angle between the spectrometer axis and the gamma-rays producing photoelectrons in the acceptance cone. An estimate of $\langle\cos\theta\rangle$ can be made if the scattering of the photoelectrons is neglected and if the angular distribution of the photoelectrons is simply taken to be a delta-function at the angle

$$\omega=\cos^{-1}\beta_e$$

with the direction of the gamma-ray, where β_e is the velocity of the photoelectron in units of the velocity of light. Then for the geometry in question, with θ_0 the acceptance angle of the spectrometer

$$\langle\cos\theta\rangle=[\cos(\theta_0+\omega)\cos(\theta_0-\omega)]^{\frac{1}{2}}.$$

Table V gives the calculations leading to the values of δ, assuming that the residual nucleus has not been stopped before the emission of the gamma-ray. The scattering experienced by the photoelectrons will in general reduce the Doppler shift, since radiation emitted at large angles to the center of mass motion will contribute appreciably to the spectrum. In an experimental comparison of the gamma-ray from the decay of Be^7 with that accompanying the inelastic scattering of protons by Li^7, the Doppler shift was found to be 1.6 kev[20] for the same geometrical arrangement used here.

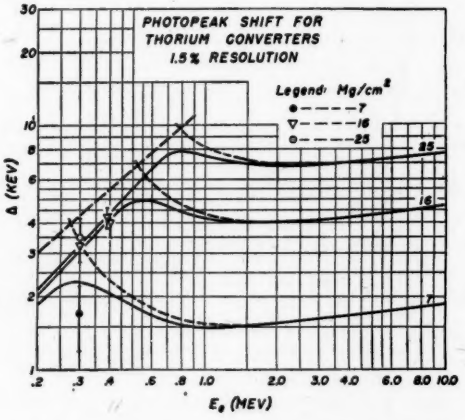

FIG. 11. Peak shift correction for converter thickness as a function of initial photoelectron energy.

[20] Rasmussen, Lauritsen, and Lauritsen, Phys. Rev. 75, 199 (1949).

TABLE V. Doppler shifts.

Reaction	Bombarding voltage (Mev)	v/c	ω	$\langle\cos\theta\rangle$†	δ (kev)
$Li^7(p\,p')Li^{7*}$	1.05	.0059	38.5°	.78	2.2
$Be^9(d\,n)B^{10*}$	.96	.0058	27.1°	.86	3.6

† $\theta_0=13°$.

TABLE VI. Gamma-ray and excitation energies.

Reaction	$E\gamma$ (kev)	δ (kev)	ΔE_{level} (kev)
$Li^7(p\,p')Li^{7*}$	478.3± .6	1.6± .7	476.7± .9
$Be^9(d\,n)B^{10*}$	716.4± .8	2.6±1.0†	713.8±1.3
$Co^{60}(\beta^-)Ni^{60*}$ (a)	1172.4±1.8	0	1172.4±1.8
$Co^{60}(\beta^-)Ni^{60*}$ (b)	1330.9±2.1	0	1330.9±2.1

† Taken as $\approx 1.6/2.2\times 3.6$.

The calculated shift for B^{10*} has been reduced by the same proportion in the computation of the final values, even though at this higher energy the scattering is certainly less important. Table VI presents the final values, using the means of Tables III and IV, and including the estimated Doppler shifts.

The present value for the excited state of Li^7 is slightly lower than the value 478.5±1.5 kev given by Elliott and Bell[21] for $B^{10}(n\alpha)Li^{7*}$ but as the probable errors overlap, the difference is hardly significant. The Co^{60} values are about 15 kev higher than those obtained by Jensen, Laslett, and Pratt[16,*]; the reason for this discrepancy is not clear. A preliminary crystal spectrometer determination of these lines, kindly communicated to us by Professor DuMond and Dr. Lind is in good agreement with the values quoted here.

It is a pleasure to acknowledge the many helpful suggestions and active assistance of Professor R. F. Christy in connection with this problem. We are also indebted to Professors C. C. Lauritsen and W. A. Fowler for valuable advice and consultations. This work was assisted by the joint program of the ONR and the AEC.

[21] L. G. Elliott and R. E. Bell, Phys. Rev. **74**, 1869 (1948).

* *Note added in proof:* More recent work by the authors, kindly communicated to us by Professor Laslett has led to values which, when adjusted by use of the *average* energy loss, agree well with those cited here. The agreement is less good if the shift is calculated from the most probable energy loss, but is still within the combined probable errors.

PHYSICAL REVIEW VOLUME 76, NUMBER 6 SEPTEMBER 15, 1949

Penetration and Diffusion of X-Rays through Thick Barriers. II. The Asymptotic Behavior when Pair Production Is Important*

U. FANO
National Bureau of Standards, Washington, D. C.

(Received May 16, 1949)

The methods of a previous paper are modified to cover the high energy x-rays which are strongly absorbed by pair production. The variation of intensity with depth of penetration is then expected to follow a law of the type $x^{-5/6}\exp(-\mu_m x+bx^{\frac{1}{2}})$.

THE factors governing the approach to spectral equilibrium in the penetration of hard x-rays have been discussed in a previous paper,[1] which will be referred to as I. It was found that the trend of the total x-ray intensity at great depth of penetration depends essentially upon the progressive formation and decay of those secondary components that are least absorbed.†

The earlier treatment assumed that the primary x-rays are less absorbed than any of their secondaries. This obtains in lead only up to energies of about 3 Mev, in lighter elements up to higher energies. At very high energies absorption by pair production becomes increasingly important and secondary scattered x-rays may be more penetrating than the primaries. Under these conditions the softer x-ray components still approach an equilibrium, but this equilibrium state is now controlled by the formation and decay of the hardest secondary components. The energy of these components corresponds to the minimum of the plot of absorption coefficient *vs.* photon energy,[2] and may be much lower than the energy of the primaries. (The present analysis *disregards the bremsstrahlung* of the electrons generated by pair production.)

* Work supported by the Applied Mathematics Branch of the ONR.

[1] Bethe, Fano, and Karr, Phys. Rev. **76**, 538 (1949).

† *Note added in proof:* The results derived in I are closely related to those derived by Wick (Phys. Rev. **75**, 738 (1949)) in his treatment of the analogous neutron problem. Wick also took into account the effect of small angular deflections and his methods are now being applied to the x-ray problem. This effect tends to modify the values of the constants in (13 *a* and *c*) without changing the structure of these formulas. Finally, it is understood that some of the results reported in I were also obtained by Greuling (unpublished).

[2] See, e.g., W. Heitler, *Quantum Theory of Radiation* (Oxford University Press, London, 1944), p. 216.

This paper deals with the approach to equilibrium by a method which holds under broader conditions than the method used in the earlier work. However, we rely on the same principles as in I, namely:

(a) Use of special approximations in the limited energy range of the hardest components which control the equilibrium.
(b) Disregard of the deflections associated with scattering, since these deflections are small for the hardest components.

The latter assumption, amounting to the adoption of a "one-dimensional" model, is not as realistic in the present context as it was in I, since the hardest components themselves may have undergone an appreciable deflection in the course of previous scattering. Therefore, the results to be obtained here need reviewing in the framework of a more comprehensive treatment which is now being developed. However, the asymptotic behavior of the "one-dimensional model" is inherently an essential ingredient of the behavior of more realistic systems.

The mathematical treatment of this paper is more flexible than that of I. It makes use of a simplifying assumption somewhat less restrictive than the previous one ($K(\mu', \mu)=$const). The solution that will be given here preserves a qualitative significance, even though little accuracy, in the low energy range. The purpose of this note is just to point out qualitative features. The derivation of a more accurate solution requires a more detailed calculation which is now in progress.

CALCULATION

We start from a "one-dimensional" equation governing the diffusion and degradation of photons, which is equivalent to (1) I. It is convenient to adopt here a different choice of variables—namely, to indicate:

(1) the energy of photons by their wave-length λ, expressed in Compton units, and
(2) their spectral distribution by a "spectral energy density" $Y(x, \lambda)$. (With reference to the "integral photon spectrum" referred to in I, $Y=-\nu\partial I/\partial\nu=\lambda\partial I/\partial\lambda$.)

The function Y is governed by the equation

$$\partial Y/\partial x=-\mu(\lambda)Y+\int_{\lambda_0}^{\lambda} k(\lambda', \lambda)Y(x, \lambda')d\lambda', \quad (1)$$

where:

$$k(\lambda', \lambda)=(\tfrac{3}{8})\mu_{T\lambda}\{\lambda'^2+\lambda^2+\lambda'\lambda[(\lambda-\lambda')^2-2(\lambda-\lambda')]\}/\lambda^2. \quad (1')$$

$\mu_{T\lambda}$ = absorption coefficient for Thomson scattering.
μ = total narrow beam absorption coefficient at wave-length λ.

The initial condition is:

$$Y(0, \lambda)=\lambda_0\delta(\lambda-\lambda_0). \quad (1'')$$

The solution of (1) is represented by the method of Laplace transformation as a superposition of spectral distributions—each of which decays as an exponential function of x:

$$Y(x, \lambda)=(1/2\pi i)\int_{a-i\infty}^{a+i\infty} dp\, y(p, \lambda)\exp(-px)+\lambda_0\delta(\lambda-\lambda_0)\exp(-\mu_0 x). \quad (2)$$

The last term of (2) represents the primary radiation. The "Laplace Transform" $y(p, \lambda)$ is governed by the equation:

$$(\mu-p)y(p, \lambda)=\int_{\lambda_0}^{\lambda} k(\lambda', \lambda)y(p, \lambda')d\lambda'+\lambda_0 k(\lambda_0, \lambda)/(\mu_0-p). \quad (3)$$

At this point we introduce the main simplifying assumption (referred to as (a) above), of attributing to $k(\lambda', \lambda)$ a constant value C. This value may be taken equal to $k(\lambda, \lambda)=(\frac{3}{4})\mu_{T\lambda}$ or a little lower. (The earlier choice of the independent variable λ and of the dependent variable Y was designed so that the assumption $k(\lambda', \lambda)=C$ is not too unrealistic. In fact $k(\lambda', \lambda)$ remains of the order of magnitude of $\mu_{T\lambda}$ for all values of λ' and λ.)

Equation (3) reduces now to:

$$(\mu-p)y(p,\lambda)=C\int_{\lambda_0}^{\lambda} y(p, \lambda')d\lambda'+C\lambda_0/(\mu_0-p). \quad (3')$$

Simple differentiation reduces (3′) to a first order linear differential equation whose solution is:

$$y(p, \lambda)=C\lambda_0\exp\left[C\int_{\lambda_0}^{\lambda} d\lambda'/(\mu(\lambda')-p)\right]\Big/(\mu-p)(\mu_0-p). \quad (4)$$

Equation (2), with the expression (4) of y, describes the spectral distribution at all depths x. It constitutes an approximate formal solution of the "one-dimensional" penetration and degradation problem governed by (1).

ASYMPTOTIC BEHAVIOR OF THE SOLUTION

There is a standard method for studying the values of the "inverse transform" (2) at great depths, that is, for large x. This is to deform the path of complex integration over p way to the right in the complex plane, where the factor, $\exp(-px)$ becomes very small; however, the deformation should not bring the path through any region where y becomes very large. Such a region lies on the positive real axis of p, where the denominators $\mu-p$ in (4) vanish.

Accordingly, the path of integration can be so deformed (Fig. 1) that the main contribution to the integral comes from a section of the path in the proximity of

a "saddle point" at $p=p_s$.[3] This point is located on the real axis a little to the left of μ_s, where μ_s is the *smallest value of* $\mu(\lambda')$ in the range of integration of λ' in (4), from λ_0 to λ. (The distance of p_s from μ_s decreases as x increases and it turns out that the product $(\mu_s-p_s)x$ is either a number of the order of 1 or a slowly increasing function of x.)

In the case, studied in I, where the primary radiation of wave-length λ_0 is harder than any of its secondaries, the smallest value of $\mu(\lambda')$ is found at the very start of the integration: $\mu_s=\mu(\lambda_0)=\mu_0$. The function $\mu(\lambda')$ for any material has a minimum value μ_m at some wave-length λ_m. Therefore, in general,

$$\mu_s=\mu(\lambda_m)=\mu_m \quad \text{for} \quad \lambda_0\leq\lambda_m, \tag{5a}$$

$$\mu_s=\mu(\lambda_0)=\mu_0 \quad \text{for} \quad \lambda_0\geq\lambda_m. \tag{5b}$$

(The case where $\lambda<\lambda_m$ is not interesting in the present connection.)

At great depths of penetration, the values of p which contribute substantially to the integral in (2) still depend on the value of x, but they are confined to the proximity of μ_s within a distance $\sim\mu_s-p_s$. Therefore, this dependence on x will not affect substantially the factor $(\mu-p)$ in (4) or those *portions* of the integral in (4) where $\mu(\lambda')-p\gg\mu_s-p$ (assuming that $\lambda\gg\lambda_s$). Now, these portions of (4) are the very ones that depend on λ. It follows that the whole integral in (2) depends on λ and x through separate factors of the expression (4). In other words, under the conditions stated, $Y(\lambda, x)$ becomes the product of a function of λ and a function of x, that is, the spectral distribution becomes independent of the depth of penetration. This constitutes a sort of "equilibrium" (within the meaning of (b) in I).

The concept just outlined may be formulated mathematically by various devices. For example, one may represent the factor $1/(\mu(\lambda')-p)$ in the integral of (4) as the sum of two functions: one function which matches $1/(\mu-p)$ accurately for $\lambda'\sim\lambda_s$, has a simple form and vanishes when $\lambda'\gtrless\gtrless\lambda_s$, and another function which vanishes for $\lambda'\sim\lambda_s$ and is therefore practically independent of p. The function $\mu(\lambda')$ may be matched, for

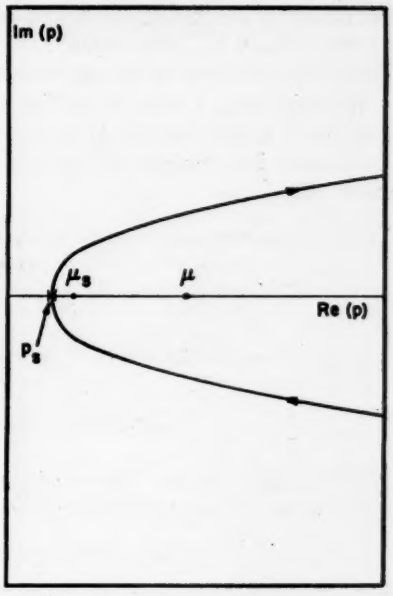

FIG. 1. Schematic representation of the "saddle point" of the integrand and of the "steepest descent" path of integration over the complex variable p in Eq. (4).

$\lambda'\sim\lambda_s$ by a three-term power expansion:

$$\mu(\lambda')\sim\mu_s+\dot{\mu}_s(\lambda'-\lambda_s)+(d^2\mu/d\lambda^2)_s(\lambda'-\lambda_s)^2/2,$$

where $\dot{\mu}_s=(d\mu/d\lambda')_{\lambda'=\lambda_s}$. We write then:

$$\begin{aligned}1/[\mu(\lambda')-p]&=1/[\mu_s-p+\dot{\mu}_s(\lambda'-\lambda_s)\\&\quad+(d^2\mu/d\lambda^2)_s(\lambda'-\lambda_s)^2/2]+\{1/[\mu(\lambda')-p]\\&\quad-1/[\mu_s-p+\dot{\mu}_s(\lambda'-\lambda_s)\\&\qquad+(d^2\mu/d\lambda^2)_s(\lambda'-\lambda_s)^2/2]\}.\end{aligned} \tag{6}$$

Little error is incurred by replacing the variable p by μ_s within the curly brackets. The quantity $\{\ \}$ may then be integrated over λ' from λ_0 to λ, numerically if necessary. The result of the integration is some function

$$\begin{aligned}Q(\lambda_0, \lambda)=\int_{\lambda_0}^{\lambda} d\lambda'\{&1/[\mu(\lambda')-\mu_s]\\&-1/[\dot{\mu}_s(\lambda'-\lambda_s)+(d^2\mu/d\lambda^2)_s(\lambda'-\lambda_s)^2/2]\},\end{aligned} \tag{7}$$

which needs no further investigation at this point.

The remaining integral yields:

$$\begin{aligned}\int_{\lambda_0}^{\lambda} d\lambda'/[\mu_s-p+\dot{\mu}_s(\lambda'-\lambda_s)+(d^2\mu/d\lambda^2)_s(\lambda'-\lambda_s)^2/2]&=T_1+T_2\\&=[\dot{\mu}_s^2-2(d^2\mu/d\lambda^2)_s(\mu_s-p)]^{-\frac{1}{2}}\log\frac{\dot{\mu}_s+(d^2\mu/d\lambda^2)_s(\lambda-\lambda_s)-[\dot{\mu}_s^2-2(d^2\mu/d\lambda^2)_s(\mu_s-p)]^{\frac{1}{2}}}{\dot{\mu}_s+(d^2\mu/d\lambda^2)_s(\lambda-\lambda_s)+[\dot{\mu}_s^2-2(d^2\mu/d\lambda^2)_s(\mu_s-p)]^{\frac{1}{2}}}\\&\quad-[\dot{\mu}_s^2-2(d^2\mu/d\lambda^2)_s(\mu_s-p)]^{-\frac{1}{2}}\log\frac{\dot{\mu}_s+(d^2\mu/d\lambda^2)_s(\lambda_0-\lambda_s)-[\dot{\mu}_s^2-2(d^2\mu/d\lambda^2)_s(\mu_s-p)]^{\frac{1}{2}}}{\dot{\mu}_s+(d^2\mu/d\lambda^2)_s(\lambda_0-\lambda_s)+[\dot{\mu}_s^2-2(d^2\mu/d\lambda^2)_s(\mu_s-p)]^{\frac{1}{2}}}.\end{aligned} \tag{8}$$

The term T_1 may be simplified, when $\lambda\gg\lambda_s$, by expanding the logarithm. It reduces to:

$$T_1\sim-2/[\dot{\mu}_s+(d^2\mu/d\lambda^2)_s(\lambda-\lambda_s)] \quad (\text{for } \lambda\gg\lambda_s). \tag{9a}$$

This term may be added to $Q(\lambda_0, \lambda)$ and treated accordingly.

The term T_2 is independent of λ and it determines the asymptotic dependence of Y on x. This term takes different, simple, forms when the primary radiation is

[3] See, e.g., H. and B. S. Jeffreys, Mathematical Physics (Cambridge University Press, London, 1946), Chapter 17.

not nearly of the most penetrating variety, that is when $\lambda_0 \gg \lambda_m$ or $\lambda_0 \ll \lambda_m$, also when $\lambda_0 = \lambda_m$. The former of these cases is the same as was treated in I.

When $\lambda_0 \gg \lambda_m$, $\lambda_s = \lambda_0$ according to (5a). When λ_0 is sufficiently larger than λ_m, $\dot{\mu}_s^2 = \dot{\mu}_0^2 \gg 2(d^2\mu/d\lambda^2)_0(\mu_0 - p)$. Expansion into powers of $2(d^2\mu/d\lambda^2)_0(\mu_0 - p)/\dot{\mu}_0^2$ reduces then T_2 to:

$$T_2 \sim -(1/\dot{\mu}_0) \log[(\mu_0 - p)(d^2\mu/d\lambda^2)_0/\dot{\mu}_0^2], \quad (\text{for } \lambda_0 \gg \lambda_m). \quad (10a)$$

When λ_0 approaches λ_m, $\dot{\mu}_0$ tends to zero. The expression $[\dot{\mu}_0^2 - 2(d^2\mu/d\lambda^2)_0(\mu_0 - p)]^{\frac{1}{2}}$ vanishes before λ_0 reaches λ_m, and thereafter it becomes imaginary. At $\lambda_0 = \lambda_m$, $\dot{\mu}_0 = \dot{\mu}_s = \dot{\mu}_m = 0$, the argument of the log is $-1 = e^{-\pi i}$ and T_2 reduces to

$$T_2 = \pi[2(d^2\mu/d\lambda^2)_m(\mu_m - p)]^{-\frac{1}{2}}. \quad (10b)$$

When λ_0 decreases below λ_m, $\lambda_s = \lambda_m$ according to (5b), $\dot{\mu}_s = \dot{\mu}_m = 0$, and T_2 takes the form:

$$T_2 = i[2(d^2\mu/d\lambda^2)_m(\mu_m - p)]^{-\frac{1}{2}} \log \frac{(d^2\mu/d\lambda^2)_m(\lambda_0 - \lambda_m) - i[2(d^2\mu/d\lambda^2)_m(\mu_m - p)]^{\frac{1}{2}}}{(d^2\mu/d\lambda^2)_m(\lambda_0 - \lambda_m) + i[2(d^2\mu/d\lambda^2)_m(\mu_m - p)]^{\frac{1}{2}}}$$
$$= [2(d^2\mu/d\lambda^2)_m(\mu_m - p)]^{-\frac{1}{2}}\{2\pi - \arctan[(d^2\mu/d\lambda^2)_m^{\frac{1}{2}}(\mu_m - p)^{\frac{1}{2}}/(d^2\mu/d\lambda^2)_m(\lambda_m - \lambda_0)]\}. \quad (8a)$$

When $\lambda_0 \ll \lambda_m$ the last term becomes very small and, inclusive of the factor in front, it reduces to:

$$\sim 1/(d^2\mu/d\lambda^2)_m(\lambda_m - \lambda_0). \quad (9b)$$

This term, like (9a), is independent of p; it may be added to $Q(\lambda_0, \lambda)$ and treated accordingly. The significant part of (8) is then simply:

$$T_2 \sim 2\pi[2(d^2\mu/d\lambda^2)_m(\mu_m - p)]^{-\frac{1}{2}}, \quad \text{for } (\lambda_0 \gg \lambda_m). \quad (10c)$$

The preceding considerations lead us to write the spectral distribution (2) in the form:

$$V(x, \lambda) = \lambda_0 \delta(\lambda - \lambda_0) \exp(-\mu_0 x) + [C\lambda_0/(\mu - \mu_s)] \exp[CQ(\lambda_0, \lambda) + CT_1] F(x, \lambda_0), \quad (\text{for } \lambda \gg \lambda_s); \quad (11)$$

with

$$F(x, \lambda_0) = (1/2\pi i) \int_{a-i\infty}^{a+i\infty} dp \times \exp[-px + CT_2(p, \lambda_0)]/(\mu_0 - p). \quad (11')$$

The integral in (11′) may be evaluated by steepest descent for each value of x and for the different relationships between μ and λ which correspond to different absorbing materials. When the energy of the primary photons is much smaller than that of the most penetrating ones (i.e., $\lambda_0 \gg \lambda_m$) T_2 takes the form (10a), and the integration yields exactly:

$$F(x, \lambda_0) = [1/\Gamma(C/\dot{\mu}_0 + 1)](\dot{\mu}_0^2 x/(d^2\mu/d\lambda^2)_0)^{C/\dot{\mu}_0} \times \exp(-\mu_0 x). \quad (12a)$$

This asymptotic behavior coincides with that obtained in (5) I, as it should. In the opposite case, when $\lambda_0 \ll \lambda_m$ and T_2 takes the form (10c), evaluation by steepest descent yields:

$$F(x, \lambda_0) \sim (2/3\pi)^{\frac{1}{2}}[2\pi^2 C^2/(d^2\mu/d\lambda^2)_m(\mu_0 - \mu_m)] \times [(d^2\mu/d\lambda^2)_m/4\pi^2 C^2 x]^{5/6} \exp[-\mu_m x + 3(\pi^2 C^2 x/2(d^2\mu/d\lambda^2)_m)^{\frac{1}{2}}]. \quad (12c)$$

The structure of these formulas is brought out by expressing them respectively as:

$$F(x, \lambda_0) = \text{const. } x^{K_0} \exp(-\mu_0 x), \quad (13a)$$

$$F(x, \lambda_0) = \text{const. } x^{-5/6} \exp(-\mu_m x + bx^{\frac{1}{2}}),^4 \quad (13c)$$

where $K_0 = C/\dot{\mu}_0$ and $b = 3(\pi^2 C^2/2(d^2\mu/d\lambda^2)_m)^{\frac{1}{3}}$. Both formulas contain the factor $\exp(-\mu_s x)$, where μ_s stands for μ_0 or μ_m respectively, which represents the decay of the most penetrating component under consideration. The remaining factor x^{K_0} or respectively $x^{-5/6}\exp(bx^{\frac{1}{2}})$ represents the effect of the accumulation of the secondary components barely softer than the most penetrating ones. Notice that K_0 and b depend on the balance between the generation of softer components, which is represented by C, and the corresponding loss of penetrating power, which depends on the derivatives of μ.

The solution obtained here has much the same significance as the solution derived in I and discussed at the end of that paper. The solution (11) is completely defined for all values of $\lambda \gg \lambda_s$, but it has no great claim to accuracy for large values of λ because of the assumptions made, namely that $k(\lambda', \lambda) = C$ and that the effect of deflections can be disregarded.

It is a pleasure for me to acknowledge the cooperation of my colleague P. R. Karr. I also wish to thank Dr. F. H. Murray of the Oak Ridge National Laboratory for many helpful discussions.

[4] This formula has also been obtained independently by Dr. Henry Hurwitz, Jr., who has kindly informed me of his results.

On the Gyromagnetic Ratio and Spectroscopic Splitting Factor of Ferromagnetic Substances

CHARLES KITTEL
Bell Telephone Laboratories, Murray Hill, New Jersey
(Received May 13, 1949)

A discussion is given of the connection between the results of microwave resonance absorption experiments and gyromagnetic ratio experiments on ferromagnetic substances. A review of the experimental data indicates that the microwave experiments usually give $g>2$, while gyromagnetic measurements usually give values of the related quantity g' which are <2. The analogous situation obtaining in paramagnetic salts is explained by means of a simple example, and the application of the argument to ferromagnetic substances is indicated. The validity of the use of g in the macroscopic equations of motion in the resonance experiment is justified as a consequence of the approximate mutual cancellation of the orbital and lattice angular momenta. A critical discussion is given of other attempts to explain the $g \neq g'$ effect.

I. INTRODUCTION

THE purpose of this paper is to discuss the connection between the results of determinations of the gyromagnetic ratio of ferromagnetic substances and the results of microwave magnetic resonance absorption experiments on these substances. Further, a critical analysis will be given of the various attempts to "explain away" the apparently anomalous result of the resonance absorption experiments, namely the fact that the values of the g-factor deduced from the absorption experiments are usually >2, whereas the gyromagnetic experiments usually give values <2. We are concerned in this paper with an explanation of the differences between the two types of experiments. In the existing literature there is rather little discussion of the detailed theory of gyromagnetic effects: Gorter and Kahn[1] have treated the paramagnetic case, and Polder[2] has suggested the extension of their considerations to the ferromagnetic case. Broer[3] has discussed the diamagnetic case with particular reference to superconductors. Our arguments may be considered as an extension and justification of the suggestion made by Polder in the references cited.

In a microwave resonance absorption experiment one determines the separation $\hbar\omega$ between adjacent energy eigenvalues of the specimen in a constant magnetic field H. The classical theory[4] of the effect gives as the resonance condition

$$\hbar\omega = g\mu_B H_{eff}, \tag{1}$$

where the effective magnetic field H_{eff} is given by

$$H_{eff} = (BH)^{\frac{1}{2}} \tag{2}$$

for a plane specimen with the static magnetic field parallel to the plane of the specimen; and by

$$H_{eff} = H - 4\pi M_s, \tag{3}$$

for a plane specimen with the static magnetic field normal to the plane of the specimen; while in general

$$H_{eff} = \{[H_z + (N_y - N_z)M_z][H_z + (N_x - N_z)M_z]\}^{\frac{1}{2}} \tag{4}$$

for an ellipsoid with demagnetizing factors N_x, N_y, N_z; here H_z is the static field. The effective field to be used in the resonance condition Eq. (1) differs from the applied field H because of the effect of the magnetic moment interactions within the specimen; these interactions give a dynamic demagnetization coupling which shifts the resonance condition in the manner prescribed by the effective field equations. The results of the classical theory of the effective field have been confirmed by the quantum-mechanical calculations of Van Vleck[5] and Polder[2] who worked with the complete microscopic Hamiltonian of the spin system; quantum-mechanical calculations by Luttinger and Kittel,[6] and Richardson,[7] give identical results starting from a macroscopic Hamiltonian. It is of course to be expected from the correspondence principle that the classical results will not be altered by quantization, since we are concerned here with large quantum numbers, of the order of 10^{15} or more.

We shall consider Eq. (1) as the definition of g, which will be called the *spectroscopic splitting factor*. That is, the g-value resulting from a microwave absorption experiment is to be calculated by substituting in the equation $\hbar\omega = g\mu_B H_{eff}$ the experimental frequency ω and the experimental effective field H_{eff} as given by the appropriate special case of Eq. (4), taking H to be the static magnetic field strength at the resonance maximum.[8] This definition of g involves the implicit assumption that the effective field equation is valid

[1] C. J. Gorter and B. Kahn, Physica **7**, 753–764 (1940).
[2] D. Polder, Phys. Rev. **73**, 1116 (1948); Phil. Mag. **40**, 99–115 (1949); see also the comments by J. H. Van Vleck, Physica **15**, 197–206 (1949).
[3] L. J. F. Broer, Physica **13**, 473–478 (1947).
[4] C. Kittel, Phys. Rev. **71**, 270–271 (1947); **73**, 155–161 (1948).
[5] J. H. Van Vleck, unpublished.
[6] J. M. Luttinger and C. Kittel, Helv. Phys. Acta **21**, 480–482 (1948).
[7] J. M. Richardson, Phys. Rev. **75**, 1630 (1949).
[8] It is supposed merely for ease in discussion that the crystalline anisotropy energy of the substance is zero; the effect of finite anisotropy is discussed in the author's 1948 paper. Professor J. H. Van Vleck has kindly pointed out that a term was neglected in Eq. (26) of the latter paper, so that Eq. (25b) should read

$$N_y' = (\tfrac{3}{2} + \tfrac{1}{2}\cos 4\theta)(K_1/M_s^2),$$

and the K_1 term in Eq. (27b) should be corrected similarly.

TABLE I. Comparison of representative experimental values of spectroscopic splitting factor (g) and magnetomechanical ratio. (g') for ferromagnetic substances.*

	Microwave resonance g	Gyromagnetic experiments g'
Iron	2.12–2.17	1.93
Cobalt	2.22	1.87
Nickel	2.19–2.42	1.92
Magnetite	2.20	1.93
Heusler alloy	2.01	2.00
Permalloy	2.07–2.14	1.91
Supermalloy	2.12–2.23	—

* The values of g' are taken from the summary by S. J. Barnett, Proc. Am. Acad. 75, 109 (1944). The values of g are based largely on J. H. E. Griffiths, reference 13, and unpublished data kindly communicated by Dr. Griffiths; also on various papers and unpublished measurements by W. A. Yager and his collaborators, to which detailed reference is made in the text. The value of g for magnetite is from L. R. Bickford, Jr., Phys. Rev. 76, 137 (1949). For Permalloy, g is from Kip and Arnold, reference 14.

under more general conditions that envisaged by any of the previous derivations of the effective field equation.[2,4–7] A more general derivation is given in Section IV.

In a gyromagnetic experiment one determines the change of magnetic moment resulting from a change of angular momentum, as in the Barnett experiment; or else one determines the change of angular momentum resulting from a change of magnetic moment, as in the Einstein-de Haas experiment. In either case we define the *magnetomechanical factor* g' by the equation

$$g'(e/2mc)=\Delta M/\Delta J, \tag{5}$$

where M is the magnetization and J is the angular momentum per unit volume. We shall require later the following more explicit statement of this relation. One actually observes the angular velocity (and, hence, the angular momentum) of the lattice of the specimen; because of conservation of angular momentum the change of angular momentum of the lattice ΔJ_{lat} is equal but opposite to the sum of the changes in the angular momenta* J_{spin} and J_{orb} associated with the spin and orbital motion of the atomic electrons:

$$\Delta J_{\text{lat}}=-\Delta(J_{\text{spin}}+J_{\text{orb}}). \tag{6}$$

We have supposed here that, unlike the microwave case, the changes of J_{spin} and J_{orb} are non-radiative, but proceed by relaxation effects entirely internal to the specimen. We now make the additional assumption that the magnetic moment associated with the rotation of the lattice may be neglected; this assumption may introduce fractional errors of the order of less than $m/M_H\approx 1/2000$; an error of this magnitude is not detectable with present experimental technique. Thus we may set

$$\Delta M=\Delta(M_{\text{spin}}+M_{\text{orb}}), \tag{7}$$

so that Eq. (5) becomes

$$g'\frac{e}{2mc}=\frac{\Delta(M_{\text{spin}}+M_{\text{orb}})}{\Delta(J_{\text{spin}}+J_{\text{orb}})}, \tag{8}$$

* For convenience in writing we shall imagine that we are always dealing with unit volume of material.

apart from questions of algebraic sign. We are omitting diamagnetic effects throughout.

Because the following sections of this paper are concerned largely with the differences which exist between g and g' it may be well here to prove that $g=g'$ for a solid in which the individual atoms are not subjected to any *non-central* electric fields from neighboring atoms in the solid: this amounts in effect to the assumption that the electrostatic field intensity caused by neighbors is zero over the volume of the atom under consideration. A consequence of this assumption is that the orbital and spin angular momenta are not coupled to the lattice, although the orbit and spin may be coupled to each other. We permit only a fictitious small coupling to the lattice in order to make possible the exchange of angular momentum between the electronic and lattice systems which occurs in the gyromagnetic experiments, but we neglect the momentum exchange in the microwave experiments. On the above model the resonance absorption effect will be described by the equation of motion

$$d(\mathbf{J}_{\text{spin}}+\mathbf{J}_{\text{orb}})/dt=(\mathbf{M}_{\text{spin}}+\mathbf{M}_{\text{orb}})\times\mathbf{H}; \tag{9}$$

on substituting Eq. (8), we have

$$d(\mathbf{M}_{\text{spin}}+\mathbf{M}_{\text{orb}})/dt=g'(e/2mc)(\mathbf{M}_{\text{spin}}+\mathbf{M}_{\text{orb}})\times\mathbf{H}, \tag{10}$$

which leads in the usual way to the resonance condition

$$\omega=g'(e/2mc)H_{\text{eff}}, \tag{11}$$

or

$$\hbar\omega=g'\mu_B H_{\text{eff}}; \tag{12}$$

this is identical with Eq. (1) if

$$g'=g. \tag{13}$$

We have thus shown that the spectroscopic splitting factor is equal to the magnetomechanical factor when the electronic angular momentum is not coupled to the crystal lattice. We shall show below that for numerous solid substances the electronic angular momentum is coupled to the lattice, and that to a good approximation one should in calculating the resonance condition omit J_{orb} from the left side of Eq. (9), while Eq. (8) is unaltered. In this situation g will no longer be equal to g', but we have (Eq. 37))

$$\frac{g'}{g}=\frac{J_{\text{spin}}}{J_{\text{spin}}+J_{\text{orb}}}, \tag{14}$$

which may be greater or less than unity depending on the sign of the spin-orbit coupling constant.

In some ways g is similar to the effective mass in the theory of metals; in both cases hidden momentum transfer processes are present and are important.

II. EXPERIMENTAL VALUES OF g AND g'

A summary of the results of experimental measurements of g and g' is given in Table I. It may be noted that $g>2$ and $g'<2$ in every instance except for Heusler

alloy, where $g \cong g' \cong 2.00$. A possible explanation of the unique position of Heusler alloy will be suggested in Section III. We now proceed to give a detailed discussion of certain fundamental aspects of the experimental results.

Shape Dependence of Effective Field Equation

Perhaps the most convincing test of Eq. (4) for the effective field is provided by a comparison of g-values from the parallel [Eq. (2)] and normal [Eq. (3)] field experiments, as first suggested to the author by Professor C. J. Gorter. The experiments were performed on Supermalloy at 1.25 cm by Kittel, Yager, and Merritt,[9] and resonance was obtained at the widely different field strengths of 4880 oersteds with the field parallel to the plane sample and 15,500 oersteds with the field normal to the sample; the corresponding g values as calculated using Eqs. (2) and (3) are

$$g_{\parallel}=2.17; \quad g_{\perp}=2.23.$$

These values are quite sensitive to the value of the saturation magnetization, and the uncertainty in this quantity may perhaps account for the small differences between $g_{\perp}$ and $g_{\parallel}$. Unpublished results of Yager on nickel at 1.25 cm give

$$g_{\parallel}=2.19\text{–}2.22; \quad g_{\perp}=2.26.$$

An additional but less critical test of the theory is furnished by the measurements of Hewitt[10] on two specimens of zinc-manganese ferrite, one a plane and the other a small sphere. Application of the appropriate effective field equations leads to

$$g_{\text{plane}}=2.12; \quad g_{\text{sphere}}=2.16.$$

Frequency Dependence

The clearest test of the frequency dependence of Eq. (1) is provided by Supermalloy. At 1.25 cm Yager and Bozorth,[11] and Yager,[12] find $g=2.17$. At 3 cm Yager finds, in unpublished work, $g=2.17$. The resonance in Supermalloy is exceptionally sharp; so that the agreement of the g-values at the two wave-lengths is quite a critical confirmation of the theory. For iron, the measurements of Griffiths[13] give $g=2.12$ at 1.25 cm and 2.03 at 3 cm, while for nickel the measurements give $g=2.27$ at 1.25 cm and 2.40 at 3 cm; here, however, the g-values are subject to considerable uncertainty because the resonance peaks are relatively wide. For Permalloy, Kip and Arnold[14] find $g=2.08\pm0.03$ at 3 cm and $g=2.12\pm0.03$ at 1.25 cm.

[9] Kittel, Yager, and Merritt, Amsterdam Conference on the Physics of Metals, 1948; Physica **15**, 256–257 (1949).
[10] W. H. Hewitt, Jr., Phys. Rev. **73**, 1118–1119 (1948).
[11] W. A. Yager and R. M. Bozorth, Phys. Rev. **72**, 80–81 (1947).
[12] W. A. Yager, Phys. Rev. **75**, 316–317 (1949).
[13] J. H. E. Griffiths, Nature **158**, 670 (1946).
[14] A. F. Kip and R. D. Arnold, R. L. E. Progress Report, M.I.T., October 15, 1948, pp. 31–32.

TABLE II. Comparison of g-values of paramagnetic salts from susceptibility measurements and from microwave resonance absorption measurements.

Substance	g (Susceptibility)	g (Resonance absorption)
$NiSiF_6 \cdot 6H_2O$	2.25[a]	2.29–2.36[b]
$NH_4Cr(SO_4)_2 \cdot 12H_2O$	1.98–2.00[a,d]	1.99[e,f]
$MnSO_4 \cdot 4H_2O$	1.99[g]	1.98[h]
$K_2Cu(SO_4)_2 \cdot 6H_2O$		
$\parallel$ axis	2.42[i]	2.42[j]
$\perp$ axis	2.05[i]	2.09[j]

[a] J. Becquerel and W. Opechowski, Physica **6**, 1039–1056 (1939).
[b] Holden, Kittel, and Yager, Phys. Rev. **75**, 1443 (1949).
[c] A. Serres, Ann. de physique **17**, 5 (1932).
[d] W. J. de Haas and C. J. Gorter, Proc. Amsterdam Acad. **33**, 676 (1930).
[e] Whitmer, Weidner, Hsiang, and Weiss, Phys. Rev. **74**, 1478–1484 (1948).
[f] Yager, Merritt, Holden, and Kittel, Phy. Rev. **75**, 1630 (1949).
[g] Kamerlingh Onnes and Oosterhuis, Comm., Leiden 129b.
[h] Cummerow, Halliday, and Moore, Phys. Rev. **72**, 1233–1240 (1947).
[i] D. Polder, Physica **9**, 709 (1942).
[j] R. D. Arnold and A. F. Kip, Phys. Rev. **75**, 1199–1205 (1949).

Temperature Dependence

The data on the temperature dependence of g are scanty. We have unpublished results of Yager on Supermalloy in the temperature range between liquid nitrogen (−196°C) and 300°C. The Curie point is about 400°C. The data on one sample suggests a very gradual increase in g from about 2.1 at −190°C to 2.17 at 300°C, but this conclusion is rather uncertain because of possible errors in the values of the saturation magnetization. For Permalloy, Kip and Arnold[14] find $g=2.14\pm0.075$ at room temperature, and $g=2.07\pm0.08$ at liquid nitrogen temperature.

III. ATOMIC MECHANISM RESULTING IN INEQUALITY OF g AND g'

We shall first give a calculation for a particular case in order to exhibit in as explicit a form as possible the mechanism by which one obtains $g \neq g'$. The calculation is given primarily with an educational motive: calculations based on similar principles but in a rather formal setting occur in the theory of paramagnetism and appear to have been given first by Schlapp and Penney.[15] In paramagnetic salts of the iron group it is quite often found that the observed susceptibilities lead to values of the Curie constant somewhat different from the Bose-Stoner "spin-only" values. The Curie constant is proportional to g^2, so that one may obtain values of g from susceptibility measurements, as well as from resonance absorption measurements. Table II gives a comparison of g-values obtained by these two methods, and it is seen that harmonious agreement prevails. Schlapp and Penney were concerned with the explanation of the departure of the susceptibility from the values predicted by the spin-only theory.

The mechanism by which one accounts for $g \neq g'$ in paramagnetic salts is rather special and unusual, and perhaps this aspect is not generally appreciated. It is a

[15] R. Schlapp and W. G. Penney, Phys. Rev. **42**, 666 (1932).

result of the combined effects of spin-orbit interaction and the crystalline electric field, but it does not occur in an important way for a crystalline field of purely cylindrical symmetry. Let us consider the behavior of an atom in a ^2F state in an electric field of cubic symmetry. It is supposed that the strength of the electric field is sufficient to destroy the coupling of the **L** vector to the **S** vector, but is not sufficient to destroy the Russell-Saunders coupling in which the individual **l** vectors form a resultant **L**. In a cubic field the seven orbital states split into groups of 1, 3, and 3; we suppose that the non-degenerate orbital state is lowest.** There is also the twofold spin degeneracy. We may take the zero-order ground state wave functions as

$$\Psi=(1/\sqrt{2})(\psi_2-\psi_{-2})\begin{pmatrix}\alpha\\ \beta\end{pmatrix}. \tag{15}$$

Here ψ_2 has $L=3$; $M_L=2$; α and β are the spin functions for $m_s=\pm\frac{1}{2}$. This combination may readily be seen to be satisfactory, since ψ_2 depends on angle as $z(x+iy)^2$ and ψ_{-2} as $z(x-iy)^2$; the combination $\psi_2-\psi_{-2}$ depends on angle as xyz, which is a one-dimensional representation of the cubic group and therefore meets our need for a non-degenerate orbital function with $L=3$. The combination,

$$(1/\sqrt{2})(\psi_2+\psi_{-2}),$$

belongs to one of the threefold degenerate orbital levels separated by an energy difference Δ from the ground state. The spin-orbit interaction operator

$$\lambda\mathbf{L}\cdot\mathbf{S}=\lambda\{L_zS_z+\tfrac{1}{2}(A_LB_S+B_LA_S)\}, \tag{16}$$

where A and B are the usual raising and lowering operators, mixes various upper states in with the ground state. It turns out that for our purposes only the λL_zS_z part of the operator is important. This mixes states of the same spin and produces first order effects on g and g'; the remaining terms in Eq. (16) give only second order effects, which may usually be neglected. A simple perturbation calculation gives

$$\Psi^\alpha=[(1/\sqrt{2})(\psi_2-\psi_{-2})+(\epsilon/\sqrt{2})(\psi_2+\psi_{-2})]\alpha, \tag{17}$$

and

$$\Psi^\beta=[(1/\sqrt{2})(\psi_2-\psi_{-2})-(\epsilon/\sqrt{2})(\psi_2+\psi_{-2})]\beta, \tag{18}$$

where $\epsilon=-\lambda/\Delta$, and Δ is the level separation in the crystal field. We have neglected terms which arise from the $A_LB_S+B_LA_S$ part of the spin-orbit operator, and also the ϵ^2 correction to the normalization factor.

It may be noted that

$$(\psi_2-\psi_{-2}|L_z|\psi_2-\psi_{-2})=0 \tag{19}$$

and

$$(\psi_2+\psi_{-2}|L_z|\psi_2+\psi_{-2})=0; \tag{20}$$

however,

$$(\Psi^\alpha|L_z|\Psi^\alpha)=4\epsilon, \tag{21}$$

$$(\Psi^\beta|L_z|\Psi^\beta)=-4\epsilon. \tag{22}$$

It is seen that the spin-orbit interaction is effective in endowing the ground states with an orbital angular momentum component because of interference effects between the $(\psi_2-\psi_{-2})$ and $(\psi_2+\psi_{-2})$ terms. An instructive way to understand the behavior of the wave functions is to write the orbital part of Eq. (17) as $2^{-\frac{1}{2}}[(1+\epsilon)\psi_2-(1-\epsilon)\psi_{-2}]$, which shows that the term ψ_2 with positive momentum outweighs the term ψ_{-2} which has negative momentum. The expectation values of the energy in a magnetic field are

$$(\Psi^\alpha|L+2S_z|\Psi^\alpha)\mu_BH=(1+4\epsilon)\mu_BH; \tag{23}$$

$$(\Psi^\beta|L_z+2S_z|\Psi^\beta)\mu_BH=-(1+4\epsilon)\mu_BH; \tag{24}$$

so that the energy difference is

$$\Delta E=\hbar\omega=2(1+4\epsilon)\mu_BH, \tag{25}$$

or

$$g=2(1+4\epsilon). \tag{26}$$

The magnetomechanical factor is

$$g'=\frac{(\Psi^\alpha|L_z+2S_z|\Psi^\alpha)}{(\Psi^\alpha|L_z+S_z|\Psi^\alpha)}=\frac{(1+4\epsilon)}{(\frac{1}{2}+4\epsilon)} \tag{27}$$

or, for $\epsilon\ll1$,

$$g'\cong2(1-4\epsilon). \tag{28}$$

Thus we have demonstrated for a particular case the mechanism by which g may be expected to be larger than two if g' is less than two. The relationship stated here was first pointed out in a general way by Gorter and Kahn, who give a comparison with experiment for the paramagnetic salts on which gyromagnetic measurements were made by Sucksmith.

The algebraic sign of $\epsilon(=-\lambda/\Delta)$ is opposite to the algebraic sign of the spin-orbit constant λ, since the splitting Δ is defined so as to be positive. Now λ is positive[16] for an electronic shell which is less than half full, and negative for a shell more than half-full. We then expect ϵ to be positive for paramagnetic salts containing Fe^{++}, Co^{++}, Ni^{++}, and Cu^{++} ions; and this conclusion is generally confirmed by experiment; ϵ also appears to be positive for the ferromagnetic metals Fe, Co and Ni, and their alloys. At Mn^{++} the $3d$ shell is approximately half-filled so that ϵ should be quite small, again in agreement with experiments on paramagnetic manganous salts. We have perhaps in this circumstance the explanation of the equality of g and g' for Heusler alloy (Cu_2AlMn), if we wish to consider manganous ions as the magnetic moment carriers in the alloy. It may be of interest to measure g-values in the Fe-Mn alloy system, and particularly in the ferromagnetic compounds of Mn and Cr, such as MnBi, MnP, CrTe, etc. In the mixed ferrites one might expect

** This assumption is made so that we may study the situation which occurs when the orbital momentum is quenched, in the zeroth-order approximation. Presumably in ferromagnetic materials the orbital momentum is quenched by exchange interactions if it is not quenched by the ordinary crystalline field.

[16] E. U. Condon and G. H. Shortley, *Theory of Atomic Spectra* (Cambridge University Press, New York, 1935), p. 210.

g to vary with composition, perhaps in a predictable way.

The translation of the example worked out in this section to an actual ferromagnetic metal offers very considerable difficulties because of the inadequacy of present treatments of the wave functions of $3d$ shell electrons in metals. The quenching of the orbital angular momentum may occur largely through exchange effects, as Van Vleck has suggested, rather than through crystal field effects. Brooks[17] has carried out a calculation of g on an itinerant electron model, according to which the quenching occurs by exchange effects, but his results are somewhat inconclusive. It does not appear to be practical to make more detailed calculations at present. It is well to emphasize that the $g \neq g'$ effect can be understood for paramagnetic salts, and in principle nothing fundamentally new appears to be added (apart from exchange quenching) on going to the metal; one adds only the grave computational difficulties associated with the breakdown of simple atomic coupling schemes.** There appears further to be a residual discrepancy, as for small departures from 2.00 one expects g to be as much larger than 2.00 as g' is smaller than 2.00. This relation is definitely not satisfied by the available data. Further theoretical consideration needs to be given to this discrepancy.

The experimental values of g may be used in breaking down the number of effective Bohr magnetons per atom into the separate contributions from spin and orbit.

It should be pointed out that there is no contradiction involved in having $g>2$ in a material for which the crystalline anisotropy energy may be zero, as in Supermalloy. This may be appreciated on the theory of anisotropy given by Brooks,[17] for example.

IV. MACROSCOPIC CONSEQUENCES OF ATOMIC MECHANISM

In the preceding section we have shown how an individual atomic system may have $g \neq g'$ as a consequence of incomplete quenching of the orbital angular momentum. We shall now discuss the effect on the macroscopic equations of motion, with the idea of justifying the use of the effective field equations which were originally derived for the central field case. In a magnetic dipole transition the z component of the total angular momentum of the system changes by $+\hbar$ in absorption:

$$\Delta J^z = +\hbar. \tag{29}$$

For wave functions of the form of Eqs. (17) and (18) which describe individual atomic systems,

$$\Delta J_{\text{spin}}{}^z = +\hbar \tag{30}$$

in absorption, and

$$\Delta J_{\text{orb}}{}^z = 4\epsilon\hbar. \tag{31}$$

Now by definition

$$\Delta J = \Delta J_{\text{spin}} + \Delta J_{\text{orb}} + \Delta J_{\text{lat}} \tag{32}$$

so that we must have

$$\Delta J_{\text{lat}}{}^z = -\Delta J_{\text{orb}}{}^z, \tag{33}$$

and, by symmetry, similar relations apply to the x and y components. That is, the model adopted for describing an individual atomic system leads to the conclusion that in a resonance absorption experiment the orbital angular momentum changes are neutralized by compensating changes in the lattice angular momentum. The latter could in principle be observed on a freely-suspended specimen, but is probably undetectable in practice. The accuracy of Eq. (33) is limited by only the neglect of terms in ϵ^2 as a consequency of the neglect of terms in β in the wave function Ψ^α.

The macroscopic equation of motion

$$\frac{d}{dt}(\mathbf{J}_{\text{spin}} + \mathbf{J}_{\text{orb}} + \mathbf{J}_{\text{lat}}) = (\mathbf{M}_{\text{spin}} + \mathbf{M}_{\text{orb}} + \mathbf{M}_{\text{lat}}) \times \mathbf{H} \tag{34}$$

reduces to

$$\frac{d}{dt}\mathbf{J}_{\text{spin}} = (\mathbf{M}_{\text{spin}} + \mathbf{M}_{\text{orb}}) \times \mathbf{H} \tag{35}$$

on application of Eq. (33) and neglecting M_{lat} as before. Eq. (35) leads to the resonance condition $\hbar\omega = g\mu_B H_{\text{eff}}$ if we set

$$g\frac{e}{2mc} = \frac{M_{\text{spin}} + M_{\text{orb}}}{J_{\text{spin}}}, \tag{36}$$

which is equivalent to the expression for g resulting from the microscopic calculation. The expression Eq. (4) for the effective field holds also for the present calculations. We have further

$$\frac{g'}{g} = \frac{J_{\text{spin}}}{J_{\text{spin}} + J_{\text{orb}}}. \tag{37}$$

We thus see that different combinations of momenta are involved in the Einstein-de Haas experiment, for which $\Delta J = 0$, and in the resonance absorption experiments, for which $\Delta J = \hbar$. The discussion of this section justifies the use of g, instead of g', in discussing resonance absorption on either classical or quantum equations of motion. In the gyromagnetic experiments direct spin lattice relaxation effects are important; we neglect relaxation effects in the discussion of microwave resonance, to the present approximation.

V. DISCUSSION OF OTHER EXPLANATIONS

In this paper we have supposed that the $g \neq g'$ effect is a real effect. Other authors have suggested that the effect is not real, but that the difference between g and

[17] H. Brooks, Phys. Rev. **58**, 909–918 (1940). In this reference g and g' are somewhat confused; g is actually calculated, although it is spoken of as if it were g'.

** It may be that the coupling schemes are simpler in the ferromagnetic oxides than in the metals; Néel has for example given an explanation of many properties of the ferrites on the basis of R-S coupling schemes.

g' is only apparent, being caused by experimental disturbances of various kinds.

Birks[18] has suggested that the resonance maximum is shifted by random anisotropy line shape distortion effects associated with the polycrystalline nature of the material. This hypothesis fails to account for the best-established high g-value in the field, that of Supermalloy, where the line width is very narrow. Birks supposed that rolling anisotropy was responsible for the high g-value of Supermalloy; unpublished measurements by Yager give too small a value of the rolling anisotropy for this supposition to be adequate. Deliberately cold-rolling Supermalloy broadened the resonance, but did not shift the position of the maximum,[12] contrary to the behavior predicted by Birks.

Rado[19] has suggested that a certain expression which occurs in the theory of the approach to magnetic saturation[20] in polycrystalline materials may be interpreted as an effective field for the purpose of ferromagnetic resonance. This identification is not justified, and leads to incorrect results, as may be confirmed by examining the simple limiting case of zero anisotropy; and also in the case of large H, where Rado proposes that $H=4\pi M_s/3$ be used in place of H in the effective field equations. The Lorentz term $(4\pi/3)M_s$ should not, however, be included in the effective field equation, as proved earlier.[4] On experimental grounds the fact that g appears to be independent of frequency to a fair accuracy in the case of Supermalloy may be cited against the Rado hypothesis. Further, the behavior of Heusler alloy would be quite anomalous on this hypothesis. W. F. Brown[21] has raised essentially the same objectives as we have here.

Griffiths[22] has obtained results on thin ferromagnetic films which indicate that g decreases as the films become thinner and approaches 2.00 for films below a critical thickness of the order of 0.5 micron. These results have not yet been satisfactorily explained, and it may be that the explanation is to be found in differences between the physical properties of actual thin films and the mathematical model of a thin film. The results at first sight may suggest that exchange force effects caused by non-uniform magnetization accompanying eddy-currents may play a significant part in the resonance process. Theoretical calculations by Polder[2] and by the author indicate that it is not to be expected that significant exchange effects enter for the eddy-current skin depths characteristic of existing measurements, although they may enter at very low temperatures in pure metals. Certainly the high g-values in the semiconducting ferrites cannot be ascribed to exchange-eddy current effects of this type. Further, the exchange effect would be accompanied by a line-broadening: the sharp line in Supermalloy therefore rules out a shift in the resonance maximum due to non-uniform magnetization.

ACKNOWLEDGMENTS

I wish to express my appreciation to W. A. Yager for permission to refer to his various unpublished measurements. I wish further to thank W. Shockley and S. O. Morgan for the encouragement and support which they have lent to the research activity on ferromagnetic resonance, and G. H. Wannier and P. W. Anderson for several stimulating discussions. J. H. Van Vleck and H. Brooks have kindly made a number of useful suggestions on the manuscript.

[18] J. B. Birks, Phys. Rev. **74**, 988 (1948). Birks' interpretation of his own data is somewhat questionable because of the presumably unknown shape effect of the individual particles in the wax compacts.

[19] G. T. Rado, Phys. Rev. **75**, 893–894 (1949).

[20] T. Holstein and H. Primakoff, Phys. Rev. **59**, 388–394 (1941); identical results were obtained independently by L. Néel, J. de Physique **9**, 193–199 (1948).

[21] W. F. Brown, Phys. Rev. **75**, 1959 (1949).

[22] J. H. E. Griffiths, Oxford Conference on Microwave Spectroscopy, July, 1948.

PHYSICAL REVIEW VOLUME 76, NUMBER 6 SEPTEMBER 15, 1949

The Theory of Positrons

R. P. FEYNMAN
Department of Physics, Cornell University, Ithaca, New York
(Received April 8, 1949)

The problem of the behavior of positrons and electrons in given external potentials, neglecting their mutual interaction, is analyzed by replacing the theory of holes by a reinterpretation of the solutions of the Dirac equation. It is possible to write down a complete solution of the problem in terms of boundary conditions on the wave function, and this solution contains automatically all the possibilities of virtual (and real) pair formation and annihilation together with the ordinary scattering processes, including the correct relative signs of the various terms.

In this solution, the "negative energy states" appear in a form which may be pictured (as by Stückelberg) in space-time as waves traveling away from the external potential backwards in time. Experimentally, such a wave corresponds to a positron approaching the potential and annihilating the electron. A particle moving forward in time (electron) in a potential may be scattered forward in time (ordinary scattering) or backward (pair annihilation). When moving backward (positron) it may be scattered backward in time (positron scattering) or forward (pair production). For such a particle the amplitude for transition from an initial to a final state is analyzed to any order in the potential by considering it to undergo a sequence of such scatterings.

The amplitude for a process involving many such particles is the product of the transition amplitudes for each particle. The exclusion principle requires that antisymmetric combinations of amplitudes be chosen for those complete processes which differ only by exchange of particles. It seems that a consistent interpretation is only possible if the exclusion principle is adopted. The exclusion principle need not be taken into account in intermediate states. Vacuum problems do not arise for charges which do not interact with one another, but these are analyzed nevertheless in anticipation of application to quantum electrodynamics.

The results are also expressed in momentum-energy variables. Equivalence to the second quantization theory of holes is proved in an appendix.

1. INTRODUCTION

THIS is the first of a set of papers dealing with the solution of problems in quantum electrodynamics. The main principle is to deal directly with the solutions to the Hamiltonian differential equations rather than with these equations themselves. Here we treat simply the motion of electrons and positrons in given external potentials. In a second paper we consider the interactions of these particles, that is, quantum electrodynamics.

The problem of charges in a fixed potential is usually treated by the method of second quantization of the electron field, using the ideas of the theory of holes. Instead we show that by a suitable choice and interpretation of the solutions of Dirac's equation the problem may be equally well treated in a manner which is fundamentally no more complicated than Schrödinger's method of dealing with one or more particles. The various creation and annihilation operators in the conventional electron field view are required because the number of particles is not conserved, i.e., pairs may be created or destroyed. On the other hand charge is conserved which suggests that if we follow the charge, not the particle, the results can be simplified.

In the approximation of classical relativistic theory the creation of an electron pair (electron A, positron B) might be represented by the start of two world lines from the point of creation, 1. The world lines of the positron will then continue until it annihilates another electron, C, at a world point 2. Between the times t_1 and t_2 there are then three world lines, before and after only one. However, the world lines of C, B, and A together form one continuous line albeit the "positron part" B of this continuous line is directed backwards in time. Following the charge rather than the particles corresponds to considering this continuous world line as a whole rather than breaking it up into its pieces. It is as though a bombardier flying low over a road suddenly sees three roads and it is only when two of them come together and disappear again that he realizes that he has simply passed over a long switchback in a single road.

This over-all space-time point of view leads to considerable simplification in many problems. One can take into account at the same time processes which ordinarily would have to be considered separately. For example, when considering the scattering of an electron by a potential one automatically takes into account the effects of virtual pair productions. The same equation, Dirac's, which describes the deflection of the world line of an electron in a field, can also describe the deflection (and in just as simple a manner) when it is large enough to reverse the time-sense of the world line, and thereby correspond to pair annihilation. Quantum mechanically the direction of the world lines is replaced by the direction of propagation of waves.

This view is quite different from that of the Hamiltonian method which considers the future as developing continuously from out of the past. Here we imagine the entire space-time history laid out, and that we just become aware of increasing portions of it successively. In a scattering problem this over-all view of the complete scattering process is similar to the S-matrix viewpoint of Heisenberg. The temporal order of events during the scattering, which is analyzed in such detail by the Hamiltonian differential equation, is irrelevant. The relation of these viewpoints will be discussed much more fully in the introduction to the second paper, in which the more complicated interactions are analyzed.

The development stemmed from the idea that in nonrelativistic quantum mechanics the amplitude for a given process can be considered as the sum of an ampli-

tude for each space-time path available.[1] In view of the fact that in classical physics positrons could be viewed as electrons proceeding along world lines toward the past (reference 7) the attempt was made to remove, in the relativistic case, the restriction that the paths must proceed always in one direction in time. It was discovered that the results could be even more easily understood from a more familiar physical viewpoint, that of scattered waves. This viewpoint is the one used in this paper. After the equations were worked out physically the proof of the equivalence to the second quantization theory was found.[2]

First we discuss the relation of the Hamiltonian differential equation to its solution, using for an example the Schrödinger equation. Next we deal in an analogous way with the Dirac equation and show how the solutions may be interpreted to apply to positrons. The interpretation seems not to be consistent unless the electrons obey the exclusion principle. (Charges obeying the Klein-Gordon equations can be described in an analogous manner, but here consistency apparently requires Bose statistics.)[3] A representation in momentum and energy variables which is useful for the calculation of matrix elements is described. A proof of the equivalence of the method to the theory of holes in second quantization is given in the Appendix.

2. GREEN'S FUNCTION TREATMENT OF SCHRÖDINGER'S EQUATION

We begin by a brief discussion of the relation of the non-relativistic wave equation to its solution. The ideas will then be extended to relativistic particles, satisfying Dirac's equation, and finally in the succeeding paper to interacting relativistic particles, that is, quantum electrodynamics.

The Schrödinger equation

$$i\partial\psi/\partial t=H\psi, \tag{1}$$

describes the change in the wave function ψ in an infinitesimal time Δt as due to the operation of an operator $\exp(-iH\Delta t)$. One can ask also, if $\psi(\mathbf{x}_1, t_1)$ is the wave function at $\mathbf{x}_1$ at time t_1, what is the wave function at time $t_2>t_1$? It can always be written as

$$\psi(\mathbf{x}_2, t_2)=\int K(\mathbf{x}_2, t_2; \mathbf{x}_1, t_1)\psi(\mathbf{x}_1, t_1)d^3\mathbf{x}_1, \tag{2}$$

where K is a Green's function for the linear Eq. (1). (We have limited ourselves to a single particle of coordinate $\mathbf{x}$, but the equations are obviously of greater generality.) If H is a constant operator having eigenvalues E_n, eigenfunctions ϕ_n so that $\psi(\mathbf{x}, t_1)$ can be expanded as $\sum_n C_n\phi_n(\mathbf{x})$, then $\psi(\mathbf{x}, t_2)=\exp(-iE_n(t_2-t_1))\times C_n\phi_n(\mathbf{x})$. Since $C_n=\int\phi_n^*(\mathbf{x}_1)\psi(\mathbf{x}_1, t_1)d^3\mathbf{x}_1$, one finds (where we write 1 for $\mathbf{x}_1$, t_1 and 2 for $\mathbf{x}_2$, t_2) in this case

$$K(2, 1)=\sum_n \phi_n(\mathbf{x}_2)\phi_n^*(\mathbf{x}_1)\exp(-iE_n(t_2-t_1)), \tag{3}$$

for $t_2>t_1$. We shall find it convenient for $t_2<t_1$ to define $K(2, 1)=0$ (Eq. (2) is then not valid for $t_2<t_1$). It is then readily shown that in general K can be defined by that solution of

$$(i\partial/\partial t_2-H_2)K(2, 1)=i\delta(2, 1), \tag{4}$$

which is zero for $t_2<t_1$, where $\delta(2, 1)=\delta(t_2-t_1)\delta(x_2-x_1)\times\delta(y_2-y_1)\delta(z_2-z_1)$ and the subscript 2 on H_2 means that the operator acts on the variables of 2 of $K(2, 1)$. When H is not constant, (2) and (4) are valid but K is less easy to evaluate than (3).[4]

We can call $K(2, 1)$ the total amplitude for arrival at $\mathbf{x}_2$, t_2 starting from $\mathbf{x}_1$, t_1. (It results from adding an amplitude, $\exp iS$, for each space time path between these points, where S is the action along the path.[1]) The transition amplitude for finding a particle in state $\chi(\mathbf{x}_2, t_2)$ at time t_2, if at t_1 it was in $\psi(\mathbf{x}_1, t_1)$, is

$$\int\chi^*(2)K(2, 1)\psi(1)d^3\mathbf{x}_1d^3\mathbf{x}_2. \tag{5}$$

A quantum mechanical system is described equally well by specifying the function K, or by specifying the Hamiltonian H from which it results. For some purposes the specification in terms of K is easier to use and visualize. We desire eventually to discuss quantum electrodynamics from this point of view.

To gain a greater familiarity with the K function and the point of view it suggests, we consider a simple perturbation problem. Imagine we have a particle in a weak potential $U(\mathbf{x}, t)$, a function of position and time. We wish to calculate $K(2, 1)$ if U differs from zero only for t between t_1 and t_2. We shall expand K in increasing powers of U:

$$K(2, 1)=K_0(2, 1)+K^{(1)}(2, 1)+K^{(2)}(2, 1)+\cdots. \tag{6}$$

To zero order in U, K is that for a free particle, $K_0(2, 1)$.[4] To study the first order correction $K^{(1)}(2, 1)$, first consider the case that U differs from zero only for the infinitesimal time interval Δt_3 between some time t_3 and $t_3+\Delta t_3(t_1<t_3<t_2)$. Then if $\psi(1)$ is the wave function at $\mathbf{x}_1$, t_1, the wave function at $\mathbf{x}_3$, t_3 is

$$\psi(3)=\int K_0(3, 1)\psi(1)d^3\mathbf{x}_1, \tag{7}$$

since from t_1 to t_3 the particle is free. For the short interval Δt_3 we solve (1) as

$$\psi(\mathbf{x}, t_3+\Delta t_3)=\exp(-iH\Delta t_3)\psi(\mathbf{x}, t_3)$$
$$=(1-iH_0\Delta t_3-iU\Delta t_3)\psi(\mathbf{x}, t_3),$$

[1] R. P. Feynman, Rev. Mod. Phys. **20**, 367 (1948).

[2] The equivalence of the entire procedure (including photon interactions) with the work of Schwinger and Tomonaga has been demonstrated by F. J. Dyson, Phys. Rev. **75**, 486 (1949).

[3] These are special examples of the general relation of spin and statistics deduced by W. Pauli, Phys. Rev. **58**, 716 (1940).

[4] For a non-relativistic free particle, where $\phi_n=\exp(i\mathbf{p}\cdot\mathbf{x})$, $E_n=\mathbf{p}^2/2m$, (3) gives, as is well known

$$K_0(2, 1)=\int\exp[-(i\mathbf{p}\cdot\mathbf{x}_1-i\mathbf{p}\cdot\mathbf{x}_2)-i\mathbf{p}^2(t_2-t_1)/2m]d^3\mathbf{p}(2\pi)^{-3}$$
$$=(2\pi im^{-1}(t_2-t_1))^{-\frac{1}{2}}\exp(\tfrac{1}{2}im(\mathbf{x}_2-\mathbf{x}_1)^2(t_2-t_1)^{-1})$$

for $t_2>t_1$, and $K_0=0$ for $t_2<t_1$.

where we put $H=H_0+U$, H_0 being the Hamiltonian of a free particle. Thus $\psi(\mathbf{x}, t_3+\Delta t_3)$ differs from what it would be if the potential were zero (namely $(1-iH_0\Delta t_3)\psi(\mathbf{x}, t_3)$) by the extra piece

$$\Delta\psi=-iU(\mathbf{x}_3, t_3)\cdot\psi(\mathbf{x}_3, t_3)\Delta t_3, \tag{8}$$

which we shall call the amplitude scattered by the potential. The wave function at 2 is given by

$$\psi(\mathbf{x}_2, t_2)=\int K_0(\mathbf{x}_2, t_2; \mathbf{x}_3, t_3+\Delta t_3)\psi(\mathbf{x}_3, t_3+\Delta t_3)d^3\mathbf{x}_3,$$

since after $t_3+\Delta t_3$ the particle is again free. Therefore the change in the wave function at 2 brought about by the potential is (substitute (7) into (8) and (8) into the equation for $\psi(\mathbf{x}_2, t_2)$):

$$\Delta\psi(2)=-i\int K_0(2, 3)U(3)K_0(3, 1)\psi(1)d^3\mathbf{x}_1d^3\mathbf{x}_3\Delta t_3.$$

In the case that the potential exists for an extended time, it may be looked upon as a sum of effects from each interval Δt_3 so that the total effect is obtained by integrating over t_3 as well as $\mathbf{x}_3$. From the definition (2) of K then, we find

$$K^{(1)}(2, 1)=-i\int K_0(2, 3)U(3)K_0(3, 1)d\tau_3, \tag{9}$$

where the integral can now be extended over all space and time, $d\tau_3=d^3\mathbf{x}_3dt_3$. Automatically there will be no contribution if t_3 is outside the range t_1 to t_2 because of our definition, $K_0(2, 1)=0$ for $t_2<t_1$.

We can understand the result (6), (9) this way. We can imagine that a particle travels as a free particle from point to point, but is scattered by the potential U. Thus the total amplitude for arrival at 2 from 1 can be considered as the sum of the amplitudes for various alternative routes. It may go directly from 1 to 2 (amplitude $K_0(2, 1)$, giving the zero order term in (6)). Or (see Fig. 1(a)) it may go from 1 to 3 (amplitude $K_0(3, 1)$), get scattered there by the potential (scattering amplitude $-iU(3)$ per unit volume and time) and then go from 3 to 2 (amplitude $K_0(2, 3)$). This may occur for any point 3 so that summing over these alternatives gives (9).

Again, it may be scattered twice by the potential (Fig. 1(b)). It goes from 1 to 3 ($K_0(3, 1)$), gets scattered there ($-iU(3)$) then proceeds to some other point, 4, in space time (amplitude $K_0(4, 3)$) is scattered again ($-iU(4)$) and then proceeds to 2 ($K_0(2, 4)$). Summing over all possible places and times for 3, 4 find that the second order contribution to the total amplitude $K^{(2)}(2, 1)$ is

$$(-i)^2\int\int K_0(2, 4)U(4)K_0(4, 3)\times U(3)K_0(3, 1)d\tau_3d\tau_4. \tag{10}$$

This can be readily verified directly from (1) just as (9) was. One can in this way obviously write down any of the terms of the expansion (6).[5]

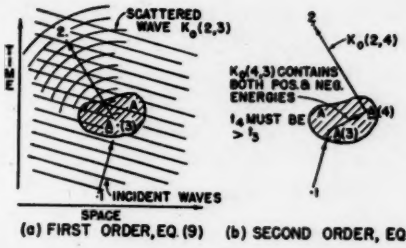

FIG. 1. The Schrödinger (and Dirac) equation can be visualized as describing the fact that plane waves are scattered successively by a potential. Figure 1 (a) illustrates the situation in first order. $K_0(2, 3)$ is the amplitude for a free particle starting at point 3 to arrive at 2. The shaded region indicates the presence of the potential A which scatters at 3 with amplitude $-iA(3)$ per cm³sec. (Eq. (9)). In (b) is illustrated the second order process (Eq. (10)), the waves scattered at 3 are scattered again at 4. However, in Dirac one-electron theory $K_0(4, 3)$ would represent electrons both of positive and of negative energies proceeding from 3 to 4. This is remedied by choosing a different scattering kernel $K_+(4, 3)$, Fig. 2.

3. TREATMENT OF THE DIRAC EQUATION

We shall now extend the method of the last section to apply to the Dirac equation. All that would seem to be necessary in the previous equations is to consider H as the Dirac Hamiltonian, ψ as a symbol with four indices (for each particle). Then K_0 can still be defined by (3) or (4) and is now a 4–4 matrix which operating on the initial wave function, gives the final wave function. In (10), $U(3)$ can be generalized to $A_4(3)-\boldsymbol{\alpha}\cdot\mathbf{A}(3)$ where A_4, $\mathbf{A}$ are the scalar and vector potential (times e, the electron charge) and $\boldsymbol{\alpha}$ are Dirac matrices.

To discuss this we shall define a convenient relativistic notation. We represent four-vectors like $\mathbf{x}$, t by a symbol x_μ, where $\mu=1, 2, 3, 4$ and $x_4=t$ is real. Thus the vector and scalar potential (times e) $\mathbf{A}$, A_4 is A_μ. The four matrices $\boldsymbol{\beta\alpha}$, $\boldsymbol{\beta}$ can be considered as transforming as a four vector γ_μ (our γ_μ differs from Pauli's by a factor i for $\mu=1, 2, 3$). We use the summation convention $a_\mu b_\mu=a_4b_4-a_1b_1-a_2b_2-a_3b_3=a\cdot b$. In particular if a_μ is any four vector (but not a matrix) we write $\boldsymbol{a}=a_\mu\gamma_\mu$ so that $\boldsymbol{a}$ is a matrix associated with a vector ($\boldsymbol{a}$ will often be used in place of a_μ as a symbol for the vector). The γ_μ satisfy $\gamma_\mu\gamma_\nu+\gamma_\nu\gamma_\mu=2\delta_{\mu\nu}$ where $\delta_{44}=+1$, $\delta_{11}=\delta_{22}=\delta_{33}=-1$, and the other $\delta_{\mu\nu}$ are zero. As a consequence of our summation convention $\delta_{\mu\nu}a_\nu=a_\mu$ and $\delta_{\mu\mu}=4$. Note that $\boldsymbol{ab}+\boldsymbol{ba}=2a\cdot b$ and that $\boldsymbol{a}^2=a_\mu a_\mu=a\cdot a$ is a pure number. The symbol $\partial/\partial x_\mu$ will mean $\partial/\partial t$ for $\mu=4$, and $-\partial/\partial x$, $-\partial/\partial y$, $-\partial/\partial z$ for $\mu=1, 2, 3$. Call $\nabla=\gamma_\mu\partial/\partial x_\mu=\boldsymbol{\beta}\partial/\partial t+\boldsymbol{\beta\alpha}\cdot\nabla$. We shall imagine

[5] We are simply solving by successive approximations an integral equation (deducible directly from (1) with $H=H_0+U$ and (4) with $H=H_0$),

$$\psi(2)=-i\int K_0(2, 3)U(3)\psi(3)d\tau_3+\int K_0(2, 1)\psi(1)d^3\mathbf{x}_1,$$

where the first integral extends over all space and all times t_3 greater than the t_1 appearing in the second term, and $t_2>t_1$.

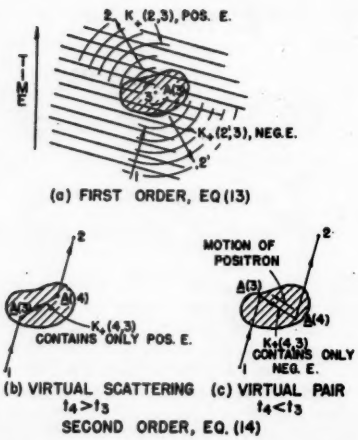

FIG. 2. The Dirac equation permits another solution $K_+(2, 1)$ if one considers that waves scattered by the potential can proceed backwards in time as in Fig. 2 (a). This is interpreted in the second order processes (b), (c), by noting that there is now the possibility (c) of virtual pair production at 4, the positron going to 3 to be annihilated. This can be pictured as similar to ordinary scattering (b) except that the electron is scattered backwards in time from 3 to 4. The waves scattered from 3 to 2′ in (a) represent the possibility of a positron arriving at 3 from 2′ and annihilating the electron from 1. This view is proved equivalent to hole theory: electrons traveling backwards in time are recognized as positrons.

hereafter, purely for relativistic convenience, that ϕ_n^* in (3) is replaced by its adjoint $\bar{\phi}_n=\phi_n^*\beta$.

Thus the Dirac equation for a particle, mass m, in an external field $A=A_\mu\gamma_\mu$ is

$$(i\nabla-m)\psi=A\psi, \tag{11}$$

and Eq. (4) determining the propagation of a free particle becomes

$$(i\nabla_2-m)K_+(2, 1)=i\delta(2, 1), \tag{12}$$

the index 2 on ∇_2 indicating differentiation with respect to the coordinates $x_{2\mu}$ which are represented as 2 in $K_+(2, 1)$ and $\delta(2, 1)$.

The function $K_+(2, 1)$ is defined in the absence of a field. If a potential A is acting a similar function, say $K_+^{(A)}(2, 1)$ can be defined. It differs from $K_+(2, 1)$ by a first order correction given by the analogue of (9) namely

$$K_+^{(1)}(2, 1)=-i\int K_+(2, 3)A(3)K_+(3, 1)d\tau_3, \tag{13}$$

representing the amplitude to go from 1 to 3 as a free particle, get scattered there by the potential (now the matrix $A(3)$ instead of $U(3)$) and continue to 2 as free. The second order correction, analogous to (10) is

$$K_+^{(2)}(2, 1)=-\int\int K_+(2, 4)A(4)\times K_+(4, 3)A(3)K_+(3, 1)d\tau_4 d\tau_3, \tag{14}$$

and so on. In general $K_+^{(A)}$ satisfies

$$(i\nabla_2-A(2)-m)K_+^{(A)}(2, 1)=i\delta(2, 1), \tag{15}$$

and the successive terms (13), (14) are the power series expansion of the integral equation

$$K_+^{(A)}(2, 1)=K_+(2, 1)-i\int K_+(2, 3)A(3)K_+^{(A)}(3, 1)d\tau_3, \tag{16}$$

which it also satisfies.

We would now expect to choose, for the special solution of (12), $K_+=K_0$ where $K_0(2, 1)$ vanishes for $t_2<t_1$ and for $t_2>t_1$ is given by (3) where ϕ_n and E_n are the eigenfunctions and energy values of a particle satisfying Dirac's equation, and ϕ_n^* is replaced by $\bar{\phi}_n$.

The formulas arising from this choice, however, suffer from the drawback that they apply to the one electron theory of Dirac rather than to the hole theory of the positron. For example, consider as in Fig. 1(a) an electron after being scattered by a potential in a small region 3 of space time. The one electron theory says (as does (3) with $K_+=K_0$) that the scattered amplitude at another point 2 will proceed toward positive times with both positive and negative energies, that is with both positive and negative rates of change of phase. No wave is scattered to times previous to the time of scattering. These are just the properties of $K_0(2, 3)$.

On the other hand, according to the positron theory negative energy states are not available to the electron after the scattering. Therefore the choice $K_+=K_0$ is unsatisfactory. But there are other solutions of (12). We shall choose the solution defining $K_+(2, 1)$ so that *$K_+(2, 1)$ for $t_2>t_1$ is the sum of (3) over positive energy states only.* Now this new solution must satisfy (12) for all times in order that the representation be complete. It must therefore differ from the old solution K_0 by a solution of the homogeneous Dirac equation. It is clear from the definition that the difference K_0-K_+ is the sum of (3) over all negative energy states, as long as $t_2>t_1$. But this difference must be a solution of the homogeneous Dirac equation for all times and must therefore be represented by the same sum over negative energy states also for $t_2<t_1$. Since $K_0=0$ in this case, it follows that our new kernel, *$K_+(2, 1)$, for $t_2<t_1$ is the negative of the sum (3) over negative energy states.* That is,

$$\begin{aligned} K_+(2, 1)&=\textstyle\sum_{POS\ E_n}\phi_n(2)\bar{\phi}_n(1)\times\exp(-iE_n(t_2-t_1)) \quad \text{for} \quad t_2>t_1 \\ &=-\textstyle\sum_{NEG\ E_n}\phi_n(2)\bar{\phi}_n(1)\times\exp(-iE_n(t_2-t_1)) \quad \text{for} \quad t_2<t_1. \end{aligned} \tag{17}$$

With this choice of K_+ our equations such as (13) and (14) will now give results equivalent to those of the positron hole theory.

That (14), for example, is the correct second order expression for finding at 2 an electron originally at 1 according to the positron theory may be seen as follows (Fig. 2). Assume as a special example that $t_2>t_1$ and that the potential vanishes except in interval t_2-t_1 so that t_4 and t_3 both lie between t_1 and t_2.

First suppose $t_4>t_3$ (Fig. 2(b)). Then (since $t_3>t_1$)

the electron assumed originally in a positive energy state propagates in that state (by $K_+(3, 1)$) to position 3 where it gets scattered ($A(3)$). It then proceeds to 4, which it must do as a positive energy electron. This is correctly described by (14) for $K_+(4, 3)$ contains only positive energy components in its expansion, as $t_4 > t_3$. After being scattered at 4 it then proceeds on to 2, again necessarily in a positive energy state, as $t_2 > t_4$.

In positron theory there is an additional contribution due to the possibility of virtual pair production (Fig. 2(c)). A pair could be created by the potential $A(4)$ at 4, the electron of which is that found later at 2. The positron (or rather, the hole) proceeds to 3 where it annihilates the electron which has arrived there from 1.

This alternative is already included in (14) as contributions for which $t_4 < t_3$, and its study will lead us to an interpretation of $K_+(4, 3)$ for $t_4 < t_3$. The factor $K_+(2, 4)$ describes the electron (after the pair production at 4) proceeding from 4 to 2. Likewise $K_+(3, 1)$ represents the electron proceeding from 1 to 3. $K_+(4, 3)$ must therefore represent the propagation of the positron or hole from 4 to 3. That it does so is clear. The fact that in hole theory the hole proceeds in the manner of and electron of negative energy is reflected in the fact that $K_+(4, 3)$ for $t_4 < t_3$ is (minus) the sum of only negative energy components. In hole theory the real energy of these intermediate states is, of course, positive. This is true here too, since in the phases $\exp(-iE_n(t_4 - t_3))$ defining $K_+(4, 3)$ in (17), E_n is negative but so is $t_4 - t_3$. That is, the contributions vary with t_3 as $\exp(-i|E_n|(t_3 - t_4))$ as they would if the energy of the intermediate state were $|E_n|$. The fact that the entire sum is taken as negative in computing $K_+(4, 3)$ is reflected in the fact that in hole theory the amplitude has its sign reversed in accordance with the Pauli principle and the fact that the electron arriving at 2 has been exchanged with one in the sea.[6] To this, and to higher orders, all processes involving virtual pairs are correctly described in this way.

The expressions such as (14) can still be described as a passage of the electron from 1 to 3 ($K_+(3, 1)$), scattering at 3 by $A(3)$, proceeding to 4 ($K_+(4, 3)$), scattering again, $A(4)$, arriving finally at 2. The scatterings may, however, be toward both future and past times, an electron propagating backwards in time being recognized as a positron.

This therefore suggests that negative energy components created by scattering in a potential be considered as waves propagating from the scattering point toward the past, and that such waves represent the propagation of a positron annihilating the electron in the potential.[7]

With this interpretation real pair production is also described correctly (see Fig. 3). For example in (13) if $t_1 < t_3 < t_2$ the equation gives the amplitude that if at time t_1 one electron is present at 1, then at time t_2 just one electron will be present (having been scattered at 3) and it will be at 2. On the other hand if t_2 is less than t_3, for example, if $t_2 = t_1 < t_3$, the same expression gives the amplitude that a pair, electron at 1, positron at 2 will annihilate at 3, and subsequently no particles will be present. Likewise if t_2 and t_1 exceed t_3 we have (minus) the amplitude for finding a single pair, electron at 2, positron at 1 created by $A(3)$ from a vacuum. If $t_1 > t_3 > t_2$, (13) describes the scattering of a positron. All these amplitudes are relative to the amplitude that a vacuum will remain a vacuum, which is taken as unity. (This will be discussed more fully later.)

The analogue of (2) can be easily worked out.[8] It is,

$$\psi(2) = \int K_+(2, 1) N(1) \psi(1) d^3V_1, \tag{18}$$

where d^3V_1 is the volume element of the closed 3-dimensional surface of a region of space time containing

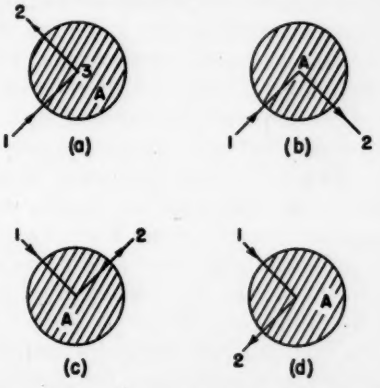

FIG. 3. Several different processes can be described by the same formula depending on the time relations of the variables t_2, t_1. Thus $P_s|K_+^{(A)}(2, 1)|^2$ is the probability that: (a) An electron at 1 will be scattered at 2 (and no other pairs form in vacuum). (b) Electron at 1 and positron at 2 annihilate leaving nothing. (c) A single pair at 1 and 2 is created from vacuum. (d) A positron at 2 is scattered to 1. ($K_+^{(A)}(2, 1)$ is the sum of the effects of scattering in the potential to all orders. P_s is a normalizing constant.)

[6] It has often been noted that the one-electron theory apparently gives the same matrix elements for this process as does hole theory. The problem is one of interpretation, especially in a way that will also give correct results for other processes, e.g., self-energy.

[7] The idea that positrons can be represented as electrons with proper time reversed relative to true time has been discussed by the author and others, particularly by Stückelberg. E. C. C. Stückelberg, Helv. Phys. Acta **15**, 23 (1942); R. P. Feynman, Phys. Rev. **74**, 939 (1948). The fact that classically the action (proper time) increases continuously as one follows a trajectory is reflected in quantum mechanics in the fact that the phase, which is $|E_n||t_2 - t_1|$, always increases as the particle proceeds from one scattering point to the next.

[8] By multiplying (12) on the right by $(-i\nabla_1 - m)$ and noting that $\nabla_1\delta(2, 1) = -\nabla_2\delta(2, 1)$ show that $K_+(2, 1)$ also satisfies $K_+(2, 1)(-i\nabla_1 - m) = i\delta(2, 1)$, where the ∇_1 operates on variable 1 in $K_+(2, 1)$ but is written after that function to keep the correct order of the γ matrices. Multiply this equation by $\psi(1)$ and Eq. (11) (with $A = 0$, calling the variables 1) by $K_+(2, 1)$, subtract and integrate over a region of space-time. The integral on the left-hand side can be transformed to an integral over the surface of the region. The right-hand side is $\psi(2)$ if the point 2 lies within the region, and is zero otherwise. (What happens when the 3-surface contains a light line and hence has no unique normal need not concern us as these points can be made to occur so far away from 2 that their contribution vanishes.)

point 2, and $N(1)$ is $N_\mu(1)\gamma_\mu$ where $N_\mu(1)$ is the *inward* drawn unit normal to the surface at the point 1. That is, the wave function $\psi(2)$ (in this case for a free particle) is determined at any point inside a four-dimensional region if its values on the surface of that region are specified.

To interpret this, consider the case that the 3-surface consists essentially of all space at some time say $t=0$ previous to t_2, and of all space at the time $T>t_2$. The cylinder connecting these to complete the closure of the surface may be very distant from $\mathbf{x}_2$ so that it gives no appreciable contribution (as $K_+(2,1)$ decreases exponentially in space-like directions). Hence, if $\gamma_4=\beta$, since the inward drawn normals N will be β and $-\beta$,

$$\psi(2)=\int K_+(2,1)\beta\psi(1)d^3\mathbf{x}_1 - \int K_+(2,1')\beta\psi(1')d^3\mathbf{x}_{1'}, \quad (19)$$

where $t_1=0$, $t_{1'}=T$. Only positive energy (electron) components in $\psi(1)$ contribute to the first integral and only negative energy (positron) components of $\psi(1')$ to the second. That is, the amplitude for finding a charge at 2 is determined both by the amplitude for finding an electron previous to the measurement and by the amplitude for finding a positron after the measurement. This might be interpreted as meaning that even in a problem involving but one charge the amplitude for finding the charge at 2 is not determined when the only thing known in the amplitude for finding an electron (or a positron) at an earlier time. There may have been no electron present initially but a pair was created in the measurement (or also by other external fields). The amplitude for this contingency is specified by the amplitude for finding a positron in the future.

We can also obtain expressions for transition amplitudes, like (5). For example if at $t=0$ we have an electron present in a state with (positive energy) wave function $f(\mathbf{x})$, what is the amplitude for finding it at $t=T$ with the (positive energy) wave function $g(\mathbf{x})$? The amplitude for finding the electron anywhere after $t=0$ is given by (19) with $\psi(1)$ replaced by $f(\mathbf{x})$, the second integral vanishing. Hence, the transition element to find it in state $g(\mathbf{x})$ is, in analogy to (5), just ($t_2=T$, $t_1=0$)

$$\int \bar{g}(\mathbf{x}_2)\beta K_+(2,1)\beta f(\mathbf{x}_1)d^3\mathbf{x}_1 d^3\mathbf{x}_2, \quad (20)$$

since $g^*=\bar{g}\beta$.

If a potential acts somewhere in the interval between 0 and T, K_+ is replaced by $K_+^{(A)}$. Thus the first order effect on the transition amplitude is, from (13),

$$-i\int \bar{g}(\mathbf{x}_2)\beta K_+(2,3)A(3)K_+(3,1)\beta f(\mathbf{x}_1)d^3\mathbf{x}_1 d^3\mathbf{x}_2. \quad (21)$$

Expressions such as this can be simplified and the 3-surface integrals, which are inconvenient for relativistic calculations, can be removed as follows. Instead of defining a state by the wave function $f(\mathbf{x})$, which it has at a given time $t_1=0$, we define the state by the function $f(1)$ of four variables $\mathbf{x}_1$, t_1 which is a solution of the free particle equation for all t_1 and is $f(\mathbf{x}_1)$ for $t_1=0$. The final state is likewise defined by a function $g(2)$ over-all space-time. Then our surface integrals can be performed since $\int K_+(3,1)\beta f(\mathbf{x}_1)d^3\mathbf{x}_1=f(3)$ and $\int \bar{g}(\mathbf{x}_2)\beta d^3\mathbf{x}_2 K_+(2,3)=\bar{g}(3)$. There results

$$-i\int \bar{g}(3)A(3)f(3)d\tau_3, \quad (22)$$

the integral now being over-all space-time. The transition amplitude to second order (from (14)) is

$$-\int\int \bar{g}(2)A(2)K_+(2,1)A(1)f(1)d\tau_1 d\tau_2, \quad (23)$$

for the particle arriving at 1 with amplitude $f(1)$ is scattered ($A(1)$), progresses to 2, ($K_+(2,1)$), and is scattered again ($A(2)$), and we then ask for the amplitude that it is in state $g(2)$. If $g(2)$ is a negative energy state we are solving a problem of annihilation of electron in $f(1)$, positron in $g(2)$, etc.

We have been emphasizing scattering problems, but obviously the motion in a fixed potential V, say in a hydrogen atom, can also be dealt with. If it is first viewed as a scattering problem we can ask for the amplitude, $\phi_k(1)$, that an electron with original free wave function was scattered k times in the potential V either forward or backward in time to arrive at 1. Then the amplitude after one more scattering is

$$\phi_{k+1}(2)=-i\int K_+(2,1)V(1)\phi_k(1)d\tau_1. \quad (24)$$

An equation for the total amplitude

$$\psi(1)=\sum_{k=0}^{\infty}\phi_k(1)$$

for arriving at 1 either directly or after any number of scatterings is obtained by summing (24) over all k from 0 to ∞;

$$\psi(2)=\phi_0(2)-i\int K_+(2,1)V(1)\psi(1)d\tau_1. \quad (25)$$

Viewed as a steady state problem we may wish, for example, to find that initial condition ϕ_0 (or better just the ψ) which leads to a periodic motion of ψ. This is most practically done, of course, by solving the Dirac equation,

$$(i\nabla-m)\psi(1)=V(1)\psi(1), \quad (26)$$

deduced from (25) by operating on both sides by $i\nabla_2-m$, thereby eliminating the ϕ_0, and using (12). This illustrates the relation between the points of view.

For many problems the total potential $A+V$ may be split conveniently into a fixed one, V, and another, A, considered as a perturbation. If $K_+^{(V)}$ is defined as in

(16) with V for A, expressions such as (23) are valid and useful with K_+ replaced by $K_+^{(V)}$ and the functions $f(1)$, $g(2)$ replaced by solutions for all space and time of the Dirac Eq. (26) in the potential V (rather than free particle wave functions).

4. PROBLEMS INVOLVING SEVERAL CHARGES

We wish next to consider the case that there are two (or more) distinct charges (in addition to pairs they may produce in virtual states). In a succeeding paper we discuss the interaction between such charges. Here we assume that they do not interact. In this case each particle behaves independently of the other. We can expect that if we have two particles a and b, the amplitude that particle a goes from $\mathbf{x}_1$ at t_1, to $\mathbf{x}_3$ at t_3 while b goes from $\mathbf{x}_2$ at t_2 to $\mathbf{x}_4$ at t_4 is the product

$$K(3,4;1,2)=K_{+a}(3,1)K_{+b}(4,2).$$

The symbols a, b simply indicate that the matrices appearing in the K_+ apply to the Dirac four component spinors corresponding to particle a or b respectively (the wave function now having 16 indices). In a potential K_{+a} and K_{+b} become $K_{+a}^{(A)}$ and $K_{+b}^{(A)}$ where $K_{+a}^{(A)}$ is defined and calculated as for a single particle. They commute. Hereafter the a, b can be omitted; the space time variable appearing in the kernels suffice to define on what they operate.

The particles are identical however and satisfy the exclusion principle. The principle requires only that one calculate $K(3,4;1,2)-K(4,3;1,2)$ to get the net amplitude for arrival of charges at 3, 4. (It is normalized assuming that when an integral is performed over points 3 and 4, for example, since the electrons represented are identical, one divides by 2.) This expression is correct for positrons also (Fig. 4). For example the amplitude that an electron and a positron found initially at $\mathbf{x}_1$ and $\mathbf{x}_4$ (say $t_1=t_4$) are later found at $\mathbf{x}_3$ and $\mathbf{x}_2$ (with $t_2=t_3>t_1$) is given by the same expression

$$K_+^{(A)}(3,1)K_+^{(A)}(4,2)-K_+^{(A)}(4,1)K_+^{(A)}(3,2). \quad (27)$$

The first term represents the amplitude that the electron proceeds from 1 to 3 and the positron from 4 to 2 (Fig. 4(c)), while the second term represents the interfering amplitude that the pair at 1, 4 annihilate and what is found at 3, 2 is a pair newly created in the potential. The generalization to several particles is clear. There is an additional factor $K_+^{(A)}$ for each particle, and antisymmetric combinations are always taken.

No account need be taken of the exclusion principle in intermediate states. As an example consider again expression (14) for $t_2>t_1$ and suppose $t_4<t_3$ so that the situation represented (Fig. 2(c)) is that a pair is made at 4 with the electron proceeding to 2, and the positron to 3 where it annihilates the electron arriving from 1. It may be objected that if it happens that the electron created at 4 is in the same state as the one coming from 1, then the process cannot occur because of the exclusion principle and we should not have included it in our term (14). We shall see, however, that considering the exclusion principle also requires another change which reinstates the quantity.

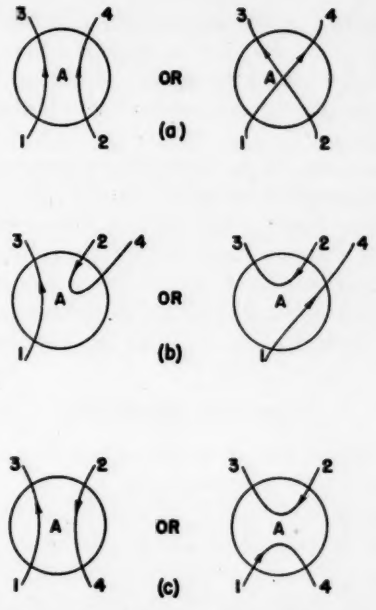

FIG. 4. Some problems involving two distinct charges (in addition to virtual pairs they may produce): $P_v|K_+^{(A)}(3,1)K_+^{(A)}(4,2)-K_+^{(A)}(4,1)K_+^{(A)}(3,2)|^2$ is the probability that: (a) Electrons at 1 and 2 are scattered to 3, 4 (and no pairs are formed). (b) Starting with an electron at 1 a single pair is formed, positron at 2, electrons at 3, 4. (c) A pair at 1, 4 is found at 3, 2, etc. The exclusion principle requires that the amplitudes for processes involving exchange of two electrons be subtracted.

For we are computing amplitudes relative to the amplitude that a vacuum at t_1 will still be a vacuum at t_2. We are interested in the alteration in this amplitude due to the presence of an electron at 1. Now one process that can be visualized as occurring in the vacuum is the creation of a pair at 4 followed by a re-annihilation of the *same* pair at 3 (a process which we shall call a closed loop path). But if a real electron is present in a certain state 1, those pairs for which the electron was created in state 1 in the vacuum must now be excluded. We must therefore subtract from our relative amplitude the term corresponding to this process. But this just reinstates the quantity which it was argued should not have been included in (14), the necessary minus sign coming automatically from the definition of K_+. It is obviously simpler to disregard the exclusion principle completely in the intermediate states.

All the amplitudes are relative and their squares give the relative probabilities of the various phenomena. Absolute probabilities result if one multiplies each of the probabilities by P_v, the true probability that if one has no particles present initially there will be none finally. This quantity P_v can be calculated by normalizing the relative probabilities such that the sum of the probabilities of all mutually exclusive alternatives is unity. (For example if one starts with a vacuum one can calculate the relative probability that there remains a

vacuum (unity), or one pair is created, or two pairs, etc. The sum is P_v^{-1}.) Put in this form the theory is complete and there are no divergence problems. Real processes are completely independent of what goes on in the vacuum.

When we come, in the succeeding paper, to deal with interactions between charges, however, the situation is not so simple. There is the possibility that virtual electrons in the vacuum may interact electromagnetically with the real electrons. For that reason processes occurring in the vacuum are analyzed in the next section, in which an independent method of obtaining P_v is discussed.

5. VACUUM PROBLEMS

An alternative way of obtaining absolute amplitudes is to multiply all amplitudes by C_v, the vacuum to vacuum amplitude, that is, the absolute amplitude that there be no particles both initially and finally. We can assume $C_v=1$ if no potential is present during the interval, and otherwise we compute it as follows. It differs from unity because, for example, a pair could be created which eventually annihilates itself again. Such a path would appear as a closed loop on a space-time diagram. The sum of the amplitudes resulting from all such single closed loops we call L. To a first approximation L is

$$L^{(1)}=-\frac{1}{2}\int\int Sp[K_+(2,1)A(1)\times K_+(1,2)A(2)]d\tau_1 d\tau_2. \quad (28)$$

For a pair could be created say at 1, the electron and positron could both go on to 2 and there annihilate. The spur, Sp, is taken since one has to sum over all possible spins for the pair. The factor $\frac{1}{2}$ arises from the fact that the same loop could be considered as starting at either potential, and the minus sign results since the interactors are each $-iA$. The next order term would be[9]

$$L^{(2)}=+(i/3)\int\int\int Sp[K_+(2,1)A(1)\times K_+(1,3)A(3)K_+(3,2)A(2)]d\tau_1 d\tau_2 d\tau_3,$$

etc. The sum of all such terms gives L.[10]

In addition to these single loops we have the possibility that two independent pairs may be created and each pair may annihilate itself again. That is, there may be formed in the vacuum two closed loops, and the contribution in amplitude from this alternative is just the product of the contribution from each of the loops considered singly. The total contribution from all such pairs of loops (it is still consistent to disregard the exclusion principle for these virtual states) is $L^2/2$ for in L^2 we count every pair of loops twice. The total vacuum-vacuum amplitude is then

$$C_v=1-L+L^2/2-L^3/6+\cdots=\exp(-L), \quad (30)$$

the successive terms representing the amplitude from zero, one, two, etc., loops. The fact that the contribution to C_v of single loops is $-L$ is a consequence of the Pauli principle. For example, consider a situation in which two pairs of particles are created. Then these pairs later destroy themselves so that we have two loops. The electrons could, at a given time, be interchanged forming a kind of figure eight which is a single loop. The fact that the interchange must change the sign of the contribution requires that the terms in C_v appear with alternate signs. (The exclusion principle is also responsible in a similar way for the fact that the amplitude for a pair creation is $-K_+$ rather than $+K_+$.) Symmetrical statistics would lead to

$$C_v=1+L+L^2/2=\exp(+L).$$

The quantity L has an infinite imaginary part (from $L^{(1)}$, higher orders are finite). We will discuss this in connection with vacuum polarization in the succeeding paper. This has no effect on the normalization constant for the probability that a vacuum remain vacuum is given by

$$P_v=|C_v|^2=\exp(-2\cdot\text{real part of } L),$$

from (30). This value agrees with the one calculated directly by renormalizing probabilities. The real part of L appears to be positive as a consequence of the Dirac equation and properties of K_+ so that P_v is less than one. Bose statistics gives $C_v=\exp(+L)$ and consequently a value of P_v greater than unity which appears meaningless if the quantities are interpreted as we have done here. Our choice of K_+ apparently requires the exclusion principle.

Charges obeying the Klein-Gordon equation can be equally well treated by the methods which are discussed here for the Dirac electrons. How this is done is discussed in more detail in the succeeding paper. The real part of L comes out negative for this equation so that in this case Bose statistics appear to be required for consistency.[3]

[9] This term actually vanishes as can be seen as follows. In any spur the sign of all γ matrices may be reversed. Reversing the sign of γ in $K_+(2,1)$ changes it to the transpose of $K_+(1,2)$ so that the order of all factors and variables is reversed. Since the integral is taken over all τ_1, τ_2, and τ_3 this has no effect and we are left with $(-1)^3$ from changing the sign of A. Thus the spur equals its negative. Loops with an odd number of potential interactors give zero. Physically this is because for each loop the electron can go around one way or in the opposite direction and we must add these amplitudes. But reversing the motion of an electron makes it behave like a positive charge thus changing the sign of each potential interaction, so that the sum is zero if the number of interactions is odd. This theorem is due to W. H. Furry, Phys. Rev. 51, 125 (1937).

[10] A closed expression for L in terms of $K_+^{(A)}$ is hard to obtain because of the factor $(1/n)$ in the nth term. However, the perturbation in L, ΔL due to a small change in potential ΔA, is easy to express. The $(1/n)$ is canceled by the fact that ΔA can appear in any of the n potentials. The result after summing over n by (13), (14) and using (16) is

$$\Delta L=-i\int Sp[(K_+^{(A)}(1,1)-K_+(1,1))\Delta A(1)]d\tau_1. \quad (29)$$

The term $K_+(1,1)$ actually integrates to zero.

6. ENERGY-MOMENTUM REPRESENTATION

The practical evaluation of the matrix elements in some problems is often simplified by working with momentum and energy variables rather than space and time. This is because the function $K_+(2,1)$ is fairly complicated but we shall find that its Fourier transform is very simple, namely $(i/4\pi^2)(\not p-m)^{-1}$ that is

$$K_+(2,1)=(i/4\pi^2)\int(\not p-m)^{-1}\exp(-ip\cdot x_{21})d^4p, \quad (31)$$

where $p\cdot x_{21}=p\cdot x_2-p\cdot x_1=p_\mu x_{2\mu}-p_\mu x_{1\mu}$, $\not p=p_\mu\gamma_\mu$, and d^4p means $(2\pi)^{-2}dp_1dp_2dp_3dp_4$, the integral over all p. That this is true can be seen immediately from (12), for the representation of the operator $i\nabla-m$ in energy (p_4) and momentum ($p_{1,2,3}$) space is $\not p-m$ and the transform of $\delta(2,1)$ is a constant. The reciprocal matrix $(\not p-m)^{-1}$ can be interpreted as $(\not p+m)(p^2-m^2)^{-1}$ for $p^2-m^2=(\not p-m)(\not p+m)$ is a pure number not involving γ matrices. Hence if one wishes one can write

$$K_+(2,1)=i(i\nabla_2+m)I_+(2,1),$$

where

$$I_+(2,1)=(2\pi)^{-2}\int(p^2-m^2)^{-1}\exp(-ip\cdot x_{21})d^4p, \quad (32)$$

is not a matrix operator but a function satisfying

$$\Box_2^2I_+(2,1)-m^2I_+(2,1)=\delta(2,1), \quad (33)$$

where $-\Box_2^2=(\nabla_2)^2=(\partial/\partial x_{2\mu})(\partial/\partial x_{2\mu})$.

The integrals (31) and (32) are not yet completely defined for there are poles in the integrand when $p^2-m^2=0$. We can define how these poles are to be evaluated by the rule that *m is considered to have an infinitesimal negative imaginary part.* That is m, is replaced by $m-i\delta$ and the limit taken as $\delta\to0$ from above. This can be seen by imagining that we calculate K_+ by integrating on p_4 first. If we call $E=+(m^2+p_1^2+p_2^2+p_3^2)^{\frac{1}{2}}$ then the integrals involve p_4 essentially as $\int\exp(-ip_4(t_2-t_1))dp_4(p_4^2-E^2)^{-1}$ which has poles at $p_4=+E$ and $p_4=-E$. The replacement of m by $m-i\delta$ means that E has a small negative imaginary part; the first pole is below, the second above the real axis. Now if $t_2-t_1>0$ the contour can be completed around the semicircle below the real axis thus giving a residue from the $p_4=+E$ pole, or $-(2E)^{-1}\exp(-iE(t_2-t_1))$. If $t_2-t_1<0$ the upper semicircle must be used, and $p_4=-E$ at the pole, so that the function varies in each case as required by the other definition (17).

Other solutions of (12) result from other prescriptions. For example if p_4 in the factor $(p^2-m^2)^{-1}$ is considered to have a positive imaginary part K_+ becomes replaced by K_0, the Dirac one-electron kernel, zero for $t_2<t_1$. Explicitly the function is[11] ($\mathbf{x}$, $t=x_{21\mu}$)

$$I_+(\mathbf{x},t)=-(4\pi)^{-1}\delta(s^2)+(m/8\pi s)H_1^{(2)}(ms), \quad (34)$$

where $s=+(t^2-\mathbf{x}^2)^{\frac{1}{2}}$ for $t^2>\mathbf{x}^2$ and $s=-i(x^2-t^2)^{\frac{1}{2}}$ for $t^2<x^2$, $H_1^{(2)}$ is the Hankel function and $\delta(s^2)$ is the Dirac delta function of s^2. It behaves asymptotically as $\exp(-ims)$, decaying exponentially in space-like directions.[12]

By means of such transforms the matrix elements like (22), (23) are easily worked out. A free particle wave function for an electron of momentum $\not p_1$ is $u_1\exp(-ip_1\cdot x)$ where u_1 is a constant spinor satisfying the Dirac equation $\not p_1u_1=mu_1$ so that $p_1^2=m^2$. The matrix element (22) for going from a state $\not p_1$, u_1 to a state of momentum $\not p_2$, spinor u_2, is $-4\pi^2i(\bar u_2\not a(q)u_1)$ where we have imagined $\mathbf{A}$ expanded in a Fourier integral

$$\mathbf{A}(1)=\int\mathbf{a}(q)\exp(-iq\cdot x_1)d^4q,$$

and we select the component of momentum $q=\not p_2-\not p_1$.

The second order term (23) is the matrix element between u_1 and u_2 of

$$-4\pi^2i\int(\not a(\not p_2-\not p_1-\not q))(\not p_1+\not q-m)^{-1}\not a(q)d^4q, \quad (35)$$

since the electron of momentum $\not p_1$ may pick up q from the potential $\not a(q)$, propagate with momentum $\not p_1+q$ (factor $(\not p_1+\not q-m)^{-1}$) until it is scattered again by the potential, $\not a(\not p_2-\not p_1-\not q)$, picking up the remaining momentum, $\not p_2-\not p_1-\not q$, to bring the total to $\not p_2$. Since all values of q are possible, one integrates over q.

These same matrices apply directly to positron problems, for if the time component of, say, $\not p_1$ is negative the state represents a positron of four-momentum $-\not p_1$, and we are describing pair production if $\not p_2$ is an electron, i.e., has positive time component, etc.

The probability of an event whose matrix element is $(\bar u_2Mu_1)$ is proportional to the absolute square. This may also be written $(\bar u_1\bar Mu_2)(\bar u_2Mu_1)$, where $\bar M$ is M with the operators written in opposite order and explicit appearance of i changed to $-i$ ($\bar M$ is β times the complex conjugate transpose of βM). For many problems we are not concerned about the spin of the final state. Then we can sum the probability over the two u_2 corresponding to the two spin directions. This is not a complete set because $\not p_2$ has another eigenvalue, $-m$. To permit summing over all states we can insert the projection operator $(2m)^{-1}(\not p_2+m)$ and so obtain $(2m)^{-1}(\bar u_1\bar M(\not p_2+m)Mu_1)$ for the probability of transition from $\not p_1$, u_1, to $\not p_2$ with arbitrary spin. If the incident state is unpolarized we can sum on its spins too, and obtain

$$(2m)^{-2}Sp[(\not p_1+m)\bar M(\not p_2+m)M] \quad (36)$$

for (twice) the probability that an electron of arbitrary spin with momentum $\not p_1$ will make transition to $\not p_2$. The expressions are all valid for positrons when $\not p$'s with

[11] $I_+(\mathbf{x},t)$ is $(2i)^{-1}(D_1(\mathbf{x},t)-iD(\mathbf{x},t))$ where D_1 and D are the functions defined by W. Pauli, Rev. Mod. Phys. 13, 203 (1941).

[12] If the $-i\delta$ is kept with m here too the function I_+ approaches zero for infinite positive and negative times. This may be useful in general analyses in avoiding complications from infinitely remote surfaces.

negative energies are inserted, and the situation interpreted in accordance with the timing relations discussed above. (We have used functions normalized to $(\bar{u}u)=1$ instead of the conventional $(\bar{u}\beta u)=(u^*u)=1$. On our scale $(\bar{u}\beta u)=$energy$/m$ so the probabilities must be corrected by the appropriate factors.)

The author has many people to thank for fruitful conversations about this subject, particularly H. A. Bethe and F. J. Dyson.

APPENDIX

a. Deduction from Second Quantization

In this section we shall show the equivalence of this theory with the hole theory of the positron.[2] According to the theory of second quantization of the electron field in a given potential,[13] the state of this field at any time is represented by a wave function χ satisfying

$$i\partial\chi/\partial t=H\chi,$$

where $H=\int\Psi^*(\mathbf{x})(\boldsymbol{\alpha}\cdot(-i\boldsymbol{\nabla}-\mathbf{A})+A_4+m\beta)\Psi(\mathbf{x})d^3\mathbf{x}$ and $\Psi(\mathbf{x})$ is an operator annihilating an electron at position $\mathbf{x}$, while $\Psi^*(\mathbf{x})$ is the corresponding creation operator. We contemplate a situation in which at $t=0$ we have present some electrons in states represented by ordinary spinor functions $f_1(\mathbf{x})$, $f_2(\mathbf{x})$, $\cdots$ assumed orthogonal, and some positrons. These are described as holes in the negative energy sea, the electrons which would normally fill the holes having wave functions $p_1(\mathbf{x})$, $p_2(\mathbf{x})$, $\cdots$. We ask, at time T what is the amplitude that we find electrons in states $g_1(\mathbf{x})$, $g_2(\mathbf{x})$, $\cdots$ and holes at $q_1(\mathbf{x})$, $q_2(\mathbf{x})$, $\cdots$. If the initial and final state vectors representing this situation are χ_i and χ_f respectively, we wish to calculate the matrix element

$$R=\left(\chi_f^*\exp\left(-i\int_0^T H dt\right)\chi_i\right)=(\chi_f^*S\chi_i). \tag{37}$$

We assume that the potential A differs from zero only for times between 0 and T so that a vacuum can be defined at these times. If χ_0 represents the vacuum state (that is, all negative energy states filled, all positive energies empty), the amplitude for having a vacuum at time T, if we had one at $t=0$, is

$$C_v=(\chi_0^*S\chi_0), \tag{38}$$

writing S for $\exp(-i\int_0^T Hdt)$. Our problem is to evaluate R and show that it is a simple factor times C_v, and that the factor involves the $K_+^{(A)}$ functions in the way discussed in the previous sections.

To do this we first express χ_i in terms of χ_0. The operator

$$\Phi^*=\int\Psi^*(\mathbf{x})\phi(\mathbf{x})d^3\mathbf{x}, \tag{39}$$

creates an electron with wave function $\phi(\mathbf{x})$. Likewise $\Phi=\int\phi^*(\mathbf{x})\Psi(\mathbf{x})d^3\mathbf{x}$ annihilates one with wave function $\phi(\mathbf{x})$. Hence state χ_i is $\chi_i=F_1^*F_2^*\cdots P_1P_2\cdots\chi_0$ while the final state is $G_1^*G_2^*\cdots Q_1Q_2\cdots\chi_0$ where F_i, G_i, P_i, Q_i are operators defined like Φ, in (39), but with f_i, g_i, p_i, q_i replacing ϕ; for the initial state would result from the vacuum if we created the electrons in f_1, f_2, $\cdots$ and annihilated those in p_1, p_2, $\cdots$. Hence we must find

$$R=(\chi_0^*\cdots Q_2^*Q_1^*\cdots G_2G_1SF_1^*F_2^*\cdots P_1P_2\cdots\chi_0). \tag{40}$$

To simplify this we shall have to use commutation relations between a Φ^* operator and S. To this end consider $\exp(-i\int_0^t Hdt')\Phi^*\times\exp(+i\int_0^t Hdt')$ and expand this quantity in terms of $\Psi^*(\mathbf{x})$, giving $\int\Psi^*(\mathbf{x})\phi(\mathbf{x},t)d^3\mathbf{x}$, (which defines $\phi(\mathbf{x},t)$). Now multiply this equation by $\exp(+i\int_0^t Hdt')\cdots\exp(-i\int_0^t Hdt')$ and find

$$\int\Psi^*(\mathbf{x})\phi(\mathbf{x})d^3\mathbf{x}=\int\Psi^*(\mathbf{x},t)\phi(\mathbf{x},t)d^3\mathbf{x}, \tag{41}$$

where we have defined $\Psi(\mathbf{x},t)$ by $\Psi(\mathbf{x},t)=\exp(+i\int_0^t Hdt')\Psi(\mathbf{x})\times\exp(-i\int_0^t Hdt')$. As is well known $\Psi(\mathbf{x},t)$ satisfies the Dirac equation, (differentiate $\Psi(\mathbf{x},t)$ with respect to t and use commutation relations of H and Ψ)

$$i\partial\Psi(\mathbf{x},t)/\partial t=(\boldsymbol{\alpha}\cdot(-i\boldsymbol{\nabla}-\mathbf{A})+A_4+m\beta)\Psi(\mathbf{x},t). \tag{42}$$

Consequently $\phi(\mathbf{x},t)$ must also satisfy the Dirac equation (differentiate (41) with respect to t, use (42) and integrate by parts).

That is, if $\phi(\mathbf{x},T)$ is that solution of the Dirac equation at time T which is $\phi(\mathbf{x})$ at $t=0$, and if we define $\Phi^*=\int\Psi^*(\mathbf{x})\phi(\mathbf{x})d^3\mathbf{x}$ and $\Phi'^*=\int\Psi^*(\mathbf{x})\phi(\mathbf{x},T)d^3\mathbf{x}$ then $\Phi'^*=S\Phi^*S^{-1}$, or

$$S\Phi^*=\Phi'^*S. \tag{43}$$

The principle on which the proof will be based can now be illustrated by a simple example. Suppose we have just one electron initially and finally and ask for

$$r=(\chi_0^*GSF^*\chi_0). \tag{44}$$

We might try putting F^* through the operator S using (43), $SF^*=F'^*S$, where f' in $F'^*=\int\Psi^*(\mathbf{x})f'(\mathbf{x})d^3\mathbf{x}$ is the wave function at T arising from $f(\mathbf{x})$ at 0. Then

$$r=(\chi_0^*GF'^*S\chi_0)=\int g^*(\mathbf{x})f'(\mathbf{x})d^3\mathbf{x}\cdot C_v-(\chi_0^*F'^*GS\chi_0), \tag{45}$$

where the second expression has been obtained by use of the definition (38) of C_v and the general commutation relation

$$GF^*+F^*G=\int g^*(\mathbf{x})f(\mathbf{x})d^3\mathbf{x},$$

which is a consequence of the properties of $\Psi(\mathbf{x})$ (the others are $FG=-GF$ and $F^*G^*=-G^*F^*$). Now $\chi_0^*F'^*$ in the last term in (45) is the complex conjugate of $F'\chi_0$. Thus if f' contained only positive energy components, $F'\chi_0$ would vanish and we would have reduced r to a factor times C_v. But F', as worked out here, does contain negative energy components created in the potential A and the method must be slightly modified.

Before putting F^* through the operator we shall add to it another operator F''^* arising from a function $f''(x)$ containing *only negative* energy components and so chosen that the resulting f' has *only positive* ones. That is we want

$$S(F_{\text{pos}}^*+F_{\text{neg}}''^*)=F_{\text{pos}}'^*S, \tag{46}$$

where the "pos" and "neg" serve as reminders of the sign of the energy components contained in the operators. This we can now use in the form

$$SF_{\text{pos}}^*=F_{\text{pos}}'^*S-SF_{\text{neg}}''^*. \tag{47}$$

In our one electron problem this substitution replaces r by two terms

$$r=(\chi_0^*GF_{\text{pos}}'^*S\chi_0)-(\chi_0^*GSF_{\text{neg}}''^*\chi_0).$$

The first of these reduces to

$$r=\int g^*(\mathbf{x})f_{\text{pos}}'(\mathbf{x})d^3\mathbf{x}\cdot C_v,$$

as above, for $F_{\text{pos}}'\chi_0$ is now zero, while the second is zero since the creation operator $F_{\text{neg}}''^*$ gives zero when acting on the vacuum state as all negative energies are full. This is the central idea of the demonstration.

The problem presented by (46) is this: Given a function $f_{\text{pos}}(\mathbf{x})$ at time 0, to find the amount, f_{neg}'', of negative energy component which must be added in order that the solution of Dirac's equation at time T will have only positive energy components, f_{pos}'. This is a boundary value problem for which the kernel $K_+^{(A)}$ is designed. We know the positive energy components initially, f_{pos}, and the negative ones finally (zero). The positive ones finally are therefore (using (19))

$$f_{\text{pos}}'(\mathbf{x}_2)=\int K_+^{(A)}(2,1)\beta f_{\text{pos}}(\mathbf{x}_1)d^3\mathbf{x}_1, \tag{48}$$

where $t_2=T$, $t_1=0$. Similarly, the negative ones initially are

$$f_{\text{neg}}''(\mathbf{x}_2)=\int K_+^{(A)}(2,1)\beta f_{\text{pos}}(\mathbf{x}_1)d^3\mathbf{x}_1-f_{\text{pos}}(\mathbf{x}_2), \tag{49}$$

where t_2 approaches zero from above, and $t_1=0$. The $f_{\text{pos}}(\mathbf{x}_2)$ is

[13] See, for example, G. Wentzel, *Einfuhrung in die Quantentheorie der Wellenfelder* (Franz Deuticke, Leipzig, 1943), Chapter V.

subtracted to keep in $f_{neg}''(\mathbf{x}_2)$ only those waves which return from the potential and not those arriving directly at t_2 from the $K_+(2,1)$ part of $K_+^{(A)}(2,1)$, as $t_2 \to 0$. We could also have written

$$f_{neg}''(\mathbf{x}_2) = \int [K_+^{(A)}(2,1) - K_+(2,1)] \beta f_{pos}(\mathbf{x}_1) d^3\mathbf{x}_1. \quad (50)$$

Therefore the one-electron problem, $r = \int g^*(\mathbf{x}) f_{pos}'(\mathbf{x}) d^3\mathbf{x} \cdot C_v$, gives by (48)

$$r = C_v \int g^*(\mathbf{x}_2) K_+^{(A)}(2,1) \beta f(\mathbf{x}_1) d^3\mathbf{x}_1 d^3\mathbf{x}_2,$$

as expected in accordance with the reasoning of the previous sections (i.e., (20) with $K_+^{(A)}$ replacing K_+).

The proof is readily extended to the more general expression R, (40), which can be analyzed by induction. First one replaces F_1^* by a relation such as (47) obtaining two terms

$$R = (\chi_0^* \cdots Q_2^* Q_1^* \cdots G_2 G_1 F_{1pos}'^* S F_2^* \cdots P_1 P_2 \cdots \chi_0) - (\chi_0^* \cdots Q_2^* Q_1^* \cdots G_2 G_1 S F_{1neg}''^* F_2^* \cdots P_1 P_2 \cdots \chi_0).$$

In the first term the order of $F_{1pos}'^*$ and G_1 is then interchanged, producing an additional term $\int g_1^*(\mathbf{x}) f_{1pos}'(\mathbf{x}) d^3\mathbf{x}$ times an expression with one less electron in initial and final state. Next it is exchanged with G_2 producing an addition $-\int g_2^*(\mathbf{x}) f_{1pos}'(\mathbf{x}) d^3\mathbf{x}$ times a similar term, etc. Finally on reaching the Q_1^* with which it anticommutes it can be simply moved over to juxtaposition with χ_0^* where it gives zero. The second term is similarly handled by moving $F_{1neg}''^*$ through anti commuting F_2^*, etc., until it reaches P_1. Then it is exchanged with P_1 to produce an additional simpler term with a factor $\mp \int p_1^*(\mathbf{x}) f_{1neg}''(\mathbf{x}) d^3\mathbf{x}$ or $\mp \int p_1^*(\mathbf{x}_2) K_+^{(A)}(2,1) \beta f_1(\mathbf{x}_1) d^3\mathbf{x}_1 d^3\mathbf{x}_2$ from (49), with $t_2 = t_1 = 0$ (the extra $f_1(\mathbf{x}_2)$ in (49) gives zero as it is orthogonal to $p_1(\mathbf{x}_2)$). This describes in the expected manner the annihilation of the pair, electron f_1, positron p_1. The $F_{neg}''^*$ is moved in this way successively through the P's until it gives zero when acting on χ_0. Thus R is reduced, with the expected factors (and with alternating signs as required by the exclusion principle), to simpler terms containing two less operators which may in turn be further reduced by using F_2^* in a similar manner, etc. After all the F^* are used the Q^*'s can be reduced in a similar manner. They are moved through the S in the opposite direction in such a manner as to produce a purely negative energy operator at time 0, using relations analogous to (46) to (49). After all this is done we are left simply with the expected factor times C_v (assuming the net charge is the same in initial and final state.)

In this way we have written the solution to the general problem of the motion of electrons in given potentials. The factor C_v is obtained by normalization. However for photon fields it is desirable to have an explicit form for C_v in terms of the potentials. This is given by (30) and (29) and it is readily demonstrated that this also is correct according to second quantization.

b. Analysis of the Vacuum Problem

We shall calculate C_v from second quantization by induction considering a series of problems each containing a potential distribution more nearly like the one we wish. Suppose we know C_v for a problem like the one we want and having the same potentials for time t between some t_0 and T, but having potential zero for times from 0 to t_0. Call this $C_v(t_0)$, the corresponding Hamiltonian H_{t_0} and the sum of contributions for all single loops, $L(t_0)$. Then for $t_0 = T$ we have zero potential at all times, no pairs can be produced, $L(T) = 0$ and $C_v(T) = 1$. For $t_0 = 0$ we have the complete problem, so that $C_v(0)$ is what is defined as C_v in (38). Generally we have,

$$C_v(t_0) = \left(\chi_0^* \exp\left(-i\int_0^T H_{t_0} dt\right)\chi_0\right) = \left(\chi_0^* \exp\left(-i\int_{t_0}^T H_{t_0} dt\right)\chi_0\right),$$

since H_{t_0} is identical to the constant vacuum Hamiltonian H_T for $t < t_0$ and χ_0 is an eigenfunction of H_T with an eigenvalue (energy of vacuum) which we can take as zero.

The value of $C_v(t_0 - \Delta t_0)$ arises from the Hamiltonian $H_{t_0 - \Delta t_0}$ which differs from H_{t_0} just by having an extra potential during the short interval Δt_0. Hence, to first order in Δt_0, we have

$$C_v(t_0 - \Delta t_0) = \left(\chi_0^* \exp\left(-i\int_{t_0 - \Delta t_0}^T H_{t_0 - \Delta t_0} dt\right)\chi_0\right) = \left(\chi_0^* \exp\left(-i\int_{t_0}^T H_{t_0} dt\right)\left[1 - i\Delta t_0 \int \Psi^*(\mathbf{x}) \times (-\boldsymbol{\alpha} \cdot \mathbf{A}(\mathbf{x}, t_0) + A_4(\mathbf{x}, t_0))\Psi(\mathbf{x}) d^3\mathbf{x}\right]\chi_0\right);$$

we therefore obtain for the derivative of C_v the expression

$$-dC_v(t_0)/dt_0 = -i\left(\chi_0^* \exp\left(-i\int_{t_0}^T H_{t_0} dt\right) \times \int \Psi^*(\mathbf{x}) \beta A(\mathbf{x}, t_0) \Psi(\mathbf{x}) d^3\mathbf{x} \chi_0\right), \quad (51)$$

which will be reduced to a simple factor times $C_v(t_0)$ by methods analogous to those used in reducing R. The operator Ψ can be imagined to be split into two pieces Ψ_{pos} and Ψ_{neg} operating on positive and negative energy states respectively. The Ψ_{pos} on χ_0 gives zero so we are left with two terms in the current density, $\Psi_{pos}^* \boldsymbol{\beta A} \Psi_{neg}$ and $\Psi_{neg}^* \boldsymbol{\beta A} \Psi_{neg}$. The latter $\Psi_{neg}^* \boldsymbol{\beta A} \Psi_{neg}$ is just the expectation value of $\boldsymbol{\beta A}$ taken over all negative energy states (minus $\Psi_{neg} \boldsymbol{\beta A} \Psi_{neg}^*$ which gives zero acting on χ_0). This is the effect of the vacuum expectation current of the electrons in the sea which we should have subtracted from our original Hamiltonian in the customary way.

The remaining term $\Psi_{pos}^* \boldsymbol{\beta A} \Psi_{neg}$, or its equivalent $\Psi_{pos}^* \boldsymbol{\beta A} \Psi$ can be considered as $\Psi^*(\mathbf{x}) \mathbf{f}_{pos}(\mathbf{x})$ where $\mathbf{f}_{pos}(\mathbf{x})$ is written for the positive energy component of the operator $\boldsymbol{\beta A} \Psi(\mathbf{x})$. Now this operator, $\Psi^*(\mathbf{x}) \mathbf{f}_{pos}(\mathbf{x})$, or more precisely just the $\Psi^*(\mathbf{x})$ part of it, can be pushed through the $\exp(-i\int_{t_0}^T H dt)$ in a manner exactly analogous to (47) when f is a function. (An alternative derivation results from the consideration that the operator $\Psi(\mathbf{x}, t)$ which satisfies the Dirac equation also satisfies the linear integral equations which are equivalent to it.) That is, (51) can be written by (48), (50),

$$-dC_v(t_0)/dt_0 = -i\left(\chi_0^* \int\int \Psi^*(\mathbf{x}_2) K_+^{(A)}(2,1) \times \exp\left(-i\int_{t_0}^T H dt\right) \boldsymbol{A}(1) \Psi(\mathbf{x}_1) d^3\mathbf{x}_1 d^3\mathbf{x}_2 \chi_0\right) + i\left(\chi_0^* \exp\left(-i\int_{t_0}^T H dt\right) \int\int \Psi^*(\mathbf{x}_2) [K_+^{(A)}(2,1) - K_+(2,1)] \boldsymbol{A}(1) \Psi(\mathbf{x}_1) d^3\mathbf{x}_1 d^3\mathbf{x}_2 \chi_0\right),$$

where in the first term $t_2 = T$, and in the second $t_2 \to t_0 = t_1$. The (A) in $K_+^{(A)}$ refers to that part of the potential $\boldsymbol{A}$ after t_0. The first term vanishes for it involves (from the $K_+^{(A)}(2,1)$) only positive energy components of Ψ^*, which give zero operating into χ_0^*. In the second term only negative components of $\Psi^*(\mathbf{x}_2)$ appear. If, then $\Psi^*(\mathbf{x}_2)$ is interchanged in order with $\Psi(\mathbf{x}_1)$ it will give zero operating on χ_0, and only the term,

$$-dC_v(t_0)/dt_0 = +i\int Sp[(K_+^{(A)}(1,1) - K_+(1,1))\boldsymbol{A}(1)] d^3\mathbf{x}_1 \cdot C_v(t_0), \quad (52)$$

will remain, from the usual commutation relation of Ψ^* and Ψ.

The factor of $C_v(t_0)$ in (52) times $-\Delta t_0$ is, according to (29) (reference 10), just $L(t_0 - \Delta t_0) - L(t_0)$ since this difference arises from the extra potential $\Delta \boldsymbol{A} = \boldsymbol{A}$ during the short time interval Δt_0. Hence $-dC_v(t_0)/dt_0 = +(dL(t_0)/dt_0) C_v(t_0)$ so that integration from $t_0 = T$ to $t_0 = 0$ establishes (30).

Starting from the theory of the electromagnetic field in second quantization, a deduction of the equations for quantum electrodynamics which appear in the succeeding paper may be worked out using very similar principles. The Pauli-Weisskopf theory of the Klein-Gordon equation can apparently be analyzed in essentially the same way as that used here for Dirac electrons.

On Total Absorption in Spectra with Overlapping Lines*

FRANK MATOSSI, ROBERT MAYER,** AND EMMA RAUSCHER**
Naval Ordnance Laboratory, White Oak, Silver Spring, Maryland
(Received April 27, 1949)

Total absorption of overlapping lines of equal width but different distances and intensities is calculated. The possibility of deviations from the "root-law" of Ladenburg and Reiche is discussed.

I. INTRODUCTION

IN a paper on selective absorption, Ladenburg and Reiche[1] discussed the total absorption of a limited frequency range in selectively absorbing matter. Their computations are based on Drude's dispersion theory and on the assumption that absorption will take place only within an isolated absorption line the width of which shall be small in comparison with the frequency range considered. The restricting supposition of an isolated absorption line has been eliminated by Elsasser;[2] he substitutes the concept of an infinite number of lines of equal intensity, equal width, and equal mutual distance. He gives an explicit result for the limiting cases in which the ratio of line width and line distance is very small or very large; in general, the computation leads to an integral the evaluation of which is possible only approximately. The present paper deals with a still more general case. The absorption lines may all be equally broad, their width shall be small relative to the considered frequency range as in the previous theories; number, intensities, and mutual distances, however, may be chosen arbitrarily with some slight restrictions developed in Section IIC.

II. TOTAL ABSORPTION BY TWO OVERLAPPING LINES

A. Fundamentals

To find the total absorption A, as defined by Ladenburg and Reiche, within a frequency range from $\omega_1-\delta$ to $\omega_1+\delta$ along a path of the length z, we have to solve the integral

$$A=(1/2\delta)\int_{1-\delta}^{\omega_1+\delta}[1-\exp(-K(\omega)z)]d\omega, \qquad (1)$$

this formula being based upon the Bouguer-Lambert absorption law for homogeneous radiation.

Restricting ourselves at first to the overlapping of only two absorption lines within the range $\omega_1-\delta\leqslant\omega\leqslant\omega_1+\delta$, the absorption coefficient $K(\omega)$ can be written as

$$K(\omega)=a_1/[(\omega-\omega_1)^2+b_1^2]+a_2/[(\omega-\omega_2)^2+b_2^2]$$

with

$$a_i=2\pi N_i b_i e_i^2/n_0 m_i c. \qquad (2)$$

Here, N_i means the number of particles per unit volume responsible for the absorption line; e_i and m_i are charge and mass of these particles; $\omega_i=2\pi c/\lambda_i$ is their eigenfrequency and n_0, the refractive index of the absorbing material as it would be without the existence of absorption in the frequency range considered. In general, the half-widths $2b_i$ of the lines, being a measure of the damping of the vibrations, will be different from one another; it is, however, assumed that all widths are equal. b_i may also be described as the damping factor in the equation of an oscillation

$$\partial^2\xi/\partial t^2+\omega_i^2\xi+b_i\partial\xi/\partial t=0.$$

If we introduce $u=(\omega-\omega_1)/b$ as a new integration variable, and $v=(\omega-\omega_2)/b$ as an abbreviation, we have, instead of Eq. (1),

$$2\delta A=B_2$$
$$=b\int_{-\delta/b}^{\delta/b}\left[1-\exp\left(-\frac{a_1}{b^2(1+u^2)}-\frac{a_2}{b^2(1+v^2)}\right)\right]du. \qquad (3)$$

The index at B indicates the number of overlapping lines. v is to be considered as a function of u.

Putting further

$$u=\tan\varphi,\ v=\tan\psi,\ r_1=a_1z/b^2,\ r_2=a_2z/b^2,\ \delta'=\operatorname{arctg}(\delta/b),$$

and taking into account that

$$\cos^2\psi=\cos^2\varphi/[1-2(\omega_2-\omega_1)\sin\varphi\cos\varphi/b+(\omega_2-\omega_1)^2\cos^2\varphi/b^2]=k\cos^2\varphi,$$

we have

$$B_2=b\int_{-\delta'}^{\delta'}[1-\exp(-(r_1+kr_2)\cos^2\varphi)](d\varphi/\cos^2\varphi). \qquad (4)$$

With the abbreviations

$$(\omega_2-\omega_1)/b=l,\quad 1\mp 2l\sin\varphi\cos\varphi+l^2\cos^2\varphi=1/k_\pm,$$

Eq. (4) becomes

$$B_2=b\int_0^{\delta'}[1-\exp(-(r_1+k_+r_2)\cos^2\varphi)](d\varphi/\cos^2\varphi)$$
$$+b\int_0^{\delta'}[1-\exp(-(r_1+k_-r_2)\cos^2\varphi)](d\varphi/\cos^2\varphi)$$
$$=B_2^+ + B_2^-. \qquad (4a)$$

* The original paper was prepared in the winter of 1944–1945 at the IInd Institute of Physics of the University of Graz, Austria; the circumstances having prevented the publication, the manuscript has been revised and completed. Short review in Naturwiss. 33, 219 (1946).

** University of Graz, Austria.

[1] R. Ladenburg and F. Reiche, Ann. d. Physik 42, 181 (1913).

[2] W. M. Elsasser, Phys. Rev. 54, 126 (1938).

B. Approximate Solution

To obtain an approximate value for B_2, we look for a differential equation. Differentiating B_2 twice with respect to the variables r_1, r_2, and l in any order, the denominator with $\cos^2\varphi$, which would cause a strong increase of the integrand for $\varphi\approx\pi/2$, disappears, and a factor $\cos^2\varphi$ is added to the exponential function. We have

$$(\partial^2 B_2/\partial r_1\partial r_2)=b\int_0^{\delta'} k\cos^2\varphi\exp[-(r_1+kr_2)\cos^2\varphi]d\varphi$$
$$=b\int_0^{\delta'} k\phi d\varphi;$$
$$(\partial^2 B_2/\partial r_1\partial l)=br_1\int_0^{\delta'}(\partial k/\partial l)\phi d\varphi.$$

It is to be seen without difficulty that B_2 satisfies the differential equation

$$\frac{\partial^2 F}{\partial r_1\partial l}=r_1\frac{\partial^2 F}{\partial r_1\partial r_2}\frac{\partial\chi}{\partial l}\Big/\chi \quad\text{with}\quad \chi=\int_0^{\delta'} k d\varphi, \qquad (5)$$

if ϕ is slowly variable in comparison with k and $\partial k/\partial l$. Calculating $(\partial\phi/\partial\varphi)/(\partial k/\partial\varphi)$ and $(\partial\phi/\partial\varphi)/(\partial^2 k/\partial\varphi\partial l)$, it can be shown that this condition will be satisfied only if l is not too small. For this trivial case $l=0$, however, we shall fit B_2 to the exact value by boundary conditions. Therefore, the approximation will be sufficient also in this case. The accuracy of the approximation of B_2 by F becomes worse also for small values of r, but the superposition of lines of practically disappearing intensity is not at all of interest.

The general integral of (5) is

$$F=f(r_1+C\chi r_2)+g(r_1)+h(r_2)+j(r_2,l)+m(l), \qquad (5a)$$

in which f, g, h, j, m are arbitrary functions of their arguments and C is a constant.

As boundary conditions we assume the case of a single isolated absorption line, treated by Ladenburg and Reiche, by putting $r_2=0$. With these authors supposing the frequency range to be much larger than the line width,[3] we directly assume their result. Therefore, for $r_2=0$, we obtain

$$B_2^{\pm}(r_1,0,l)=(1/2)b\pi\exp(-r_1/2)$$
$$\times[I_0(ir_1/2)-iI_1(ir_1/2)], \qquad (6)$$

in which I_0 and I_1 are the Bessel functions of the orders 0 and 1. From (6) and (5a), it follows at once that

$$m(l)=0,\quad j(0,l)=0,\quad h(0)=0.$$

If the two lines are coinciding ($l=0$), the variables r_1 and r_2 must necessarily appear as a sum, and we have

$$B_2^{\pm}(r_1,r_2,0)=(1/2)b\pi(r_1+r_2)\exp[-(r_1+r_2)/2]$$
$$\times[I_0(i(r_1+r_2)/2)-iI_1(i(r_1+r_2)/2)]. \qquad (6a)$$

[3] Then the integration limits may be infinite, because the contribution to absorption from the range $\omega>\omega_1+\delta$ may be neglected.

This condition is compatible with the general solution only if

$$g(r_1)=0,\quad j(r_2,0)=0,\quad h(r_2)=0,\quad C=1/\chi(0).$$

Abbreviating

$$x\exp(-x/2)=R_1(x),\quad I_0-iI_1=R_2,$$

we can now write

$$B_2=B_2^{+}+B_2^{-}=(1/2)b\pi R_1(r_1+C_+\chi_+r_2)$$
$$\times R_2(i(r_1+C_+\chi_+r_2)/2)+j_+(r_2,l)$$
$$+(1/2)b\pi R_1(r_1+C_-\chi_-r_2)$$
$$\times R_2(i(r_1+C_-\chi_-r_2)/2)+j_-(r_2,l) \qquad (7)$$

with the condition $j(r_2,l)=0$ for $r_2=0$ or $l=0$.

In transforming the original integral (1), r_1 has been distinguished, φ being chosen as an integration variable in (2). If we would have determined ψ as a function of φ and integrated over ψ as an independent variable, we would have come to the form

$$B_2=b\int_{-\delta'}^{\delta'}[1-\exp(-(kr_1+r_2)\cos^2\varphi)](d\psi/\cos^2\psi) \qquad (8)$$

in which

$$1/k=1+2l\sin\psi\cos\psi+l^2\cos^2\psi.$$

This manner of writing B_2 can be derived from the former one by interchanging k_+ and k_- in the terms B_2^{+} and B_2^{-} and putting them as factors of r_1 instead of r_2. Thus we have, on the one hand,

$$B_2^{+}=(1/2)b\pi R_1(r_1+C_+\chi_+r_2)R_2(i(r_1+C_+\chi_+r_2)/2)$$
$$+j_+'(r_2,l) \qquad (8a)$$

and, on the other hand,

$$B_2^{+}=(1/2)b\pi R_1(C_-\chi_-r_1+r_2)R_2(i(C_-\chi_-r_1+r_2)/2)$$
$$+j_+''(r_1,l); \qquad (8b)$$

j is subject to the conditions

$$j'(0,l)=0,\quad j'(r_2,0)=0,\quad j''(0,l)=0,\quad j''(r_1,0)=0. \qquad (9)$$

Equaling (8a) and (8b) for $r_1=0$, we obtain

$$j_+'(r_2,l)=(1/2)b\pi[R_1(r_2)R_2(ir_2/2)$$
$$-R_1(C_+\chi_+r_2)R_2(iC_+\chi_+r_2/2)]$$

and a corresponding expression for $j_-'(r_2,l)$.

Finally, we obtain for B_2 the formula

$$2B_2/b\pi=R_1(r_1+C_+\chi_+r_2)R_2(i(r_1+C_+\chi_+r_2)/2)$$
$$+R_1(r_1+C_-\chi_-r_2)R_2(i(r_1+C_-\chi_-r_2)/2)$$
$$+2R_1(r_2)R_2(ir_2/2)$$
$$-R_1(C_+\chi_+r_2)R_2(iC_+\chi_+r_2/2)$$
$$-R_1(C_-\chi_-r_2)R_2(iC_-\chi_-r_2/2), \qquad (10)$$

in which χ_+, χ_- are given by

$$\chi_{\pm}=\arctan[(\delta/b)/(1\mp l\delta/b+l^2)]. \qquad (11)$$

If δ/b can be considered as being infinite, we can write

$$\chi_{\pm}=\mp\arctan 1/l.$$

If $l=1$ and $\delta/b=\infty$, then $\chi_{\pm}=\mp\pi/4$.

The assumption $\delta/b=\infty$ or $b/\delta=0$ is not permitted if $l\ll 1$ is comparable with b/δ. Then, i.e., in the case

of very closely neighboring lines, we can write

$$\chi_{\pm}=\arctan 1/(b/\delta\pm l).$$

Expanding in series yields

$$\chi_{\pm}=\mp\pi/2\pm(b/\delta\mp l)\mp(b/\delta\mp l)^3/3\pm\cdots,$$

hence,

$$\chi_{l=0}=\mp\pi/2\pm(b/\delta)\mp(b/\delta)^3/3\pm\cdots\simeq\pm\pi/2 \quad (12)$$

and, therefore, $C_-=-C_+\simeq 2/\pi$.

If b/δ is finite and $l>1$, expanding in series is possible too, if the absolute value of the denominator exceeds 1:

$$\chi_{\pm}=1/[b(1+l^2)/\delta\mp l]-1/3[b(1+l^2)/\delta\mp l]^3+\cdots.$$

This series converges well enough only if the arguments are not too close to 1.

In the case $1\ll l\ll\delta/b$, χ is nearly zero. Values of l, which come near to δ/b or which even exceed it, are to be excluded, for then the lines would not be entirely in the integration interval. Then, the assumption that the integration limits may be extended to infinity is not justified any longer.

The expression (10) for B_2 can be simplified for small or for large values of r. Expanding the function R_2, we have for $r\ll 1$: $R_2(ix)=1$ (and $R_1(x)=x$) and for $r>10$: $R_2(ix)=(2/\pi x)^{\frac{1}{2}}e^x$.

With these approximate expressions for R_2, we obtain $B_2/b\pi=r_1+r_2$ for $r\ll 1$,

$$B_2/b\pi^{\frac{1}{2}}=(r_1+C_+\chi_+r_2)^{\frac{1}{2}}+(r_1+C_-\chi_-r_2)^{\frac{1}{2}}+2r_2^{\frac{1}{2}} -(C_+\chi_+r_2)^{\frac{1}{2}}-(C_-\chi_-r_2)^{\frac{1}{2}} \text{ for } r>10. \quad (13)$$

C. Restrictions and Discussion

In (6) and (6a), we assumed as boundary values of $B_2(r_1, 0, l)$ and $B_2(r_1, r_2, 0)$ the results of Ladenburg and Reiche. The restrictions given by these authors, therefore, are valid also for our problem; they may be summed up briefly:

1. The integration interval must be small with respect to the doubled absorption frequencies, $\delta\ll 2\omega_i$.

2. The limit of δ against lower values is given by $\delta\gg br^{\frac{1}{2}}$ and already $\delta\gg b$. These relations are equivalent to saying that the integration interval must be large with respect to the width of an absorption line.

3. The absorption should be moderately strong, $r\ll 4\pi z/\lambda_i$. Hence, for $\lambda=6\mu$ and $z=1$ cm, we must confine r to $r\ll 2\times 10^4$.

The influence of the overlapping of the lines is comprised within the terms with χ. For large values of l, i.e., for lines being practically isolated from one another, χ can be neglected according to (10a). In this case, we need only add the Ladenburg and Reiche expressions for total absorption.

For large r values, Ladenburg and Reiche's "root-law" is certainly valid also for overlapping lines as far as the dependence on the path-length z is concerned.

Concerning, however, the dependence on pressure, which is given by the dependence of line-width on pressure ($b\sim p$), the root-law is valid only as far as χ is independent of b. In any other case, we have, through the influence of χ, a deviation from the $p^{\frac{1}{2}}$-law, at least in principle. Summerfield and Strong[4] found for ozone that overlapping may lead to proportionality with the fourth root of p, and we ourselves obtained a similar dependence with water vapor.[5] But, according to the theoretical results, the dependence on pressure may obey this special law only within a limited pressure range. With regard to the statements in Section IIB, deviations from the $p^{\frac{1}{2}}$-law might be possible mainly if δ/b is not too large and if l does not assume extremely high or low values.

Of course, there might be deviations from the root-law, if the proportionality of b with the pressure is not maintained. Indeed, there have been indications that the assumption of damping by impacts only ($b\sim p$) does not always hold and that a "coupling effect" might be superimposed,[6] which would give $b\sim p^{\frac{1}{2}}$, and this would lead to $A\sim p^{\frac{1}{2}}$ even if there is no overlapping. The discussion of the observations with water vapor and of a numerical evaluation of our formulas[5] has shown that this possibility cannot be excluded. Nothing, however, is known about the superposition of the two damping effects, either theoretically or experimentally.

III. OVERLAPPING OF n LINES

The results obtained in the preceding sections have to be generalized for the overlapping of several lines. As the starting integral for the overlapping of n lines, we now have

$$B_n=\int_{\omega_1-\delta}^{\omega_1+\delta}\left[1-\exp\left(-\frac{a_1 z}{(\omega-\omega_1)^2+b^2} -\sum_{\sigma=2}^{n}\frac{a_\sigma z}{(\omega-\omega_\sigma)^2+b^2}\right)\right]d\omega.$$

With $a_\sigma z/b^2=r_\sigma$ and $(\omega-\omega_\sigma)/b=\tan\varphi_\sigma$, we obtain

$$B_n=b\int_{-\delta'}^{\delta'}d\varphi_1 \times\left[1-\exp\left(\left(-r_1-\sum_{\sigma=2}^{n}r_\sigma k_\sigma\right)\cos^2\varphi_1\right)\right]\Big/\cos^2\varphi_1.$$

At first, we deal with 3 lines. In analogy to (4a), we write

$$B_3=b\int_0^{\delta'}d\varphi_1[1-\exp(-(r_1+k_{2+}r_2 +k_{3+}r_3)\cos^2\varphi_1)]/\cos^2\varphi_1 +b\int_0^{\delta'}d\varphi_1[1-\exp(-(r_1+k_{2-}r_2 +k_{3-}r_3)\cos^2\varphi_1)]/\cos^2\varphi_1=B_3^{+}+B_3^{-}, \quad (14)$$

[4] M. Summerfield and J. Strong, Phys. Rev. **60**, 162 (1941). Experimental curves, see J. Strong, J. Frank. Inst. **231**, 121 (1941).

[5] F. Matossi and E. Rauscher, Zeits. f. Physik **125**, 418 (1949).

[6] G. Becker, Zeits. f. Physik **34**, 255 (1925); H. Becker, Zeits. f. Physik **59**, 583 (1930); J. Holtsmark, Zeits. f. Physik **34**, 722 (1925).

in which

$$1/k_{i\pm}=1\mp 2l_{i1}\sin\varphi_1\cos\varphi_1+l_{i1}^2\cos^2\varphi_1,$$
$$l_{ik}=(\omega_i-\omega_k)/b,\quad \tan\varphi_i=u-(\omega_i-\omega_1)/b.$$

In Eq. (14), φ_2 and φ_3 are considered as functions of φ_1. Were, however, φ_2 or φ_3 independent variables, we would obtain (14a) and (14b) with the same right as (14):

$$B_3=b\int_0^{\delta'}d\varphi_2[1-\exp(-(k_{1+}'r_1+r_2+k_{3+}'r_3)\cos^2\varphi_2)]/\cos^2\varphi_2$$
$$+b\int_0^{\delta'}d\varphi_2[1-\exp(-(k_{1-}'r_1+r_2+k_{3-}'r_3)\cos^2\varphi_2)]/\cos^2\varphi_2;\quad (14a)$$

$$B_3=b\int_0^{\delta'}d\varphi_3[1-\exp(-(k_{1+}''r_1+k_{2+}''r_2+r_3)\cos^2\varphi_3)]/\cos^2\varphi_3$$
$$+b\int_0^{\delta'}d\varphi_3[1-\exp(-(k_{1-}''r_1+k_{2-}''r_2+r_3)\cos^2\varphi_3)]/\cos^2\varphi_3.\quad (14b)$$

In k_i' and k_i'', the quantities l_{i2}, φ_2 and l_{i3}, φ_3 are substituted for l_{i1}, φ_1 in k_i.

Under similar conditions as in Section II, we obtain for B_3 the differential equations

$$\frac{\partial^2F}{\partial r_1\partial l_{\sigma 1}}=r_\sigma\frac{\partial^2F}{\partial r_1\partial r_\sigma}\frac{\partial\chi_{\sigma 1}}{\partial l_{\sigma 1}}\Big/\chi_{\sigma 1}\quad(\sigma=2,3);$$
$$\frac{\partial^2F'}{\partial r_2\partial l_{\sigma 2}}=r_\sigma\frac{\partial^2F'}{\partial r_2\partial r_\sigma}\frac{\partial\chi_{\sigma 2}}{\partial l_{\sigma 2}}\Big/\chi_{\sigma 2}\quad(\sigma=1,3);$$
$$\frac{\partial^2F''}{\partial r_3\partial l_{\sigma 3}}=r_\sigma\frac{\partial^2F''}{\partial r_3\partial r_\sigma}\frac{\partial\chi_{\sigma 3}}{\partial l_{\sigma 3}}\Big/\chi_{\sigma 3}\quad(\sigma=1,2).$$

In a similar manner as above, we obtain from (14), (14a), and (14b) the expressions

$$B_3^+=f(r_1+C\chi_{21}^+r_2+C\chi_{31}^+r_3)+K_3^+(r_2,r_3,l_{21},l_{31}),\quad (15)$$
$$B_3^+=f(r_2+C\chi_{12}^+r_1+C\chi_{32}^+r_3)+K_3'^+(r_1,r_3,l_{12},l_{32}),\quad (15a)$$
$$B_3^+=f(r_3+C\chi_{13}^+r_1+C\chi_{23}^+r_2)+K_3''^+(r_1,r_2,l_{13},l_{23}).\quad (15b)$$

K_3^+ must be determined under the condition $K_3''^+(0,0,l_{13},l_{23})=0$. Because the result must be indifferent to a change of the reference line, the three expressions (15) are equivalent. Equaling (15) and (15a) yields, for $r_1=0$:

$$f(C\chi_{21}r_2)+(C\chi_{31}r_3)+K_3(r_2,r_3,l_{21},l_{31})=f(r_2+C\chi_{32}r_3)+K_3'(0,r_3,l_{12},l_{32}).$$

In the same manner, by equaling (15a) and (15b) for $r_1=r_2=0$:

$$f(C\chi_{32}r_3)+K_3'(0,r_3,l_{12},l_{32})=f(r_3)+K_3''(l_{13},l_{23})=f(r_3).$$

Hence

$$K_3(r_2,r_3,l_{21},l_{31})=f(r_2+C\chi_{32}r_3)+f(r_3)-f(C\chi_{21}r_2+C\chi_{31}r_3)-f(C\chi_{32}r_3)$$

and, therefore,

$$B_3^+=f(r_1+C_+\chi_{21}^+r_2+C_+\chi_{31}^+r_3)+f(r_2+C_+\chi_{32}^+r_3)+f(r_3)-f(C_+\chi_{21}^+r_2+C_+\chi_{31}^+r_3)-f(C_+\chi_{32}^+r_3)\quad (16)$$

with a corresponding formula for B_3^-.

In a similar way, we find for B_4^+ or B_4^-:

$$B_4=f(r_1+C\chi_{21}r_2+C\chi_{31}r_3+C\chi_{41}r_4)+f(r_2+C\chi_{32}r_3+C\chi_{42}r_4)+f(r_3+C\chi_{43}r_4)+f(r_4)-f(C\chi_{21}r_2+C\chi_{31}r_3+C\chi_{41}r_4)-f(C\chi_{32}r_3+C\chi_{42}r_4)-f(C\chi_{43}r_4),$$

in which the indices + and − are to be inserted, respectively.

The overlapping of n lines thus leads to the general formula

$$B_n=\sum_{\tau=1}^{n}f\Big(r_\tau+\sum_{\sigma=\tau+1}^{n}C_+\chi_{\sigma\tau}^+r_\sigma\Big)-\sum_{\tau=1}^{n-1}f\Big(\sum_{\sigma=\tau+1}^{n}C_+\chi_{\sigma\tau}^+r_\sigma\Big)+\sum_{\tau=1}^{n}f\Big(r_\tau+\sum_{\sigma=\tau+1}^{n}C_-\chi_{\sigma\tau}^-r_\sigma\Big)-\sum_{\tau=1}^{n-1}f\Big(\sum_{\sigma=\tau+1}^{n}C_-\chi_{\sigma\tau}^-r_\sigma\Big),\quad (17)$$

the total absorption being given by $A_n=B_n/2\delta$.

The meaning of the quantities in Eq. (17) may be stated here again, for the sake of convenience:

$$2f(x)=b\pi xe^{-x/2}[I_0(ix/2)-iI_1(ix/2)]=b\pi R_1(x)[R_2(ix/2)];$$

I_0 and I_1 are the Bessel functions of the orders 0 and 1; if x is very large, $f(x)$ becomes $b(\pi x)^{\frac{1}{2}}$; if x is very small, $f(x)=b\pi x/2$;

$$\chi_{\sigma\tau}^{\mp}=\arctan[(\delta/b)/(1\mp l_{\sigma\tau}\delta/b+l_{\sigma\tau}^2)];$$
$$C_-=-C_+=2/\pi,\quad l_{\sigma\tau}=(\omega_\sigma-\omega_\tau)/b,$$
$$r_\sigma=a_\sigma z/b^2,\quad a_\sigma=2\pi N_\sigma e_\sigma^2 b/n_\sigma m_\sigma c;$$

N_σ, e_σ, m_σ = number per unit volume, charge and mass of the particles to which the absorption line $\omega_\sigma=2\pi c/\lambda_\sigma$ is due, n_σ = "normal" refractive index at $\omega=\omega_\sigma$; b = half half-width of every line, z = path-length of absorbing matter, δ = frequency range equivalent to half the spectrometer slit-width; $\delta'=\arctan(\delta/b)$.

The general discussion and the restrictions in Section IIC are valid also for the case of n lines. In spectra with many lines, it may occur that some lines come near the edge of the slit. Then restriction II interferes and there must be "edge-disturbances" of, however, so much less importance as there are more lines within the interval.

Finally, we mention that formula (17) may be simplified by always calculating with integrals from $-\delta'$ to δ' instead of dividing B into B^+ and B^-. Then only the first two terms of (17) with a factor 2 remain, in which now

$$\chi=\pi+\arctan[2(\delta/b)/(1-(\delta/b)^2+l_{\sigma\tau}^2)] \quad \text{and} \quad C=1/\pi;$$

the indices + or − are of course superfluous now.

Whether there is a considerable numerical difference between these two approximations, has not been investigated. We ourselves (reference 5) utilized Eq. (17), which, in principle, appears to be the better approximation: still further division of the integrals would give still better solutions which, however, could not be handled well.

IV. SUMMARY

The computation of "total absorption," as defined by Ladenburg and Reiche, is extended to the case of overlapping lines which all are equally broad, but which have different distances and different, not too large, intensities. The method is elaborated in detail for the overlapping of two lines in Section II; the general case is dealt with briefly in Section III. Final results: Eqs. (10) and (13) for two lines, Eq. (17) for n lines; restricting assumptions, see Section IIC. The total absorption is proportional to the square root of the path-length also with overlapping lines, as long as this "root-law" is valid for a single line. But there might be deviations from the $p^{\frac{1}{2}}$-law under certain circumstances explained at the end of Section II.

PHYSICAL REVIEW VOLUME 76, NUMBER 6 SEPTEMBER 15, 1949

The Equations of Codazzi and the Relations between Electromagnetism and Gravitation

ANTONIO GIÃO
Lisbon, Portugal

(Received October 4, 1949)

The aim of this paper is to show that, quite independently of any physical theory, the general equations of Codazzi on differential geometry lead to fundamental relations between the electromagnetic and the gravitational fields as soon as the external metric tensor of space-time is interpreted as an electromagnetic tensor. When the important special case of quasi static fields is considered, we get for a *rotating body with no permanent magnetization:* (1) The relation, previously studied by the author, between magnetic moment and angular momentum which explains the general features of stellar and terrestrial magnetism as well as the magnetic moment of the neutron; (2) a relation between gravitation and the electrostatic field, such that any massive body creates an electrostatic field by its own gravitation. *The mean electrostatic fields of celestial bodies, including the earth, can be ascribed to this effect.* When the gravitation produced by a given body is negligible (as in the laboratory) the equations of Codazzi show that the familiar Coulomb field is merely a consequence of the very rapid vibrations of the components g_{4i} $(i=1, 2, 3)$ of the internal metric tensor. Finally, for an uncharged body with permanent magnetization it can be shown that the curl of the g_{4i} and the magnetic field are related as cause and effect.

We think that these results are a confirmation of a fundamental result of our unified field theory: *That the geometrization of electromagnetism must necessarily be achieved by the external metric of space-time.*

1. EQUATIONS OF GAUSS AND CODAZZI

ANY space (l_N) with an arbitrary number (N) of dimensions can be considered as a hypersurface of an enveloping space l_{N+1} of $N+1$ dimensions. The space l_N has then an external as well as an internal metric (to which the second and the first fundamental quadratic forms correspond respectively). These two metrics are well defined by the equation of l_N in l_{N+1} and by the internal metric which can be imposed on l_{N+1}. When l_N is a differentiable variety, the internal (g_{ik}) and the external (ω_{ik}) metric tensors (both symmetric) must necessarily satisfy the fundamental compatibility equations of Gauss and Codazzi.[1,2] Denoting by

R_{ijkl} the Riemann-Christoffel tensor of l_N;
$\bar{R}_{\alpha\beta\gamma\delta}$ the Riemann-Christoffel tensor of l_{N+1} *taken on* l_N;
n^α the contravariant components of the unit normal to l_N;
x^i general coordinates in l_N $(i=1, 2, \cdots, N)$;
X^μ general coordinates in l_{N+1} $(\mu=1, 2, \cdots, N+1)$,

and putting

$$X_{,i}^{\mu}\equiv\partial X^\mu/\partial x^i,$$

the equations of Gauss and Codazzi, for an l_N embedded in a l_{N+1} take the form

$$R_{ijkl}-(\omega_{ik}\omega_{jl}-\omega_{il}\omega_{jk})=\bar{R}_{\alpha\beta\gamma\delta}X_{,i}^{\alpha}X_{,j}^{\beta}X_{,k}^{\gamma}X_{,l}^{\delta}, \quad (1)$$

$$\omega_{ik,j}-\omega_{ij,k}=\bar{R}_{\alpha\beta\gamma\delta}n^\alpha X_{,i}^{\beta}X_{,k}^{\gamma}X_{,j}^{\delta}. \quad (2)$$

(The comma denotes a covariant differentiation.) When

[1] A. Gião, Comptes Rendus **224**, 1813 (1947); **225**, 924 (1947); **226**, 645, 1298, 2126 (1948). *Gazeta de Mat.* (Lisbon), **34** (1947) and **35** (1948).
[2] A. Gião, Portugaliae Physica **2**, 1–98 (1946). Portugaliae Mathematica **5**, 145–192 (1946); **6**, 67–114 (1947); **7**, 1–43 (1948). Bull. Soc. Port. Math. (*A*), 29–40 (1947).

l_N is a space of class 1, that is to say a space which can be embedded in an Euclidean or pseudo-Euclidean l_{N+1}, the right members of Eqs. (1) and (2) vanish identically.

Here we are specially interested in Eq. (2) of Codazzi. Since

$$\omega_{ij,k}=\frac{\partial\omega_{ij}}{\partial x^k}-\omega_{jl}\left\{\begin{matrix}l\\ik\end{matrix}\right\}-\omega_{il}\left\{\begin{matrix}l\\jk\end{matrix}\right\},$$

the $\left\{\begin{matrix}l\\ik\end{matrix}\right\}$ being the Christoffel symbols of second kind formed with the g_{ik}, the equations of Codazzi can be written as follows

$$\frac{\partial\omega_{ik}}{\partial x^j}-\frac{\partial\omega_{ij}}{\partial x^k}-\left(\omega_{kl}\left\{\begin{matrix}l\\ij\end{matrix}\right\}-\omega_{jl}\left\{\begin{matrix}l\\ik\end{matrix}\right\}\right)=\bar{R}_{\alpha\beta\gamma\delta}n^\alpha X_{,i}{}^\beta X_{,k}{}^\gamma X_{,j}{}^\delta.$$

Putting

$$2A_k{}^i\equiv g^{li}\omega_{lk}, \tag{3}$$

we can also write

$$\frac{\partial\omega_{ik}}{\partial x^j}-\frac{\partial\omega_{ij}}{\partial x^k}-\left[A_k{}^h\left(\frac{\partial g_{ih}}{\partial x^j}-\frac{\partial g_{ij}}{\partial x^h}+\frac{\partial g_{jh}}{\partial x^i}\right)-A_j{}^h\left(\frac{\partial g_{ih}}{\partial x^k}-\frac{\partial g_{ik}}{\partial x^h}+\frac{\partial g_{kh}}{\partial x^i}\right)\right]=\bar{R}_{\alpha\beta\gamma\delta}n^\alpha X_{,i}{}^\beta X_{,k}{}^\gamma X_{,j}{}^\delta,$$

which reduces to

$$\frac{\partial\omega_{ik}}{\partial x^j}-\frac{\partial\omega_{ij}}{\partial x^k}=A_k{}^h\left(\frac{\partial g_{ih}}{\partial x^j}-\frac{\partial g_{ij}}{\partial x^h}+\frac{\partial g_{jh}}{\partial x^i}\right)-A_j{}^h\left(\frac{\partial g_{ih}}{\partial x^k}-\frac{\partial g_{ik}}{\partial x^h}+\frac{\partial g_{kh}}{\partial x^i}\right), \tag{4}$$

for a space l_N of class 1.

2. FOUR-DIMENSIONAL SPACE OF CLASS 1

Let us consider a four-dimensional space of class 1 and calculate by the corresponding Codazzi equations (Eq. (4)) the quantities:

$$\frac{\partial\omega_{4l}}{\partial x^j}-\frac{\partial\omega_{4j}}{\partial x^l}\quad(j,l=1,2,3)$$

and

$$\frac{\partial\omega_{44}}{\partial x^i}-\frac{\partial\omega_{4i}}{\partial x^4}\quad(i=1,2,3).$$

i, j, l denoting a cyclic permutation of 1, 2, 3, we obtain on the one hand

$$\begin{aligned}\frac{\partial\omega_{4l}}{\partial x^j}-\frac{\partial\omega_{4j}}{\partial x^l}&=(A_j{}^j+A_l{}^l)\left(\frac{\partial g_{4l}}{\partial x^j}-\frac{\partial g_{4j}}{\partial x^l}\right)\\&+A_l{}^i\left(\frac{\partial g_{4i}}{\partial x^j}-\frac{\partial g_{4j}}{\partial x^i}\right)+A_j{}^i\left(\frac{\partial g_{4l}}{\partial x^i}-\frac{\partial g_{4i}}{\partial x^l}\right)\\&+\left(A_l{}^4\frac{\partial g_{44}}{\partial x^j}-A_j{}^4\frac{\partial g_{44}}{\partial x^l}\right)+(A_l{}^l-A_j{}^j)\frac{\partial g_{jl}}{\partial x^4}\\&+\left(A_l{}^i\frac{\partial g_{ij}}{\partial x^4}-A_j{}^i\frac{\partial g_{il}}{\partial x^4}\right)+\left(A_l{}^j\frac{\partial g_{jj}}{\partial x^4}-A_j{}^l\frac{\partial g_{ll}}{\partial x^4}\right),\end{aligned}$$

and on the other hand

$$\begin{aligned}\frac{\partial\omega_{44}}{\partial x^i}-\frac{\partial\omega_{4i}}{\partial x^4}&=A_4{}^j\left(\frac{\partial g_{4j}}{\partial x^i}-\frac{\partial g_{4i}}{\partial x^j}\right)+A_4{}^l\left(\frac{\partial g_{4l}}{\partial x^i}-\frac{\partial g_{4i}}{\partial x^l}\right)\\&+A_4{}^h\frac{\partial g_{ih}}{\partial x^4}+A_i{}^h\left(\frac{\partial g_{44}}{\partial x^h}-2\frac{\partial g_{4h}}{\partial x^4}\right)+A_4{}^4\left(\frac{\partial g_{44}}{\partial x^i}-\frac{\partial g_{4i}}{\partial x^4}\right).\end{aligned}$$

In the very important special case of *quasi static* metric fields, that is to say when all the derivatives of g_{ik} and ω_{ik} with respect to the "temporal" variable x^4 vanish, excepting the temporal derivatives of g_{4i} and ω_{4i} $(i=1, 2, 3)$, the preceding relations become:

$$\begin{aligned}\frac{\partial\omega_{4l}}{\partial x^j}-\frac{\partial\omega_{4j}}{\partial x^l}&=(A_j{}^j+A_l{}^l)\left(\frac{\partial g_{4l}}{\partial x^j}-\frac{\partial g_{4j}}{\partial x^l}\right)\\&+A_l{}^i\left(\frac{\partial g_{4i}}{\partial x^j}-\frac{\partial g_{4j}}{\partial x^i}\right)+A_j{}^i\left(\frac{\partial g_{4l}}{\partial x^i}-\frac{\partial g_{4i}}{\partial x^l}\right)\\&+\left(A_l{}^4\frac{\partial g_{44}}{\partial x^j}-A_j{}^4\frac{\partial g_{44}}{\partial x^l}\right),\end{aligned} \tag{5}$$

and

$$\begin{aligned}\frac{\partial\omega_{44}}{\partial x^i}-\frac{\partial\omega_{4i}}{\partial x^4}&=A_4{}^j\left(\frac{\partial g_{4j}}{\partial x^i}-\frac{\partial g_{4i}}{\partial x^j}\right)+A_4{}^l\left(\frac{\partial g_{4l}}{\partial x^i}-\frac{\partial g_{4i}}{\partial x^l}\right)\\&+A_4{}^4\frac{\partial g_{44}}{\partial x^i}+\sum_1^3{}_h A_i{}^h\left(\frac{\partial g_{44}}{\partial x^h}-2\frac{\partial g_{4h}}{\partial x^4}\right).\end{aligned} \tag{6}$$

The mean curvature χ of the four-dimensional space is given by $4\chi\equiv g^{ik}\omega_{ik}$ and putting $\omega_{ik}\equiv\chi g_{ik}+\bar{\omega}_{ik}$ we get from (3):

$$2A_k{}^i=\chi\delta_k{}^i+g^{li}\bar{\omega}_{lk}. \tag{3a}$$

For a space such that the $\bar{\omega}_{ik}$ $(i\neq k)$ are small quantities against χ (all spaces with slight variable mean curvature obey this condition), the components of the tensor $A_k{}^i$ (for $i\neq k$) are, according to (3a), small quantities against $A_i{}^i$. Equations (5) and (6) can then be simplified

as follows:

$$\frac{\partial\omega_{4l}}{\partial x^j}-\frac{\partial\omega_{4j}}{\partial x^l}=(A_j{}^j+A_l{}^l)\left(\frac{\partial g_{4l}}{\partial x^j}-\frac{\partial g_{4j}}{\partial x^l}\right), \tag{7}$$

and

$$\frac{\partial\omega_{44}}{\partial x^i}-\frac{\partial\omega_{4i}}{\partial x^4}=(A_4{}^4+A_i{}^i)\frac{\partial g_{44}}{\partial x^i}-2A_i{}^i\frac{\partial g_{4i}}{\partial x^4}. \tag{8}$$

3. THE EXTERNAL METRIC TENSOR AND THE ELECTROMAGNETIC FIELD

The preceding sections are quite independent of any physical theory. In order to give them an essential physical meaning, one needs only to interpret physically the external metric tensor ω_{ik}, since it is well known that g_{ik} is the gravitational tensor. According to our unified field theory,[2] space-time is a four-dimensional hypersurface of class 1 and ω_{ik} is the tensor of the electromagnetic (electromotive) field. Moreover,[2] between the electric field intensity (E_i), the magnetic field intensity (H_i; $i=1, 2, 3$) and the components of the external metric tensor the following fundamental relations hold:

$$H_i=\frac{1}{\chi_0(-1)^{\frac{1}{2}}}\frac{(m_0)_e c^2}{e}\left(\frac{\partial\omega_{4l}}{\partial x^j}-\frac{\partial\omega_{4j}}{\partial x^l}+\frac{\partial\omega_{jl}}{\partial x^4}\right), \tag{9}$$

and

$$E_i=-\frac{1}{2\chi_0}\frac{(m_0)_e c^2}{e}\left(\frac{\partial\omega_{44}}{\partial x_i}-2\frac{\partial\omega_{4i}}{\partial x^4}\right), \tag{10}$$

where χ_0 is a positive constant (mean curvature of the isotropic and homogeneous space-time nearest to the real space-time), $(m_0)_e$ and e the rest mass and electric charge of the electron. It must be remarked that the field (9), (10) behaves as a tensor F_{jl} only for pure spatial coordinate changes, and this tensor is antisymmetric (as the tensor of the Maxwellian field) only when the metric is static.

For a quasi static field the relations (9) and (10) reduce to:

$$\left.\begin{aligned} H_i&=\frac{1}{\chi_0(-1)^{\frac{1}{2}}}\frac{(m_0)_e c^2}{e}\left(\frac{\partial\omega_{4l}}{\partial x^j}-\frac{\partial\omega_{4j}}{\partial x^l}\right),\\ E_i&=-\frac{1}{2\chi_0}\frac{(m_0)_e c^2}{e}\left(\frac{\partial\omega_{44}}{\partial x^i}-2\frac{\partial\omega_{4i}}{\partial x^4}\right),\end{aligned}\right\} \tag{11}$$

and Eqs. (7) and (8) give then:

$$H_i=\frac{1}{\chi_0(-1)^{\frac{1}{2}}}\frac{(m_0)_e c^2}{e}(A_j{}^j+A_l{}^l)\left(\frac{\partial g_{4l}}{\partial x^j}-\frac{\partial g_{4j}}{\partial x^l}\right), \tag{12a}$$

$$E_i=-\frac{1}{2\chi_0}\frac{(m_0)_e c^2}{e}\left[(A_4{}^4+A_i{}^i)\frac{\partial g_{44}}{\partial x^i}-2A_i{}^i\frac{\partial g_{4i}}{\partial x^4}-\frac{\partial\omega_{4i}}{\partial x^4}\right]. \tag{12b}$$

These equations will now be applied to the analysis of the relations between the electromagnetic and the gravitational fields. For this purpose, special cases will be considered which give a clear understanding of the main characteristics of these relations.

4. SPHERICAL ROTATING BODY WITH NO PERMANENT MAGNETIZATION

Let us consider a rotating sphere of mass M and constant angular momentum M_{rot}. There is no permanent magnetization and the angular velocity Ω of each particle is parallel to the axis of rotation, but $|\Omega|$ as well the density μ are arbitrarily distributed in the mass. Denoting by γ a numerical coefficient (≤ 1), by K the gravitational constant, by r the spatial distance from the center ($x^1=x^2=x^3=0$) of the sphere and by u^i the components of the unit vector of the axis of rotation, the well known Einstein equations for the internal metric field give[1] the following expression for the statical part of the g_{4i} ($i=1, 2, 3$) of the rotating sphere:

$$g_{4i}=2\frac{K}{c^3(-1)^{\frac{1}{2}}}\gamma M_{\text{rot}}\frac{1}{r^3}(u^i x^l-x^i u^l), \tag{13}$$

[$\gamma=1$ when $|\Omega|$ and μ are spatially constant or have a spherical symmetry inside the sphere. It can be shown[3] that $\gamma>0.6$ for the earth]. Concerning the non-statical part $g_{4i}{}^*$ of the g_{4i} ($i=1, 2, 3$) we shall only assume that

$$g_{4i}{}^*=h(r, x^4)\partial r/\partial x^i. \tag{14}$$

Equations (12a) and (12b) then become

$$H_i=\frac{2}{\chi_0}\frac{(m_0)_e}{ec}K\gamma M_{\text{rot}}\left\{\frac{\partial}{\partial x^l}\left[\frac{1}{r^3}(u^l x^i-u^i x^l)\right]-\frac{\partial}{\partial x^j}\left[\frac{1}{r^3}(u^i x^j-u^j x^i)\right]\right\}(A_j{}^j+A_l{}^l), \tag{15}$$

and

$$E_i=-\frac{1}{2\chi_0}\frac{(m_0)_e c^2}{e}\left[(A_4{}^4+A_i{}^i)\frac{\partial g_{44}}{\partial x^i}-2A_i{}^i\frac{\partial h}{\partial x^4}\frac{\partial r}{\partial x^i}-\frac{\partial\omega_{4i}}{\partial x^4}\right]. \tag{16}$$

(a) The Magnetic Field of the Rotating Sphere

In order to derive this static field from (15) we must take the large scale temporal mean of both sides of this equation. From (3a) we get $A_j{}^j+A_l{}^l\cong\chi$ when the $\tilde{\omega}_{ik}$ are small quantities against χ. Writting $A_j{}^j+A_l{}^l\equiv\xi+\xi'$, where ξ' corresponds to the rapid changing part $g_{4i}{}^*$ of g_{4i}, we see that the large scale temporal mean $\langle[A_j{}^j+A_l{}^l]\rangle_{Av}$ of $A_j{}^j+A_l{}^l$ is simply

$$\langle[A_j{}^j+A_l{}^l]\rangle_{Av}=\xi.$$

[3] Comptes Rendus **226**, 1298 (1948).

Formula (15) then gives

$$\mathbf{H}=2\frac{\xi}{\chi_0}\frac{(m_0)_e}{ec}K\gamma M_{\text{rot}}\,\text{curl}\left[\mathbf{u}\times\nabla\left(\frac{1}{r}\right)\right]. \tag{17}$$

According to classical electromagnetism the magnetic moment M_{magn} which corresponds to the field (17) is related to $\mathbf{H}$ by

$$\mathbf{H}=M_{\text{magn}}\,\text{curl}[\mathbf{u}\times\nabla(1/r)]. \tag{18}$$

Comparing (17) and (18) we get finally

$$M_{\text{magn}}=2\frac{\xi}{\chi_0}\frac{(m_0)_e}{ec}K\gamma M_{\text{rot}}. \tag{19}$$

This is the very important formula explaining the general features of the magnetic fields of the stars and the earth as a fundamental consequence of their rotation. It explains also[4] the magnetic moments of the proton and the neutron. The recently discovered stars with periodic magnetic fields[5] can also be explained by (19), for it can be shown[6] that $\xi=\pm\lambda^2\chi_0$, and that in general λ is a periodic function of time. Formula (19) has been previously derived by the author from his unified field theory, quite independently of the Codazzi equations, and its consequences have been thoroughly studied.[1] For this reason we will only point out here the important fact that (19) is a mere consequence of the Codazzi equations when the external metric tensor is interpreted (by Eqs. (9) and (10)) as an electromagnetic tensor.

This result brings new evidence to our unified theory and we regard it as a good proof of the fundamental character of the creation of magnetism by rotation, even without any electrical charge.

(b) The Electrostatic Field

The force of gravitation G_i (per unity mass) is related to g_{44} by the well-known formula of the relativity theory:

$$G_i=-\frac{c^2}{2}\frac{\partial g_{44}}{\partial x^i}.$$

Introducing this in (16) we get

$$E_i=\frac{1}{\chi_0}\frac{(m_0)_e}{e}\left[(A_4{}^4+A_i{}^i)G_i+c^2A_i{}^i\frac{\partial h}{\partial x^4}\frac{\partial r}{\partial x^i}+\frac{c^2}{2}\frac{\partial\omega_{4i}}{\partial x^4}\right].$$

Since, according to (3a), $A_4{}^4+A_i{}^i\cong\chi=(\xi+\xi')$, and as ω_{4i} are bounded functions, we obtain for the large scale temporal mean value $\langle(E_{\text{st}})_i\rangle_{Av}$ of E_i, i.e., the electrostatic field:

$$\mathbf{E}_{\text{st}}=\frac{\xi}{\chi_0}\frac{(m_0)_e}{e}\left\{\mathbf{G}+\frac{c^2}{\xi}\left\langle\left[\xi'\frac{\partial h}{\partial x^4}\right]\right\rangle_{Av}\frac{\mathbf{r}}{r}\right\}. \tag{20}$$

The mean value of $\xi'\partial h/\partial x^4$ can be deduced from the equations of the metric fields. When, as in the present case, the T_{4i} components of the energy-momentum tensor correspond to the static part of g_{4i}, the non-static part $g_{4i}{}^*$ obeys the following linearized Einstein equation:

$$\Box g_{4i}{}^*=-(8\pi K/c^2)Tg_{4i}{}^*. \tag{21}$$

Taking (14) into account and putting

$$h(r,x^4)=f(x^4)\varphi(r)$$

the solution of (21) for a point outside the material sphere is:

$$(1/(-1)^{\frac{1}{2}})g_{4i}{}^*=\varphi(r)(\partial r/\partial x^i)\sin(c\sigma t),$$

with an appropriate time origin and σ denoting a constant. The electrostatic field will then be given by

$$\mathbf{E}_{\text{st}}=\frac{\xi}{\chi_0}\frac{(m_0)_e}{e}\left\{\mathbf{G}+\frac{c^2\sigma}{\xi}\langle[\varphi\xi'\cos(c\sigma t)]\rangle_{Av}\frac{\mathbf{r}}{r}\right\}. \tag{22}$$

The spatial variation of $\varphi\xi'$ is determined by the equation $\text{div}\mathbf{E}_{\text{st}}=0$ of the electrostatic field outside the charges. As $\text{div}\mathbf{G}=0$ outside the material sphere, we get the condition $\text{div}[(\mathbf{r}/r)\varphi(r)\xi'(r,t)]=0$, which leads to

$$(\partial(\varphi\xi')/\partial r)+(2/r)\varphi\xi'=0.$$

The solution is

$$\varphi\xi'=(a(t)/r^2),$$

and (22) becomes:

$$\mathbf{E}_{\text{st}}=\frac{\xi}{\chi_0}\frac{(m_0)_e}{e}\left\{\mathbf{G}+\frac{c^2\sigma}{\xi}\langle[a(t)\cos(c\sigma t)]\rangle_{Av}\frac{\mathbf{r}}{r^3}\right\}.$$

The function $a(t)$ is of course a periodic function with the same period as $g_{4i}{}^*$. Hence, by a Fourier expansion $\langle a(t)\cos(c\sigma t)\rangle_{Av}=\alpha$ with

$$\alpha=c\sigma\int_0^{2\pi/c\sigma}a(t)\cos(c\sigma t)dt.$$

Putting $c^2\sigma\alpha=\eta$ (constant) we get finally

$$\mathbf{E}_{\text{st}}=\frac{\xi}{\chi_0}\frac{(m_0)_e}{e}\left[\mathbf{G}+\frac{\eta}{\xi}\frac{\mathbf{r}}{r^3}\right]. \tag{23}$$

Since $\mathbf{G}=-KM\mathbf{r}/r^3$, (23) can still be written as follows:

$$\mathbf{E}_{\text{st}}=\frac{\xi}{\chi_0}\frac{(m_0)_e}{e}\left[1-\frac{\eta}{KM\xi}\right]\mathbf{G}. \tag{24}$$

This is the required relation between the electrostatic

[4] Portugaliae Mathematica 7, 1–43 (1948).
[5] H. W. Babcock, Astronom. Soc. Pac. 59, 260 (1947).
[6] Comptes Rendus 226, 2126 (1948).

field and gravitation. We are inclined to think that (24), which is a consequence of the Codazzi equations, reveals *the real cause of the maintenance of the mean electrostatic field of the earth. This cause is merely the gravitation of the earth's mass*, and we conclude also from (24) that *any massive body must have an electric charge.*

According to Blackett,[7] who compared the magnetic moment M_{magn} and the angular momentum of the earth, the sun and the star 78Vir: $M_{\text{magn}}/M_{\text{rot}} = \beta(K)^{\frac{1}{2}}/2c$, β denoting a numerical coefficient ($\beta \sim 1$). This value of $M_{\text{magn}}/M_{\text{rot}}$ corresponds to

$$\xi/\chi_0 = \beta l/4(m_0)_e(K)^{\frac{1}{2}},$$

and it is quite natural to suppose that the ratio E/G is also nearly constant for the different celestial bodies. Denoting by R the radius of the bodies and by the subscript zero the values of the different quantities for the earth, Eq. (24) then gives the following relation for the electrostatic field at the surface of the stars:

$$\mathbf{E}_{st} = (\mathbf{E}_{st})_0 \frac{M}{M_0}\left(\frac{R_0}{R}\right)^2 = (\mathbf{E}_{st})_0 \frac{\bar{\mu}}{\bar{\mu}_0}\frac{R}{R_0} \tag{25}$$

the $\bar{\mu}$ denoting the mean densities. Hence, for instance: $(\mathbf{E}_{st})_{sun} = 28(\mathbf{E}_{st})_0$.

An alternative way of presenting (24) or (25) is to replace the electrostatic field intensity by the corresponding charges Q or potentials V. We obtain from (24)

$$Q = -\frac{2\xi}{\chi_0}\frac{(m_0)_e}{e}\left(1 - \frac{\eta}{KM\xi}\right)KM, \tag{26}$$

and (25) gives:

$$Q = Q_0(M/M_0), \tag{27}$$

and

$$V = V_0(\bar{\mu}/\bar{\mu}_0)(R/R_0)^2. \tag{28}$$

As this relation can be applied to the stars, we see that many stars must exist with the very strong electric potential required to give rise to the expulsion of cosmic rays.

When, as in the laboratory, the gravitation created by the body is quite negligible, Eq. (23) reduces to:

$$\mathbf{E}_{st} = \frac{\eta}{\chi_0}\frac{(m_0)_e}{e}\frac{\mathbf{r}}{r^3}. \tag{29}$$

This is the familiar Coulomb field of a sphere with the electric charge $Q = (\eta/\chi_0)(m_0)_e/e$. Remembering the nature of the constant η, we see that the Coulomb field is a direct consequence of the very rapid vibrations undergone by the g_{4i} ($i = 1, 2, 3$) components of the metric tensor corresponding to any charged body.

[7] P. S. Blackett, Nature 159, 658–666 (1947).

5. STATIC FIELD OF A MAGNET

As a last special case illustrating the fundamental links of electromagnetism and gravitation, we consider a constant magnet whose magnetization may be of the permanent and of the induced types. For pure spatial coordinate transformations the g_{4i} ($i = 1, 2, 3$) and the T_{4i} ($i = 1, 2, 3$) components of the energy-momentum tensor are spatial vectors which will be denoted by $\mathbf{g}_4$ and $\mathbf{T}_4$. Clearly, Eq. (12a) can be applied to the case under examination. Taking into account that $A_j{}^j + A_l{}^l \cong \xi$ we get:

$$\mathbf{H} = \frac{\xi}{\chi_0(-1)^{\frac{1}{2}}}\frac{(m_0)_e c^2}{e}\operatorname{curl}\mathbf{g}_4. \tag{30}$$

The equations of the internal metric field give

$$\Delta\mathbf{g}_4 = (8\pi K/c^2)(\mathbf{T}_4 - \tfrac{1}{2}T\mathbf{g}_4) \equiv [8\pi K/c^2]\mathbf{T}_4^*, \tag{31}$$

and reduce to

$$\Delta\mathbf{g}_4 = 0, \tag{32}$$

for a point outside the magnet. The solution of (32) must be compatible with the Maxwell equation $\operatorname{curl}\mathbf{H} = 0$ for a magnetostatic field outside its sources. From (30) we then derive the conditions:

$$\operatorname{curl}\operatorname{curl}\mathbf{g}_4 = 0; \quad \nabla(\operatorname{div}\mathbf{g}_4) = 0.$$

The appropriate solution of (32) is therefore

$$\mathbf{g}_4 = \mathbf{a} \times \nabla(1/r),$$

$\mathbf{a}$ being a constant vector and r the distance from the "center of gravity" of the magnet. Equation (30) then gives:

$$\mathbf{H} = [\xi/\chi_0(-1)^{\frac{1}{2}}][(m_0)_e c^2/e]\operatorname{curl}[\mathbf{a} \times \nabla(1/r)]. \tag{33}$$

Comparing this result with the classical formula of the magnetostatic field for points outside the magnet and sufficiently far from it, we see at once that $\mathbf{a}$ is related to the magnetic moment $\mathbf{M}_{\text{magn}}$ of the magnet by:

$$\mathbf{a} = [\chi_0(-1)^{\frac{1}{2}}/\xi][e/(m_0)_e c^2]\mathbf{M}_{\text{magn}}. \tag{34}$$

Taking (31) into account (34) can be written as follows:

$$8\pi K[(m_0)_e/e]\xi/\chi_0 \int_v \mathbf{T}_4^* dv = \mathbf{M}_{\text{magn}}, \tag{35}$$

v denoting the volume of the magnet. This relation gives the material momentum $\int_v \mathbf{T}_4^* dv$ produced by the magnetization, but it must be remarked that this momentum is by no means associated with a macroscopic material current. It is the material counterpart of the well known electromagnetic momentum in the canonical equations of motion.

It would be rather easy to generalize the preceding results for points inside the magnet.

Space-Time Approach to Quantum Electrodynamics

R. P. FEYNMAN
Department of Physics, Cornell University, Ithaca, New York
(Received May 9, 1949)

In this paper two things are done. (1) It is shown that a considerable simplification can be attained in writing down matrix elements for complex processes in electrodynamics. Further, a physical point of view is available which permits them to be written down directly for any specific problem. Being simply a restatement of conventional electrodynamics, however, the matrix elements diverge for complex processes. (2) Electrodynamics is modified by altering the interaction of electrons at short distances. All matrix elements are now finite, with the exception of those relating to problems of vacuum polarization. The latter are evaluated in a manner suggested by Pauli and Bethe, which gives finite results for these matrices also. The only effects sensitive to the modification are changes in mass and charge of the electrons. Such changes could not be directly observed. Phenomena directly observable, are insensitive to the details of the modification used (except at extreme energies). For such phenomena, a limit can be taken as the range of the modification goes to zero. The results then agree with those of Schwinger. A complete, unambiguous, and presumably consistent, method is therefore available for the calculation of all processes involving electrons and photons.

The simplification in writing the expressions results from an emphasis on the over-all space-time view resulting from a study of the solution of the equations of electrodynamics. The relation of this to the more conventional Hamiltonian point of view is discussed. It would be very difficult to make the modification which is proposed if one insisted on having the equations in Hamiltonian form.

The methods apply as well to charges obeying the Klein-Gordon equation, and to the various meson theories of nuclear forces. Illustrative examples are given. Although a modification like that used in electrodynamics can make all matrices finite for all of the meson theories, for some of the theories it is no longer true that all directly observable phenomena are insensitive to the details of the modification used.

The actual evaluation of integrals appearing in the matrix elements may be facilitated, in the simpler cases, by methods described in the appendix.

THIS paper should be considered as a direct continuation of a preceding one[1] (I) in which the motion of electrons, neglecting interaction, was analyzed, by dealing directly with the *solution* of the Hamiltonian differential equations. Here the same technique is applied to include interactions and in that way to express in simple terms the solution of problems in quantum electrodynamics.

For most practical calculations in quantum electrodynamics the solution is ordinarily expressed in terms of a matrix element. The matrix is worked out as an expansion in powers of $e^2/\hbar c$, the successive terms corresponding to the inclusion of an increasing number of virtual quanta. It appears that a considerable simplification can be achieved in writing down these matrix elements for complex processes. Furthermore, each term in the expansion can be written down and understood directly from a physical point of view, similar to the space-time view in I. It is the purpose of this paper to describe how this may be done. We shall also discuss methods of handling the divergent integrals which appear in these matrix elements.

The simplification in the formulae results mainly from the fact that previous methods unnecessarily separated into individual terms processes that were closely related physically. For example, in the exchange of a quantum between two electrons there were two terms depending on which electron emitted and which absorbed the quantum. Yet, in the virtual states considered, timing relations are not significant. Olny the order of operators in the matrix must be maintained. We have seen (I), that in addition, processes in which virtual pairs are produced can be combined with others in which only positive energy electrons are involved. Further, the effects of longitudinal and transverse waves can be combined together. The separations previously made were on an unrelativistic basis (reflected in the circumstance that apparently momentum but not energy is conserved in intermediate states). When the terms are combined and simplified, the relativistic invariance of the result is self-evident.

We begin by discussing the solution in space and time of the Schrödinger equation for particles interacting instantaneously. The results are immediately generalizable to delayed interactions of relativistic electrons and we represent in that way the laws of quantum electrodynamics. We can then see how the matrix element for any process can be written down directly. In particular, the self-energy expression is written down.

So far, nothing has been done other than a restatement of conventional electrodynamics in other terms. Therefore, the self-energy diverges. A modification[2] in interaction between charges is next made, and it is shown that the self-energy is made convergent and corresponds to a correction to the electron mass. After the mass correction is made, other real processes are finite and insensitive to the "width" of the cut-off in the interaction.[3]

Unfortunately, the modification proposed is not completely satisfactory theoretically (it leads to some difficulties of conservation of energy). It does, however, seem consistent and satisfactory to define the matrix

[1] R. P. Feynman, Phys. Rev. **76**, 749 (1949), hereafter called I.

[2] For a discussion of this modification in classical physics see R. P. Feynman, Phys. Rev. **74** 939 (1948), hereafter referred to as A.

[3] A brief summary of the methods and results will be found in R. P. Feynman, Phys. Rev. **74**, 1430 (1948), hereafter referred to as B.

element for all real processes as the limit of that computed here as the cut-off width goes to zero. A similar technique suggested by Pauli and by Bethe can be applied to problems of vacuum polarization (resulting in a renormalization of charge) but again a strict physical basis for the rules of convergence is not known.

After mass and charge renormalization, the limit of zero cut-off width can be taken for all real processes. The results are then equivalent to those of Schwinger[4] who does not make explicit use of the convergence factors. The method of Schwinger is to identify the terms corresponding to corrections in mass and charge and, previous to their evaluation, to remove them from the expressions for real processes. This has the advantage of showing that the results can be strictly independent of particular cut-off methods. On the other hand, many of the properties of the integrals are analyzed using formal properties of invariant propagation functions. But one of the properties is that the integrals are infinite and it is not clear to what extent this invalidates the demonstrations. A practical advantage of the present method is that ambiguities can be more easily resolved; simply by direct calculation of the otherwise divergent integrals. Nevertheless, it is not at all clear that the convergence factors do not upset the physical consistency of the theory. Although in the limit the two methods agree, neither method appears to be thoroughly satisfactory theoretically. Nevertheless, it does appear that we now have available a complete and definite method for the calculation of physical processes to any order in quantum electrodynamics.

Since we can write down the solution to any physical problem, we have a complete theory which could stand by itself. It will be theoretically incomplete, however, in two respects. First, although each term of increasing order in $e^2/\hbar c$ can be written down it would be desirable to see some way of expressing things in finite form to all orders in $e^2/\hbar c$ at once. Second, although it will be physically evident that the results obtained are equivalent to those obtained by conventional electrodynamics the mathematical proof of this is not included. Both of these limitations will be removed in a subsequent paper (see also Dyson[4]).

Briefly the genesis of this theory was this. The conventional electrodynamics was expressed in the Lagrangian form of quantum mechanics described in the Reviews of Modern Physics.[5] The motion of the field oscillators could be integrated out (as described in Section 13 of that paper), the result being an expression of the delayed interaction of the particles. Next the modification of the delta-function interaction could be made directly from the analogy to the classical case.[2] This was still not complete because the Lagrangian method had been worked out in detail only for particles obeying the non-relativistic Schrödinger equation. It was then modified in accordance with the requirements of the Dirac equation and the phenomenon of pair creation. This was made easier by the reinterpretation of the theory of holes (I). Finally for practical calculations the expressions were developed in a power series in $e^2/\hbar c$. It was apparent that each term in the series had a simple physical interpretation. Since the result was easier to understand than the derivation, it was thought best to publish the results first in this paper. Considerable time has been spent to make these first two papers as complete and as physically plausible as possible without relying on the Lagrangian method, because it is not generally familiar. It is realized that such a description cannot carry the conviction of truth which would accompany the derivation. On the other hand, in the interest of keeping simple things simple the derivation will appear in a separate paper.

The possible application of these methods to the various meson theories is discussed briefly. The formulas corresponding to a charge particle of zero spin moving in accordance with the Klein Gordon equation are also given. In an Appendix a method is given for calculating the integrals appearing in the matrix elements for the simpler processes.

The point of view which is taken here of the interaction of charges differs from the more usual point of view of field theory. Furthermore, the familiar Hamiltonian form of quantum mechanics must be compared to the over-all space-time view used here. The first section is, therefore, devoted to a discussion of the relations of these viewpoints.

1. COMPARISON WITH THE HAMILTONIAN METHOD

Electrodynamics can be looked upon in two equivalent and complementary ways. One is as the description of the behavior of a field (Maxwell's equations). The other is as a description of a direct interaction at a distance (albeit delayed in time) between charges (the solutions of Lienard and Wiechert). From the latter point of view light is considered as an interaction of the charges in the source with those in the absorber. This is an impractical point of view because many kinds of sources produce the same kind of effects. The field point of view separates these aspects into two simpler problems, production of light, and absorption of light. On the other hand, the field point of view is less practical when dealing with close collisions of particles (or their action on themselves). For here the source and absorber are not readily distinguishable, there is an intimate exchange of quanta. The fields are so closely determined by the motions of the particles that it is just as well not to separate the question into two problems but to consider the process as a direct interaction. Roughly, the field point of view is most practical for problems involv-

[4] J. Schwinger, Phys. Rev. 74, 1439 (1948), Phys. Rev. 75, 651 (1949). A proof of this equivalence is given by F. J. Dyson, Phys. Rev. 75, 486 (1949).

[5] R. P. Feynman, Rev. Mod. Phys. 20, 367 (1948). The application to electrodynamics is described in detail by H. J. Groenewold, Koninklijke Nederlandsche Akademia van Weteschappen. Proceedings Vol. LII, 3 (226) 1949.

ing real quanta, while the interaction view is best for the discussion of the virtual quanta involved. We shall emphasize the interaction viewpoint in this paper, first because it is less familiar and therefore requires more discussion, and second because the important aspect in the problems with which we shall deal is the effect of virtual quanta.

The Hamiltonian method is not well adapted to represent the direct action at a distance between charges because that action is delayed. The Hamiltonian method represents the future as developing out of the present. If the values of a complete set of quantities are known now, their values can be computed at the next instant in time. If particles interact through a delayed interaction, however, one cannot predict the future by simply knowing the present motion of the particles. One would also have to know what the motions of the particles were in the past in view of the interaction this may have on the future motions. This is done in the Hamiltonian electrodynamics, of course, by requiring that one specify besides the present motion of the particles, the values of a host of new variables (the coordinates of the field oscillators) to keep track of that aspect of the past motions of the particles which determines their future behavior. The use of the Hamiltonian forces one to choose the field viewpoint rather than the interaction viewpoint.

In many problems, for example, the close collisions of particles, we are not interested in the precise temporal sequence of events. It is not of interest to be able to say how the situation would look at each instant of time during a collision and how it progresses from instant to instant. Such ideas are only useful for events taking a long time and for which we can readily obtain information during the intervening period. For collisions it is much easier to treat the process as a whole.[6] The Møller interaction matrix for the the collision of two electrons is not essentially more complicated than the nonrelativistic Rutherford formula, yet the mathematical machinery used to obtain the former from quantum electrodynamics is vastly more complicated than Schrödinger's equation with the e^2/r_{12} interaction needed to obtain the latter. The difference is only that in the latter the action is instantaneous so that the Hamiltonian method requires no extra variables, while in the former relativistic case it is delayed and the Hamiltonian method is very cumbersome.

We shall be discussing the solutions of equations rather than the time differential equations from which they come. We shall discover that the solutions, because of the over-all space-time view that they permit, are as easy to understand when interactions are delayed as when they are instantaneous.

As a further point, relativistic invariance will be self-evident. The Hamiltonian form of the equations develops the future from the instantaneous present. But for different observers in relative motion the instantaneous present is different, and corresponds to a different 3-dimensional cut of space-time. Thus the temporal analyses of different observers is different and their Hamiltonian equations are developing the process in different ways. These differences are irrelevant, however, for the solution is the same in any space time frame. By forsaking the Hamiltonian method, the wedding of relativity and quantum mechanics can be accomplished most naturally.

We illustrate these points in the next section by studying the solution of Schrödinger's equation for nonrelativistic particles interacting by an instantaneous Coulomb potential (Eq. 2). When the solution is modified to include the effects of delay in the interaction and the relativistic properties of the electrons we obtain an expression of the laws of quantum electrodynamics (Eq. 4).

2. THE INTERACTION BETWEEN CHARGES

We study by the same methods as in I, the interaction of two particles using the same notation as I. We start by considering the non-relativistic case described by the Schrödinger equation (I, Eq. 1). The wave function at a given time is a function $\psi(\mathbf{x}_a, \mathbf{x}_b, t)$ of the coordinates $\mathbf{x}_a$ and $\mathbf{x}_b$ of each particle. Thus call $K(\mathbf{x}_a, \mathbf{x}_b, t; \mathbf{x}_a', \mathbf{x}_b', t')$ the amplitude that particle a at $\mathbf{x}_a'$ at time t' will get to $\mathbf{x}_a$ at t while particle b at $\mathbf{x}_b'$ at t' gets to $\mathbf{x}_b$ at t. If the particles are free and do not interact this is

$$K(\mathbf{x}_a, \mathbf{x}_b, t; \mathbf{x}_a', \mathbf{x}_b', t') = K_{0a}(\mathbf{x}_a, t; \mathbf{x}_a', t') K_{0b}(\mathbf{x}_b, t; \mathbf{x}_b', t')$$

where K_{0a} is the K_0 function for particle a considered as free. In *this* case we can obviously define a quantity like K, but for which the time t need not be the same for particles a and b (likewise for t'); e.g.,

$$K_0(3, 4; 1, 2) = K_{0a}(3, 1) K_{0b}(4, 2) \tag{1}$$

can be thought of as the amplitude that particle a goes from $\mathbf{x}_1$ at t_1 to $\mathbf{x}_3$ at t_3 and that particle b goes from $\mathbf{x}_2$ at t_2 to $\mathbf{x}_4$ at t_4.

When the particles do interact, one can only define the quantity $K(3, 4; 1, 2)$ precisely if the interaction vanishes between t_1 and t_2 and also between t_3 and t_4. In a real physical system such is not the case. There is such an enormous advantage, however, to the concept that we shall continue to use it, imagining that we can neglect the effect of interactions between t_1 and t_2 and between t_3 and t_4. For practical problems this means choosing such long time intervals $t_3 - t_1$ and $t_4 - t_2$ that the extra interactions near the end points have small relative effects. As an example, in a scattering problem it may well be that the particles are so well separated initially and finally that the interaction at these times is negligible. Again energy values can be defined by the average rate of change of phase over such long time intervals that errors initially and finally can be neglected. Inasmuch as any physical problem can be defined in terms of scattering processes we do not lose much in

[6] This is the viewpoint of the theory of the S matrix of Heisenberg.

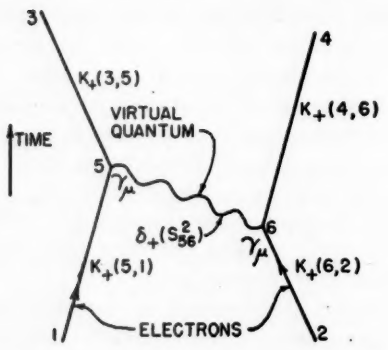

FIG. 1. The fundamental interaction Eq. (4). Exchange of one quantum between two electrons.

a general theoretical sense by this approximation. If it is not made it is not easy to study interacting particles relativistically, for there is nothing significant in choosing $t_1=t_3$ if $\mathbf{x}_1\neq\mathbf{x}_3$, as absolute simultaneity of events at a distance cannot be defined invariantly. It is essentially to avoid this approximation that the complicated structure of the older quantum electrodynamics has been built up. We wish to describe electrodynamics as a delayed interaction between particles. If we can make the approximation of assuming a meaning to $K(3,4;1,2)$ the results of this interaction can be expressed very simply.

To see how this may be done, imagine first that the interaction is simply that given by a Coulomb potential e^2/r where r is the distance between the particles. If this be turned on only for a very short time Δt_0 at time t_0, the first order correction to $K(3,4;1,2)$ can be worked out exactly as was Eq. (9) of I by an obvious generalization to two particles:

$$K^{(1)}(3,4;1,2)=-ie^2\int\int K_{0a}(3,5)K_{0b}(4,6)r_{56}^{-1}\times K_{0a}(5,1)K_{0b}(6,2)d^3\mathbf{x}_5 d^3\mathbf{x}_6\Delta t_0,$$

where $t_5=t_6=t_0$. If now the potential were on at all times (so that strictly K is not defined unless $t_4=t_3$ and $t_1=t_2$), the first-order effect is obtained by integrating on t_0, which we can write as an integral over both t_5 and t_6 if we include a delta-function $\delta(t_5-t_6)$ to insure contribution only when $t_5=t_6$. Hence, the first-order effect of interaction is (calling $t_5-t_6=t_{56}$):

$$K^{(1)}(3,4;1,2)=-ie^2\int\int K_{0a}(3,5)K_{0b}(4,6)r_{56}^{-1}\times\delta(t_{56})K_{0a}(5,1)K_{0b}(6,2)d\tau_5 d\tau_6, \quad (2)$$

where $d\tau=d^3\mathbf{x}dt$.

We know, however, in classical electrodynamics, that the Coulomb potential does not act instantaneously, but is delayed by a time r_{56}, taking the speed of light as unity. This suggests simply replacing $r_{56}^{-1}\delta(t_{56})$ in (2) by something like $r_{56}^{-1}\delta(t_{56}-r_{56})$ to represent the delay in the effect of b on a.

This turns out to be not quite right,[7] for when this interaction is represented by photons they must be of only positive energy, while the Fourier transform of $\delta(t_{56}-r_{56})$ contains frequencies of both signs. It should instead be replaced by $\delta_+(t_{56}-r_{56})$ where

$$\delta_+(x)=\int_0^\infty e^{-i\omega x}d\omega/\pi=\lim_{\epsilon\to 0}\frac{(\pi i)^{-1}}{x-i\epsilon}=\delta(x)+(\pi ix)^{-1}. \quad (3)$$

This is to be averaged with $r_{56}^{-1}\delta_+(-t_{56}-r_{56})$ which arises when $t_5<t_6$ and corresponds to a emitting the quantum which b receives. Since

$$(2r)^{-1}(\delta_+(t-r)+\delta_+(-t-r))=\delta_+(t^2-r^2),$$

this means $r_{56}^{-1}\delta(t_{56})$ is replaced by $\delta_+(s_{56}^2)$ where $s_{56}^2=t_{56}^2-r_{56}^2$ is the square of the relativistically invariant interval between points 5 and 6. Since in classical electrodynamics there is also an interaction through the vector potential, the complete interaction (see A, Eq. (1)) should be $(1-(\mathbf{v}_5\cdot\mathbf{v}_6)\delta_+(s_{56}^2)$, or in the relativistic case,

$$(1-\boldsymbol{\alpha}_a\cdot\boldsymbol{\alpha}_b)\delta_+(s_{56}^2)=\beta_a\beta_b\gamma_{a\mu}\gamma_{b\mu}\delta_+(s_{56}^2).$$

Hence we have for electrons obeying the Dirac equation,

$$K^{(1)}(3,4;1,2)=-ie^2\int\int K_{+a}(3,5)K_{+b}(4,6)\gamma_{a\mu}\gamma_{b\mu}\times\delta_+(s_{56}^2)K_{+a}(5,1)K_{+b}(6,2)d\tau_5 d\tau_6, \quad (4)$$

where $\gamma_{a\mu}$ and $\gamma_{b\mu}$ are the Dirac matrices applying to the spinor corresponding to particles a and b, respectively (the factor $\beta_a\beta_b$ being absorbed in the definition, I Eq. (17), of K_+).

This is our fundamental equation for electrodynamics. It describes the effect of exchange of one quantum (therefore first order in e^2) between two electrons. It will serve as a prototype enabling us to write down the corresponding quantities involving the exchange of two or more quanta between two electrons or the interaction of an electron with itself. It is a consequence of conventional electrodynamics. Relativistic invariance is clear. Since one sums over μ it contains the effects of both longitudinal and transverse waves in a relativistically symmetrical way.

We shall now interpret Eq. (4) in a manner which will permit us to write down the higher order terms. It can be understood (see Fig. 1) as saying that the amplitude for "a" to go from 1 to 3 and "b" to go from 2 to 4 is altered to first order because they can exchange a quantum. Thus, "a" can go to 5 (amplitude $K_+(5,1)$)

[7] It, and a like term for the effect of a on b, leads to a theory which, in the classical limit, exhibits interaction through half-advanced and half-retarded potentials. Classically, this is equivalent to purely retarded effects within a closed box from which no light escapes (e.g., see A, or J. A. Wheeler and R. P. Feynman, Rev. Mod. Phys. 17, 157 (1945)). Analogous theorems exist in quantum mechanics but it would lead us too far astray to discuss them now.

emit a quantum (longitudinal, transverse, or scalar $\gamma_{a\mu}$) and then proceed to 3 ($K_+(3,5)$). Meantime "b" goes to 6 ($K_+(6,2)$), absorbs the quantum ($\gamma_{b\mu}$) and proceeds to 4 ($K_+(4,6)$). The quantum meanwhile proceeds from 5 to 6, which it does with amplitude $\delta_+(s_{56}^2)$. We must sum over all the possible quantum polarizations μ and positions and times of emission 5, and of absorption 6. Actually if $t_5 > t_6$ it would be better to say that "a" absorbs and "b" emits but no attention need be paid to these matters, as all such alternatives are automatically contained in (4).

The correct terms of higher order in e^2 or involving larger numbers of electrons (interacting with themselves or in pairs) can be written down by the same kind of reasoning. They will be illustrated by examples as we proceed. In a succeeding paper they will all be deduced from conventional quantum electrodynamics.

Calculation, from (4), of the transition element between positive energy free electron states gives the Möller scattering of two electrons, when account is taken of the Pauli principle.

The exclusion principle for interacting charges is handled in exactly the same way as for non-interacting charges (I). For example, for two charges it requires only that one calculate $K(3,4;1,2)-K(4,3;1,2)$ to get the net amplitude for arrival of charges at 3 and 4. It is disregarded in intermediate states. The interference effects for scattering of electrons by positrons discussed by Bhabha will be seen to result directly in this formulation. The formulas are interpreted to apply to positrons in the manner discussed in I.

As our primary concern will be for processes in which the quanta are virtual we shall not include here the detailed analysis of processes involving real quanta in initial or final state, and shall content ourselves by only stating the rules applying to them.[8] The result of the analysis is, as expected, that they can be included by the same line of reasoning as is used in discussing the virtual processes, provided the quantities are normalized in the usual manner to represent single quanta. For example, the amplitude that an electron in going from 1 to 2 absorbs a quantum whose vector potential, suitably normalized, is $c_\mu \exp(-ik\cdot x)=C_\mu(x)$ is just the expression (I, Eq. (13)) for scattering in a potential with $\boldsymbol{A}$ (3) replaced by $\boldsymbol{C}$ (3). Each quantum interacts only once (either in emission or in absorption), terms like (I, Eq. (14)) occur only when there is more than one quantum involved. The Bose statistics of the quanta can, in all cases, be disregarded in intermediate states. The only effect of the statistics is to change the weight of initial or final states. If there are among quanta, in the initial state, some n which are identical then the weight of the state is $(1/n!)$ of what it would be if these quanta were considered as different (similarly for the final state).

3. THE SELF-ENERGY PROBLEM

Having a term representing the mutual interaction of a pair of charges, we must include similar terms to represent the interaction of a charge with itself. For under some circumstances what appears to be two distinct electrons may, according to I, be viewed also as a single electron (namely in case one electron was created in a pair with a positron destined to annihilate the other electron). Thus to the interaction between such electrons must correspond the possibility of the action of an electron on itself.[9]

This interaction is the heart of the self energy problem. Consider to first order in e^2 the action of an electron on itself in an otherwise force free region. The amplitude $K(2,1)$ for a single particle to get from 1 to 2 differs from $K_+(2,1)$ to first order in e^2 by a term

$$K^{(1)}(2,1)=-ie^2\int\int K_+(2,4)\gamma_\mu K_+(4,3)\gamma_\mu \times K_+(3,1)d\tau_3 d\tau_4 \delta_1(s_{43}^2). \quad (6)$$

It arises because the electron instead of going from 1 directly to 2, may go (Fig. 2) first to 3, ($K_+(3,1)$), emit a quantum (γ_μ), proceed to 4, ($K_+(4,3)$), absorb it (γ_μ), and finally arrive at 2 ($K_+(2,4)$). The quantum must go from 3 to 4 ($\delta_+(s_{43}^2)$).

This is related to the self-energy of a free electron in the following manner. Suppose initially, time t_1, we have an electron in state $f(1)$ which we imagine to be a positive energy solution of Dirac's equation for a free particle. After a long time t_2-t_1 the perturbation will alter

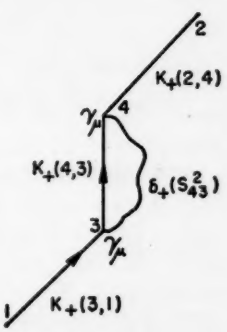

FIG. 2. Interaction of an electron with itself, Eq. (6).

[8] Although in the expressions stemming from (4) the quanta are virtual, this is not actually a theoretical limitation. One way to deduce the correct rules for real quanta from (4) is to note that in a closed system all quanta can be considered as virtual (i.e., they have a known source and are eventually absorbed) so that in such a system the present description is complete and equivalent to the conventional one. In particular, the relation of the Einstein A and B coefficients can be deduced. A more practical direct deduction of the expressions for real quanta will be given in the subsequent paper. It might be noted that (4) can be rewritten as describing the action on a, $K^{(1)}(3,1)=i\int K_+(3,5)\times \boldsymbol{A}(5)K_+(5,1)d\tau_5$ of the potential $A_\mu(5)=e^2\int K_+(4,6)\delta_+(s_{56}^2)\gamma_\mu \times K_+(6,2)d\tau_6$ arising from Maxwell's equations $-\Box^2 A_\mu=4\pi j_\mu$ from a "current" $j_\mu(6)=e^2K_+(4,6)\gamma_\mu K_+(6,2)$ produced by particle b in going from 2 to 4. This is virtue of the fact that δ_+ satisfies

$$-\Box_2^2\delta_+(s_{21}^2)=4\pi\delta(2,1). \quad (5)$$

[9] These considerations make it appear unlikely that the contention of J. A. Wheeler and R. P. Feynman, Rev. Mod. Phys. 17, 157 (1945), that electrons do not act on themselves, will be a successful concept in quantum electrodynamics.

the wave function, which can then be looked upon as a superposition of free particle solutions (actually it only contains f). The amplitude that $g(2)$ is contained is calculated as in (I, Eq. (21)). The diagonal element ($g=f$) is therefore

$$\int\int \bar{f}(2)\beta K^{(1)}(2,1)\beta f(1)d^3\mathbf{x}_1 d^3\mathbf{x}_2. \quad (7)$$

The time interval $T=t_2-t_1$ (and the spatial volume V over which one integrates) must be taken very large, for the expressions are only approximate (analogous to the situation for two interacting charges).[10] This is because, for example, we are dealing incorrectly with quanta emitted just before t_2 which would normally be reabsorbed at times after t_2.

If $K^{(1)}(2,1)$ from (6) is actually substituted into (7) the surface integrals can be performed as was done in obtaining I, Eq. (22) resulting in

$$-ie^2\int\int \bar{f}(4)\gamma_\mu K_+(4,3)\gamma_\mu f(3)\delta_+(s_{43}^2)d\tau_3 d\tau_4. \quad (8)$$

Putting for $f(1)$ the plane wave $u\exp(-ip\cdot x_1)$ where p_μ is the energy (p_4) and momentum of the electron ($p^2=m^2$), and u is a constant 4-index symbol, (8) becomes

$$-ie^2\int\int (\bar{u}\gamma_\mu K_+(4,3)\gamma_\mu u) \times\exp(ip\cdot(x_4-x_3))\delta_+(s_{43}^2)d\tau_3 d\tau_4,$$

the integrals extending over the volume V and time interval T. Since $K_+(4,3)$ depends only on the difference of the coordinates of 4 and 3, $x_{43\mu}$, the integral on 4 gives a result (except near the surfaces of the region) independent of 3. When integrated on 3, therefore, the result is of order VT. The effect is proportional to V, for the wave functions have been normalized to unit volume. If normalized to volume V, the result would simply be proportional to T. This is expected, for if the effect were equivalent to a change in energy ΔE, the amplitude for arrival in f at t_2 is altered by a factor $\exp(-i\Delta E(t_2-t_1))$, or to first order by the difference $-i(\Delta E)T$. Hence, we have

$$\Delta E=e^2\int (\bar{u}\gamma_\mu K_+(4,3)\gamma_\mu u)\exp(ip\cdot x_{43})\delta_+(s_{43}^2)d\tau_4, \quad (9)$$

integrated over all space-time $d\tau_4$. This expression will be simplified presently. In interpreting (9) we have tacitly assumed that the wave functions are normalized so that $(u^*u)=(\bar{u}\gamma_4 u)=1$. The equation may therefore be made independent of the normalization by writing the left side as $(\Delta E)(\bar{u}\gamma_4 u)$, or since $(\bar{u}\gamma_4 u)=(E/m)(\bar{u}u)$ and $m\Delta m=E\Delta E$, as $\Delta m(\bar{u}u)$ where Δm is an equivalent change in mass of the electron. In this form invariance is obvious.

One can likewise obtain an expression for the energy shift for an electron in a hydrogen atom. Simply replace K_+ in (8), by $K_+^{(V)}$, the exact kernel for an electron in the potential, $V=\beta e^2/r$, of the atom, and f by a wave function (of space and time) for an atomic state. In general the ΔE which results is not real. The imaginary part is negative and in $\exp(-i\Delta ET)$ produces an exponentially decreasing amplitude with time. This is because we are asking for the amplitude that an atom initially with no photon in the field, will still appear after time T with no photon. If the atom is in a state which can radiate, this amplitude must decay with time. The imaginary part of ΔE when calculated does indeed give the correct rate of radiation from atomic states. It is zero for the ground state and for a free electron.

In the non-relativistic region the expression for ΔE can be worked out as has been done by Bethe.[11] In the relativistic region (points 4 and 3 as close together as a Compton wave-length) the $K_+^{(V)}$ which should appear in (8) can be replaced to first order in V by K_+ plus $K_+^{(1)}(2,1)$ given in I, Eq. (13). The problem is then very similar to the radiationless scattering problem discussed below.

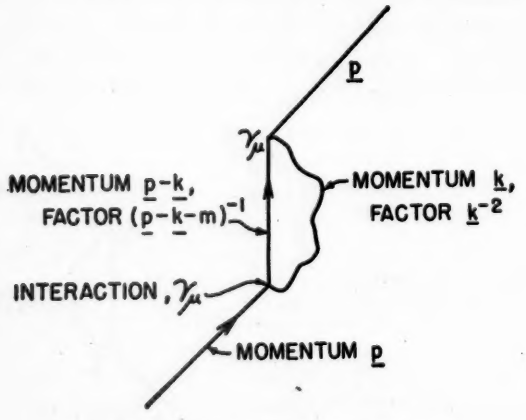

FIG. 3. Interaction of an electron with itself. Momentum space, Eq. (11).

4. EXPRESSION IN MOMENTUM AND ENERGY SPACE

The evaluation of (9), as well as all the other more complicated expressions arising in these problems, is very much simplified by working in the momentum and energy variables, rather than space and time. For this we shall need the Fourier Transform of $\delta_+(s_{21}^2)$ which is

$$-\delta_+(s_{21}^2)=\pi^{-1}\int \exp(-ik\cdot x_{21})k^{-2}d^4k, \quad (10)$$

which can be obtained from (3) and (5) or from I, Eq. (32) noting that $I_+(2,1)$ for $m^2=0$ is $\delta_+(s_{21}^2)$ from

[10] This is discussed in reference 5 in which it is pointed out that the concept of a wave function loses accuracy if there are delayed self-actions.

[11] H. A. Bethe, Phys. Rev. 72, 339 (1947).

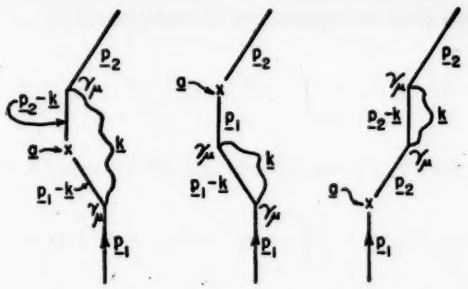

FIG. 4. Radiative correction to scattering, momentum space.

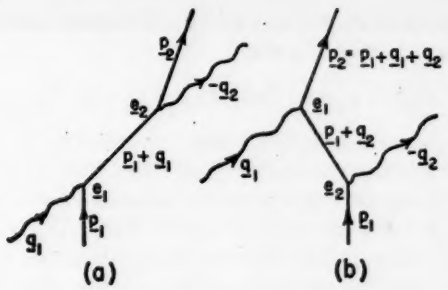

FIG. 5. Compton scattering, Eq. (15).

I, Eq. (34): The k^{-2} means $(k\cdot k)^{-1}$ or more precisely the limit as $\delta\to 0$ of $(k\cdot k+i\delta)^{-1}$. Further d^4k means $(2\pi)^{-2}dk_1dk_2dk_3dk_4$. If we imagine that quanta are particles of zero mass, then we can make the general rule that all poles are to be resolved by considering the masses of the particles and quanta to have infinitesimal negative imaginary parts.

Using these results we see that the self-energy (9) is the matrix element between $\bar{u}$ and u of the matrix

$$(e^2/\pi i)\int \gamma_\mu(p-k-m)^{-1}\gamma_\mu k^{-2}d^4k, \qquad (11)$$

where we have used the expression (I, Eq. (31)) for the Fourier transform of K_+. This form for the self-energy is easier to work with than is (9).

The equation can be understood by imagining (Fig. 3) that the electron of momentum p emits (γ_μ) a quantum of momentum k, and makes its way now with momentum $p-k$ to the next event (factor $(p-k-m)^{-1}$) which is to absorb the quantum (another γ_μ). The amplitude of propagation of quanta is k^{-2}. (There is a factor $e^2/\pi i$ for each virtual quantum). One integrates over all quanta. The reason an electron of momentum p propagates as $1/(p-m)$ is that this operator is the reciprocal of the Dirac equation operator, and we are simply solving this equation. Likewise light goes as $1/k^2$, for this is the reciprocal D'Alembertian operator of the wave equation of light. The first γ_μ represents the current which generates the vector potential, while the second is the velocity operator by which this potential is multiplied in the Dirac equation when an external field acts on an electron.

Using the same line of reasoning, other problems may be set up directly in momentum space. For example, consider the scattering in a potential $A=A_\mu\gamma_\mu$ varying in space and time as $a\exp(-iq\cdot x)$. An electron initially in state of momentum $p_1=p_{1\mu}\gamma_\mu$ will be deflected to state p_2 where $p_2=p_1+q$. The zero-order answer is simply the matrix element of a between states 1 and 2. We next ask for the first order (in e^2) radiative correction due to virtual radiation of one quantum. There are several ways this can happen. First for the case illustrated in Fig. 4(a), find the matrix:

$$(e^2/\pi i)\int \gamma_\mu(p_2-k-m)^{-1}a(p_1-k-m)^{-1}\gamma_\mu k^{-2}d^4k. \qquad (12)$$

For in this case, first[12] a quantum of momentum k is emitted (γ_μ), the electron then having momentum p_1-k and hence propagating with factor $(p_1-k-m)^{-1}$. Next it is scattered by the potential (matrix a) receiving additional momentum q, propagating on then (factor $(p_2-k-m)^{-1}$) with the new momentum until the quantum is reabsorbed (γ_μ). The quantum propagates from emission to absorption (k^{-2}) and we integrate over all quanta (d^4k), and sum on polarization μ. When this is integrated on k_4, the result can be shown to be exactly equal to the expressions (16) and (17) given in B for the same process, the various terms coming from residues of the poles of the integrand (12).

Or again if the quantum is both emitted and reabsorbed before the scattering takes place one finds (Fig. 4(b))

$$(e^2/\pi i)\int a(p_1-m)^{-1}\gamma_\mu(p_1-k-m)^{-1}\gamma_\mu k^{-2}d^4k, \qquad (13)$$

or if both emission and absorption occur after the scattering, (Fig. 4(c))

$$(e^2/\pi i)\int \gamma_\mu(p_2-k-m)^{-1}\gamma_\mu(p_2-m)^{-1}ak^{-2}d^4k. \qquad (14)$$

These terms are discussed in detail below.

We have now achieved our simplification of the form of writing matrix elements arising from virtual processes. Processes in which a number of real quanta is given initially and finally offer no problem (assuming correct normalization). For example, consider the Compton effect (Fig. 5(a)) in which an electron in state p_1 absorbs a quantum of momentum q_1, polarization vector $e_{1\mu}$ so that its interaction is $e_{1\mu}\gamma_\mu=e_1$, and emits a second quantum of momentum $-q_2$, polarization e_2 to arrive in final state of momentum p_2. The matrix for

[12] First, next, etc., here refer not to the order in true time but to the succession of events along the trajectory of the electron. That is, more precisely, to the order of appearance of the matrices in the expressions.

this process is $e_2(p_1+q_1-m)^{-1}e_1$. The total matrix for the Compton effect is, then,

$$e_2(p_1+q_1-m)^{-1}e_1+e_1(p_1+q_2-m)^{-1}e_2, \quad (15)$$

the second term arising because the emission of e_2 may also precede the absorption of e_1 (Fig. 5(b)). One takes matrix elements of this between initial and final electron states ($p_1+q_1=p_2-q_2$), to obtain the Klein Nishina formula. Pair annihilation with emission of two quanta, etc., are given by the same matrix, positron states being those with negative time component of p. Whether quanta are absorbed or emitted depends on whether the time component of q is positive or negative.

5. THE CONVERGENCE OF PROCESSES WITH VIRTUAL QUANTA

These expressions are, as has been indicated, no more than a re-expression of conventional quantum electrodynamics. As a consequence, many of them are meaningless. For example, the self-energy expression (9) or (11) gives an infinite result when evaluated. The infinity arises, apparently, from the coincidence of the δ-function singularities in $K_+(4, 3)$ and $\delta_+(s_{43}^2)$. Only at this point is it necessary to make a real departure from conventional electrodynamics, a departure other than simply rewriting expressions in a simpler form.

We desire to make a modification of quantum electrodynamics analogous to the modification of classical electrodynamics described in a previous article, A. There the $\delta(s_{12}^2)$ appearing in the action of interaction was replaced by $f(s_{12}^2)$ where $f(x)$ is a function of small width and great height.

The obvious corresponding modification in the quantum theory is to replace the $\delta_+(s^2)$ appearing the quantum mechanical interaction by a new function $f_+(s^2)$. We can postulate that if the Fourier transform of the classical $f(s_{12}^2)$ is the integral over all k of $F(k^2)\exp(-ik\cdot x_{12})d^4k$, then the Fourier transform of $f_+(s^2)$ is the same integral taken over only positive frequencies k_4 for $t_2>t_1$ and over only negative ones for $t_2<t_1$ in analogy to the relation of $\delta_+(s^2)$ to $\delta(s^2)$. The function $f(s^2)=f(x\cdot x)$ can be written* as

$$f(x\cdot x)=(2\pi)^{-2}\int_{k_4=0}^{\infty}\int \sin(k_4|x_4|)\times\cos(\mathbf{K}\cdot\mathbf{x})dk_4d^3\mathbf{K}g(k\cdot k),$$

where $g(k\cdot k)$ is k_4^{-1} times the density of oscillators and may be expressed for positive k_4 as (A, Eq. (16))

$$g(k^2)=\int_0^{\infty}(\delta(k^2)-\delta(k^2-\lambda^2))G(\lambda)d\lambda,$$

where $\int_0^{\infty}G(\lambda)d\lambda=1$ and G involves values of λ large compared to m. This simply means that the amplitude for propagation of quanta of momentum k is

$$-F_+(k^2)=\pi^{-1}\int_0^{\infty}(k^{-2}-(k^2-\lambda^2)^{-1})G(\lambda)d\lambda,$$

rather than k^{-2}. That is, writing $F_+(k^2)=-\pi^{-1}k^{-2}C(k^2)$,

$$-f_+(s_{12}^2)=\pi^{-1}\int \exp(-ik\cdot x_{12})k^{-2}C(k^2)d^4k. \quad (16)$$

Every integral over an intermediate quantum which previously involved a factor d^4k/k^2 is now supplied with a convergence factor $C(k^2)$ where

$$C(k^2)=\int_0^{\infty}-\lambda^2(k^2-\lambda^2)^{-1}G(\lambda)d\lambda. \quad (17)$$

The poles are defined by replacing k^2 by $k^2+i\delta$ in the limit $\delta\to 0$. That is λ^2 may be assumed to have an infinitesimal negative imaginary part.

The function $f_+(s_{12}^2)$ may still have a discontinuity in value on the light cone. This is of no influence for the Dirac electron. For a particle satisfying the Klein Gordon equation, however, the interaction involves gradients of the potential which reinstates the δ function if f has discontinuities. The condition that f is to have no discontinuity in value on the light cone implies $k^2C(k^2)$ approaches zero as k^2 approaches infinity. In terms of $G(\lambda)$ the condition is

$$\int_0^{\infty}\lambda^2G(\lambda)d\lambda=0. \quad (18)$$

This condition will also be used in discussing the convergence of vacuum polarization integrals.

The expression for the self-energy matrix is now

$$(e^2/\pi i)\int\gamma_\mu(p-k-m)^{-1}\gamma_\mu k^{-2}d^4kC(k^2), \quad (19)$$

which, since $C(k^2)$ falls off at least as rapidly as $1/k^2$, converges. For practical purposes we shall suppose hereafter that $C(k^2)$ is simply $-\lambda^2/(k^2-\lambda^2)$ implying that some average (with weight $G(\lambda)d\lambda$) over values of λ may be taken afterwards. Since in all processes the quantum momentum will be contained in at least one extra factor of the form $(p-k-m)^{-1}$ representing propagation of an electron while that quantum is in the field, we can expect all such integrals with their convergence factors to converge and that the result of all such processes will now be finite and definite (excepting the processes with closed loops, discussed below, in which the diverging integrals are over the momenta of the electrons rather than the quanta).

The integral of (19) with $C(k^2)=-\lambda^2(k^2-\lambda^2)^{-1}$ noting that $p^2=m^2$, $\lambda\gg m$ and dropping terms of order m/λ, is (see Appendix A)

$$(e^2/2\pi)[4m(\ln(\lambda/m)+\tfrac{1}{2})-p(\ln(\lambda/m)+5/4)]. \quad (20)$$

* This relation is given incorrectly in A, equation just preceding 16.

When applied to a state of an electron of momentum $\boldsymbol{p}$ satisfying $\boldsymbol{pu}=m\boldsymbol{u}$, it gives for the change in mass (as in B, Eq. (9))

$$\Delta m=m(e^2/2\pi)(3\ln(\lambda/m)+\tfrac{3}{4}). \tag{21}$$

6. RADIATIVE CORRECTIONS TO SCATTERING

We can now complete the discussion of the radiative corrections to scattering. In the integrals we include the convergence factor $C(\boldsymbol{k}^2)$, so that they converge for large $\boldsymbol{k}$. Integral (12) is also not convergent because of the well-known infra-red catastrophy. For this reason we calculate (as discussed in B) the value of the integral assuming the photons to have a small mass $\lambda_{\min}\ll m\ll\lambda$. The integral (12) becomes

$$(e^2/\pi i)\int\gamma_\mu(\boldsymbol{p}_2-\boldsymbol{k}-m)^{-1}\boldsymbol{a}(\boldsymbol{p}_1-\boldsymbol{k}-m)^{-1}\times\gamma_\mu(\boldsymbol{k}^2-\lambda_{\min}{}^2)^{-1}d^4kC(\boldsymbol{k}^2-\lambda_{\min}{}^2),$$

which when integrated (see Appendix B) gives $(e^2/2\pi)$ times

$$\left[2\left(\ln\frac{m}{\lambda_{\min}}-1\right)\left(1-\frac{2\theta}{\tan2\theta}\right)+\theta\tan\theta+\frac{4}{\tan2\theta}\int_0^\theta\alpha\tan\alpha d\alpha\right]\boldsymbol{a}+\frac{1}{4m}(\boldsymbol{qa}-\boldsymbol{aq})\frac{2\theta}{\sin2\theta}+r\boldsymbol{a}, \tag{22}$$

where $(q^2)^{\frac{1}{2}}=2m\sin\theta$ and we have assumed the matrix to operate between states of momentum $\boldsymbol{p}_1$ and $\boldsymbol{p}_2=\boldsymbol{p}_1+\boldsymbol{q}$ and have neglected terms of order $\lambda_{\min}/m$, m/λ, and q^2/λ^2. Here the only dependence on the convergence factor is in the term $r\boldsymbol{a}$, where

$$r=\ln(\lambda/m)+9/4-2\ln(m/\lambda_{\min}). \tag{23}$$

As we shall see in a moment, the other terms (13), (14) give contributions which just cancel the $r\boldsymbol{a}$ term. The remaining terms give for small $\boldsymbol{q}$,

$$(e^2/4\pi)\left(\frac{1}{2m}(\boldsymbol{qa}-\boldsymbol{aq})+\frac{4\boldsymbol{q}^2}{3m^2}\boldsymbol{a}\left(\ln\frac{m}{\lambda_{\min}}-\frac{3}{8}\right)\right), \tag{24}$$

which shows the change in magnetic moment and the Lamb shift as interpreted in more detail in B.[13]

We must now study the remaining terms (13) and (14). The integral on $\boldsymbol{k}$ in (13) can be performed (after multiplication by $C(\boldsymbol{k}^2)$) since it involves nothing but the integral (19) for the self-energy and the result is allowed to operate on the initial state $\boldsymbol{u}_1$, (so that $\boldsymbol{p}_1\boldsymbol{u}_1=m\boldsymbol{u}_1$). Hence the factor following $\boldsymbol{a}(\boldsymbol{p}_1-m)^{-1}$ will be just Δm. But, if one now tries to expand $1/(\boldsymbol{p}_1-m)=(\boldsymbol{p}_1+m)/(\boldsymbol{p}_1{}^2-m^2)$ one obtains an infinite result, since $\boldsymbol{p}_1{}^2=m^2$. This is, however, just what is expected physically. For the quantum can be emitted and absorbed at any time previous to the scattering. Such a process has the effect of a change in mass of the electron in the state 1. It therefore changes the energy by ΔE and the amplitude to first order in ΔE by $-i\Delta E\cdot t$ where t is the time it is acting, which is infinite. That is, the major effect of this term would be canceled by the effect of change of mass Δm.

The situation can be analyzed in the following manner. We suppose that the electron approaching the scattering potential $\boldsymbol{a}$ has not been free for an infinite time, but at some time far past suffered a scattering by a potential $\boldsymbol{b}$. If we limit our discussion to the effects of Δm and of the virtual radiation of one quantum between two such scatterings each of the effects will be finite, though large, and their difference is determinate. The propagation from $\boldsymbol{b}$ to $\boldsymbol{a}$ is represented by a matrix

$$\boldsymbol{a}(\boldsymbol{p}'-m)^{-1}\boldsymbol{b}, \tag{25}$$

in which one is to integrate possibly over $\boldsymbol{p}'$ (depending on details of the situation). (If the time is long between $\boldsymbol{b}$ and $\boldsymbol{a}$, the energy is very nearly determined so that $\boldsymbol{p}'^2$ is very nearly m^2.)

We shall compare the effect on the matrix (25) of the virtual quanta and of the change of mass Δm. The effect of a virtual quantum is

$$(e^2/\pi i)\int\boldsymbol{a}(\boldsymbol{p}'-m)^{-1}\gamma_\mu(\boldsymbol{p}'-\boldsymbol{k}-m)^{-1}\times\gamma_\mu(\boldsymbol{p}'-m)^{-1}\boldsymbol{b}k^{-2}d^4kC(\boldsymbol{k}^2), \tag{26}$$

while that of a change of mass can be written

$$\boldsymbol{a}(\boldsymbol{p}'-m)^{-1}\Delta m(\boldsymbol{p}'-m)^{-1}\boldsymbol{b}, \tag{27}$$

and we are interested in the difference (26)–(27). A simple and direct method of making this comparison is just to evaluate the integral on $\boldsymbol{k}$ in (26) and subtract from the result the expression (27) where Δm is given in (21). The remainder can be expressed as a multiple $-r(\boldsymbol{p}'^2)$ of the unperturbed amplitude (25);

$$-r(\boldsymbol{p}'^2)\boldsymbol{a}(\boldsymbol{p}'-m)^{-1}\boldsymbol{b}. \tag{28}$$

This has the same result (to this order) as replacing the potentials $\boldsymbol{a}$ and $\boldsymbol{b}$ in (25) by $(1-\frac{1}{2}r(\boldsymbol{p}'^2))\boldsymbol{a}$ and

[13] That the result given in B in Eq. (19) was in error was repeatedly pointed out to the author, in private communication, by V. F. Weisskopf and J. B. French, as their calculation, completed simultaneously with the author's early in 1948, gave a different result. French has finally shown that although the expression for the radiationless scattering B, Eq. (18) or (24) above is correct, it was incorrectly joined onto Bethe's non-relativistic result. He shows that the relation $\ln2k_{\max}-1=\ln\lambda_{\min}$ used by the author should have been $\ln2k_{\max}-5/6=\ln\lambda_{\min}$. This results in adding a term $-(1/6)$ to the logarithm in B, Eq. (19) so that the result now agrees with that of J. B. French and V. F. Weisskopf, Phys. Rev. **75**, 1240 (1949) and N. H. Kroll and W. E. Lamb, Phys. Rev. **75**, 388 (1949). The author feels unhappily responsible for the very considerable delay in the publication of French's result occasioned by this error. This footnote is appropriately numbered.

$(1-\frac{1}{2}r(\not{p}'^2))b$. In the limit, then, as $\not{p}'^2 \to m^2$ the net effect on the scattering is $-\frac{1}{2}ra$ where r, the limit of $r(\not{p}'^2)$ as $\not{p}'^2 \to m^2$ (assuming the integrals have an infrared cut-off), turns out to be just equal to that given in (23). An equal term $-\frac{1}{2}ra$ arises from virtual transitions after the scattering (14) so that the entire ra term in (22) is canceled.

The reason that r is just the value of (12) when $q^2=0$ can also be seen without a direct calculation as follows: Let us call $\not{p}$ the vector of length m in the direction of $\not{p}'$ so that if $\not{p}'^2=m(1+\epsilon)^2$ we have $\not{p}'=(1+\epsilon)\not{p}$ and we take ϵ as very small, being of order T^{-1} where T is the time between the scatterings b and a. Since $(\not{p}'-m)^{-1}=(\not{p}'+m)/(\not{p}'^2-m^2)\approx(\not{p}+m)/2m^2\epsilon$, the quantity (25) is of order ϵ^{-1} or T. We shall compute corrections to it only to its own order (ϵ^{-1}) in the limit $\epsilon \to 0$. The term (27) can be written approximately[14] as

$$(e^2/\pi i)\int a(\not{p}'-m)^{-1}\gamma_\mu(\not{p}-\not{k}-m)^{-1} \times\gamma_\mu(\not{p}'-m)^{-1}b k^{-2}d^4kC(k^2),$$

using the expression (19) for Δm. The net of the two effects is therefore approximately[15]

$$-(e^2/\pi i)\int a(\not{p}'-m)^{-1}\gamma_\mu(\not{p}-\not{k}-m)^{-1}\epsilon\not{p}(\not{p}-\not{k}-m)^{-1} \times\gamma_\mu(\not{p}'-m)^{-1}b k^{-2}d^4kC(k^2),$$

a term now of order $1/\epsilon$ (since $(\not{p}'-m)^{-1}\approx(\not{p}+m)\times(2m^2\epsilon)^{-1}$) and therefore the one desired in the limit. Comparison to (28) gives for r the expression

$$(\not{p}_1+m/2m)\int \gamma_\mu(\not{p}_1-\not{k}-m)^{-1}(\not{p}_1 m^{-1})(\not{p}_1-\not{k}-m)^{-1} \times\gamma_\mu k^{-2}d^4kC(k^2). \quad (29)$$

The integral can be immediately evaluated, since it is the same as the integral (12), but with $q=0$, for a replaced by $\not{p}_1/m$. The result is therefore $r\cdot(\not{p}_1/m)$ which when acting on the state u_1 is just r, as $\not{p}_1 u_1=mu_1$. For the same reason the term $(\not{p}_1+m)/2m$ in (29) is effectively 1 and we are left with $-r$ of (23).[16]

In more complex problems starting with a free electron the same type of term arises from the effects of a virtual emission and absorption both previous to the other processes. They, therefore, simply lead to the same factor r so that the expression (23) may be used directly and these renormalization integrals need not be computed afresh for each problem.

In this problem of the radiative corrections to scattering the net result is insensitive to the cut-off. This means, of course, that by a simple rearrangement of terms previous to the integration we could have avoided the use of the convergence factors completely (see for example Lewis[17]). The problem was solved in the manner here in order to illustrate how the use of such convergence factors, even when they are actually unnecessary, may facilitate analysis somewhat by removing the effort and ambiguities that may be involved in trying to rearrange the otherwise divergent terms.

The replacement of δ_+ by f_+ given in (16), (17) is not determined by the analogy with the classical problem. In the classical limit only the real part of δ_+ (i.e., just δ) is easy to interpret. But by what should the imaginary part, $1/(\pi i s^2)$, of δ_+ be replaced? The choice we have made here (in defining, as we have, the location of the poles of (17)) is arbitrary and almost certainly incorrect. If the radiation resistance is calculated for an atom, as the imaginary part of (8), the result depends slightly on the function f_+. On the other hand the light radiated at very large distances from a source is independent of f_+. The total energy absorbed by distant absorbers will not check with the energy loss of the source. We are in a situation analogous to that in the classical theory if the entire f function is made to contain only retarded contributions (see A, Appendix). One desires instead the analogue of $\langle F\rangle_{\text{ret}}$ of A. This problem is being studied.

One can say therefore, that this attempt to find a consistent modification of quantum electrodynamics is incomplete (see also the question of closed loops, below). For it could turn out that any correct form of f_+ which will guarantee energy conservation may at the same time not be able to make the self-energy integral finite. The desire to make the methods of simplifying the calculation of quantum electrodynamic processes more widely available has prompted this publication before an analysis of the correct form for f_+ is complete. One might try to take the position that, since the energy discrepancies discussed vanish in the limit $\lambda\to\infty$, the correct physics might be considered to be that obtained by letting $\lambda\to\infty$ after mass renormalization. I have no proof of the mathematical consistency of this procedure, but the presumption is very strong that it is satisfactory. (It is also strong that a satisfactory form for f_+ can be found.)

7. THE PROBLEM OF VACUUM POLARIZATION

In the analysis of the radiative corrections to scattering one type of term was not considered. The potential

[14] The expression is not exact because the substitution of Δm by the integral in (19) is valid only if $\not{p}$ operates on a state such that $\not{p}$ can be replaced by m. The error, however, is of order $a(\not{p}'-m)^{-1}(\not{p}-m)(\not{p}'-m)^{-1}b$ which is $a((1+\epsilon)\not{p}+m)(\not{p}-m)\times((1+\epsilon)\not{p}+m)\not{p}(2\epsilon+\epsilon^2)^{-2}m^{-4}$. But since $\not{p}^2=m^2$, we have $\not{p}(\not{p}-m)=-m(\not{p}-m)=(\not{p}-m)\not{p}$ so the net result is approximately $a(\not{p}-m)b/4m^2$ and is not of order $1/\epsilon$ but smaller, so that its effect drops out in the limit.

[15] We have used, to first order, the general expansion (valid for any operators A, B)

$$(A+B)^{-1}=A^{-1}-A^{-1}BA^{-1}+A^{-1}BA^{-1}BA^{-1}-\cdots$$

with $A=\not{p}-\not{k}-m$ and $B=\not{p}'-\not{p}=\epsilon\not{p}$ to expand the difference of $(\not{p}'-\not{k}-m)^{-1}$ and $(\not{p}-\not{k}-m)^{-1}$.

[16] The renormalization terms appearing B, Eqs. (14), (15) when translated directly into the present notation do not give twice (29) but give this expression with the central $\not{p}_1 m^{-1}$ factor replaced by $m\gamma_4/E_1$ where $E_1=p_{1\mu}$ for $\mu=4$. When integrated it therefore gives $ra((\not{p}_1+m)/2m)(m\gamma_4/E_1)$ or $ra-ra(m\gamma_4/E_1)(\not{p}_1-m)/2m$. (Since $\not{p}_1\gamma_4+\gamma_4\not{p}_1=2E_1$) which gives just ra, since $\not{p}_1 u_1=mu_1$.

[17] H. W. Lewis, Phys. Rev. 73, 173 (1948).

which we can assume to vary as $a_\mu \exp(-iq\cdot x)$ creates a pair of electrons (see Fig. 6), momenta p_a, $-p_b$. This pair then reannihilates, emitting a quantum $q=p_b-p_a$, which quantum scatters the original electron from state 1 to state 2. The matrix element for this process (and the others which can be obtained by rearranging the order in time of the various events) is

$$-(e^2/\pi i)(\bar{u}_2\gamma_\mu u_1)\int Sp[(p_a+q-m)^{-1}\times\gamma_\nu(p_a-m)^{-1}\gamma_\mu]d^4p_a q^{-2}C(q^2)a_\nu. \quad (30)$$

This is because the potential produces the pair with amplitude proportional to $a_\nu\gamma_\nu$, the electrons of momenta p_a and $-(p_a+q)$ proceed from there to annihilate, producing a quantum (factor γ_μ) which propagates (factor $q^{-2}C(q^2)$) over to the other electron, by which it is absorbed (matrix element of γ_μ between states 1 and 2 of the original electron $(\bar{u}_2\gamma_\mu u_1)$). All momenta p_a and spin states of the virtual electron are admitted, which means the spur and the integral on d^4p_a are calculated.

One can imagine that the closed loop path of the positron-electron produces a current

$$4\pi j_\mu = J_{\mu\nu}a_\nu, \quad (31)$$

which is the source of the quanta which act on the second electron. The quantity

$$J_{\mu\nu}=-(e^2/\pi i)\int Sp[(p+q-m)^{-1}\times\gamma_\nu(p-m)^{-1}\gamma_\mu]d^4p, \quad (32)$$

is then characteristic for this problem of polarization of the vacuum.

One sees at once that $J_{\mu\nu}$ diverges badly. The modification of δ to f alters the amplitude with which the current j_μ will affect the scattered electron, but it can do nothing to prevent the divergence of the integral (32) and of its effects.

One way to avoid such difficulties is apparent. From one point of view we are considering all routes by which a given electron can get from one region of space-time to another, i.e., from the source of electrons to the apparatus which measures them. From this point of view the closed loop path leading to (32) is unnatural. It might be assumed that the only paths of meaning are those which start from the source and work their way in a continuous path (possibly containing many time reversals) to the detector. Closed loops would be excluded. We have already found that this may be done for electrons moving in a fixed potential.

Such a suggestion must meet several questions, however. The closed loops are a consequence of the usual hole theory in electrodynamics. Among other things, they are required to keep probability conserved. The probability that no pair is produced by a potential is not unity and its deviation from unity arises from the imaginary part of $J_{\mu\nu}$. Again, with closed loops excluded, a pair of electrons once created cannot annihilate one another again, the scattering of light by light would be zero, etc. Although we are not experimentally sure of these phenomena, this does seem to indicate that the closed loops are necessary. To be sure, it is always possible that these matters of probability conservation, etc., will work themselves out as simply in the case of interacting particles as for those in a fixed potential. Lacking such a demonstration the presumption is that the difficulties of vacuum polarization are not so easily circumvented.[18]

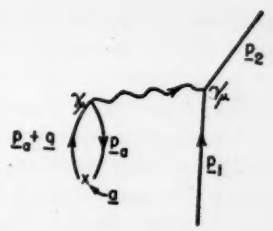

FIG. 6. Vacuum polarization effect on scattering, Eq. (30).

An alternative procedure discussed in *B* is to assume that the function $K_+(2,1)$ used above is incorrect and is to be replaced by a modified function K_+' having no singularity on the light cone. The effect of this is to provide a convergence factor $C(p^2-m^2)$ for *every* integral over electron momenta.[19] This will multiply the integrand of (32) by $C(p^2-m^2)C((p+q)^2-m^2)$, since the integral was originally $\delta(p_a-p_b+q)d^4p_a d^4p_b$ and both p_a and p_b get convergence factors. The integral now converges but the result is unsatisfactory.[20]

One expects the current (31) to be conserved, that is $q_\mu j_\mu=0$ or $q_\mu J_{\mu\nu}=0$. Also one expects no current if a_ν is a gradient, or $a_\nu=q_\nu$ times a constant. This leads to the condition $J_{\mu\nu}q_\nu=0$ which is equivalent to $q_\mu J_{\mu\nu}=0$ since $J_{\mu\nu}$ is symmetrical. But when the expression (32) is integrated with such convergence factors it does not satisfy this condition. By altering the kernel from K to another, K', which does not satisfy the Dirac equation we have lost the gauge invariance, its consequent current conservation and the general consistency of the theory.

One can see this best by calculating $J_{\mu\nu}q_\nu$ directly from (32). The expression within the spur becomes $(p+q-m)^{-1}q(p-m)^{-1}\gamma_\mu$ which can be written as the difference of two terms: $(p-m)^{-1}\gamma_\mu-(p+q-m)^{-1}\gamma_\mu$. Each of these terms would give the same result if the integration d^4p were without a convergence factor, for

[18] It would be very interesting to calculate the Lamb shift accurately enough to be sure that the 20 megacycles expected from vacuum polarization are actually present.

[19] This technique also makes self-energy and radiationless scattering integrals finite even without the modification of δ_+ to f_+ for the radiation (and the consequent convergence factor $C(k^2)$ for the quanta). See B.

[20] Added to the terms given below (33) there is a term $\frac{1}{4}(\lambda^2-2\mu^2+\frac{1}{3}q^2)\delta_{\mu\nu}$ for $C(k^2)=-\lambda^2(k^2-\lambda^2)^{-1}$, which is not gauge invariant. (In addition the charge renormalization has $-7/6$ added to the logarithm.)

the first can be converted into the second by a shift of the origin of p, namely $p'=p+q$. This does not result in cancelation in (32) however, for the convergence factor is altered by the substitution.

A method of making (32) convergent without spoiling the gauge invariance has been found by Bethe and by Pauli. The convergence factor for light can be looked upon as the result of superposition of the effects of quanta of various masses (some contributing negatively). Likewise if we take the factor $C(p^2-m^2)=-\lambda^2(p^2-m^2-\lambda^2)^{-1}$ so that $(p^2-m^2)^{-1}C(p^2-m^2)=(p^2-m^2)^{-1}-(p^2-m^2-\lambda^2)^{-1}$ we are taking the difference of the result for electrons of mass m and mass $(\lambda^2+m^2)^{\frac{1}{2}}$. But we have taken this difference for *each* propagation between interactions with photons. They suggest instead that once created with a certain mass the electron should continue to propagate with this mass through all the potential interactions until it closes its loop. That is if the quantity (32), integrated over some finite range of p, is called $J_{\mu\nu}(m^2)$ and the corresponding quantity over the same range of p, but with m replaced by $(m^2+\lambda^2)^{\frac{1}{2}}$ is $J_{\mu\nu}(m^2+\lambda^2)$ we should calculate

$$J_{\mu\nu}{}^P=\int_0^\infty [J_{\mu\nu}(m^2)-J_{\mu\nu}(m^2+\lambda^2)]G(\lambda)d\lambda, \quad (32')$$

the function $G(\lambda)$ satisfying $\int_0^\infty G(\lambda)d\lambda=1$ and $\int_0^\infty G(\lambda)\lambda^2 d\lambda=0$. Then in the expression for $J_{\mu\nu}{}^P$ the range of p integration can be extended to infinity as the integral now converges. The result of the integration using this method is the integral on $d\lambda$ over $G(\lambda)$ of (see Appendix C)

$$J_{\mu\nu}{}^P=-\frac{e^2}{\pi}(q_\mu q_\nu-\delta_{\mu\nu}q^2)\left(-\frac{1}{3}\ln\frac{\lambda^2}{m^2}-\left[\frac{4m^2+2q^2}{3q^2}\left(1-\frac{\theta}{\tan\theta}\right)-\frac{1}{9}\right]\right), \quad (33)$$

with $q^2=4m^2\sin^2\theta$.

The gauge invariance is clear, since $q_\mu(q_\mu q_\nu-q^2\delta_{\mu\nu})=0$. Operating (as it always will) on a potential of zero divergence the $(q_\mu q_\nu-\delta_{\mu\nu}q^2)a_\nu$ is simply $-q^2a_\mu$, the D'Alembertian of the potential, that is, the current producing the potential. The term $-\frac{1}{3}(\ln(\lambda^2/m^2))(q_\mu q_\nu-q^2\delta_{\mu\nu})$ therefore gives a current proportional to the current producing the potential. This would have the same effect as a change in charge, so that we would have a difference $\Delta(e^2)$ between e^2 and the experimentally observed charge, $e^2+\Delta(e^2)$, analogous to the difference between m and the observed mass. This charge depends logarithmically on the cut-off, $\Delta(e^2)/e^2=-(2e^2/3\pi)\ln(\lambda/m)$. After this renormalization of charge is made, no effects will be sensitive to the cut-off.

After this is done the final term remaining in (33), contains the usual effects[21] of polarization of the vacuum. It is zero for a free light quantum ($q^2=0$). For small q^2 it behaves as $(2/15)q^2$ (adding $-\frac{1}{5}$ to the logarithm in the Lamb effect). For $q^2>(2m)^2$ it is complex, the imaginary part representing the loss in amplitude required by the fact that the probability that no quanta are produced by a potential able to produce pairs ($(q^2)^{\frac{1}{2}}>2m$) decreases with time. (To make the necessary analytic continuation, imagine m to have a small negative imaginary part, so that $(1-q^2/4m^2)^{\frac{1}{2}}$ becomes $-i(q^2/4m^2-1)^{\frac{1}{2}}$ as q^2 goes from below to above $4m^2$. Then $\theta=\pi/2+iu$ where $\sinh u=+(q^2/4m^2-1)^{\frac{1}{2}}$, and $-1/\tan\theta=i\tanh u=+i(q^2-4m^2)^{\frac{1}{2}}(q^2)^{-\frac{1}{2}}$.)

Closed loops containing a number of quanta or potential interactions larger than two produce no trouble. Any loop with an odd number of interactions gives zero (I, reference 9). Four or more potential interactions give integrals which are convergent even without a convergence factor as is well known. The situation is analogous to that for self-energy. Once the simple problem of a single closed loop is solved there are no further divergence difficulties for more complex processes.[22]

8. LONGITUDINAL WAVES

In the usual form of quantum electrodynamics the longitudinal and transverse waves are given separate treatment. Alternately the condition $(\partial A_\mu/\partial x_\mu)\Psi=0$ is carried along as a supplementary condition. In the present form no such special considerations are necessary for we are dealing with the solutions of the equation $-\Box^2 A_\mu=4\pi j_\mu$ with a current j_μ which is conserved $\partial j_\mu/\partial x_\mu=0$. That means at least $\Box^2(\partial A_\mu/\partial x_\mu)=0$ and in fact our solution also satisfies $\partial A_\mu/\partial x_\mu=0$.

To show that this is the case we consider the amplitude for emission (real or virtual) of a photon and show that the divergence of this amplitude vanishes. The amplitude for emission for photons polarized in the μ direction involves matrix elements of γ_μ. Therefore what we have to show is that the corresponding matrix elements of $q_\mu\gamma_\mu=q$ vanish. For example, for a first order effect we would require the matrix element of q between two states p_1 and $p_2=p_1+q$. But since $q=p_2-p_1$ and $(\bar{u}_2 p_1 u_1)=m(\bar{u}_2 u_1)=(\bar{u}_2 p_2 u_1)$ the matrix element vanishes, which proves the contention in this case. It also vanishes in more complex situations (essentially because of relation (34), below) (for example, try putting $e_2=q_2$ in the matrix (15) for the Compton Effect).

To prove this in general, suppose a_i, $i=1$ to N are a set of plane wave disturbing potentials carrying momenta q_i (e.g., some may be emissions or absorptions of the same or different quanta) and consider a matrix for the transition from a state of momentum p_0 to p_N such

[21] E. A. Uehling, Phys. Rev. 48, 55 (1935), R. Serber, Phys. Rev. 48, 49 (1935).

[22] There are loops completely without external interactions. For example, a pair is created virtually along with a photon. Next they annihilate, absorbing this photon. Such loops are disregarded on the grounds that they do not interact with anything and are thereby completely unobservable. Any indirect effects they may have via the exclusion principle have already been included.

as $\boldsymbol{a}_N\prod_{i=1}^{N-1}(\boldsymbol{p}_i-m)^{-1}\boldsymbol{a}_i$ where $\boldsymbol{p}_i=\boldsymbol{p}_{i-1}+\boldsymbol{q}_i$ (and in the product, terms with larger i are written to the left). The most general matrix element is simply a linear combination of these. Next consider the matrix between states $\boldsymbol{p}_0$ and $\boldsymbol{p}_N+\boldsymbol{q}$ in a situation in which not only are the $\boldsymbol{a}_i$ acting but also another potential $\boldsymbol{a}\exp(-i\boldsymbol{q}\cdot x)$ where $\boldsymbol{a}=\boldsymbol{q}$. This may act previous to all $\boldsymbol{a}_i$, in which case it gives $\boldsymbol{a}_N\prod(\boldsymbol{p}_i+\boldsymbol{q}-m)^{-1}\boldsymbol{a}_i(\boldsymbol{p}_0+\boldsymbol{q}-m)^{-1}\boldsymbol{q}$ which is equivalent to $+\boldsymbol{a}_N\prod(\boldsymbol{p}_i+\boldsymbol{q}-m)^{-1}\boldsymbol{a}_i$ since $+(\boldsymbol{p}_0+\boldsymbol{q}-m)^{-1}\boldsymbol{q}$ is equivalent to $(\boldsymbol{p}_0+\boldsymbol{q}-m)^{-1}\times(\boldsymbol{p}_0+\boldsymbol{q}-m)$ as $\boldsymbol{p}_0$ is equivalent to m acting on the initial state. Likewise if it acts after all the potentials it gives $\boldsymbol{q}(\boldsymbol{p}_N-m)^{-1}\boldsymbol{a}_N\prod(\boldsymbol{p}_i-m)^{-1}\boldsymbol{a}_i$ which is equivalent to $-\boldsymbol{a}_N\prod(\boldsymbol{p}_i-m)^{-1}\boldsymbol{a}_i$ since $\boldsymbol{p}_N+\boldsymbol{q}-m$ gives zero on the final state. Or again it may act between the potential $\boldsymbol{a}_k$ and $\boldsymbol{a}_{k+1}$ for each k. This gives

$$\sum_{k=1}^{N-1}\boldsymbol{a}_N\prod_{i=k+1}^{N-1}(\boldsymbol{p}_i+\boldsymbol{q}-m)^{-1}\boldsymbol{a}_i(\boldsymbol{p}_k+\boldsymbol{q}-m)^{-1}\times\boldsymbol{q}(\boldsymbol{p}_k-m)^{-1}\boldsymbol{a}_k\prod_{j=1}^{k-1}(\boldsymbol{p}_j-m)^{-1}\boldsymbol{a}_j.$$

However,

$$(\boldsymbol{p}_k+\boldsymbol{q}-m)^{-1}\boldsymbol{q}(\boldsymbol{p}_k-m)^{-1}=(\boldsymbol{p}_k-m)^{-1}-(\boldsymbol{p}_k+\boldsymbol{q}-m)^{-1},\quad(34)$$

so that the sum breaks into the difference of two sums, the first of which may be converted to the other by the replacement of k by $k-1$. There remain only the terms from the ends of the range of summation,

$$+\boldsymbol{a}_N\prod_{i=1}^{N-1}(\boldsymbol{p}_i-m)^{-1}\boldsymbol{a}_i-\boldsymbol{a}_N\prod_{i=1}^{N-1}(\boldsymbol{p}_i+\boldsymbol{q}-m)^{-1}\boldsymbol{a}_i.$$

These cancel the two terms originally discussed so that the entire effect is zero. Hence any wave emitted will satisfy $\partial A_\mu/\partial x_\mu=0$. Likewise longitudinal waves (that is, waves for which $A_\mu=\partial\phi/\partial x_\mu$ or $\boldsymbol{a}=\boldsymbol{q}$) cannot be absorbed and will have no effect, for the matrix elements for emission and absorption are similar. (We have said little more than that a potential $A_\mu=\partial\varphi/\partial x_\mu$ has no effect on a Dirac electron since a transformation $\psi'=\exp(-i\phi)\psi$ removes it. It is also easy to see in coordinate representation using integrations by parts.)

This has a useful practical consequence in that in computing probabilities for transition for unpolarized light one can sum the squared matrix over all four directions rather than just the two special polarization vectors. Thus suppose the matrix element for some process for light polarized in direction e_μ is $e_\mu M_\mu$. If the light has wave vector q_μ we know from the argument above that $q_\mu M_\mu=0$. For unpolarized light progressing in the z direction we would ordinarily calculate $M_x{}^2+M_y{}^2$. But we can as well sum $M_x{}^2+M_y{}^2+M_z{}^2-M_t{}^2$ for $q_\mu M_\mu$ implies $M_t=M_z$ since $q_t=q_z$ for free quanta. This shows that unpolarized light is a relativistically invariant concept, and permits some simplification in computing cross sections for such light.

Incidentally, the virtual quanta interact through terms like $\gamma_\mu\cdots\gamma_\mu\boldsymbol{k}^{-2}d^4k$. Real processes correspond to poles in the formulae for virtual processes. The pole occurs when $\boldsymbol{k}^2=0$, but it looks at first as though in the sum on all four values of μ, of $\gamma_\mu\cdots\gamma_\mu$ we would have four kinds of polarization instead of two. Now it is clear that only two perpendicular to $\boldsymbol{k}$ are effective.

The usual elimination of longitudinal and scalar virtual photons (leading to an instantaneous Coulomb potential) can of course be performed here too (although it is not particularly useful). A typical term in a virtual transition is $\gamma_\mu\cdots\gamma_\mu\boldsymbol{k}^{-2}d^4k$ where the $\cdots$ represent some intervening matrices. Let us choose for the values of μ, the time t, the direction of vector part $\mathbf{K}$, of $\boldsymbol{k}$, and two perpendicular directions 1, 2. We shall not change the expression for these two 1, 2 for these are represented by transverse quanta. But we must find $(\gamma_t\cdots\gamma_t)-(\gamma_{\mathbf{K}}\cdots\gamma_{\mathbf{K}})$. Now $\boldsymbol{k}=k_4\gamma_t-K\gamma_{\mathbf{K}}$, where $K=(\mathbf{K}\cdot\mathbf{K})^{\frac{1}{2}}$, and we have shown above that $\boldsymbol{k}$ replacing the γ_μ gives zero.[23] Hence $K\gamma_{\mathbf{K}}$ is equivalent to $k_4\gamma_t$ and

$$(\gamma_t\cdots\gamma_t)-(\gamma_{\mathbf{K}}\cdots\gamma_{\mathbf{K}})=((K^2-k_4{}^2)/K^2)(\gamma_t\cdots\gamma_t),$$

so that on multiplying by $\boldsymbol{k}^{-2}d^4k=d^4k(k_4{}^2-K^2)^{-1}$ the net effect is $-(\gamma_t\cdots\gamma_t)d^4k/K^2$. The γ_t means just scalar waves, that is, potentials produced by charge density. The fact that $1/K^2$ does not contain k_4 means that k_4 can be integrated first, resulting in an instantaneous interaction, and the $d^3\mathbf{K}/K^2$ is just the momentum representation of the Coulomb potential, $1/r$.

9. KLEIN GORDON EQUATION

The methods may be readily extended to particles of spin zero satisfying the Klein Gordon equation,[24]

$$\Box^2\psi-m^2\psi=i\partial(A_\mu\psi)/\partial x_\mu+iA_\mu\partial\psi/\partial x_\mu-A_\mu A_\mu\psi.\quad(35)$$

[23] A little more care is required when both γ_μ's act on the same particle. Define $\boldsymbol{x}=k_4\gamma_t+K\gamma_{\mathbf{K}}$, and consider $(\boldsymbol{k}\cdots\boldsymbol{x})+(\boldsymbol{x}\cdots\boldsymbol{k})$. Exactly this term would arise if a system, acted on by potential $\boldsymbol{x}$ carrying momentum $-\boldsymbol{k}$, is disturbed by an added potential $\boldsymbol{k}$ of momentum $+\boldsymbol{k}$ (the reversed sign of the momenta in the intermediate factors in the second term $\boldsymbol{x}\cdots\boldsymbol{k}$ has no effect since we will later integrate over all $\boldsymbol{k}$). Hence as shown above the result is zero, but since $(\boldsymbol{k}\cdots\boldsymbol{x})+(\boldsymbol{x}\cdots\boldsymbol{k})=k_4{}^2(\gamma_t\cdots\gamma_t)-K^2(\gamma_{\mathbf{K}}\cdots\gamma_{\mathbf{K}})$ we can still conclude $(\gamma_{\mathbf{K}}\cdots\gamma_{\mathbf{K}})=k_4{}^2K^{-2}(\gamma_t\cdots\gamma_t)$.

[24] The equations discussed in this section were deduced from the formulation of the Klein Gordon equation given in reference 5, Section 14. The function ψ in this section has only one component and is not a spinor. An alternative formal method of making the equations valid for spin zero and also for spin 1 is (presumably) by use of the Kemmer-Duffin matrices β_μ, satisfying the commutation relation

$$\beta_\mu\beta_\nu\beta_\sigma+\beta_\sigma\beta_\nu\beta_\mu=\delta_{\mu\nu}\beta_\sigma+\delta_{\sigma\nu}\beta_\mu.$$

If we interpret $\boldsymbol{a}$ to mean $a_\mu\beta_\mu$, rather than $a_\mu\gamma_\mu$, for any a_μ, all of the equations in momentum space will remain formally identical to those for the spin 1/2; with the exception of those in which a denominator $(\boldsymbol{p}-m)^{-1}$ has been rationalized to $(\boldsymbol{p}+m)(\boldsymbol{p}^2-m^2)^{-1}$ since $\boldsymbol{p}^2$ is no longer equal to a number, $p\cdot p$. But $\boldsymbol{p}^3$ does equal $(p\cdot p)\boldsymbol{p}$ so that $(\boldsymbol{p}-m)^{-1}$ may now be interpreted as $(m\boldsymbol{p}+m^2+\boldsymbol{p}^2-p\cdot p)(p\cdot p-m^2)^{-1}m^{-1}$. This implies that equations in coordinate space will be valid of the function $K_+(2,1)$ is given as $K_+(2,1)=[(i\nabla_2+m)-m^{-1}(\nabla_2{}^2+\Box_2{}^2)]iI_+(2,1)$ with $\nabla_2=\beta_\mu\partial/\partial x_{2\mu}$. This is all in virtue of the fact that the many component wave function ψ (5 components for spin 0, 10 for spin 1) satisfies $(i\nabla-m)\psi=A\psi$ which is formally identical to the Dirac Equation. See W. Pauli, Rev. Mod. Phys. **13**, 203 (1940).

The important kernel is now $I_+(2, 1)$ defined in (I, Eq. (32)). For a free particle, the wave function $\psi(2)$ satisfies $+\Box^2\psi - m^2\psi = 0$. At a point, 2, inside a space time region it is given by

$$\psi(2) = \int [\psi(1)\partial I_+(2, 1)/\partial x_{1\mu} - (\partial\psi/\partial x_{1\mu}) I_+(2, 1)] N_\mu(1) d^3V_1,$$

(as is readily shown by the usual method of demonstrating Green's theorem) the integral being over an entire 3-surface boundary of the region (with normal vector N_μ). Only the positive frequency components of ψ contribute from the surface preceding the time corresponding to 2, and only negative frequencies from the surface future to 2. These can be interpreted as electrons and positrons in direct analogy to the Dirac case.

The right-hand side of (35) can be considered as a source of new waves and a series of terms written down to represent matrix elements for processes of increasing order. There is only one new point here, the term in $A_\mu A_\mu$ by which two quanta can act at the same time. As an example, suppose three quanta or potentials, $a_\mu \exp(-iq_a\cdot x)$, $b_\mu \exp(-iq_b\cdot x)$, and $c_\mu \exp(-iq_c\cdot x)$ are to act in that order on a particle of original momentum $p_{0\mu}$ so that $p_a = p_0 + q_a$ and $p_b = p_a + q_b$; the final momentum being $p_c = p_b + q_c$. The matrix element is the sum of three terms ($p^2 = p_\mu p_\mu$) (illustrated in Fig. 7)

$$\begin{aligned}&(p_c\cdot c + p_b\cdot c)(p_b^2 - m^2)^{-1}(p_b\cdot b + p_a\cdot b) \times (p_a^2 - m^2)^{-1}(p_a\cdot a + p_0\cdot a)\\ &-(p_c\cdot c + p_b\cdot c)(p_b^2 - m^2)^{-1}(b\cdot a)\\ &-(c\cdot b)(p_a^2 - m^2)^{-1}(p_a\cdot a + p_0\cdot a).\end{aligned} \tag{36}$$

The first comes when each potential acts through the perturbation $i\partial(A_\mu\psi)/\partial x_\mu + iA_\mu\partial\psi/\partial x_\mu$. These gradient operators in momentum space mean respectively the momentum after and before the potential A_μ operates. The second term comes from b_μ and a_μ acting at the same instant and arises from the $A_\mu A_\mu$ term in (a). Together b_μ and a_μ carry momentum $q_{b\mu} + q_{a\mu}$ so that after $b\cdot a$ operates the momentum is $p_0 + q_a + q_b$ or p_b. The final term comes from c_μ and b_μ operating together in a similar manner. The term $A_\mu A_\mu$ thus permits a new type of process in which two quanta can be emitted (or absorbed, or one absorbed, one emitted) at the same time. There is no $a\cdot c$ term for the order a, b, c we have assumed. In an actual problem there would be other terms like (36) but with alterations in the order in which the quanta a, b, c act. In these terms $a\cdot c$ would appear.

As a further example the self-energy of a particle of momentum p_μ is

$$(e^2/2\pi i m)\int [(2p-k)_\mu((p-k)^2 - m^2)^{-1} \times (2p-k)_\mu - \delta_{\mu\mu}] d^4k k^{-2} C(k^2),$$

where the $\delta_{\mu\mu} = 4$ comes from the $A_\mu A_\mu$ term and represents the possibility of the simultaneous emission and absorption of the same virtual quantum. This integral without the $C(k^2)$ diverges quadratically and would not converge if $C(k^2) = -\lambda^2/(k^2 - \lambda^2)$. Since the interaction occurs through the gradients of the potential, we must use a stronger convergence factor, for example $C(k^2) = \lambda^4(k^2 - \lambda^2)^{-2}$, or in general (17) with $\int_0^\infty \lambda^2 G(\lambda) d\lambda = 0$. In this case the self-energy converges but depends quadratically on the cut-off λ and is not necessarily small compared to m. The radiative corrections to scattering after mass renormalization are insensitive to the cut-off just as for the Dirac equation.

When there are several particles one can obtain Bose statistics by the rule that if two processes lead to the same state but with two electrons exchanged, their amplitudes are to be added (rather than subtracted as for Fermi statistics). In this case equivalence to the second quantization treatment of Pauli and Weisskopf should be demonstrable in a way very much like that given in I (appendix) for Dirac electrons. The Bose statistics mean that the sign of contribution of a closed loop to the vacuum polarization is the opposite of what it is for the Fermi case (see I). It is ($p_b = p_a + q$)

$$J_{\mu\nu} = \frac{e^2}{2\pi i m}\int [(p_{b\mu} + p_{a\mu})(p_{b\nu} + p_{a\nu})(p_a^2 - m^2)^{-1} \times (p_b^2 - m^2)^{-1} - \delta_{\mu\nu}(p_a^2 - m^2)^{-1} - \delta_{\mu\nu}(p_b^2 - m^2)^{-1}] d^4p_a$$

giving,

$$J_{\mu\nu}{}^P = \frac{e^2}{\pi}(q_\mu q_\nu - \delta_{\mu\nu}q^2)\left[\frac{1}{6}\ln\frac{\lambda^2}{m^2} + \frac{1}{9} - \frac{4m^2 - q^2}{3q^2}\left(1 - \frac{\theta}{\tan\theta}\right)\right],$$

the notation as in (33). The imaginary part for $(q^2)^{\frac{1}{2}} > 2m$ is again positive representing the loss in the probability of finding the final state to be a vacuum, associated with the possibilities of pair production. Fermi statistics would give a gain in probability (and also a charge renormalization of opposite sign to that expected).

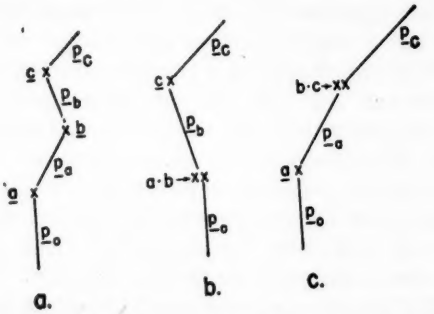

FIG. 7. Klein-Gordon particle in three potentials, Eq. (36). The coupling to the electromagnetic field is now, for example, $p_0\cdot a + p_a\cdot a$, and a new possibility arises, (b), of simultaneous interaction with two quanta $a\cdot b$. The propagation factor is now $(p\cdot p - m^2)^{-1}$ for a particle of momentum p_μ.

10. APPLICATION TO MESON THEORIES

The theories which have been developed to describe mesons and the interaction of nucleons can be easily expressed in the language used here. Calculations, to lowest order in the interactions can be made very easily for the various theories, but agreement with experimental results is not obtained. Most likely all of our present formulations are quantitatively unsatisfactory. We shall content ourselves therefore with a brief summary of the methods which can be used.

The nucleons are usually assumed to satisfy Dirac's equation so that the factor for propagation of a nucleon of momentum $\boldsymbol{p}$ is $(\boldsymbol{p}-M)^{-1}$ where M is the mass of the nucleon (which implies that nucleons can be created in pairs). The nucleon is then assumed to interact with mesons, the various theories differing in the form assumed for this interaction.

First, we consider the case of neutral mesons. The theory closest to electrodynamics is the theory of vector mesons with vector coupling. Here the factor for emission or absorption of a meson is $g\gamma_\mu$ when this meson is "polarized" in the μ direction. The factor g, the "mesonic charge," replaces the electric charge e. The amplitude for propagation of a meson of momentum $\boldsymbol{q}$ in intermediate states is $(\boldsymbol{q}^2-\mu^2)^{-1}$ (rather than $\boldsymbol{q}^{-2}$ as it is for light) where μ is the mass of the meson. The necessary integrals are made finite by convergence factors $C(\boldsymbol{q}^2-\mu^2)$ as in electrodynamics. For scalar mesons with scalar coupling the only change is that one replaces the γ_μ by 1 in emission and absorption. There is no longer a direction of polarization, μ, to sum upon. For pseudoscalar mesons, pseudoscalar coupling replace γ_μ by $\gamma_5=i\gamma_x\gamma_y\gamma_z\gamma_t$. For example, the self-energy matrix of a nucleon of momentum $\boldsymbol{p}$ in this theory is

$$(g^2/\pi i)\int \gamma_5(\boldsymbol{p}-\boldsymbol{k}-M)^{-1}\gamma_5 d^4k(\boldsymbol{k}^2-\mu^2)^{-1}C(\boldsymbol{k}^2-\mu^2).$$

Other types of meson theory result from the replacement of γ_μ by other expressions (for example by $\frac{1}{2}(\gamma_\mu\gamma_\nu-\gamma_\nu\gamma_\mu)$ with a subsequent sum over all μ and ν for virtual mesons). Scalar mesons with vector coupling result from the replacement of γ_μ by $\mu^{-1}\boldsymbol{q}$ where $\boldsymbol{q}$ is the final momentum of the nucleon minus its initial momentum, that is, it is the momentum of the meson if absorbed, or the negative of the momentum of a meson emitted. As is well known, this theory with neutral mesons gives zero for all processes, as is proved by our discussion on longitudinal waves in electrodynamics. Pseudoscalar mesons with pseudo-vector coupling corresponds to γ_μ being replaced by $\mu^{-1}\gamma_5\boldsymbol{q}$ while vector mesons with tensor coupling correspond to using $(2\mu)^{-1}(\gamma_\mu\boldsymbol{q}-\boldsymbol{q}\gamma_\mu)$. These extra gradients involve the danger of producing higher divergencies for real processes. For example, $\gamma_5\boldsymbol{q}$ gives a logarithmically divergent interaction of neutron and electron.[25] Although these divergencies can be held by strong enough convergence factors, the results then are sensitive to the method used for convergence and the size of the cut-off values of λ. For low order processes $\mu^{-1}\gamma_5\boldsymbol{q}$ is equivalent to the pseudoscalar interaction $2M\mu^{-1}\gamma_5$ because if taken between free particle wave functions of the nucleon of momenta $\boldsymbol{p}_1$ and $\boldsymbol{p}_2=\boldsymbol{p}_1+\boldsymbol{q}$, we have

$$(\bar{u}_2\gamma_5\boldsymbol{q}u_1)=(\bar{u}_2\gamma_5(\boldsymbol{p}_2-\boldsymbol{p}_1)u_1)=-(\bar{u}_2\boldsymbol{p}_2\gamma_5u_1)-(\bar{u}_2\gamma_5\boldsymbol{p}_1u_1)=-2M(\bar{u}_2\gamma_5u_1)$$

since γ_5 anticommutes with $\boldsymbol{p}_2$ and $\boldsymbol{p}_2$ operating on the state 2 equivalent to M as is $\boldsymbol{p}_1$ on the state 1. This shows that the γ_5 interaction is unusually weak in the non-relativistic limit (for example the expected value of γ_5 for a free nucleon is zero), but since $\gamma_5^2=1$ is not small, pseudoscalar theory gives a more important interaction in second order than it does in first. Thus the pseudoscalar coupling constant should be chosen to fit nuclear forces including these important second order processes.[26] The equivalence of pseudoscalar and pseudovector coupling which holds for low order processes therefore does not hold when the pseudoscalar theory is giving its most important effects. These theories will therefore give quite different results in the majority of practical problems.

In calculating the corrections to scattering of a nucleon by a neutral vector meson field (γ_μ) due to the effects of virtual mesons, the situation is just as in electrodynamics, in that the result converges without need for a cut-off and depends only on gradients of the meson potential. With scalar (1) or pseudoscalar (γ_5) neutral mesons the result diverges logarithmically and so must be cut off. The part sensitive to the cut-off, however, is directly proportional to the meson potential. It may thereby be removed by a renormalization of mesonic charge g. After this renormalization the results depend only on gradients of the meson potential and are essentially independent of cut-off. This is in addition to the mesonic charge renormalization coming from the production of virtual nucleon pairs by a meson, analogous to the vacuum polarization in electrodynamics. But here there is a further difference from electrodynamics for scalar or pseudoscalar mesons in that the polarization also gives a term in the induced current proportional to the meson potential representing therefore an additional renormalization of the *mass of the meson* which usually depends quadratically on the cut-off.

Next consider charged mesons in the absence of an electromagnetic field. One can introduce isotopic spin operators in an obvious way. (Specifically replace the neutral γ_5, say, by $\tau_i\gamma_5$ and sum over $i=1, 2$ where $\tau_1=\tau_++\tau_-$, $\tau_2=i(\tau_+-\tau_-)$ and τ_+ changes neutron to proton (τ_+ on proton$=0$) and τ_- changes proton to neutron.) It is just as easy for practical problems simply to keep track of whether the particle is a proton or a neutron on a diagram drawn to help write down the

[25] M. Slotnick and W. Heitler, Phys. Rev. 75, 1645 (1949).

[26] H. A. Bethe, Bull. Am. Phys. Soc. 24, 3, Z3 (Washington, 1949).

matrix element. This excludes certain processes. For example in the scattering of a negative meson from q_1 to q_2 by a neutron, the meson q_2 must be emitted first (in order of operators, not time) for the neutron cannot absorb the negative meson q_1 until it becomes a proton. That is, in comparison to the Klein Nishina formula (15), only the analogue of second term (see Fig. 5(b)) would appear in the scattering of negative mesons by neutrons, and only the first term (Fig. 5(a)) in the neutron scattering of positive mesons.

The source of mesons of a given charge is not conserved, for a neutron capable of emitting negative mesons may (on emitting one, say) become a proton no longer able to do so. The proof that a perturbation q gives zero, discussed for longitudinal electromagnetic waves, fails. This has the consequence that vector mesons, if represented by the interaction γ_μ would not satisfy the condition that the divergence of the potential is zero. The interaction is to be taken[27] as $\gamma_\mu-\mu^{-2}q_\mu q$ in emission and as γ_μ in absorption if the real emission of mesons with a non-zero divergence of potential is to be avoided. (The correction term $\mu^{-2}q_\mu q$ gives zero in the neutral case.) The asymmetry in emission and absorption is only apparent, as this is clearly the same thing as subtracting from the original $\gamma_\mu\cdots\gamma_\mu$, a term $\mu^{-2}q\cdots q$. That is, if the term $-\mu^{-2}q_\mu q$ is omitted the resulting theory describes a combination of mesons of spin one and spin zero. The spin zero mesons, coupled by vector coupling q, are removed by subtracting the term $\mu^{-2}q\cdots q$.

The two extra gradients $q\cdots q$ make the problem of diverging integrals still more serious (for example the interaction between two protons corresponding to the exchange of two charged vector mesons depends quadratically on the cut-off if calculated in a straightforward way). One is tempted in this formulation to choose simply $\gamma_\mu\cdots\gamma_\mu$ and accept the admixture of spin zero mesons. But it appears that this leads in the conventional formalism to negative energies for the spin zero component. This shows one of the advantages of the method of second quantization of meson fields over the present formulation. There such errors of sign are obvious while here we seem to be able to write seemingly innocent expressions which can give absurd results. Pseudovector mesons with pseudovector coupling correspond to using $\gamma_5(\gamma_\mu-\mu^{-2}q_\mu q)$ for absorption and $\gamma_5\gamma_\mu$ for emission for both charged and neutral mesons.

In the presence of an electromagnetic field, whenever the nucleon is a proton it interacts with the field in the way described for electrons. The meson interacts in the scalar or pseudoscalar case as a particle obeying the Klein-Gordon equation. It is important here to use the method of calculation of Bethe and Pauli, that is, a virtual meson is assumed to have the same "mass" during all its interactions with the electromagnetic field. The result for mass μ and for $(\mu^2+\lambda^2)^{\frac{1}{2}}$ are subtracted and the difference integrated over the function $G(\lambda)d\lambda$. A separate convergence factor is not provided for each meson propagation between electromagnetic interactions, otherwise gauge invariance is not insured. When the coupling involves a gradient, such as $\gamma_5 q$ where q is the final minus the initial momentum of the nucleon, the vector potential A must be subtracted from the momentum of the proton. That is, there is an additional coupling $\pm\gamma_5 A$ (plus when going from proton to neutron, minus for the reverse) representing the new possibility of a simultaneous emission (or absorption) of meson and photon.

Emission of positive or absorption of negative virtual mesons are represented in the same term, the sign of the charge being determined by temporal relations as for electrons and positrons.

Calculations are very easily carried out in this way to lowest order in g^2 for the various theories for nucleon interaction, scattering of mesons by nucleons, meson production by nuclear collisions and by gamma-rays, nuclear magnetic moments, neutron electron scattering, etc., However, no good agreement with experiment results, when these are available, is obtained. Probably all of the formulations are incorrect. An uncertainty arises since the calculations are only to first order in g^2, and are not valid if $g^2/\hbar c$ is large.

The author is particularly indebted to Professor H. A. Bethe for his explanation of a method of obtaining finite and gauge invariant results for the problem of vacuum polarization. He is also grateful for Professor Bethe's criticisms of the manuscript, and for innumerable discussions during the development of this work. He wishes to thank Professor J. Ashkin for his careful reading of the manuscript.

APPENDIX

In this appendix a method will be illustrated by which the simpler integrals appearing in problems in electrodynamics can be directly evaluated. The integrals arising in more complex processes lead to rather complicated functions, but the study of the relations of one integral to another and their expression in terms of simpler integrals may be facilitated by the methods given here.

---

[27] The vector meson field potentials φ_μ satisfy

$$-\partial/\partial x_\nu(\partial\varphi_\mu/\partial x_\nu-\partial\varphi_\nu/\partial x_\mu)-\mu^2\varphi_\mu=-4\pi s_\mu,$$

where s_μ, the source for such mesons, is the matrix element of γ_μ between states of neutron and proton. By taking the divergence $\partial/\partial x_\mu$ of both sides, conclude that $\partial\varphi_\nu/\partial x_\nu=4\pi\mu^{-2}\partial s_\nu/\partial x_\nu$ so that the original equation can be rewritten as

$$\Box^2\varphi_\mu-\mu^2\varphi_\mu=-4\pi(s_\mu+\mu^{-2}\partial/\partial x_\mu(\partial s_\nu/\partial x_\nu)).$$

The right hand side gives in momentum representation $\gamma_\mu-\mu^{-2}q_\mu q_\nu\gamma_\nu$ the left yields the $(q^2-\mu^2)^{-1}$ and finally the interaction $s_\mu\varphi_\mu$ in the Lagrangian gives the γ_μ on absorption.

Proceeding in this way find generally that particles of spin one can be represented by a four-vector u_μ (which, for a free particle of momentum q satisfies $q\cdot u=0$). The propagation of virtual particles of momentum q from state ν to μ is represented by multiplication by the 4–4 matrix (or tensor) $P_{\mu\nu}=(\delta_{\mu\nu}-\mu^{-2}q_\mu q_\nu)\times(q^2-\mu^2)^{-1}$. The first-order interaction (from the Proca equation) with an electromagnetic potential $a\exp(-ik\cdot x)$ corresponds to multiplication by the matrix $E_{\mu\nu}=(q_2\cdot a+q_1\cdot a)\delta_{\mu\nu}-q_{2\nu}a_\mu-q_{1\mu}a_\nu$ where q_1 and $q_2=q_1+k$ are the momenta before and after the interaction. Finally, two potentials a, b may act simultaneously, with matrix $E'_{\mu\nu}=-(a\cdot b)\delta_{\mu\nu}+b_\mu a_\nu$.

As a typical problem consider the integral (12) appearing in the first order radiationless scattering problem:

$$\int \gamma_\mu(\not p_2-\not k-m)^{-1}a(\not p_1-\not k-m)^{-1}\gamma_\mu k^{-2}d^4kC(k^2), \qquad (1a)$$

where we shall take $C(k^2)$ to be typically $-\lambda^2(k^2-\lambda^2)^{-1}$ and d^4k means $(2\pi)^{-2}dk_1dk_2dk_3dk_4$. We first rationalize the factors $(\not p-\not k-m)^{-1}=(\not p-\not k+m)((p-k)^2-m^2)^{-1}$ obtaining,

$$\int \gamma_\mu(\not p_2-\not k+m)a(\not p_1-\not k+m)\gamma_\mu k^{-2}d^4kC(k^2) \times((p_1-k)^2-m^2)^{-1}((p_2-k)^2-m^2)^{-1}. \qquad (2a)$$

The matrix expression may be simplified. It appears to be best to do so *after* the integrations are performed. Since $AB=2A\cdot B-BA$ where $A\cdot B=A_\mu B_\mu$ is a number commuting with all matrices, find, if R is any expression, and A a vector, since $\gamma_\mu A=-A\gamma_\mu+2A_\mu$,

$$\gamma_\mu AR\gamma_\mu=-A\gamma_\mu R\gamma_\mu+2RA. \qquad (3a)$$

Expressions between two γ_μ's can be thereby reduced by induction. Particularly useful are

$$\begin{aligned}\gamma_\mu\gamma_\mu&=4\\ \gamma_\mu A\gamma_\mu&=-2A\\ \gamma_\mu AB\gamma_\mu&=2(AB+BA)=4A\cdot B\\ \gamma_\mu ABC\gamma_\mu&=-2CBA\end{aligned} \qquad (4a)$$

where A, B, C are any three vector-matrices (i.e., linear combinations of the four γ's).

In order to calculate the integral in (2a) the integral may be written as the sum of three terms (since $k=k_\sigma\gamma_\sigma$),

$$\gamma_\mu(\not p_2+m)a(\not p_1+m)\gamma_\mu J_1-[\gamma_\mu\gamma_\sigma a(\not p_1+m)\gamma_\mu +\gamma_\mu(\not p_2+m)a\gamma_\sigma\gamma_\mu]J_2+\gamma_\mu\gamma_\sigma a\gamma_\tau\gamma_\mu J_3, \qquad (5a)$$

where

$$J_{(1;2;3)}=\int(1;k_\sigma;k_\sigma k_\tau)k^{-2}d^4kC(k^2) \times((p_2-k)^2-m^2)^{-1}((p_1-k)^2-m^2)^{-1}. \qquad (6a)$$

That is for J_1 the $(1;k_\sigma;k_\sigma k_\tau)$ is replaced by 1, for J_2 by k_σ, and for J_3 by $k_\sigma k_\tau$.

More complex processes of the first order involve more factors like $((p_3-k)^2-m^2)^{-1}$ and a corresponding increase in the number of k's which may appear in the numerator, as $k_\sigma k_\tau k_\nu\cdots$. Higher order processes involving two or more virtual quanta involve similar integrals but with factors possibly involving $k+k'$ instead of just k, and the integral extending on $k^{-2}d^4kC(k^2)k'^{-2}d^4k'C(k'^2)$. They can be simplified by methods analogous to those used on the first order integrals.

The factors $(\not p-\not k)^2-m^2$ may be written

$$(\not p-\not k)^2-m^2=k^2-2p\cdot k-\Delta, \qquad (7a)$$

where $\Delta=m^2-p^2$, $\Delta_1=m_1^2-p_1^2$, etc., and we can consider dealing with cases of greater generality in that the different denominators need not have the same value of the mass m. In our specific problem (6a), $p_1^2=m^2$ so that $\Delta_1=0$, but we desire to work with greater generality.

Now for the factor $C(k^2)/k^2$ we shall use $-\lambda^2(k^2-\lambda^2)^{-1}k^{-2}$. This can be written as

$$-\lambda^2/(k^2-\lambda^2)k^2=k^{-2}C(k^2)=-\int_0^{\lambda^2}dL(k^2-L)^{-2}. \qquad (8a)$$

Thus we can replace $k^{-2}C(k^2)$ by $(k^2-L)^{-2}$ and at the end integrate the result with respect to L from zero to λ^2. We can for many practical purposes consider λ^2 very large relative to m^2 or p^2. When the original integral converges even without the convergence factor, it will be obvious since the L integration will then be convergent to infinity. If an infra-red catastrophe exists in the integral one can simply assume quanta have a small mass $\lambda_{\min}$ and extend the integral on L from $\lambda^2_{\min}$ to λ^2, rather than from zero to λ^2.

We then have to do integrals of the form

$$\int(1;k_\sigma;k_\sigma k_\tau)d^4k(k^2-L)^{-2}(k^2-2p_1\cdot k-\Delta_1)^{-1} \times(k^2-2p_2\cdot k-\Delta_2)^{-1}, \qquad (9a)$$

where by $(1;k_\sigma;k_\sigma k_\tau)$ we mean that in the place of this symbol either 1, or k_σ, or $k_\sigma k_\tau$ may stand in different cases. In more complicated problems there may be more factors $(k^2-2p_i\cdot k-\Delta_i)^{-1}$ or other powers of these factors (the $(k^2-L)^{-2}$ may be considered as a special case of such a factor with $p_i=0$, $\Delta_i=L$) and further factors like $k_\sigma k_\tau k_\rho\cdots$ in the numerator. The poles in all the factors are made definite by the assumption that L, and the Δ's have infinitesimal negative imaginary parts.

We shall do the integrals of successive complexity by induction. We start with the simplest convergent one, and show

$$\int d^4k(k^2-L)^{-3}=(8iL)^{-1}. \qquad (10a)$$

For this integral is $\int(2\pi)^{-2}dk_4d^3\mathbf{K}(k_4^2-\mathbf{K}\cdot\mathbf{K}-L)^{-3}$ where the vector $\mathbf{K}$, of magnitude $K=(\mathbf{K}\cdot\mathbf{K})^{\frac12}$ is k_1, k_2, k_3. The integral on k_4 shows third order poles at $k_4=+(K^2+L)^{\frac12}$ and $k_4=-(K^2+L)^{\frac12}$. Imagining, in accordance with our definitions, that L has a small negative imaginary part only the first is below the real axis. The contour can be closed by an infinite semi-circle below this axis, without change of the value of the integral since the contribution from the semi-circle vanishes in the limit. Thus the contour can be shrunk about the pole $k_4=+(K^2+L)^{\frac12}$ and the resulting k_4 integral is $-2\pi i$ times the residue at this pole. Writing $k_4=(K^2+L)^{\frac12}+\epsilon$ and expanding $(k_4^2-K^2-L)^{-3}=\epsilon^{-3}(\epsilon+2(K^2+L)^{\frac12})^{-3}$ in powers of ϵ, the residue, being the coefficient of the term ϵ^{-1}, is seen to be $6(2(K^2+L)^{\frac12})^{-5}$ so our integral is

$$-(3i/32\pi)\int_0^\infty 4\pi K^2dK(K^2+L)^{-5/2}=(3/8i)(1/3L)$$

establishing (10a).

We also have $\int k_\sigma d^4k(k^2-L)^{-3}=0$ from the symmetry in the k space. We write these results as

$$(8i)\int(1;k_\sigma)d^4k(k^2-L)^{-3}=(1;0)L^{-1}, \qquad (11a)$$

where in the brackets $(1;k_\sigma)$ and $(1;0)$ corresponding entries are to be used.

Substituting $k=k'-p$ in (11a), and calling $L-p^2=\Delta$ shows that

$$(8i)\int(1;k_\sigma)d^4k(k^2-2p\cdot k-\Delta)^{-3}=(1;p_\sigma)(p^2+\Delta)^{-1}. \qquad (12a)$$

By differentiating both sides of (12a) with respect to Δ, or with respect to p_τ there follows directly

$$(24i)\int(1;k_\sigma;k_\sigma k_\tau)d^4k(k^2-2p\cdot k-\Delta)^{-4} =-(1;p_\sigma;p_\sigma p_\tau-\tfrac12\delta_{\sigma\tau}(p^2+\Delta))(p^2+\Delta)^{-2}. \qquad (13a)$$

Further differentiations give directly successive integrals including more k factors in the numerator and higher powers of $(k^2-2p\cdot k-\Delta)$ in the denominator.

The integrals so far only contain one factor in the denominator. To obtain results for two factors we make use of the identity

$$a^{-1}b^{-1}=\int_0^1 dx(ax+b(1-x))^{-2}, \qquad (14a)$$

(suggested by some work of Schwinger's involving Gaussian integrals). This represents the product of two reciprocals as a parametric integral over one and will therefore permit integrals with two factors to be expressed in terms of one. For other powers of a, b, we make use of all of the identities, such as

$$a^{-2}b^{-1}=\int_0^1 2xdx(ax+b(1-x))^{-3}, \qquad (15a)$$

deducible from (14a) by successive differentiations with respect to a or b.

To perform an integral, such as

$$(8i)\int(1;k_\sigma)d^4k(k^2-2p_1\cdot k-\Delta_1)^{-2}(k^2-2p_2\cdot k-\Delta_2)^{-1}, \qquad (16a)$$

write, using (15a),

$$(k^2-2p_1\cdot k-\Delta_1)^{-a}(k^2-2p_2\cdot k-\Delta_2)^{-1}=\int_0^1 2xdx(k^2-2p_x\cdot k-\Delta_x)^{-3},$$

where

$$p_x=xp_1+(1-x)p_2 \quad \text{and} \quad \Delta_x=x\Delta_1+(1-x)\Delta_2, \tag{17a}$$

(note that Δ_x is *not* equal to $m^2-p_x^2$) so that the expression (16a) is $(8i)\int_0^1 2xdx\int(1;k_\sigma)d^4k(k^2-2p_x\cdot k-\Delta_x)^{-3}$ which may now be evaluated by (12a) and is

$$(16a)=\int_0^1(1;p_{x\sigma})2xdx(p_x^2+\Delta_x)^{-1}, \tag{18a}$$

where p_x, Δ_x are given in (17a). The integral in (18a) is elementary, being the integral of ratio of polynomials, the denominator of second degree in x. The general expression although readily obtained is a rather complicated combination of roots and logarithms.

Other integrals can be obtained again by parametric differentiation. For example differentiation of (16a), (18a) with respect to Δ_2 or $p_{2\tau}$ gives

$$(8i)\int(1;k_\sigma;k_\sigma k_\tau)d^4k(k^2-2p_1\cdot k-\Delta_1)^{-a}(k^2-2p_2\cdot k-\Delta_2)^{-2}$$
$$=-\int_0^1(1;p_{x\sigma};p_{x\sigma}p_{x\tau}-\tfrac{1}{2}\delta_{\sigma\tau}(p_x^2+\Delta_x))$$
$$\times 2x(1-x)dx(p_x^2+\Delta_x)^{-2}, \tag{19a}$$

again leading to elementary integrals.

As an example, consider the case that the second factor is just $(k^2-L)^{-2}$ and in the first put $p_1=p$, $\Delta_1=\Delta$. Then $p_x=xp$, $\Delta_x=x\Delta+(1-x)L$. There results

$$(8i)\int(1;k_\sigma;k_\sigma k_\tau)d^4k(k^2-L)^{-2}(k^2-2p\cdot k-\Delta)^{-2}$$
$$=-\int_0^1(1;xp_\sigma;x^2p_\sigma p_\tau-\tfrac{1}{2}\delta_{\sigma\tau}(x^2p^2+\Delta_x))$$
$$\times 2x(1-x)dx(x^2p^2+\Delta_x)^{-2}. \tag{20a}$$

Integrals with three factors can be reduced to those involving two by using (14a) again. They, therefore, lead to integrals with two parameters (e.g., see application to radiative correction to scattering below).

The methods of calculation given in this paper are deceptively simple when applied to the lower order processes. For processes of increasingly higher orders the complexity and difficulty increases rapidly, and these methods soon become impractical in their present form.

A. Self-Energy

The self-energy integral (19) is

$$(e^2/\pi i)\int\gamma_\mu(p-k-m)^{-1}\gamma_\mu k^{-2}d^4kC(k^2), \tag{19}$$

so that it requires that we find (using the principle of (8a)) the integral on L from 0 to λ^2 of

$$\int\gamma_\mu(p-k+m)\gamma_\mu d^4k(k^2-L)^{-2}(k^2-2p\cdot k)^{-1},$$

since $(p-k)^2-m^2=k^2-2p\cdot k$, as $p^2=m^2$. This is of the form (16a) with $\Delta_1=L$, $p_1=0$, $\Delta_2=0$, $p_2=p$ so that (18a) gives, since $p_x=(1-x)p$, $\Delta_x=xL$,

$$(8i)\int(1;k_\sigma)d^4k(k^2-L)^{-2}(k^2-2p\cdot k)^{-1}$$
$$=\int_0^1(1;(1-x)p_\sigma)2xdx((1-x)^2m^2+xL)^{-1},$$

or performing the integral on L, as in (8),

$$(8i)\int(1;k_\sigma)d^4kk^{-2}C(k^2)(k^2-2p\cdot k)^{-1}$$
$$=\int_0^1(1;(1-x)p_\sigma)2dx\ln\frac{x\lambda^2+(1-x)^2m^2}{(1-x)^2m^2}.$$

Assuming now that $\lambda^2\gg m^2$ we neglect $(1-x)^2m^2$ relative to $x\lambda^2$ in the argument of the logarithm, which then becomes $(\lambda^2/m^2)(x/(1-x)^2)$. Then since $\int_0^1dx\ln(x(1-x)^{-2})=1$ and $\int_0^1(1-x)dx\ln(x(1-x)^{-2})=-(1/4)$ find

$$(8i)\int(1;k_\sigma)k^{-2}C(k^2)d^4k(k^2-2p\cdot k)^{-1}$$
$$=\left(2\ln\frac{\lambda^2}{m^2}+2;p_\sigma\left(\ln\frac{\lambda^2}{m^2}-\frac{1}{2}\right)\right),$$

so that substitution into (19) (after the $(p-k-m)^{-1}$ in (19) is replaced by $(p-k+m)(k^2-2p\cdot k)^{-1}$) gives

$$(19)=(e^2/8\pi)\gamma_\mu[(p+m)(2\ln(\lambda^2/m^2)+2)$$
$$-p(\ln(\lambda^2/m^2)-\tfrac{1}{2})]\gamma_\mu$$
$$=(e^2/8\pi)[8m(\ln(\lambda^2/m^2)+1)-p(2\ln(\lambda^2/m^2)+5)], \tag{20}$$

using (4a) to remove the γ_μ's. This agrees with Eq. (20) of the text, and gives the self-energy (21) when p is replaced by m.

B. Corrections to Scattering

The term (12) in the radiationless scattering, after rationalizing the matrix denominators and using $p_1^2=p_2^2=m^2$ requires the integrals (9a), as we have discussed. This is an integral with three denominators which we do in two stages. First the factors $(k^2-2p_1\cdot k)$ and $(k^2-2p_2\cdot k)$ are combined by a parameter y;

$$(k^2-2p_1\cdot k)^{-1}(k^2-2p_2\cdot k)^{-1}=\int_0^1 dy(k^2-2p_y\cdot k)^{-2},$$

from (14a) where

$$p_y=yp_1+(1-y)p_2. \tag{21a}$$

We therefore need the integrals

$$(8i)\int(1;k_\sigma;k_\sigma k_\tau)d^4k(k^2-L)^{-2}(k^2-2p_y\cdot k)^{-2}, \tag{22a}$$

which we will then integrate with respect to y from 0 to 1. Next we do the integrals (22a) immediately from (20a) with $p=p_y$, $\Delta=0$:

$$(22a)=-\int_0^1\int_0^1(1;xp_{y\sigma};x^2p_{y\sigma}p_{y\tau}$$
$$-\tfrac{1}{2}\delta_{\sigma\tau}(x^2p_y^2+(1-x)L))2x(1-x)dx(x^2p_y^2+L(1-x))^{-2}dy.$$

We now turn to the integrals on L as required in (8a). The first term, (1), in $(1;k_\sigma;k_\sigma k_\tau)$ gives no trouble for large L, but if L is put equal to zero there results $x^{-2}p_y^{-2}$ which leads to a diverging integral on x as $x\to 0$. This infra-red catastrophe is analyzed by using $\lambda_{\min}^2$ for the lower limit of the L integral. For the last term the upper limit of L must be kept as λ^2. Assuming $\lambda_{\min}^2\ll p_y^2\ll\lambda^2$ the x integrals which remain are trivial, as in the self-energy case. One finds

$$-(8i)\int(k^2-\lambda_{\min}^2)^{-1}d^4kC(k^2-\lambda_{\min}^2)(k^2-2p_1\cdot k)^{-1}(k^2-2p_2\cdot k)^{-1}$$
$$=\int_0^1 p_y^{-2}dy\ln(p_y^2/\lambda_{\min}^2) \tag{23a}$$

$$-(8i)\int k_\sigma k^{-2}d^4kC(k^2)(k^2-2p_1\cdot k)^{-1}(k^2-2p_2\cdot k)^{-1}$$
$$=2\int_0^1 p_{y\sigma}p_y^{-2}dy, \tag{24a}$$

$$-(8i)\int k_\sigma k_\tau k^{-2}d^4kC(k^2)(k^2-2p_1\cdot k)^{-1}(k^2-2p_2\cdot k)^{-1}$$
$$=\int_0^1 p_{y\sigma}p_{y\tau}p_y^{-2}dy-\tfrac{1}{2}\delta_{\sigma\tau}\int_0^1 dy\ln(\lambda^2p_y^{-2})+\tfrac{1}{4}\delta_{\sigma\tau}. \tag{25a}$$

The integrals on y give,

$$\int_0^1 p_y^{-2}dy\ln(p_y^2\lambda_{\min}^{-2})=4(m^2\sin2\theta)^{-1}\left[\theta\ln(m\lambda_{\min}^{-1})\right.$$
$$\left.-\int_0^\theta\alpha\tan\alpha d\alpha\right], \tag{26a}$$

$$\int_0^1 p_{y\sigma}p_y^{-2}dy=\theta(m^2\sin2\theta)^{-1}(p_{1\sigma}+p_{2\sigma}), \tag{27a}$$

$$\int_0^1 p_{y\sigma}p_{y\tau}p_y^{-2}dy=\theta(2m^2\sin2\theta)^{-1}(p_{1\sigma}+p_{1\tau})(p_{2\sigma}+p_{2\tau})$$
$$+q^{-2}q_\sigma q_\tau(1-\theta\operatorname{ctn}\theta), \tag{28a}$$

$$\int_0^1 dy\ln(\lambda^2p_y^{-2})=\ln(\lambda^2/m^2)+2(1-\theta\operatorname{ctn}\theta). \tag{29a}$$

These integrals on y were performed as follows. Since $\not p_2=\not p_1+\not q$ where q is the momentum carried by the potential, it follows from $p_2^2=p_1^2=m^2$ that $2p_1\cdot q=-q^2$ so that since $p_y=p_1+q(1-y)$, $p_y^2=m^2-q^2y(1-y)$. The substitution $2y-1=\tan\alpha/\tan\theta$ where θ is defined by $4m^2\sin^2\theta=q^2$ is useful for it means $p_y^2=m^2\sec^2\alpha/\sec^2\theta$ and $p_y^{-2}dy=(m^2\sin 2\theta)^{-1}d\alpha$ where α goes from $-\theta$ to $+\theta$.

These results are substituted into the original scattering formula (2a), giving (22). It has been simplified by frequent use of the fact that $\not p_1$ operating on the initial state is m, and likewise $\not p_2$ when it appears at the left is replacable by m. (Thus, to simplify:

$$\gamma_\mu\not p_2 a\not p_1\gamma_\mu=-2\not p_1 a\not p_2 \text{ by (4a)},$$
$$=-2(\not p_2-\not q)a(\not p_1+\not q)=-2(m-\not q)a(m+\not q).$$

A term like $\not q a\not q=-q^2a+2(a\cdot q)\not q$ is equivalent to just $-q^2a$ since $\not q=\not p_2-\not p_1=m-m$ has zero matrix element.) The renormalization term requires the corresponding integrals for the special case $q=0$.

C. Vacuum Polarization

The expressions (32) and (32′) for $J_{\mu\nu}$ in the vacuum polarization problem require the calculation of the integral

$$J_{\mu\nu}(m^2)=-\frac{e^2}{\pi i}\int Sp[\gamma_\mu(\not p-\tfrac{1}{2}\not q+m)\gamma_\nu(\not p+\tfrac{1}{2}\not q+m)]d^4p$$
$$\times((p-\tfrac{1}{2}q)^2-m^2)^{-1}((p+\tfrac{1}{2}q)^2-m^2)^{-1}, \quad (32)$$

where we have replaced p by $p-\frac{1}{2}q$ to simplify the calculation somewhat. We shall indicate the method of calculation by studying the integral,

$$I(m^2)=\int p_\sigma p_\tau d^4p((p-\tfrac{1}{2}q)^2-m^2)^{-1}((p+\tfrac{1}{2}q)^2-m^2)^{-1}.$$

The factors in the denominator, $p^2-p\cdot q-m^2+\frac{1}{4}q^2$ and $p^2+p\cdot q-m^2+\frac{1}{4}q^2$ are combined as usual by (8a) but for symmetry we substitute $x=\frac{1}{2}(1+\eta)$, $(1-x)=\frac{1}{2}(1-\eta)$ and integrate η from -1 to $+1$:

$$I(m^2)=\int_{-1}^{+1}p_\sigma p_\tau d^4p(p^2-\eta p\cdot q-m^2+\tfrac{1}{4}q^2)^{-2}d\eta/2. \quad (30a)$$

But the integral on p will not be found in our list for it is badly divergent. However, as discussed in Section 7, Eq. (32′) we do not wish $I(m^2)$ but rather $\int_0^\infty[I(m^2)-I(m^2+\lambda^2)]G(\lambda)d\lambda$. We can calculate the difference $I(m^2)-I(m^2+\lambda^2)$ by first calculating the derivative $I'(m^2+L)$ of I with respect to m^2 at m^2+L and later integrating L from zero to λ^2. By differentiating (30a), with respect to m^2 find,

$$I'(m^2+L)=\int_{-1}^{+1}p_\sigma p_\tau d^4p(p^2-\eta p\cdot q-m^2-L+\tfrac{1}{4}q^2)^{-3}d\eta.$$

This still diverges, but we can differentiate again to get

$$I''(m^2+L)=3\int_{-1}^{+1}p_\sigma p_\tau d^4p(p^2-\eta p\cdot q-m^2-L+\tfrac{1}{4}q^2)^{-4}d\eta$$
$$=-(8i)^{-1}\int_{-1}^{+1}(\tfrac{1}{4}\eta^2q_\sigma q_\tau D^{-3}-\tfrac{1}{2}\delta_{\sigma\tau}D^{-1})d\eta \quad (31a)$$

(where $D=\frac{1}{4}(\eta^2-1)q^2+m^2+L$), which now converges and has been evaluated by (13a) with $p=\frac{1}{2}\eta q$ and $\Delta=m^2+L-\frac{1}{4}q^2$. Now to get I' we may integrate I'' with respect to L as an indefinite integral and *we may choose any convenient arbitrary constant.* This is because a constant C in I' will mean a term $-C\lambda^2$ in $I(m^2)-I(m^2+\lambda^2)$ which vanishes since we will integrate the results times $G(\lambda)d\lambda$ and $\int_0^\infty\lambda^2G(\lambda)d\lambda=0$. This means that the logarithm appearing on integrating L in (31a) presents no problem. We may take

$$I'(m^2+L)=(8i)^{-1}\int_{-1}^{+1}[\tfrac{1}{4}\eta^2q_\sigma q_\tau D^{-1}+\tfrac{1}{2}\delta_{\sigma\tau}\ln D]d\eta+C\delta_{\sigma\tau},$$

a subsequent integral on L and finally on η presents no new problems. There results

$$-(8i)\int p_\sigma p_\tau d^4p((p-\tfrac{1}{2}q)^2-m^2)^{-1}((p+\tfrac{1}{2}q)^2-m^2)^{-1}$$
$$=(q_\sigma q_\tau-\delta_{\sigma\tau}q^2)\left[\frac{1}{9}-\frac{4m^2-q^2}{3q^2}\left(1-\frac{\theta}{\tan\theta}\right)+\frac{1}{6}\ln\frac{\lambda^2}{m^2}\right]$$
$$+\delta_{\sigma\tau}[(\lambda^2+m^2)\ln(\lambda^2m^{-2}+1)-C'\lambda^2], \quad (32a)$$

where we assume $\lambda^2\gg m^2$ and have put some terms into the arbitrary constant C' which is independent of λ^2 (but in principle could depend on q^2) and which drops out in the integral on $G(\lambda)d\lambda$. We have set $q^2=4m^2\sin^2\theta$.

In a very similar way the integral with m^2 in the numerator can be worked out. It is, of course, necessary to differentiate this m^2 also when calculating I' and I''. There results

$$-(8i)\int m^2d^4p((p-\tfrac{1}{2}q)^2-m^2)^{-1}((p+\tfrac{1}{2}q)^2-m^2)^{-1}$$
$$=4m^2(1-\theta\operatorname{ctn}\theta)-q^2/3+2(\lambda^2+m^2)\ln(\lambda^2m^{-2}+1)-C''\lambda^2), \quad (33a)$$

with another unimportant constant C''. The complete problem requires the further integral,

$$-(8i)\int(1;p_\sigma)d^4p((p-\tfrac{1}{2}q)^2-m^2)^{-1}((p+\tfrac{1}{2}q)^2-m^2)^{-1}$$
$$=(1,0)(4(1-\theta\operatorname{ctn}\theta)+2\ln(\lambda^2m^{-2})). \quad (34a)$$

The value of the integral (34a) times m^2 differs from (33a), of course, because the results on the right are not actually the integrals on the left, but rather equal their actual value minus their value for $m^2=m^2+\lambda^2$.

Combining these quantities, as required by (32), dropping the constants C', C'' and evaluating the spur gives (33). The spurs are evaluated in the usual way, noting that the spur of any odd number of γ matrices vanishes and $Sp(AB)=Sp(BA)$ for arbitrary A, B. The $Sp(1)=4$ and we also have

$$\tfrac{1}{4}Sp[(\not p_1+m_1)(\not p_2-m_2)]=p_1\cdot p_2-m_1m_2, \quad (35a)$$

$$\tfrac{1}{4}Sp[(\not p_1+m_1)(\not p_2-m_2)(\not p_3+m_3)(\not p_4-m_4)]$$
$$=(p_1\cdot p_2-m_1m_2)(p_3\cdot p_4-m_3m_4)$$
$$-(p_1\cdot p_3-m_1m_3)(p_2\cdot p_4-m_2m_4)$$
$$+(p_1\cdot p_4-m_1m_4)(p_2\cdot p_3-m_2m_3), \quad (36a)$$

where p_i, m_i are arbitrary four-vectors and constants.

It is interesting that the terms of order $\lambda^2\ln\lambda^2$ go out, so that the charge renormalization depends only logarithmically on λ^2. This is not true for some of the meson theories. Electrodynamics is suspiciously unique in the mildness of its divergence.

D. More Complex Problems

Matrix elements for complex problems can be set up in a manner analogous to that used for the simpler cases. We give three illustrations; higher order corrections to the Møller scatter-

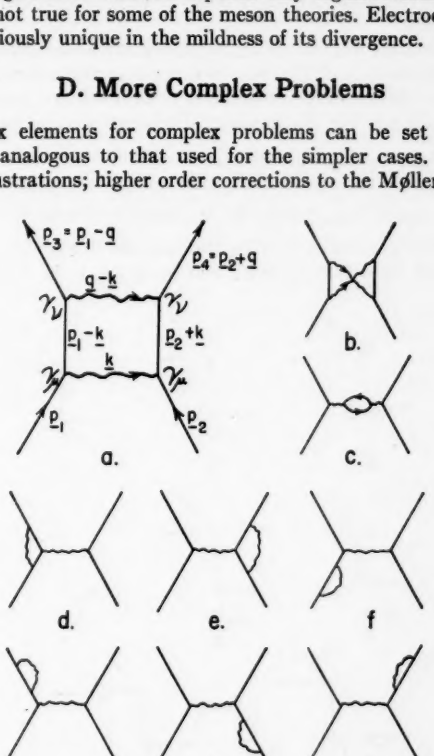

FIG. 8. The interaction between two electrons to order $(e^2/\hbar c)^2$. One adds the contribution of every figure involving two virtual quanta, Appendix D.

ing, to the Compton scattering, and the interaction of a neutron with an electromagnetic field.

For the Møller scattering, consider two electrons, one in state u_1 of momentum p_1 and the other in state u_2 of momentum p_2. Later they are found in states u_3, p_3 and u_4, p_4. This may happen (first order in $e^2/\hbar c$) because they exchange a quantum of momentum $q=p_1-p_3=p_4-p_2$ in the manner of Eq. (4) and Fig. 1. The matrix element for this process is proportional to (translating (4) to momentum space)

$$(\bar{u}_4\gamma_\mu u_2)(\bar{u}_3\gamma_\mu u_1)q^{-2}. \tag{37a}$$

We shall discuss corrections to (37a) to the next order in $e^2/\hbar c$. (There is also the possibility that it is the electron at 2 which finally arrives at 3, the electron at 1 going to 4 through the exchange of quantum of momentum p_3-p_2. The amplitude for this process, $(\bar{u}_4\gamma_\mu u_1)(\bar{u}_3\gamma_\mu u_2)(p_3-p_2)^{-2}$, must be subtracted from (37a) in accordance with the exclusion principle. A similar situation exists to each order so that we need consider in detail only the corrections to (37a), reserving to the last the subtraction of the same terms with 3, 4 exchanged.)

One reason that (37a) is modified is that two quanta may be exchanged, in the manner of Fig. 8a. The total matrix element for all exchanges of this type is

$$(e^2/\pi i)\int(\bar{u}_3\gamma_\nu(p_1-k-m)^{-1}\gamma_\mu u_1)(\bar{u}_4\gamma_\nu(p_2+k-m)^{-1}\gamma_\mu u_2)\cdot k^{-2}(q-k)^{-2}d^4k, \tag{38a}$$

as is clear from the figure and the general rule that electrons of momentum p contribute in amplitude $(p-m)^{-1}$ between interactions γ_μ, and that quanta of momentum k contribute k^{-2}. In integrating on d^4k and summing over μ and ν, we add all alternatives of the type of Fig. 8a. If the time of absorption, γ_μ, of the quantum k by electron 2 is later than the absorption, γ_ν, of $q-k$, this corresponds to the virtual state p_2+k being a positron (so that (38a) contains over thirty terms of the conventional method of analysis).

In integrating over all these alternatives we have considered all possible distortions of Fig. 8a which preserve the order of events along the trajectories. We have not included the possibilities corresponding to Fig. 8b, however. Their contribution is

$$(e^2/\pi i)\int(\bar{u}_3\gamma_\nu(p_1-k-m)^{-1}\gamma_\mu u_1)\times(\bar{u}_4\gamma_\mu(p_2+q-k-m)^{-1}\gamma_\nu u_2)k^{-2}(q-k)^{-2}d^4k, \tag{39a}$$

as is readily verified by labeling the diagram. The contributions of all possible ways that an event can occur are to be added. This means that one adds with equal weight the integrals corresponding to each topologically distinct figure.

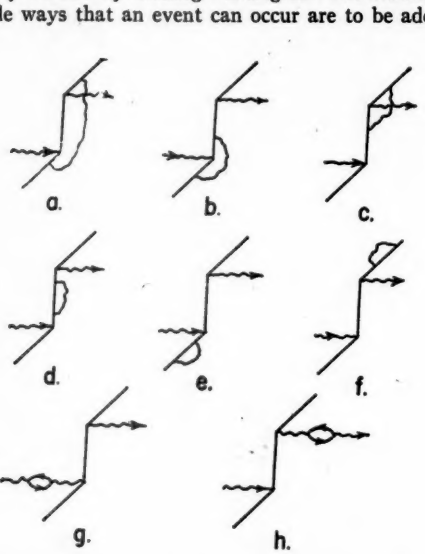

FIG. 9. Radiative correction to the Compton scattering term (a) of Fig. 5. Appendix D.

To this same order there are also the possibilities of Fig. 8d which give

$$(e^2/\pi i)\int(\bar{u}_3\gamma_\nu(p_3-k-m)^{-1}\gamma_\mu(p_1-k-m)^{-1}\gamma_\nu u_1)\times(\bar{u}_4\gamma_\mu u_2)k^{-2}q^{-2}d^4k.$$

This integral on k will be seen to be precisely the integral (12) for the radiative corrections to scattering, which we have worked out. The term may be combined with the renormalization terms resulting from the difference of the effects of mass change and the terms, Figs. 8f and 8g. Figures 8e, 8h, and 8i are similarly analyzed.

Finally the term Fig. 8c is clearly related to our vacuum polarization problem, and when integrated gives a term proportional to $(\bar{u}_4\gamma_\mu u_2)(\bar{u}_3\gamma_\nu u_1)J_{\mu\nu}q^{-4}$. If the charge is renormalized the term $\ln(\lambda/m)$ in $J_{\mu\nu}$ in (33) is omitted so there is no remaining dependence on the cut-off.

The only new integrals we require are the convergent integrals (38a) and (39a). They can be simplified by rationalizing the denominators and combining them by (14a). For example (38a) involves the factors $(k^2-2p_1\cdot k)^{-1}(k^2+2p_2\cdot k)^{-1}k^{-2}(q^2+k^2-2q\cdot k)^{-2}$. The first two may be combined by (14a) with a parameter x, and the second pair by an expression obtained by differentiation (15a) with respect to b and calling the parameter y. There results a factor $(k^2-2p_x\cdot k)^{-3}(k^2+yq^2-2yq\cdot k)^{-4}$ so that the integrals on d^4k now involve two factors and can be performed by the methods given earlier in the appendix. The subsequent integrals on the parameters x and y are complicated and have not been worked out in detail.

Working with charged mesons there is often a considerable reduction of the number of terms. For example, for the interaction between protons resulting from the exchange of two mesons only the term corresponding to Fig. 8b remains. Term 8a, for example, is impossible, for if the first proton emits a positive meson the second cannot absorb it directly for only neutrons can absorb positive mesons.

As a second example, consider the radiative correction to the Compton scattering. As seen from Eq. (15) and Fig. 5 this scattering is represented by two terms, so that we can consider the corrections to each one separately. Figure 9 shows the types of terms arising from corrections to the term of Fig. 5a. Calling k the momentum of the virtual quantum, Fig. 9a gives an integral

$$\int\gamma_\mu(p_2-k-m)^{-1}e_2(p_1+q_1-k-m)^{-1}e_1(p_1-k-m)^{-1}\gamma_\mu k^{-2}d^4k,$$

convergent without cut-off and reducible by the methods outlined in this appendix.

The other terms are relatively easy to evaluate. Terms b and c of Fig. 9 are closely related to radiative corrections (although somewhat more difficult to evaluate, for one of the states is not that of a free electron, $(p_1+q)^2\neq m^2$). Terms e, f are renormalization terms. From term d must be subtracted explicitly the effect of mass Δm, as analyzed in Eqs. (26) and (27) leading to (28) with $p'=p_1+q$, $a=e_2$, $b=e_1$. Terms g, h give zero since the vacuum polarization has zero effect on free light quanta, $q_1^2=0$, $q_2^2=0$. The total is insensitive to the cut-off λ.

The result shows an infra-red catastrophe, the largest part of the effect. When cut-off at $\lambda_{\min}$, the effect proportional to $\ln(m/\lambda_{\min})$ goes as

$$(e^2/\pi)\ln(m/\lambda_{\min})(1-2\theta\operatorname{ctn}2\theta), \tag{40a}$$

times the uncorrected amplitude, where $(p_2-p_1)^2=4m^2\sin^2\theta$. This is the same as for the radiative correction to scattering for a deflection p_2-p_1. This is physically clear since the long wave quanta are not effected by short-lived intermediate states. The infra-red effects arise[28] from a final adjustment of the field from the asymptotic coulomb field characteristic of the electron of

[28] F. Bloch and A. Nordsieck, Phys. Rev. **52**, 54 (1937).

momentum p_1 before the collision to that characteristic of an electron moving in a new direction p_2 after the collision.

The complete expression for the correction is a very complicated expression involving transcendental integrals.

As a final example we consider the interaction of a neutron with an electromagnetic field in virtue of the fact that the neutron may emit a virtual negative meson. We choose the example of pseudoscalar mesons with pseudovector coupling. The change in amplitude due to an electromagnetic field $A=a\exp(-iq\cdot x)$ determines the scattering of a neutron by such a field. In the limit of small q it will vary as $qa-aq$ which represents the interaction of a particle possessing a magnetic moment. The first-order interaction between an electron and a neutron is given by the same calculation by considering the exchange of a quantum between the electron and the nucleon. In this case a_μ is q^{-2} times the matrix element of γ_μ between the initial and final states of the electron, the states differing in momentum by q.

The interaction may occur because the neutron of momentum p_1 emits a negative meson becoming a proton which proton interacts with the field and then reabsorbs the meson (Fig. 10a). The matrix for this process is $(p_2=p_1+q)$,

$$\int(\gamma_5 k)(p_2-k-M)^{-1}a(p_1-k-M)^{-1}(\gamma_5 k)(k^2-\mu^2)^{-1}d^4k. \quad (41a)$$

Alternatively it may be the meson which interacts with the field. We assume that it does this in the manner of a scalar potential satisfying the Klein Gordon Eq. (35), (Fig. 10b)

$$-\int(\gamma_5 k_2)(p_1-k_1-M)^{-1}(\gamma_5 k_1)(k_2^2-\mu^2)^{-1}\times(k_2\cdot a+k_1\cdot a)(k_1^2-\mu^2)^{-1}d^4k_1, \quad (42a)$$

where we have put $k_2=k_1+q$. The change in sign arises because the virtual meson is negative. Finally there are two terms arising from the $\gamma_5 a$ part of the pseudovector coupling (Figs. 10c, 10d)

$$\int(\gamma_5 k)(p_2-k-M)^{-1}(\gamma_5 a)(k^2-\mu^2)^{-1}d^4k, \quad (43a)$$

and

$$\int(\gamma_5 a)(p_1-k-M)^{-1}(\gamma_5 k)(k^2-\mu^2)^{-1}d^4k. \quad (44a)$$

Using convergence factors in the manner discussed in the section on meson theories each integral can be evaluated and the results combined. Expanded in powers of q the first term gives the magnetic moment of the neutron and is insensitive to the cut-off, the next gives the scattering amplitude of slow electrons on neutrons, and depends logarithmically on the cut-off.

The expressions may be simplified and combined somewhat before integration. This makes the integrals a little easier and also shows the relation to the case of pseudoscalar coupling. For example in (41a) the final $\gamma_5 k$ can be written as $\gamma_5(k-p_1+M)$ since $p_1=M$ when operating on the initial neutron state. This is

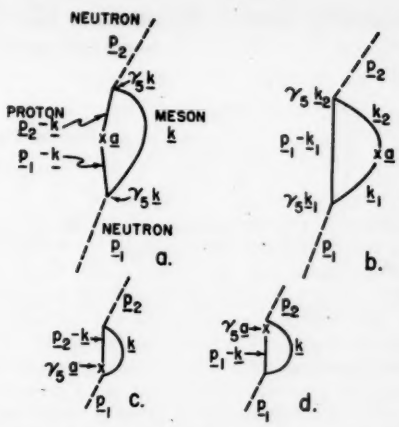

FIG. 10. According to the meson theory a neutron interacts with an electromagnetic potential a by first emitting a virtual charged meson. The figure illustrates the case for a pseudoscalar meson with pseudovector coupling. Appendix D.

$(p_1-k-M)\gamma_5+2M\gamma_5$ since γ_5 anticommutes with p_1 and k. The first term cancels the $(p_1-k-M)^{-1}$ and gives a term which just cancels (43a). In a like manner the leading factor $\gamma_5 k$ in (41a) is written as $-2M\gamma_5-\gamma_5(p_2-k-M)$, the second term leading to a simpler term containing no $(p_2-k-M)^{-1}$ factor and combining with a similar one from (44a). One simplifies the $\gamma_5 k_1$ and $\gamma_5 k_2$ in (42a) in an analogous way. There finally results terms like (41a), (42a) but with pseudoscalar coupling $2M\gamma_5$ instead of $\gamma_5 k$, no terms like (43a) or (44a) and a remainder, representing the difference in effects of pseudovector and pseudoscalar coupling. The pseudoscalar terms do not depend sensitively on the cut-off, but the difference term depends on it logarithmically. The difference term affects the electron-neutron interaction but not the magnetic moment of the neutron.

Interaction of a proton with an electromagnetic potential can be similarly analyzed. There is an effect of virtual mesons on the electromagnetic properties of the proton even in the case that the mesons are neutral. It is analogous to the radiative corrections to the scattering of electrons due to virtual photons. The sum of the magnetic moments of neutron and proton for charged mesons is the same as the proton moment calculated for the corresponding neutral mesons. In fact it is readily seen by comparing diagrams, that for arbitrary q, the scattering matrix to *first order in the electromagnetic potential* for a proton according to neutral meson theory is equal, if the mesons were charged, to the sum of the matrix for a neutron and the matrix for a proton. This is true, for any type or mixtures of meson coupling, to all orders in the coupling (neglecting the mass difference of neutron and proton).

Quantum Electrodynamics. III. The Electromagnetic Properties of the Electron —Radiative Corrections to Scattering

JULIAN SCHWINGER

Harvard University, Cambridge, Massachusetts

(Received May 26, 1949)

The discussion of vacuum polarization in the previous paper of this series was confined to that produced by the field of a prescribed current distribution. We now consider the induction of current in the vacuum by an electron, which is a dynamical system and an entity indistinguishable from the particles associated with vacuum fluctuations. The additional current thus attributed to an electron implies an alteration in its electromagnetic properties which will be revealed by scattering in a Coulomb field and by energy level displacements. This paper is concerned with the computation of the second-order corrections to the current operator and the application to electron scattering. Radiative corrections to energy levels will be treated in the next paper of the series. Following a canonical transformation which effectively renormalizes the electron mass, the correction to the current operator produced by the coupling with the electromagnetic field is developed in a power series, of which first- and second-order terms are retained. One thus obtains second-order modifications in the current operator which are of the same general nature as the previously treated vacuum polarization current, save for a contribution that has the form of a dipole current. The latter implies a fractional increase of $\alpha/2\pi$ in the spin magnetic moment of the electron. The only flaw in the second-order current correction is a logarithmic divergence attributable to an infra-red catastrophe. It is remarked that, in the presence of an external field, the first-order current correction will introduce a compensating divergence. Thus, the second-order corrections to particle electromagnetic properties cannot be completely stated without regard for the manner of exhibiting them by an external field. Accordingly, we consider in the second section the interaction of three systems, the matter field, the electromagnetic field, and a given current distribution. It is shown that this situation can be described in terms of an external potential coupled to the current operator, as modified by the interaction with the vacuum electromagnetic field. Application is made to the scattering of an electron by an external field, in which the latter is regarded as a small perturbation. It is found convenient to calculate the total rate at which collisions occur and then identify the cross sections for individual events. The correction to the cross section for radiationless scattering is determined by the second-order correction to the current operator, while scattering that is accompanied by single quantum emission is a consequence of the first-order current correction. The final object of calculation is the differential cross section for scattering through a given angle with a prescribed maximum energy loss, which is completely free of divergences. Detailed evaluations are given in two situations, the essentially elastic scattering of an electron, in which only a small fraction of the kinetic energy is radiated, and the scattering of a slowly moving electron with unrestricted energy loss. The Appendix is devoted to an alternative treatment of the polarization of the vacuum by an external field. The conditions imposed on the induced current by the charge conservation and gauge invariance requirements are examined. It is found that the fulfillment of these formal properties requires the vanishing of an integral that is not absolutely convergent, but naturally vanishes for reasons of symmetry. This null integral is then used to simplify the expression for the induced current in such a manner that direct calculation yields a gauge invariant result. The induced current contains a logarithmically divergent multiple of the external current, which implies that a non-vanishing total charge, proportional to the external charge, is induced in the vacuum. The apparent contradiction with charge conservation is resolved by showing that a compensating charge escapes to infinity. Finally, the expression for the electromagnetic mass of the electron is treated with the methods developed in this paper.

A COVARIANT form of quantum electrodynamics has been developed, and applied to two elementary vacuum fluctuation phenomena in the previous articles of this series.[1] These applications were the polarization of the vacuum, expressing the modifications in the properties of an electromagnetic field arising from its interaction with the matter field vacuum fluctuations, and the electromagnetic mass of the electron, embodying the corrections to the mechanical properties of the matter field, in its single particle aspect, that are produced by the vacuum fluctuations of the electromagnetic field. In these problems, the divergences that mar the theory are found to be concealed in unobservable charge and mass renormalization factors.

The previous discussion of the polarization of the vacuum was concerned with a given current distribution, one that is not affected by the dynamical reactions of the electron-positron matter field. We shall now consider the more complicated situation in which the original current is that ascribed to an electron or positron—a dynamical system, and an entity indistinguishable from the particles associated with the matter field vacuum fluctuations. The changed electromagnetic properties of the particle will be exhibited in an external field, and may be compared with the experimental indications of deviations from the Dirac theory that were briefly discussed in I. To avoid a work of excessive length, this discussion will be given in two papers. In this paper we shall construct the current operator as modified, to the second order, by the coupling with the vacuum electromagnetic field. This will be applied to compute the radiative correction to the scattering of an electron by a Coulomb field.[2] The second paper will deal with the effects of radiative corrections on energy levels.

1. SECOND-ORDER CORRECTIONS TO THE CURRENT OPERATOR

We shall evaluate the second-order modifications of the current operator produced by the coupling between

[1] Julian Schwinger, "Quantum Electrodynamics. I," Phys. Rev. 74, 1439 (1948); "Quantum Electrodynamics. II," Phys. Rev. 75, 651 (1949).

[2] A short account of the results has already been published, Julian Schwinger, Phys. Rev. 75, 898 (1949).

the matter and electromagnetic fields. The latter is described by

$$i\hbar c\frac{\delta\Psi[\sigma]}{\delta\sigma(x)}=\mathcal{H}(x)\Psi[\sigma],$$

$$\mathcal{H}(x)=-\frac{1}{c}j_\mu(x)A_\mu(x). \tag{1.1}$$

Among the effects produced by this coupling is the electromagnetic mass of the electron, as contained in the self-energy operator $\mathcal{H}_{1,0}(x)$. In order to describe the electron in terms of the experimental mass, we write (1.1) as

$$i\hbar c\frac{\delta\Psi[\sigma]}{\delta\sigma(x)}=(\mathcal{H}_{1,0}(x)+\mathcal{K}(x))\Psi[\sigma], \tag{1.2}$$

where

$$\mathcal{K}(x)=\mathcal{H}(x)-\mathcal{H}_{1,0}(x). \tag{1.3}$$

The canonical transformation

$$\Psi[\sigma]\rightarrow W[\sigma]\Psi[\sigma],$$

$$i\hbar c\frac{\delta W[\sigma]}{\delta\sigma(x)}=\mathcal{H}_{1,0}(x)W[\sigma], \tag{1.4}$$

then replaces (1.2) with

$$i\hbar c\frac{\delta\Psi[\sigma]}{\delta\sigma(x)}=W^{-1}[\sigma]\mathcal{K}(x)W[\sigma]\Psi[\sigma], \tag{1.5}$$

while the operator representing the current becomes $W^{-1}[\sigma]j_\mu(x)W[\sigma]$. Now, as we have shown in II, the spinor $W^{-1}[\sigma]\psi(x)W[\sigma]$ obeys the Dirac equation for a particle of mass $m=m_0+\delta m$, the experimental mass of the electron. Accordingly, the expectation value of the current operator can be computed as

$$\langle j_\mu(x)\rangle=(\Psi[\sigma],j_\mu(x)\Psi[\sigma]), \tag{1.6}$$

where

$$i\hbar c\frac{\delta\Psi[\sigma]}{\delta\sigma(x)}=\mathcal{K}(x)\Psi[\sigma], \tag{1.7}$$

with the understanding that the experimental electron mass is to be employed.

If a solution of the latter equation is constructed in the form

$$\Psi[\sigma]=U[\sigma]\Psi_0, \tag{1.8}$$

the expectation value of the current operator becomes

$$\langle j_\mu(x)\rangle=(\Psi_0,U^{-1}[\sigma]j_\mu(x)U[\sigma]\Psi_0)=(\Psi_0,\mathbf{j}_\mu(x)\Psi_0), \tag{1.9}$$

in which the latter version describes the effect of the coupling between the fields by changing the current operator into

$$\mathbf{j}_\mu(x)=U^{-1}[\sigma]j_\mu(x)U[\sigma]. \tag{1.10}$$

The unitary operator $U[\sigma]$ obeys the equation of motion

$$i\hbar c\frac{\delta U[\sigma]}{\delta\sigma(x)}=\mathcal{K}(x)U[\sigma], \tag{1.11}$$

which may be supplemented by the boundary condition

$$U[-\infty]=1, \tag{1.12}$$

in accordance with the supposition that coupling between the two fields is adiabatically established in the remote past.

The operator $\mathbf{j}_\mu(x)$ can now be evaluated by remarking that

$$\mathbf{j}_\mu(x)=j_\mu(x)+\int_{-\infty}^{\sigma}d\omega'\frac{\delta}{\delta\sigma'(x')}(U^{-1}[\sigma']j_\mu(x)U[\sigma'])$$

$$=j_\mu(x)-\frac{i}{\hbar c}\int_{-\infty}^{\sigma}d\omega'U^{-1}[\sigma'][j_\mu(x),\mathcal{K}(x')]U[\sigma']. \tag{1.13}$$

This process can be continued according to

$$\int_{-\infty}^{\sigma}d\omega'U^{-1}[\sigma'][j_\mu(x),\mathcal{K}(x')]U[\sigma']=\int_{-\infty}^{\sigma}d\omega'[j_\mu(x),\mathcal{K}(x')]$$

$$+\int_{-\infty}^{\sigma}d\omega'\int_{-\infty}^{\sigma'}d\omega''\frac{\delta}{\delta\sigma''(x'')}(U^{-1}[\sigma'''][j_\mu(x),\mathcal{K}(x')]U[\sigma'']), \tag{1.14}$$

and yields $\mathbf{j}_\mu(x)$ in the form of an infinite series,

$$\mathbf{j}_\mu(x)=j_\mu(x)+\left(-\frac{i}{\hbar c}\right)\int_{-\infty}^{\sigma}d\omega'[j_\mu(x),\mathcal{K}(x')]+\left(-\frac{i}{\hbar c}\right)^2\int_{-\infty}^{\sigma}d\omega'\int_{-\infty}^{\sigma'}d\omega''[[j_\mu(x),\mathcal{K}(x')],\mathcal{K}(x'')]+\cdots. \tag{1.15}$$

An equivalent procedure, which exhibits $\mathbf{j}_\mu(x)$ in a form that is more symmetrical between past and future, is

based on the following observation,

$$\int_{-\infty}^{\infty} d\omega' \epsilon[\sigma,\sigma'] \frac{\delta}{\delta\sigma'(x')} (U^{-1}[\sigma'] j_\mu(x) U[\sigma']) = \int_{-\infty}^{\sigma} d\omega' \frac{\delta}{\delta\sigma'(x')} (U^{-1}[\sigma'] j_\mu(x) U[\sigma'])$$

$$+ \int_{\infty}^{\sigma} d\omega' \frac{\delta}{\delta\sigma'(x')} (U^{-1}[\sigma'] j_\mu(x) U[\sigma']) = (\mathbf{j}_\mu(x) - j_\mu(x)) + (\mathbf{j}_\mu(x) - U^{-1}[\infty] j_\mu(x) U[\infty]), \quad (1.16)$$

or

$$\mathbf{j}_\mu(x) = \tfrac{1}{2}(j_\mu(x) + S^{-1} j_\mu(x) S) + \left(-\frac{i}{2\hbar c}\right) \int_{-\infty}^{\infty} d\omega' \epsilon[\sigma,\sigma'] U^{-1}[\sigma'] [j_\mu(x), \mathcal{K}(x')] U[\sigma'], \quad (1.17)$$

where

$$S = U[\infty], \quad U[-\infty] = 1 \quad (1.18)$$

is the collision operator which describes the real transitions that permanently alter the state of the system. This process can be continued and finally yields

$$\mathbf{j}_\mu(x) = \tfrac{1}{2}(k_\mu(x) + S^{-1} k_\mu(x) S), \quad (1.19)$$

in which

$$k_\mu(x) = j_\mu(x) + \left(-\frac{i}{2\hbar c}\right) \int_{-\infty}^{\infty} d\omega' \epsilon[\sigma,\sigma'] [j_\mu(x), \mathcal{K}(x')]$$

$$+ \left(-\frac{i}{2\hbar c}\right)^2 \int_{-\infty}^{\infty} d\omega' d\omega'' \epsilon[\sigma,\sigma'] \epsilon[\sigma',\sigma''] [[j_\mu(x), \mathcal{K}(x')], \mathcal{K}(x'')] + \cdots. \quad (1.20)$$

The further terms in the series are not required to compute the second-order correction of the current operator.

The collision operator S can be constructed in a similar manner. Thus,

$$S - 1 = \int_{-\infty}^{\infty} d\omega \frac{\delta}{\delta\sigma(x)} U[\sigma] = -\frac{i}{\hbar c} \int_{-\infty}^{\infty} d\omega \mathcal{K}(x) U[\sigma], \quad (1.21)$$

and

$$U[\sigma] - \tfrac{1}{2}(S+1) = \frac{1}{2} \int_{-\infty}^{\infty} d\omega' \epsilon[\sigma,\sigma'] \frac{\delta}{\delta\sigma'(x')} U[\sigma'] = -\frac{i}{2\hbar c} \int_{-\infty}^{\infty} d\omega' \epsilon[\sigma,\sigma'] \mathcal{K}(x') U[\sigma'], \quad (1.22)$$

whence,

$$S - 1 = \left(-\frac{i}{2\hbar c}\right) \int_{-\infty}^{\infty} d\omega \mathcal{K}(x)(S+1) + 2\left(-\frac{i}{2\hbar c}\right)^2 \int_{-\infty}^{\infty} d\omega d\omega' \epsilon[\sigma,\sigma'] \mathcal{K}(x) \mathcal{K}(x') U[\sigma']. \quad (1.23)$$

Continuing in this manner, we obtain

$$\frac{S-1}{S+1} = \left(-\frac{i}{2\hbar c}\right) \int_{-\infty}^{\infty} d\omega \mathcal{K}(x) + \left(-\frac{i}{2\hbar c}\right)^2 \int_{-\infty}^{\infty} d\omega d\omega' \epsilon[\sigma,\sigma'] \mathcal{K}(x) \mathcal{K}(x') + \cdots. \quad (1.24)$$

Only the indicated terms need be retained for the desired degree of approximation. In view of the absence of real first-order effects, as expressed by

$$\int_{-\infty}^{\infty} \mathcal{K}(x) d\omega = 0, \quad (1.25)$$

the leading terms in (1.24) are of the second order:

$$\frac{S-1}{S+1} = -\frac{i}{2\hbar c} \int_{-\infty}^{\infty} d\omega \left[-\frac{i}{4\hbar c} \int_{-\infty}^{\infty} \epsilon(x-x') [\mathcal{K}(x), \mathcal{K}(x')] d\omega' - \mathcal{K}_{1,0}(x) \right]. \quad (1.26)$$

According to (II 3.14) and (II 3.71), (the vacuum term $\mathcal{K}_{0,0}$ is of no consequence),

$$-\frac{i}{4\hbar c} \int_{-\infty}^{\infty} \epsilon(x-x') [\mathcal{K}(x), \mathcal{K}(x')] d\omega' = \mathcal{K}_{1,0}(x) + \mathcal{K}_{2,0}(x) + \mathcal{K}_{1,1}(x), \quad (1.27)$$

whence,

$$\frac{S-1}{S+1} = -\frac{i}{2\hbar c} \int_{-\infty}^{\infty} [\mathcal{K}_{2,0}(x) + \mathcal{K}_{1,1}(x)] d\omega, \quad (1.28)$$

which describes the real effects involving either two particles or one particle and a light quantum. Since we shall be concerned only with second-order effects referring to a single particle and the absence of light quanta, such real processes do not come into play and S is effectively unity. Consequently, the current operator is modified only by virtual processes, and is completely symmetrical between past and future. Thus, to the desired order of approximation,

$$\mathbf{j}_\mu(x)=j_\mu(x)-\frac{i}{2\hbar c}\int_{-\infty}^{\infty}d\omega'\epsilon[\sigma,\sigma'][j_\mu(x),\mathcal{H}(x')]+\frac{i}{2\hbar c}\int_{-\infty}^{\infty}d\omega'\epsilon[\sigma,\sigma'][j_\mu(x),\mathcal{H}_{1,0}(x')]$$

$$+\left(-\frac{i}{2\hbar c}\right)^2\int_{-\infty}^{\infty}d\omega'd\omega''\epsilon[\sigma,\sigma']\epsilon[\sigma',\sigma'']][[i_\mu(x),\mathcal{H}(x')],\mathcal{H}(x'')]. \tag{1.29}$$

The correction to the current operator may now be written

$$\mathbf{j}_\mu(x)-j_\mu(x)=\delta j_\mu{}^{(1)}(x)+\delta j_\mu{}^{(2)}(x), \tag{1.30}$$

where

$$\delta j_\mu{}^{(1)}(x)=\frac{i}{2\hbar c^2}\int_{-\infty}^{\infty}d\omega'\epsilon(x-x')[j_\mu(x),j_\nu(x')]A_\nu(x'), \tag{1.31}$$

and

$$(\delta j_\mu{}^{(2)}(x))_{1,0}=-\frac{1}{4\hbar^2c^4}\int_{-\infty}^{\infty}d\omega'd\omega''\epsilon[\sigma,\sigma']\epsilon[\sigma',\sigma'']][[j_\mu(x),j_\nu(x')]A_\nu(x'),j_\lambda(x'')A_\lambda(x'')]_{1,0}$$

$$+\frac{i}{2\hbar c}\int_{-\infty}^{\infty}d\omega'\epsilon(x-x')[j_\mu(x),\mathcal{H}_{1,0}(x')]_1 \tag{1.32}$$

are the first- and second-order corrections, respectively. In the latter, the subscripts emphasize that we are only concerned with second-order effects involving a single particle and no light quanta. To simplify (1.32), note that

$$[[j_\mu(x),j_\nu(x')]A_\nu(x'),j_\lambda(x'')A_\lambda(x'')]_{1,0}=\tfrac{1}{2}[A_\nu(x'),A_\lambda(x'')]\{[j_\mu(x),j_\nu(x')],j_\lambda(x'')\}_1$$

$$+\tfrac{1}{2}\{A_\nu(x'),A_\lambda(x'')\}_0[[j_\mu(x),j_\nu(x')],j_\lambda(x'')]_1, \tag{1.33}$$

whence

$$(\delta j_\mu{}^{(2)}(x))_{1,0}=\frac{i}{4\hbar c^3}\int_{-\infty}^{\infty}d\omega'd\omega''\epsilon(x-x')\,\bar{D}(x'-x'')\{[j_\mu(x),j_\nu(x')],j_\nu(x'')\}_1$$

$$-\frac{1}{8\hbar c^3}\int_{-\infty}^{\infty}d\omega'd\omega''\epsilon[\sigma,\sigma']\epsilon[\sigma',\sigma'']D^{(1)}(x'-x'')[[j_\mu(x),j_\nu(x')],j_\nu(x'')]_1+\frac{i}{2\hbar c}\int_{-\infty}^{\infty}d\omega'\epsilon(x-x')[i_\mu(x),\mathcal{H}_{1,0}(x')]_1, \tag{1.34}$$

in consequence of

$$-\tfrac{1}{2}\epsilon(x'-x'')[A_\nu(x'),A_\lambda(x'')]=ihc\delta_{\nu\lambda}\bar{D}(x'-x'') \tag{1.35}$$

and

$$\{A_\nu(x'),A_\lambda(x'')\}_0=\hbar c\delta_{\nu\lambda}D^{(1)}(x'-x''). \tag{1.36}$$

The double commutator in (1.34) is easily evaluated,

$$[[j_\mu(x),j_\nu(x')],j_\nu(x'')]=-e^3c^3[\bar{\psi}(x)\gamma_\mu S(x-x')\gamma_\nu\psi(x')-\bar{\psi}(x')\gamma_\nu S(x'-x)\gamma_\mu\psi(x),\bar{\psi}(x'')\gamma_\nu\psi(x'')]$$

$$=ie^3c^3(\bar{\psi}(x)\gamma_\mu S(x-x')\gamma_\nu S(x'-x'')\gamma_\nu\psi(x'')+\bar{\psi}(x'')\gamma_\nu S(x''-x')\gamma_\nu S(x'-x)\gamma_\mu\psi(x)$$

$$-\bar{\psi}(x')\gamma_\nu S(x'-x)\gamma_\mu S(x-x'')\gamma_\nu\psi(x'')-\bar{\psi}(x'')\gamma_\nu S(x''-x)\gamma_\mu S(x-x')\gamma_\nu\psi(x')). \tag{1.37}$$

The one-particle part of $\{[j_\mu(x),j_\nu(x')],j_\nu(x'')\}$ can be constructed in the manner employed in II. We have only to notice that $[j_\mu(x),j_\nu(x')]$ has a non-vanishing vacuum expectation value. Thus,

$$\{[j_\mu(x),j_\nu(x')],j_\nu(x'')\}_1-2[j_\mu(x),j_\nu(x')]_0j_\nu(x'')$$

$$=-e^3c^3\{(\bar{\psi}(x)\gamma_\mu S(x-x')\gamma_\nu\psi(x')-\bar{\psi}(x')\gamma_\nu S(x'-x)\gamma_\mu\psi(x))_1,(\bar{\psi}(x'')\gamma_\nu\psi(x''))_1\}_1$$

$$=-e^3c^3(\bar{\psi}(x)\gamma_\mu S(x-x')\gamma_\nu\{\psi(x'),\bar{\psi}(x'')\}_0\gamma_\nu\psi(x'')-\bar{\psi}(x'')\gamma_\nu\{\psi(x''),\bar{\psi}(x')\}_0\gamma_\nu S(x'-x)\gamma_\mu\psi(x)$$

$$-\bar{\psi}(x')\gamma_\nu S(x'-x)\gamma_\mu\{\psi(x),\bar{\psi}(x'')\}_0\gamma_\nu\psi(x'')+\bar{\psi}(x'')\gamma_\nu\{\psi(x''),\bar{\psi}(x)\}_0\gamma_\mu S(x-x')\gamma_\nu\psi(x'))_1, \tag{1.38}$$

and

$$\{[j_\mu(x),j_\nu(x')],j_\nu(x'')\}_1=2[j_\mu(x),j_\nu(x')]_0 j_\nu(x'')$$
$$+e^3c^3(\bar\psi(x)\gamma_\mu S(x-x')\gamma_\nu S^{(1)}(x'-x'')\gamma_\nu\psi(x'')-\bar\psi(x'')\gamma_\nu S^{(1)}(x''-x')\gamma_\nu S(x'-x)\gamma_\mu\psi(x)$$
$$-\bar\psi(x')\gamma_\nu S(x'-x)\gamma_\mu S^{(1)}(x-x'')\gamma_\nu\psi(x'')+\bar\psi(x'')\gamma_\nu S^{(1)}(x''-x)\gamma_\mu S(x-x')\gamma_\nu\psi(x'))_1. \quad (1.39)$$

On inserting (1.37) and (1.39) into (1.34), we obtain

$$(\delta j_\mu^{(2)}(x))_{1,0}=\frac{i}{2\hbar c^2}\int_{-\infty}^{\infty}d\omega'd\omega''\epsilon(x-x')[j_\mu(x),j_\nu(x')]_0\bar D(x'-x'')j_\nu(x'')$$

$$-\frac{ie^3}{2\hbar}\int_{-\infty}^{\infty}d\omega'd\omega''(\bar\psi(x')\gamma_\nu\bar S(x'-x)\gamma_\mu S^{(1)}(x-x'')\gamma_\nu\psi(x'')+\bar\psi(x')\gamma_\nu S^{(1)}(x'-x)\gamma_\mu\bar S(x-x'')\gamma_\nu\psi(x''))_1\bar D(x'-x'')$$

$$-\frac{ie^3}{2\hbar}\int_{-\infty}^{\infty}d\omega'd\omega''(\bar\psi(x')\gamma_\nu\bar S(x'-x)\gamma_\mu\bar S(x-x'')\gamma_\nu\psi(x''))_1D^{(1)}(x'-x'')$$

$$+\frac{ie}{\hbar}\int_{-\infty}^{\infty}d\omega'(\bar\psi(x)\gamma_\mu\bar S(x-x')\phi(x')+\bar\phi(x')\bar S(x'-x)\gamma_\mu\psi(x))_1$$
$$-\frac{e}{2\hbar}\int_{-\infty}^{\infty}d\omega'\epsilon(x-x')(\bar\psi(x)\gamma_\mu[\psi(x),\mathfrak{K}_{1,0}(x')]+[\bar\psi(x),\mathfrak{K}_{1,0}(x')]\gamma_\mu\psi(x))_1, \quad (1.40)$$

where (see II (3.78))

$$\phi(x)=-\frac{e^2}{2}\int_{-\infty}^{\infty}d\omega'\gamma_\nu(\bar D(x-x')S^{(1)}(x-x')+D^{(1)}(x-x')\bar S(x-x'))\gamma_\nu\psi(x')$$
$$=\delta mc^2\psi(x). \quad (1.41)$$

The third term of (1.40) is derived from

$$\frac{ie^3}{8\hbar}\int_{-\infty}^{\infty}d\omega'd\omega''(\epsilon[\sigma,\sigma']-\epsilon[\sigma,\sigma''])\epsilon[\sigma',\sigma'']\bar\psi(x')\gamma_\nu S(x'-x)\gamma_\mu S(x-x'')\gamma_\nu\psi(x''))_1D^{(1)}(x'-x'') \quad (1.42)$$

with the aid of the identity

$$(\epsilon[\sigma,\sigma']-\epsilon[\sigma,\sigma''])\epsilon[\sigma',\sigma'']=\epsilon[\sigma,\sigma']\epsilon[\sigma,\sigma'']-1, \quad (1.43)$$

and the null value of

$$\int_{-\infty}^{\infty}d\omega'd\omega''(\bar\psi(x')\gamma_\nu S(x'-x)\gamma_\mu S(x-x'')\gamma_\nu\psi(x''))_1D^{(1)}(x'-x'')$$
$$=-\frac{1}{\hbar c}\int_{-\infty}^{\infty}d\omega'd\omega''(\bar\psi(x')\gamma_\nu\{\psi(x'),\bar\psi(x)\}\gamma_\mu\{\psi(x),\bar\psi(x'')\}\gamma_\lambda\psi(x''))_1\{A_\nu(x'),A_\lambda(x'')\}_0. \quad (1.44)$$

The latter is an immediate consequence of (1.25), expressing the absence of real first-order transitions.

The insertion of the expression for $\mathfrak{K}_{1,0}(x)$, (II (3.77)),

$$\mathfrak{K}_{1,0}(x)=\tfrac{1}{2}(\bar\psi(x)\phi(x)+\bar\phi(x)\psi(x))_1, \quad (1.45)$$

enables the last two terms of (1.40) to be combined into

$$\frac{ie}{2\hbar}(\bar\psi(x)\gamma_\mu\chi(x)+\bar\chi(x)\gamma_\mu\psi(x))_1, \quad (1.46)$$

where

$$\chi(x)=\int_{-\infty}^{\infty}d\omega'\left[\bar S(x-x')\phi(x')+\frac{i}{2}\epsilon(x-x')\{\psi(x),\bar\phi(x')\}\psi(x')\right]. \quad (1.47)$$

It will first be observed that the integrand of (1.47) vanishes, in virtue of the relation $\phi(x)=\delta mc^2\psi(x)$, since

$$\frac{i}{2}\epsilon(x-x')\{\psi(x),\bar\phi(x')\}\psi(x')=-\bar S(x-x')\delta mc^2\psi(x'). \quad (1.48)$$

On the other hand, integrals of the form

$$\int_{-\infty}^{\infty} d\omega' \bar{S}(x-x')\psi(x') \tag{1.49}$$

are divergent, since $\psi(x')$ and $\bar{S}(x-x')$, respectively, obey homogeneous and inhomogeneous equations associated with the same differential operator. It is convenient to express the latter integral as the limit of the finite quantity obtained by an alteration of the differential equation satisfied by $\psi(x)$, in which the mass parameter κ is replaced by $\kappa+\delta\kappa$ and the limit $\delta\kappa\to 0$ is taken. The differential equations

$$\left(\gamma_\mu \frac{\partial}{\partial x_\mu'} + \kappa + \delta\kappa\right)\psi(x') = 0, \quad \frac{\partial}{\partial x_\mu'}\bar{S}(x-x')\gamma_\mu - \kappa\bar{S}(x-x') = \delta(x-x'), \tag{1.50}$$

imply the relation

$$\frac{\partial}{\partial x_\mu'}[\bar{S}(x-x')\gamma_\mu\psi(x')] + \delta\kappa\bar{S}(x-x')\psi(x') = \delta(x-x')\psi(x), \tag{1.51}$$

whence

$$\int_{-\infty}^{\infty} d\omega' \bar{S}(x-x')\psi(x') = \operatorname*{Lim}_{\delta\kappa\to 0}\frac{1}{\delta\kappa}\psi(x). \tag{1.52}$$

It may be inferred that a non-vanishing value will be obtained for $\chi(x)$ if the spinor, of which (1.47) is a linear function, is subject to the Dirac equation with the mass parameter $\kappa+\delta\kappa$, and $\delta\kappa$ is allowed to approach zero. Indeed, according to (1.48) and (1.52),

$$\begin{aligned}\chi(x) &= \operatorname*{Lim}_{\delta\kappa\to 0}\int_{-\infty}^{\infty} d\omega' \bar{S}(x-x')(\phi(x') - \delta mc^2\psi(x')) \\ &= \operatorname*{Lim}_{\delta\kappa\to 0}\frac{1}{\delta\kappa}(\phi(x) - \delta mc^2\psi(x)),\end{aligned} \tag{1.53}$$

or

$$\chi(x) = \operatorname*{Lim}_{\delta\kappa\to 0}\frac{1}{\delta\kappa}\left[-\frac{e^2}{2}\int_{-\infty}^{\infty} d\omega'\gamma_\nu(\bar{D}(x-x')S^{(1)}(x-x') + D^{(1)}(x-x')\bar{S}(x-x'))\gamma_\nu\psi(x') - \delta mc^2\psi(x)\right]. \tag{1.54}$$

A suitable representation of the solution of the Dirac equation with an altered mass parameter, $\psi_{\kappa+\delta\kappa}(x')$, in terms of the actual spinor, $\psi_\kappa(x')$, is provided by

$$\psi_{\kappa+\delta\kappa}(x') = \psi_\kappa(x') + \frac{\delta\kappa}{\kappa}(x_\lambda' - x_\lambda)\frac{\partial}{\partial x_\lambda'}\psi_\kappa(x') \tag{1.55}$$

since

$$\begin{aligned}\left(\gamma_\mu\frac{\partial}{\partial x_\mu'} + \kappa\right)\psi_{\kappa+\delta\kappa}(x') &= \frac{\delta\kappa}{\kappa}\gamma_\mu\frac{\partial}{\partial x_\mu'}\psi_\kappa(x') \\ &= -\delta\kappa\psi_\kappa(x'),\end{aligned} \tag{1.56}$$

which establishes the validity of (1.55) to the first order in $\delta\kappa$. The latter is so constructed that $\psi_{\kappa+\delta\kappa}(x)=\psi_\kappa(x)$, whence,

$$\chi(x) = \frac{e^2}{2\kappa}\int_{-\infty}^{\infty} d\omega'\gamma_\nu(\bar{D}(x-x')S^{(1)}(x-x') + D^{(1)}(x-x')\bar{S}(x-x'))\gamma_\nu(x_\lambda - x_\lambda')\frac{\partial}{\partial x_\lambda'}\psi(x'). \tag{1.57}$$

The resulting expression for the second-order correction to the current operator is

$$(\delta j_\mu^{(2)}(x))_{1,0} = \frac{i}{2\hbar c^2}\int_{-\infty}^{\infty} d\omega'\epsilon(x-x')[j_\mu(x), j_\nu(x')]_0\delta A_\nu(x') - \frac{ie^3}{2\hbar}\int_{-\infty}^{\infty} d\omega' d\omega''(\bar{\psi}(x')K_\mu(x'-x, x-x'')\psi(x''))_1, \tag{1.58}$$

where

$$\delta A_\mu(x) = \frac{1}{c}\int_{-\infty}^{\infty} d\omega'\,\bar{D}(x-x')j_\mu(x'), \tag{1.59}$$

and

$$K_\mu(x'-x, x-x'') = K_\mu^{(1)}(x'-x, x-x'') + K_\mu^{(2)}(x'-x, x-x''). \tag{1.60}$$

Here

$$K_\mu^{(1)}(\xi,\eta) = \gamma_\nu(\bar{S}(\xi)\gamma_\mu S^{(1)}(\eta)\,\bar{D}(\xi+\eta) + S^{(1)}(\xi)\gamma_\mu\bar{S}(\eta)\,\bar{D}(\xi+\eta) + \bar{S}(\xi)\gamma_\mu\bar{S}(\eta)D^{(1)}(\xi+\eta))\gamma_\nu \tag{1.61}$$

and

$$K_\mu^{(2)}(\xi,\eta)=-\gamma_\mu\delta(\xi)\frac{1}{2\kappa}\frac{\partial}{\partial\eta_\lambda}\eta_\lambda\gamma_\nu(\bar{D}(\eta)S^{(1)}(\eta)+D^{(1)}(\eta)\bar{S}(\eta))\gamma_\nu-\frac{1}{2\kappa}\frac{\partial}{\partial\xi_\lambda}\xi_\lambda\gamma_\nu(\bar{D}(\xi)S^{(1)}(\xi)+D^{(1)}(\xi)\bar{S}(\xi))\gamma_\nu\delta(\eta)\gamma_\mu. \quad (1.62)$$

An equivalent form can be given in terms of the functions

$$S_\pm(x)=\bar{S}(x)\pm\frac{i}{2}S^{(1)}(x),$$

$$D_\pm(x)=\bar{D}(x)\pm\frac{i}{2}D^{(1)}(x). \quad (1.63)$$

Thus,

$$K_\mu^{(1)}(\xi,\eta)=\frac{1}{i}\gamma_\nu(S_+(\xi)\gamma_\mu S_+(\eta)D_+(\xi+\eta)-S_-(\xi)\gamma_\mu S_-(\eta)D_-(\xi+\eta))\gamma_\nu, \quad (1.64)$$

and

$$K_\mu^{(2)}(\xi,\eta)=-\gamma_\mu\delta(\xi)\frac{1}{2\kappa}\frac{\partial}{\partial\eta_\lambda}\eta_\lambda\frac{1}{i}\gamma_\nu(D_+(\eta)S_+(\eta)-D_-(\eta)S_-(\eta))\gamma_\nu$$
$$-\frac{1}{2\kappa}\frac{\partial}{\partial\xi_\lambda}\xi_\lambda\frac{1}{i}\gamma_\nu(D_+(\xi)S_+(\xi)-D_-(\xi)S_-(\xi))\gamma_\nu\delta(\eta)\gamma_\mu. \quad (1.65)$$

The first term of (1.58) is the current induced by the electromagnetic field that accompanies a given current distribution, as discussed in II. It is the second part of (1.58), expressing the additional effects involved when the current is associated with the matter field, rather than an external system, that merits our attention.

In order to evaluate $K_\mu(x'-x,x-x'')$, we shall substitute Fourier integral representations for the various functions involved, (II (A.10), (A.31)),

$$\bar{S}(x)=\frac{1}{(2\pi)^4}\int(dk)e^{ikx}(i\gamma k-\kappa)\frac{1}{k^2+\kappa^2},$$

$$S^{(1)}(x)=\frac{1}{(2\pi)^3}\int(dk)e^{ikx}(i\gamma k-\kappa)\delta(k^2+\kappa^2),$$

$$\bar{D}(x)=\frac{1}{(2\pi)^4}\int(dk)e^{ikx}\frac{1}{k^2},$$

$$D^{(1)}(x)=\frac{1}{(2\pi)^3}\int(dk)e^{ikx}\delta(k^2), \quad (1.66)$$

in which the principal part of $1/(k^2+\kappa^2)$ and $1/k^2$ is understood. We have employed the simplified notation ab to denote $a_\mu b_\mu$, the scalar product of two four-vectors. The functions (1.63) have the following Fourier integral representations,

$$S_\pm(x)=\frac{1}{(2\pi)^4}\int(dk)e^{ikx}(i\gamma k-\kappa)\left(\frac{1}{k^2+\kappa^2}\pm\pi i\delta(k^2+\kappa^2)\right),$$

$$D_\pm(x)=\frac{1}{(2\pi)^4}\int(dk)e^{ikx}\left(\frac{1}{k^2}\pm\pi i\delta(k^2)\right). \quad (1.67)$$

These expressions can be written more compactly by observing that

$$\operatorname*{Lim}_{\epsilon\to+0}\frac{1}{\xi\mp i\epsilon}=\operatorname*{Lim}_{\epsilon\to+0}\left(\frac{\xi}{\xi^2+\epsilon^2}\pm i\frac{\epsilon}{\xi^2+\epsilon^2}\right)$$

$$=\frac{1}{\xi}\pm\pi i\delta(\xi), \quad (1.68)$$

whence,

$$S_{\pm}(x)=\frac{1}{(2\pi)^4}\int(dk)e^{ikx}(i\gamma k-\kappa)\frac{1}{k^2+\kappa^2\mp i\epsilon},$$

$$D_{\pm}(x)=\frac{1}{(2\pi)^4}\int(dk)e^{ikx}\frac{1}{k^2\mp ie}, \tag{1.69}$$

in which the limit $\epsilon\rightarrow+0$ is understood.

The form obtained for $K_\mu^{(1)}$ from (1.61), is

$$K_\mu^{(1)}(x'-x,x-x'')=\frac{1}{(2\pi)^{11}}\int(dk)(dk')(dk'')e^{i(k+k')(x'-x)}e^{i(k+k'')(x-x'')}$$
$$\times\gamma_\nu(i\gamma k'-\kappa)\gamma_\mu(i\gamma k''-\kappa)\gamma_\nu\left[\frac{\delta(k'^2+\kappa^2)}{(k''^2+\kappa^2)k^2}+\frac{\delta(k''^2+\kappa^2)}{(k'^2+\kappa^2)k^2}+\frac{\delta(k^2)}{(k'^2+\kappa^2)(k''^2+\kappa^2)}\right]. \tag{1.70}$$

It is convenient to replace k_μ' and k_μ'' by

$$p_\mu'=k_\mu+k_\mu', \quad p_\mu''=k_\mu+k_\mu'', \tag{1.71}$$

which enter directly in the coordinate dependence of the Fourier integral. Since $K_\mu^{(1)}(x'-x,x-x'')$ is to be multiplied by $\bar\psi(x')$, $\psi(x'')$ and integrated with respect to x' and x'', only such values of p_μ' and p_μ'' occur for which

$$p'^2+\kappa^2=p''^2+\kappa^2=0. \tag{1.72}$$

As a result of this transformation,

$$K_\mu^{(1)}(x'-x,x-x'')=\frac{1}{(2\pi)^{11}}\int(dk)(dp')(dp'')e^{ip'(x'-x)}e^{ip''(x-x'')}\gamma_\nu(i\gamma(p'-k)-\kappa)\gamma_\mu(i\gamma(p''-k)-\kappa)\gamma_\nu$$
$$\times\left[\frac{\delta(k^2-2kp')}{(2kp'-2kp'')(2kp')}+\frac{\delta(k^2-2kp'')}{(2kp''-2kp')(2kp'')}+\frac{\delta(k^2)}{(2kp')(2kp'')}\right]. \tag{1.73}$$

The last factor in (1.73) can be simplified by writing it as

$$\frac{1}{2k(p'-p'')}\left[\frac{1}{2kp'}(\delta(k^2-2kp')-\delta(k^2))-\frac{1}{2kp''}(\delta(k^2-2kp'')-\delta(k^2))\right], \tag{1.74}$$

and observing that

$$\frac{1}{2kp}(\delta(k^2-2kp)-\delta(k^2))=-\int_0^1 du\delta'(k^2-2kpu), \tag{1.75}$$

whence (1.74) becomes

$$-\frac{1}{2k(p'-p'')}\int_0^1 du[\delta'(k^2-2kp'u)-\delta'(k^2-2kp''u)]. \tag{1.76}$$

This, in turn, can be represented more compactly as

$$\frac{1}{2}\int_{-1}^1 dv\int_0^1 udu\delta''(k^2-k(p'+p''+(p'-p'')v)u). \tag{1.77}$$

Therefore,

$$K_\mu^{(1)}(x'-x,x-x'')=\frac{1}{2(2\pi)^{11}}\int_{-1}^1 dv\int_0^1 udu\int(dk)(dp')(dp'')e^{ip'(x'-x)}e^{ip''(x-x'')}$$
$$\times\gamma_\nu(i\gamma(p'-k)-\kappa)\gamma_\mu(i\gamma(p''-k)-\kappa)\gamma_\nu\delta''(k^2-k(p'+p''+(p'-p'')v)u). \tag{1.78}$$

If the expression (1.64) is employed for $K_\mu^{(1)}$, the bracketed factors in (1.70) and (1.73) are replaced by

$$\frac{1}{\pi}Im\frac{1}{k'^2+\kappa^2-i\epsilon}\cdot\frac{1}{k''^2+\kappa^2-i\epsilon}\cdot\frac{1}{k^2-i\epsilon}=\frac{1}{\pi}Im\frac{1}{k^2-2kp'-i\epsilon}\cdot\frac{1}{k^2-2kp''-i\epsilon}\cdot\frac{1}{k^2-i\epsilon}. \tag{1.79}$$

However,

$$\frac{1}{k^2-2kp'-i\epsilon}\,\frac{1}{k^2-2kp''-i\epsilon}\,\frac{1}{k^2-i\epsilon}=\frac{1}{2k(p'-p'')}\Big[\frac{1}{2kp'}\Big(\frac{1}{k^2-2kp'-i\epsilon}-\frac{1}{k^2-i\epsilon}\Big)$$
$$-\frac{1}{2kp''}\Big(\frac{1}{k^2-2kp''-i\epsilon}-\frac{1}{k^2-i\epsilon}\Big)\Big], \tag{1.80}$$

and, on extracting the imaginary part divided by π, we again encounter (1.74).

The second part of K_μ, (1.62), can also be readily expressed in Fourier integral form

$$K_\mu{}^{(2)}(x'-x,x-x'')=\frac{1}{(2\pi)^{11}}\int(dk)(dp')(dp'')e^{ip'(x'-x)}e^{ip''(x-x'')}\Big[\frac{1}{2\kappa}p_\lambda{}'\frac{\partial}{\partial p_\lambda{}'}\gamma_\nu(i\gamma(p'-k)-\kappa)\gamma_\nu\Big(\frac{\delta((k-p')^2+\kappa^2)}{k^2}$$
$$+\frac{\delta(k^2)}{(k-p')^2+\kappa^2}\Big)\gamma_\mu+\gamma_\mu\frac{1}{2\kappa}p_\lambda{}''\frac{\delta}{\partial p_\lambda{}''}\gamma_\nu(i\gamma(p''-k)-\kappa)\gamma_\nu\Big(\frac{\delta((k-p'')^2+\kappa^2)}{k^2}+\frac{\delta(k^2)}{(k-p'')^2+\kappa^2}\Big)\Big]. \tag{1.81}$$

To evaluate the derivatives with respect to $p_\lambda{}'$ and $p_\lambda{}''$, we observe that

$$p_\lambda\frac{\partial}{\partial p_\lambda}(i\gamma(p-k)+\kappa)(i\gamma(p-k)-\kappa)f((p-k)^2+\kappa^2)=0, \tag{1.82}$$

where $f(x)$ is $\delta(x)$ or $1/x$. On differentiating and multiplying to the left by $i\gamma(p-k)-\kappa$, we obtain

$$p_\lambda\frac{\partial}{\partial p_\lambda}(i\gamma(p-k)-\kappa)f((p-k)^2+\kappa^2)=(i\gamma(p-k)-\kappa)i\gamma p(i\gamma(p-k)-\kappa)\frac{f(k^2-2kp)}{k^2-2kp}. \tag{1.83}$$

Consequently,

$$p_\lambda\frac{\partial}{\partial p_\lambda}\gamma_\nu(i\gamma(p-k)-\kappa)\gamma_\nu\Big(\frac{\delta((p-k)^2+\kappa^2)}{k^2}+\frac{\delta(k^2)}{(p-k)^2+\kappa^2}\Big)$$
$$=-\gamma_\nu(i\gamma(p-k)-\kappa)i\gamma p(i\gamma(p-k)-\kappa)\gamma_\nu\Big(\frac{\delta'(k^2-2kp)}{k^2}-\frac{(\delta k^2)}{(2kp)^2}\Big), \tag{1.84}$$

in virtue of the delta-function property

$$\delta'(x)=-\frac{\delta(x)}{x}. \tag{1.85}$$

Furthermore,

$$\frac{\delta'(k^2-2kp)}{k^2}-\frac{\delta(k^2)}{(2kp)^2}=-\frac{\partial}{\partial(2kp)}\Big(\frac{\delta(k^2-2kp)}{k^2}-\frac{\delta(k^2)}{2kp}\Big)=-\int_0^1 udu\delta''(k^2-2kpu), \tag{1.86}$$

according to (1.75). Therefore, (1.81) becomes

$$K_\mu{}^{(2)}(x'-x,x-x'')=\frac{1}{(2\pi)^{11}}\int_0^1 udu\int(dk)(dp')(dp'')e^{ip'(x'-x)}e^{ip''(x-x'')}$$
$$\times\Big[\delta''(k^2-2kp'u)\frac{1}{2\kappa}\gamma_\nu(i\gamma(p'-k)-\kappa)i\gamma p'(i\gamma(p'-k)-\kappa)\gamma_\nu\gamma_\mu$$
$$+\gamma_\mu\frac{1}{2\kappa}\gamma_\nu(i\gamma(p'-k)-\kappa)i\gamma p''(i\gamma(p''-k)-\kappa)\gamma_\nu\delta''(k^2-2kp''u)\Big]. \tag{1.87}$$

The transformation

$$k_\mu\to k_\mu+(p_\mu{}'+p_\mu{}''+(p_\mu{}'-p_\mu{}'')v)\frac{u}{2} \tag{1.88}$$

now brings the delta-function of (1.78) into the form

$$\delta''(k^2+\lambda^2u^2), \tag{1.89}$$

where

$$\lambda^2=\kappa^2\left(1+\frac{(p'-p'')^2}{4\kappa^2}(1-v^2)\right), \tag{1.90}$$

in virtue of the relations

$$\left(\frac{p'+p''}{2}\right)^2+\left(\frac{p'-p''}{2}\right)^2+\kappa^2=0, \quad (p'+p'')(p'-p'')=0. \tag{1.91}$$

As a consequence of this transformation, the factor involving the Dirac matrices in (1.78) becomes

$$\gamma_\nu\left(i\gamma\left(p'-\frac{p'+p''}{2}u-\frac{p'-p''}{2}uv\right)-\kappa\right)\gamma_\mu\left(i\gamma\left(p''-\frac{p'+p''}{2}u-\frac{p'-p''}{2}uv\right)-\kappa\right)\gamma_\nu-\gamma_\mu k^2. \tag{1.92}$$

In writing this result we have exploited the symmetry of the delta-function (1.89), in connection with the k integration, and discarded terms linear in k_λ, while replacing $k_\lambda k_\sigma$ by $\frac{1}{4}\delta_{\lambda\sigma}k^2$. The following property of the Dirac matrices has also been used,

$$\gamma_\lambda\gamma_\mu\gamma_\lambda=-2\gamma_\mu. \tag{1.93}$$

The factor (1.92) can be further simplified by omitting the terms linear in v, which will vanish on integration, and rearranging the remaining terms to obtain

$$4\kappa^2\gamma_\mu(1-u-\tfrac{1}{2}u^2)-\gamma_\mu k^2+2\kappa(u-u^2)\sigma_{\mu\nu}(p_\nu'-p_\nu'')+2(p'-p'')^2\gamma_\mu\left(1-u+\frac{1-v^2}{4}u^2\right)$$

$$+i(1-u^2v^2)(p_\mu'-p_\mu'')((i\gamma p'+\kappa)-(i\gamma p''+\kappa))-2(1-u)\Big[(i\gamma p'+\kappa)\left(\kappa(1+u)\gamma_\mu+ip_\mu''+i\frac{1-u}{2}(p_\mu'+p_\mu'')\right)$$

$$-(i\gamma p'+\kappa)\gamma_\mu(i\gamma p''+\kappa)+\left(\kappa(1+u)\gamma_\mu+ip_\mu'+i\frac{1-u}{2}(p_\mu'+p_\mu'')\right)(i\gamma p''+\kappa)\Big]. \tag{1.94}$$

Now, a right-hand factor $i\gamma p''+\kappa$ is equivalent to $-\gamma_\lambda(\partial/\partial x_\lambda'')+\kappa$ operating on $K_\mu(x'-x,x-x'')$, which annihilates $\psi(x'')$ on integration by parts. Similarly, a left-hand factor $i\gamma p'+\kappa$ annihilates $\bar\psi(x')$. As a consequence of the Dirac equation, therefore,

$$K_\mu^{(1)}(x'-x,x-x'')=\frac{1}{(2\pi)^{11}}\int_{-1}^{1}dv\int_0^1 udu\int(dk)(dp')(dp'')e^{ip'(x'-x)}e^{ip''(x-x'')}\delta''(k^2+\lambda^2u^2)$$

$$\times\Big[2\kappa^2\gamma_\mu(1-u-\tfrac{1}{2}u^2)-\tfrac{1}{2}\gamma_\mu k^2+\kappa(u-u^2)\sigma_{\mu\nu}(p_\nu'-p_\nu'')+(p'-p'')^2\gamma_\mu\left(1-u+\frac{1-v^2}{4}u^2\right)\Big]. \tag{1.95}$$

Transformations analogous to (1.88) can be introduced in the two terms of (1.87), namely $k_\mu\to k_\mu+p_\mu'u$, and $k_\mu\to k_\mu+p_\mu''u$. Both delta functions then become $\delta''(k^2+\kappa^2u^2)$, while the factors involving the Dirac matrices simplify according to

$$\frac{1}{2\kappa}\gamma_\nu(i\gamma(p-k)-\kappa)i\gamma p(i\gamma(p-k)-\kappa)\gamma_\nu\to-2\kappa^2(1-u-\tfrac{1}{2}u^2)+\tfrac{1}{2}k^2-(2\kappa^2(1-u+\tfrac{1}{2}u^2)+\tfrac{1}{2}k^2)\frac{1}{\kappa}(i\gamma p+\kappa), \tag{1.96}$$

where p is p' or p'' for the two terms of (1.87). In consequence of the Dirac equation, therefore,

$$K_\mu^{(2)}(x'-x,x-x'')=-\frac{2}{(2\pi)^{11}}\int_0^1 udu\int(dk)(dp')(dp'')e^{ip'(x'-x)}e^{p''(x-x'')}\delta''(k^2+\kappa^2u^2)$$

$$\times[2\kappa^2\gamma_\mu(1-u-\tfrac{1}{2}u^2)-\tfrac{1}{2}\gamma_\mu k^2]. \tag{1.97}$$

To combine $K_\mu^{(1)}$ and $K_\mu^{(2)}$, it is sufficient to perform an integration by parts with respect to v for the first two terms of (1.95), as indicated by

$$\int_{-1}^{1}dv\delta''(k^2+\lambda^2u^2)=2\delta''(k^2+\kappa^2u^2)-\int_1^1 dvv\frac{\partial}{\partial v}\delta''(k^2+\lambda^2u^2). \tag{1.98}$$

The integrated terms precisely cancel $K_\mu^{(2)}$. If the v differentiation is explicitly performed for the second term of (1.95), the k integral thus encountered is

$$\int (dk)k^2\delta'''(k^2+\lambda^2u^2)=\frac{1}{2}\int (dk)k_\nu\frac{\partial}{\partial k_\nu}\delta''(k^2+\lambda^2u^2)$$

$$=-2\int (dk)\delta''(k^2+\lambda^2u^2). \tag{1.99}$$

Hence,

$$K_\mu(x'-x,x-x'')=\frac{1}{(2\pi)^{11}}\int_{-1}^{1}dv\int_0^1 udu\int (dk)(dp')(dp'')e^{ip'(x'-x)}e^{ip''(x-x'')}\left[(p'-p'')^2\gamma_\mu\left(1-u+\frac{1+v^2}{4}u^2\right)\right.$$

$$\left.+\kappa(u-u^2)\sigma_{\mu\nu}(p_\nu'-p_\nu'')-2\kappa^2\gamma_\mu(1-u-\tfrac{1}{2}u^2)v\frac{\partial}{\partial v}\right]\delta''(k^2+\lambda^2u^2). \tag{1.100}$$

The integration with respect to k may now be effected. According to the integral representation,

$$\delta(k^2+\lambda^2u^2)=\frac{1}{2\pi}\int_{-\infty}^{\infty}dwe^{iw(k^2+\lambda^2u^2)}, \tag{1.101}$$

we have

$$\int (dk)\delta''(k^2+\lambda^2u^2)=-\frac{1}{2\pi}\int_{-\infty}^{\infty}w^2dwe^{iw\lambda^2u^2}\int (dk)e^{iwk^2}$$

$$=-\frac{\pi i}{2}\int_{-\infty}^{\infty}dw\frac{w}{|w|}e^{iw\lambda^2u^2}$$

$$=\frac{\pi}{\lambda^2u^2}. \tag{1.102}$$

However, it should be noticed that we are then required to evaluate integrals with respect to u of the form

$$\int_0^1 u^{n+1}du\int (dk)\delta''(k^2+\lambda^2u^2)=\frac{\pi}{\lambda^2}\int_0^1 u^{n-1}du, \tag{1.103}$$

in which n may be 0, 1 or 2. For $n=0$, the integral is logarithmically divergent.

In order to ascertain the significance of this divergence, we shall interchange the operations used in obtaining (1.103), thus producing a more easily interpreted divergent k integral. For $n=0$, (1.103) reads

$$\frac{1}{2\lambda^2}\int (dk)\int_0^1 du\frac{\partial}{\partial u}\delta'(k^2+\lambda^2u^2)=\frac{1}{2\lambda^2}\int (dk)[\delta'(k^2+\lambda^2)-\delta'(k^2)]. \tag{1.104}$$

One may express this invariant integral, in three-dimensional notation, as

$$\frac{1}{2\lambda^2}\int (d\mathbf{k})dk_0\frac{1}{2k_0}\frac{\partial}{\partial k_0}[\delta(k_0^2-\mathbf{k}^2)-\delta(k_0^2-\mathbf{k}^2-\lambda^2)]=\frac{1}{4\lambda^2}\int (d\mathbf{k})dk_0\frac{1}{k_0^2}[\delta(k_0^2-\mathbf{k}^2)-\delta(k_0^2-\mathbf{k}^2-\lambda^2)], \tag{1.105}$$

in which the delta-functions describe the energy-momentum relations of a light quantum, and of a particle with mass $\hbar\lambda/c$. On performing the k_0 integration, (1.105) becomes

$$\frac{1}{4\lambda^2}\int (d\mathbf{k})\left[\frac{1}{|\mathbf{k}|^3}-\frac{1}{(\mathbf{k}^2+\lambda^2)^{\frac{3}{2}}}\right]=\frac{\pi}{\lambda^2}\left[\int_0^\infty dk\left(\frac{1}{k}-\frac{1}{(k^2+\lambda^2)^{\frac{1}{2}}}\right)+1\right], \tag{1.106}$$

in which form it is evident that the divergence is associated with zero frequency light quanta—an "infra-red catastrophe." As we shall later demonstrate, this divergence is entirely spurious, and is removed on properly including the effects of $\delta j_\mu^{(1)}(x)$, the first-order correction to the current operator. The divergent integral (1.106) can

be expressed in terms of an invariant minimum light quantum wave number, $k_{\min}$, as

$$\frac{\pi}{\lambda^2}\left(\log\frac{\lambda}{2k_{\min}}+1\right). \tag{1.107}$$

With the k and u integrations thus performed, $K_\mu(x'-x,x-x'')$ becomes

$$K_\mu(x'-x,x-x'')=\frac{1}{(2\pi)^{10}}\int_0^1 dv\int (dp')(dp'')\exp\left[i\frac{p'+p''}{2}(x'-x'')\right]\exp\left[i(p''-p')\left(x-\frac{x'+x''}{2}\right)\right]$$
$$\times\left[\frac{(p'-p'')^2}{\kappa^2}\gamma_\mu\frac{1+v^2}{2}\left(\log\frac{\kappa}{2k_{\min}}+1+\tfrac{1}{2}\log\left(1+\frac{(p'-p'')^2}{4\kappa^2}(1-v^2)\right)\right)-\frac{(p'-p'')^2}{4\kappa^2}\gamma_\mu\right.$$
$$\left.+\frac{1}{2\kappa}\sigma_{\mu\nu}(p_\nu'-p_\nu'')\right]\frac{1}{1+((p'-p'')^2/4\kappa^2)(1-v^2)}, \tag{1.108}$$

in which we have evaluated the third term of (1.100) by writing

$$\frac{1}{1+((p'-p'')^2/4\kappa^2)(1-v^2)}=1-\frac{((p'-p'')^2/4\kappa^2)(1-v^2)}{1+((p'-p'')^2/4\kappa^2)(1-v^2)}, \tag{1.109}$$

and performing the v differentiation for the term obtained from the first part of (1.109), while reversing the integration by parts for the term produced by the second part of (1.109). It will now be observed that the integrand of (1.108) involves only $p_\lambda'-p_\lambda''$. It is then useful to introduce the new variables

$$P_\lambda=\frac{p_\lambda'+p_\lambda''}{2},\quad p_\lambda=p_\lambda''-p_\lambda', \tag{1.110}$$

since the P integration can be immediately performed, yielding $\delta(x'-x'')$. In this way, we obtain

$$K_\mu(x'-x,x-x'')=-\frac{1}{8\pi^2}\gamma_\mu\delta(x'-x'')\frac{1}{\kappa^2}\Box^2\left[\log\frac{\kappa}{2k_{\min}}(F_0(x-x')+F_1(x-x'))\right.$$
$$\left.+\tfrac{1}{2}F_0(x-x')+F_1(x-x')+\tfrac{1}{2}G(x-x')\right]+\frac{i}{8\pi^2}\delta(x'-x'')\sigma_{\mu\nu}\frac{\partial}{\partial x_\nu}F_0(x-x'), \tag{1.111}$$

where

$$F_n(x)=\int_0^1 dv v^{2n}\frac{1}{(2\pi)^4}\int (dp)\frac{e^{ipx}}{1+(p^2/4k^2)(1-v^2)}$$
$$=16\kappa^2\int_0^1 dv\frac{v^{2n}}{(1-v^2)^2}\bar{\Delta}\left(\frac{2}{(1-v^2)^{\frac{1}{2}}}x\right) \tag{1.112}$$

and

$$G(x)=\int_0^1 dv(1+v^2)\frac{1}{(2\pi)^4}\int (dp)e^{ipx}\frac{\log(1+(p^2/4\kappa^2)(1-v^2))}{1+(p^2/4\kappa^2)(1-v^2)}$$
$$=8\Box^2\int_0^1 dv\frac{1+v^2}{1-v^2}\int_0^1\frac{udu}{1-u^2}\left[\frac{1}{u^2}\bar{\Delta}\left(\frac{2}{(1-v^2)^{\frac{1}{2}}u}x\right)-\bar{\Delta}\left(\frac{2}{(1-v^2)^{\frac{1}{2}}}x\right)\right]. \tag{1.113}$$

Finally, then,

$$-\frac{ie^3}{2\hbar}\int d\omega'd\omega''(\bar{\psi}(x')K_\mu(x'-x,x-x'')\psi(x''))_1=\frac{\alpha}{4\pi}\log\frac{\kappa}{2k_{\min}}\frac{1}{\kappa^2}\Box^2\int[F_0(x-x')+F_1(x-x')]j_\mu(x')d\omega'$$
$$+\frac{\alpha}{4\pi}\frac{1}{\kappa^2}\Box^2\int[\tfrac{1}{2}F_0(x-x')+F_1(x-x')+\tfrac{1}{2}G(x-x')]j_\mu(x')d\omega'+\frac{\alpha}{2\pi}c\frac{\partial}{\partial x_\nu}\int F_0(x-x')m_{\mu\nu}(x')d\omega', \tag{1.114}$$

in which

$$m_{\mu\nu}(x)=\frac{e}{2\kappa}(\bar{\psi}(x)\sigma_{\mu\nu}\psi(x))_1$$

$$=\frac{e}{2\kappa}\tfrac{1}{2}[\bar{\psi}(x)\sigma_{\mu\nu}\psi(x)-\bar{\psi}'(x)\sigma_{\mu\nu}\psi'(x)]. \tag{1.115}$$

Expressed in the same notation, the first term of (1.58) is (see II (2.44)),

$$\frac{i}{2\hbar c^2}\int d\omega'\epsilon(x-x')[j_\mu(x),j_\nu(x')]_0\delta A_\nu(x')=-\frac{\alpha}{4\pi}\frac{1}{\kappa^2}\Box^2\int[F_1(x-x')-\tfrac{1}{3}F_2(x-x')]j_\mu(x')d\omega', \tag{1.116}$$

from which we have omitted the charge renormalization term, with the understanding that the value of e is to be correspondingly altered. A rederivation of this result, employing methods akin to those presented in this paper, is given in the Appendix. Evidently the new contributions to the one particle current operator, as given in (1.114), are of the same general nature as the previously considered effect, (1.116), with the exception of the last term in (1.114). This is an addition to the current vector of the form

$$c(\partial/\partial x)_\nu\delta m_{\mu\nu}(x), \tag{1.117}$$

where

$$\delta m_{\mu\nu}(x)=\alpha/2\pi\int F_0(x-x')m_{\mu\nu}(x')d\omega'. \tag{1.118}$$

A current vector of this type can be interpreted as a dipole current, derived from an antisymmetrical dipole tensor $\delta m_{\mu\nu}$ which combines electric and magnetic dipole moment densities. The tensor $m_{\mu\nu}$ is that characteristic of the Dirac theory, in which intrinsic dipole moments are related to the antisymmetrical spin tensor $\sigma_{\mu\nu}$, the factor of proportionality being

$$\mu_0=e/2\kappa=e\hbar/2mc, \tag{1.119}$$

the Bohr magneton. According to (1.118), the correction to the dipole tensor at a point involves an average of $m_{\mu\nu}$ over the vicinity of that point. If all quantities are slowly varying, relative to $\hbar/mc$ and $\hbar/mc^2$ as units of length and time, an expansion in ascending powers of $\Box^2$ can be constructed, as in II (2.47). For this purpose, it is sufficient to expand the denominator in the first form of (1.112), thus obtaining

$$F_n(x)=\frac{1}{2n+1}\delta(x)$$

$$+\frac{1}{(2n+1)(2n+3)}\frac{1}{2\kappa^2}\Box^2\delta(x)+\cdots. \tag{1.120}$$

Hence,

$$\delta m_{\mu\nu}(x)=\frac{\alpha}{2\pi}\left[m_{\mu\nu}(x)+\frac{1}{6\kappa^2}\Box^2 m_{\mu\nu}(x)+\cdots\right], \tag{1.121}$$

and, under conditions that permit the neglect of all but the first term in this series, an electron will act as though it possessed an additional spin magnetic moment[3]

$$\delta\mu=(\alpha/2\pi)\mu_0. \tag{1.122}$$

The comparison of this prediction with experiment will be discussed in the sequel to this paper.

The final result for the second-order correction to the one particle current operator is

$$(\delta j_\mu{}^{(2)}(x))_{1,0}=\frac{\alpha}{4\pi}\log\frac{\kappa}{2k_{\min}}\frac{1}{\kappa^2}\Box^2\int[F_0(x-x')+F_1(x-x')]j_\mu(x')d\omega'$$

$$+\frac{\alpha}{4\pi}\frac{1}{\kappa^2}\Box^2\int[\tfrac{1}{2}F_0(x-x')+\tfrac{1}{3}F_2(x-x')+\tfrac{1}{2}G(x-x')]j_\mu(x')d\omega'+c\frac{\partial}{\partial x_\nu}\delta m_{\mu\nu}(x). \tag{1.123}$$

Under conditions of slow variation ($(1/\kappa^2)\Box^2 j_\mu$, $m_{\mu\nu}\ll j_\mu, m_{\mu\nu}$), this reduces to

$$(\delta j_\mu{}^{(2)}(x))_{1,0}=\frac{\alpha}{3\pi}\left(\log\frac{\kappa}{2k_{\min}}+\frac{17}{40}\right)\frac{1}{\kappa^2}\Box^2 j_\mu(x)+\frac{\alpha}{2\pi}c\frac{\partial}{\partial x_\nu}m_{\mu\nu}(x), \tag{1.124}$$

in virtue of (1.120), and the analogous expansion of $G(x)$,

$$G(x)=-\frac{1}{5\kappa^2}\Box^2\delta(x)+\cdots. \tag{1.125}$$

It will be noted that the total charge computed from $(\delta j_\mu{}^{(2)}(x))_{1,0}$ is zero, in agreement with evident charge conservation requirements, and the formal property that the operator of total charge commutes with all

[3] This result was announced at the January, 1948 meeting of the American Physical Society. The formula is misprinted in a published note, J. Schwinger, Phys. Rev. 73, 416 (1948). The misprint has unfortunately been copied by L. Rosenfeld in his book, *Nuclear Forces* (Interscience Publishers, Inc., New York, 1949), p. 438.

one-particle operators. The apparent contradiction between these statements and the existence of the charge renormalization term is discussed in the Appendix, where it is shown that a compensating charge is created at infinity.

Our result, (1.123), is marred only by the appearance of the logarithmic divergence associated with zero frequency quanta. It should be remarked, however, that $(\delta j_\mu^{(2)}(x))_{1,0}$ is not a complete description of the radiative corrections under discussion. In order to measure the correction to the current, it is necessary to impose an external field. This will induce the emission of quanta, as described by $\delta j_\mu^{(1)}(x)$, among the effects of which is a compensating low frequency divergence. It will be apparent that, as a consequence of the "infra-red catastrophe," the second-order corrections to particle electromagnetic properties cannot be completely stated without regard for the manner of exhibiting them by an external field. We therefore turn to a discussion of the behavior of a single particle in an external field, as modified by the vacuum fluctuations of the electromagnetic field.

2. RADIATIVE CORRECTIONS TO ELECTRON SCATTERING

We shall now be concerned with the interaction of three systems—the matter field, the electromagnetic field, and a given current distribution. The latter may be associated with a nucleus or a macroscopic apparatus, two situations in which the reaction on the current distribution may have a negligible effect. A description of this state of affairs, in the interaction representation, is given by

$$ihc\frac{\delta\Psi[\sigma]}{\delta\sigma(x)}=\left[-\frac{1}{c}(j_\mu(x)+J_\mu(x))A_\mu(x)\right]\Psi[\sigma], \tag{2.1a}$$

$$\left[\frac{\partial A_\mu(x')}{\partial x_\mu'}-\frac{1}{c}\int_\sigma D(x'-x)(j_\mu(x)+J_\mu(x))d\sigma_\mu\right]\Psi[\sigma]=0, \tag{2.1b}$$

where $j_\mu(x)$ and $J_\mu(x)$ are the current vectors associated with the matter field and the external system, respectively. Both current distributions are coupled to the electromagnetic field, as characterized by $A_\mu(x)$. An equally valid way of stating matters is in terms of an external electromagnetic field acting on the matter field current distribution:

$$ihc\frac{\delta\Psi[\sigma]}{\delta\sigma(x)}=\left[-\frac{1}{c}j_\mu(x)(A_\mu(x)+A_\mu^{(e)}(x))\right]\Psi[\sigma], \tag{2.2a}$$

$$\left[\frac{\partial A_\mu(x')}{\partial x_\mu'}-\frac{1}{c}\int_\sigma D(x'-x)j_\mu(x)d\sigma_\mu\right]\Psi[\sigma]=0, \tag{2.2b}$$

where

$$\Box^2A_\mu^{(e)}(x)=-\frac{1}{c}J_\mu(x),\quad \frac{\partial A_\mu^{(e)}(x)}{\partial x_\mu}=0. \tag{2.3}$$

The equivalence of the two descriptions is established by showing that (2.2) is obtained from (2.1) by a canonical transformation, namely,

$$\Psi[\sigma]\rightarrow e^{-iJ[\sigma]}\Psi[\sigma], \tag{2.4}$$

with $J[\sigma]$ determined by

$$\hbar c\frac{\delta J[\sigma]}{\delta\sigma(x)}=-\frac{1}{c}J_\mu(x)A_\mu(x). \tag{2.5}$$

The functional $J[\sigma]$ is explicitly exhibited as

$$J[\sigma]=-\frac{1}{\hbar c^2}\int_{-\infty}^{\sigma}J_\mu(x')A_\mu(x')d\omega', \tag{2.6}$$

in which the choice of lower limit corresponds to selecting the retarded potentials for the electromagnetic field generated by the given current distribution. The equation of motion satisfied by the new state vector is

$$ihc\frac{\delta\Psi[\sigma]}{\delta\sigma(x)}+ihce^{iJ[\sigma]}\frac{\delta e^{-iJ[\sigma]}}{\delta\sigma(x)}\Psi[\sigma]=\left[-\frac{1}{c}(j_\mu(x)+J_\mu(x))e^{iJ[\sigma]}A_\mu(x)e^{-iJ[\sigma]}\right]\Psi[\sigma]. \tag{2.7}$$

Now

$$e^{iJ[\sigma]}A_\mu(x)e^{-iJ[\sigma]}=A_\mu(x)+i[J[\sigma],A_\mu(x)]-\tfrac{1}{2}[J[\sigma],[J[\sigma],A_\mu(x)]]+\cdots$$

$$=A_\mu(x)-\frac{1}{c}\int_{-\infty}^{\sigma}D(x-x')J_\mu(x')d\omega'$$

$$=A_\mu(x)+A_\mu{}^{(e)}(x), \tag{2.8}$$

in which the series ends after two terms since the components of $J_\mu(x)$ are mutually commutative, in view of the prescribed nature of this current distribution. It is easily seen that

$$A_\mu{}^{(e)}(x)=-\frac{1}{c}\int_{-\infty}^{\sigma}D(x-x')J_\mu(x')d\omega' \tag{2.9}$$

obeys (2.3). Indeed,

$$\Box^2A_\mu{}^{(e)}(x)=-\frac{1}{c}\frac{\partial}{\partial x_\nu}\int_{-\infty}^{\sigma}\frac{\partial D(x-x')}{\partial x_\nu'}J_\mu(x')d\omega'$$

$$=-\frac{1}{c}\int_{\sigma}d\sigma_\nu'\frac{\partial D(x-x')}{\partial x_\nu'}J_\mu(x')$$

$$=-\frac{1}{c}J_\mu(x), \tag{2.10}$$

and

$$\frac{\partial A_\mu{}^{(e)}(x)}{\partial x_\mu}=-\frac{1}{c}\int_{-\infty}^{\sigma}d\omega'\frac{\partial}{\partial x_\mu'}(D(x-x')J_\mu(x'))$$

$$=0. \tag{2.11}$$

Furthermore,

$$ihce^{iJ[\sigma]}\frac{\delta e^{-iJ[\sigma]}}{\delta\sigma(x)}=hc\frac{\delta J[\sigma]}{\delta\sigma(x)}+\frac{ihc}{2}\left[J[\sigma],\frac{\delta J[\sigma]}{\delta\sigma(x)}\right]+\cdots$$

$$=-\frac{1}{c}J_\mu(x)A_\mu(x)-\frac{1}{2c}J_\mu(x)A_\mu{}^{(e)}(x), \tag{2.12}$$

and the transformed equation of motion therefore reads

$$ihc\frac{\delta\Psi[\sigma]}{\delta\sigma(x)}=\left[-\frac{1}{c}j_\mu(x)(A_\mu(x)+A_\mu{}^{(e)}(x))-\frac{1}{2c}J_\mu(x)A_\mu{}^{(e)}(x)\right]\Psi[\sigma], \tag{2.13}$$

which is equivalent to (2.2a), since the term $-(1/2c)J_\mu(x)A_\mu{}^{(e)}(x)$, describing the self-action of the given current distribution, has no dynamical consequences and can be omitted.

In a similar way, the supplementary condition (2.1b) is transformed into

$$\left[e^{iJ[\sigma]}\frac{\partial A_\mu(x')}{\partial x_\mu'}e^{-iJ[\sigma]}-\frac{1}{c}\int_{\sigma}D(x'-x)(j_\mu(x)+J_\mu(x))d\sigma_\mu\right]\Psi[\sigma]=0, \tag{2.14}$$

wherein

$$e^{iJ[\sigma]}\frac{\partial A_\mu(x')}{\partial x_\mu'}e^{-iJ[\sigma]}=\frac{\partial A_\mu(x')}{\partial x_\mu'}+i\left[J[\sigma],\frac{\partial A_\mu(x')}{\partial x_\mu'}\right]=\frac{\partial A_\mu(x')}{\partial x_\mu'}-\frac{1}{c}\int_{-\infty}^{\sigma}\frac{\partial D(x'-x'')}{\partial x_\mu'}J_\mu(x'')d\omega''. \tag{2.15}$$

However,

$$-\frac{1}{c}\int_{-\infty}^{\sigma}\frac{\partial D(x'-x'')}{\partial x_\mu'}J_\mu(x'')d\omega''=\frac{1}{c}\int_{-\infty}^{\sigma}\frac{\partial}{\partial x_\mu''}(D(x'-x'')J_\mu(x''))d\omega''=\frac{1}{c}\int_{\sigma}D(x'-x)J_\mu(x)d\sigma_\mu, \tag{2.16}$$

which verifies (2.2b).

One can bring (2.2) into a form which enables the results of the previous section to be utilized. The mass renormalization transformation

$$\Psi[\sigma]\rightarrow W[\sigma]\Psi[\sigma],\quad ihc\frac{[\delta W\sigma]}{\delta\sigma(x)}=\mathfrak{K}_{1,0}(x)W[\sigma], \tag{2.17}$$

replaces (2.2a) with

$$ihc\frac{\delta\Psi[\sigma]}{\delta\sigma(x)}=[\mathcal{K}(x)+\mathcal{K}^{(e)}(x)]\Psi[\sigma], \tag{2.18}$$

where (see (1.3))

$$\mathcal{K}(x)=\mathcal{H}(x)-\mathcal{H}_{1,0}(x), \tag{2.19}$$

$$\mathcal{K}^{(e)}(x)=-\frac{1}{c}j_\mu(x)A_\mu{}^{(e)}(x), \tag{2.20}$$

and the Dirac equation for $\psi(x)$ now involves the experimental mass. The further transformation

$$\Psi[\sigma]=U[\sigma]\Phi[\sigma], \tag{2.21}$$

where

$$ihc\frac{\delta U[\sigma]}{\delta\sigma(x)}=\mathcal{K}(x)U[\sigma],\quad U[-\infty]=1, \tag{2.22}$$

is the analog of (1.8), save that $\Phi[\sigma]$ varies in the presence of an external field,

$$\begin{aligned}ihc\frac{\delta\Phi[\sigma]}{\delta\sigma(x)}&=U^{-1}[\sigma]\mathcal{K}^{(e)}(x)U[\sigma]\Phi[\sigma]\\&=-\frac{1}{c}\mathbf{j}_\mu(x)A_\mu{}^{(e)}(x)\Phi[\sigma],\end{aligned} \tag{2.23}$$

in response to the coupling with the current operator $\mathbf{j}_\mu(x)$. The latter contains the modifications produced by the vacuum electromagnetic field. The supplementary condition (2.2b) appears as

$$\left[U^{-1}[\sigma]\frac{\partial A_\mu(x')}{\partial x_\mu'}U[\sigma]-\frac{1}{c}\int_\sigma D(x'-x)\mathbf{j}_\mu(x)d\sigma_\mu\right]\Phi[\sigma]=0, \tag{2.24}$$

in consequence of these transformations. However,

$$\begin{aligned}U^{-1}[\sigma]\frac{\partial A_\mu(x')}{\partial x_\mu'}U[\sigma]-\frac{\partial A_\mu(x')}{\partial x_\mu'}&=\int_{-\infty}^{\sigma}d\omega''\frac{\delta}{\delta\sigma''(x'')}\left(U^{-1}[\sigma'']\frac{\partial A_\mu(x')}{\partial x_\mu'}U[\sigma'']\right)\\&=\frac{i}{\hbar c^2}\int_{-\infty}^{\sigma}d\omega''U^{-1}[\sigma'']\left[\frac{\partial A_\mu(x')}{\partial x_\mu'},A_\nu(x'')\right]j_\nu(x'')U[\sigma'']=\frac{1}{c}\int_{-\infty}^{\sigma}d\omega''\frac{\partial}{\partial x_\mu''}(D(x'-x'')\mathbf{j}_\mu(x''))\\&=\frac{1}{c}\int_\sigma D(x'-x)\mathbf{j}_\mu(x)d\sigma_\mu,\end{aligned} \tag{2.25}$$

so that the supplementary condition associated with (2.23) is simply

$$\frac{\partial A_\mu(x')}{\partial x_\mu'}\Phi[\sigma]=0. \tag{2.26}$$

As the first application of (2.23), we shall consider the scattering of an electron produced by its interaction with an external field, in which the latter is regarded as a small perturbation.[4] We shall restrict the external potential to be that of a time independent field, which will eventually be specialized to the Coulomb field of a stationary nucleus.

A solution of (2.23) can be constructed in the form

$$\Phi[\sigma]=R[\sigma]\Phi_1, \tag{2.27}$$

where

$$ihc\frac{\delta R[\sigma]}{\delta\sigma(x)}=H(x)R[\sigma], \tag{2.28}$$

and

$$R[\sigma]\to 1,\quad \sigma\to-\infty. \tag{2.29}$$

[4] Radiative corrections to scattering have been discussed by many authors. That a finite correction is obtained after a renormalization of charge and mass was independently observed by Z. Koba and S. Tomonaga, Prog. Theor. Phys. 3, 290 (1948); H. W. Lewis, Phys. Rev. 73, 173 (1948); and J. Schwinger, Phys. Rev. 73, 416 (1948). See also R. P. Feynman, Phys. Rev. 74, 1430 (1948).

The state vector Φ_1 characterizes the initial state of the system, composed of one electron with definite energy and momentum, and no light quanta. The total probability, per unit time, that a scattering process occurs, can be obtained by evaluating the time rate of decrease of the probability that the system remain in the initial state,

$$w=-c\int dv\frac{\delta}{\delta\sigma(x)}|(\Phi_1,\Phi[\sigma])|^2=-c\int dv\frac{\delta}{\delta\sigma(x)}|(\Phi_1,R[\sigma]\Phi_1)|^2. \tag{2.30}$$

The integration is extended over the surface $t=$ const., with dv the three-dimensional volume element. Now

$$i\hbar c\frac{\delta}{\delta\sigma(x)}|(\Phi_1,R[\sigma]\Phi_1)|^2=(\Phi_1,R^{-1}[\sigma]\Phi_1)(\Phi_1,\boldsymbol{H}(x)R[\sigma]\Phi_1)-(\Phi_1,R[\sigma]\Phi_1)(\Phi_1,R^{-1}[\sigma]\boldsymbol{H}(x)\Phi_1). \tag{2.31}$$

In view of the treatment of $\boldsymbol{H}(x)$ as a small perturbation, it is sufficient to write

$$R[\sigma]=1-\frac{i}{\hbar c}\int_{-\infty}^{\sigma}\boldsymbol{H}(x')d\omega',\quad R^{-1}[\sigma]=1+\frac{i}{\hbar c}\int_{-\infty}^{\sigma}\boldsymbol{H}(x')d\omega'. \tag{2.32}$$

It will also be useful to introduce

$$\boldsymbol{H}'(x)=\boldsymbol{H}(x)-(\Phi_1,\boldsymbol{H}(x)\Phi_1), \tag{2.33}$$

which possesses a vanishing diagonal matrix element for the initial state, and obtain

$$R[\sigma]=\exp\left[-\frac{i}{\hbar c}\int_{-\infty}^{\sigma}(1|\boldsymbol{H}(x')|1)d\omega'\right]\left(1-\frac{i}{\hbar c}\int_{-\infty}^{\sigma}\boldsymbol{H}'(x')d\omega'\right). \tag{2.34}$$

The phase factor evidently has no effect in (2.31), and can be omitted. The latter is also unaffected if $\boldsymbol{H}(x)$ is replaced by $\boldsymbol{H}'(x)$. Hence to the accuracy of first-order perturbation theory, we have

$$-\frac{\delta}{\delta\sigma(x)}|(\Phi_1,R[\sigma]\Phi_1)|^2=\frac{1}{\hbar^2c^2}\left(1\left|\boldsymbol{H}'(x)\int_{-\infty}^{\sigma}\boldsymbol{H}'(x')d\omega'+\int_{-\infty}^{\sigma}\boldsymbol{H}'(x')d\omega'\boldsymbol{H}'(x)\right|1\right), \tag{2.35}$$

and

$$w=\frac{1}{\hbar^2c}\int dvdv'\left(1\left|\boldsymbol{H}'(x)\int_{\infty}^{x_0}\boldsymbol{H}'(x')dx_0'+\int_{-\infty}^{x_0}\boldsymbol{H}'(x')dx_0'\boldsymbol{H}'(x)\right|1\right). \tag{2.36}$$

We may now remark that a diagonal matrix element for a state of definite energy must be invariant with respect to time displacements, whence

$$\int dvdv'\left(1\left|\int_{\infty}^{x_0}\boldsymbol{H}'(x')dx_0'\boldsymbol{H}'(x)\right|1\right)=\int dvdv'\left(1\left|\boldsymbol{H}'(x)\int_{x_0}^{\infty}\boldsymbol{H}'(x')dx_0'\right|1\right), \tag{2.37}$$

and

$$w=\frac{1}{\hbar^2c}\int dvdv'\left(1\left|\boldsymbol{H}'(x)\int_{-\infty}^{\infty}\boldsymbol{H}'(x')dx_0'\right|1\right). \tag{2.38}$$

This result is perfectly equivalent to the more conventional perturbation formula in which the rate of transition from the initial state is expressed as a sum of transition rates to all possible final states of equal energy. The energy conservation law is here expressed by the time integration, and the summation over all states other than the original is provided for by the removal from $\boldsymbol{H}(x)$ of the diagonal matrix element. Our basic formula for calculating the transition rate for scattering of a particle by a time independent potential is thus

$$w=\frac{1}{\hbar^2c^3}\int dvdv'A_\mu^{(e)}(\mathbf{r})A_\nu^{(e)}(\mathbf{r}')\left(1\left|\mathbf{j}_\mu(x)\int_{-\infty}^{\infty}\mathbf{j}_\nu(x')dx_0'\right|1\right). \tag{2.39}$$

We have not indicated that the diagonal matrix element is to be subtracted from $\mathbf{j}_\mu(x)$, since it is sufficient to remove, in the final result, those transitions in which no change of state occurs.

We have shown in the first section that, to the second order in e,

$$\mathbf{j}_\mu(x)=j_\mu(x)+\delta j_\mu^{(1)}(x)+\delta j_\mu^{(2)}(x), \tag{2.40}$$

where

$$\delta j_\mu^{(1)}(x)=\frac{i}{2\hbar c^2}\int_{-\infty}^{\infty}\epsilon(x-x')[j_\mu(x),j_\nu(x')]_1 A_\nu(x')d\omega'$$

$$=\frac{ie^2}{\hbar}\int_{-\infty}^{\infty}[\bar\psi(x)\gamma_\mu\bar S(x-x')\gamma_\nu\psi(x')+\bar\psi(x')\gamma_\nu\bar S(x'-x)\gamma_\mu\psi(x)]_1 A_\nu(x')d\omega', \tag{2.41}$$

and

$$(\delta j_\mu^{(2)}(x))_{1,0}=iec\int_{-\infty}^{\infty}[\bar\psi(x')\Gamma_\mu(x-x')\psi(x')]_1 d\omega'. \tag{2.42}$$

Here

$$\Gamma_\mu(x)=\frac{\alpha}{4\pi}\gamma_\mu\log\frac{\kappa}{2k_{\min}}-\frac{1}{\kappa^2}\Box^2(F_0(x)+F_1(x))+\frac{\alpha}{4\pi}\gamma_\mu\frac{1}{\kappa^2}\Box^2(\tfrac{1}{2}F_0(x)+\tfrac{1}{3}F_2(x)+\tfrac{1}{2}G(x))-i\frac{\alpha}{4\pi}\sigma_{\mu\nu}\frac{1}{\kappa}\frac{\partial}{\partial x_\nu}F_0(x). \tag{2.43}$$

It is only the indicated portion of $\delta j_\mu^{(2)}(x)$, referring to one particle and no light quanta, that need be retained to compute the second-order correction to the scattering cross section for an external field, since only this part of $\delta j_\mu^{(2)}(x)$ is coherent with $j_\mu(x)$.

The total rate of transition from the initial state can now be written as

$$w=w_0+w_1, \tag{2.44}$$

where

$$w_0=\frac{1}{\hbar^2c^3}\int dvdv' A_\mu^{(e)}(\mathbf{r})A_\nu^{(e)}(\mathbf{r}')\left(1\left|(j_\mu(x)+(\delta j_\mu^{(2)}(x))_{1,0})\int_{-\infty}^{\infty}(j_\nu(x')+(\delta j_\nu^{(2)}(x'))_{1,0})dx_0'\right|1\right) \tag{2.45}$$

describes the rate of radiationless scattering, while

$$w_1=\frac{1}{\hbar^2c^3}\int dvdv' A_\mu^{(e)}(\mathbf{r})A_\nu^{(e)}(\mathbf{r}')\left(1\left|\delta j_\mu^{(1)}(x)\int_{-\infty}^{\infty}\delta j_\nu^{(1)}(x')dx_0'\right|1\right) \tag{2.46}$$

accounts for scattering that is accompanied by single quantum emission.

To indicate the manner in which the perturbation formulas are to be used, we consider the evaluation of

$$\int_{-\infty}^{\infty}(1|j_\mu(x)j_\nu(x')|1)dx_0'. \tag{2.47}$$

This can be written as

$$-e^2c^2\int_{-\infty}^{\infty}(1|\bar\psi(x)\gamma_\mu\psi(x)\bar\psi(x')\gamma_\nu\psi(x')|1)dx_0', \tag{2.48}$$

in which it is understood that one omits the processes in which $\bar\psi(x)\psi(x)$, or $\bar\psi(x')\psi(x')$ induces no change in state. Now $\psi(x')$ can either annul the original electron, in which case $\bar\psi(x')\psi(x')$ causes an electron transition to some final state, or $\psi(x')$ generates a positron, in which event $\bar\psi(x')\psi(x')$ induces the creation of a pair. However, the latter process is incompatible with the energy conservation that is enforced by the time integration, and can therefore be omitted. Hence, it only occurs that $\psi(x')$ annihilates the original electron, whence $\psi(x')\Phi_1$ is a multiple of the vacuum state vector. The same comment applies to $\bar\psi^\dagger(x)\Phi_1=\gamma_4\psi(x)\Phi_1$. Therefore, only the vacuum expectation value of the operator $\psi(x)\bar\psi(x')$ is required in (2.48). Furthermore, since only one state of the matter field is initially excited, as described by the wave function ue^{ipz}, we arrive at the result

$$\int_{-\infty}^{\infty}(1|j_\mu(x)j_\nu(x')|1)dx_0'=\frac{e^2c^2}{(2\pi)^2}\int(dq)\delta(q_0-p_0)\delta(q^2+\kappa^2)\bar u\gamma_\mu(i\gamma q-\kappa)\gamma_\nu u e^{i(\mathbf{p}-\mathbf{q})\cdot(\mathbf{r}'-\mathbf{r})}, \tag{2.49}$$

on employing the relation

$$\langle\psi_\alpha(x)\bar\psi_\beta(x')\rangle_0=-iS_{\alpha\beta}^{(+)}(x-x')=-\frac{1}{(2\pi)^3}\int_{q_0>0}(dq)\delta(q^2+\kappa^2)(i\gamma q-\kappa)_{\alpha\beta}e^{iq(x-x')}. \tag{2.50}$$

Before further simplifying this expression, we shall consider the analogous evaluations of

$$\int_{-\infty}^{\infty}(1|j_\mu(x)(\delta j_\nu^{(2)}(x'))_{1,0}|1)dx_0' \tag{2.51a}$$

and

$$\int_{-\infty}^{\infty}(1|(\delta j_\mu^{(2)}(x))_{1,0}j_\nu(x')|1)dx_0' \tag{2.51b}$$

which describe the radiationless corrections to the scattering process. Now (2.51a) can be written

$$-e^2c^2\int_{-\infty}^{\infty}dx_0'\int d\omega''(1|\bar\psi(x)\gamma_\mu\psi(x)\bar\psi(x'')\Gamma_\nu(x'-x'')\psi(x'')|1), \tag{2.52}$$

which, according to the arguments presented in connection with (2.47), becomes

$$-e^2c^2\int_{-\infty}^{\infty}dx_0'\int d\omega''\bar u\gamma_\mu\langle\psi(x)\bar\psi(x'')\rangle_0\Gamma_\nu(x'-x'')ue^{ip(x''-x)}$$

$$=\frac{e^2c^2}{(2\pi)^3}\int_{-\infty}^{\infty}dx_0'\int d\omega''\int_{q_0>0}(dq)\delta(q^2+\kappa^2)\bar u\gamma_\mu(i\gamma q-\kappa)\Gamma_\nu(x'-x'')ue^{i(p-q)(x''-x)}. \tag{2.53}$$

On introducing the Fourier transform of $\Gamma_\nu(x)$:

$$\Gamma_\nu(p-q)=\int e^{-i(p-q)x}\Gamma_\nu(x)d\omega, \tag{2.54}$$

we obtain

$$\int_{-\infty}^{\infty}(1|j_\mu(x)(\delta j_\nu^{(2)}(x'))_{1,0}|1)dx_0'=\frac{e^2c^2}{(2\pi)^2}\int(dq)\delta(q_0-p_0)\delta(q^2+\kappa^2)\bar u\gamma_\mu(i\gamma q-\kappa)\Gamma_\nu(p-q)ue^{i(\mathbf{p}-\mathbf{q})\cdot(\mathbf{r}'-\mathbf{r})}. \tag{2.55}$$

The result of combining (2.49) and (2.55) with the analogous evaluation of (2.51b) is expressed by

$$w_0=\frac{1}{(2\pi)^2}\frac{e^2}{\hbar^2c}\int dq_0(d\mathbf{q})\delta(q_0-p_0)\delta(q^2+\kappa^2)\int e^{-i(\mathbf{p}-\mathbf{q})\cdot\mathbf{r}}A_\mu^{(e)}(\mathbf{r})dv\int e^{i(\mathbf{p}-\mathbf{q})\cdot\mathbf{r}'}A_\nu^{(e)}(\mathbf{r}')dv'$$

$$\times\bar u(\gamma_\mu+\Gamma_\mu(q-p))(i\gamma q-\kappa)(\gamma_\nu+\Gamma_\nu(p-q))u. \tag{2.56}$$

On performing the integration with respect to q_0 and $|\mathbf{q}|$, we obtain w_0 in the form of an integral extended over all directions of the vector $\mathbf{q}$, other than the incident direction:

$$w_0=\frac{1}{8\pi^2}\frac{e^2}{\hbar^2c}\int d\Omega|\mathbf{p}|\int e^{-i(\mathbf{p}-\mathbf{q})\cdot\mathbf{r}}A_\mu^{(e)}(\mathbf{r})dv\int e^{i(\mathbf{p}-\mathbf{q})\cdot\mathbf{r}'}A_\nu^{(e)}(\mathbf{r}')dv'\bar u(\gamma_\mu+\Gamma_\mu(q-p))(i\gamma q-\kappa)(\gamma_\nu+\Gamma_\nu(p-q))u. \tag{2.57}$$

This must be interpreted as the rate of transition from the initial state, expressed as the probability per unit time for a deflection into an arbitrary element of solid angle. A further simplification can be introduced by averaging (2.57) with respect to the two spin states in which the incident electron may occur. For this purpose, we require the average of $u_\alpha\bar u_\beta$ for the two polarization states associated with a given energy and momentum. It can be inferred from the anticommutator

$$\{\psi_\alpha(x),\bar\psi_\beta(x')\}=\frac{1}{i}S_{\alpha\beta}(x-x')=-\frac{1}{(2\pi)^3}\int(dp)\delta(p^2+\kappa)\epsilon(p)(i\gamma p-\kappa)_{\alpha\beta}e^{ip(x-x')}, \tag{2.58}$$

which exhibits, with equal weight, the contributions of all states of a particle, that

$$\langle u_\alpha\bar u_\beta\rangle=A(i\gamma p-\kappa)_{\alpha\beta}, \tag{2.59}$$

for a state with wave number four-vector p_μ. The constant A is conveniently evaluated for our purpose in terms of the expectation value of the particle flux vector in the initial state,

$$\mathbf{S}^{(inc)}=(1|ic(\bar\psi(x)\boldsymbol{\gamma}\psi(x))_1|1)$$

$$=ic\bar u\boldsymbol{\gamma}u. \tag{2.60}$$

Thus,

$$\mathbf{S}^{(inc)}=ic\boldsymbol{\gamma}_{\beta\alpha}u_\alpha\bar u_\beta\rightarrow icATr\boldsymbol{\gamma}(i\gamma p-\kappa)$$

$$=-4cA\mathbf{p}, \tag{2.61}$$

so that

$$\langle u_\alpha \bar{u}_\beta \rangle = -\frac{1}{4c}\frac{|\mathbf{S}^{(inc)}|}{|\mathbf{p}|}(i\gamma p-\kappa)_{\alpha\beta}. \tag{2.62}$$

This leads to the following expression for the total rate of transition from the initial state,

$$w_0=\frac{1}{8\pi^2}\frac{e^2}{\hbar^2c^2}|\mathbf{S}^{(inc)}|\int d\Omega\left|\int e^{i(\mathbf{p}-\mathbf{q})\cdot\mathbf{r}}\frac{Ze}{4\pi r}dv\right|^2 \tfrac{1}{4}Tr[(i\gamma p-\kappa)(\gamma_4+\Gamma_4(q-p))(i\gamma q-\kappa)(\gamma_4+\Gamma_4(p-q))], \tag{2.63}$$

in which we have also specialized to the Coulomb potential of a stationary nucleus. We may now infer that the differential cross section for radiationless scattering through the angle ϑ into a unit solid angle is

$$\frac{d\sigma_0(\vartheta)}{d\Omega}=2\left[\frac{Z\alpha}{(\mathbf{p}-\mathbf{q})^2}\right]^2\tfrac{1}{4}Tr[(i\gamma p-\kappa)(\gamma_4+\Gamma_4(q-p))(i\gamma q-\kappa)(\gamma_4+\Gamma_4(p-q))]. \tag{2.64}$$

The Fourier transform of Γ_4 is conveniently written in the form

$$\Gamma_4(p-q)=-\frac{\alpha}{4\pi}\gamma_4\left[4\lambda^2A(\lambda)+\frac{i}{\kappa}\boldsymbol{\gamma}\cdot(\mathbf{p}-\mathbf{q})F_0(\lambda)\right], \tag{2.65}$$

where

$$A(\lambda)=\log\frac{\kappa}{2k_{\min}}(F_0(\lambda)+F_1(\lambda))+\tfrac{1}{2}(F_0(\lambda)+\tfrac{2}{3}F_2(\lambda)+G(\lambda)). \tag{2.66}$$

Here

$$\lambda=\frac{|\mathbf{p}-\mathbf{q}|}{2\kappa}=\frac{|\mathbf{p}|}{\kappa}\sin\frac{\vartheta}{2}, \tag{2.67}$$

and

$$F_0(\lambda)=\int_0^1\frac{dv}{1+\lambda^2(1-v^2)}=\frac{\log((1+\lambda^2)^{\frac{1}{2}}+\lambda)}{(1+\lambda^2)^{\frac{1}{2}}\lambda} \tag{2.68a}$$

$$F_1(\lambda)=\int_0^1\frac{v^2dv}{1+\lambda^2(1-v^2)}=\left(1+\frac{1}{\lambda^2}\right)F_0(\lambda)-\frac{1}{\lambda^2} \tag{2.68b}$$

$$F_2(\lambda)=\int_0^1\frac{v^4dv}{1+\lambda^2(1-v^2)}=\left(1+\frac{1}{\lambda^2}\right)F_1(\lambda)-\frac{1}{3\lambda^2}. \tag{2.68c}$$

The more complicated transform, $G(\lambda)$ is not required in the following development. The trace of the Dirac matrices contained in (2.64) is easily computed:

$$\tfrac{1}{4}Tr[(i\gamma p-\kappa)(\gamma_4+\Gamma_4(q-p))(i\gamma q-\kappa)(\gamma_4+\Gamma_4(p-q))]=2(p_0^2-\kappa^2\lambda^2)\left(1-\frac{2\alpha}{\pi}\lambda^2A(\lambda)\right)-\frac{2\alpha}{\pi}\kappa^2\lambda^2F_0(\lambda), \tag{2.69}$$

whence

$$\frac{d\sigma_0(\vartheta)}{d\Omega}=\left(\frac{Z\alpha}{2|\mathbf{p}|\beta}\csc^2\frac{\vartheta}{2}\right)^2\left(1-\beta^2\sin^2\frac{\vartheta}{2}\right)\left[1-\frac{2\alpha}{\pi}\lambda^2A(\lambda)-\frac{\alpha}{\pi}\frac{\kappa^2}{p_0^2-\kappa^2\lambda^2}\lambda^2F_0(\lambda)\right] \tag{2.70}$$

in which $\beta=|\mathbf{p}|/p_0$ is the speed of the particle relative to c.

To evaluate the rate at which transitions occur accompanied by radiation, we consider

$$\left(1\left|\delta j_\mu^{(1)}(x)\int_{-\infty}^{\infty}\delta j_\nu^{(1)}(x')dx_0'\right|1\right)=-\frac{e^4}{\hbar^2}\int d\omega''d\omega'''\left(1\left|[\bar{\psi}(x)\gamma_\mu\bar{S}(x-x'')\gamma_\lambda\psi(x'')+\bar{\psi}(x'')\gamma_\lambda\bar{S}(x''-x)\gamma_\mu\psi(x)]_1\right.\right.$$

$$\left.\left.\times\int_{-\infty}^{\infty}dx_0'[\bar{\psi}(x')\gamma_\nu\bar{S}(x'-x''')\gamma_\sigma\psi(x''')+\bar{\psi}(x''')\gamma_\sigma\bar{S}(x'''-x')\gamma_\nu\psi(x')]_1A_\lambda(x'')A_\sigma(x''')\right|1\right). \tag{2.71}$$

Since the state vector Φ_1 is characterized by an absence of quanta, only the following vacuum expectation value is required for the electromagnetic field,

$$\langle A_\lambda(x'')A_\sigma(x''')\rangle_0=i\hbar c\delta_{\lambda\sigma}D^{(+)}(x''-x''')=\frac{\hbar c}{(2\pi)^3}\delta_{\lambda\sigma}\int_{k_0>0}(dk)\delta(k^2)e^{ik(x''-x''')}. \tag{2.72}$$

The matter field operators are treated as before, with the result

$$\left(1\left|\delta j_\mu^{(1)}(x)\int_{-\infty}^{\infty}\delta j_\mu^{(1)}(x')dx_0'\right|1\right)=\frac{e^4}{\hbar^2}\frac{\hbar c}{(2\pi)^6}\int_{q_0,k_0>0}(dq)\delta(q^2+\kappa^2)(dk)\delta(k^2)\int_{-\infty}^{\infty}dx_0'e^{i(p-q-k)(x'-x)}$$
$$\times\bar{u}(\gamma_\mu\bar{S}(q+k)\gamma_\lambda+\gamma_\lambda\bar{S}(p-k)\gamma_\mu)(i\gamma q-\kappa)(\gamma_\nu\bar{S}(p-k)\gamma_\lambda+\gamma_\lambda\bar{S}(q+k)\gamma_\nu)u. \quad (2.73)$$

Here

$$\bar{S}(q+k)=\int e^{-i(q+k)x}\bar{S}(x)d\omega=\frac{i\gamma(q+k)-\kappa}{2qk} \quad (2.74)$$

and

$$\bar{S}(p-k)=-\frac{i\gamma(p-k)-\kappa}{2pk} \quad (2.75)$$

are Fourier transforms of $\bar{S}(x)$. The integration with respect to x_0' imposes the energy conservation law

$$p_0=q_0+k_0, \quad (2.76)$$

which is evidently that of a light quantum emission process. The integration with respect to q_0 and the magnitude of $\mathbf{q}$ can now be performed, leaving one with an expression for w_1 in the form of an integral extended over all directions of the scattered electron, and all light quanta, as restricted by energy conservation. On averaging with respect to the polarization of the incident electron, and specializing to the Coulomb field of a nucleus, one obtains

$$w_1=\frac{\alpha}{\pi^2}|\mathbf{S}^{(inc)}|\int_{k_0>0}d\Omega(dk)\delta(k^2)\frac{|\mathbf{q}|}{|\mathbf{p}|}\left[\frac{Z\alpha}{(\mathbf{p}-\mathbf{q}-\mathbf{k})^2}\right]^2\tfrac{1}{4}Tr\left[(i\gamma p-\kappa)\right.$$
$$\left.\times\left(\gamma_4\frac{i\gamma(q+k)-\kappa}{2qk}\gamma_\lambda-\gamma_\lambda\frac{i\gamma(p-k)-\kappa}{2pk}\gamma_4\right)(i\gamma q-\kappa)\left(\gamma_4\frac{i\gamma(p-k)-\kappa}{2pk}\gamma_\lambda-\gamma_\lambda\frac{i\gamma(q+k)-\kappa}{2qk}\gamma_4\right)\right]. \quad (2.77)$$

It may then be inferred that the differential cross section for radiative scattering through the angle ϑ, in which the energy loss does not exceed ΔE, is

$$\frac{d\sigma_1(\vartheta,\Delta E)}{d\Omega}=\frac{\alpha}{\pi^2}\int_{k_0=0}^{k_0=K}(dk)\delta(k^2)\frac{|\mathbf{q}|}{|\mathbf{p}|}\left[\frac{Z\alpha}{(\mathbf{p}-\mathbf{q}-\mathbf{k})^2}\right]^2\tfrac{1}{4}Tr\left[(i\gamma p-\kappa)\right.$$
$$\left.\times\left(\gamma_4\left(\frac{q_\lambda}{qk}-\frac{p_\lambda}{pk}\right)+\gamma_4\frac{\gamma k}{2qk}\gamma_\lambda+\gamma_\lambda\frac{\gamma k}{2pk}\gamma_4\right)(i\gamma q-\kappa)\left(\gamma_4\left(\frac{q_\lambda}{qk}-\frac{p_\lambda}{pk}\right)+\gamma_\lambda\frac{\gamma k}{2qk}\gamma_4+\gamma_4\frac{\gamma k}{2pk}\gamma_\lambda\right)\right], \quad (2.78)$$

where

$$K=\Delta E/\hbar c. \quad (2.79)$$

We shall first consider the simple situation in which the emitted radiation exerts a negligible reaction on the electron. That is to say, we shall treat the essentially elastic scattering of an electron, in which only a small fraction of the electron kinetic energy is radiated. Under these circumstances, which are expressed by $\Delta E\ll W=E-mc^2$, (2.79) simplifies to

$$\frac{d\sigma_1(\vartheta,\Delta E)}{d\Omega}=\left(\frac{Z\alpha}{2|\mathbf{p}|\beta}\csc^2\frac{\vartheta}{2}\right)^2\left(1-\beta^2\sin^2\frac{\vartheta}{2}\right)\frac{\alpha}{2\pi^2}\int_{k_0=0}^{k_0=K}(dk)\delta(k^2)\left(\frac{p}{pk}-\frac{q}{qk}\right)^2. \quad (2.80)$$

Now

$$\left(\frac{p}{pk}-\frac{q}{qk}\right)^2=\frac{(p-q)^2}{(pk)(qk)}+\kappa^2\left(\frac{2}{(pk)(qk)}-\frac{1}{(pk)^2}-\frac{1}{(qk)^2}\right), \quad (2.81)$$

and

$$\frac{1}{(pk)(qk)}=\frac{1}{(q-p)k}\left(\frac{1}{pk}-\frac{1}{qk}\right)=\frac{1}{2}\int_{-1}^{1}\frac{dv}{\left[\left(\frac{p+q}{2}+\frac{p-q}{2}v\right)k\right]^2}, \quad (2.82)$$

from which one deduces, on integration by parts, that

$$\frac{2}{(pk)(qk)}-\frac{1}{(pk)^2}-\frac{1}{(qk)^2}=-\int_{-1}^{1}dvv\frac{\partial}{\partial v}\frac{1}{\left[\left(\frac{p+q}{2}+\frac{p-q}{2}v\right)k\right]^2}. \quad (2.83)$$

Therefore,

$$\int (dk)\delta(k^2)\left(\frac{p}{pk}-\frac{q}{qk}\right)^2=\kappa^2\int_{-1}^{1}dv\left(\frac{(p-q)^2}{2\kappa^2}-v\frac{\partial}{\partial v}\right)\int (dk)\frac{\delta(k^2)}{\left[\left(\frac{p+q}{2}+\frac{p-q}{2}v\right)k\right]^2}. \tag{2.84}$$

The k integration in the latter equation can be written as

$$-\int (dk)\frac{\delta(k^2)}{\left(\frac{p+q}{2}+\frac{p-q}{2}v\right)^2}\left(\frac{p+q}{2}+\frac{p-q}{2}v\right)_\lambda\frac{\partial}{\partial k_\lambda}\frac{1}{\left(\frac{p+q}{2}+\frac{p-q}{2}v\right)k}$$

$$=\frac{1}{\kappa^2}\frac{1}{1+[(p-q)^2/4\kappa^2](1-v^2)}\left[\int (dk)\frac{\partial}{\partial k_\lambda}\left[\delta(k^2)\frac{\left(\frac{p+q}{2}+\frac{p-q}{2}v\right)_\lambda}{\left(\frac{p+q}{2}+\frac{p-q}{2}v\right)k}\right]-2\int (dk)\delta'(k^2)\right]. \tag{2.85}$$

However,

$$-2\int (dk)\delta'(k^2)=\int\frac{(dk)}{k_0}\frac{\partial}{\partial k_0}\delta(k^2)=\int (dk)\frac{\partial}{\partial k_0}\left(\frac{\delta(k^2)}{k_0}\right)+\int\frac{(dk)}{k_0^2}\delta(k^2), \tag{2.86}$$

so that

$$\int (dk)\delta(k^2)\left(\frac{p}{pk}-\frac{q}{qk}\right)^2=\int_{-1}^{1}dv\left(\frac{(p-q)^2}{2\kappa^2}-v\frac{\partial}{\partial v}\right)\frac{1}{1+[(p-q)^2/4\kappa^2](1-v^2)}\left[\int\frac{(dk)}{k_0^2}\delta(k^2)\right.$$

$$\left.+\int (dk)\frac{\partial}{\partial k_0}\left\{\delta(k^2)\left[\frac{\left(\frac{p+q}{2}+\frac{p-q}{2}v\right)_0}{\left(\frac{p+q}{2}+\frac{p-q}{2}v\right)k}+\frac{1}{k_0}\right]\right\}\right], \tag{2.87}$$

in which we have discarded terms that obviously vanish on integration over the domain $0<k_0<K$.

The first bracketed integral in (2.87), when expressed in three-dimensional notation, becomes

$$\int\frac{(d\mathbf{k})dk_0}{k_0^2}\delta(\mathbf{k}^2-k_0^2)=2\pi\int_{k_{\min}}^{k}\frac{dk_0}{k_0}=2\pi\log\frac{K}{k_{\min}}, \tag{2.88}$$

in which we have again introduced an invariant minimum light quantum wave number to characterize a logarithmic divergence associated with the "infra-red catastrophe." A similar expression of the second bracketed integral in (2.87) yields.

$$\int (d\mathbf{k})\delta(\mathbf{k}^2-K^2)\left[\frac{1}{K}-\frac{p_0}{p_0K-\left(\frac{\mathbf{p}+\mathbf{q}}{2}+\frac{\mathbf{p}-\mathbf{q}}{2}v\right)\cdot\mathbf{k}}\right]$$

$$=2\pi\left[1-\frac{1}{2}\frac{p_0}{(\mathbf{p}^2-[(\mathbf{p}-\mathbf{q})^2/4](1-v^2))^{\frac{1}{2}}}\log\frac{p_0+(\mathbf{p}^2-[(\mathbf{p}-\mathbf{q})^2/4](1-v^2))^{\frac{1}{2}}}{p_0-(\mathbf{p}^2-[(\mathbf{p}-\mathbf{q})^2/4](1-v^2))^{\frac{1}{2}}}\right]. \tag{2.89}$$

Therefore,

$$\int_{k_0=0}^{k_0=K}(dk)\delta(k^2)(p/pk-q/qk)^2$$

$$=4\pi\int_0^1 dv\left(\frac{(\mathbf{p}-\mathbf{q})^2}{2\kappa^2}-v\frac{\partial}{\partial v}\right)\frac{1}{1+[(\mathbf{p}-\mathbf{q})^2/4\kappa^2](1-v^2)}\left[\log\frac{K}{k_{\min}}+1-\frac{1}{2\beta\xi}\log\frac{1+\beta\xi}{1-\beta\xi}\right], \tag{2.90}$$

where

$$\xi=\left(1-\sin^2\frac{\vartheta}{2}(1-v^2)\right)^{\frac{1}{2}}. \tag{2.91}$$

We may now employ the identity

$$\frac{1-1/2\beta\xi\log(1+\beta\xi/1-\beta\xi)}{1+[(\mathbf{p}-\mathbf{q})^2/4\kappa^2](1-v^2)}=\frac{1}{2}\frac{\log(1+[(\mathbf{p}-\mathbf{q})^2/4\kappa^2](1-v^2))}{1+[(\mathbf{p}-\mathbf{q})^2/4\kappa^2](1-v^2)}-\frac{\log(2p_0/\kappa)-1}{1+[(\mathbf{p}-\mathbf{q})^2/4\kappa^2](1-v^2)}$$

$$+\frac{\kappa^2}{p_0^2}\frac{1}{2\beta\xi}\left[\frac{\log\frac{1-\beta\xi}{2}}{1+\beta\xi}-\frac{\log\frac{1+\beta\xi}{2}}{1-\beta\xi}\right] \tag{2.92}$$

to cast (2.90) into the form

$$\int_{k_0=0}^{k_0=K}(dk)\delta(k^2)\left(\frac{p}{pk}-\frac{q}{qk}\right)^2=4\pi\frac{\mathbf{p}^2}{\kappa^2}\sin^2\frac{\vartheta}{2}\left[\left(\log\frac{K}{k_{\min}}-\log\frac{2p_0}{\kappa}+1\right)(F_0+F_1)+F_1+\tfrac{1}{2}G+H\right], \tag{2.93}$$

where

$$H=\left(1+\frac{1}{2\lambda^2}\right)\frac{\kappa^2}{p_0^2}\int_0^1\frac{dv}{\beta\xi}\left[\frac{\log\frac{1-\beta\xi}{2}}{1+\beta\xi}-\frac{\log\frac{1+\beta\xi}{2}}{1-\beta\xi}\right]-\frac{1}{2\lambda^2}\frac{\kappa^2}{p_0^2}\frac{1}{\beta}\left[\frac{\log\frac{1-\beta}{2}}{1+\beta}-\frac{\log\frac{1+\beta}{2}}{1-\beta}\right]. \tag{2.94}$$

The function H approaches a constant in the limit of small velocities,

$$\beta\ll 1:\quad H=\frac{4}{3}(\log 2-1)-\frac{1}{9}. \tag{2.95}$$

At high energies, H is approximated by

$$p_0/\kappa\gg 1:\quad H=-\frac{\kappa^2}{p_0^2}f(\vartheta), \tag{2.96}$$

with

$$f(\vartheta)=\frac{1}{\sin\vartheta/2}\int_{\cos\vartheta/2}^1\left[\frac{\log\frac{1+\xi}{2}}{1-\xi}-\frac{\log\frac{1-\xi}{2}}{1+\xi}\right]\frac{d\xi}{(\xi^2-\cos^2(\vartheta/2))^{\frac{1}{2}}}. \tag{2.97}$$

This integral can be performed analytically for $\vartheta=\pi$,

$$f(\pi)=\pi^2/12, \tag{2.98}$$

but must be evaluated numerically for other angles. An approximation in excess, which has the correct asymptotic form at small angles, is provided by

$$f(\vartheta)\sim\left(\frac{2}{\cos(\vartheta/2)(1+\cos(\vartheta/2))^3}\right)^{\frac{1}{2}}\left[\log\frac{1}{2(1-\cos(\vartheta/2))}+\frac{1-\cos(\vartheta/2)}{2}+1\right]. \tag{2.99}$$

This formula is reasonably accurate even for $\vartheta=\pi/2$, where the value yielded by (2.99) exceeds by only 8.6 percent the following result of a numerical calculation:

$$f(\pi/2)=1.167. \tag{2.100}$$

The total differential cross section for scattering through the angle ϑ, in which the energy loss does not exceed ΔE, is

$$\frac{d\sigma(\vartheta,\Delta E)}{d\Omega}=\frac{d\sigma_0(\vartheta)}{d\Omega}+\frac{d\sigma_1(\vartheta,\Delta E)}{d\Omega}=\left(\frac{Z\alpha}{2|\mathbf{p}|\beta}\csc^2\frac{\vartheta}{2}\right)^2\left(1-\beta^2\sin^2\frac{\vartheta}{2}\right)(1-\delta(\vartheta,\Delta E)), \tag{2.101}$$

where $\delta(\vartheta,\Delta E)$ is the desired fractional decrease in the cross section produced by radiative effects. For essentially elastic scattering, we obtain

$$\delta(\vartheta,\Delta E\ll W)=\frac{2\alpha}{\pi}\beta^2\frac{p_0^2}{\kappa^2}\sin^2\frac{\vartheta}{2}\left[\left(\log\frac{E}{\Delta E}-1\right)(F_0+F_1)+\frac{1}{2}F_0-F_1+\frac{1}{3}F_2-H+\frac{1}{2}\frac{\kappa^2/p_0^2}{1-\beta^2\sin^2(\vartheta/2)}F_0\right], \tag{2.102}$$

on combining (2.70) with (2.80). It will be noted that the infra-red catastrophe, as characterized by $k_{\min}$ has disappeared. However, it is possible, in principle, to consider the limit $\Delta E \to 0$, which would make δ diverge logarithmically. It is well known that this difficulty stems from the neglect of processes involving more than one low frequency quantum.[5] Actually, the essentially elastic scattering cross section must approach zero as $\Delta E \to 0$; that is, it never happens that a scattering event is unaccompanied by the emission of quanta. This is described by replacing the radiative correction factor $1-\delta$ with $e^{-\delta}$, which has the proper limiting behavior as $\Delta E \to 0$. The further terms in the series expansion of $e^{-\delta}$ express the effects of higher order processes involving the multiple emission of soft quanta. However, for practical purposes, such a refinement is unnecessary. The accuracy with which the energy of a particle can be measured is such that the limit $\Delta E \to 0$ cannot be realized, and δ will be small in comparison with unity under presently accessible circumstances.

For a slowly moving particle,

$$\beta \ll 1: \delta(\vartheta, \Delta E \ll W) = \frac{8\alpha}{3\pi}\beta^2 \sin^2\frac{\vartheta}{2}\left[\log\frac{mc^2}{2\Delta E} + \frac{19}{30}\right], \quad (2.103)$$

according to (2.95), the limiting form of H and the corresponding limiting form of F_n:

$$\lambda \ll 1: \quad F_n = \frac{1}{2n+1}. \quad (2.104)$$

The radiative correction thus increases linearly with the kinetic energy of the particle. In the extreme relativistic region, on the other hand,

$$\frac{p_0}{\kappa}\sin\frac{\vartheta}{2} \gg 1:$$

$$\delta(\vartheta, \Delta E \ll W) = \frac{4\alpha}{\pi}\left[\left(\log\frac{E}{\Delta E} - \frac{13}{12}\right)\left(\log\frac{2p_0}{K}\sin\frac{\vartheta}{2} - \frac{1}{2}\right) + \frac{17}{72} + \frac{1}{2}\sin^2\frac{\vartheta}{2} - f(\vartheta)\right], \quad (2.105)$$

which has a logarithmic dependence on the particle energy. The asymptotic form (2.105) is quite accurate for even moderate energies. Thus, with $\vartheta = \pi/2$, $\Delta E = 10$ kev and $W = 3.1$ Mev, which corresponds to $(p_0/\kappa) \times \sin\vartheta/2 = 5$, the value of δ computed from (2.105) differs from the correct value,

$$\delta = 8.6\ 10^{-2}, \quad (2.106)$$

by only a fraction of a percent. It is evident from this numerical result that radiative corrections to scattering cross sections can be quite appreciable. For the particular conditions chosen, ΔE can be materially increased (but still subject to $\Delta E \ll W$), without seriously impairing δ. Thus, with $\Delta E = 40$ kev, $\delta = 6.3\ 10^{-2}$, while $\Delta E = 80$ kev yields $\delta = 5.1\ 10^{-2}$. As to the energy dependence of δ, we remark that with a given accuracy in the determination of the energy, $\Delta E/E$, δ varies linearly with the logarithm of the energy. Thus, with $\Delta E/E = 0.04/3.6 = 1.1\ 10^{-2}$, an increase in the total energy by a factor of four produces an addition of $4.4\ 10^{-2}$ to δ, whence $\delta = 11\ 10^{-2}$ for $W = 14$ Mev, and $\delta = 15\ 10^{-2}$ for $W = 57$ Mev.

The angular dependence of δ at relativistic energies is not fully described by the asymptotic formula (2.105), since the underlying condition, $(p_0/\kappa)\sin\vartheta/2 \ll 1$, cannot be maintained with diminishing ϑ. Indeed, δ is proportional to $\sin^2\vartheta/2$ at angles such that $(p_0/\kappa)\sin\vartheta/2 \ll 1$. However (2.105) can be used over a wide angular range, even at moderate energies. Thus, with $W = 3.1$ Mev, $\Delta E = 40$ kev, and $\vartheta = \pi/4$, which corresponds to $(p_0/\kappa)\sin\vartheta/2 = 2.7$, the value of δ deduced from (2.105) exceeds by only 2 percent the correct value, $\delta = 4.2\ 10^{-2}$. We may note that under the same energy conditions, but with $\vartheta = 3\pi/4$, $\delta = 7.2\ 10^{-2}$. The angular dependence of δ may be particularly suitable for an experimental test of these predictions, which involve the relativistic aspects of the radiative corrections to the electromagnetic properties of the electron.

We have thus far considered only the essentially elastic scattering of an electron, in which radiative corrections arise primarily from virtual processes. If we wish to compute the differential cross section for scattering with an arbitrary maximum energy loss ΔE, it is only necessary to augment the essentially elastic cross section, in which the maximum energy loss is $\Delta E' \ll W$, by the cross section for scattering with the emission of a light quantum in the energy range from $\Delta E'$ to ΔE. The latter process involves the well-known bremsstrahlung cross section which, of course, is the content of (2.79). This will be illustrated by the calculation of the differential cross section for the scattering of a slowly moving electron, irrespective of the final energy. The differential cross section per unit solid angle for scattering of an electron through the angle ϑ, in which a light quantum is emitted in the energy range from $\Delta E'$ to W, is

$$\frac{\alpha}{\pi^2}\int_{\Delta E'/\hbar c}^{W/\hbar c}\frac{dk_0}{k_0}\int d\omega\frac{|\mathbf{q}|}{|\mathbf{p}|}\left[\frac{Z\alpha}{(\mathbf{p}-\mathbf{q})^2}\right]^2\left[(\mathbf{p}-\mathbf{q})^2 - (\mathbf{n}\cdot(\mathbf{p}-\mathbf{q}))^2\right], \quad (2.107)$$

according to the non-relativistic limit of (2.78). Here $d\omega$ is an element of solid angle associated with the direction of the unit vector $\mathbf{n} = \mathbf{k}/k_0$, and

$$|\mathbf{q}| = (\mathbf{p}^2 - 2\kappa k_0)^{\frac{1}{2}}. \quad (2.108)$$

[5] F. Bloch and A. Nordsieck, Phys. Rev. **52**, 54 (1937).

On performing the integration over all emission directions of the light quantum, and introducing the new variable of integration, $x=|\mathbf{q}|/|\mathbf{p}|$, (2.107) becomes

$$\frac{8\alpha}{3\pi}\left(\frac{Z\alpha}{|\mathbf{p}|}\right)^2\int_0^{(1-\Delta E'/W)^{\frac{1}{2}}}\frac{x}{1+x^2-2x\cos\vartheta}\frac{2xdx}{1-x^2}$$
$$=\left(\frac{Z\alpha}{2|\mathbf{p}|\beta}\csc^2\frac{\vartheta}{2}\right)^2\frac{8\alpha}{3\pi}\beta^2\sin^2\frac{\vartheta}{2}\left[\log\frac{W}{\Delta E'}-\int_0^1\frac{1-x}{1+x^2-2x\cos\vartheta}\frac{2xdx}{1+x}\right]. \quad (2.109)$$

Thus the contribution to δ produced by emission of quanta with energies in the range from $\Delta E'$ to W is

$$-\frac{8\alpha}{3\pi}\beta^2\sin^2\frac{\vartheta}{2}\left[\log\frac{4W}{\Delta E'}-(\pi-\vartheta)\tan\frac{\vartheta}{2}-\frac{\cos\vartheta}{\cos^2\vartheta/2}\log\csc\frac{\vartheta}{2}\right]. \quad (2.110)$$

On adding this to $\delta(\vartheta,\Delta E')$, as given by (2.103), we obtain the desired result:

$$\beta\ll 1:\quad \delta(\vartheta,W)=\frac{8\alpha}{3\pi}\beta^2\sin^2\frac{\vartheta}{2}\left[\log\frac{1}{4\beta^2}+\frac{19}{30}+(\pi-\vartheta)\tan\frac{\vartheta}{2}+\frac{\cos\vartheta}{\cos^2\vartheta/2}\log\csc\frac{\vartheta}{2}\right]. \quad (2.111)$$

It may be remarked, finally, that the analogous meso-nuclear phenomenon, the radiative correction to nucleon-nucleon scattering associated with virtual meson emission, will be a relatively more significant effect in view of the stronger couplings involved. This may well be the explanation of the discrepancy between the observed neutron-proton scattering cross section for high energy neutrons and the larger theoretical values computed from various assumed interaction potentials.[6]

APPENDIX

In this section, we shall first give an alternative treatment of the polarization of the vacuum by an external field, employing the methods developed in the preceding pages. It is desired to compute the expectation value of $j_\mu(x)$,

$$\langle j_\mu(x)\rangle=(\Psi[\sigma],j_\mu(x)\Psi[\sigma]), \quad (A.1)$$

where $\Psi[\sigma]$ obeys

$$i\hbar c\frac{\delta\Psi[\sigma]}{\delta\sigma(x)}=-\frac{1}{c}j_\mu(x)A_\mu(x)\Psi[\sigma], \quad (A.2)$$

and $A_\mu(x)$ is the potential of a prescribed current distribution. The physical situation can be described as follows. In the remote past, the matter field is uncoupled from the external electromagnetic field, and the state vector is that of the vacuum,

$$\Psi[-\infty]=\Psi_0. \quad (A.3)$$

It is supposed that the coupling is adiabatically switched on, and that the external field does not induce real pair creation. The latter restriction implies that the final state of the matter field, after the coupling is adiabatically switched off, is simply Ψ_0, whence

$$\Psi[\infty]-\Psi[-\infty]=(S-1)\Psi_0=0. \quad (A.4)$$

A solution of (A.2), in the form

$$\Psi[\sigma]=U[\sigma]\Psi_0, \quad (A.5)$$

may be constructed, where

$$i\hbar c\frac{\delta U[\sigma]}{\delta\sigma(x)}=-\frac{1}{c}j_\mu(x)A_\mu(x)U[\sigma], \quad (A.6)$$

and

$$U[\infty]=S,\quad U[-\infty]=1. \quad (A.7)$$

The current induced in the vacuum is then written as

$$\langle j_\mu(x)\rangle=\langle U^{-1}[\sigma]j_\mu(x)U[\sigma]\rangle_0. \quad (A.8)$$

Now

$$\tfrac{1}{2}\int_{-\infty}^{\infty}d\omega'\epsilon[\sigma,\sigma']\frac{\delta}{\delta\sigma'(x')}U^{-1}[\sigma']j_\mu(x)U[\sigma']=U^{-1}[\sigma]j_\mu(x)U[\sigma]-\tfrac{1}{2}(j_\mu(x)+S^{-1}j_\mu(x)S), \quad (A.9)$$

whence

$$U^{-1}[\sigma]j_\mu(x)U[\sigma]=\tfrac{1}{2}(j_\mu(x)+S^{-1}j_\mu(x)S)+\frac{i}{2\hbar c^2}\int_{-\infty}^{\infty}d\omega'\epsilon[\sigma,\sigma']U^{-1}[\sigma'][j_\mu(x),j_\nu(x')]U[\sigma']A_\nu(x'). \quad (A.10)$$

On placing $U[\sigma']=1$ on the right side of (A.10), one obtains the first approximation in a treatment that regards the disturbance of the vacuum as small. Hence,

$$\langle j_\mu(x)\rangle=\frac{i}{2\hbar c^2}\int_{-\infty}^{\infty}d\omega'\epsilon(x-x')[j_\mu(x),j_\nu(x')]_0A_\nu(x'), \quad (A.11)$$

in view of (A.4) and the absence of a current in the unperturbed vacuum. We shall, for convenience, write this formula as

$$\langle j_\mu(x)\rangle=\frac{4e^2}{\hbar}\int G_{\mu\nu}(x-x')A_\nu(x')d\omega', \quad (A.12)$$

where, according to II (2.10),

$$G_{\mu\nu}(x-x')=\tfrac{1}{8}Tr[S^{(1)}(x'-x)\gamma_\mu\bar{S}(x-x')\gamma_\nu+\bar{S}(x'-x)\gamma_\mu S^{(1)}(x-x')\gamma_\nu]. \quad (A.13)$$

The introduction of the Fourier integral representations for the functions $S^{(1)}$ and $\bar{S}$, combined with the trace evaluation (see II (2.10))

$$\tfrac{1}{8}Tr[(-i\gamma k'+\kappa)\gamma_\mu(i\gamma k''+\kappa)\gamma_\nu+(-i\gamma k''+\kappa)\gamma_\mu(i\gamma k'+\kappa)\gamma_\nu]=k_\mu'k_\nu''+k_\nu'k_\mu''-\delta_{\mu\nu}(k'k''-\kappa^2), \quad (A.14)$$

[6] A summary is given by L. Rosenfeld, Nuclear Forces (Interscience Publishers, Inc., New York, 1949), pp. 450, 454.

yields the following expression for $G_{\mu\nu}(x)$,

$$G_{\mu\nu}(x)=\frac{1}{(2\pi)^7}\int(dk')(dk'')e^{i(k'+k'')x}\frac{\delta(k''^2+\kappa^2)}{k'^2+\kappa^2}[k_\mu' k_\nu''+k_\nu' k_\mu''-\delta_{\mu\nu}(k'k''-\kappa^2)]. \tag{A.15}$$

It is instructive to examine the conditions imposed on $G_{\mu\nu}(x)$ by the related requirements of charge conservation and gauge invariance. The former evidently demands that

$$\frac{\partial}{\partial x_\mu}G_{\mu\nu}(x)=0. \tag{A.16}$$

The requirement of gauge invariance is that the induced current be unaffected by the gauge transformation

$$A_\mu(x)\rightarrow A_\mu(x)-\frac{\partial\Lambda(x)}{\partial x_\mu}, \tag{A.17}$$

or that

$$\int G_{\mu\nu}(x-x')\frac{\partial\Lambda(x')}{\partial x_\nu'}d\omega'=\int\frac{\partial}{\partial x_\nu}G_{\mu\nu}(x-x')\Lambda(x')d\omega'=0, \tag{A.18}$$

in which the absence of an integrated term is a consequence of the adiabatic removal of the coupling in the remote past and future. Evidently (A.18) is satisfied in virtue of (A.16), since

$$G_{\mu\nu}(x)=G_{\nu\mu}(x). \tag{A.19}$$

On computing $\partial G_{\mu\nu}(x)/\partial x_\mu$ from (A.15), we obtain

$$\frac{\partial}{\partial x_\mu}G_{\mu\nu}(x)=\frac{i}{(2\pi)^7}\int(dk')(dk'')e^{i(k'+k'')x}k_\nu''\delta(k''^2+\kappa^2)$$

$$=\frac{i}{(2\pi)^7}\int(dk)e^{ikx}\int(dk'')k_\nu''\delta(k''^2+\kappa^2), \tag{A.20}$$

where

$$k_\mu=k_\mu'+k_\mu'', \tag{A.21}$$

which is indeed zero if

$$\int(dk'')k_\nu''\delta(k''^2+\kappa^2)=0. \tag{A.22}$$

Although the latter integral is strictly divergent, the value of zero is unambiguously obtained from any limiting process in which the delta-function is replaced by a suitable non-singular function. In this sense, the requirements of charge conservation and gauge invariance are satisfied. It may be noted that the same integral is encountered in evaluating the current in the unperturbed vacuum, II (1.73),

$$\langle j_\mu(x)\rangle_0=\frac{iec}{2}Tr\gamma_\mu S^{(1)}(0)$$

$$=\frac{2ec}{(2\pi)^4}\int(dk'')k_\mu''\delta(k''^2+\kappa^2), \tag{A.23}$$

which must also be zero.

We return to the evaluation of $G_{\mu\nu}(x)$, and utilize the identity

$$k'k''-\kappa^2=2\frac{(kk')(kk'')}{k^2}-(k'^2+\kappa^2)\frac{kk''}{k^2}-(k''^2+\kappa^2)\frac{kk'}{k^2} \tag{A.24}$$

to simplify (A.15). The third term in the latter expression makes no contribution in view of the null value of $(k''^2+\kappa^2)\delta(k''^2+\kappa^2)$, while the second term produces a contribution of $G_{\mu\nu}(x)$ of the form.

$$\int(dk)(dk'')e^{ikx}\frac{kk''}{k^2}\delta(k''^2+\kappa^2), \tag{A.25}$$

which must also be zero, in consequence of (A.22). Hence,

$$G_{\mu\nu}(x)=\frac{1}{(2\pi)^7}\int(dk')(dk'')e^{ikx}\left(\frac{\delta(k'^2+\kappa^2)}{k''^2+\kappa^2}+\frac{\delta(k''^2+\kappa^2)}{k'^2+\kappa^2}\right)\left(\frac{k_\mu' k_\nu''+k_\nu' k_\mu''}{2}-\delta_{\mu\nu}\frac{(kk')(kk'')}{k^2}\right). \tag{A.26}$$

The delta-function factor can be simplified in the manner introduced in the text:

$$\frac{\delta(k'^2+\kappa^2)}{k''^2+\kappa^2}+\frac{\delta(k''^2+\kappa^2)}{k'^2+\kappa^2}=\frac{1}{k''^2-k'^2}(\delta(k'^2+\kappa^2)-\delta(k''^2+\kappa^2))=-\tfrac{1}{2}\int_{-1}^{1}dv\delta'\left(\frac{k'^2+k''^2}{2}+\frac{k'^2-k''^2}{2}v+\kappa^2\right). \tag{A.27}$$

The introduction of the new variables k_μ and p_μ, as defined by

$$k_\mu'=\tfrac{1}{2}k_\mu+\left(p_\mu-\frac{v}{2}k_\mu\right)$$

$$k_\mu''=\tfrac{1}{2}k_\mu-\left(p_\mu-\frac{v}{2}k_\mu\right), \tag{A.28}$$

then brings $G_{\mu\nu}(x)$ into the form

$$G_{\mu\nu}(x)=-\frac{1}{8(2\pi)^7}\int_{-1}^{1}dv(1-v^2)\int(dk)(dp)e^{ikx}(k_\mu k_\nu-\delta_{\mu\nu}k^2)\delta'\left(p^2+\kappa^2+\frac{k^2}{4}(1-v^2)\right), \tag{A.29}$$

where, in virtue of the dependence of the delta-function on p^2 alone, terms linear in p_μ have been discarded, and $p_\mu p_\nu$ has been replaced by $\frac{1}{4}\delta_{\mu\nu}p^2$. It is thereby shown that

$$G_{\mu\nu}(x)=\left(\frac{\partial}{\partial x_\nu}\frac{\partial}{\partial x_\nu}-\delta_{\mu\nu}\Box^2\right)G(x), \tag{A.30}$$

with

$$G(x)=\frac{1}{8(2\pi)^7}\int_{-1}^{1}dv(1-v^2)\int(dk)(dp)e^{ikx}\delta'\left(p^2+\kappa^2+\frac{k^2}{4}(1-v^2)\right). \tag{A.31}$$

The divergent and convergent parts of $G(x)$ can be separated by a partial integration with respect to v,

$$G(x)=\frac{1}{6(2\pi)^4}\int(dp)\delta'(p^2+\kappa^2)\delta(x)-\Box^2\frac{1}{8(2\pi)^7}\int_0^1 v^2\left(1-\frac{v^2}{3}\right)dv\int(dk)e^{ikx}\int(dp)\delta''\left(p^2+\kappa^2+\frac{k^2}{4}(1-v^2)\right). \tag{A.32}$$

The invariant, logarithmically divergent integral that occurs in the first term of (A.32) can be expressed in three-dimensional notation as

$$\int (dp)\delta'(p^2+\kappa^2) = -\int (d\mathbf{p})dp_0 \frac{1}{2p_0}\frac{\partial}{\partial p_0}\delta(p_0^2-\mathbf{p}^2-\kappa^2) = -\tfrac{1}{2}\int \frac{(d\mathbf{p})}{(\mathbf{p}^2+\kappa^2)^{\frac{1}{2}}} = -2\pi \operatorname*{Lim}_{P\to\infty}\left(\log\frac{P_0+P}{\kappa}-1\right), \tag{A.33}$$

where

$$P_0 = (P^2+\kappa^2)^{\frac{1}{2}}. \tag{A.34}$$

The convergent second integral of (A.32) is then obtained by differentiating (A.33) with respect to κ^2 and replacing the latter by $\kappa^2+(k^2/4)(1-v^2)$,

$$\int (dp)\delta''\left(p^2+\kappa^2+\frac{k^2}{4}(1-v^2)\right) = \frac{\pi}{\kappa^2+(k^2/4)(1-v^2)}. \tag{A.35}$$

With these evaluations, $G(x)$ becomes

$$G(x) = -\frac{1}{24\pi^2}\operatorname*{Lim}_{P\to\infty}\left(\log\frac{P_0+P}{\kappa}-1\right)\delta(x) - \frac{1}{64\pi^2}\frac{1}{\kappa^2}\Box^2(F_1(x)-\tfrac{1}{3}F_2(x)), \tag{A.36}$$

where

$$F_n(x) = \int_0^1 v^{2n}dv\frac{1}{(2\pi)^4}\int (dk)\frac{e^{ikx}}{1+(k^2/4\kappa^2)(1-v^2)}. \tag{A.37}$$

Finally, we may insert (A.30) into (A.12) and integrate by parts to obtain

$$\langle j_\mu(x)\rangle = 16\pi\alpha\int G(x-x')J_\nu(x')d\omega', \tag{A.38}$$

where $J_\mu(x)$ is the current vector that generates the external electromagnetic field. The expression of $G(x)$ contained in (A.36) then yields

$$\langle j_\mu(x)\rangle = -\frac{2\alpha}{3\pi}\operatorname*{Lim}_{P\to\infty}\left(\log\frac{P_0+P}{\kappa}-1\right)J_\mu(x) - \frac{\alpha}{4\pi}\frac{1}{\kappa^2}\Box^2\int (F_1(x-x')-\tfrac{1}{3}F_2(x-x'))J_\mu(x')d\omega', \tag{A.39}$$

in which the first term represents the logarithmically divergent renormalization of charge.

It should be remarked that the existence of a charge renormalization term would appear to contradict the conservation of charge, since it implies that a non-vanishing total charge is induced in the vacuum. Indeed, a formal evaluation of the total induced charge would yield zero,

$$\begin{aligned}\frac{1}{c}\int \langle j_\mu(x)\rangle d\sigma_\mu &= \frac{i}{2\hbar c^2}\int \epsilon(x-x')\left[\frac{1}{c}\int j_\mu(x)d\sigma_\mu, j_\nu(x')\right]_0 A_\nu(x')d\omega' \\ &= 0,\end{aligned} \tag{A.40}$$

since the operator of the total charge commutes with the current vector at an arbitrary point. The expression of $\langle j_\mu(x)\rangle$ as

$$\langle j_\mu(x)\rangle = \frac{\partial}{\partial x_\nu}\frac{4e^2}{\hbar}\int G(x-x')F_{\mu\nu}(x')d\omega', \tag{A.41}$$

where

$$F_{\mu\nu} = \frac{\partial}{\partial x_\mu}A_\nu - \frac{\partial}{\partial x_\nu}A_\mu, \tag{A.42}$$

is formally consistent with the result since

$$\begin{aligned}\frac{1}{c}\int \langle j_\mu(x)\rangle d\sigma_\mu &= \frac{2e^2}{\hbar}\int\left(d\sigma_\mu\frac{\partial}{\partial x_\nu} - d\sigma_\nu\frac{\partial}{\partial x_\mu}\right)\int G(x-x')F_{\mu\nu}(x')d\omega' \\ &= 0,\end{aligned} \tag{A.43}$$

in view of the theorem

$$\int\left(d\sigma_\mu\frac{\partial}{\partial x_\nu}F(x) - d\sigma_\nu\frac{\partial}{\partial x_\mu}F(x)\right) = 0. \tag{A.44}$$

However, it is evident that these formal manipulations are only justified if the integrand in (A.44) decreases sufficiently rapidly in space-like directions, which is not fulfilled for the field strengths generated by a charge distribution of non-vanishing total charge.

This difficulty can be avoided by treating the actual electromagnetic field as the limit of a spatially confined field, for which the total induced charge is zero. A convenient way to accomplish this is to introduce a finite light quantum mass, which is eventually allowed to vanish. We thus write the potentials generated by the given charge distribution as

$$A_\mu(x) = \frac{1}{c}\int \bar{D}(x-x')J_\mu(x')d\omega', \quad \frac{\partial A_\mu(x)}{\partial x_\mu} = 0, \tag{A.45}$$

where

$$\bar{D}(x) = \operatorname*{Lim}_{\epsilon\to 0}\frac{1}{(2\pi)^4}\int \frac{e^{ikx}}{k^2+\epsilon^2}(dk). \tag{A.46}$$

The induced current can then be exhibited in the form

$$\begin{aligned}\langle j_\mu(x)\rangle &= -\frac{4e^2}{\hbar c}\int G(x-x')\Box'^2\bar{D}(x'-x'')J_\mu(x'')d\omega'd\omega'' \\ &= \frac{4e^2}{\hbar c}\frac{1}{(2\pi)^4}\int e^{ik\xi}G(k)k^2\bar{D}(k)J_\mu(x-\xi)(dk)(d\xi),\end{aligned} \tag{A.47}$$

in which the second version involves the Fourier transforms of the functions, $G(x)$ and $\bar{D}(x)$,

$$\begin{aligned}G(k) &= \frac{1}{(4\pi)^2}\int_{-1}^{1}dv(1-v^2)\int (dp)\delta'\left(p^2+\kappa^2+\frac{k^2}{4}(1-v^2)\right) \\ \bar{D}(k) &= \operatorname*{Lim}_{\epsilon\to 0}\frac{1}{k^2+\epsilon^2}.\end{aligned} \tag{A.48}$$

The total induced charge can then be calculated in terms of the total external charge,

$$Q=\frac{1}{c}\int J_\mu(x-\xi)d\sigma_\mu, \tag{A.49}$$

which expression is independent of ξ. Therefore,

$$\frac{1}{c}\int\langle j_\mu(x)\rangle d\sigma_\mu=\frac{4e^2}{\hbar c}Q\int G(k)k^2\bar{D}(k)\delta(k)(dk)$$

$$=\frac{4e^2}{\hbar c}Q\operatorname*{Lim}_{\epsilon\to 0}\left(\frac{k^2}{k^2+\epsilon^2}G(k)\right)_{k_\mu=0}. \tag{A.50}$$

If ϵ is placed equal to zero before evaluating the Fourier transforms at $k_\mu=0$, we obtain the previously computed non-vanishing induced charge

$$\delta Q=\frac{4e^2}{\hbar c}Q[G(k)]_{k_\mu=0}=\frac{\alpha}{3\pi^2}Q\int(dp)\delta'(p^2+\kappa^2). \tag{A.51}$$

On the other hand, if the limiting process $\epsilon\to 0$ is reserved to the end of the calculation, we evidently find $\delta Q=0$.

The implications of this limiting process may be further indicated by noting that, in the first term of (A.39), $J_\mu(x)$ will be replaced by

$$J_\mu(x)-e^2cA_\mu(x), \tag{A.52}$$

in virtue of the differential equation

$$(\Box^2-\epsilon^2)A_\mu(x)=-\frac{1}{c}J_\mu(x) \tag{A.53}$$

obeyed by the potential (A.45). Now (A.52) reduces to $J_\mu(x)$ at any point as $\epsilon\to 0$. Yet the total charge computed from (A.52) is zero. This is illustrated by the charge density associated, according to (A.52), with a point charge at the origin:

$$\operatorname*{Lim}_{\epsilon\to 0}\left(\delta(\mathbf{r})-\epsilon^2\frac{e^{-\epsilon r}}{4\pi r}\right). \tag{A.54}$$

We may conclude that in the process of vacuum polarization, a non-vanishing, and indeed divergent charge is attached to the original charge distribution, and a compensating charge is created at infinity.

We shall finally apply the computational methods of this paper to evaluate the invariant expression for the electromagnetic mass,

$$\delta mc^2\psi(x)=-\frac{e^2}{2}\int\gamma_\mu[\bar{D}(x-x')S^{(1)}(x-x')+D^{(1)}(x-x')\bar{S}(x-x')]\gamma_\mu\psi(x')d\omega'. \tag{A.55}$$

The insertion of the Fourier integral representations yields

$$\delta mc^2\psi(x)=-\frac{e^2}{2}\frac{1}{(2\pi)^7}\int(dk)(dk')e^{i(k+k')(x-x')}\gamma_\mu(i\gamma k'-\kappa)\gamma_\mu\left(\frac{\delta(k'^2+\kappa^2)}{k^2}+\frac{\delta(k^2)}{k'^2+\kappa^2}\right)\psi(x')d\omega'. \tag{A.56}$$

This becomes

$$-\frac{e^2}{2}\frac{1}{(2\pi)^7}\int(dk)(dp)e^{ip(x-x')}\gamma_\mu(i\gamma(p-k)-\kappa)\gamma_\mu\left(\frac{\delta(k^2-2pk)}{2pk}-\frac{\delta(k^2)}{2pk}\right)\psi(x')d\omega' \tag{A.57}$$

on introducing

$$p_\mu=k_\mu+k_\mu', \tag{A.58}$$

which is effectively subject to the restriction

$$p^2+\kappa^2=0, \tag{A.59}$$

in view of the wave equation satisfied by $\psi(x')$. Now

$$\frac{1}{2pk}[\delta(k^2-2pk)-\delta(k^2)]=-\int_0^1\delta'(k^2-2pku)du, \tag{A.60}$$

and

$$\gamma_\mu(i\gamma(p-k)-\kappa)\gamma_\mu=-2(i\gamma(p-k)+2\kappa), \tag{A.61}$$

whence

$$\delta mc^2\psi(x)=\frac{e^2}{(2\pi)^7}\int(dk)(dp)\int_0^1 du e^{ip(x-x')}(i\gamma k-\kappa)\delta'(k^2-2pku)\psi(x')d\omega', \tag{A.62}$$

in which we have employed the fact that $i\gamma p+\kappa$ is equivalent to $\gamma_\mu(\partial/\partial x_\mu')+\kappa$ applied to $\psi(x')$ and is thus effectively equal to zero. The transformation

$$k_\mu\to k_\mu+p_\mu u \tag{A.63}$$

then yields

$$\delta mc^2\psi(x)=\frac{e^2}{(2\pi)^7}\int(dk)(dp)\int_0^1 du e^{ip(x-x')}(i\gamma pu-\kappa)\delta'(k^2+\kappa^2u^2)\psi(x')d\omega'$$

$$=-\frac{e^2}{(2\pi)^3}\kappa\int_0^1 du\int(dk)(1+u)\delta'(k^2+\kappa^2u^2)\psi(x). \tag{A.64}$$

Hence,

$$\delta m/m=-\frac{\alpha}{2\pi^2}\int_0^1(1+u)du\int(dk)\delta'(k^2+\kappa^2u^2)=-\frac{3\alpha}{4\pi^2}\int(dk)\delta'(k^2+\kappa^2)+\frac{\alpha}{2\pi^2}\int_0^1(2u^2+u^3)du\kappa^2\int(dk)\delta''(k^2+\kappa^2u^2), \tag{A.65}$$

and

$$\delta m/m=\frac{3\alpha}{2\pi}\operatorname*{Lim}_{K\to\infty}\left(\log\frac{K_0+K}{\kappa}-\tfrac{1}{4}\right), \tag{A.66}$$

according to the integrals (A.33) and (A.35).

On the Electromagnetic Properties of Nucleons

SIDNEY BOROWITZ AND WALTER KOHN
Harvard University, Cambridge, Massachusetts

(Received May 31, 1949)

The methods recently developed by Schwinger for dealing with problems in quantum electrodynamics have been applied to an investigation of the electromagnetic properties of nucleons in interaction with pseudoscalar mesons. The calculated values of the magnetic moments of the neutron and proton are in agreement with results previously obtained by Case, Luttinger, and Slotnick and Heitler using different calculational procedures. Our result for the neutron-electron interaction is identical with that obtained by Case. Included in this paper are the anomalous proton-electron interaction and a qualitative discussion of the scattering of high energy nucleons. The large coupling constants necessary to fit any of the experimental data show that the results obtained by a second order perturbation calculation are not quantitatively reliable.

I. INTRODUCTION

THE methods recently developed in quantum electrodynamics[1–3] may be applied to a study of the changes in the electromagnetic properties of nucleons which result from their coupling to a symmetrical pseudoscalar meson field. Several[4–6] papers on this topic have appeared recently, in which the anomalous moments of the neutron and proton as well as the neutron-electron interaction were discussed. In these papers, the nucleon, meson, as well as the external electromagnetic fields were introduced at the start of the calculations and the electromagnetic properties of the nucleons were deduced from the energy of the system.

When the external field is a given space-time function, the electromagnetic properties of the nucleons are described by the current operator of the nucleon-meson system. We shall therefore first calculate the modifications of this operator due to the coupling of the nucleon to the meson vacuum field. It is then simple to examine the behavior of the system in an external electromagnetic field. This technique is in close analogy to Schwinger's treatment of the electromagnetic properties of electrons.[3]

Our results for the magnetic moments and the neutron-electron interaction are in agreement with those previously reported; we have also calculated the anomalous proton-electron interaction. Further, we have investigated qualitatively the interaction of high energy nucleons with an electromagnetic field. It is found that meson theory leads to effective anomalous magnetic moments which decrease in magnitude with increasing momentum transfer of the nucleon.

This paper, as well as the previous ones,[4–6] is based on a covariant perturbation theory carried to the second order of the coupling constant.

[1] J. S. Schwinger, Phys. Rev. **74**, 1439 (1948), hereafter referred to as *I*.
[2] J. S. Schwinger, Phys. Rev. **75**, 651 (1949), hereafter referred to as *II*.
[3] J. S. Schwinger, Phys. Rev., this issue, hereafter referred to as *III*.
[4] K. Case, Phys. Rev. **76**, 1 (1949).
[5] J. Luttinger, Helv. Phys. Acta **21**, 483 (1948).
[6] M. Slotnick and W. Heitler, Phys. Rev. **75**, 1645 (1949).

II. PRELIMINARIES

The following notation will be used: The symbol ϕ stands for the three operators ϕ_1, ϕ_2, ϕ_3, and represents the field variables of the symmetrical pseudoscalar meson.[7] The Dirac spinor ψ and its adjoint $\bar{\psi}$ denote the nucleon field; μ and κ are the inverse Compton wave-lengths of the mesons and nucleons respectively; $\gamma_\mu(\mu=1, 2, 3, 4)$ and γ_5 are the usual Dirac matrices; τ represents the three isotopic spin matrices τ_1, τ_2, and τ_3; g is the coupling constant.

The Lagrangian density of the nucleon and meson fields with pseudoscalar coupling is[8]

$$\mathfrak{L}=-\tfrac{1}{2}[(\partial\phi(x)/\partial x_\mu)(\partial\phi(x)/\partial x_\mu)+\mu^2\phi(x)\phi(x)] -\hbar c\bar{\psi}(x)(\gamma_\mu(\partial/\partial x_\mu)+\kappa)\psi(x) +ig\bar{\psi}(x)\gamma_5\tau\psi(x)\phi(x), \quad (2.1)$$

where $\phi\phi$ is the "scalar product" $\sum_{i=1}^{3}\phi_i\phi_i$, and $(\partial\phi/\partial x_\mu)\times(\partial\phi/\partial x_\mu)$ and $\tau\phi$ have an analogous meaning. Repeated Greek letter subscripts are to be summed from 1 to 4 throughout. The coordinate x stands for x_1, x_2, x_3, $x_4(=ict)$.

In the interaction representation, the state vector $\Psi[\sigma]$ obeys the equation of motion

$$i\hbar c\{\delta\Psi[\sigma]/\delta\sigma(x)\}=\mathfrak{IC}(x)\Psi[\sigma], \quad (2.2)$$

where

$$\mathfrak{IC}(x)=-ig\psi(x)\gamma_5\tau\psi(x)\phi(x). \quad (2.3)$$

The field operators satisfy the commutation relations

$$[\phi_i(x), \phi_j(x')]=i\hbar cD(x-x')\delta_{ij}, \quad (2.4)$$

and

$$\{\bar{\psi}_\alpha(x), \psi_\beta(x')\}=(1/i)S_{\alpha\beta}(x-x') =(1/i)[\gamma_\mu(\partial/\partial x_\mu)-\kappa]_{\alpha\beta}\Delta(x-x'), \quad (2.5)$$

where $D(x)$ and $\Delta(x)$ are the usual invariant functions associated with the meson and nucleon fields respectively.[1]

[7] N. Kemmer, Proc. Cambr. Phil. Soc. **34**, 354 (1938).
[8] We deliberately have not symmetrized the theory to avoid the additional terms arising from the charge conjugate expressions. This procedure does not affect the result; see F. J. Dyson, Phys. Rev. **75**, 486 (1949).

The current operator in this representation consists of a nucleon and meson part

$$j_\mu(x)=j_\mu^{(n)}(x)+j_\mu^{(m)}(x), \tag{2.6}$$

where

$$j_\mu^{(n)}(x)=iec\bar{\psi}(x)\gamma_\mu((1+\tau_3)/2)\psi(x);$$
$$j_\mu^{(m)}(x)=-(ie/\hbar)\phi(x)T_3[\partial\phi(x)/\partial x_\mu]. \tag{2.7}$$

Here T_3 is the operator which generates infinitesimal rotations about the third axis in the ϕ-space according to

$$\phi(x)\rightarrow(1+i\epsilon T_3)\phi(x).$$

It can be represented by the matrix

$$T_3=\begin{bmatrix}0 & -i & 0\\ i & 0 & 0\\ 0 & 0 & 0\end{bmatrix}. \tag{2.8}$$

We are interested in the current operator in the Heisenberg representation, which is given by $j_\mu(x)+\delta j_\mu(x)$ with[9]

$$\delta j_\mu(x)=-(i/2\hbar c)^2\int_{-\infty}^{\infty}\epsilon[\sigma,\sigma']\epsilon[\sigma',\sigma'']\times[[j_\mu(x),\mathcal{H}(x')],\mathcal{H}(x'')]d\omega'd\omega''$$
$$+(i/2\hbar c)\int_{-\infty}^{\infty}\epsilon[\sigma,\sigma'][j_\mu(x),\mathcal{H}_{1,0}(x')]d\omega', \tag{2.9}$$

correct to second order in "g".[10]

The function $\epsilon[\sigma,\sigma']=\pm1$ according to whether the surface σ follows or precedes σ'. $\mathcal{H}_{1,0}(x)$ is that part of the interaction Hamiltonian which contains the mass renormalization,[11] δM, of the nucleon,

$$\mathcal{H}_{1,0}(x)=\tfrac{1}{2}(\bar{\psi}(x)\chi(x)+\bar{\chi}(x)\psi(x)), \tag{2.10}$$

where

$$\chi(x)=\delta Mc^2\psi(x) \tag{2.11}$$

III. MODIFICATION OF THE NUCLEON CURRENT

When one substitutes $j_\mu=j_\mu^{(n)}+j_\mu^{(m)}$ in Eq. (2.9), the expression for δj_μ separates into a contribution from the nucleon current and one from the meson current. The expression for the nucleon part is strictly analogous to *III*, Eq. (1.32). One may therefore take over Eqs. (1.58), (1.61), and (1.62) of *III* with the following substitutions:

$$\gamma_\mu\rightarrow\gamma_\mu\left(\frac{1+\tau_3}{2}\right)\qquad e^2\rightarrow g^2$$
$$\gamma_\nu\rightarrow\gamma_5\qquad A_\nu\rightarrow\phi. \tag{3.1}$$

The term corresponding to the first term in *III*, Eq. (1.58) vanishes in our case since, with pseudoscalar coupling the meson particles and anti-particles have the same "mesonic charge."[4] Thus, in a nucleon vacuum,

$$\langle[j_\mu^{(n)},\mathcal{H}(x')]\rangle=0, \tag{3.2}$$

where the symbol $\langle\,\rangle$ indicates the expectation value. We note, too, that the Fourier representations of $\bar{D}(x)$ and $D^{(1)}(x)$ differ from those of the electromagnetic field due to the nonvanishing meson mass:

$$\bar{D}(x)=1/(2\pi)^4\int(dk)e^{ikx}(1/(k^2+\mu^2)), \tag{3.3}$$

$$D^{(1)}(x)=1/(2\pi)^3\int(dk)e^{ikx}\delta(k^2+\mu^2). \tag{3.4}$$

Thus we obtain, in the present case,

$$(\delta j_\mu^{(n)}(x))_{1,0}=-(ieg^2/2\hbar)\int d\omega'd\omega''\bar{\psi}(x')\times K_\mu(x'-x;x-x'')\psi(x''), \tag{3.5}$$

where

$$K_\mu=K_\mu^{(1)}+K_\mu^{(2)},$$

with

$$K_\mu^{(1)}=\frac{1}{(2\pi)^{11}}\int(dk')(dk'')(dk)\times\left[\gamma_5\tau(i\gamma k'-\kappa)\gamma_\mu\frac{1+\tau_3}{2}(i\gamma k''-\kappa)\gamma_5\tau\right]$$
$$\times\left\{\frac{\delta(k''^2+\kappa^2)}{(k'^2+\kappa^2)(k^2+\mu^2)}+\frac{\delta(k'^2+\kappa^2)}{(k''^2+\kappa^2)(k^2+\mu^2)}+\frac{\delta(k^2+\mu^2)}{(k'^2+\kappa^2)(k''^2+\kappa^2)}\right\}\exp[i(k'+k)(x'-x)]\times\exp[i(k''+k)(x-x'')], \tag{3.6}$$

and

$$K_\mu^{(2)}=-\frac{1}{(2\pi)^{11}}\int(dk')(dk'')(dk)\times\left\{\frac{3-\tau_3}{2}+2\tau_3\right\}\gamma_\mu\frac{1}{2\kappa}\frac{\partial}{\partial(x-x'')_\lambda}(x-x'')_\lambda$$
$$\times\exp[i(k''+k)(x-x'')]\exp[ik'(x'-x)]\times\gamma_5(i\gamma(k''-\kappa))\gamma_5\times\left\{\frac{\delta(k''^2+\kappa^2)}{k^2+\mu^2}+\frac{\delta(k^2+\mu^2)}{k''^2+\kappa^2}\right\} \tag{3.7}$$

+term with k' and k'', $(x-x')$ and $(x'-x)$ interchanged. In Eqs. (3.6) and (3.7) terms of the type ab denote $\sum_{\nu=1}^{4}a_\nu b_\nu$; in Eq. (3.7) we have used the relation

$$(1+\tau_3)/2\cdot\tau\cdot\tau=(3-\tau_3)/2+2\tau_3.$$

The calculation of $K_\mu^{(1)}$ and that part of $K_\mu^{(2)}$ which contains $(3-\tau_3)/2$ proceeds in analogy with the corre-

[9] See *III*, Eq. (1.32).

[10] We omit the first order correction to the current since its expectation value in a meson vacuum vanishes.

[11] The derivation of this is precisely analogous to the derivation of *II*, Eq. (3.77).

sponding calculation in *III*, to give

$$K_\mu=\frac{3-\tau_3}{2}\frac{1}{\kappa}\frac{1}{8\pi^2}\delta(x'-x'')M_\mu^{(n)} -\frac{3-\tau_3}{4}\frac{\delta(x'-x'')}{4\pi^2}\cdot\frac{1}{\kappa^2}C_\mu^{(n)}+R_\mu^{(n)}, \quad (3.8)$$

where

$$M_\mu^{(n)}=\sigma_{\mu\nu}\frac{\partial}{\partial x_\nu}F_0(x-x'); \quad \left(\sigma_{\mu\nu}=\frac{\gamma_\mu\gamma_\nu-\gamma_\nu\gamma_\mu}{2i}\right), \quad (3.9)$$

$$C_\mu^{(n)}=\gamma_\mu\Box^2(F_0(x-x')+F_1(x-x') +G_0(x-x')-G_1(x-x')), \quad (3.10)$$

$$R_\mu^{(n)}=-\frac{1}{(2\pi)^{11}}\int(dk')(dk'')(dk)\gamma_\mu 2\tau_3(1/2\kappa) \times\frac{\partial}{\partial(x-x')_\lambda}(x-x'')_\lambda\exp[i(k''+k)(x-x'')] \times\exp[ik'(x'-x)]\left\{\frac{\delta(k'^2+\kappa^2)}{k^2+\mu^2}+\frac{\delta(k^2+\mu^2)}{k'^2+\kappa^2}\right\} \quad (3.11)$$

+term with k' and k'', $(x-x'')$ and $(x'-x)$ interchanged. The functions F_l and G_l are defined as follows:

$$F_l(x)=\frac{1}{(2\pi)^4}\int(dp)e^{ipx}\int_0^1 v^{2l}dv\int_0^1 du \times\frac{u}{1+(\mu^2/\kappa^2)((1-u)/u^2)+(p^2/4\kappa^2)(1-v^2)}, \quad (3.12)$$

$$G_l(x)=\frac{1}{(2\pi)^4}\int(dp)e^{ipx}\int_0^1 v^{2l}dv\int_0^1 du \times\frac{u}{1+(\mu^2/\kappa^2)((1-u)/u^2)+(p^2/4\kappa^2)(1-v^2)} \times\frac{1}{1+(\mu^2/\kappa^2)((1-u)/u^2)}. \quad (3.13)$$

Thus the correction to the current operator arising from the nucleon current is, from Eq. (3.5),

$$\begin{aligned}(\delta j_\mu^{(n)}(x))_{1,0} &=-\frac{g^2}{4\pi\hbar c}\cdot\frac{1}{2\pi}\cdot\frac{ec}{2\kappa} \times\int\bar\psi(x')\frac{3-\tau_3}{2}M_\mu^{(n)}(x-x')\psi(x')d\omega', \\ &+\frac{g^2}{4\pi\hbar c}\cdot\frac{1}{2\pi}\cdot\frac{1}{4\kappa^2}\cdot\frac{iec}{4\pi} \times\int\bar\psi(x')\frac{3-\tau_3}{2}C_\mu^{(n)}(x-x')\psi(x')d\omega', \\ &-(ieg^2/2\hbar)\int\bar\psi(x')R_\mu^{(n)}(x'-x;x-x'') \times\psi(x'')d\omega'd\omega''. \end{aligned} \quad (3.14)$$

It is clear from Eqs. (3.9) and (3.10), that the first term of Eq. (3.14) is a polarization current giving rise to an anomalous magnetic moment and the second term is a convection current. This convection current does not correspond to an additional nucleon charge since its space integral vanishes. The third term, however, involving $R_\mu^{(n)}$, is the change of the nucleon charge due to the interaction. Since the total charge is conserved, we should expect that it will be cancelled by a term occurring in the correction to the meson current operator (see Section IV).

IV. MODIFICATION OF THE MESON CURRENT

On substituting the meson current $j_\mu^{(m)}$, Eq. (2.7), into Eq. (2.9), we obtain

$$(\delta j_\mu^{(m)}(x))_{1,0}=\left(-\frac{i}{\hbar c}\right)^2\int_{-\infty}^{\infty}\epsilon[\sigma,\sigma']\epsilon[\sigma',\sigma''] \times[[j_\mu^{(m}(x),\mathfrak{IC}(x')],\mathfrak{IC}(x'')]_{1,0}d\omega'd\omega''. \quad (4.1)$$

Using the notation $'$ to indicate the argument x', we first evaluate the commutator

$$\begin{aligned}[j_\mu^{(m)},\mathfrak{IC}'] &=-\frac{eg}{\hbar}\left[\phi T_3\frac{\partial\varphi}{\partial x_\mu},\bar\psi'\gamma_5\tau\phi'\right] \\ &=-iegc\left(\phi T_3\frac{\partial}{\partial x_\mu}D(x-x')\bar\psi'\gamma_5\tau\psi' -\bar\psi'\gamma_5\tau\psi'D(x'-x)T_3\frac{\partial\varphi}{\partial x_\mu}\right). \end{aligned} \quad (4.2)$$

In Eq. (4.2), T_3 can be eliminated with the aid of the following relations:

$$\begin{aligned}\bar\psi\phi T_3\tau\psi &=-\bar\psi[\tau_3/2,\tau]\phi\psi, \\ \bar\psi\tau T_3\phi\psi &=\bar\psi[\tau_3/2,\tau]\phi\psi. \end{aligned} \quad (4.3)$$

These are a consequence of the invariance of the "scalar product" $\bar\psi\tau\psi\phi$ under a rotation about the third axis of the isotopic spin space in which

$$\begin{aligned}&\psi\rightarrow[1+(i\epsilon/2)\tau_3]\psi, \\ &\bar\psi\rightarrow\bar\psi[1-(i\epsilon/2)\tau_3], \\ &\phi\rightarrow(1+i\epsilon T_3)\phi. \end{aligned} \quad (4.4)$$

One can also verify Eq. (4.3) by choosing the representation (2.8) of T_3 and the usual isotopic spin matrices. Equation (4.2) then becomes

$$[j_\mu^{(m)},\mathfrak{IC}']=\frac{iegc}{2}\left(\phi\bar\psi'\gamma_5[\tau_3,\tau]\psi'\frac{\partial}{\partial x_\mu}D(x-x') +\bar\psi'\gamma_5[\tau_3,\tau]\psi'\frac{\partial\phi}{\partial x_\mu}D(x-x')\right). \quad (4.5)$$

Calculating next the second commutator with $\mathfrak{K}''$, we obtain

$$[[j_\mu^{(m)}, \mathfrak{K}'], \mathfrak{K}'']_{1,0}$$
$$=\frac{eg^2c}{2}\Bigg(\left[\phi_i\bar{\psi}'\gamma_5[\tau_3, \tau_i]\psi', \bar{\psi}''\gamma_5\tau_j\psi''\phi_j''\right]\frac{\partial}{\partial x_\mu}D(x-x')$$
$$+\left[\bar{\psi}'\gamma_5[\tau_3, \tau_i]\psi'\frac{\partial\phi_i}{\partial x_\mu}, \bar{\psi}''\gamma_5\tau_j\psi''\phi_j\right]D(x'-x)\Bigg)_{1,0}$$
$$=\frac{eg^2c}{4}\Bigg([\bar{\psi}'\gamma_5[\tau_3, \tau_i]\psi', \bar{\psi}''\gamma_5\tau_j\psi'']_1\{\phi_i, \phi_j''\}_0$$
$$+\{\bar{\psi}'\gamma_5[\tau_3, \tau_i]\psi', \bar{\psi}''\gamma_5\tau_j\psi''\}_1$$
$$\times[\phi_i, \phi_j'']\Bigg)\frac{\partial}{\partial x_\mu}D(x-x')$$
$$+\frac{eg^2c}{4}\Bigg([\bar{\psi}'\gamma_5[\tau_3, \tau_i]\psi', \bar{\psi}''\gamma_5\tau_j\psi'']_1\left\{\frac{\partial\phi_i}{\partial x_\mu}, \phi_j''\right\}_0$$
$$+\{\bar{\psi}'\gamma_5[\tau_3, \tau_i]\psi', \bar{\psi}''\gamma_5\tau_j\psi''\}_1\left[\frac{\partial\phi_i}{\partial x_\mu}, \phi_j''\right]\Bigg). \quad (4.6)$$

The subscript 0 indicates the expectation value in the meson vacuum; the subscript 1, the one-particle part of the nucleon operators.

The reduction of Eq. (4.6) is straightforward and requires the following information in addition to Eq. (4.3) and the commutation relations, all of which is contained in *II* and *III*:

$$\{\phi_i, \phi_j'\}_0=\hbar cD^{(1)}(x-x')\delta_{ij}. \quad (4.7)$$

$$\{\bar{\psi}A\psi, \bar{\psi}'B\psi'\}_1=(\bar{\psi}AS^{(1)}(x-x')B\psi') +(\bar{\psi}'BS^{(1)}(x-x')A\psi). \quad (4.8)$$

$$[\epsilon(x-x')-\epsilon(x-x'')]\epsilon(x'-x'') =\epsilon(x-x')\epsilon(x-x'')-1. \quad (4.9)$$

$S^{(1)}(x)$, $D^{(1)}(x)$ are even functions.

$S(x)$, $D(x)$ are odd functions.

$$\bar{D}(x)=-\tfrac{1}{2}\epsilon(x)D(x). \quad (4.10)$$

$$\bar{S}(x)=-\tfrac{1}{2}\epsilon(x)S(x). \quad (4.11)$$

In using Eq. (4.9), the term which -1 multiplies will be discarded since only virtual processes occur.

As a result of this reduction one finds

$$(\delta j_\mu^{(m)}(x))_{1,0}=-\frac{ieg^2}{\hbar}\int\bar{\psi}(x')\tau_3L_\mu(x'-x; x-x'') \times\psi(x'')dx'dx'', \quad (4.12)$$

and

$$L_\mu=\gamma_5\{\mathfrak{s}[\bar{S}(x''-x')\bar{D}(x'-x)(\partial/\partial x_\mu)D^{(1)}(x-x'')] +\mathfrak{s}[\bar{S}(x''-x')(\partial/\partial x_\mu')\bar{D}(x'-x)D^{(1)}(x-x'')]\}\gamma_5. \quad (4.13)$$

The symbol $\mathfrak{s}$ denotes the operation of interchanging the superscript $^{(1)}$ in turn with each of the superscripts $^-$ and summing. Thus Eq. (4.13) contains six terms.

We now write the $\bar{S}$ and $\bar{D}$ functions as Fourier Integrals (see *III*, Eq. (1.66)) and commute through the γ_5's. This leads to the expression

$$L_\mu=-\frac{1}{(2\pi)^{11}}\int(dk)(dk')(dk'')e^{ik(x'-x'')} \times e^{ik'(x'-x)}e^{ik''(x-x'')}(i\gamma k+\kappa)i(k'+k'')_\mu \times\left\{\frac{\delta(k''^2+\mu^2)}{(k^2+\kappa^2)(k'^2+\mu^2)}+\frac{\delta(k'^2+\kappa^2)}{(k^2+\kappa^2)(k''^2+\mu^2)} +\frac{\delta(k^2+\kappa^2)}{(k'^2+\mu^2)(k''^2+\mu^2)}\right\}. \quad (4.14)$$

Introducing next new variables p' and p'' according to the equations

$$k'=p'-k, \quad k''=p''-k, \quad (4.14')$$

we obtain

$$L_\mu=-\frac{1}{(2\pi)^{11}}\int(dk)(dp')(dp'')e^{ip'(x'-x)} \times e^{ip''(x-x'')}(i\gamma k+\kappa)i(p'+p''-2k)_\mu \times\left[\frac{\delta(k^2-2kp''+\mu^2-\kappa^2)}{(k^2+\kappa^2)(k^2-2kp'+\mu^2-\kappa^2)} +\frac{\delta(k^2-2kp'+\mu^2-\kappa^2)}{(k^2+\kappa^2)(k^2-2kp''+\mu^2-\kappa^2)} +\frac{\delta(k^2+\kappa^2)}{(k^2-2kp'+\mu^2-\kappa^2)(k^2-2kp''+\mu^2-\kappa^2)}\right]. \quad (4.15)$$

The expression in square brackets can be reduced as in *III* and gives,

$$\frac{1}{2}\int_{-1}^{1}dv\int_0^1 udu(\delta''[k^2+\kappa^2-(2\kappa^2-\mu^2)u -\mu k(p'+p''+(p'-p'')v)]. \quad (4.16)$$

We eliminate the terms in the δ'' function which are linear in k by the transformation

$$k\rightarrow k+\frac{u}{2}(p'+p''+(p'-p'')v), \quad (4.17)$$

upon which it becomes, in virtue of *III*, Eq. (1.91),

$$\delta''\left[k^2+\kappa^2-(2\kappa^2-\mu^2)u +\kappa^2u^2\left(1+\frac{(p'-p'')^2}{4\kappa^2}(1-v^2)\right)\right]. \quad (4.18)$$

The factor $(i\gamma k+\kappa)i(p'+p''-2k)_\mu$ in Eq. (4.15) becomes, under the transformation (4.17),

$$(i\gamma k+\kappa)i(p'+p''-2k)_\mu$$
$$=\left[i\gamma k+\frac{i\gamma\mu}{2}(p'+p''+(p'-p'')v)+\kappa\right]$$
$$\times i[p'+p''-2ku(p'+p''+(p'-p'')v)]_\mu. \quad (4.19)$$

This expression can be considerably simplified by observing that as a result of integration, terms linear in k and v will vanish and $k_\lambda k_\sigma$ is equivalent to $\frac{1}{4}k^2\delta_{\lambda\sigma}$. Further, since the operators in Eq. (4.19) operate on field variables which obey the Dirac Equation for a free particle we may set $(i\gamma p'+\kappa)$ and $(i\gamma p''+\kappa)=0$ (see *III*, discussion of Eq. (1.94)). The expression (4.19) then becomes

$$(\gamma_\mu k^2/2)+i\kappa(1-u)^2(p'+p'')_\mu. \quad (4.20)$$

In virtue of the Dirac equation, we can separate $(p'+p'')_\mu$ into a convection and a polarization part, *viz.*

$$(p'+p'')_\mu=-1/i\kappa[2\kappa^2\gamma_\mu-\kappa\sigma_{\mu\nu}(p''-p')_\nu]. \quad (4.21)$$

Finally then we have

$$L_\mu=-\frac{1}{(2\pi)^{11}}\cdot\frac{1}{2}\int(dp')(dp'')(dk)e^{ip'(x'-x)}e^{ip''(x-x'')}$$
$$\times\int_0^1 udu\int_1^1 dv\Big[(1-u)^2\sigma_{\mu\nu}(p''-p')_\nu\kappa$$
$$-2(1-u)^2\kappa^2\gamma_\mu+\frac{\gamma_\mu k^2}{2}\Big]$$
$$\times\delta''\Big[k^2+\kappa^2-(2\kappa^2-\mu^2)u$$
$$+\kappa^2u^2\left(1+\frac{(p'-p'')^2}{4\kappa^2}(1-v^2)\right)\Big]. \quad (4.22)$$

The part of L_μ which contributes to the polarization current is

$$L_\mu{}^{(P)}=-\frac{1}{(2\pi)^{11}}\cdot\frac{1}{2}\int(dp')(dp'')(dk)$$
$$\times e^{ip'(x'-x)}e^{ip''(x-x'')}$$
$$\times\int_0^1 udu\int_{-1}^1 dv[(1-u)^2\sigma_{\mu\nu}(p''-p')_\nu\kappa]$$
$$\times\delta''\Big[k^2+\kappa^2-(2\kappa^2-\mu^2)u$$
$$+\kappa^2u^2\left(1+\frac{(p'-p'')^2}{4\kappa^2}(1-v^2)\right)\Big]. \quad (4.23)$$

Performing the integration over k as in *III*, Eq. (1.102) and changing the integral over v to an integral from 0 to 1, we obtain

$$L_\mu{}^{(P)}=-\frac{\pi}{(2\pi)^{11}}\frac{1}{\kappa}\int(dp')(dp'')e^{ip'(x'-x)}e^{ip''(x-x'')}$$
$$\times\int_0^1 udu\int_0^1 dv\frac{(1-u)^2\sigma_{\mu\nu}(p''-p')_\nu}{d}, \quad (4.24)$$

where we have used the abbreviation

$$(1-u)^2+\frac{\mu^2}{\kappa^2}u+\frac{(p'-p'')^2}{4\kappa^2}(1-v^2)=d. \quad (4.24a)$$

We now introduce the variables

$$P_\mu=(p_\mu'+p_\mu'')/2;\quad p_\mu=p_\mu''-p_\mu', \quad (4.25)$$

and integrate over P, obtaining

$$L_\mu{}^{(P)}=-\frac{1}{8\pi^2}\frac{1}{i\kappa}\delta(x'-x'')M_\mu{}^{(m)}(x-x'), \quad (4.26)$$

where

$$M_\mu{}^{(m)}(x-x')=\sigma_{\mu\nu}\frac{\partial}{\partial x_\nu}E_0(x-x'),$$

and

$$E_0(x-x')=\frac{1}{(2\pi)^4}\int_0^1 udu\int_0^1 dv$$
$$\times\int\frac{(dp)e^{ip(x-x')}(1-u)^2}{d}. \quad (4.27)$$

One treats the remaining terms of Eq. (4.22), which contribute to the convection current, by integrating by parts with respect to v, which results in

$$L_\mu{}^{(C)}=-\frac{1}{(2\pi)^{11}}\int(dk)(dp')(dp'')$$
$$\times\exp[ip'(x'-x)]\exp[ip''(x-x'')]$$
$$\cdot\int_0^1 udu(\gamma_\mu k^2-2(1-u)^2\kappa^2\gamma_\mu)$$
$$\cdot\delta''(k^2+\kappa^2-(2\kappa^2-\mu^2)u+\kappa^2u^2)$$
$$+\frac{1}{2}\cdot\frac{1}{(2\pi)^{11}}\int(dk)(dp')(dp'')e^{ip'(x'-x)}$$
$$\times e^{ip''(x-x'')}\cdot\int_0^1 udu\int_0^1 dv$$
$$\cdot\left(\frac{\gamma_\mu k^2}{2}-2(1-u)^2\kappa^2\gamma_\mu\right)v$$
$$\times\frac{\partial}{\partial v}\delta''\Big[k^2+\kappa^2-(2\kappa^2-\mu^2)u$$
$$+\kappa^2u^2\left(1+\frac{(p'-p'')^2}{4\kappa^2}(1-v^2)\right)\Big]. \quad (4.28)$$

We first evaluate the second term of $L_\mu^{(C)}$, which contains $(\gamma_\mu k^2/2-2(1-u^2)\kappa^2\gamma_\mu)$ as a factor. For the part proportional to k^2 we carry out the v differentiation which gives

$$-\frac{v^2u^2}{4}(p'-p'')^2k^2\gamma_\mu\delta'''\Big[k^2+\kappa^2-(2\kappa^2-\mu^2)u+\kappa^2u^2\Big(1+\frac{(p'-p'')^2}{4\kappa^2}(1-v^2)\Big)\Big]. \quad (4.29)$$

The integral of this expression over k, is equal to the integral over k of

$$\frac{v^2u^2}{2}(p'-p'')^2\gamma_\mu\delta''\Big[k^2+\kappa^2-(2\kappa^2-\mu^2)u+\kappa^2u^2\Big(1+\frac{(p'-p'')^2}{4\kappa^2}(1-v^2)\Big)\Big], \quad (4.30)$$

(see *III*, Eq. (1.99)). Substituting Eq. (4.30) into Eq. (4.28), we can now carry out the k integration for the entire second term of Eq. (4.28) leading to

$$\frac{\pi}{2(2\pi)^{11}}\cdot\frac{1}{\kappa^2}\int(dp')(dp'')e^{ip(x'-x)}e^{ip''(x-x'')}\times\int_0^1 udu\int_0^1 dv\Big(\frac{v^2u^2}{2}(p'-p'')^2\gamma_\mu-2(1-u)^2\kappa^2\gamma_\mu v\frac{\partial}{\partial v}\Big)\frac{1}{d}. \quad (4.31)$$

To eliminate the derivative with respect to v, we write

$$\frac{1}{d}=\frac{1}{(1-u)^2+(\mu^2/\kappa^2)u}-\frac{[(p'-p'')^2/4\kappa^2](1-v^2)[1/((1-u)^2+(\mu^2/\kappa^2)u)]}{d}. \quad (4.32)$$

The differentiation of the first term gives 0. The second term can be integrated by parts with respect to v, and we note that the boundary terms vanish.

On introducing the variables of Eq. (4.25) in Eq. (4.31), we can carry out the integration over P, obtaining finally

$$L_\mu^{(C)}=[1/(8\pi)^2]\delta(x'-x'')(1/2\kappa^2)\times C_\mu^{(m)}(x-x')+B_\mu^{(m)}, \quad (4.33)$$

where

$$C_\mu^{(m)}(x-x')=\gamma_\mu[-\Box^2(J_1(x-x')+I_0(x-x')-I_1(x-x'))], \quad (4.34)$$

$$J_1(x-x')=\frac{1}{(2\pi)^4}\int_0^1 u^3du\int_0^1 dv\times\int(dp)\frac{\exp[ip(x-x')]}{d}, \quad (4.35)$$

$$I_1(x-x')=\frac{1}{(2\pi)^4}\int_0^1(1-u)^2u^3du\int_0^1 v^{2l}\int(dp)\times\frac{\exp[ip(x-x')]}{d}\cdot\frac{1}{1+(2-\mu^2/\kappa^2)u+u^2}, \quad (4.36)$$

and $B_\mu^{(m)}$ is the first term of Eq. (4.28).

Substituting Eqs. (4.26) and (4.33) into Eq. (4.12), we find for the correction to the current operator arising from the meson current,

$$(\delta j_\mu^{(m)}(x))_{1,0}=\frac{g^2}{4\pi\hbar c}\cdot\frac{1}{\pi}\cdot\frac{ec}{2\kappa}\int\bar\psi(x')\tau_3\times M_\mu^{(m)}(x-x')\psi(x')d\omega'-\frac{g^2}{4\pi\hbar c}\cdot\frac{1}{\pi}\cdot\frac{iec}{4\kappa^2}\int\bar\psi(x')\tau_3\times C_\mu^{(m)}(x-x')\psi(x')d\omega'-\frac{ieg^2}{\hbar}\int\bar\psi(x')B_\mu^{(m)}(x'-x;x-x'')\times\psi(x'')d\omega'd\omega''. \quad (4.37)$$

The last term in Eq. (4.37) has the transformation properties of a convection current and may be interpreted as the charge carried by the meson field by virtue of its interaction with the nucleon. As indicated at the conclusion of Section III, the contributions of $B_\mu^{(m)}$ and $R_\mu^{(n)}$ to δj_μ cancel each other. Since their individual contributions are divergent, it is essential that they be evaluated using the same physical variables. In arriving at the expression for $B_\mu^{(m)}$ (the first term in Eq. (4.28)), we replaced the variable k'', associated with the momentum of the meson, by the variable $p''=k+k''$. Hence in simplifying $R_\mu^{(n)}$, we must again eliminate the meson momentum, this time k, by the same substitution $p''=k+k''$. This is in contrast to the treatment of the part of $K_\mu^{(2)}$ proportional to $(3-\tau_3)/2$ in which the nucleon momentum k'' was replaced by p''.

V. ANOMALOUS MAGNETIC MOMENTS

The coupling between a nucleon and the meson vacuum leads to observable effects in the presence of an external electromagnetic field, in virtue of the additional interaction

$$\delta H=-\frac{1}{c}(\delta j_\mu)_{1,0}A_\mu. \quad (5.1)$$

Here $(\delta j_\mu)_{1,0}$ is the total correction to the current operator given by the sum of Eqs. (3.14) and (4.37), and A_μ is the external electromagnetic field.

As a first application, we turn to the question of the anomalous magnetic moments of the neutron and proton. For this purpose we pick out from $(\delta j_\mu)_{1,0}$ the polarization part, $\delta j_\mu^{(P)}$,* which has the form $\sigma_{\mu\nu}(\partial/\partial x_\nu)$, i.e.,

$$\delta j_\mu^{(P)}=-\frac{g^2}{4\pi\hbar c}\cdot\frac{1}{2\pi}\cdot\frac{ec}{2\kappa}\times\int\bar\psi(x')\frac{3-\tau_3}{2}M_\mu^{(n)}(x-x')\psi(x')d\omega'$$
$$+\frac{g^2}{4\pi\hbar c}\frac{1}{\pi}\cdot\frac{ec}{2\kappa}\times\int\bar\psi(x')\tau M_\mu^{(m)}(x-x')\psi(x')d\omega'$$
$$=-\frac{g^2}{4\pi\hbar c}\cdot\frac{1}{2\pi}\cdot\frac{e}{2\kappa}\cdot c\frac{\partial}{\partial x_\nu}\frac{1}{(2\pi)^4}\times\int d\omega'(dp)\bar\psi(x')\left[\frac{3-\tau_3}{2}f_1(p^2)+\tau_3 f_2(p^2)\right]\cdot\sigma_{\mu\nu}\psi(x')e^{ip(x-x')},\quad(5.2)$$

where

$$f_1(p^2)=\int_0^1 dv\int_0^1 du\times\frac{u^3}{u^2+\eta(1-u)+(p^2u^2/4\kappa^2)(1-v^2)},\quad(5.3)$$

$$f_2(p^2)=-2\int_0^1 dv\int_0^1 du\times\frac{(1-u)u^2}{u^2+\eta(1-u)+(p^2/4\kappa^2)(1-u)^2(1-v^2)}.\quad(5.4)$$

Here η is the square of the ratio of meson to nucleon mass, $(\mu/\kappa)^2$.

The functions $f_1(p^2)$ and $f_2(p^2)$ can be expanded in powers of p^2/κ^2; noting that a p^2 is equivalent to the operator $-\Box^2$ applied to $e^{ip(x-x')}$, we have

$$f_1=\int_0^1 du\frac{u^3}{u^2+\eta(1-u)}\times\left\{1+\frac{1}{6(u^2+\eta(1-u))}\frac{\Box^2}{\kappa^2}+\cdots\right\},\quad(5.5)$$

$$f_2=-2\int_0^1 du\frac{(1-u)u^2}{u^2+\eta(1-u)}\times\left\{1+\frac{(1-u)^2}{6(u^2+\eta(1-u))}\frac{\Box^2}{\kappa^2}+\cdots\right\}.\quad(5.6)$$

* From here on, we shall dispense with the notation, $(\ )_{1,0}$ since in all applications to be discussed we shall be concerned only with the one nucleon, no meson part of the current operators.

Since we are interested in the operator (5.1), we may, by an integration by parts, transfer the differential operators $\Box^2$, $\Box^4$, etc., to the A_μ. If the variation of A_μ in space and time is small within a Compton wavelength of the nucleon, all terms in Eqs. (5.5) and (5.6) except the first may be neglected. Under these conditions the integration over p in Eq, (5.3) may be easily carried out to give $(2\pi)^4\delta(x-x')$. Therefore

$$\delta j_\mu^{(P)}=-\frac{g^2}{4\pi\hbar c}\frac{1}{2\pi}\frac{e}{2\kappa}c\frac{\partial}{\partial x_\nu}\times\bar\psi(x)\left\{\frac{3-\tau_3}{2}f_1(0)+\tau_3 f_2(0)\right\}\sigma_{\mu\nu}\psi(x).\quad(5.7)$$

This corresponds to additional magnetic moments

$$\lambda=-\frac{g^2}{4\pi\hbar c}\cdot\frac{1}{2\pi}\left\{\frac{3-\tau_3}{2}f_1(0)+\tau_3 f_2(0)\right\}\mu_0,\quad(5.8)$$

where μ_0 is the nuclear magneton $e/2\kappa$, and $\tau_3=\pm1$ for a proton and neutron respectively. Thus for the proton, the additional moment is

$$\lambda_P=-\frac{g^2}{4\pi\hbar c}\frac{\mu_0}{2\pi}\int_0^1 du\left\{\frac{u^3-2(1-u)u^2}{u^2+\eta(1-u)}\right\}$$
$$=\frac{g^2}{4\pi\hbar c}\frac{\mu_0}{\pi}\left\{\frac{1}{4}-\frac{3\eta}{2}+\frac{1}{4}(5\eta-3\eta^2)\log\frac{1}{\eta}-\frac{(\eta)^{\frac12}}{2}\left\{\frac{4-11\eta+3\eta^2}{(4-\eta)^{\frac12}}\right\}\cos^{-1}\frac{(\eta)^{\frac12}}{2}\right\}.\quad(5.9)$$

Similarly, the anomalous neutron moment is

$$\lambda_N=-\frac{g^2}{4\pi\hbar c}\frac{\mu_0}{\pi}\int_0^1 du\left\{\frac{u^3+(1-u)u^2}{u^2+\eta(1-u)}\right\}$$
$$=-\frac{g^2}{4\pi\hbar c}\frac{\mu_0}{\pi}\left\{1+\frac{\eta}{2}\log\frac{1}{\eta}-\frac{(\eta)^{\frac12}}{(4-\eta)^{\frac12}}(2-\eta)\cos^{-1}\frac{\eta^{\frac12}}{2}\right\}.\quad(5.10)$$

With a meson mass of $282m_e$, these expressions are in qualitative agreement with experiment in the following respects: (1) The anomalous moments are finite and have the correct sign. (2) The neutron moment is larger in absolute magnitude than the anomalous proton moment.

Quantitatively, however, the agreement with experiment is very poor. The calculated ratio $\delta\mu_N/\delta\mu_p$, which is independent of the coupling constant, is equal approximately to -8, whereas its experimental value is -1.07. From Eq. (4.12), we see that the computed contributions of the meson current to the anomalous

moments are equal and opposite for neutron and proton. The large ratio $\delta\mu_N/\delta\mu_p$ is then due to the fact that the contribution to the moments from the nucleon current is of the same order of magnitude. This rather unexpected result indicates that in our model the mesons are tightly bound to the nucleon and are spread over a nucleon rather than a meson Compton wave-length.

In adjusting the coupling constant $(g^2/4\pi\hbar c)$ to fit the experimental value of either the neutron or proton moment, one meets the difficulty characteristic of weak coupling methods in nuclear problems: The values needed are 7 and 52 respectively, which shows clearly that our results, obtained from a second order perturbation calculation, are quantitatively not trustworthy.

VI. NUCLEON ELECTRON INTERACTIONS

We turn next to a discussion of the interactions of nucleons with electrons which arise as the result of the coupling of the nucleon and meson fields. Thus there exists an interaction between a neutron and an electron as well as a correction to the Coulomb potential between a proton and an electron. The neutron electron interaction has been experimentally measured in scattering experiments by E. Fermi, I. I. Rabi and their coworkers.[12,13] The anomalous proton electron interaction contributes a small part (theoretically estimated at less than $\frac{1}{2}$ megacycle) to the Lamb shift.

An electron will, of course, interact with the entire additional current of the nucleons. However, the effect with which we are concerned here, and which has been measured in the above mentioned experiments, is the interaction of an electron with the convection part only. According to Eqs. (3.14) and (4.37), the latter is given by

$$\begin{aligned}\delta j_\mu^{(C)}=&\frac{g^2}{4\pi\hbar c}\cdot\frac{1}{\kappa^2}\cdot\frac{iec}{4\pi}\\&\times\int\bar\psi(x')\frac{3-\tau_3}{2}C_\mu^{(n)}(x-x')\psi(x')d\omega\\&-\frac{g^2}{4\pi\hbar c}\cdot\frac{1}{\kappa^2}\cdot\frac{iec}{4\pi}\\&\times\int\bar\psi(x')\tau C_\mu^{(m)}(x-x')\psi(x')d\omega'\\=&\frac{g^2}{4\pi\hbar c}\cdot\frac{1}{4\kappa^2}\cdot\frac{iec}{\pi}\cdot\frac{1}{(2\pi)^4}\Box^2\\&\times\int d\omega'(dp)\bar\psi(x)\left\{\frac{3-\tau_3}{2}f_3(p^2)\right.\\&\left.+\tau_3 f_4(p^2)\right\}\gamma_\mu\psi(x')\cdot\exp[ip(x-x')],\end{aligned}\tag{6.1}$$

where

$$\begin{aligned}f_3(p^2)=&\frac{1}{4}\int_0^1 dv\int_0^1 du\left\{\frac{(1+v^2)u^3}{u^2+\eta(1-u)+(p^2u^2/4\kappa^2)(1-v^2)}\right.\\&+\frac{(1-v^2)u^5}{u^2+\eta(1-u)+(p^2u^2/4\kappa^2)(1-v^2)}\\&\left.\cdot\frac{1}{u^2+\eta(1-u)}\right\},\end{aligned}\tag{6.2}$$

$$\begin{aligned}f_4(p^2)=&-\int_0^1 dv\int_0^1 du\\&\times\left\{\frac{-v^2(1-u)^3}{u^2+\eta(1-u)+(p^2/4\kappa^2)(1-u)^2(1-v^2)}\right.\\&+\frac{(1-v^2)u^2(1-u)^3}{u^2+\eta(1-u)+(p^2/4\kappa^2)(1-u)^2(1-v^2)}\\&\left.\cdot\frac{1}{u^2+\eta(1-u)}\right\}.\end{aligned}\tag{6.3}$$

The interaction density of this current with the electromagnetic field of the electrons, A_μ, is given by the expression

$$\delta H^{(C)}=-(1/c)\delta j_\mu^{(C)}\cdot A_\mu.\tag{6.4}$$

As in Section V, the $\Box^2$ occurring in the expression (6.1) for $\delta j_\mu^{(C)}$, may be transferred by an integration of parts to A_μ. The slow variation of the quantity $\Box^2 A_\mu=-(e/c)I_\mu$ where I_μ is the electron particle current, allows us to replace the argument p^2 in the functions f_3 and f_4 by 0. Thus we have effectively

$$\begin{aligned}\delta j_\mu^{(C)}=&\frac{g^2}{4\pi\hbar c}\cdot\frac{1}{4\kappa^2}\cdot\frac{iec}{\pi}\Box^2\bar\psi(x)\left\{\frac{3-\tau_3}{2}f_3(0)\right.\\&\left.+\tau_3 f_4(0)\right\}\gamma_\mu\psi(x)=-\tfrac{1}{6}Q\Box^2 i_\mu.\end{aligned}\tag{6.5}$$

The quantity,

$$Q=-\frac{g^2}{4\pi\hbar c}\cdot\frac{3}{2\kappa^2}\cdot\frac{e}{\pi}\left\{\frac{3-\tau_3}{2}f_3(0)+\tau_3 f_4(0)\right\},\tag{6.6}$$

has the dimensions of charge$\times$(length)^2; i_μ is the unperturbed nucleon particle current,

$$i_\mu=ic\bar\psi(x)\gamma_\mu\psi(x).\tag{6.7}$$

When the relative motion of nucleon and electron is slow, we need consider only the 4−4 term of the interaction (6.4). Thus we have

$$\begin{aligned}\delta H^{(C)}&=(1/6c)Q\Box^2 i_\mu A_\mu\\&=-(eQ/6c^2)i_\mu I_\mu\\&\cong(eQ/6)d_{nucl}\cdot d_{el},\end{aligned}\tag{6.8}$$

where the d's are particle densities. The interaction

[12] E. Fermi and L. Marshall, Phys. Rev. **72**, 1139 (1947).
[13] Rainwater, Rabi, and Havens, Jr., Phys. Rev. **72**, 634 (1947); Phys. Rev. **75**, 1295 (1949).

(6.8) corresponds to a short range potential V between the nucleon and electron whose space integral is

$$\int V d\tau = \frac{eQ}{6} \text{ erg-cm}^3. \tag{6.9}$$

If one takes the meson mass as $282m_e$, Eqs. (6.9), (6.2), and (6.3) yield for the proton

$$\begin{aligned}\frac{eQ_P}{6} &= \frac{g^2}{4\pi\hbar c}\cdot\frac{1}{4\kappa^2}\cdot\frac{e^2}{6\pi}\int_0^1 du\left(\frac{2u^3+2(1-u)^3}{u^2+\eta(1-u)}\right.\\ &\qquad\left.+\frac{u^5-4u^2(1-u)^3}{[u^2+\eta(1-u)]^2}\right)\\ &= \frac{g^2}{4\pi\hbar c}\frac{e^2}{2\pi\kappa^2}\left\{\frac{1}{4-\eta}\left(-\frac{17}{6}+\frac{131\eta}{24}-\frac{5\eta^2}{2}\right)\right.\\ &\qquad+\left(\frac{1}{4}-\frac{7\eta}{6}+\frac{5\eta^2}{8}\right)\log\frac{1}{\eta}+\frac{\eta^{\frac{1}{2}}}{(4-\eta)^{\frac{1}{2}}}\\ &\qquad\left.\times\left(\frac{35}{3}-\frac{22\eta}{3}+\frac{59\eta^2}{6}-\frac{5\eta^3}{4}\right)\cos^{-1}\frac{\eta^{\frac{1}{2}}}{2}\right\} \qquad (6.10)\\ &= 0.97\times10^{-46}\frac{g^2}{4\pi\hbar c} \text{ erg-cm}^3.\end{aligned}$$

while for the neutron

$$\begin{aligned}\frac{eQ_N}{6} &= \frac{g^2}{4\pi\hbar c}\cdot\frac{1}{4\kappa^2}\cdot\frac{e^2}{3\pi}\int_0^1 du\left\{\frac{2u^3-(1-u)^3}{u^2+\eta(1-u)}\right.\\ &\qquad\left.+\frac{u^5+2u^2(1-u)^3}{[u^2+\eta(1-u)]^2}\right\}\\ &= -\frac{g^2}{4\pi\hbar c}\cdot\frac{e^2}{2\pi\kappa^2}\left\{\frac{1}{4-\eta}\left(-\frac{13}{3}+\frac{4\eta}{3}\right)\right.\\ &\qquad+\left(\frac{1}{4}-\frac{2\eta}{3}\right)\log\frac{1}{\eta}+\frac{\eta^{\frac{1}{2}}}{(4-\eta)^{\frac{1}{2}}}\\ &\qquad\left.\times\left(\frac{35}{3}-\frac{17\eta}{3}+\frac{4\eta^2}{3}\right)\cos^{-1}\frac{\eta^{\frac{1}{2}}}{2}\right\}\\ &= -0.26\times10^{-46}\frac{g^2}{4\pi\hbar c} \text{ erg-cm}^3.^{**} \qquad (6.11)\end{aligned}$$

The experimental values of $(eQ_N/6)$ lie between -7 and -30×10^{-46} erg-cm^3 corresponding to coupling constants between 27 and 115. If one takes a coupling constant of 50 to estimate $(eQ_P/6)$, one finds $(eQ_P/6) = 48\times10^{-46}$ erg-cm^3. This repulsive interaction displaces the $^2S_{\frac{1}{2}}$ level of hydrogen upwards by about 0.2 megacycles and thus makes a very small contribution to the 1062 ± 5 megacycles of the Lamb shift.[14]

The quantity Q can be given the following physical interpretation. Due to the interaction of the "bare" nucleons with the meson vacuum, the physical neutron and proton have associated with them a charge cloud of total charge 0 and e respectively. The anomalous nucleon electron interaction stems from the fact that this charge is spread out rather than concentrated at a point. Let us denote the difference between the actual charge distribution of a physical nucleon and that of a point nucleon by $\delta\rho$. One can then calculate the total interaction energy of the charge distribution $\delta\rho$ with an electron distribution, $-ed_{el}$, which may be taken as constant over the dimensions of the nucleon. One finds directly the value

$$d_{el}\int V d\tau = (ed_{el}/6)\int \delta\rho r^2 d\tau. \tag{6.12}$$

Comparing Eqs. (6.12) and (6.9) we see that

$$Q = \int \delta\rho r^2 d\tau, \tag{6.13}$$

i.e., Q is the monopole moment of the charge distribution of the physical nucleon. Clearly the square root of $|Q/e|$ is a measure of the spread of the nucleon charge. Taking a coupling constant of 50, we find

$$|Q_N/e|^{\frac{1}{2}} = 5\times10^{-14} \text{ cm}, \tag{6.14}$$

a distance intermediate between the nucleon and meson Compton wave-lengths.

VII. REMARKS ON HIGH ENERGY SCATTERING

In the last two sections we have considered processes in which the external field varied so slowly that an expansion of δj_μ in powers of $\Box^2/\kappa^2$ was possible. On the other hand, when treating the collisions of high energy nucleons with an external field this procedure will, at best, converge very slowly and hence is not suitable.

Let us first consider the scattering of a nucleon due to its anomalous polarization current $\delta j_\mu^{(P)}$, Eq. (5.2), If we are interested in the matrix element of the interaction, $-1/c\int \delta j_\mu^{(P)} A_\mu d\tau$, between initial and final states in which the nucleon has energy-momentum vectors $p^{(1)}$ and $p^{(2)}$ respectively, only the following Fourier components of ψ' and $\bar\psi'$ come into play:

$$\begin{aligned}\psi' &\to a_1 \exp[ip^{(1)}x'],\\ \bar\psi' &\to \bar a_2 \exp[-ip^{(2)}x'].\end{aligned} \tag{7.1}$$

** *Note added in proof:* The neutron-electron interaction given in Eq. (6.11) is in agreement with the result of K. Case, reference 4. On the other hand our results for the neutron-electron and proton-electron interactions, Eqs. (6.11) and (6.10), differ from those published by M. Slotnick and W. Heitler, reference 6. The difference is due to the fact that in their work the contribution of the nucleon current to the interaction potentials is negligibly small compared to the meson contribution, while in our calculations both are of the same order of magnitude. Professor Heitler has suggested in a letter that the discrepancy may be due to a different handling of the divergences. However, up to the present, the disagreement has not yet been resolved.

[14] W. E. Lamb and R. C. Retherford, Phys. Rev. **72**, 241 (1947). R. C. Retherford and W. E. Lamb, Phys. Rev. **75**, 1325 (1949).

Hence an integration of $\delta j_\mu^{(P)}$ over x' gives $(2\pi)^4\delta(\Delta p)$ where Δp denotes the momentum transfer $(p^{(1)}-p^{(2)})$. Integrating next over p gives

$$\delta j_\mu^{(P)}\rightarrow -\frac{g^2}{4\pi\hbar c}\frac{1}{2\pi}\mu_0 c\frac{\partial}{\partial x_\nu}\bar{a}_2\exp[-ip^{(2)}x]\times\left\{\frac{3-\tau_3}{2}f_1(\Delta p^2)+\tau_3 f_2(\Delta p^2)\right\}\cdot\sigma_{\mu\nu}a_1\exp[ip^{(1)}x]. \quad (7.2)$$

Thus, for this transition the effective polarization current is

$$\delta j_\mu^{(P)}=-\frac{g^2}{4\pi\hbar c}\frac{1}{2\pi}\mu_0 c\frac{\partial}{\partial x_\nu}\bar{\psi}(x)\left\{\frac{3-\tau_3}{2}f_1(\Delta p^2)+\tau_3 f_2(\Delta p^2)\right\}\sigma_{\mu\nu}\psi(x). \quad (7.3)$$

In precisely the same way we find for the convection current

$$\delta j_\mu^{(C)}=\frac{g^2}{4\pi\hbar c}\cdot\frac{1}{4\kappa^2}\frac{iec}{\pi}\Box^2\bar{\psi}(x)\left\{\frac{3-\tau_3}{2}f_3(\Delta p^2)+\tau_3 f_4(\Delta p^2)\right\}\gamma_\mu\psi(x). \quad (7.4)$$

These expressions exhibit the dependence of the effective current operators on the energy-momentum transfer of the nucleons.

We may note in particular, that as a consequence of Eq. (7.3), the effective anomalous nucleon moments, λ, in a process involving an energy-momentum transfer Δp are

$$\lambda=F(\Delta p^2)\lambda_0, \quad (7.5)$$

where λ_0 are the static moments and

$$F(\Delta p^2)=\frac{((3-\tau_3)/2)f_1(\Delta p^2)+\tau_3 f_2(\Delta p^2)}{((3-\tau_3)/2)f_1(0)+\tau_3 f_2(0)}. \quad (7.5')$$

Here $\tau_3=\pm 1$ for the proton and neutron respectively. For large p^2, $F(\Delta p^2)$ decreases like $(\log(\Delta p^2)/\Delta p)^2$.

Several authors have observed that a fixed Pauli-type dipole moment leads to very large scattering cross sections of high energy nucleons.[15,16] For example, the scattering cross section due to a fixed anomalous moment, λ_0, of a fast nucleon by an external Coulomb field is independent of the energy. However, when one takes into account $F(\Delta p^2)$, Eq. (7.5), the differential cross section is reduced by a factor of the order $((\log E)/E)^4$ where E is the energy of the incident nucleon, except for very small angles where Δp^2 is small. A similar reduction of the cross section is to be expected in other processes such as Bremsstrahlung.

VIII. CONCLUSION

A covariant perturbation calculation for nucleons in interaction with pseudoscalar mesons has been carried out to the second order. The results for the magnetic moments of the neutron and proton as well as the nucleon-electron interaction are finite and some predictions concerning the scattering of high energy nucleons can be made. Some qualitative aspects of the theory are correct but the quantitative agreement with experiment is very poor. The large values of the coupling constant required to fit the experimental data show that the results obtained by our second order perturbation calculation are quantitatively unreliable and indicate that higher order calculations would not be promising. To test the correctness of the meson hypothesis, some method more suitable for dealing with strong coupling is required.

We wish to take this opportunity to express our sincere appreciation to Professor J. Schwinger for the many discussions of his work on the "Electromagnetic Properties of the Electron," before publication, as well as for numerous suggestions as to how his methods could be adapted to nuclear problems. We also wish to thank Dr. K. Case for sending us a copy of his paper prior to publication.

[15] W. Pauli, Rev. Mod. Phys. **13**, 203 (1941).
[16] J. L. Powell, Phys. Rev. **75**, 32 (1949).

Motion in a Constant Magnetic Field

M. H. JOHNSON AND B. A. LIPPMANN
Nucleonics Division, Naval Research Laboratory, Washington, D. C.
(Received May 9, 1949)

The motion of a charged particle in a constant magnetic field is treated in both relativistic and non-relativistic quantum theory. Operators representing the center of the orbit, which obey the commutation law for conjugate variables, are introduced and their connections with energy, angular momentum, and magnetic moment studied. Energy eigenfunctions in an operator form are obtained by factorization. Previously derived eigenfunctions in coordinate space are obtained and are shown to be eigenfunctions for the operators for the center of the orbit as well as for the energy. Corresponding relativistic eigenfunctions are derived by a simple device which enables one to construct solutions of the Dirac equation from solutions of the Schrödinger equation.

I. INTRODUCTION

THE motion of a charged particle in a constant magnetic field has been treated in the quantum theory by many authors.[1] In the present work two new features have been added, a more complete interpretation of certain operator integration constants and a general method for the construction of energy eigenfunctions.

In a well-known paper, Kennard[1] integrated the NR[2] operator equations of motion and obtained the operators as explicit functions of time. We, however, will effect the integration by finding operators which are constants of the motion. In so simple a mechanical problem, the difference in procedure would appear to be trivial. Actually the second procedure can be easily extended to relativistic motion and leads naturally to a discussion of certain integration constants, namely the coordinates for the center of the orbit, which obey commutation relations typical of conjugate variables. These topics as well as the relation between the center of the orbit, energy, angular momentum, and magnetic moment are the subject matter of Section II.

Most of the work cited above[1] has been concerned with stationary solutions of the wave equation. The solutions may be in a variety of forms because of the infinite degeneracy, expressed in classical mechanics by the fact that the axes of helical orbits with the same energy may lie anywhere in the plane perpendicular to $\mathbf{H}$. As we shall see, this degeneracy in the quantum theory is connected with the existence of the integration constants mentioned above and, indeed, the integration constants may be conveniently used to classify the eigenfunctions.

A general operator solution for the energy eigenfunctions can be obtained by formulating the problem in terms of the kinetic momenta, $\boldsymbol{\pi}$,

$$\boldsymbol{\pi}=\mathbf{p}+e\mathbf{A}/c. \tag{1}$$

The Hamiltonian, together with the commutation relations satisfied by $\boldsymbol{\pi}$, which then define the eigenvalue problem, no longer contain $\mathbf{r}$. The system of equations is formally identical with the harmonic oscillator[3] and the eigenfunctions can be deduced in a familiar way by the factorization technique. Details of this method are given in Section III where it is also shown that previously obtained eigenfunctions can be easily derived from the operator solution. The method is extended to relativistic motion by a simple device for constructing solutions of the Dirac equation from solutions of the Schrödinger equation.

II. INTEGRALS OF THE EQUATIONS OF MOTION

The NR equations of motion may be derived from the Hamiltonian

$$H=(1/2m)\pi^2, \tag{2}$$

where $\boldsymbol{\pi}$ it related to the linear momentum by Eq. (1) and therefore satisfies the commutation relation

$$\boldsymbol{\pi}\times\boldsymbol{\pi}=-(ie\hbar/c)\mathbf{H}. \tag{3}$$

The equations of motion can be obtained from the definition of a time derivative

$$\hbar\dot{B}=i[H, B], \tag{4}$$

where $[a, b]$ is the commutator $ab-ba$. Remembering that $\mathbf{H}$ is along the z axis[2] it follows that

$$\dot{\pi}_x=-(e\mathfrak{H}/mc)\pi_y=-\omega\pi_y, \tag{5a}$$

$$\dot{\pi}_y=(e\mathfrak{H}/mc)\pi_x=\omega\pi_x, \tag{5b}$$

$$\dot{\pi}_z=0, \tag{5c}$$

$$m\dot{\mathbf{r}}=\boldsymbol{\pi}. \tag{6}$$

[1] Non-relativistic motion and wave functions are discussed by: E. H. Kennard, Zeits. f. Physik **44**, 326 (1927); G. C. Darwin, Proc. Roy. Soc. **117**, 258 (1928); L. Landau, Zeits. f. Physik **64**, 629 (1930); L. Page, Phys. Rev. **36**, 444 (1930); Uhlenbeck and Young, Phys. Rev. **36**, 1721 (1930). Relativistic wave functions are discussed by: I. I. Rabi, Zeits. f. Physik **49**, 507 (1928); M. S. Plesset, Phys. Rev. **36**, 1728 (1930); I. D. Huff, Phys. Rev. **38**, 501 (1931).

[2] Notation: NR is an abbreviation for non-relativistic. By an energy representation is meant any representation whose basis is a complete set of energy eigenfunctions. The constant magnetic field, $\mathbf{H}$, of magnitude $\mathfrak{H}$, is taken along the z axis and is derived from a vector potential $\mathbf{A}$. The mass and charge of the particle are m and $-e$, respectively. Its momentum and position are designated by $\mathbf{p}$ and $\mathbf{r}$. The quantity $\hbar$ is Planck's constant divided by 2π. The velocity of light is c and Gaussian units are used throughout.

[3] This was first observed by Landau who thereby obtained the eigenvalues of the energy in the NR motion.

It is immediately evident that π_z is constant, the motion along the z axis is that of a free particle.

Two integration constants for the transverse motion result when π_x and π_y are eliminated between Eqs. (5) and (6)

$$d/dt(\pi_x+m\omega y)=0, \tag{7a}$$

$$d/dt(\pi_y-m\omega x)=0, \tag{7b}$$

whence

$$y_0=y+\pi_x/m\omega, \tag{8a}$$

$$x_0=x-\pi_y/m\omega. \tag{8b}$$

The integration constants x_0 and y_0 necessarily commute with the Hamiltonian. It is easily verified that they also commute with both π_x and π_y so that with respect to the Hamiltonian they behave as unit operators. However, they do not commute with each other,

$$[x_0, y_0]=i\hbar c/e\mathcal{H}=i\lambda^2. \tag{9}$$

The length λ is characteristic for the quantum mechanical treatment of this problem.

Equations (5) through (8) have the same form as the corresponding classical equations. We will therefore identify the operators x_0 and y_0 with the coordinates for the center of the orbit. In agreement with this interpretation the expectation value of x_0 in an energy representation[2] is equal to the expectation value of x.[4]

The commutation relation (9) is identical in form with the commutation relation satisfied by a coordinate and its canonically conjugate momentum variable. A well-known consequence is that the eigenvalues of x_0 and y_0 coincide with the continuum of real numbers. Since x_0 and y_0 behave as unit operators with respect to Hamiltonian, each energy state must include an infinite manifold of eigenfunctions corresponding to the eigenvalues of x_0 or y_0 or of some function of x_0 and y_0. Thus the energy is infinitely degenerate, just as in classical mechanics, because it does not depend on the location of the center of the orbit in the xy plane.

In Section III eigenfunctions corresponding to eigenvalues of x_0 will be given explicitly. Eigenfunctions corresponding to eigenvalues of r_0^2,

$$r_0^2=x_0^2+y_0^2, \tag{10}$$

will also be given. Because the characteristic value problem contained in Eqs. (9) and (10) is formally identical with the one-dimensional harmonic oscillator, we can immediately conclude the eigenvalues of r_0^2 are $\lambda^2(2l+1)$ where l is any positive integer. The "zero point" value of r_0^2 indicates that the origin of a coordinate system can only coincide with the center of the orbit to an accuracy of λ.

The commutation relation, Eq. (8), also implies that

$$\Delta x_0\Delta y_0\gtrsim\lambda^2/2, \tag{11}$$

where Δx_0 and Δy_0 are the uncertainties in any possible experimentally determined values of x_0 and y_0 from which the orbit may be predicted. If the radius, r_1, is introduced by means of Eq. (8)

$$r_1^2=(x-x_0)^2+(y-y_0)^2 =(m\omega)^{-2}(\pi_x^2+\pi_y^2)=2H_t/m\omega^2, \tag{12}$$

where H_t is the transverse energy. Thus, in an energy representation, r_1^2 is exactly known and the uncertainty in locating points on the orbit is solely due to the uncertainty in locating the center of the orbit.

A measurement of the orbit's center may, for example, be made by simultaneously determining the transverse coordinates and momenta which are subject to the uncertainty relations

$$\Delta x\Delta p_x\gtrsim\hbar/2;\quad \Delta y\Delta p_y\gtrsim\hbar/2. \tag{13}$$

The coordinates of the orbit's center can then be calculated from Eqs. (8) expressed in terms of the canonical momenta[5]

$$x_0=x/2-p_y/m\omega, \tag{14a}$$

$$y_0=y/2+p_x/m\omega. \tag{14b}$$

The uncertainties in x_0 and y_0 are arising from the uncertainties in Eq. (13) are then necessarily related by Eq. (11).

The energy eigenvalues can be written as

$$E=E_n+p^2/2m, \tag{15}$$

where p is an eigenvalue of π_z and E_n is an eigenvalue of the transverse energy

$$H_t=1/2m(\pi_x^2+\pi_y^2). \tag{16}$$

Equation (16) and Eq. (3) again define an eigenvalue problem identical with the one-dimensional harmonic oscillator so that

$$E_n=\hbar\omega(n+1/2), \tag{17}$$

where n is any positive integer.

The angular momentum, L_z, about the z axis is

$$L_z=(\mathbf{r}\times\mathbf{p})_z=x\pi_y-y\pi_x-(m\omega/2)(x^2+y^2). \tag{18}$$

Hence by Eqs. (3), (5), and (6)

$$\dot{L}_z=\dot{x}\pi_y-\dot{y}\pi_x+x\dot{\pi}_y-y\dot{\pi}_x -(m\omega/2)(x\dot{x}+\dot{x}x+y\dot{y}+\dot{y}y)=0,$$

and L_z is an integral of the motion. However, it can be expressed in terms of r_1^2 and r_0^2 by Eqs. (8) and (12)

$$\begin{aligned}L_z&=m\omega[x(x-x_0)+y(y-y_0)-\tfrac{1}{2}(x^2+y^2)]\\&=(m\omega/2)(r_1^2-r_0^2),\end{aligned} \tag{19}$$

which is the same as the classical relation between these quantities. Since r_1^2 is proportional to the energy by

[4] In an energy representation the expectation value of a time derivative of a quantity which does not involve z is zero because the diagonal elements of a commutator with H then vanish. According to Eqs. (5a) and (5b) π_z and π_y are such derivatives.

[5] Here, as in what follows, the vector potential $(\mathbf{H}\times\mathbf{r})/2$ has been used. Any other vector potential can only differ by the addition of ∇f where f is the gauge. If another vector potential were used, the equations of motion can be brought back to our form by the contact transformation $S=\exp(ief/\hbar c)$.

Eq. (12), L_z is not an independent integral of the motion From Eqs. (17) and (10), its eigenvalues are $\hbar(n-l)$.

The magnetic moment, defined by

$$M=-\frac{\partial H}{\partial \mathcal{H}}=m^{-1}\left(\pi_x\frac{\partial \pi_x}{\partial \mathcal{H}}+\pi_y\frac{\partial \pi_y}{\partial \mathcal{H}}\right)$$
$$=-(e/mc)(x\pi_y-y\pi_x) \quad (20)$$

is not a constant of the motion. However, again using Eq. (8),

$$M=-(e\omega/c)[r_1^2+x_0(x-x_0)+y_0(y-y_0)]. \quad (21)$$

In an energy representation the expectation values of $x-x_0$ and $y-y_0$ are zero so that the expectation value of M is given by the energy through Eq. (12).

The relativistic equations of motion follow from the Dirac Hamiltonian which, in conventional notation, is

$$H=c\boldsymbol{\alpha}\cdot\boldsymbol{\pi}+\beta mc^2. \quad (22)$$

By application of Eqs. (3) and (4)

$$\dot{\pi}_x=-e\mathcal{H}\alpha_y, \quad (23a)$$

$$\dot{\pi}_y=e\mathcal{H}\alpha_x, \quad (23b)$$

$$\dot{\pi}_z=0, \quad (23c)$$

$$\dot{\mathbf{r}}=c\boldsymbol{\alpha}. \quad (24)$$

If $\boldsymbol{\alpha}$ is eliminated between Eqs. (23) and (24), Eqs. (7) and (8) are obtained again. Therefore the previous discussion of the integration constants x_0 and y_0 applies without change to the relativistic motion with the exception of Eq. (12) and the accompanying remark. (The quantity r_1^2 is no longer a constant of motion.)

To complete the equations of motion, expressions for the time derivative of $\boldsymbol{\alpha}$ and β must be added. With the help of Eqs. (3) and (4) and of the commutation relations for $\boldsymbol{\alpha}$ and β

$$\hbar\dot{\beta}=-2ic\boldsymbol{\alpha}\cdot\boldsymbol{\pi}\beta, \quad (25)$$

$$\hbar\dot{\boldsymbol{\alpha}}=2c\boldsymbol{\pi}\times\boldsymbol{\sigma}+2imc^2\boldsymbol{\alpha}\beta, \quad (26)$$

where

$$\boldsymbol{\sigma}=-i(\alpha_y\alpha_z,\ \alpha_z\alpha_x,\ \alpha_x\alpha_y), \quad (27a)$$

$$\hbar\dot{\boldsymbol{\sigma}}=2c\boldsymbol{\pi}\times\boldsymbol{\alpha}. \quad (27b)$$

It is convenient to use

$$H^2=c^2\pi^2+m^2c^4+e\hbar c\mathcal{H}\sigma_z, \quad (28)$$

rather than H, to discuss energy eigenvalues. Taking π_z diagonal with the eigenvalue p and σ_z diagonal with the eigenvalue $s(=\pm1)$,

$$H^2=2mc^2H_t+c^2p^2+m^2c^4+e\hbar c\mathcal{H}s. \quad (29a)$$

With the aid of Eq. (17) the energy eigenvalues are now given by

$$E=\pm[c^2p^2+m^2c^4+e\hbar c\mathcal{H}(2n+s+1)]^{\frac{1}{2}}. \quad (29b)$$

The energy states are symmetrically arranged about zero and, with the exception of $n=0$ and $s=-1$, are doubly degenerate.

The total angular momentum along the z axis is

$$J_z=(\mathbf{r}\times\mathbf{p})_z+\hbar\sigma_z/2$$
$$=x\pi_y-y\pi_x-(m\omega/2)(x^2+y^2)+\hbar\sigma_z/2 \quad (30)$$

and is easily shown to be constant in virtue of Eqs. (22), (23), and (26). Expressing x and y in terms of x_0 and y_0 by Eq. (8)

$$J_z=(2m\omega)^{-1}(\pi_x^2+\pi_y^2+e\hbar\mathcal{H}\sigma_z/c)-m\omega r_0^2/2$$
$$=(2e\mathcal{H}c)^{-1}(H^2-c^2\pi_z^2-m^2c^4)-m\omega r_0^2/2. \quad (31)$$

Again J_z is not an independent integral of motion and its eigenvalues, according to Eqs. (10) and (29), are $\hbar(n-l+s/2)$.

The magnetic moment

$$M=-\frac{\partial H}{\partial \mathcal{H}}=-c\boldsymbol{\alpha}\cdot\frac{\partial \boldsymbol{\pi}}{\partial \mathcal{H}}=e(\alpha_x y-\alpha_y x) \quad (32)$$

is not constant. In virtue of Eq. (23)

$$M=\mathcal{H}^{-1}(y\dot{\pi}_y+x\dot{\pi}_x)$$
$$=\mathcal{H}^{-1}[d/dt(x\pi_x+y\pi_y)-H+c\alpha_z\pi_z+\beta mc^2], \quad (33)$$

which can be written

$$M=\mathcal{H}^{-1}\{d/dt(x\pi_x+y\pi_y)-[d/dt(\alpha_z\pi_z+\beta mc)$$
$$+H^2-c^2\pi_z^2-m^2c^4]H^{-1}\}. \quad (34a)$$

The expectation[6] value, $\bar{M}$, in an energy representation, is given by the last term since the expectation value of the time derivatives is zero,

$$\bar{M}=-(E^2-c^2p^2-m^2c^4)/E. \quad (34b)$$

It is noteworthy that $\bar{M}$ is positive for negative energy states. This can be understood by the characteristic behavior of negative states in which the acceleration is in the opposite direction to the applied force.

III. ENERGY EIGENFUNCTIONS

The eigenvalue problem for the Hamiltonian H_t (Eq. 16) and the commutation relations for π_x and π_y (Eq. 31) is the familiar one-dimensional harmonic oscillator and the eigenfunctions may be obtained by factorization.[7] It is convenient to use the notation

$$\pi_\pm=\pi_x\pm i\pi_y. \quad (35)$$

Then if ψ_n is an eigenfunction for H_t, so also are $\pi_+\psi_n$ and $\pi_-\psi_n$ for the eigenvalues $\hbar\omega(n+1+\frac{1}{2})$ and $\hbar\omega(n-1+\frac{1}{2})$, respectively. By expressing the normalization integral for ψ_n in terms of that for ψ_{n+1} or ψ_{n-1}, it is easily seen that for a series of eigenfunctions nor-

[6] Equation (34b) can be immediately obtained from the theorem (cf. W. Pauli, Handbuch der Physik 24, No. 1, 161) that the diagonal elements of $\partial H/\partial\mathcal{H}$ in an energy representation are equal to $\partial E/\partial\mathcal{H}$. Using Eq. (29b) for E, Eq. (34b) results.

[7] P. A. M. Dirac, Quantum Mechanics (Oxford Press, 1947), 3rd Ed., p. 136.

malized in the same way,

$$\psi_n=(2n)^{-\frac{1}{2}}(\lambda\pi_+/\hbar)\psi_{n-1}, \tag{36a}$$

$$\psi_{n-1}=(2n)^{-\frac{1}{2}}(\lambda\pi_-/\hbar)\psi_n. \tag{36b}$$

The lowest state function must be a solution of $\pi_-\psi_0=0$. The energy eigenfunctions are therefore determined by the equations

$$\psi_n=(2^n n!)^{-\frac{1}{2}}(\lambda\pi_+/\hbar)^n\psi_0, \tag{37a}$$

$$\pi_-\psi_0=0, \tag{37b}$$

$$\pi_z\psi_0=p\psi_0, \tag{37c}$$

and its eigenvalues are given by Eq. (17).

Equation (37) may be used to find the eigenfunctions in either coordinate or momentum space. We will confine our attention to the first case for which, according to Eq. (1),

$$\pi_\pm=-i\hbar[\partial/\partial x\pm i(\partial/\partial y)+2/\lambda(x\pm iy)], \tag{38a}$$

$$\pi_z=-i\hbar(\partial/\partial z). \tag{38b}$$

The solution of Eqs. (37b) and (37c) is readily found.

$$\psi_0=f(x-iy)\exp[ipz/\hbar-(x^2+y^2)/4\lambda^2], \tag{39}$$

where f is an arbitrary function.

The appearance of an arbitrary function in Eq. (37a) corresponds to the infinite degeneracy already discussed and allows us to impose other conditions on ψ_0. First we will consider eigenfunctions for x_0. Since x_0 commutes with π_+, this requirement is a condition on ψ_0

$$x_0\psi_0=a\psi_0, \tag{40a}$$

where a is the eigenvalue of x_0. Making use of Eq. (14a)

$$(x/2+i\lambda^2\partial/\partial y)\psi_0=a\psi_0 \tag{40b}$$

or

$$f'=-(x-iy+2a)(a\lambda^2)^{-1}f. \tag{40c}$$

The solution of Eq. (40c) gives

$$\psi_{0,a}=(\pi\lambda^2)^{-\frac{1}{4}}\exp[-(2\lambda)^{-2}\times(x^2+y^2-2a^2+(x-iy-2a)^2)+ipz/\hbar]. \tag{40d}$$

The normalization constant has been chosen to make the charge density unity after integration over x. Upon inserting Eq. (40d) into Eq. (37a) we obtain the desired eigenfunctions. The resulting expression after repeated application of the identity

$$\pi_+\exp(x^2+y^2/4\lambda^2)=[\exp(x^2+y^2/4\lambda^2)](-i\hbar)(\partial/\partial x+i(\partial/\partial y) \tag{41}$$

is

$$\psi_{n,a}=((\pi)^{\frac{1}{2}}\lambda 2^n n!)^{-\frac{1}{2}}(-i\lambda)^n\times[\exp(2\lambda)^{-2}(x^2+y^2+2a^2)](\partial/\partial x+i\partial/\partial y)^n\times\exp[-(2\lambda)^{-2}(2x^2+2y^2+(x-iy-2a)^2)+ipz/\hbar]. \tag{42}$$

If now $\exp(x+iy-2a/2\lambda)^2$ is inserted before the differential operator and the reciprocal of this quantity is inserted after the differential operator, $\psi_{n,a}$ is unchanged because $\partial/\partial x+i\partial/\partial y$ commutes with any function of $x+iy$. We then obtain

$$\psi_{n,a}=(i/\sqrt{2})^n((\pi)^{\frac{1}{2}}\lambda n!)^{-\frac{1}{2}}\cdot\times\exp[(2\lambda^2)^{-1}(iy(x-2a)-(x-a)^2)+ipz/\hbar]\times H_n(x-a/\lambda), \tag{43}$$

$$H_n(\xi)=(-1)^n e^{\xi^2}(\partial/\partial\xi)^n e^{-\xi^2}.$$

These are the eigenfunctions used by Landau and by Uhlenbeck and Young.[1]

We will next consider solutions which are eigenfunctions for r_0^2. Again, since r_0^2 commutes with π_+, this requirement is a condition on ψ_0

$$r_0^2\psi_0=\lambda^2(2l+1)\psi_0, \tag{44a}$$

where $\lambda^2(2l+1)$ are the eigenvalues of r_0^2 (l any positive integer).[8] From Eq. (14)

$$x_0^2+y_0^2=(1/4)(x^2+y^2)+i\lambda^2\left(x\frac{\partial}{\partial y}-y\frac{\partial}{\partial x}\right)-\lambda^4\left(\frac{\partial^2}{\partial x^2}+\frac{\partial^2}{\partial y^2}\right). \tag{44b}$$

Inserting Eq. (39) into Eq. (44),

$$(x-iy)f'=lf. \tag{44c}$$

The solution of Eq. (44c) gives

$$\psi_{0,l}=(2^{l+1}\pi l!)^{-\frac{1}{2}}\lambda^{-1}(x-iy/\lambda)^l\times\exp[-(x^2+y^2/4\lambda^2)+ipz/\hbar], \tag{44d}$$

where the normalization is to unit charge density after integrating over x and y. After repeated use of the identity in Eq. (41) we find

$$\psi_{n,l}=(-i)^n(2^{n+l+1}\pi l!n!)^{-\frac{1}{2}}\lambda^{-1}\times\exp\left[\frac{x^2+y^2}{4\lambda^2}+ipz/\hbar\right]\left(\frac{\partial}{\partial x}+i\frac{\partial}{\partial y}\right)^n\times\left(\frac{x-iy}{\lambda}\right)^l\exp[-(x^2+y^2)/2\lambda^2]. \tag{45}$$

If polar variables, ρ, ϕ, are introduced[9]

$$\psi_{n,l}=i^n(2^{n+l-1}\pi l!n!)^{-\frac{1}{2}}\lambda^{-1}(\rho/\lambda)^{n-l}\times\exp[-\rho^2/4\lambda^2+ipz/\hbar+i(n-l)\phi]\cdot\mathfrak{L}^l_{n,l}(\rho^2/2\lambda^2), \tag{46}$$

$$\mathfrak{L}_{n,l}(\xi)=(-1)^n e^{\xi}(\partial/\partial\xi)^n\xi^l e^{-\xi}.$$

---

[8] Since eigenfunctions for H and r_0^2 are necessarily eigenfunctions for L_z (cf. Eq. (19)), the condition can also be written as

$$\partial\psi_0/\partial\varphi=-l\psi_0$$

from which Eq. (44d) immediately follows.

[9] Since $f(x+y)$ commutes with $\partial/\partial x+i\partial/\partial y$ each derivative may be multiplied by $(x+iy)^{-1}$ and $(x-iy)^l$ multiplied by $(x+iy)^l$ provided a factor $(x+iy)^{n-l}$ is placed on the left of the differential operator. The function to the right of the differential operator then depends only on ρ^2. Now

$$(x+iy)^{-1}(\partial/\partial x+i\partial/\partial y)=\rho^{-1}(\partial/\partial\rho+i\rho^{-1}\partial/\partial\varphi).$$

Since ϕ does not appear explicitly, $\partial/\partial\varphi$ may be set equal to zero. When $\rho^{-1}(\partial/\partial\rho)$ is expressed as a derivative with respect to ρ^2 Eq. (46) is obtained.

These functions are related to the solutions given by Page.[1] They are clearly eigenfunctions for L_z with the eigenvalues $\hbar(n-l)$.

The interpretation of our eigenfunctions is obvious from their derivation. The solutions of Eq. (43) correspond to a uniform distribution of orbits with the same energy whose centers lie on the line $x=a$ while the solutions of Eq. (46) correspond to a uniform distribution of orbits whose centers lie on the circle $\rho=\lambda(2l+1)^{\frac{1}{2}}$. The connection between the solutions may be obtained by expanding $\psi_{0,a}$ as a power series in $x-iy$. The terms in the expansion are the functions $\psi_{0,l}$.

The relativistic eigenfunctions are solutions of the Dirac equation

$$H\Phi=E\Phi, \tag{47}$$

where H is given by Eq. (22). Solutions of Eq. (47) may be constructed from solutions of the second order equation

$$(H^2-E^2)\mathrm{X}=(H-E)(H+E)\mathrm{X}=0. \tag{48}$$

Clearly if X is a solution of Eq. (48) then

$$\Phi=(H+E)\mathrm{X} \tag{49}$$

is a solution of Eq. (47). Equation (49) is an empty identity if X is also solution of the first-order equation.

If X are eigenfunctions for σ_z

$$\sigma_z\mathrm{X}_s=s\mathrm{X}_s \tag{50}$$

for the eigenvalues $s=\pm1$, the second order equation becomes (using H^2 from Eq. (28))

$$\{H_s+(1/2mc^2)(c^2p^2+m^2c^4+e\hbar c\mathfrak{H}s-E^2)\}\mathrm{X}_s=0. \tag{51}$$

Then X_1 and X_{-1} satisfy separate differential equations which are formally identical with the NR wave equation, the eigenvalues of E being given by Eq. (29b).

The spinors X_s are not yet completely specified. We may, among other possibilities, take them to be eigenfunctions for β with the eigenvalue 1.

$$\beta\mathrm{X}_s=\mathrm{X}_s.$$

In this way we obtain the two spinors

$$\mathrm{X}_{1,n-1}=\begin{pmatrix}\psi_{n-1}\\0\\0\\0\end{pmatrix};\quad \mathrm{X}_{-1,n}=\begin{pmatrix}0\\\psi_n\\0\\0\end{pmatrix}, \tag{52}$$

where ψ_n are the NR eigenfunctions given by Eq. (37a). The eigenvalues of the energy corresponding to the spinors of Eq. (52) are

$$E=\pm[c^2p^2+m^2c^4+2e\hbar c\mathfrak{H}n]^{\frac{1}{2}}. \tag{53}$$

The energy eigenfunctions are now given by Eq. (49)

$$\begin{aligned}
\Phi_{1,n-1}&=(H+E)\begin{pmatrix}\psi_{n-1}\\0\\0\\0\end{pmatrix}G^{-1}=\begin{pmatrix}(mc^2+E)\psi_{n-1}\\0\\c\pi_z\psi_{n-1}\\c\pi_+\psi_{n-1}\end{pmatrix}G^{-1}=\begin{pmatrix}(mc^2+E)\psi_{n-1}\\0\\cp\psi_{n-1}\\(2e\hbar c\mathfrak{H}n)^{\frac{1}{2}}\psi_n\end{pmatrix}G^{-1},\\
\Phi_{-1,n}&=(H+E)\begin{pmatrix}0\\\psi_n\\0\\0\end{pmatrix}G^{-1}=\begin{pmatrix}0\\(mc^2+E)\psi_n\\c\pi_-\psi_n\\-c\pi_z\psi_n\end{pmatrix}G^{-1}=\begin{pmatrix}0\\(mc^2+E)\psi_n\\(2e\hbar c\mathfrak{H}n)^{\frac{1}{2}}\psi_{n-1}\\-cp\psi_n\end{pmatrix}G^{-1},
\end{aligned} \tag{54}$$

$$G=[2E(E+mc^2)]^{\frac{1}{2}}.$$

The four spinors of Eq. (54) (two for the positive sign and two for the negative sign in Eq. (53)) may be constructed from any ortho-normal set of energy eigenfunctions for the NR motion.

Special relativistic solutions can now be obtained from the previous solution of the NR problem. In particular eigenfunctions for x_0 (Huff[1]) are obtained by using Eq. (43) for ψ_n while eigenfunctions for r_0^2 (Rabi[1]) are obtained by using Eq. (46) for ψ_n. The only difference between our solutions and those previously given is in the initial choice of the spinor X; to obtain the latter, symmetric and antisymmetric combinations of the spinors in Eq. (52) must be used.

The Optical Detection of Radiofrequency Resonance*

F. BITTER
Research Laboratory of Electronics, Massachusetts Institute of Technology, Cambridge, Massachusetts
(Received May 31, 1949)

Calculations are made of the frequency, intensity, and polarization of the light emitted by an atom in a $^2P-^2S$ transition in a weak magnetic field having an oscillating component. Near resonance, or when the frequency of the oscillating component approaches the Larmor frequency of one of the two states involved in the radiation process, all of the quantities calculated are modified. Qualitatively similar results are to be expected for other transitions. Observations in very weak fields would be of particular interest because they would give information on nuclear spins as well as atomic g-factors. Under such conditions, the Zeemann components will in general not be resolvable. There will, however, be a change in the polarization of the edges of a spectral line at resonance. It is shown that very small changes in this polarization structure are theoretically detectable.

A HOPE of drastically extending our knowledge of nuclear structure lies in further application of the resonance method, i.e., the direct measurement of the spacing between the hyperfine-structure components of an energy level. A new method is here proposed to detect the condition of resonance when it is established—namely a change in the radiation emitted by an atom when it is subjected to an oscillating field at the resonance frequency in the above sense.

For simplicity, the discussion is confined to the resonance line ($^2P-^2S$) of an atom having one optical electron, and it is further assumed that there is no hyperfine structure. The resonance to be investigated is that corresponding to the Larmor frequency of the system in very weak fields, or, in other words, corresponding to the Zeemann splitting of one of the levels concerned. Although this discussion specifically excludes nuclear effects, it is clear that any method of following the ordinary Zeemann effect into the region of very weak fields will produce information about nuclear moments when the Zeemann splitting becomes of the same order of magnitude as any hyperfine structures which may exist.

The wave functions describing an atom in a magnetic field having an oscillating component are known.[1] They are the solutions of the Schroedinger time-dependent equation, and contain one arbitrary constant which is usually so chosen as to define the initial state of the system. In an atomic-beam experiment, for instance, this constant specifies the state of the system when it enters the oscillating field, and the solution makes it possible to specify the probability of finding the system in any particular state at any subsequent time. The problem here proposed is physically somewhat different. Consider a gas of the atoms under consideration at extremely low pressures so that collision effects may be neglected. All the atoms in the container holding the gas are subjected to the same field. In this case, the arbitrary constant in the wave function of the atoms in the ground state must be so chosen that, if the oscillating field is slowly removed, the wave functions go over into the normal wave functions for the atom in a constant magnetic field.

For an atom having $J=\frac{1}{2}$, the desired solutions are

$$\frac{1}{\sqrt{2}}\left\{\left[\frac{-\delta}{(1+\delta^2)^{\frac{1}{2}}}+1\right]^{\frac{1}{2}}\psi_{\frac{1}{2}}+\left[\frac{\delta}{(1+\delta^2)^{\frac{1}{2}}}+1\right]^{\frac{1}{2}}\psi_{-\frac{1}{2}}\right\} \quad (1)$$

$$\frac{1}{\sqrt{2}}\left\{\left[\frac{\delta}{(1+\delta^2)^{\frac{1}{2}}}+1\right]^{\frac{1}{2}}\psi_{\frac{1}{2}}-\left[\frac{-\delta}{(1+\delta^2)^{\frac{1}{2}}}+1\right]^{\frac{1}{2}}\psi_{-\frac{1}{2}}\right\} \quad (2)$$

where δ is a number measuring the approach to resonance and defined below. At resonance $\delta=0$; on one side it is positive, and on the other negative. It is evident that these are the desired solutions in the sense that, far from resonance, they reduce to the standard forms describing the system for $m=\frac{1}{2}$ and $m=-\frac{1}{2}$. The mean

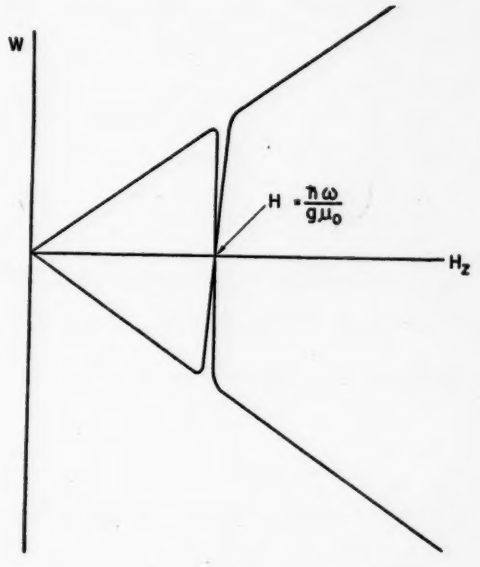

FIG. 1. Zeeman splitting of $J=\frac{1}{2}$ level in the presence of an oscillating field whose frequency is $\omega/2\pi$.

* This work has been supported in part by the Signal Corps, the Air Materiel Command, and ONR.

[1] I. I. Rabi, Phys. Rev. **51**, 652 (1937); F. Bloch and I. I. Rabi, Rev. Mod. Phys. **17**, 237 (1945).

value of the energy of the system in these states is

$$W=\pm\frac{g\mu_0 H_z}{2}\left[\frac{\delta+H_0/H_z}{(1+\delta^2)^{\frac{1}{2}}}\right]; \tag{3}$$

where μ_0 is one Bohr magneton; H_z is the constant magnetic field; $\delta=H_z/H_0\times(\omega-\omega_0)/\omega_0$; H_0 is the amplitude of the rotating magnetic field. This field is at right angles to the constant field; ω is the angular velocity of the rotating field; ω_0 is the Larmor frequency $g\mu_0 H_z/\hbar$; and $ge/2mc$ is the gyromagnetic ratio. The derivation of Eqs. (1)–(3) is given in Appendix A.

We are now in a position to consider the effect of the rotating magnetic field H_0 on the Zeemann effect. The resonance line width in the above discussion is determined entirely by the amplitude of the rotating field. In actual gases, the levels will be broadened due to other causes. Investigations of resonance in the ground state will be of particular interest because of the sharpness of these levels.

From Eq. (3) it is clear that the energy levels have their normal positions except near resonance, where the level corresponding to $m=\frac{1}{2}$ changes places with the level corresponding to $m=-\frac{1}{2}$. A schematic plot of the effect on the energy levels is shown in Fig. 1, and the effect on the position of the Zeemann components is shown in Fig. 2.

The intensity and state of polarization of the lines can be readily computed. For the sake of brevity, we write a and b for the coefficients of the spin-wave functions in Eqs. (1) and (2), and x^2, y^2, and z^2 for numbers proportional to the squares of the components of the electric dipole moments along the x-, y-, and z-axes. The results are

$$\left.\begin{array}{llll} {}^2P_{3/2}-{}^2S_{\frac{1}{2}} & m=\frac{3}{2}\text{ to }\frac{1}{2} & x^2=y^2=3a^2 & z^2=0 \\ & \frac{3}{2}\text{ to }-\frac{1}{2} & x^2=y^2=3b^2 & z^2=0 \\ & \frac{1}{2}\text{ to }\frac{1}{2} & x^2=y^2=\ b^2 & z^2=4a^2 \\ & \frac{1}{2}\text{ to }-\frac{1}{2} & x^2=y^2=\ a^2 & z^2=4b^2 \end{array}\right\}, \tag{4}$$

$$\left.\begin{array}{llll} {}^2P_{\frac{1}{2}}-{}^2S_{\frac{1}{2}} & \frac{1}{2}\text{ to }\frac{1}{2} & x^2=y^2=2b^2 & z^2=2a^2 \\ & \frac{1}{2}\text{ to }-\frac{1}{2} & x^2=y^2=2a^2 & z^2=2b^2 \end{array}\right\}.$$

These results state that the resultant intensity and the polarization of all the light given off in any direction is independent of δ, and is the same in all directions. Further, since on one side of resonance $a=0$ and $b=1$, while on the other side of resonance $a=1$ and $b=0$, it would seem from Eq. (4) that there are certain differences in the Zeemann effect above and below resonance. When the interchange of the energy levels is taken into account, it appears that the Zeemann effect presents exactly the same appearance on either side of resonance.

Equation (4) does, however, predict certain changes in the position, intensity, and degree of polarization of spectral lines in the vicinity of resonance. The following consideration indicates that these changes will not be easy to detect experimentally. With specially constructed light sources having a very small Doppler effect, and with the best available instruments, usable resolving powers of 10^6 can be achieved. Since visible light has a frequency of the order of 0.5×10^{-15}, we have for the smallest resolvable frequency difference between two spectral lines

$$\frac{\Delta\nu}{\nu}=\frac{\Delta\nu}{0.5\times10^{-15}}=10^{-6}, \tag{5}$$

$$\Delta\nu=0.5\times10^{9}.$$

This is of the order of magnitude of the frequencies to be applied. It is therefore clear that the detail of the predicted phenomena will not be easy to observe. The presence of resonance can, however, be detected without resolving the Zeemann components, as may be seen from the following argument. Consider, for example, the polarization structure of the line resulting from the transition ${}^2P_{\frac{1}{2}}$ to ${}^2S_{\frac{1}{2}}$ in a field which is too weak to produce an observable resolution of the components. Although the line as a whole would be unpolarized, the edges would show a slight excess of σ-polarization, and the center of the line a slight excess of π-polarization. At resonance, this polarization structure disappears. Resonance might be detected by noting a change in this polarization structure. Extremely small effects of this kind can be observed by means of an optical system which transmits only the excess polarized light at the edge of a line, and by modulating the amplitude of this transmitted component by going in and out of resonance at some selectable frequency. The limitations of such a scheme are further discussed in Appendix B.

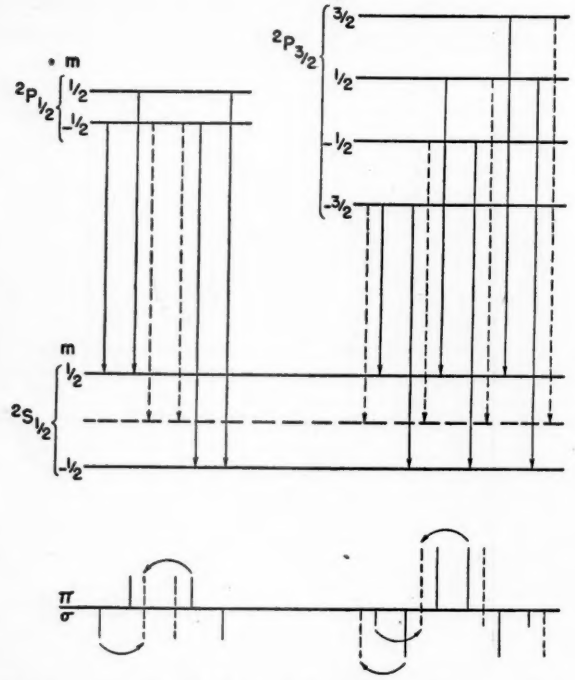

FIG. 2. ——— Normal Zeemann lines; — — — Zeemann lines at resonance in the ${}^2S_{\frac{1}{2}}$ state.

APPENDIX A

The equation to be solved is

$$i\hbar\dot{\psi}=g\frac{\mu_0}{2}(\sigma_1H_1+\sigma_2H_2+\sigma_3H_3),$$

where

σ are the spin matrices;
$H_1=H_0\cos\omega t$;
$H_2=H_0\sin\omega t$;
$H_3=H_z$.

The normalized solutions are

$$\psi=C_{\frac{1}{2}}\psi_{\frac{1}{2}}+C_{-\frac{1}{2}}\psi_{-\frac{1}{2}},$$
$$C_{\frac{1}{2}}=A_1\sin\alpha e^{ip_1t}+A_2\cos\alpha e^{ip_2t},$$
$$C_{-\frac{1}{2}}=-A_2\sin\alpha e^{-ip_2t}+A_1\cos\alpha e^{-ip_1t},$$
α=integration constant,
$$p_1=-\frac{\omega}{2}+\frac{H_0}{H_z}\frac{\omega_0}{2}(\delta^2+1)^{\frac{1}{2}},$$
$$p_2=-\frac{\omega}{2}-\frac{H_0}{H_z}\frac{\omega_0}{2}(\delta^2+1)^{\frac{1}{2}},$$
$$A_1=\left[\frac{\delta+(\delta^2+1)^{\frac{1}{2}}}{2(\delta^2+1)^{\frac{1}{2}}}\right]^{\frac{1}{2}},$$
$$A_2=\left[\frac{-\delta+(\delta^2+1)^{\frac{1}{2}}}{2(\delta^2+1)^{\frac{1}{2}}}\right]^{\frac{1}{2}}.$$

The expression for the energy is found by evaluating

$$W=-(\hbar/i)\bar{\psi}\dot{\psi}.$$

In general, the energy is a function of the time, and this is interpreted as periodic emission and absorption from the rotating field. This is not true for the particular solutions in which we are interested, corresponding to $\alpha=0$ or $\pi/2$.

As we have seen, above and below resonance the magnetic moment is parallel or antiparallel to the constant field H_z. At resonance $\delta=0$, and the expression for the energy becomes, according to Eq. (3),

$$\pm g(\mu_0/2)H_0,$$

that is, the magnetic moment is parallel or antiparallel to the oscillating field H_0. No work is done on the atom by the rotating field, and therefore the energy is constant.

APPENDIX B

The problem is to detect a very small amount of polarized light in the presence of unpolarized light. The intensity of the polarized component alone may be modulated, for instance, by passing the light first through a rotating polaroid and then through a fixed polaroid.** If such light is used to activate an electron-multiplier tube whose output contains a tuned amplifier, very small amounts of polarization can be detected. Let the current through the output of the tube be

$$Gi_0(1+f\cos\omega t),$$

where f=fraction of total light falling on the tube which is originally polarized, and therefore modulated, and G=gain of tube.

The signal-to-noise ratio across a tuned circuit through which this current flows may be estimated as follows:

signal voltage$=L(di/dt)=GLfi_0\omega\sin\omega t$;
noise voltage$=GRi_0(2eb/i_0)^{\frac{1}{2}}$;
b=band width of amplifier;
signal/noise$=Qf(i_0/2eb)^{\frac{1}{2}}$.

Intense light sources are advantageous. Assuming that the light intensity can be increased to the point for which the limiting factor is the tube current $i_{\max}=i_{0\max}G$, we see that the smallest detectable fraction of polarized light is

$$f=1/Q(G2eb/i_{\max})^{\frac{1}{2}}$$

for $Q=100$, $G=10^6$, $i_{\max}=1$ ma, $b=1$ cycle/sec., $f\sim10^{-7}$.

** More elegant ways of doing this by means of a vibrating glass block have been developed by Prof. H. Mueller of the Massachusetts Institute of Technology.

Mean Square Angles of Bremsstrahlung and Pair Production

MARTIN STEARNS
Laboratory of Nuclear Studies, Cornell University, Ithaca, New York

(Received June 6, 1949)

The mean square angles of bremsstrahlung and pair production have been derived and formulas for them are given in terms of the energies of the particles involved, the target material, and the maximum angle up to which the integration is taken. Calculations from these formulas have been made for incident energies between 50 and 300 Mev and for a maximum angle of 20°, and these have been graphed (Figs. 4 and 5). It is shown that the root-mean-square angle of bremsstrahlung goes as $\mu/E_0 \ln E_0/\mu$, and similarly for pair production. The dependence of the mean square on the maximum angle of integration is briefly discussed.

QUANTITIVE expressions for the mean square angles of bremsstrahlung and pair production have been derived, under assumptions to be discussed later. It was thought that, as measures of the angular dispersion in these fundamental processes, the mean squares might be useful in several ways. They enter, for example, in the detailed calculations on the lateral spread of cosmic-ray showers. They contribute to the dispersion of the gamma-ray beams from betatrons and synchrotrons. They can be used in estimating an optimum target thickness for gamma-ray spectrographs and electron accelerators.

We shall show that for high energies the root-mean-square angle of bremsstrahlung goes as $\mu/E_0 \ln E_0/\mu$ (where μ is the rest mass of the electron and E_0 is its initial energy) rather than as μ/E_0,— and similarly for pair production. Formulas for these mean squares are given as functions of the energies of the particles involved, the target material, Z, and the maximum angle up to which the mean square is taken. We have calculated and graphed the root-mean-square angles of bremsstrahlung and pair production for three different values of Z and a maximum angle of 20° (Figs. 4 and 5).

BREMSSTRAHLUNG

Following the notation of Bethe and Heitler,[1] we let E_0 be the energy of the incident electron, E the energy of the electron after it radiates, and $k=E_0-E$ the energy of the quantum radiated. The angle between the direction of the incident electron and that of the emitted quantum is θ, and it is the mean square of this angle[2] that is derived.

In the derivation, the integration over small values of θ had to be treated in a manner different from the integration over the larger values of θ; thus, the formula for the mean square, Eq. (2), is given as a sum of two terms. This comes about because for small values of θ, say θ less than some angle β, the impact parameter is generally large and the screening of the nucleus by the atomic electrons is important; for $\theta>\beta$, however, the impact parameter is small and screening is negligible.

The screening effect of the atomic electrons, on the basis of the Fermi-Thomas model of the atom,[3] is determined by a quantity γ, where

$$\gamma=100\mu k/E_0Ez^{\frac{1}{3}}. \tag{1}$$

For $\gamma<1$ the screening is important, whereas for $\gamma\gg1$ the screening can be practically neglected. The first term of our expression, therefore, being the integration of θ^2 over the region of screening, is naturally given as a function of γ.

For $\theta>\beta$ (no screening) the distribution of Hough[4] was used, and the integration of θ^2 over this distribution from $\theta=\beta$ to $\theta=\theta_{\max}$ gives the second term.

The mean square of θ over the interval $0<\theta<\theta_{\max}$ is

$$\bar{\theta}^2=\frac{4\mu^2}{E_0^2}\left\{\frac{(1+\alpha^2)g_1(\gamma,z)-4\alpha g_2(\gamma,z)}{(1+\alpha^2)[f_1(\gamma)-4/3\ln z]-\frac{2}{3}\alpha[f_2(\gamma)-4/3\ln z]}+\frac{A\ln(\theta_{\max}/\beta)+B\ln[(1-\alpha)\theta^2_{\max}+\alpha^2/(1-\alpha)\beta^2+\alpha^2]}{\text{same denominator}}\right\}, \tag{2}$$

where

$$\alpha=E/E_0, \tag{3}$$

$$\beta=2(\mu E/E_0k)^{\frac{1}{2}}, \tag{4}$$

$$\begin{cases}A=2(1+\alpha^2)\ln(2E_0E/\mu k)-\alpha(2+\alpha)-1\\ B=[(2-\alpha)(4-4\alpha-\alpha^2)/16(1-\alpha)].\end{cases} \tag{5}$$

The restrictions on Eq. (2) are

$$\begin{cases}E_0, E, k\gg\mu\\ \mu/4E_0\ll E/k\leqslant(\pi^2/144)E_0/\mu\\ \beta<\theta_{\max}<60°.\end{cases} \tag{6}$$

The denominator of Eq. (2) will be recognized, apart from some minor factors, as the total cross section for bremsstrahlung, and it appears because of the normalization. The functions $f_1(\gamma)$ and $f_2(\gamma)$ are given in several papers[5] but we reproduce them here for convenience (Fig. 1). $g_1(\gamma,z)$ and $g_2(\gamma,z)$ are functions of Z as well as γ, and we have graphed them for the three values $Z=4$, 30, and 90 (Figs. 2 and 3).

[1] H. Bethe and W. Heitler, Proc. Roy. Soc. **146**, 83 (1934).

[2] Bethe and Heitler use θ_0 for our θ.

[3] H. Bethe, Proc. Camb. Phil. Soc. **30**, 524 (1934).

[4] P. V. C. Hough, Phys. Rev. **74**, 80 (1948).

[5] B. Rossi and K. Greisen, Rev. Mod. Phys. **13**, 240 (1941). H. Bethe and W. Heitler, Proc. Roy. Soc. **146**, 83 (1934).

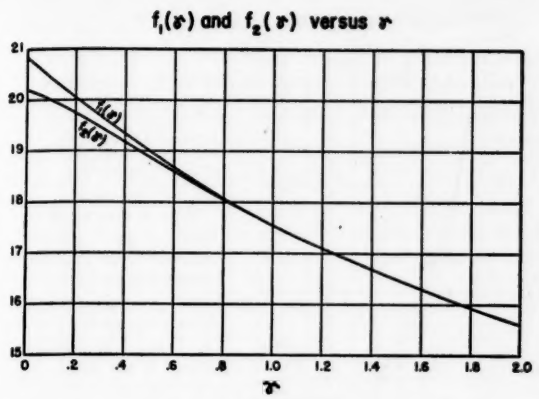

FIG. 1. $f_1(\gamma)$ and $f_2(\gamma)$ *vs.* γ.

Using Eq. (2), we have calculated and graphed the root-mean-square angle of bremsstrahlung as a function of E/E_0. This was done for the three values of $Z=4$, 30, 90, and in each case for $\theta_{max}=20°$. Since it can be easily shown, from an examination of Eq. (2), that in the limit of high energies, the root-mean-square angle goes as $\mu/E_0 \ln E_0/\mu$, it was only natural to choose this as an angular unit. If this is done the root-mean-square angle is very insensitive to energy, even in the range extending from 50 to 300 Mev. In fact, for a given Z, one curve will give the root-mean-square angle in this energy interval with an accuracy of 3 percent. The direction the curve would take for higher energies is indicated by the point for $E_0=5000$ Mev, $Z=90$, $E/E_0=\frac{1}{2}$.

It is of some interest to know how the mean square goes as a function of θ since we integrate up to θ_{max}. In the second term of Eq. (2), i.e., $A \ln(\theta_{max}/\beta)+B \ln[\cdots]$, the $A \ln(\theta_{max}/\beta)$ is by far the most important, usually accounting for more than 90 percent of the term. β is an arbitrary angle, designed to join the calculation with screening to that with zero screening and thus would be expected to drop out when the two intervals are joined. If we define a minimum angle, θ_{min}, to take care of the atomic screening, such as is done in elastic scattering, and if we recognize that the first term of Eq. (2) must be a function of θ_{min} and β such as to cancel the β in the second term, we see that Eq. (2) must take the form

$$C[\ln(\beta/\theta_{min})+\ln(\theta_{max}/\beta)]=C \ln(\theta_{max}/\theta_{min}),$$

where

$$C=\frac{4(\mu^2/E_0^2)A}{(1+\alpha^2)[f_1(\gamma)-4/3 \ln z]-\frac{2}{3}\alpha[f_2(\gamma)-4/3 \ln z]}.$$

This gives a convenient method for getting the root-mean-square angle from the curves in Fig. 4 for θ_{max} different from 20°. For $\theta_{max}<20°$, one need only subtract $C \ln(20°/\theta_{max})$ from the value of the curve, and for $\theta_{max}>20°$ one need only add $C \ln(\theta_{max}/20°)$ to this value. If the angles are not too extreme the error in this approximation will be less than 10 percent.

The choice of θ_{max} is, unfortunately, ambiguous. In general, as θ increases, the impact parameter becomes smaller, and one would expect a natural upper limit for θ when *nuclear* screening takes effect. However, in the case of bremsstrahlung, it has not been possible to determine this limit; and in any event, because the bremsstrahlung distribution goes down only inversely as θ^3, one must be careful in interpreting a mean square at the larger angles.[6] Since for many practical cases the angular spread due to bremsstrahlung will be compared with that due to multiple elastic scattering, one might take for θ_{max} that angle at which the cross section for multiple scattering has dropped to a very low value. In other experiments the geometry of the set-up may suggest a different angle.

PAIR PRODUCTION

Because of the Born approximation, electron and positron coordinates enter symmetrically in the probability distribution, and it is to be expected that the mean angle between the positron and photon should equal

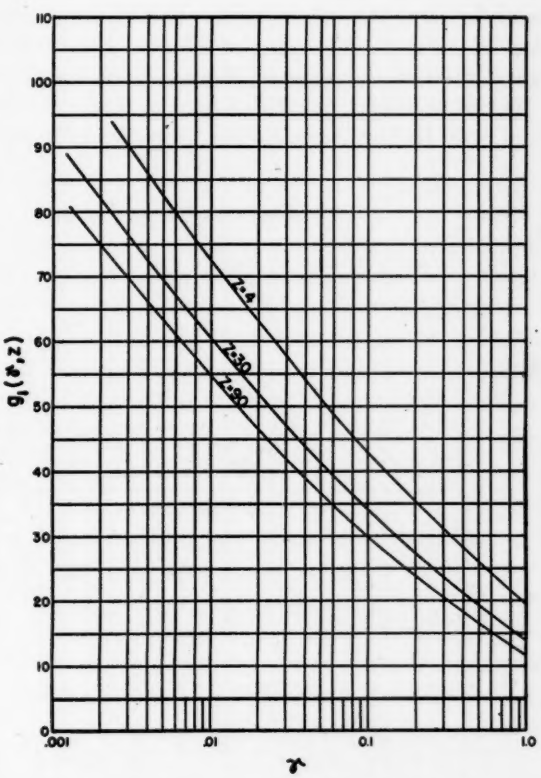

FIG. 2. $g_1(\gamma,z)$ *vs.* γ for values of $Z=4$, 30, and 90.

[6] Because of the inverse θ^3 distribution at the larger angles the root mean square of θ will be larger than the *average* value. Somd calculations have indicated that for an incident energy of arouny 150 Mev and θ_{max} about 15°, the root mean square is roughle twice the average angle. For a discussion of an upper limit for θ due to nuclear screening, particularly in the case of pair production, see the Hough article, reference 4.

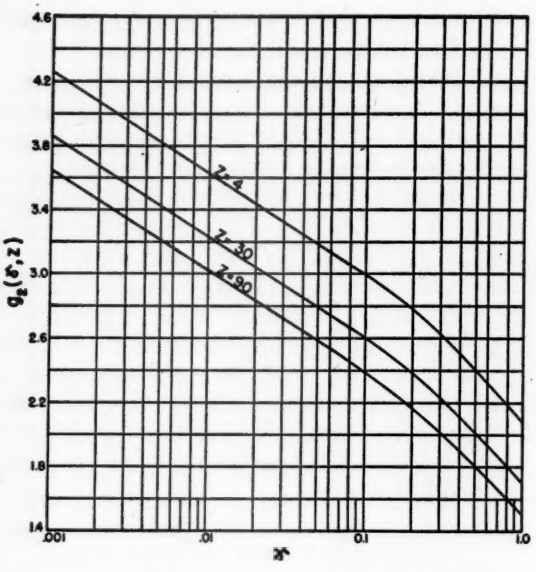

FIG. 3. $g_2(\gamma,z)$ *vs.* γ for values of $Z=4$, 30, and 90.

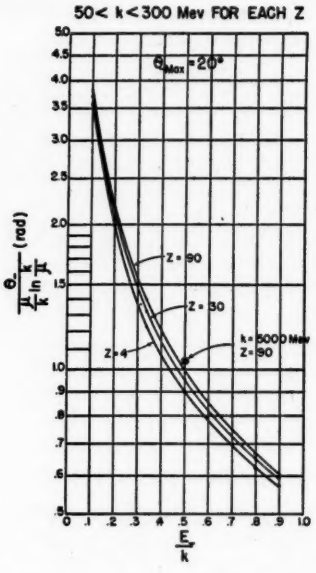

FIG. 5. Root-mean-square angle of pair production *vs.* E_-/k. θ_- is the angle between the incident quantum and the electron and has been divided by $\mu/k\ln(k/\mu)$ to make the curves insensitive to energy. $\theta_{-\max}=20°$.

the mean angle between electron and photon. Thus, though in this section we shall write the expression for the mean square angle between *electron* and photon, it is understood to apply as well to that of the positron.

Let E_- and θ_- refer to the electron's energy and angle relative to the photon's direction, and let E_+ and θ_+ represent similar quantities for the positron. Then Bethe and Heitler have shown that the probability distribution for pair production is to be obtained from that of bremsstrahlung by substituting $-E_+$, E_-, and θ_- for E, E_0, and θ respectively. (There is also a change in the final density of states but this does not concern us because of the normalization.)

If we let

$$\gamma=100\mu k/E_+E_-z^{\frac{1}{2}},$$
$$\beta=2(\mu E_+/E_-k)^{\frac{1}{2}},$$

then $\overline{\theta_-^2}$ over the interval $0<\theta<\theta_{\max}$ is

$$\overline{\theta_-^2}=\frac{4\mu^2}{E_-^2}\left\{\frac{(1+\alpha^2)g_1(\gamma,z)+4\alpha g_2(\gamma,z)}{(1+\alpha^2)[f_1(\gamma)-4/3\ln z]+\frac{2}{3}\alpha[f_2(\gamma)-4/3\ln z]}\right.$$
$$\left.+\frac{F\ln(\theta_{-\max}/\beta)+G\ln[\alpha^2+(1+\alpha)\theta_{-\max}^2/\alpha^2+(1+\alpha)\beta^2]}{\text{same denominator}}\right\},\quad(8)$$

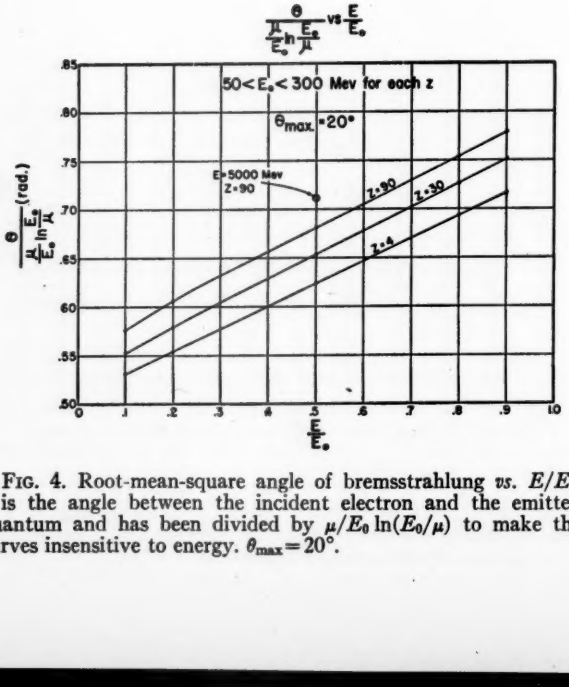

FIG. 4. Root-mean-square angle of bremsstrahlung *vs.* E/E_0. θ is the angle between the incident electron and the emitted quantum and has been divided by $\mu/E_0\ln(E_0/\mu)$ to make the curves insensitive to energy. $\theta_{\max}=20°$.

where

$$\begin{cases}\alpha=E_+/E_-\\ F=2(1+\alpha^2)\ln(2E_+E_-/\mu k)+\alpha(2-\alpha)-1\\ G=[(2+\alpha)(4+4\alpha-\alpha^2)/16(1+\alpha)].\end{cases}\quad(9)$$

The restrictions on Eq. (8) are

$$\begin{cases}E_+,\ E_-,k\gg\mu\\ \frac{1}{4}\mu/E_-\ll E_+/k\leqslant 1\\ \beta<\theta_{\max}\leqslant 60°.\end{cases}\quad(10)$$

In Fig. 5 we have graphed some root mean squares of θ_- calculated from Eq. (8). They have been done for $\theta_{-\max}=20°$ and for three Z values, 4, 30, and 90. Although Eq. (8) gives θ_- in terms of μ/E_-, it is more natural to express it in terms of μ/k, and this has been done in preparing Fig. 5. It is for this reason that the curves in Fig. 5 look different from those in Fig. 4.

In units of $\mu/k \ln k/\mu$ the root-mean-square angle of pair production, in analogy with bremsstrahlung, is roughly independent of the energy k, if k is sufficiently large. Thus, for a given Z, we need plot only one curve for the energy interval $50 \leqslant k \leqslant 300$ Mev and the error will be no more than 3 percent. The direction the curves would take for higher energies is indicated by the point for $k=5000$ Mev, $Z=90$, $E_-/k=\frac{1}{2}$.

I wish to thank Professors Robert R. Wilson and Hans A. Bethe for suggesting the calculation and their helpful advice, and Professor Bethe for his particular aid in the integration over the region of screening.

PHYSICAL REVIEW VOLUME 76, NUMBER 6 SEPTEMBER 15, 1949

The Admittance of High Frequency Gas Discharges*

EDGAR EVERHART** AND SANBORN C. BROWN
Research Laboratory of Electronics, Massachusetts Institute of Technology, Cambridge, Massachusetts

(Received May 9, 1949)

The admittance of a high frequency gaseous discharge between parallel plates has been measured as a function of pressure and discharge current. The susceptance is observed not to be proportional to the conductance. In fact the discharge susceptance changes sign from negative at low pressures and low electron densities to positive at high electron densities and high pressures. The discharge admittance is expressed as a volume integral over the complex conductivity. The non-linear relationship between discharge susceptance and conductance is shown to be a consequence of the non-uniform electron density along the direction of the field.

I. INTRODUCTION

A GASEOUS discharge may be maintained between parallel plates by a high frequency electric field of sufficient amplitude. The ratio of the h-f discharge current to the applied h-f potential is the discharge admittance and is complex because the current is seldom in phase with the applied potential. This paper develops the theory for the complex admittance and describes measurements of admittance which have been made at microwave frequencies.

There have been numerous studies of the high frequency admittance of discharges that were maintained by d.c. fields.[1] In these studies the d.c. field was much stronger than the h-f measuring field and thus controlled the discharge characteristics. In the present work, however, the h-f field maintains the discharge and is also used to measure the admittance.

At very low discharge currents and electron densities, the discharge has an admittance equivalent to that of a resistor and inductor connected in parallel between the discharge terminals. As the electron concentration is increased, the equivalent conductance and susceptance increase proportionately. However, when the electron current becomes comparable with the free-space displacement current, the real and imaginary parts of the admittance no longer increase proportionally and the discharge can become capacitive. The theory and measurements of this non-linear relationship are presented in this report. Still greater electron currents cause the space charge to oscillate with the applied field, thus producing a high frequency component to the space charge near the ends of the discharge. This shields the central portions and results in a still different behavior of discharge admittance. This last stage has been studied but is not reported here.

The discharge is created between parallel plates of close spacing and occupies a region small compared to the free-space wave-length of the exciting field. The study of a discharge of this simple geometry is a substantial step towards understanding more complicated cases. The discharge is observed to take the form of an ionized column of fairly definite radius between the parallel plates as shown in Fig. 1. The radius of the discharge r_0 is usually several times larger than the spacing δ. The first step in computing the admittance of the discharge is to determine the density distribution of the electrons between the plates.

II. SPATIAL DISTRIBUTION OF THE ELECTRONS

The diffusion equation determines the electron distribution in space. The problem is essentially the same as that solved for breakdown at microwave frequencies by Herlin and Brown,[2] except for the difference in diffusion coefficients. At high concentrations of electrons and positive ions, the d.c. space charges are such that the electrons and positive ions diffuse at equal rates, a condition known as ambipolar diffusion. The electron particle flow is given by

$$\Gamma = -D_a \operatorname{grad} n, \tag{1}$$

* This work has been supported in part by the Signal Corps the Air Materiel Command, and ONR.

** Now at Dartmouth College, Hanover, New Hampshire.

[1] A partial list includes E. V. Appleton and E. C. Childs, Phil. Mag. **10**, 969 (1930); E. V. Appleton and F. W. Chapman, Proc. Roy. Soc. **44**, 246 (1932); V. Ionescu and C. Mihul, J. de phys. et rad. **6**, 35 (1935); S. Gangopadhyaya and S. R. Khastgir, Phil. Mag. **25**, 883 (1938).

[2] M. A. Herlin and S. C. Brown, Phys. Rev. **74**, 291 (1948).

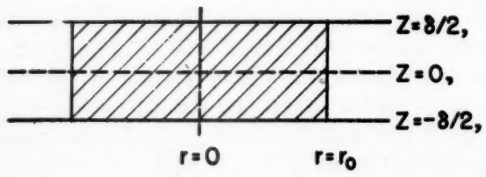

FIG. 1. Cross section of discharge showing coordinate system.

where D_a is the ambipolar diffusion coefficient,[3] and n is the electron concentration. Combining this equation with the steady-state continuity equation $\text{div}\Gamma=\nu n$, we have

$$\nabla^2 n+(\nu/D_a)n=0. \tag{2}$$

Here ν is the volume rate of production of new electrons per existing electron. This equation determines the spatial distribution of electrons within the discharge. When the diameter of the discharge is several times its length as in Fig. 1, the radial diffusion may be neglected and the problem becomes one-dimensional. The equation is then

$$n''+(\nu/D_a)n=0. \tag{3}$$

The general solution of Eq. (3) is complicated by the fact that ν is a function of the high frequency electric field which is itself a function of position due to shielding by the h-f component of the space charge. Inasmuch as we are confining the discussion to first-order effects, we neglect this and take ν to be constant independent of position.

The boundary condition $n=0$ at the edge of the discharge leads to the solution

$$n(z)=n_0\cos(\pi z/\delta), \tag{4}$$

where z is the distance along the axis normal to the plates measured from the center, as seen in Fig. 1, and n_0 is the electron concentration at $z=0$. The characteristic value $\nu/D_a=(\pi/\delta)^2$ expresses the balance between ionization and diffusion for the separation δ.

III. DISCHARGE ADMITTANCE

The complex conductivity σ_c of a system of electrons in a gas is defined as the ratio of the electron current density to the electric field. It is given by

$$\sigma_c=(ne^2/m)[(\nu_c-j\omega)/(\nu_c^2+\omega^2)], \tag{5}$$

in rationalized m.k.s. units. Here ν_c is the average electron collision frequency and ω is the applied radian frequency. A simple derivation of this formula was given by Eccles[4] in terms of an equivalent complex dielectric constant K_c, which is simply related to σ_c by the equation

$$K_c-1=\sigma_c/j\omega\epsilon_0. \tag{6}$$

Equation (5) can be derived more generally from the electron energy distribution function under the assumption that the ratio of the mean free path l to the velocity of the electron v is independent of velocity. Brode's data for electron elastic collision cross sections[5] show that this assumption is good for helium, and for this reason helium was used in our experiments. The general derivation of Eq. (5) may be obtained starting from a paper by Margenau[6] on the dispersion of ionized gases. Substituting from his Eqs. (14) and (5) into his Eq. (25) for electron current density, and making the above assumption that v/l is constant, there results

$$J=-\frac{4\pi e^2E[(v/l)-j\omega]}{3m[(v/l)^2+\omega^2]}\int_0^\infty\frac{\partial f_0}{\partial v}v^3dv. \tag{7}$$

The notation is that of Margenau except that l is here used for mean free path and J for electron current density. The constant collision frequency $\nu_c=v/l$ has made the integrand simple. A partial integration shows that

$$-\int_0^\infty(\partial f_0/\partial v)v^3dv=3n/4\pi. \tag{8}$$

Substituting Eq. (8) into Eq. (7) and dividing by the electric field, we obtain Eq. (5) for the complex conductivity.

The discharge admittance is now derived as an integral of the complex conductivity over the volume. The total current density in the discharge

$$J_T=(\sigma_c+j\omega\epsilon_0)E \tag{9}$$

includes both electron current and free-space displacement current. For regions in which the field lines are parallel, this current density J_T must be independent of z. The high frequency potential difference V_0 applied to the parallel plates is the integral of the electric field

$$V_0=\int_{-\delta/2}^{+\delta/2}Edz=J_T\int_{-\delta/2}^{+\delta/2}\frac{dz}{\sigma_c+j\omega\epsilon_0}. \tag{10}$$

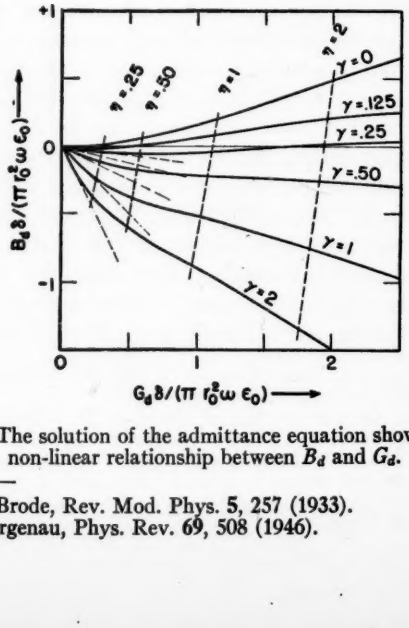

FIG. 2. The solution of the admittance equation showing the non-linear relationship between B_d and G_d.

[3] A. V. Engel and M. Steenbeck, Electrische Gasentladungen I, Julius Springer, Berlin, 1932; p. 199.
[4] W. H. Eccles, Proc. Roy. Soc. A87, 79 (1912).
[5] R. B. Brode, Rev. Mod. Phys. 5, 257 (1933).
[6] H. Margenau, Phys. Rev. 69, 508 (1946).

Neglecting fringing fields and currents, the total current carried in a discharge of radius r_0 is $I_T=\pi r_0^2 J_T$. This equation is combined with Eq. (10) to obtain the formula for total discharge admittance

$$Y_T=I_T/V_0=\pi r_0^2\Big/\int_{-\delta/2}^{+\delta/2}\frac{dz}{\sigma_c+j\omega\epsilon_0}. \tag{11}$$

The conductivity σ_c is proportional to n and has the same z dependence. Letting σ_{c0} be the complex conductivity at $z=0$ where $n=n_0$, we obtain from Eqs. (4) and (5)

$$\sigma_c=\sigma_{c0}\cos(\pi z/\delta). \tag{12}$$

In order to obtain the admittance due to the discharge alone, we subtract the admittance of the parallel plate capacitor

$$Y_0=j\pi r_0^2\omega\epsilon_0/\delta \tag{13}$$

which is present independently of the discharge. Thus,

$$Y_d=Y_T-Y_0. \tag{14}$$

The relationship $Y_d=G_d+jB_d$ defines discharge conductance G_d and discharge susceptance B_d. Equations (11), (12), and (13) are incorporated into Eq. (14) which is written in dimensionless form

$$\frac{G_d\delta}{\pi r_0^2\omega\epsilon_0}+j\frac{B_d\delta}{\pi r_0^2\omega\epsilon_0}=\frac{\delta}{\omega\epsilon_0\displaystyle\int_{-\delta/2}^{+\delta/2}[dz/\sigma_{c0}\cos(\pi z/\delta)+j\omega\epsilon_0]}-j. \tag{15}$$

Equation (15) expresses the admittance of the discharge in terms of its dimensions and the complex conductivity of the ionized medium.

In the limit of small electron concentrations where $\sigma_{c0}\ll\omega\epsilon_0$, Eq. (15) approaches

$$\left.\begin{aligned} &G_d\delta/\pi r_0^2\omega\epsilon_0+jB_d\delta/\pi r_0^2\omega\epsilon_0=2\sigma_{c0}/\pi\omega\epsilon_0,\\ \text{or}\quad &Y_d=(\text{constant})\sigma_{c0}.\end{aligned}\right\} \tag{16}$$

The requirement $\sigma_{c0}\ll\omega\epsilon_0$ is seen from Eq. (9) to be equivalent to the statement that the electron current is much smaller than the displacement current. This condition was seldom realized in our experiment and Eq. (16) was useful only at the smallest discharge currents. The form of Eq. (15) shows that there is no simple relationship between σ_{c0} and Y_d.

Inspection of Eq. (15) shows that G_d and B_d are functions of the magnitude and phase angle of 0_{c0}. We therefore introduce two dimensionless parameters η and γ defined by

$$\sigma_{c0}/\omega\epsilon_0=\eta\exp(-j\tan^{-1}\gamma), \tag{17}$$

and will describe their physical significance. It is seen from Eq. (9) that

$$\eta=|\sigma_{c0}|/\omega\epsilon_0 \tag{18}$$

is the ratio of the electron current to the displacement current at the center of the discharge. The parameter γ from Eq. (5) is

$$\gamma=\omega/\nu_c. \tag{19}$$

Although the collision frequency ν_c is nearly independent of velocity in helium, it is directly proportional to pressure p. The numerical value $\nu_c/p=2.4\times10^9$ (sec.$-$mm Hg)$^{-1}$ is obtained from the data of Brode.[5] For a given frequency then, γ is inversely proportional to pressure. In the experiment to be described, the frequency is 2950 Mc/sec. and

$$\gamma p=7.7\text{ mm Hg}. \tag{20}$$

The exact solution of Eq. (15) is shown in Fig. 2 in which G_d and B_d are plotted as functions of η and γ. The non-linear relationship between B_d and G_d is evident. At low electron concentrations the curves are tangent to the dotted straight lines calculated from Eq. (16).

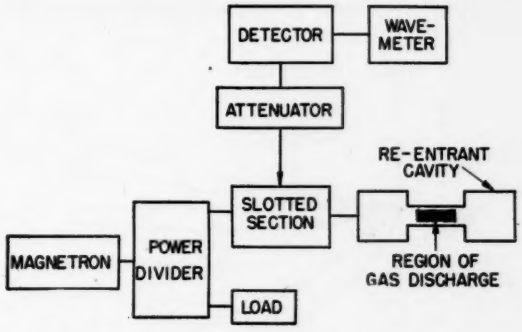

FIG. 3. A block diagram of the apparatus.

IV. EXPERIMENTAL PROCEDURE

The output of a tunable 10-cm continuous-wave magnetron passes through a power divider which sends a variable fraction of the power through a slotted section into a re-entrant resonant cavity. The slotted section, a calibrated attenuator, and a detector are used to measure the standing wave ratio and phase of the reflected wave from the cavity. Figure 3 shows a block diagram of the apparatus. The electric field is substantially constant in the parallel plate region of the cavity. The cavity is filled with helium at a known pressure. The magnetron is tuned to the resonant frequency of the cavity and the power divider is adjusted until sufficient power enters the cavity to maintain a discharge across the terminals. The discharge is localized in the form of an ionized column of finite radius as shown in the shaded region inside the cavity of Fig. 3. The width of the ionized column is measured visually with a traveling microscope.

During each experiment, the frequency and pressure

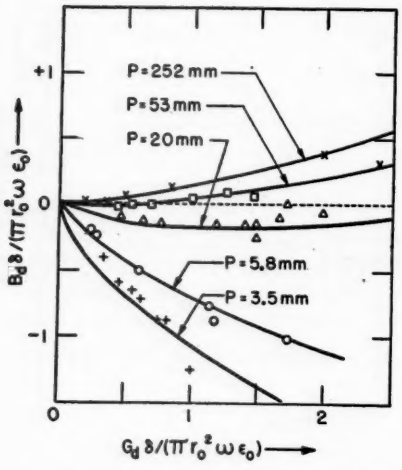

FIG. 4. Comparison of experiment and theory.

are held constant and the discharge current is varied by controlling the input power. This is equivalent to keeping γ constant while varying η. From these data, the admittance of the discharge can be computed.[7] The dimensionless discharge susceptance $B_d\delta/\pi r_0^2\omega\epsilon_0$ is plotted against the conductance $G_d\delta/\pi r_0^2\omega\epsilon_0$ at various input powers. The experiment is repeated at other pressures to obtain curves corresponding to various values of γ.

The gap δ is 10^{-3} meter, the diameter of the parallel plate region is 6.35×10^{-3} meter, the angular frequency of the applied electric field is $\omega=1.85\times10^{10}$/sec. The measurement of B_d and G_d is accurate to about three percent. The principal difficulty arises in the measurement of r_0, since the boundary of the discharge is not sharp and the discharge as a whole sometimes takes an erratic motion. Successive measurements of r_0 frequently differ by fifteen percent.

[7] S. C. Brown *et al.*, M.I.T., Research Lab. of Electronics, Tech. Rep. No. 66 (May 17, 1948).

V. CONCLUSION

The experimental points are compared with the theory in Fig. 4. For each theoretical curve, the appropriate value of γ is taken from Eq. (20). The observed non-linearity between G_d and B_d is in agreement with the present theory.

At low electron currents, the discharge admittance is proportional to the complex conductivity as shown in Eq. (16). At electron currents which are comparable with the displacement current, the discharge admittance becomes a complicated function of the complex conductivity as is Eq. (15). In fact, it is seen that the discharge can have a positive susceptance even though the imaginary part of the complex conductivity is always negative.

The detailed shape of the computed admittance curves is seen from Eq. (15) to depend upon the electron density varying as cosz. If, for example, the z dependence is taken to be parabolic, the computed admittance curves differ in detail from those of Fig. 2 although they have the same general shape and predict positive susceptance at high pressures and high discharge currents.

This positive susceptance, or increased capacitance, has been observed several times in related experiments in which the high frequency admittance of d.c. discharges has been measured.[1] There is no fundamental difference between the h-f admittance of the h-f discharge and the h-f admittance of the d.c. discharge except that the spatial electron distribution and the geometry are different in the two cases. This experiment suggests, therefore, that the increased capacitance reported in these related experiments may also be explained when the effects of the non-uniform electron distribution in space and the real part of the conductivity are accounted for in detail.

The results of the experiment reported here are consistent with the present form of the Eq. (5) for the complex conductivity of an ionized gas.

The Movement of Small Metal Particles Having Six Degrees of Freedom in Air around a Wire Carrying a Constant Electric Current

J. A. SCHEDLING
I. Physics Institute, University of Vienna, Austria
(Received August 1, 1949)

OERSTED and subsequently Ampere investigated the action of a constant electric current flowing through a wire on a magnetic needle. The author[1] has repeated these investigations in a modified manner by means of the set-up shown in Fig. 1, using small particles of iron suspended in air instead of a magnetic needle. Observer *I* (horizontal optical axis, objective n.a. 0.3) and observer *II* (vertical optical axis, objective n.a. 0.3) may simultaneously observe the paths of small particles of Stubbs steel[2] (dispersed in an electric arc) in an observation chamber in the dark field of the microscope. The direction of the illuminating beam of light is horizontal and normal to both directions of observation. Outside of the chamber two copper wires, *A* and *B*, are provided with either one carrying a constant electric current of 0 to 20 amps. d.c. The voltage between the ends of the wire (5 to 10 cm length, 2 to 4 mm diameter) is always smaller than 0.1 volt.

Observing the particles of Stubbs steel (they are of various irregular shapes, sometimes looking like long small needles and sometimes taking more sphere-like forms of the order of magnitude of 10^{-4} to 10^{-5} cm) by means of microscope *I*, as long as no wire is carrying a current, one obtains (1) particles which make the regular movement of fall in a resistant medium,[3] and (2) particles which show an additional movement in and against the direction of the geomagnetic field.[4]

If wire *A* now carries a constant electric current, observer *I* perceives particles of Stubbs steel moving in the following ways: (1) Some make the regular movement of fall which is not influenced by the magnetic field surrounding *A*. (2) Others get a horizontal component of movement which is reversible with the reversal of the current in *A*.[5] Many of these particles show a helicoidal path.[6] Figure 2 shows a photomicrograph of such a path.[7] The particle first moves nearly horizontally (path 0–1) in the field surrounding *A*. After the current has been cut off, it moves in the direction of the geomagnetic field (path 1–2). If the current in *A* is now reversed, the particle takes up its former path, but now in the opposite direction (path 2–3). Figure 3 shows a picture of such a helical path, labeled 1–2–3. Another track (4–5), which shows no reversal, appears simultaneously in this picture. The latter particle crossed the field of view after the magnetic field had been reversed and the first particle had already left the beam of light at point 3. It may be remarked that particles moving right to left and others moving left to right can be seen at the same time, both types reversing their direction with the reversal of the magnetic field. The particles often pass each other very closely; nevertheless, they run in opposite directions and reverse their respective directions with the reversal of the magnetic field. The velocities of the different particles vary more than 1:10, the average velocity being approximately of the order of magnitude of 10^{-2} cm sec.$^{-1}$. (3) Some particles behave like small magnetic needles, and are influenced by a directional moment produced by the magnetic field of *A*. The center of gravity of most of them does not show a horizontal movement. They fall vertically, demonstrating that the magnetic field used causes no translatory movement in or against the direction of the lines of force on normal dipoles. However, a few particles of the needle-like type show, apart from the directional moment, a horizontal reversible component of movement in or against the direction of the magnetic field of *A*.

Observer *II* recognizes that the movement of the particles in the field of *A* takes place in curved paths (see Fig. 4), which are concave with respect to the wire.

If wire *B* is used to build up the magnetic field, one gets the same types of movements, only the direction of the magnetic lines of force (and therefore the direction of the horizontal component of movement) is almost normal to the illuminating beam of light. Observer *I* now looks in the direction of the progression of the motion and sees the particles moving nearly in a circle, the plane of which is normal to the direction of

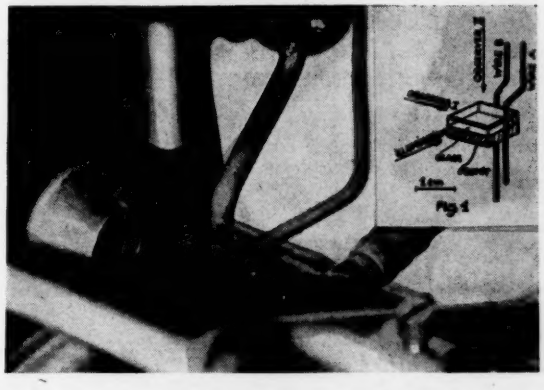

FIG. 1. Arrangement of apparatus and method of observation.

[1] J. A. Schedling, Comptes Rendus **227**, 470 (1948).
[2] Stubbs steel: 1.1 C, 0.2 Si, 0.3 Mn, 1.0 Cr, 0.1 V, rest Fe.
[3] Naturally the Brownian movement is superimposed.
[4] F. Ehrenhaft, Ann. de physique **13**, 163 (1940).
[5] F. Ehrenhaft, J. Frank. Inst. **233**, 235 (1942); Comptes Rendus **190**, 263 (1930).
[6] F. Ehrenhaft, Science **101**, 676 (1945).
[7] The pictures have been taken by Erwin Votava, Vienna.

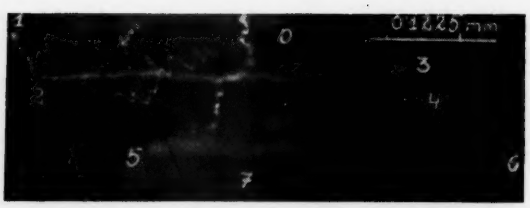

FIG. 2. Photo-micrograph of sample paths of particles of Stubbs steel. Time of exposure, approximately 5 sec. Approximate size of particles, 10^{-4} cm. Paths 0–1, 4–5, 6–7: Movement in the magnetic field of wire A. Path 1–2: Movement in the geomagnetic field. Paths 2–3, 5–6: Movement in the magnetic field of A with current in A reversed. Path 3–4: Same as 1–2.

the progression of the motion. The movement in a circle also reverses if the current in B is reversed. If wires A and B are in use, one after the other, one gets paths showing that the movement takes place in the same way, either transversal or longitudinal to the beam of light. Figure 4 shows such a path.

Investigations by means of the use of additional electrostatic fields showed that some of the particles, the movement of which has already been described, were not influenced by electrostatic fields and carried no electric charge. Other particles electrically charged, changed their electric charge under the influence of the radiation of a radioactive substance, but in spite of this they did not show any change in behavior in the magnetic field.

As already mentioned, some particles of the needle-like type show not only an orientation like a dipole in the magnetic field of the constant electric current, but also a movement of their center of gravity along the lines of force in or against the direction of the field. Stubbs steel particles of the above kind have been made the subject of a further investigation. The consecutive phases of such an experiment are schematically shown in Fig. 5 as follows: *Phase 1.* The particle shows the regular movement of fall. The geomagnetic field is compensated, and no other artificial magnetic field is applied. (Sketch 1 may depict an orientation of the particle falling in the field of gravity.) *Phase 2.* The constant electric current in wire A is cut in; the particle turns around and now lies parallel to the lines of force. Simultaneously, its center of gravity shows a movement from right to left in this particular case. *Phase 3.* With a reversal of the electric current, the particle simultaneously turns 180° and also reverses its horizontal motion, now moving from left to right. *Phase 4.* In addition, we now apply an alternating horizontal magnetic field furnished by means of two Helmholtz coils by an alternating electric current (50 cycles), parallel to the already mentioned constant magnetic field in the small area of observation. We now cut off the constant electric current. The particle shows small oscillations around the lines of force because of the field due to the a.c. in the coils, but maintains its general orientation. However, no movement in or against the lines of force can be seen. *Phase 5.* Superimposing again the magnetic field of the constant electric current, we immediately get the movement along the lines of force. Reversing the d.c. the particle reverses its translatory movement, but does not turn around 180°. (One has to maintain a suitable ratio of the magnetic field strengths of the field furnished by the constant and the alternating electric current.)

This experiment shows that such a particle reverses the direction of its translatory movement in the magnetic field with the reversal of the field, although its dipole axis has not changed its orientation in relation to the magnetic field and the illuminating beam of light during the last two phases of the experiment.

The author, assisted by E. Votava, also investigated a series of other metals also dispersed in an electric arc in air.

Copper and aluminum did not show the motion in the magnetic field of A or B. No directional moment on needle-like particles could be detected. Silver showed the same behavior, but made an intensive light positive photophoretic movement. (All observations have been

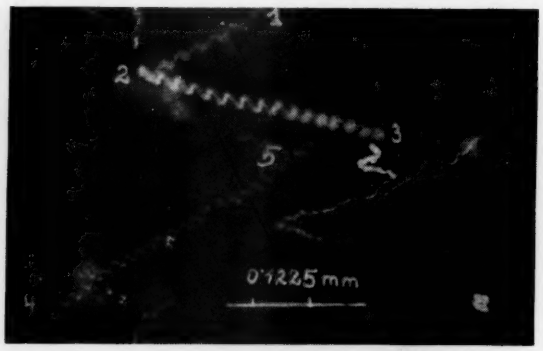

FIG. 3. Photo-micrograph of particles of Stubbs steel describing helical paths in the magnetic field of A. Time of exposure, approximately 20 sec. Path 1–2: right to left. Path 2–3: left to right, current in A reversed. Path 4–5: another particle crossing the field of view after reversal of the magnetic field.

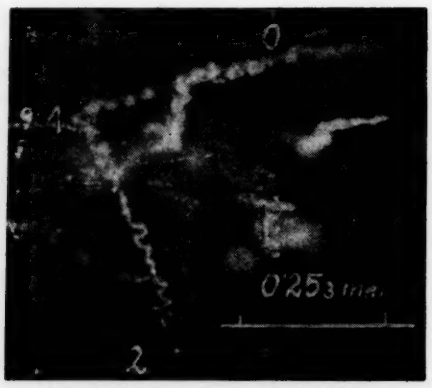

FIG. 4. Photo-micrograph of a particle of Stubbs steel. Time of exposure, approximately 10 sec. Path 0–1: motion in the field of A. Path 1–2: motion of the same particle in the field of B. (Path 0–1 coincides almost with the axis of the illuminating beam of light.)

made in the light of an arc lamp.) Particles of the above-named metals did not show helicoidal movements.

Particles of nickel and cobalt showed a pronounced movement in the magnetic field of the electric current, which was reversible with the reversal of the current. It is remarked that only a small percentage of the particles showed such movements. Particles of nickel frequently showed helicoidal motions. In a few cases, particles of cobalt also could be observed making a helical movement. For both materials, a distinct movement in the geomagnetic field exists, but no particles showing dipole behavior have been observed.

Finally, the author investigated the movement of a fine grained iron powder. The powder used was Fer Omega of French provenience. It was suspended by means of compressed air and then brought into the observation chamber. The particles showed a remarkably smooth and quiet movement (compared with the movement of particles of Stubbs steel dispersed by means of an electric arc). The picture in the dark field showed that most of them must be of a highly symmetrical form. Microscopic tests proved that a high percentage of the particles were of spherical shape. Fer Omega particles could be observed following the lines of force of the geomagnetic field in both directions. After the current in *A* or *B* had been cut in, they showed also a horizontal component of movement in both directions due to the fields of *A* or *B*. This component was reversible with the reversal of the field.

As yet helical movements have not been observed, and it has not been possible to find Fer Omega particles which behave like magnetic dipoles. The percentage of Fer Omega particles showing the above described phenomena is small in comparison to particles of Stubbs steel.

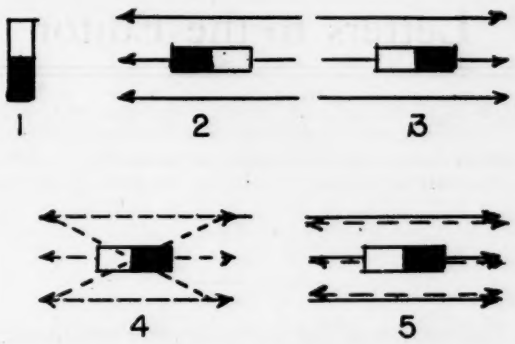

FIG. 5. Schematic diagrams illustrating different types of motion of Stubbs steel particles. (Solid arrows represent steady magnetic fields; dashed arrows, fields due to alternating current.) 1. Particle in the field of gravity (geomagnetic field compensated). 2. Particle in the horizontal magnetic field of the constant electric current (movement, e.g., right to left). 3. Particle in the horizontal magnetic field of the constant electric current, the current being reversed. 4. Particle in the horizontal magnetic field of the alternating electric current (small oscillations within the range of the dotted lines). 5. Situation as in 4. Constant magnetic field of the constant electric current (direction as in 3) again superimposed. Movement left to right as in 3.

These investigations have been carried out in the I. Physics Institute of the University of Vienna, Austria, and the author is very thankful to the Director of this institute for his kindness during the investigations.

Letters to the Editor

PUBLICATION of brief reports of important discoveries in physics may be secured by addressing them to this department. The closing date for this department is five weeks prior to the date of issue. No proof will be sent to the authors. The Board of Editors does not hold itself responsible for the opinions expressed by the correspondents. Communications should not exceed 600 words in length.

An Elaboration of the Schrödinger Formalism with Applications to Nuclear Physics

J. W. CALKIN
The Rice Institute, Houston, Texas, and Los Alamos Scientific Laboratory, Los Alamos, New Mexico
July 29, 1949

IT has been observed that much of nuclear phenomena can be discussed without a detailed potential-theoretic description of the forces between particles, but rather by boundary conditions imposed on the wave function on a surface in configuration space which contains the region in which nuclear interactions between the particles takes place.[1,2] It is our purpose here to describe a set of postulates for the wave mechanics of such systems, which give rise to such conditions naturally, as part of the definition of the Hamiltonian operator.[3] For brevity, we consider simply the problem of two bodies, whose intrinsic spin states are known. The extension of the basic ideas to the case of several bodies, the introduction of spin coordinates, etc., are readily carried out, and will be treated in more detailed discussions in the near future.

Separating the coordinates of the center of mass, we have to deal with wave functions $\psi(\mathbf{x})$ of the relative vector $\mathbf{x}$, which is defined only in the region R exterior to a spherical surface S, centered at the origin, with radius r_0. Since $\int_R|\psi|^2dR$ is then the probability of finding the "exterior" particle in the region R, it is clear that we must have, for a bound state, $\int_R|\psi|^2dR+\rho$, where ρ is the probability of the particle being interior to S. We now make the basic assumption that ρ is to have no radial dependence, but simply an angular dependence describing the relative orientation of the particles interior to S. To achieve this we assume that the states of the system are described by two-component wave functions $\psi=\{\psi,\varphi\}$, where ψ is the same as above, and φ is a function defined on S alone. We take for the inner product (ψ_1,ψ_2), $\int_R\psi_1\bar{\psi}_2+d\int_S\varphi_1\bar{\varphi}_2dS$. The constant d has the dimension of a length. We next postulate that the average value of the kinetic energy T is defined only if ψ has the form $\{\psi,\psi_S\}$ where ψ_S is the value of ψ on S. We take this average value to be

$$\bar{T}=\frac{\hbar^2}{2m}\left[\int_R|\mathrm{grad}\psi|^2dR+d\int_S|\mathrm{grad}_S\psi_S|^2dS\right],$$

where grad_S is the gradient on S. According to Green's formula, we have also

$$\bar{T}=-\frac{\hbar^2}{2m}\left[\int_R\psi\langle\nabla^2\psi\rangle_Rdr+\int_S\psi\left(\frac{\partial\bar{\psi}}{\partial r}+d\nabla_S^2\bar{\psi}_S\right)dS\right],$$

where ∇_S^2 contains only the angular terms of ∇^2. Thus the operator for T is $-(\hbar^2/2m)\{\nabla^2, d^{-1}(\partial/\partial r)|_{r=r_0}+\nabla_S^2\}$. It obviously has the requisite Hermitian character; it also has a unique spectral resolution.[3] Further, the above modification of the usual kinetic energy operator permits a corresponding modification of operators representing other forms of energy, and operators applying only to the second component of ψ are well suited to express short-range interactions. We thus obtain a Hamiltonian by adding appropriate operators to the above T and arrive at the system of equations

$$-\frac{\hbar^2}{2m}\nabla^2\psi+V\psi=E\psi \text{ in } R,\quad -\frac{\hbar^2}{2m}\left(d^{-1}\frac{\partial\psi}{\partial r}+\nabla_S^2\psi\right)+W\psi=E\psi \text{ on } S,$$

for the energy levels of the system. Here V is an operator representing the Coulomb or other field interactions, and W an operator associated with the short-range forces. In the simplest case W may be a constant; it can of course also be given the properties of an exchange operator. Its analagon after the introduction of spin coordinates can also be given a spin dependence. Indeed, a procedure entirely similar to the above can be developed for the Dirac equation. This fact and its possible consequences will be discussed later.

[1] E. P. Wigner, Am. J. Phys. **17**, 99 (1949), and references cited there.
[2] G. Breit and W. G. Bouricius, Phys. Rev. **75**, 1920 (1949).
[3] For mathematical concepts pertinent here, see J. W. Calkin, Proc. Nat. Acad. Sci. **25**, 201 (1939), and **26**, 708 (1940).

Fourth-Order Corrections in Quantum Electrodynamics and the Magnetic Moment of the Electrons

ROBERT KARPLUS* AND NORMAN M. KROLL**
Institute for Advanced Study, Princeton, New Jersey
July 27, 1949

RECENT success in the evaluation of second-order radiative corrections in quantum electrodynamics and the removal of divergences by means of charge and mass renormalization has led to the question of whether higher order corrections would also be finite and subject to a consistent and unique treatment. A procedure for carrying out such calculations to any order, together with a proof that the observable effects are always finite, has, in fact, been given by Dyson.[1] It has been deemed desirable, however, to test his procedure by applying it to a specific fourth-order calculation: first, to verify that no unforseen and insurmountable difficulties occur, and second, to obtain a quantity which could be subjected to comparison with experiment. We have chosen the magnetic moment of the electron because it promised to present the least difficulties of computation while it does contain most of the points of theoretical interest; also, it seems most accessible to experiment. This project has now been completed.

The magnetic moment was computed by evaluating the fourth-order corrections to the energy of an electron in a weak quasi-homogeneous electromagnetic field. For convenience the matrix element involved was divided into various transition schemes, the classification being that of Feynman and Dyson which groups together emission and absorption processes and electron and positron states. Individual terms arising in this way contain both ultraviolet and infra-red logarithmic divergences. These may be interpreted as effects in the fourth order of the second-order charge and wave function renormalizations on the second-order correction to the magnetic moment. On combination, the wave function renormalization effects vanish, as they must, leaving only the easily recognized ultraviolet divergent charge renormalization arising from the vacuum polarization. Actually, to avoid ambiguities arising from the cancellation between infinite integrals, we have followed the prescription of Dyson, who removes all renormalization effects from each term. A non-vanishing photon mass was introduced at this stage in order to identify and avoid infra-red divergences which remain in certain of the transition schemes. As soon as the terms are combined, however, all logarithmic dependence on the photon mass disappears, so that this quantity may safely be set equal to zero. The now finite integrals over the momentum spaces of the virtual particles were reduced by Feynman's techniques[2] to integrals over fine auxiliary variables. This final integration is straightforward but tedious. We have found the correction to the magnetic moment to be

$$-(\alpha^2/\pi^2)\{9(95/288)-3(17/36)\pi^2+9\pi^2\ln 2 -18\textstyle\int_0^1([\ln(1+x)]^2/x)dx-(47/4)\int_0^1([\ln(1-x)]^2/x)dx\}$$
$$\text{Bohr magnetons}=-2.973(\alpha^2/\pi^2)\text{ Bohr magnetons.}$$

This is approximately one and one-half percent of the second-order correction[3] and of the opposite sign, thus decreasing the moment.

* Frank B. Jewett, Postdoctoral Fellow.
** National Research Council Postdoctoral Fellow.
[1] F. J. Dyson, Phys. Rev. **75**, 1736 (1949).
[2] Private communication from Professor Feynman.
[3] Julian Schwinger, Phys. Rev. **73**, 416 (1948).

Hyperfine Structure of $4\,^3P-4\,^3D$ of the Spectrum of Al II

S. SUWA
Institute of Science and Technology, Komaba, Meguroku, Tokyo, Japan
July 27, 1949

WHEN the separations of a term multiplet in an atomic spectrum are so small that they are comparable with or smaller than the hyperfine splittings which are caused by the interaction between nuclear spin and outer electrons, the hyperfine structure exhibits an anomalous feature,[1] which has not yet been fully accounted for. In order to clarify this problem, study of the hyperfine structure of the group of lines of Al II ($4\,^3P-4\,^3D$) at λλ6243, 6231 and 6226 has been undertaken. The structure of these lines was studied previously by Paschen,[1] but his resolving power does not seem to be sufficient for our purpose.

The spectrum was excited in a water-cooled aluminum hollow cathode discharge tube filled with neon of a few mm Hg pressure. The hyperfine structure was examined by the use of a glass Lummer plate (thickness=4.7 mm), a quartz Lummer plate (thickness=4.4 mm) and a Fabry-Pérot etalon. The result of the measurements is given in the upper part of Fig. 1. The main components of λλ6243 and 6231 were so strong and broad (this is shown in Fig. 1 by shaded lines) that their positions relative to the other weaker components were less definite than the mutual distances of the weaker components.

The hyperfine splittings of the final levels, $4\,^3P_{2,1,0}$ are known by the work of Heyden and Ritschl;[2] they obey the usual rule on hyperfine structure. In order to explain the structure of the above-mentioned lines theoretically, we need only consider the structure of $4\,^3D$ and the transition probability from each level of $4\,^3D$ to that of $4\,^3P$. The total Hamiltonian is given by

$$H=H_0(j)+A(\mathbf{I}+\mathbf{s}),$$

where $\mathbf{I}$ and $\mathbf{s}$ are the spin of the nucleus and the $3s$-electron respectively, and A is their coupling constant. Taking into account both the multiplet and the hyperfine splitting simultaneously from the outset of the calculation of the energy levels of $4\,^3D$, secular equations were set up for each value of F, the hyperfine structure quantum number, in the scheme in which $\mathbf{J}^2$ is diagonal. These secular equations involve three parameters, A, $\alpha=H_0(^3D_3)-H_0(^3D_1)$ and $\beta=H_0(^3D_2)-H_0(^3D_1)$. α and β are differences of the diagonal elements of H_0 and represent the magnitudes of the triplet separations of $4\,^3D$. Assuming that $A=0.172$ cm^{-1},[2] the secular equations were solved numerically for various values of α and β, and at the same time the intensities of all hyperfine components were calculated.[3] The best fit for α and β was found to be -0.70 cm^{-1} and -0.31 cm^{-1}, respectively. The calculated separations of the hyperfine levels of $4\,^3D$ are given in Table I, and the hyperfine structure of the three lines obtained by this numerical calculation is given in the lower part of Fig. 1. Agreement between observation and theory is satisfactory within the limit of our resolving power.

TABLE I. Hyperfine separations of the terms $4\,^3D_{3,2,1}$.

	$^3D_1$	$^3D_2$	$^3D_3$
$F(11/2)$			0.208
$F(9/2)$		0.187	0.135
$F(7/2)$	−0.100	0.017	0.083
$F(5/2)$	−0.061	0.008	0.052
$F(3/2)$		0.004	0.029
$F(1/2)$			

$F(7/2)(^3D_1)-F(9/2)(^3D_2)=-0.210$ cm^{-1}
$F(1/2)(^3D_2)-F(11/2)(^3D_3)=-0.080$ cm^{-1}

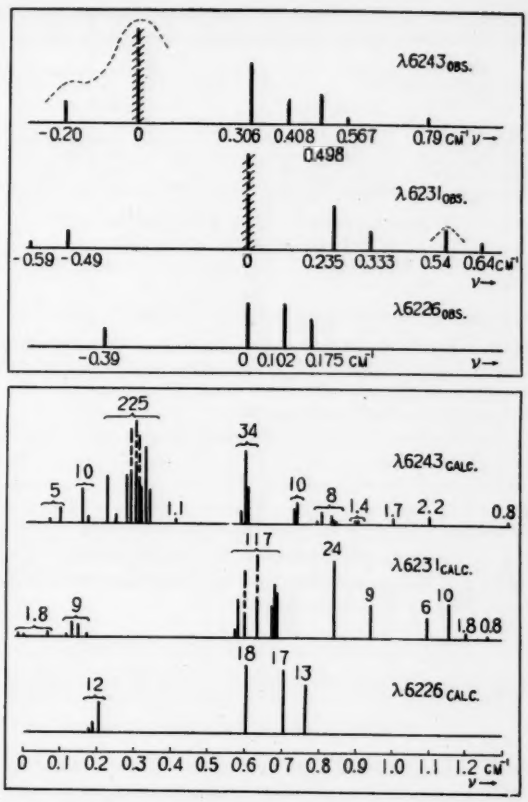

FIG. 1. Hyperfine structure of λλ6243($4\,^3P_2-4\,^3D$), 6231 ($4\,^3P_1-4\,^3D$), and 6226 ($4\,^3P_0-4\,^3D$) of Al II.

The values of α and β thus found are indeed of the same order of magnitude as the hyperfine structure constants, A, and the group of lines of Al II $4\,^3P-4\,^3D$ has proved to be a typical example in which the ordinary multiplet character is strongly perturbed by the hyperfine splittings, resulting in an unusual structure.

In conclusion the author wishes to express his sincere gratitude to Professor Murakawa for his cordial and continued guidance in this work.

[1] F. Paschen, Sitz. Preuss. Akad. Wiss. **33**, 502 (1932).
[2] M. Heyden and R. Ritschl, Zeits. f. Physik **108**, 739 (1938).
[3] P. Güttinger and W. Pauli, Zeits. f. Physik **67**, 743 (1931).

Nuclear Spin and Magnetic Moment of Cs^{135} and Cs^{137} *

DARRAGH E. NAGLE
Physics Department and Research Laboratory of Electronics, Massachusetts Institute of Technology, Cambridge, Massachusetts
July 11, 1949

AN atomic beam magnetic resonance apparatus with a mass spectrometric detector was used by Luther Davis, Jr., to measure the nuclear spin and magnetic moment of Cs 137.[1] This letter reports similar measurements made on a second aliquot of

TABLE I. $F=4$, $(-4=m_F\leftrightarrow m_F=-3)$. Resonances in Cs 133 and Cs 137.

Observed frequency megacycles·sec.$^{-1}$ f133	f137	Computed h.f.s. $\Delta\nu$ (137) (μ_I positive) megacycles·sec.$^{-1}$
45.092 ±0.020	44.934 ±0.020	10197.0 ±250
49.338 ±0.010	49.162 ±0.015	10110.0 ±130
80.289 ±0.013	79.842 ±0.026	10129.5 ±80
360.56 ±0.04	352.30 ±0.04	10123.3 ±12

Weighted average 10,125 ±9 megacycles·sec.$^{-1}$
$\mu_I=2.833\pm0.01$ nuclear magnetons

TABLE II. $F=4$, $(-4=m_F\leftrightarrow m_F=-3)$. Resonances in Cs 133 and Cs 135.

Observed frequency f133	f135	Computed h.f.s. $\Delta\nu$ (135) μ_I positive	μ_I negative
45.092 ±0.020	44.996 ±0.020	9777.0 ±240	10800 ±240
49.338 ±0.010	49.235 ±0.010	9717.0 ±100	10600 ±100
80.289 ±0.013	79.998 ±0.026	9769.0 ±80	10290 ±80
360.56 ±0.040	355.55 ±0.040	9732.1 ±9	9824 ±9
408.36 ±0.040	402.19 ±0.040	9717.0 ±7	9795 ±7

Weighted average 9724.0 ±8 megacycles·sec.$^{-1}$
$\mu_I=2.721\pm0.01$ nuclear magnetons

the original sample of fission product cesium (supplied by the Isotopes Division of the AEC), but with the mass discrimination of the spectrometer improved to the point that resonance transitions could be observed for Cs 135 in the presence of the 133 carrier, as well as the 137 transitions.

The apparatus is arranged to detect those atoms in the beam which satisfy the conditions: (1) They belong to the alkali family, and have specified mass number. (2) They undergo a change in state in the transition field which corresponds to a change of ±1 in the quantum number m_j for strong magnetic fields. Condition 1 identifies the isotope unequivocally. Condition 2 coupled with the selection rule $\Delta m_F=\pm1$ identifies the observable low frequency line as belonging to the transition

$$F=I+\tfrac{1}{2},\quad [m_F=-(I+\tfrac{1}{2})\leftrightarrow-(I-\tfrac{1}{2})=m_F].$$

In weak magnetic field the frequency of the line is very nearly

$$1.400H/(I+\tfrac{1}{2})\ \text{megacycles}\cdot\text{sec.}^{-1},$$

where H is the magnetic field in gauss and I the nuclear spin.[2,3]

Figure 1 exhibits the refocused beam intensity observed when the magnetic field is held constant and the oscillator frequency varied. With the mass spectrometer set in the 133 position the curve labeled 133 was obtained, and so forth. The background in the 133 position is principally due to fast 133 atoms in the penumbra of the beam. In the 137 position fast 137 atoms and residual ions in the spectrometer account for the background. In the 135 curve the fast 135 atoms and residual ions in the spectrometer account for part of the background, and the rest is due to 133 atoms incompletely discriminated against, as shown by the smaller maximum at the resonance frequency of the 133. The fact that all the peaks occur at nearly the same frequency shows that the spin of Cs 135, like that of 133 and 137, is 7/2.

The displacements of the 135 and 137 peaks from the 133 resonance frequency are due to differing values of the hyperfine structure separation, and permit calculation of the h.f.s. $\Delta\nu$ and the nuclear magnetic moment. The method is similar to that used by Zacharias.[4] It is assumed that μ_I is proportional to $\Delta\nu$; this might give rise to small errors in μ_I but to much smaller ones in $\Delta\nu$.[5] Using the values of Kusch, Millman, and Rabi,[6] namely,

$$\Delta\nu_{133}=9192.6\ \text{megacycles}\cdot\text{sec.}^{-1},$$
$$\mu_{133}=2.572\ \text{nuclear magnetons},$$

the values of $\Delta\nu_{135}$ and $\Delta\nu_{137}$ which best fit the Breit-Rabi formula[2] are computed from the observed resonance frequencies. This has been done for a number of values of magnetic field.

Table I presents the results for 137, which agree with the earlier ones.[1] Table II presents the results for 135, calculated alternatively for positive or negative μ_I. μ_I must be taken positive in order to obtain consistent values of $\Delta\nu$. The weighted average of the h.f.s. is computed to be 9724.0±8 megacycles·sec.$^{-1}$ and the nuclear magnetic moment 2.721 nuclear magnetons.

I wish to acknowledge the assistance of Hin Lew and the other members of the atomic beam laboratory.

* This work has been supported in part by the Signal Corps, the Air Materiel Command, and the ONR.

[1] Luther Davis, Jr., Phys. Rev. **76**, 435 (1949).
[2] G. Breit and I. I. Rabi, Phys. Rev. **38**, 2082 (1931).
[3] Thomas, Driscoll, and Hipple, Phys. Rev. **75**, 1481 (1949).
[4] J. R. Zacharias, Phys. Rev. **61**, 270 (1942).
[5] S. Millman and P. Kusch, Phys. Rev. **60**, 91 (1941).
[6] Kusch, Millman, and Rabi, Phys. Rev. **55**, 1176 (1939).

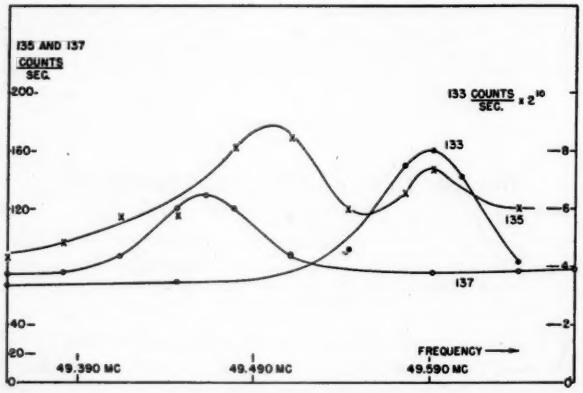

FIG. 1. Low frequency resonance transitions in Cs 133, 135, and 137.

The Energy Distribution of Fission Fragments from Pu^{239}

D. C. BRUNTON AND W. B. THOMPSON
Chalk River Laboratories, National Research Council of Canada, Chalk River, Ontario, Canada
August 1, 1949

THE energy distribution of fission fragments from Pu^{239} has been measured as a continuation of the work on U^{235} and U^{233}, reported previously.[1] The experimental arrangement was very similar to that previously described. The results, in particular the nature of the "gated" distributions, were similar to those in the other fissile materials. A comparison of these results with those of Deutsch and Ramsey[2] is shown in Table I, in which the fragment energies are uncorrected for source and collimator losses for proper comparison. The corrected values obtained in the present experiment are 94.6 and 65.2 Mev for the light and heavy frag-

TABLE I. Comparison of present experiment with Deutsch and Ramsey for fission in Pu^{239}.

	Present* experiment	Deutsch* and Ramsey
Most probable energy of light fragment (Mev)	93.3	93
Most probable energy of heavy fragment (Mev)	63.9	65
Ratio of most probable energies	1.47	1.43
Most probable mass ratio (from an equal ratio interval curve)	1.35	1.32
Width at half-maximum of high energy peak (Mev)	13.6	13
Width at half-maximum of low energy peak (Mev)	24	21
Ratio of minimum to high energy peak percent	23	11
Ratio of peak heights	1.47	1.48

* Values uncorrected for source and collimator losses.

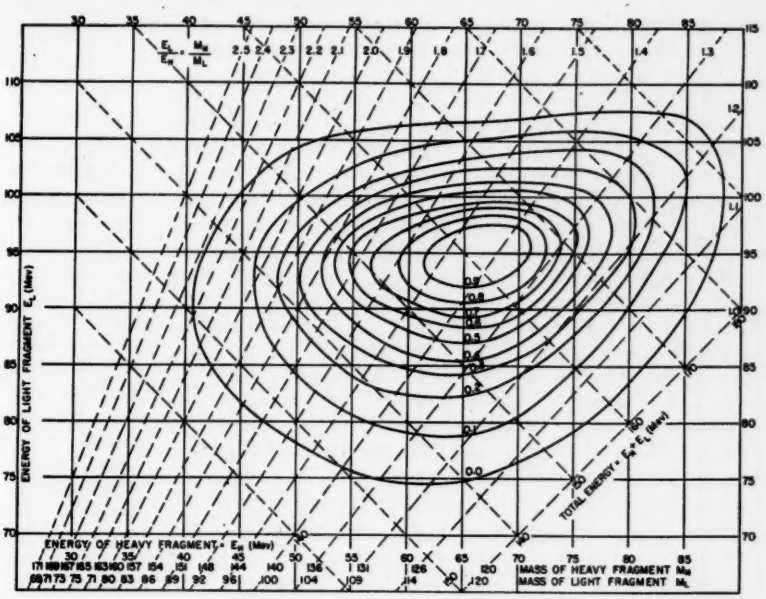
ENERGY OF LIGHT FRAGMENT, E_L (Mev)
ENERGY OF HEAVY FRAGMENT, E_H (Mev)
TOTAL ENERGY, $E_H + E_L$ (Mev)
MASS OF HEAVY FRAGMENT M_H
MASS OF LIGHT FRAGMENT M_L

FIG. 1. Fission modes in Pu^{239}. Contour lines indicate relative frequency of occurrence of the fission modes.

ments, respectively. The contour diagram for Pu^{239} is shown in Fig. 1, where, as before, the contour lines represent the relative frequency of occurrence of the fission modes. The most probable total kinetic energy was found to be a maximum at a mass ratio of 1.2 in agreement with the range measurements of Katcoff, Miskel, and Stanley.[3]

The mass diagram derived from these energy measurements is shown in Fig. 2 This curve is derived from the ratio of the energies of the two fragments with assumption of a total mass of 240 for the compound nucleus and the conservation of linear momentum. The mass curve obtained from chemical identification of the decay chains is shown for comparison.[4] It has been shown by Wilson[5] that the neutrons are evaporated from the fragments while in flight. As pointed out by Deutsch and Ramsey[2] the recoil from neutron emission gives rise to a spread in the fragment energies which results in a broader mass curve than that derived by chemical means. It is readily shown however that the energy ratio is changed on the average by less than 1 percent by neutron evaporation. Consequently, the masses obtained from a coincident pulse experiment are the primary masses *before* neutron emission while the chemical identification occurs after neutron emission For this reason a shift of several units would be expected between the two curves. The shift apparent, however, in Fig. 2 is only in the heavy fragment curve leading to the conclusion that neutron emission occurs predominantly from that fragment. This result is however contrary to the results of de Benedetti, Francis, Preston, and Bonner[6] on the angular correlation of fission neutrons. We find it difficult to account for this discrepancy by any instrumental effect but we feel that the inherent limited accuracy of our experiment leaves some doubt in our result. This effect has, however, been consistently observed with the three fissile materials studied. It is possible that a variation in w, the electron volts per ion pair for different fragments, may cause this discrepancy. However, a comparison of fission energies by ionization and calorimetric experiments shows the w is nearly the same for α-particles and fission fragments. Although accurate measurements are not available, it is, therefore, felt that this is an unlikely source of error in the mass curve presented.

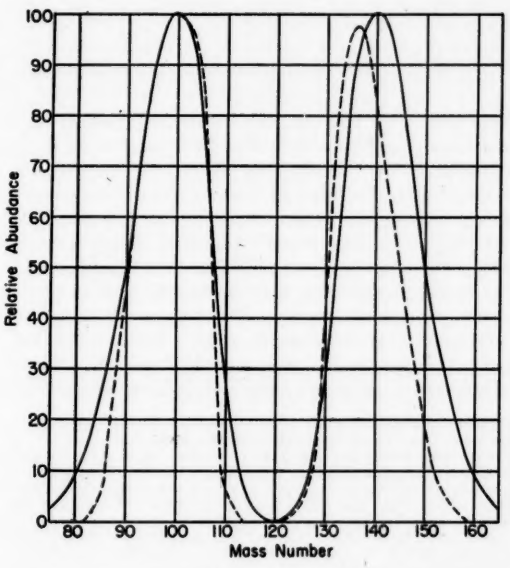

FIG. 2. Mass curves for Pu^{239}. Solid line is coincident fragment experiment; dashed line is chemical analysis.

[1] D. C. Brunton, and G. C. Hanna, Phys. Rev. **75**, 990 (1949).
[2] M. Deutsch and M. Ramsey, MDDC-945 (1945).
[3] Katcoff, Miskel, and Stanley, Phys. Rev. **74**, 631 (1948).
[4] Steinberg, Seiler, Goldstein, and Dudley, MDDC-1632 (1947).
[5] R. R. Wilson, Phys. Rev. **72**, 189 (1947).
[6] de Benedetti, Francis, Preston, and Bonner, Phys. Rev. **74**, 1645 (1948).

Altitude Dependence of Mesons of Energy between 224 and 255 Mev*

MARCELLO CONVERSI**
Institute for Nuclear Studies, University of Chicago, Chicago, Illinois
August 1, 1949

IN a series of B-29 flights recently undertaken, experiments have been carried out in order to investigate the nature of ionizing particles slowed down after penetrating a certain thickness of lead. Part of the results, as well as a short description of the apparatus employed, has been published in two previous papers.[1] A counter telescope, realized by means of double coincidences, (AB) (resolving time $\sim 2\mu$ sec.), selected a beam of

ionizing particles. In the measurements at different altitudes here reported, 15 cm of lead were interposed in the counter telescope. A 10-cm thick block of graphite was used as an "absorber" for the particles of the beam which penetrated the 15 cm of lead. The observed mesons, stopped in the absorber after traversing 15 cm of lead, had energy in the range of 224 to 255 Mev. A group of counters, C, surrounding the absorber and covering the solid angle of the counter telescope, were at the same time in "delayed coincidence" and the "anti-coincidence" with respect to the coincidences (AB). In this way, mesons responsible for the greater part of the observed delayed coincidences could be separated from other penetrating particles, responsible for part of the anticoincidences observed at high altitude (see next letter). The delayed coincidences were registered by four "channels" of the same "time width," $\Delta\theta$ (2.8 μsec.), so that four points of the decay curve corresponding to mesons stopped in the absorber were obtained. The values of $\Delta\theta$ and of the "time distance," θ (0.98 μsec.), between each channel and the next one, were fixed by delay lines. The value of the minimum delay, θ_m (1 14 μsec.), for which a coincidence was registered in the first channel, was obtained by a method analogous to the one described in a previous paper.[2] For the apparatus employed, practically all spurious delayed coincidences occurred[3] for *random* events in which a particle traversing the counter telescope, but failing to discharge counters C, was followed after a short time by another particle discharging counters C. The fraction of these spurious coincidences in the first channel was 0.5 percent near sea level and 19 percent, at the highest altitude (36,000 feet).

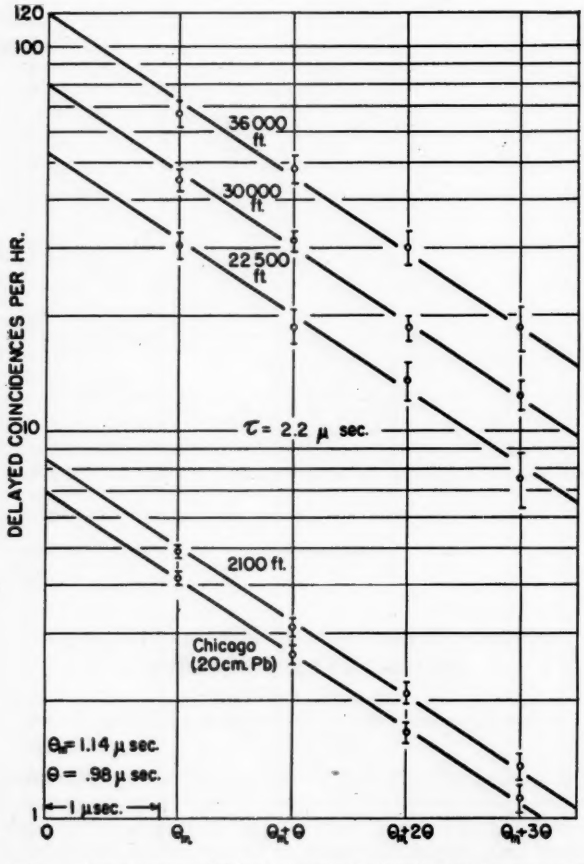

FIG. 1. Decay curves obtained at several altitudes for mesons slowed down in 10 cm of graphite after traversing 15 cm of lead. Each point of the decay curves is due to the contribution of mesons disintegrating between the instant t of the corresponding abscissa and $t+\Delta\theta$ ($\Delta\theta=2.8$ μsec.).

TABLE I. Results of measurements at several altitudes. The errors of M include the error on p.

Altitude (ft.)	600	2100	22,500	30,000	36,000
Average geomag. latitude	51°N	42°N	50°N	49°N	40°N
N (events/hr.)	6.95±0.27	8.50×0.33	53.0±3.5	79.5±3.6	120±8
M (mesons/hr.)	34.8±2.9	42.5±3.5	265±29	398±35	600±65

The value of the lifetime of the ordinary meson, deduced from an analysis of all the measurements so far performed near sea level, is $\tau=(2\ 19\pm0.07)$ μsec. The results of measurements of delayed coincidences performed at several altitudes are graphically represented in Fig. 1. All the disintegration curves are consistent with a decay constant of 2.2 μsec. An analysis of all measurements performed at 30,000 feet including those previously reported[1] gives for the decay constant the value (2.14 ± 0.12) μsec. By extrapolation to the zero time of the "most probable" 2.2-μsec. decay curve corresponding to each series of measurements, the number of mesons per hour, N, stopped in the absorber and then disintegrating within 2.8 μsec. ($\Delta\theta$) into electrons striking counters C, is obtained (Table I). The number of mesons per hour, M, stopped in the absorber after traversing the counter telescope, is then given by

$$M=N/p[1-\exp(-\Delta\theta/\tau)], \tag{1}$$

where p is the average value of the probability for a meson stopped in the graphite absorber to disintegrate into an electron discharging counters C.

Events were registered as anticoincidences when no anticoincidence counter fired within 1 1 μsec. before or 7.8 μsec. after a coincidence (AB) occurred. If the percentage of mesons decaying after 7.8 μsec. is neglected, the contribution given by mesons to the intensity, I_a, of the "true anticoincidences" (difference between the anticoincidences registered with and without absorber) is $(1-p)$ M. Results of measurements taken in Chicago (not reported in this letter) show that the ratio N/I_a does not vary appreciably under thicknesses of material greater than 20 cm of lead. This indicates that at sea level the percentage of particles different from mesons slowed down after traversing more than 20 cm of lead is negligible. In these conditions, therefore, it may be written

$$I_a=(1-p)M. \tag{2}$$

From the results of the Chicago measurements the value 0.28 ±0.015 is obtained for p through Eqs. (1) and (2). By knowing the numerical values of p, $\Delta\theta$ and τ, the absolute number of the observed mesons can be deduced for each series of measurements from Eq. (1) (see also next paper).

As shown in Fig. 1 of the next paper, the number of the observed mesons (range between 100 and 117 g/cm² of air equivalent) decreases with the atmospheric depth, x, approximately as $\exp(-x/L)$, with $L\approx280\pm10$ g/cm². Within the experimental errors an exponential dependence upon altitude but with $L\approx220$ g/cm²,[4] has been found for mesons having range between 5 and 83 g/cm² of air equivalent.[5,6] The lower rate of increase with altitude in the present case may be due, at least in part, to the more narrow angular definition of the apparatus here employed (35° maximum permitted zenith angle). The information about the production spectrum of mesons, which may be obtained from the interpretation of these results will be discussed elsewhere.

* Supported by the Joint Program of the ONR and AEC.
** On leave from the University of Rome, Italy.
[1] M. Conversi, Phys. Rev. 76, 311 (1949) and Phys. Rev. 76, 444 (1949).
[2] M. Conversi and O. Piccioni, Phys. Rev. 70, 874 (1946).
[3] The delayed coincidences registered in the 1st channel at 30,000 and 36,000 feet have been also corrected (on the basis of measurements taken without absorber) for spurious coincidences due to the lags of counters C. A detailed account of all corrections will appear in a complete report of this research.
[4] B. Rossi, Rev. Mod. Phys. 20, 547 (1948).
[5] Rossi, Sands, and Sard, Phys. Rev. 72, 120 (1947).
[6] M. Sands, Phys. Rev. 74, 1237 (1948).

Altitude Dependence of Penetrating Particles Slowed Down after Traversing 15 Cm of Lead*

MARCELLO CONVERSI**
Institute for Nuclear Studies, University of Chicago, Chicago, Illinois
August 1, 1949

IN addition to the measurements of the delayed coincidences reported in the previous paper, measurements at several altitudes of the anticoincidences have been taken simultaneously, with and without the graphite absorber. As stated in the previous letter, the "true anticoincidences," registered near sea level (Chicago) under more than 20 cm of lead, are very likely to be due only to mesons stopped in the absorber and not disintegrating into electrons which discharge within 7.8 μsec. the anticoincidence counters. At high altitude, however, a contribution, X, is given to the intensity I_a of the true anticoincidences from particles different from mesons. Equation (2) of the previous paper must be substituted, therefore, by $I_a=(1-p)M+X$.

The values of X obtained at different altitudes from this relation, on the basis of the observed counting rate of the delayed coincidences and of the anticoincidences, are reported in Table I. The intensities I_a have been obtained as a difference between the counting rates of the anticoincidences measured with and without absorber. By multiplying the values of M (see Table I of the previous paper) and of X by the factor 1.1×10^{-7}, the absolute number (per sec. cm^2 sterad.) of mesons, m, and of "X-particles," x, traversing in the vertical direction 15 cm of lead and stopped by an additional g/cm^2 of graphite, are obtained for each series of measurements. In graphically representing these results (Fig. 1), the points at 30,000 and 36,000 feet have been referred to the geomagnetic latitude (50°N) of the point at 22,500 feet. The correction has been introduced by using the latitude curves obtained at 30,000 feet, with the same apparatus, for the meson and the X-component,[1] and assuming an approximately equal latitude dependence at 36,000 feet.

As to the nature of the X-component, the following observations can be made: (1) Its large latitude effect, at 30,000 feet,[1] is comparable as far as magnitude only to the one observed, at the same altitude, for the neutron component and for "bursts."[2] (2) Its altitude dependence may be approximately represented by an exponential law, with a "mean free path," L, of about 150 g/cm^2 (Fig. 1); this value is comparatively close to the value obtained for "bursts"[3] and for star-producing radiation;[4,5] (3) No appreciable percentage of the observed anticoincidences should be due to electrons; it appears, in fact, very unlikely that a large electronic shower, able to penetrate the 15 cm of lead interposed in the counter telescope, would end in the absorber without striking any of the anticoincidence counters. (4) Previous results obtained with the same equipment[6] indicate that the excess of positive ordinary mesons at 30,000 feet would be smaller than at sea level (~20 percent) if more than 13 percent of the delayed coincidences observed with graphite absorber were due to locally produced positive π-mesons, slowed down in the absorber and disintegrating, within a fraction of μsec.,[7] into ordinary mesons of very short range;[8] hence, no large contribution should be given to the anticoincidences by negative π-mesons captured in the absorber unless the cross section for production of a π-meson is considerably larger, at the energies involved, for a negative than for a positive π-meson. These arguments lend good support to the view that the X-component is of nucleonic nature and made up essentially of protons. If the X-particles were protons they would have momentum in the range 985 to 1043 Mev/c; evidence for the presence of protons of such momentum at 30,000 feet has been given recently.[9] It is worth while observing also that the absolute number of X-particles interpreted as protons [$(2.1\pm0.13)\times10^{-5}$ per sec. cm^2 sterad., Mev/c of momentum] is in agreement with the absolute number estimated[10] on the basis of the findings of the Anderson group. Additional points would be necessary for a more exact determination of the shape of curve x, which has been represented in Fig. 1 as an exponential; the number of protons at sea level obtained by extrapolation of such an exponential is likely to be in excess.

TABLE I. Results of measurements at several altitudes.

Altitude (ft.)	2100	22,500	30,000	36,000
Average geomagnetic latit.	42°N	50°N	49°N	40°N
Antic. p. hr. with absorber	90.8±0.9	1350±19	2835±18	3986±40
True antic. p. hr. (I_a)	36.8±1.7	563±27	985±30	1136±89
X-particles per hour	6.2±3.0	372±34	638±39	704±101

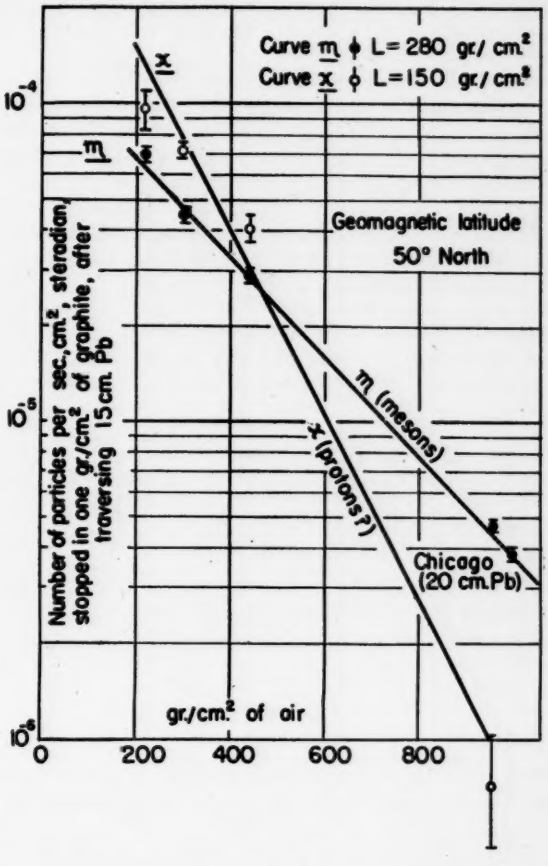

FIG. 1. Altitude dependence at 50° north geomagnetic latitude of mesons and of X-particles (protons?) stopped after traversing 15 cm of lead. The observed mesons have momentum between 315 and 348 Mev/c. If the X-particles are protons they have momentum between 985 and 1043 Mev/c.

It is a pleasure for the author to acknowledge the kind hospitality of Professor M. Schein in his laboratory, the numerous facilities granted by Professor S. K. Allison, the help of Mr. B. Jackson and the cooperation of Major W. A. Gustafson, Mr. C. L D'Ooge and of the B-29 crew through the entire period of the flight

* Supported by the Joint Program of the ONR and AEC.
** On leave from the University of Rome, Italy.
[1] M. Conversi, Phys. Rev. 76, 444 (1949).
[2] J. A. Simpson, Jr., Phys. Rev. 73, 1389 (1948); J. A. Simpson, Jr., and R. B. Uretz, Phys. Rev. 76, 569 (1949).
[3] H. Bridge and B. Rossi, Phys. Rev. 71, 379 (1947); Bridge, Rossi, and Williams, Phys. Rev. 72, 257 (1947); H. E. Tatel and J. A. Van Allen, Phys. Rev. 73, 87 (1948).
[4] Bernardini, Cortini, and Manfredini, Phys. Rev. 74, 845 (1948); 74, 1878 (1948).
[5] J. J. Lord and M. Schein, Phys. Rev. 75, 1956 (1949).
[6] M. Conversi, Phys. Rev. 76, 311 (1949).
[7] J. R. Richardson, Phys. Rev. 74, 1720 (1948).
[8] Lattes, Occhialini, and Powell, Nature 160, 486 (1947).
[9] Adams, Anderson, Lloyd, Rau, and Saxena, Rev. Mod. Phys. 20, 334 (1948); Adams, Anderson, and Cowan, Rev. Mod. Phys. 21, 562 (1948).
[10] See B. Rossi, Rev. Mod. Phys. 20, 562 (1948).

On the μ-Meson Capture

M. TAKETANI, *Tokyo, Japan,*
S. NAKAMURA, *Tokyo University, Tokyo, Japan,*
AND
M. SASAKI, *Tokyo Bunrika University, Tokyo, Japan*
July 25, 1949

SUPPLEMENT is made to the work, "On the two-meson theory" previously published.[1] It concerns the process of mu-meson capture: Firstly, Z-dependence of the capture probabilities; secondly, excitation energy of the nucleus after mu-meson capture; and thirdly, possibilities of interaction schemes between mesons, leptons, and nucleons.

The theories of mu-meson capture have already been given by various workers,[2-9] and the capture probabilities are shown to depend on, at least, the fourth power of Z. In our paper,[1] using the formula for K-electron capture.

$$1/\tau_{\mu\cdot\text{cap.}}\alpha(\alpha Z)^{2S+1}, \quad S=(1-\alpha^2Z^2)^{\frac{1}{2}}$$

which seems to be proportional to the third power of Z. However, if we take into account the Z-dependence of the unknown nuclear matrix elements, which may certainly be proportional to, at least, the first power of Z, the current result will be derived.

On the other hand, if we assume that the nuclear wave is described as a plane wave inside the nucleus and zero amplitude outside, the transition probability that the nucleon acquires the momentum $(k,\ k+dk)$ and the neutrino is emitted with the momentum $(\mathbf{p},\ \mathbf{p}+d\mathbf{p})$ will be given as follows (in the case of scalar coupling):

$$\delta(1/\tau_{\mu\cdot\text{cap.}})\sim Z^3f(y)P^2d\Omega_p\rho_k, \quad y=|\mathbf{k}+\mathbf{p}-\mathbf{k}_0|R \qquad (1)$$

where $\mathbf{k}_0$ is the average momentum of the initial protons and R is the nuclear radius. $f(y)=(y^{-1}J_{\frac{3}{2}}(y))^2$ has the value ~ 0.70 at $y=0$, and decreases rapidly as y increases, with $\exp(-y^2/4)$. Thus, the region where (1) has appreciable magnitude is confined in the small interval of $y\leq 4$. Further, the average initial momentum of protons and that of the neutrino do not depend on Z, since the latter carries away the greater part of the available energy, which enables one to put $|\mathbf{p}|\approx\kappa$, where $\kappa=m_\mu c^2/\hbar$. Accordingly, the region which contributes mainly to the probability may depend essentially on k and thus is proportional to R^{-3}. Since the final level density of k, ρ_k, is, however, proportional to R^3, the integration with respect to the final level is almost independent on Z. The only factors which show the charge dependence are the volume concentration of mu-meson in the K-orbit, together with the number of protons Z. From these facts we can roughly estimate that the total probability would behave as the fourth power of Z.

Next, if the integration with respect to angle is done, the total probability will be given as a function of nucleon momentum k. This curve has a sharp maximum at x_0, and the shape around the peak is given approximately by $\exp[-\frac{1}{4}R^2\kappa'^2(x-x_0)^2]$, where $x=k/\kappa'$, $\kappa'=\langle((p+\kappa_0)^2)_{Av}\rangle^{\frac{1}{2}}\approx 2\kappa$. The value of $R\kappa'$ is fairly large, excepting the light nuclei, and the maximum point, x_0, is given,

$$x_0=1/\tanh\tfrac{1}{2}R^2\kappa' x_0. \qquad (2)$$

For large Z, the value of x_0 is nearly equal to unity and increases slowly as Z decreases. Since the peak is sharp, we may safely identify this x_0 with the average value of momentum of the excited nucleon, which is given as follows:

$$k^2\hbar C/2M\kappa-\bar{E}=x_0^2/2^0-\bar{E}, \qquad (3)$$

where $\bar{E}$ is the average kinetic energy of the nucleon in the ground state and is 0.14 in the unit of $m_\mu c^2\cong 100$ Mev. From (3) we can see that the excitation energy is 6 Mev for large Z, and ~ 14 Mev for small Z, and slowly varying between these two values for the intermediate Z.

Finally, possible interaction schemes between elementary particles will be discussed. We have suggested a model given in Fig. 1. Alternative models, such as those shown in Fig. 2, are put forward by various workers. In the latter, a pi-meson may decay, through virtual nucleon pairs, either into leptons or into a mu-meson and a neutrino. Whereas the direct coupling between nucleons-leptons or nucleons-mu-mesons are shown to be the same,[2] the final momentum density is larger for leptons than for mu-mesons, which will make the lifetime of pi-mesons for pi-electron decay essentially faster than that for pi-mu-decay.[10] This seems to be at variances with the recent experiments of Berkeley Therefore the model given in Fig. 2 should be ruled out.

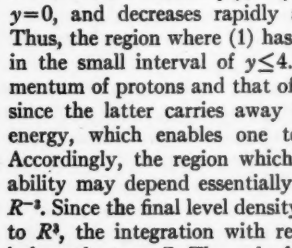

FIG. 1. Suggested interaction scheme between elementary particles.

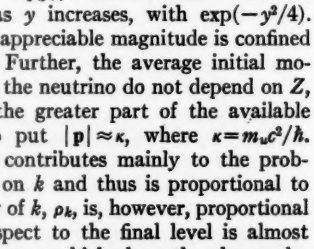

FIG. 2. Alternative interaction scheme proposed by others.

[1] Taketani, Nakamura, Ono, and Sasaki, Phys. Rev. **76**, 60 (1949).
[2] J. A. Wheeler, Phys. Rev. **71**, 320, 462 (1947); Rev. Mod. Phys. **21**, 133 (1949). J. Tiomno and J. A. Wheeler, Rev. Mod. Phys. **21**, 153 (1949).
[3] J. L. Lopes, Phys. Rev. **74**, 1722 (1948).
[4] Epstein, Finkelstein, and Oppenheimer, Phys. Rev. **73**, 1140 (1948).
[5] M. N. Rosenbluth, Phys. Rev. **75**, 532 (1949).
[6] R. E. Marshak, and H. A. Bethe, Phys. Rev. **72**, 506 (1947); R. E. Marshak, Phys. Rev. **75**, 486 (1949).
[7] T. Inoue, and S. Ogawa, Prog. Theor. Phys. **3**, 319 (1948).
[8] S. Hayakawa, Prog. Theor. Phys. **3**, 200 (1948).
[9] Y. Tanikawa, Prog. Theor. Phys. **3**, 314, 315 (1948).
[10] Of course, this conclusion may suffer some ambiguities due to divergent difficulties of present field theory and varieties of interaction types between elementary particles. Private discussions by H. Fukuda and Y. Miyamoto.

Statistical Mechanics of Mixtures of He^3 and He^4

J. DE BOER*
University of Amsterdam, Amsterdam, Netherlands
August 3, 1949

THE measurements[1] of the vapor-liquid concentration ratio of dilute solutions of He^3 and He^4 show that for temperatures *above the λ-point* these solutions behave as "perfect solutions" leading to the validity of Raoults law:

$$C^V/C^L=P_3^0/P_4^0, \qquad (1)$$

where P_3^0 and P_4^0 are the vapor pressures[2] of the pure substances He^3 and He^4.

If the mixture of He^3 and He^4 were a perfect mixture at all temperatures and concentrations, the expression for the free energy for a perfect mixture

$$F=(1-x)F_4^0+xF_3^0+RT\{x\ln x+(1-x)\ln(1-x)\}. \qquad (2)$$

F_3^0 and F_4^0 being the free energies of the pure substances and x being the relative concentration $N_3/(N_3+N_4)$ of He^3, leads to the conclusion that the temperature of the transition of phase I into II is independent of concentration $(dT/dx=0)$ and that the transition remains second order $(x^{\text{I}}=x^{\text{II}})$ at all concentrations.

According to Taconis and Beenakker[3] the vapor-liquid concentration ratio deviates from Raoult's law at temperatures *below the λ-point*, being given by

$$C^V/C^L=(1/y)(P_3^0/P_4^0), \qquad (3)$$

where $y=N_4^n/N_4$ is the ratio of the number of molecules in the "normal" state to the total number of molecules of He^4, a result which is in agreement with experiments of Daunt *et al.*[4,5] showing that the molecules of He^3 do not take part in the superflow of liquid helium II. This was explained by assuming that the He^3 molecules only mix with the normal part of He^4. If this assumption

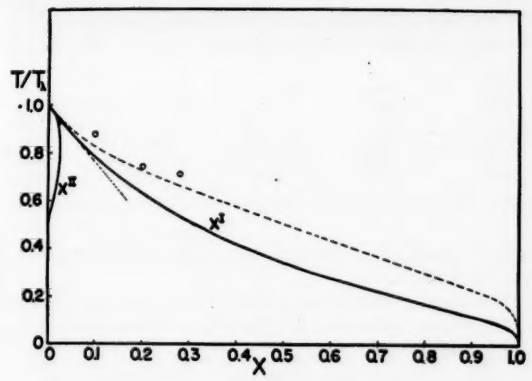

FIG. 1. Variation of concentrations x^{I} and x^{II} with temperature. The experimental points were measured by Abraham, Weinstock, and Osborne.

could be generalized to the hypothesis, that He^3 and He^4 behave like a perfect mixture of He^3 in the normal component of He^4, then the free energy (2) must be replaced by

$$F=(1-x)F_4^0+xF_3^0+RT(x/x_a)\{x_a\ln x_a+(1-x_a)\ln(1-x_a)\}, \quad (4)$$

where x_a is the "apparent" concentration; $N_3/(N_3+N_4^n)$, $y=N_4^n/N_4$ as before and where the connection between x_a, x and y is given by $x_a=x/(y+x(1-y))$.

The equations of equilibrium: $\mu_3^{\mathrm{I}}=\mu_3^{\mathrm{II}}$ and $\mu_4^{\mathrm{I}}=\mu_4^{\mathrm{II}}$ for the thermodynamic potentials of the components 3 and 4 in both phases I and II, derived from (4), lead to the result:

$$x_a^{\mathrm{I}}=x_a^{\mathrm{II}}, \quad (5a)$$

$$\ln(1-x_a^{\mathrm{I}})=-(F_4^{0\mathrm{I}}-F_4^{0\mathrm{II}})/RT(y^{\mathrm{I}}-y^{\mathrm{II}}). \quad (5b)$$

It is assumed that y is a function of temperature *only* and independent of concentration as it should be for a perfect solution. For the high temperature phase I, $y^{\mathrm{I}}=1$; whereas in the low temperature phase II, $y^{\mathrm{II}}=N_4^n/N_4=(T/T_\lambda)^\nu$ with $\nu=5.6$. Equation (5a) shows that the concentrations of He_3 in phases I and II are no longer equal. *Therefore, the transition is no longer of the second order but becomes of the first order*, the relation between the concentrations being $x^{\mathrm{I}}=x^{\mathrm{II}}/(y^{\mathrm{II}}+x^{\mathrm{II}}(1-y^{\mathrm{II}}))$. The actual calculation of the concentrations x^{I} and x^{II} as a function of the transition temperature depends on the extrapolation of the free energy curve of the high temperature phase I below $T=T_\lambda$. In Fig. 1, the results have been plotted extrapolating the entropy curve of the phase II, linearly to $\tau=0$, as has been suggested by Daunt and Mendelssohn.[6] The broken curve corresponds to a linear extrapolation of the free energy curve, as suggested in the liquid He II model of Gorter. In both cases the concentration of He_3 in the liquid phase at lower temperatures is extremely small, its value being approximately $x^{\mathrm{II}}=x^{\mathrm{I}}y^{\mathrm{II}}/(1-x^{\mathrm{I}})$. The experimental points in Fig. 1 were measured by Abraham, Weinstock, and Osborne.[7]

The general formula for the vapor-liquid concentration ratio is given by

$$C^V/C^L=(1/y)(1-x_a)^{(1-y)}(P_3^0/P_4^0) \quad (6)$$

approaching to Taconis and Beenakker's formula at low concentrations.

The first-order character of the transition of phase I into phase II, which is demonstrated in Fig. 1, leads to interesting conclusions. The fact that below temperatures of about $0.57T_\lambda$ the value of x^{II} is approximately zero makes it possible to speak in this temperature region of a pure phase II of He^4 which is in equilibrium with an ideal mixture of He^4 and He^3 in phase I If a mixture of He^3 and He^4 of concentration x is cooled down, pure liquid He^4 starts to be formed in a separate phase II at the transition temperature determined by $x=x^{\mathrm{I}}(T)$. When the temperature is decreased still more, the amount of pure liquid He^4 in phase II increases, the total fraction of substance, which at a temperature T is left as a perfect mixture in phase I, being $x/x^{\mathrm{II}}(T)$.

Of course, the present remarks must only be considered as a possibility, which is based entirely on the *hypothesis* that He^3 only mixes as a perfect mixture with the normal part of He^4 and that the interpretation in terms of the free energy expression (4) is true. A more detailed account will appear in Physica. The author is indebted to Dr. Daunt for many stimulating discussions on this subject.

* Currently visiting professor at Ohio State University, Columbus, Ohio.
** The author is very much indebted to Dr. Osborne for putting these data at his disposal before publication.

[1] Fairbank, Lane, Aldrich, and Nier, Phys. Rev. **71**, 911 (1947); Daunt, Probst, and Smyth, Phys. Rev. **74**, 495 (1948).
[2] Sydoriak, Grilley, and Hammel, Phys. Rev. **75**, 302 (1949).
[3] Taconis, Beenakker, Nier, and Aldrich, Phys. Rev. **75**, 1966 (1949).
[4] Daunt, Probst, Johnson, Aldrich, and Nier, Phys. Rev. **72**, 502 (1947).
[5] Daunt, Probst, and Johnston, J. Chem. Phys. **15**, 759 (1947).
[6] J. G. Daunt and K. Mendelssohn, Proc. Roy. Soc. A **185**, 225 (1945).
[7] Abraham, Weinstock, and Osborne, Phys. Rev. **76**, 864 (1949). The author is indebted to Dr. Osborne for putting these data at his disposal before publication.

The Beta-Spectrum of Tritium

S. C. CURRAN, J. ANGUS AND A. L. COCKROFT
Department of Natural Philosophy, University of Glasgow, Glasgow, Scotland
July 27, 1949

IN continuation of the investigation of the β-spectrum of H^3 reported elsewhere,[1] a more detailed study has been made of the shape of the spectrum near the end point. The proportional counter technique previously described[2] has again been used with a photographic method of recording and analyzing the output pulses.

This study was designed to increase the accuracy of the determination of the shape of the spectrum close to the end-point energy E_0, and also to obtain a more accurate estimate of the correction which must be made to the spectrum in view of the experimental limitations resulting from the finite resolution of the instrument.

Energy calibration was provided by a beam of K_α x-rays of molybdenum (17.4 kev). The half-width for half-intensity for this line was 900 ev (~5 percent), and the parts of the theoretical Fermi curves shown in Fig. 1 have been modified to allow for the spread arising from a resolution corresponding to this line width. The curves have been calculated for true upper energy limits (E_0) of 18.0 and 18.6 kev with a neutrino mass $\mu=0$ kev, and for $E_0=18.0$ kev and $\mu=1$ kev. They may therefore be compared directly with the observed experimental points. For $\mu=0$ the points lie between the two curves for $E_0=18.0$ and $E_0=18.6$ kev, which brings our results into rather close agreement with those of Hanna and Pontecorvo;[3] the higher energy value would also give slightly better agreement with the theoretical Fermi curve over the whole energy range previously investigated.[1] Alternatively, for $E_0=18.0$ kev, it may be assumed that μ lies between 0 and 1

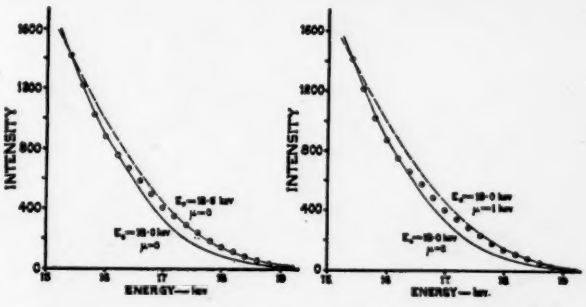

FIG. 1. Comparison of experimental and theoretical Fermi curves for tritium near the end point.

kev, in agreement with our earlier interpretation. It appears, however, that the line width is too large to allow a significant differentiation between these two cases; it has been pointed out already[2,4] that this line width arises principally from variations about the average number of ion pairs produced by the β-rays in the initial ionization process, and it is unlikely that the uncertainty will be resolved by relatively slight increases in the accuracy of measurement.

We should like to take this opportunity of thanking Professor P. I. Dee for his advice throughout the work and we are indebted to Dr. W. B. Lewis for a number of helpful comments and suggestions.

[1] Curran, Angus, and Cockroft, Nature **162**, 302 (1948); Phil. Mag. **40**, 53 (1949).
[2] Curran, Angus, and Cockroft, Phil. Mag. **40**, 36 (1949).
[3] G. C. Hanna and B. Pontecorvo, Phys. Rev. **75**, 983 (1949).
[4] Hanna, Kirkwood, and Pontecorvo, Phys. Rev. **75**, 985 (1949).

On Positive Excess of Meson Component near Sea Level

P. Bassi, E. Clementel, I. Filosofo, and G. Puppi
Centro per lo Studio degli Ioni veloci del CNR, Istituto Fisico dell'Università di Padova, Italy
August 3, 1949

THE scarcity of experimental data concerning the distribution of positive excess in the meson spectrum and the common opinion that the positive excess is closely related to the meson production by the N component, lead us to perform an experiment at sea level, in which positive and negative mesons are separated by means of a magnetic field of 14,000 gauss in air. The experimental apparatus is shown in Fig. 1.

The upper telescope consists of five channels of double coincidences 1−1, 2−2···5−5, which limits a not strictly convergent beam of cosmic rays traversing the central region of magnetic field. The field focuses particles of $pc=2\,2\cdot10^8$ ev which are revealed by counters CDE; $C'D'E'$.

Putting in S 4.7 cm of lead, fivefold coincidences register only mesons, the fourfold, besides mesons, protons and electrons. The absorber T has the object of degradating the energies of incident

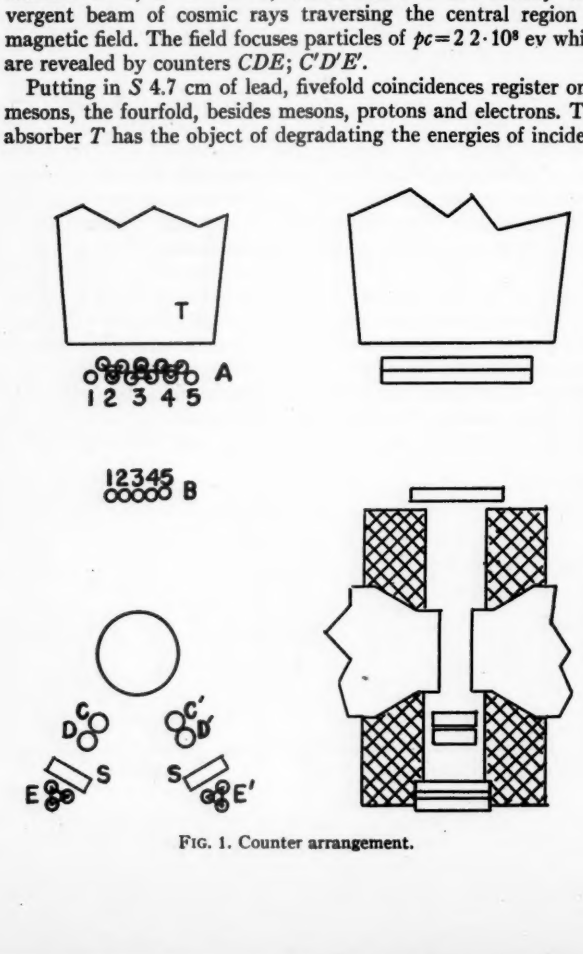

FIG. 1. Counter arrangement.

TABLE I. Experimental results for coincidence rates.

Absorber thickness (g/cm² Pb)	Counts per hour	δ	[IV−V]⁻	[IV−V]⁺
290 g/cm²	1.18±0.06	0.16±0.10	0.13±0.03	0.04±0.02
540 g/cm²	1.36±0.06	0.22±0.12	0.10±0.06	0.02±0.04
1150 g/cm²	1.14±0.05	0.25±0.07	0.20±0.04	0.04±0.05

particles. Experimental results and their probable errors are reported in Table I.

In the second column counts per hour are shown, they agree with the Wilson spectrum. In the third column, the excess as commonly defined by

$$\delta=2\frac{N_+-N_-}{N_++N_-}$$

is indicated.

The first two plots are in a good agreement with the previous data by Nereson[1] and Conversi, Pancini, and Piccioni;[2] the value of the excess in the third plot, on the contrary, is remarkably high, and indicates that, at least for energies up to 2 Bev, the excess does not decrease. This is in agreement with a recent isolated result by Brode[3] who finds an excess about 0.3 for energies from 1.4 to 2 Bev. The fourth column indicates the number of negative particles per meson whose energies are about 2.2×10^8 ev and which do not penetrate 4.7 cm of lead. They should in the first line be interpreted as knock-on electrons. The fifth column is concerned with positive particles that we may explain as protons, but the last data are less significant because of large errors.

The present results may be explained in terms of multiple meson production with the existence of two sources distributed in the atmosphere, of which the first formed by mesons created in the first collision by primary protons is substantially responsible for the excess A detailed paper will be submitted for publication in *Nuovo Cimento*.

[1] N. Nereson, Phys. Rev. **73**, 565 (1948).
[2] Conversi, Pancini, and Piccioni, Phys. Rev. **71**, 209 (1947).
[3] R. B. Brode, Phys. Rev. **76**, 468 (1949).

Heat Flow in Metals below 1°K and a New Method for Magnetic Cooling

C. V. Heer and J. G. Daunt
Mendenhall Laboratory, Ohio State University, Columbus, Ohio
August 8, 1949

MEASUREMENTS have been made of the thermal conductivities of tin and tantalum both in the superconducting and normal states in the temperature range 0.2° to 1°K and experiments have been carried out on the question of thermal contact by heat flow through superconductors in this temperature range. The preliminary results of these experiments may be of interest in connection with two stage magnetic cooling methods, such as have been proposed for the study of nuclear paramagnetism[1] and consequently are reported herewith. In addition the experiments have led to a convenient method for adiabatic magnetic cooling.

The general experimental arrangements consisted of two chromium potassium alum ellipsoids (one approximately five times the volume of the other) separated from one another by a distance of about 10 cm and connected thermally by the superconducting metal specimen under investigation. The salt-metal connection was made by high pressure molding of the salt powder. The salt ellipsoids were differentially cooled to low temperatures by the magnetic method,[2] and the thermal conductivity of the metal link between them calculated from observations of the rate

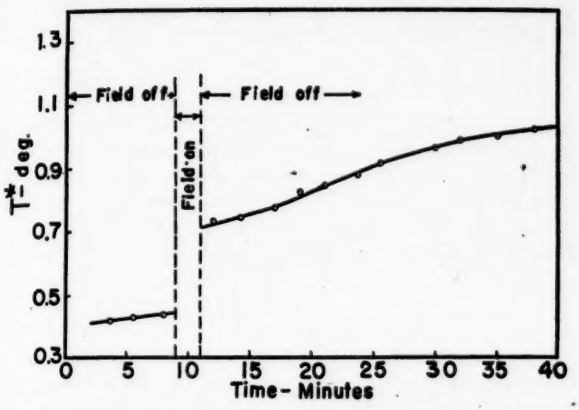

FIG. 1. Sample warm-up curve for a 3 cc chromium potassium alum ellipsoid.

of warm-up of the ellipsoids. Temperatures were calculated from ballistic mutual inductance measurements of the susceptibilities of the ellipsoids as described in previous publications.[2]

The thermal conductivity of both Sn and Ta was found to be considerably smaller in the superconducting state than in the normal state; for example for Ta the ratio of these conductivities, K_s/K_n, was found to be somewhat less than 1/60 at 0.55°K, and for Sn, $K_s/K_n \simeq 1/40$ at 0.65°K. It appeared that below 1°K the thermal conductivity of two different samples of Sn of the same purity could be expressed by $K_s = cT^3$ with $c = 1.1 \times 10^{-2}$ watt-unit. The results both for Sn and Ta were approximately such as would be expected if $K_s/K_n = (T/T_c)^2$, a relationship that can be deduced if at these low temperatures the thermal resistance is largely due to impurity scattering. Our measured values of K_s/K_n below 0.6°K were higher than those given theoretically by Heisenberg.[3]

By extrapolation our results to lower temperatures (<0.1°K) it would appear the ratio K_s/K_n would become very small, e.g., for Sn at 0.01°K, $K_s/K_n \simeq 7 \times 10^{-6}$, effectively describing the superconducting state as a thermal insulator.[4] Heat contact could therefore be made or broken, as process necessary for example for a two stage magnetic cooling system,[1] by having a metallic link either in the normal or superconducting state, a change that can easily be affected by the application of small external magnetic fields.

In experiments with magnetic cooling systems, it has been found sufficient to connect thermally the paramagnetic salt with the helium bath by a fine wire of superconducting material having a high transition temperature and dispense with the usual exchange gas. During magnetization at 1°K the wire is in the normal state and effectively conducts to the bath the heat of magnetization. On demagnetization the metallic link between the paramagnetic salt and the helium bath becomes superconductive and forms a satisfactory insulating support. Such a technique not only has the advantage of dispensing with exchange gas and its attendant equipment, but also the long periods of magnetization, which are generally required in order to pump out exchange gas, are considerably reduced. As an example of the effectiveness of this procedure we give in Fig. 1 a warm-up curve for a 3 cc chromium potassium alum ellipsoid thermally connected to a helium bath at 1.13°K through 56 cm of 0.017-cm diameter tantalum wire. From minute 0 to minute 9, the wire was in the superconducting state and the heat influx to the ellipsoid was approximately 7.3 ergs/sec. From minute 9 to minute 11 the Ta wire was transformed into the normal state by the application of a transverse field of 600 gauss. As a result the temperature of the ellipsoid rose immediately to 0.71°K, corresponding to a heat gain of 1.5×10^4 ergs. At minute 11 the wire being again in the superconducting state the heat influx to the ellipsoid fell back again to 6.7 ergs/sec.

The new technique outlined here would become still more effective if heat barriers composed of additional salt systems were employed[5] and experiments are now being carried out on this extension of the technique.

[1] Simon, Reports of Conference on Magnetism at Strasbourg, 1939 (Institut International de Cooperation Intellectuelle, 1940), Vol. III, p. 1.
[2] For further detail see J. G. Daunt and C. V. Heer, Phys. Rev. **76**, 715 (1949).
[3] W. Heisenberg, Zeits. f. Naturforschung **3a**, 65 (1948).
[4] A discussion of these possibilities has been made also by Casimir, Oak Ridge Conference on Nuclear Physics and Low Temperatures, August 7, 1948.
[5] Cooke and Hull, Proc. Roy. Soc. **181**, 83 (1942).

Ion Source for Mass Spectrography

R. F. K. HERZOG AND F. P. VIEHBÖCK
I. Physics Institute, University of Vienna, Vienna, Austria
August 1, 1949

IT is known that the cathode material of a canal-ray tube sputters during the discharge. In this case neutral molecules or negative ions only can leave the cathode because positive ions are strongly linked to the cathode by the electric field. Those few neutral molecules only, which are ionized by accident on the axis of the discharge tube, especially near the anode, may leave the tube in form of canal-rays, if they are not scattered by gas molecules. Though the number of these particles may be very small and therefore the intensity low, this process has been successfully tried in many investigations in mass spectrography.

We have improved this method very materially:

(1) There are two electric fields: First the electric field in the canal-ray tube (*A*), (see Fig. 1) which is completely separated from the electric field immediately in front of the trial-substance (*C*). The first one produces the beam (*B*) of canal-rays, which causes the sputtering. The second one has the right direction to remove and accelerate the positive ions of the trial-substance for analysis in a mass spectrograph. It is produced by the cylinders (*D*) and (*E*), which are at different voltages.

(2) The sputtering takes place in a high vacuum, because the gas-filled canal-ray tube (*A*) is separated by the narrow canal (*K*) (which has a large gas-current resistance) from the space in front of the substance. This space is connected with a pump of high pumping speed. Hereby, losses by scattering on gas molecules can be avoided almost completely.

(3) All ions will be produced on an electric equipotential-surface and will be accelerated by the same voltage. Therefore the ions get a uniform energy. Hence of producing a mass spectrogram a magnetic field alone is sufficient, which is a great advantage. But it is an advantage too for mass spectrographs with energy-focusing,

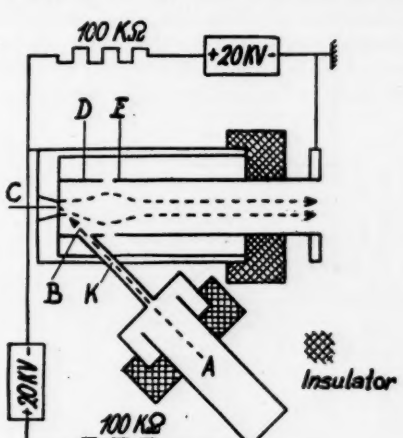

FIG. 1. Schematic diagram of suggested ion sources.

if the ions have already a nearly uniform energy, because the losses may be avoided, which always otherwise arise, if the rays hit the screen, which limits the small interval of energy.

(4) The electric field between the cylinders (D) and (E), which accelerates the positive ions of the substance, will be formed so that it works as an electron-optic lens and produces a nearly parallel beam of rays.

We have tried out such an arrangement, and found it to work most satisfactorily. The intensity is dependent on the trial-substance and was large for metals and smaller for salts. The analysis in the parabola-spectrograph shows the ions of the trial-substance and the ions of the primary canal-ray discharge, all having the same energy.

On the Spin of μ-Mesons

J. TIOMNO*
Palmer Physical Laboratory, Princeton, New Jersey
August 8, 1949

THE known processes resulting from the interaction of μ-mesons with other elementary particles:

$$\pi \rightarrow \mu + \mu_0, \quad (1)$$

$$\mu \rightarrow \mu_0 + e + \nu, \quad (2)$$

$$P + \mu^- \rightarrow N + \mu_0 \quad (3)$$

give very little indication on the spin of μ-mesons. We can only say that μ and μ_0 have both integral or half-integral spin.

As in all these processes μ appears together with μ_0 we shall assume that they are two different states of charge of the same particle and thus that they have the same spin.

The possibility of a spin $\frac{1}{2}$ for these particles has been already considered[1] (in particular if μ_0 is a neutrino). Although the hypothesis of μ_0 being a neutrino is very appealing, it seems that one should not neglect the other possibilities, in particular that it has an integer spin. From the analysis of the frequency of bursts produced by cosmic-ray mesons at sea level (mostly μ-mesons), Christy and Kusaka[2] excluded the value 1 for the spin of these mesons. If we exclude values higher than 1 (which may eventually result from an extension of Christy-Kusaka's calculations) we are left only with the values 0 and $\frac{1}{2}$.

We want to show here that a zero spin for the μ-meson with a special type of coupling with electron, neutrino and nucleons is in good agreement with the experimental results.

Let us consider first the μ-decay. We describe μ and μ_0 mesons by scalar (or pseudoscalar) fields, respectively complex (Φ) and real (φ). In order that μ-decay be a first-order process we take the interaction Lagrangean bilinear[3] in the mesonic fields; the most general one that can be formed using at most first derivatives[4] of the mesonic fields *and* of the electron-neutrino wave functions (ψ)[5] is:

$$L_{\text{int}} = \psi^+ \left\{ \left[g_1 \Phi \varphi + \frac{g_2}{\kappa} \varphi \frac{\partial \Phi}{\partial x^\sigma} \gamma_\sigma + 2 \frac{g_3}{\kappa^2} \frac{\partial \varphi}{\partial x^\rho} \frac{\partial \Phi}{\partial x^\sigma} \gamma_{\rho\sigma} \right] \tau_- + c.c. \right\} \psi, \quad (4)$$

where $\kappa = \mu c/\hbar$ and $\gamma_{\rho\sigma} = i(\gamma_\rho \gamma_\sigma - \gamma_\sigma \gamma_\rho)$, τ_- being an operator that transforms an electron into a neutrino. The probability per second of μ-decay in which the electron is produced with a momentum in the interval p_e, $p_e + dp_e$ is then proportional to:

$$dp_e \left\{ |g_1|^2 f_1\left(\frac{p_e}{\mu c}\right) + |g_2|^2 f_2\left(\frac{p_e}{\mu c}\right) + |g_3|^2 f_3\left(\frac{p_e}{\mu c}\right) + \frac{i}{2}(g_1 g_2^* - g_2 g_1^*) \cdot f_{13}\left(\frac{p_e}{\mu c}\right) \right\} \cdot \quad (5)$$

The functions f are shown, for $\mu_0 = 0$ as consistent with the experimental results,[6,7] in the upper left part of Fig. 1; the experimental points of Anderson and co-workers[7] are also plotted in an arbitrary scale. It is seen that the only one of the simple couplings which gives a spectrum in agreement with the experimental points is the one in g_2.[8] This agreement may be emphasized if one compares the integral spectrum ($\sim E_e^3[2\mu c^2 - 3E_e]$) with the experimental points, as is done in the lower part of Fig. 1.

If we consider now the capture of a μ-meson by a nucleus we calculate the nuclear excitation as in case of spin $\frac{1}{2}$,[1] using for the interaction of μ, μ_0-mesons with nucleons an expression similar to (4); we then obtain a spectrum of nuclear excitation very similar to that of the case of spin $\frac{1}{2}$ and, then, also the result that the probability for star production is very small.[9]

One then concludes that the possibility of spin zero for μ_0-mesons is in good agreement with the experimental results and should not be disregarded for the moment.

We are grateful to Drs. J. L. Lopes and L. L. Foldy for helpful discussions. This work was assisted by the joint program of the ONR and the AEC.

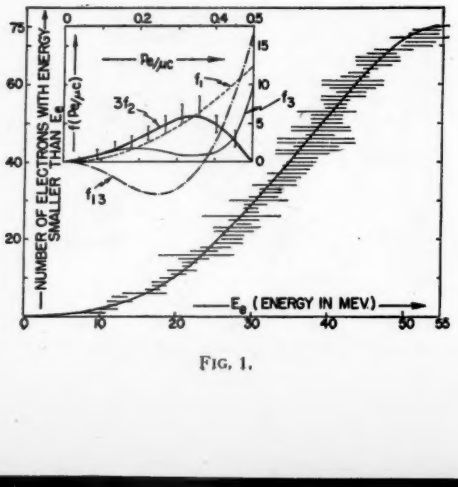

FIG. 1.

* Rockefeller Foundation fellow of the University of São Paulo, Brazil.
[1] J. Tiomno and J. A. Wheeler, Rev. Mod. Phys. **21**, 144, 153 (1949).
[2] R. F. Christy and S. Kusaka, Phys. Rev. **59**, 414 (1941).
[3] The possibility of a coupling of μ, μ_0 with the electron-neutrino field, linear in each mesonic field is easily excluded in view of the impossibility of making the process (2) significantly more probable, then:

$$\mu \rightarrow e + \nu \rightarrow e + \nu + h\nu.$$

[4] We exclude terms with two time derivatives of ϕ, φ and ψ as they lead to difficulties in the application of the usual Hamiltonian formalism.
[5] Terms with derivatives of ψ are, to first order, equivalent to terms of the kind considered in (4).
[6] C. M. G. Lattes, Phys. Rev. **75**, 1468 (1949).
[7] Leighton, Anderson, and Seriff, Phys. Rev. **75**, 1432 (1949).
[8] A rough agreement can also be obtained with $g_3 = 0$, $g_1 = ig_2$.
[9] It should be pointed out that assuming that the interaction of spinless μ-mesons with nucleons is through an intermediate κ-meson we obtain a lifetime for the $\pi - \mu$-decay of the order of 10^{-8} sec. as shown by A. S. Lodge (Nature **161**, 809 (1948)), R. Latter and R. F. Christy (Phys. Rev. **75**, 1459 (1948)) and others.

Analysis of Delayed Coincidence Counting Experiments

DANIEL BINDER
Sloane Physics Laboratory, Yale University, New Haven, Connecticut*
August 8, 1949

THE use of the delayed coincidence method for measuring short half-lives by several investigators[1-4] makes a re-examination of the basis of the experiment desirable. The coincidence counting rate *versus* delay curves exhibit two regions. The first is affected by the random delays in the counter itself, and the second is a pure exponential decrease determined by the radioactive decay. Van Name[3,5] analyzed the combination of these effects by assuming a triangular distribution for the delays in the counter but found it necessary to divide the range of artificial delays into six regions. A Gaussian distribution will be used here, and a fairly simple relation will result.

Consider a fast particle passing through both counters of a two-channel circuit at the time $t=0$. We assume that the probability that a pulse is formed between t and $t+dt$ is

$$w(t)dt=\frac{1}{(2\pi)^{\frac{1}{2}}\langle\Delta t\rangle_{Av}}\exp\left[-\frac{(t-\bar{t})^2}{2\langle\Delta t\rangle_{Av}^2}\right]dt,$$

where $\langle\Delta t\rangle_{Av}$ is the r.m.s. deviation from the mean time $\bar{t}$. If $\bar{t}_1$ and $\bar{t}_2$ are the mean statistical delays in channels 1 and 2, and t_D is the artificial delay introduced in channel 1, then, assuming the resolving time τ of the electronic circuit to be small compared to $\langle\Delta t\rangle_{Av}$ the relative coincidence rate is

$$C=2\tau\int_{-\infty}^{\infty}w_1(t)w_2(t)dt,$$

where

$$w_1(t)=\frac{1}{(2\pi)^{\frac{1}{2}}\langle\Delta t\rangle_{Av}}\exp\left[-\frac{(t-\bar{t}_1-t_D)^2}{2\langle\Delta t\rangle_{Av}^2}\right],$$

and

$$w_2(t)=\frac{1}{(2\pi)^{\frac{1}{2}}\langle\Delta t\rangle_{Av}}\exp\left[-\frac{(t-\bar{t}_2)^2}{2\langle\Delta t\rangle_{Av}^2}\right].$$

Integration gives

$$C(D)=\frac{\tau}{\pi^{\frac{1}{2}}\langle\Delta t\rangle_{Av}}\exp\left[-\left(\frac{D}{2\langle\Delta t\rangle_{Av}}\right)^2\right], \quad (1)$$

where

$$D\equiv t_D+\bar{t}_1-\bar{t}_2.$$

An excellent fit is obtained in Fig. 1 between Eq. (1) and the data of W. J. MacIntyre of this Laboratory for $\langle\Delta t\rangle_{Av}=1.85\times10^{-8}$ sec. The zero of delay is, of course, arbitrary in any measurement. The experimental points are for a proportional counter and a polystyrene scintillation counter with a P^{32} source. A similar fit is obtained for two proportional counters, supporting the assumption in the following work that $\langle\Delta t\rangle_{Av}$ is the same for the two types of counters.

Now consider two particles emitted in cascade, the first entering the counter of channel 1 and the second, the counter of channel 2 a time t' later. Then the coincidence rate is

$$C(D,t')=\frac{\tau}{\pi^{\frac{1}{2}}\langle\Delta t\rangle_{Av}}\exp\left[-\left(\frac{D-t'}{2\langle\Delta t\rangle_{Av}}\right)^2\right].$$

The probability thar the second particle is emitted between t' and $t'+dt'$ seconds later is

$$w(t')dt'=\lambda e^{-\lambda t'}dt',$$

where λ is its decay constant. Thus the relative number of coincidences as a function of D and λ is

$$C(D,\lambda)=\frac{\tau}{\pi^{\frac{1}{2}}\langle\Delta t\rangle_{Av}}\int_0^{\infty}\lambda e^{-\lambda t'}\exp\left[-\left(\frac{D-t'}{2\langle\Delta t\rangle_{Av}}\right)^2\right]dt'.$$

Finally we have

$$C(D,\lambda)=Ae^{-\lambda D}\left[1-\Phi\left(\lambda\langle\Delta t\rangle_{Av}-\frac{D}{2\langle\Delta t\rangle_{Av}}\right)\right], \quad (2)$$

where

$$A\equiv\lambda\tau\exp[\lambda^2\langle\Delta t\rangle_{Av}^2]=\text{const.}$$

and

$$\Phi(x)\equiv\frac{2}{\pi^{\frac{1}{2}}}\int_0^x\exp(-y^2)dy.$$

Note that Eq. (2) predicts a pure exponential decrease in $C(D,\lambda)$ for large D since Φ approaches -1. It may be used to find the value of D at which the curve becomes exponential when $\langle\Delta t\rangle_{Av}$ is known.

Equation (2) agrees well with MacIntyre's data[4] for the 2.3×10^{-8} sec. metastable state of Hg^{198} as shown in Fig. 2. Ten percent variations in the reported value of λ of 3×10^7 sec.$^{-1}$ cause marked differences in the theoretical coincidence rate for positive delays, thus supporting the 10 percent accuracy claimed by MacIntyre.

Equation (2) may also be used to find the shortest half-life detectable by an asymmetry in the *C versus D* curves. Computation shows that an asymmetry can still be observed with the above-mentioned equipment for a half-life of 1×10^{-8} sec., and that this disappears for 0.7×10^{-8} sec.

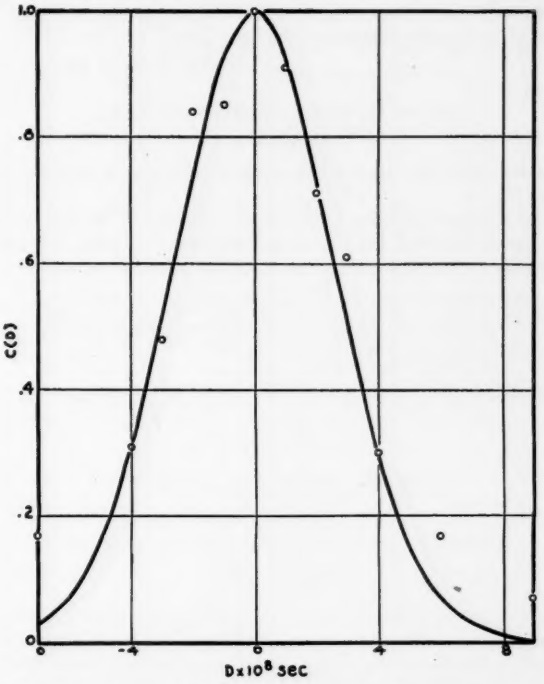

FIG. 1. $C(D)$ *versus* D with experimental points for a proportional and a polystyrene scintillation counter.

When τ is not small compared to $\langle\Delta t\rangle_{Av}$, a calculation similar to that given by Bradt and Scherrer[6] for the integral curve method may be performed. Here we have

$$C(D)=\int_{-\tau}^{\tau}dT\int_{-\infty}^{\infty}w_1(t)w_2(t-T)dt$$
$$=\tfrac{1}{2}\left[\Phi\left(\frac{\tau+D}{2\langle\Delta t\rangle_{Av}}\right)+\Phi\left(\frac{\tau+D}{2\langle\Delta t\rangle_{Av}}\right)\right] \quad (3)$$

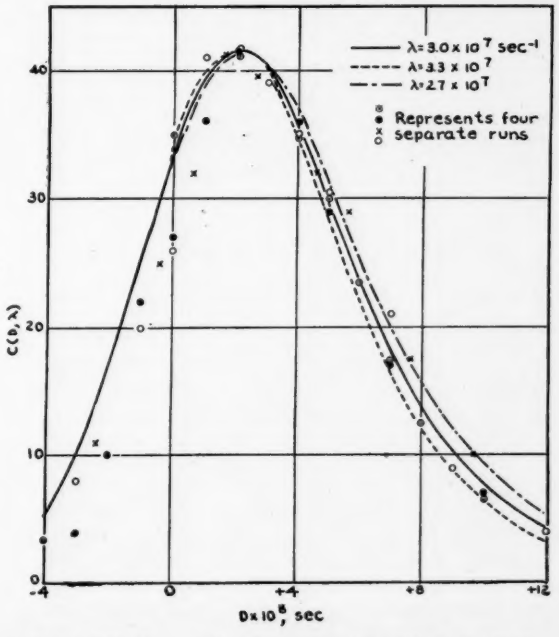

FIG. 2. $C(D,\lambda)$ *versus* D with experimental points for the Hg^{198} metastable state.

and

$$C(D,\lambda)=C(D)+\tfrac{1}{2}e^{\alpha^2/4}\{e^{\alpha x_1}[1-\Phi(x_1+\tfrac{1}{2}\alpha)] - e^{-\alpha x_2}[1+\Phi(x_2-\tfrac{1}{2}\alpha)]\}, \quad (4)$$

where

$$x_1\equiv(\tau-D)/2\langle\Delta t\rangle_{Av}, \quad x_2\equiv(\tau+D)/2\langle\Delta t\rangle_{Av}, \quad \alpha\equiv 2\lambda\langle\Delta t\rangle_{Av}.$$

Equation (4) also approaches a pure exponential decrease for large D.

The author would like to thank Mr. William J. MacIntyre for the use of his data and Professor Howard L Schultz for many discussions concerning coincidence techniques.

* Assisted by the joint program of the ONR and the AEC.
[1] S. D. Benedetti and F. K. McGowan, Phys. Rev. **74**, 728 (1948).
[2] P. T. Bittencourt and M. Goldhaber, Phys. Rev. **70**, 780 (1946).
[3] F. W. Van Name, Phys. Rev. **75**, 100 (1949).
[4] W. J. MacIntyre, Phys. Rev. **76**, 312 (1949).
[5] F. W. Van Name, Ph.D. dissertation.
[6] H. Bradt and P. Scherrer, Helv. Phys. Acta **16**, 251 (1943).

On the Half-Life of Na^{22}

L. Jackson Laslett
*Institute for Atomic Research and Department of Physics, Iowa State College, Ames, Iowa**
August 8, 1949

THE radioactivity of Na^{22}, first discovered by Frisch,[1] has been described by the present writer[2,3] as producible by the deuteron bombardment of magnesium and the half-life estimated as 3.0 years.[3] More recently, Saha[4] has given a value of 2.8 years for the half-life of this activity. During the past three years the decay of a Na^{22} sample has been followed in this laboratory and it is the purpose of the present note to report the value obtained for the half-life.

The Na^{22} sample used was produced in 1937 by the bombardment of magnesium metal with deuterons produced by the cyclotron in Professor Lawrence's laboratory at Berkeley. The magnesium target was subsequently mounted in the recess of a brass plate, covered with a mica sheet hermetically sealed to the brass, and, by means of a Lauritsen electroscope,[5] its activity was compared at intervals with that from a standard uranium oxide source

The resultant decay curves, for two different source positions, are shown in Fig. 1 and indicate a half-life of 948 days or 2.60 years.[6] It should be mentioned that diffusion of the active material from the surface into the magnesium metal would, if appreciable, result in an underestimation of the half-life, since the greater portion of the activity measured was readily absorbable (positrons). Some confirmation of the belief that diffusion and similar processes played no significant role in the present work is afforded, however, by the observation that absorption curves taken at the beginning and end of the measurements (curves 1 and 2 of the insert, Fig. 1) appeared entirely similar and were in agreement with one obtained[3] shortly after the sample was first prepared.

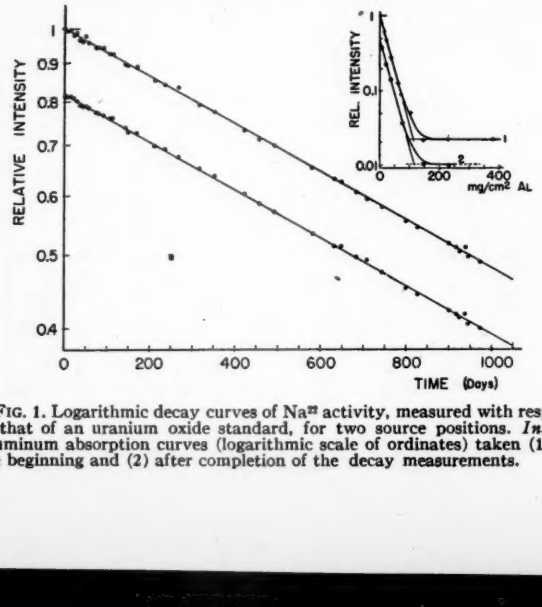

FIG. 1. Logarithmic decay curves of Na^{22} activity, measured with respect to that of an uranium oxide standard, for two source positions. *Insert*: Aluminum absorption curves (logarithmic scale of ordinates) taken (1) at the beginning and (2) after completion of the decay measurements.

It is a pleasure for the writer to indicate once again his gratitude to Professor Lawrence for the privilege of using the cyclotron in connection with the preparation of the sample used in the work reported here.

* Contribution No. 80 from the Institute for Atomic Research. Work performed at the Ames Laboratory of the AEC.
[1] O. R. Frisch, Nature **136**, 220 (1935).
[2] L. J. Laslett, Phys. Rev. **50**, 388(A) (1936).
[3] L. J. Laslett, Phys. Rev. **52**, 529 (1937).
[4] N. K. Saha, Trans. Bose Res. Inst. (Calcutta) **14**, 57 (1939–41); cited in Chem. Abstracts **42**, 450i (1948).
[5] The electroscope, manufactured by the F. C. Henson Company (Pasadena), was used to measure the ionization in a chamber approximately 2½ inches in diameter and 3 inches long, into which the radiation passed through an aluminum window of 1.2 mg/cm² surface density. The surface density of the mica covering the source was 5.2 mg/cm². We are indebted to Dr. A. F. Voigt for making available to us this electroscope in its modified form.
[6] A value of 2.6 years was provisionally communicated to Dr. G. T. Seaborg during the course of this work and has subsequently appeared in the review article of Seaborg and Perlman (Rev. Mod. Phys. **20**, 585 (1948)).

Microwave Spectrum of CF_3Cl

D. K. Coles and R. H. Hughes
Westinghouse Research Laboratories, East Pittsburgh, Pennsylvania
August 1, 1949

THE CF_3Cl rotational transitions between $J=2$ and 3 and between $J=3$ and 4 have been observed in the microwave regions around 20 kmc and 27 kmc. Thirty-one lines were measured, including five lines which are attributed to molecules in an excited vibrational state. The hyperfine structure spacing yields quadrupole coupling constants of 78.05±0.2 and 61.44±0.4 mc for CF_3Cl^{35} and CF_3Cl^{37}, respectively.

At a pressure of 0.1 mm, the line widths were approximately 5 mc, corresponding to a molecular collision cross section of 1400A².

The values of B_0 for CF_3Cl^{35} and CF_3Cl^{37} were found to be 3335.56 and 3251.51 mc, respectively. From these values one may calculate that the distance of the Cl nucleus from the center of mass of the CF_3 group is 2.129A, and that the moment of inertia of the CF_3 group about an axis through its center of mass and perpendicular to the symmetry axis is 46.31 mass units times angstroms².

If one assumes tetrahedral angles, one then obtains for the internuclear distance C−F=1.323A and C−Cl=1.765A. These are quite consistent with electron diffraction values on similar fluorochloromethanes.

Hyperfine Structure of Fe 57*

Jean Brossel
Spectroscopy Laboratory, Massachusetts Institute of Technology, Cambridge, Massachusetts
August 1, 1949

A SEARCH for the hyperfine structure of Fe 57 was carried out by means of a Fabry-Perot interferometer, crossed with a 35-foot concave grating in the Wadsworth stigmatic mounting (the blaze being in the second order).

The wave-length scale covered extended between 6000A and 2400A. No structure, broadening, or asymmetry was found. The resolution obtained would have revealed any over-all structure greater than $25\cdot10^{-3}$ cm^{-1} between 6000 and 4000A and $50\cdot10^{-3}$ cm^{-1} near 2500A. The discharge tube was a hollow cathode cooled with liquid nitrogen, the carrier being argon with a trace of helium. The spectrum was very extensive and was readily photographed. At least 400 lines were examined. Among others, the following electron configuration of Fe I were involved: $3d^74s$, $3d^64s4p$, $3d^64s4d$ and $3d^64s5s$, $3d^64s^2$, $3d^74p$. It was not found possible to excite Fe II by changing widely the conditions of the discharge.

TABLE I.

λ	Classification	$\Delta\nu_{calc.}$ 10^{-3} cm^{-1}	$\Delta\nu_{meas.}$ 10^{-3} cm^{-1}	
5446·920	$\left\{\begin{matrix} a^5F_2-z^5D_2^0 \\ (a^3F_2-z^3D_2^0)\end{matrix}\right\}$	+160		very weak—not measured
5404·144	$\left\{\begin{matrix} z^5G_4^0-e^5H_5 \\ (z^5G_3^0-f^5G_3)\end{matrix}\right\}$	+120	+117	
4210·352	$z^7D_1^0-e^7D_1$		−226	
4466·554	$\left\{\begin{matrix} b^3P_2-x_2D_3^0 \\ (a^5D_1-z^7F_0^0)\end{matrix}\right\}$	−120	−77	
3684·108	$a^3G_4-y^3D_3^0$		−227	
3682·226	$a'D_2-w'D_2^0$		+245	
3605·450	$\left\{\begin{matrix} a^5G_4-y^5H_4^0 \\ (z^7F_6^0-f^7D_5)\end{matrix}\right\}$	−400	−368	
3383·692	$\left\{\begin{matrix} a^5P_2-w^5D_1^0 \\ (b^5G_5-9_4^0)\end{matrix}\right\}$	+140		very weak—not measured same intensity
3306·356	$\left\{\begin{matrix} a^5P_1-y^5P_2^0 \\ (a'G_4-w'G_4^0)\end{matrix}\right\}$	+50	132	
3239·436	$\left\{\begin{matrix} z^7D_4^0-f^5D_4 \\ (z^7D_1^0-f^5D_1)\end{matrix}\right\}$	−220	−224	
3214·044	$\left\{\begin{matrix} z^7D_3^0-e^7P_2 \\ (z^5F_4^0-g^5G_5) \\ (z^7D_4^0-f^7D_3)\end{matrix}\right\}$	+380 +530	+360 +490	
3199·530	$\left\{\begin{matrix} z^7D_4^0-f^7D_4 \\ (a^5D_1-z^5F_2^0)\end{matrix}\right\}$	+290	+302	
3125·653	$\left\{\begin{matrix} a^5F_2-z^5D_2^0 \\ (z^7D_5^0-e^7G_4)\end{matrix}\right\}$	−30	+297	
2970·106	$\left\{\begin{matrix} a^5D_1-y^5F_2^0 \\ a^5D_2-z^3P_1^0\end{matrix}\right\}$	−210	−230	

The above results are in agreement with those reported recently[1] and similar to those concerning Ni 61.

A point which might be of interest that was noticed during the course of the research was the resolution of a few lines coinciding accidentally that have not been reported before. These lines are listed below with Russell's[2] classifications, the separations calculated from the term analysis, and the separations actually observed (see Table I). ($\Delta\nu>0$ means that the weak component has a higher frequency than the strong component from which it is measured.)

There is agreement with the Zeeman effect data of D. W. Weeks.[2]

The sample of Fe 57, enriched to 68 percent, was provided by the AEC.

* Assisted by the joint program of the ONR and the AEC.

[1] M. Gurevitch and J. G. Teasdale, Phys. Rev. **76**, 151 (1949).
[2] Russell, Moore, and Weeks, Trans. Am. Phil. Soc. **34**(II) (December 1944).

Energetic Events in Emulsions at High Altitude*

J. HORNBOSTEL AND E. O. SALANT
Brookhaven National Laboratory, Upton, Long Island, New York
August 4, 1949

IN Eastman NTB3 emulsions, exposed with planes vertical at 93,000 feet for 6 hours near Cuba (31° geomagnetic north; vertical cut-off 8 Bev[1]), many stars show straight, light tracks of minimum and near-minimum grain density, in addition, of course, to the heavy prongs visible in ordinary, less sensitive emulsions. While the light tracks can be safely ascribed to fast particles, of relativistic and near-relativistic kinetic energies, and are thought due at least in part to mesons, the portions of tracks within the emulsions are too short to decide from their appearance whether the particles are electrons, mesons or protons. Near-minimum grain densities refer to kinetic energies between 0.2 and 0.6 rest energy.

Out of 124 stars with light tracks, 76 showed, in the hemisphere above the star, a minimum ionization track, which is taken to be that of the incoming particle initiating the disintegration, either a primary proton or, in possibly a third of the events, a secondary of comparable energy, ejected from the thin (15 g/cm²) atmosphere above the plates.

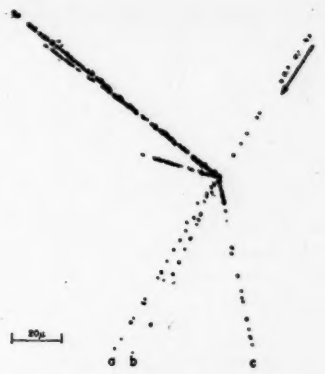

FIG. 1. Disintegration with 4 minimum ionization tracks within 43° and 4 heavy prongs. Between *a* and *b* are 3 min.-ion tracks within 20°, one dipping out of focus. Fourth track *c* is within 43° of *a*. Background removed.

Figures 1 and 2 are microphotographs of stars with some characteristic features of the light tracks (arrow indicates track of incident particle). Selecting the 47 events with 4 or more light tracks, 35 of them show 3 or more light tracks fanning out downward, roughly in the direction of the incident particle, giving the appearance of a broom. But in 10 of the broom, the handle, i.e., the incident particle, is missing, and while a few misses could arise from possible closeness to the inconvenient normal to the plate, the rest are attributable to non-ionizing radiation, presumably energetic neutrons. In the remaining 12 events, the fast particles appear uncollimated.

Outgoing light tracks in these brooms number 6 on the average, extending up to 12, and 120 of the 210 tracks have minimum ionization, the angles of near-minimum tracks being widely and rather uniformly spaced. In 27 of the brooms, there are usually 3 or 4, sometimes as many as 9, minimum ionization tracks, contained within a narrower broom, with angular spread generally between 50° and 100°. In 8 of these events, about the same number of minimum ionization tracks are in a still narrower core, of less than 20° spread. Thus it appears that the relativistic particles are more closely collimated than the near-relativistic and their angular spreads tend to fall into two groups. There is also evidence, though not yet statistically sound, for some fast particles to be created in pairs, within a few degrees of each other.

Considering, now, the stars' heavy prongs (uncollimated), 70 out of 90 of those stars with enough heavy prongs to be assigned to disintegrations of the heavy nuclei Ag, Br and I show emission of relativistic or near-relativistic particles. Very energetic stars, with up to 36 heavy prongs and 7 light tracks are observed. Even with an average of 35 Mev per prong found by Harding, Lattimore and Perkins[2] (likely to be higher at our latitude and altitude), over

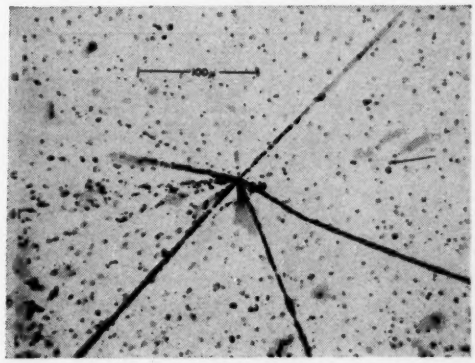

FIG. 2. Disintegration with 12 heavy prongs, 12 min. and near-min. tracks within 100°. Between *a* and *b*, 52° apart, are 8, and between *c* and *d*, 10° apart, are 5 minimum ionization tracks.

3 Bev of energy is dissipated in one such large star, if the light tracks are mesons and not electrons, and more if they are protons.

Comparing Ilford C2 emulsions on this and on a similar flight at 57° geomagnetic north (vertical cut-off 2.8 Bev),[1] production-rates of stars of 5 or more prongs was found greater by a factor of 3.6±0.4 at the northern latitude; this figure includes production during ascent and descent but not at sea-level.

We take great pleasure in acknowledging our gratitude to the Office of Naval Research for putting the balloon flight at our disposal, and to the officers and men of the USS Saipan and Mr. S. E. Golian of this laboratory, who were responsible for the success of this flight.

* Research carried out at the Brookhaven National Laboratory under the auspices of the AEC.

[1] M. S. Vallarta, Phys. Rev. **74**, 1837 (1948).
[2] Harding, Lattimore, and Perkins, Proc. Roy. Soc. A **196**, 325 (1949)

Conductivity Changes in Dielectrics during 2.5-Mev X-Radiation

F. C. Armistead, J. C. Pennock, and L. W. Mead
Massachusetts Institute of Technology, Cambridge, Massachusetts
August 3, 1949

PRELIMINARY measurements of volume conductivity have been made on three plastic dielectrics during irradiation by 2.5-Mev x-rays.

To measure the volume conductivity, a potential difference was applied across the sample and the resultant current was measured with an FP54 electrometer tube and Penick-type bridge circuit.[1] The sample, the electrometer tube, and the control grid leads were in a vacuum at 1 micron pressure in order to reduce parallel path ion current leakages and to establish easily reproducible pressure and humidity conditions at the sample.

Figure 1 shows the data taken on a sample of Okoseal, polyvinyl chloride manufactured by the Okonite Company. The conductivity of this material was found to increase very rapidly upon the start of irradiation and quickly reached an equilibrium value which was dependent on irradiation rate. This value was approximately thirty times the original conductivity at an irradiation rate of about 400 R/min. Upon stopping the irradiation, the recovery was half complete in thirty minutes, nine-tenths complete in sixteen hours.

A sample of Saran, vinylidene chloride manufactured by Dow Chemical Company, showed somewhat different characteristics. The conductivity increased slowly over a period of about two hours (2.7×10^5 R total irradiation at 2000 R/min.) until it was about three times the original conductivity. At this point the irradiation was stopped because of apparatus difficulty. The initial recovery rate was much lower than for Okoseal. After eighty-two hours recovery was complete to within the precision of measurement.

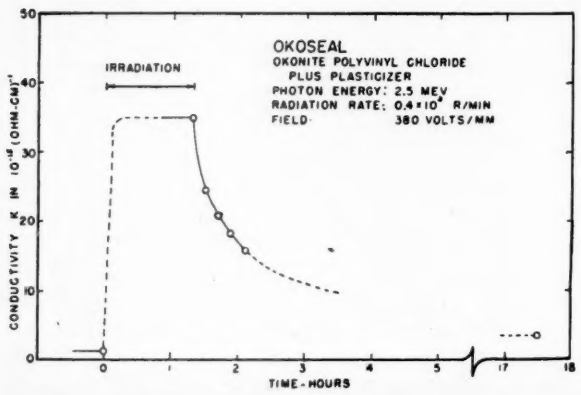

FIG. 1. Conductivity of Okoseal showing effect of irradiation.

A preliminary measurement on a sample of polystyrene showed that after a total irradiation of 5500 R at 1000 R/min., the conductivity had not risen to as much as 2×10^{-17} (ohm-cm)$^{-1}$. Assuming an initial conductivity of 10^{-20} (ohm-cm)$^{-1}$, the change was by less than a factor of 2×10^3. This result is in contrast to the report by Farmer[2] of a change by a factor of approximately 10^7 after a total irradiation of only 4000 R.

The fact that the dielectrics become conducting during irradiation is to be expected by a mechanism such as that described by Mott and Gurney,[3] whereby the passage of primary current (due directly to absorbed photons) changes the dielectric in such a way as to reduce the electrical barrier at the electrode-dielectric interface. However, the extent of change and the time constants are not readily predictable, and these measurements show that a considerable spread in the magnitude of these factors is to be expected among the various plastic dielectrics.

The authors are grateful to Professor J. G. Trump and his associates, particularly the late Mr. A. M. Clarke and Mr. K. A. Wright, for use of the x-ray generator and for their cooperation in the experiments.

This work was performed under Contract No. W-7405-eng-175 with the United States Atomic Energy Commission in connection with the M.I.T. Metallurgical Project.

[1] D. B. Penick, Rev. Sci. Inst. **6**, 115 (1935).
[2] F. T. Farmer, Nature **150**, 521 (1942).
[3] Mott and Gurney, *Electronic Processes in Ionic Crystals* (Clarendon Press, Oxford, 1940), pp. 185–188.

Heavy Particles in Cosmic-Ray Stars*

M. Blau, M. M. Block, and J. E. Nafe
Columbia University, New York, New York
July 25, 1949

IN scanning nuclear emulsions exposed for three hours at an altitude of 93,000 ft. in Minnesota ($\lambda=55°$N) the authors have observed stars with heavy particles. Although we have obtained as yet no statistics on the relative frequency of their occurrence, we have observed at least 6 stars with heavy particles ($Z\geqq3$) originating in stars both in vertical plates with no absorber and in horizontal plates under Pb (11.3 g/cm²) and Cu (11.2 g/cm²) absorber. We believe these to be secondary particles of the kind previously reported by Bonetti and Dilworth[1] and by Hodgson and Perkins.[2]

The star with three heavy particles shown in Fig. 1 is interesting in connection with publications on stars produced by heavy particles[3–5] and stars in which heavy particles are emitted. The three tracks *A*, *B* and *C* have δ-rays and are ascribed to particles with $Z\geqq3$. This star was found in a 70μ Eastman Kodak NTB emulsion impregnated with Bi in colloidal form.[6] The plate was exposed in vertical position without absorber. The orientation of the star in the emulsion is indicated by the arrow pointing to the zenith. Tracks *A* and *B* are collinear within the accuracy of our measurements and track *C* is inclined at about 30° to the direction of *B*. The track *D* of a light energetic particle lies almost parallel to *B*. Extensions of the tracks *A* and *C* were found on the adjacent identical plate but none of the tracks ends in the emulsion.

From the point of view of orientation *A* is the only one of the heavy particles which can be incoming. At first glance, therefore, the star of Fig. 1 resembles one of the type described by Bradt and Peters[5] where part of the incoming nucleon is sheared off in the collision and the remainder continues with the original momentum as a compact nucleus of reduced charge. However, the presence of the heavy particle *C* at a large angle (30°) to direction of *A*, with $Z\cong5$ and with a minimum energy of 220 Mev indicates that the event of Fig. 1 is different. Particles *B* and *C* cannot be primary particles as can be seen from the orientation of the stars. Careful δ-ray counts made independently by two observers show that *A* cannot be a primary particle but must be leaving the disintegrating nucleus. Although particle *A* does not end in the emul-

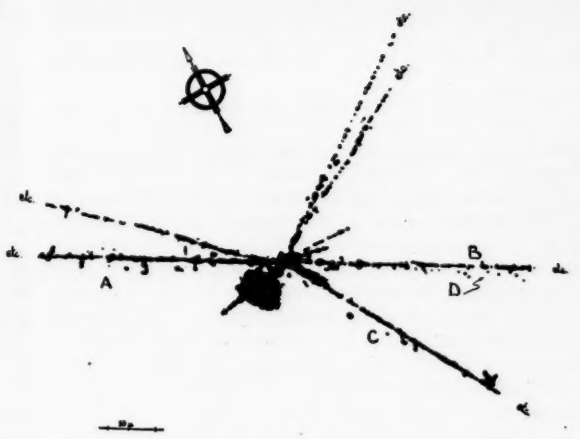

FIG. 1. A microphotograph of a star with three outgoing heavy particle tracks.

sion, the increase of the number of δ-rays per 100μ is higher by 100 percent in the last 600μ of the track than in the 600μ nearest to the star center. The particle A is therefore near the end of its range. Using the criterion of δ-ray counts for NTB plates we find for this particle $Z \cong 6$ a minimum energy of 560 Mev and a momentum of 3510 Mev/c. The energy and momentum of particle B have been evaluated approximately by the following considerations. The faint track D has a grain density (estimated from β-particles visible near the star) corresponding to a proton of about 140 Mev. To permit approximate calculations it is assumed that the particle B and the particle D have equal energy, for the alternative assumptions of equal momentum and equal energy per nucleon lead to results not consistent with δ-ray count and grain density. The δ-ray count of particle B corresponds then to a value of $Z \cong 3$. A minimum energy for particle C may be found by choosing the smallest Z consistent with the δ-ray count and by adding to the observed length of the track an amount sufficient to bring the δ-ray count down to zero. The $Z=4$ or 5 for particle C.

To estimate the energy and momentum of the incident particle only the kinetic energy of the particles A, B, C, and D is taken into account and the energy of the other particles of the star and all binding energies are neglected.** It is assumed that these low energy particles are isotropically distributed and contribute nothing to the momentum. The estimated minimum values of energy and momentum of the particles A, B, and C are given in Table I.

If the particle C is assumed to have $Z=5$, the sum of the energies is 1060 Mev and the resultant momentum is 955 Mev/c. If it is assumed also that the kinetic energy of the incident particle is 1060 Mev, the energy transfer is of the same order as the momentum transfer indicating a relativistic particle passing through the nucleus. On the other hand if 1060 Mev is taken to be the total energy of the incident particle, the energy and resultant momentum are compatible with the assumption that a τ-meson has been captured by the nucleus. Then from

$$E_{\text{total}} = E_{\text{kinetic}} + MC^2$$

and

$$P = (1/c)((E_{\text{total}})^2 - (MC^2)^2)^{\frac{1}{2}}$$

TABLE I. Estimated charge, energy, and momenta of the particles A, B, C, and D in the star of Fig. 1.

Track	Delta-rays per 100μ	Z	Energy (Mev)	Momentum (Mev/c)
A	13 (near star center) 27 (at end of track)	6	560	3500
B	6	3	140	1260
C	9	5	220	2040
D		1	140	530

the rest energy of the meson is found to be ~460 Mev and the mass ~880 electron masses. If particle C is assumed to have $Z=4$ instead of 5, the meson mass=~1170 electron masses.

The total charge freed in the star is ~25e and the exploding atom could be bromine or silver. However, it is not impossible that the explosion occurred in a Bi atom for the black spot shown in Fig. 1 is a Bi speck. The star is an illustration of Perkin's "Fission Hypothesis"[7] assuming that heavy splinters break away from the nucleus if the energy of the incident particle is comparable with the binding energy of the nucleus.

* Work done under subcontract to Brookhaven National Laboratory which is operated under a prime contract with the AEC.

** The line of reasoning which follows might be changed if minimum ionization particles were present. However, in our experience such particles are frequently accompanied by particles of lower energy observable in this emulsion.

[1] Bonetti and Dilworth, Phil. Mag. **40**, 585 (1949).
[2] Hodgson and Perkins, Nature **163**, 439 (1949).
[3] Freier, Lofgren, Ney and Oppenheimer, Phys. Rev. **74**, 1818 (1948).
[4] H. L. Bradt and B. Peters, Phys. Rev. **74**, 1829 (1948).
[5] H. L. Bradt and B. Peters, Phys. Rev. **75**, 1779 (1949).
[6] The authors wish to thank Dr. H. J. Webb and Dr. J. Spence of the Eastman Kodak Company for supplying them with this specially prepared emulsion.
[7] Harding, Lattimore, and Perkins, Proc. Roy. Soc. **196**, 325 (1949).

The Disintegration Energy of Al^{29} *

L. SEIDLITZ, E. BLEULER, AND D. J. TENDAM
Purdue University, Lafayette, Indiana
August 4, 1949

THE particular stability of nuclear systems with proton or neutron numbers 2, 8, 10, 20, 50, 82, and 126 has been explained by the occurrence of closed shells. The configurations proposed are, up to Ca^{40}: $(1s)^2(2p)^6(2s)^2(3d)^{10}$ (e.g., Feenberg and Hammack,[1] Nordheim[2]). No shell closure would occur between Ne^{20} and Ca^{40} and a regular variation of masses and decay energies with Z is expected for a sequence of nuclei of the same symmetry. A serious deviation from this behavior has been found by Bleuler and Zünti[3] in the case of the transition $Al^{28}-Si^{28}$. The upper curve of Fig 1, essentially copied from a note by Barkas,[4] shows the disintegration energies of the sequence in question. The value for Al^{28} seems about 1.3 Mev too high. Comparison of the masses of Al^{28} and Si^{28} with the values calculated by Barkas[5] indicates that the anomaly is due, most probably, to a low mass, i.e., a high binding energy, of Si^{28}. Closure of a shell at $Z=14$ could be expected, if an alternate configuration scheme, based on strong spin-orbit coupling, is assumed (Haxel, Jensen, and Suess,[6] Mayer[7]). The same shell closure should manifest itself in the decay $Al^{29}-Si^{29}$. However, the value of 2.5 Mev given by Bethe and Henderson[8] for the upper limit of the β-spectrum of Al^{29}, with no γ-radiation, would be only slightly higher than expected from

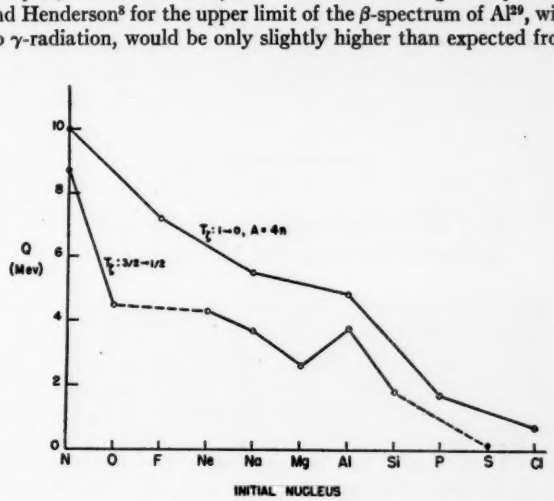

FIG. 1. Decay energies of nuclei of the same isotopic spin $T_\xi = (N-Z)/2$. Upper curve: N^{16} to Cl^{36}, lower curve: N^{17} to S^{35}.

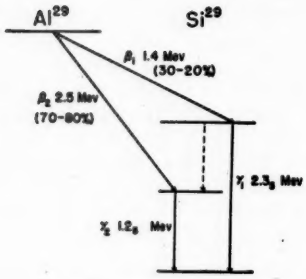

FIG. 2. Decay scheme of Al^{29}.

the sequence of similar nuclei. It seemed interesting, therefore, to redetermine the decay scheme of Al^{29}.

Al^{29} was produced by bombarding Mg with the 18-Mev α-particles of the Purdue cyclotron. The absorption curves for single counts and $\beta\gamma$-coincidences were obtained by following, for each absorber, the decay curve together with that for a standard absorber and analyzing them into the 2.30-min. and 6.56±0.06-min. periods of Al^{28} (from Mg^{25}) and Al^{29}. Contrary to previous measurements,[8] the absorption curve shows a γ-background. The analysis indicates a complex β-spectrum, consisting in the simplest case of two components of 2.5 Mev and 1.4 Mev (~30 percent). All β-transitions are followed by γ-radiation: the ratio of $\beta\gamma$-coincidences to single β-counts is constant from about 200 mg/cm² to at least 1000 mg/cm²; its value indicates (after calibration of the arrangement with Na^{24} that the 2.5-Mev β-spectrum is followed by a γ-ray of 1.2±0.2 Mev. For thinner absorbers $N_{\beta\gamma}/N_\beta$ increases slightly, corresponding to the higher γ-energy coupled with the low energy partial β-spectrum. In addition, the γ-ray energies were measured directly by coincidence absorption of the secondary electrons. Two components of 2.3_5 Mev (~20 percent) and 1.2_5 Mev can be distinguished.

The decay scheme compatible with these data is given in Fig. 2. Both β-transitions are allowed with $ft=1.6\cdot10^5$ (2.5 Mev) and $2\cdot10^4$. Cascade γ-radiation, with an intensity less than 10 percent, cannot be excluded. While the decay scheme might be subject to modifications, the total disintegration energy of 3.75±0.25 Mev seems well established. The lower curve of Fig. 1 shows the decay energies of the nuclei N^{17} to S^{35}. The value for Al^{29} is seen to be about 1.7 Mev higher than expected from the neighboring members of the sequence. This may be interpreted as confirming evidence for an especially stable structure of Si^{28} (and Si^{29}), due possibly to a shell closure at $Z=14$.

* Supported by the ONR.

[1] E. Feenberg and K. C. Hammack, Phys. Rev. **75**, 1877 (1949).
[2] L. W. Nordheim, Phys. Rev. **75**, 1894 (1949).
[3] E. Bleuler and W. Zünti, Helv. Phys. Acta **20**, 195 (1947).
[4] W. H. Barkas, Phys. Rev. **72**, 346 (1947).
[5] W. H. Barkas, Phys. Rev. **55**, 691 (1939).
[6] Haxel, Jensen, and Suess, Phys. Rev. **75**, 1766 (1949).
[7] M. G. Mayer, Phys. Rev. **75**, 1969 (1949).
[8] H. A. Bethe and W. J. Henderson, Phys. Rev. **56**, 1060 (1939).

On a New Conception of the Interaction between Charges and Electromagnetic Field

LOUIS DE BROGLIE
Institut Henri Poincaré, Paris, France
August 3, 1949

FOR the past fifteen years, I have tried to develop a form of quantum electrodynamics which I have named "wave mechanics of the photon." This theory has been set forth in several books.[1] In 1935, at the beginning of these investigations, a hypothesis was emphasized in order to avoid an infinite value for the self-energy of a charged particle. The wave mechanics of the photon discriminates between the coordinates of the charge X, Y, Z (vector $\mathbf{R}$) and the variables of the field x, y, z (vector $\mathbf{r}$). For the interaction between charge and field in a frame of reference in which the particle is at rest, the following expression is found:

$$\int\int V(\mathbf{r})\rho(R)\delta(\mathbf{r}-\mathbf{R})d\mathbf{r}d\mathbf{R}, \tag{1}$$

where δ is the Dirac function. This expression gives, as usual, an infinite value for the proper energy of the charge. I have suggested[2] that we might replace the δ-function in (1) by a function $f(\mathbf{r}-\mathbf{R})$ in the form of a very sharp, but not infinitely sharp, needle. This substitution, which would express a kind of uncertainty for the point of application of the field on the charge, would lead to a finite value of the self-energy.

Unfortunately, this idea meets difficulties from the viewpoint of relativistic invariance. Let us adopt the multi-temporal theory which introduces distinct times t and T for the field and the charge. The correct relativistic variance of the expression (1) is shown by the fact that one can write it in *any* reference frame:

$$\left|\int\int\sum_{\mu=1}^{4}A_\mu(x,y,z,t)j_\mu(X,Y,Z,T)\left(-\frac{1}{4\pi c}\frac{\partial D(0)}{\partial t}\right)\times dxdydzdXdYdZ\right|_{t=T}, \tag{2}$$

where $D(0)$ is the form for $k_0=0$ of the invariant singular function

$$D(k_0)=-\frac{1}{2\pi^2}\int\frac{\sin[kc(t-T)-\mathbf{k}(\mathbf{r}-\mathbf{R})]}{k}d\mathbf{k} \tag{3}$$

with $k^2=|\mathbf{k}|^2+k_0^2$. Indeed, for all values of k_0

$$\left|\frac{1}{c}\frac{\partial D(k_0)}{\partial t}\right|_{t=T}=-4\pi\delta(\mathbf{r}-\mathbf{R}). \tag{4}$$

But if we will substitute for the δ-function in (1) a function in the form of a sharp needle, we cannot see how the correct relativistic variance can be preserved.

I have been recently lead to a new investigation of this problem by recent papers of R. P. Feynman. Guided in my choice by the suggestions of Feynman and others,[3] I will start from the following form of Wentzel potentials (in non-rationalized units):

$$A_\mu(x,y,z,t,X,Y,Z,T)=-\epsilon\int_{-\infty}^{X_\mu}[D(0)-D(k_0)]dX_\mu, \tag{5}$$

ϵ being the electric charge of the particle. Then we have

$$\Box A_\mu=-k_0^2\epsilon\int_{-\infty}^{X_\mu}D(k_0)dX_\mu;\quad \Sigma_\nu\frac{\partial A_\nu}{\partial x_\nu}=\epsilon[D(0)-D(k_0)]. \tag{6}$$

Starting from the usual definition of the field in terms of potentials, we can easily find for the "electric field" $\mathbf{E}$ the relation

$$\mathrm{div}\mathbf{E}=-\frac{\epsilon}{c}\frac{\partial}{\partial t}[D(0)-D(k_0)]+k_0^2\epsilon\int_{-\infty}^{cT}D(k_0)d(cT). \tag{7}$$

If one makes $T=t$ (equalization of the times), one finds by (4)

$$\mathrm{div}\mathbf{E}=k_0^2\epsilon\left|\int_{-\infty}^{cT}D(k_0)d(cT)\right|_{T=t}. \tag{8}$$

The calculation in a frame of reference where the charge is at rest gives

$$\left|\int_{-\infty}^{cT}D(k_0)d(cT)\right|_{T=t}=\frac{\exp[-k_0|\mathbf{r}-\mathbf{R}|]}{|\mathbf{r}-\mathbf{R}|}. \tag{9}$$

Therefore, we see by (8) and (9) that we can replace the point charge ϵ localized at $\mathbf{R}$ by a continuous distribution of total charge ϵ with the density

$$\sigma=\epsilon f(\mathbf{r}-\mathbf{R})=\frac{\epsilon k_0^2}{4\pi}\frac{\exp[-k_0|\mathbf{r}-\mathbf{R}|]}{[\mathbf{r}-\mathbf{R}]}. \tag{10}$$

It is noteworthy that σ has the form of a Yukawa potential. Moreover, one can easily verify that the electrical distribution (10) gives at the point $\mathbf{r}$ ($\mathbf{R}$ being at the origin) the scalar potential

$$V(r)=\epsilon\frac{1-\exp[-k_0r]}{r} \tag{11}$$

equal to the difference of a Coulomb potential and a Yukawa potential. We are then lead to substitute in (1) the function $f(\mathbf{r}-\mathbf{R})$ defined by (10), and this is consistent with our 1935 assumption.

We can summarize our conclusions by saying that the interaction between electrical charges takes place with the simultaneous intervention of a photon field and a meson field, each charge reacting in an opposite manner with these two fields (more precisely, the meson charge η is equal and opposite to the electric charge ϵ). If we abstract the meson field, we are obliged to replace the point charge by the continuous distribution (10).

We have obtained our results by the multi-temporal theory. Now, using the equations of the wave mechanics of the photon, we will find them again in a very instructive manner.

In the general theory of particles of spin 1 (mere generalization of the wave mechanics of the photon) one finds[4] that the "electric field" of the particle with a proper mass $m_0=hk_0/2\pi c$ verifies the equation

$$\mathrm{div}\mathbf{E}_{k_0}=-k_0^2V_{k_0}, \tag{14}$$

V_{k_0} being the corresponding "scalar potential." The wave mechanics of the photon supposes that the photon possesses an extremely feeble, but not quite zero proper mass $\mu_0=h\gamma/2\pi c$, so that we have

$$\mathrm{div}\mathbf{E}_\gamma=-\gamma^2V_\gamma. \tag{15}$$

Let us imagine a field which is the superposition of a photon field with a constant γ and a meson field with a constant $k_0\gg\gamma$. We will find for the total "electric field"

$$\mathrm{div}\mathbf{E}=\mathrm{div}\mathbf{E}_\gamma+\mathrm{div}\mathbf{E}_{k_0}=-\gamma^2V_\gamma-k_0^2V_{k_0}. \tag{16}$$

The wave mechanics of the photon proves that the photon potential created around it by a charge placed at the origin of coordinates is[5]

$$V_\gamma=\epsilon\frac{e^{-\gamma r}}{r}-\frac{\epsilon}{\gamma^2}\delta(r). \tag{17}$$

The first term is a quasi-Coulomb potential which for $\gamma\to 0$ gives the usual Coulomb potential. I have named the second term, which is characteristic of the wave mechanics of the photon, the "coincidence potential."

For the meson potential, we have similarly

$$V_{k_0}=\eta\frac{e^{-k_0r}}{r}-\frac{\eta}{k_0^2}\delta(r) \tag{18}$$

and we assume as before that $\eta=-\epsilon$. Then, substituting (17) and (18) in (16), we find

$$\mathrm{div}\mathbf{E}=-\epsilon^2\frac{e^{-\gamma r}}{r}+\epsilon\delta(r)+k_0^2\epsilon\frac{e^{-k_0r}}{r}-\epsilon\delta(r)$$
$$=4\pi\epsilon\left[\frac{k_0^2}{4\pi}\frac{e^{-k_0r}}{r}-\frac{\gamma^2}{4\pi}\frac{e^{-\gamma r}}{r}\right]. \tag{19}$$

We can therefore overlook the meson field if we replace the point charge by a continuous distribution

$$\sigma(r)=\frac{\epsilon}{4\pi}\left[k_0^2\frac{e^{-k_0r}}{r}-\gamma^2\frac{e^{-\gamma r}}{r}\right]. \tag{20}$$

For $\gamma\to 0$, we find again the expression (10).

We must point out how the terms $\delta(r)$ disappear in (19). It is the presence of the coincidence potentials in (17) and (18) which makes possible the elimination of these terms. Now, in its usual form, the quantum electrodynamics assumes that the proper mass of the photon is rigorously equal to zero ($\gamma=0$) and consequently ignores the coincidence potential in (17). The foregoing argument shows that, of course, the coincidence potential plays a very important part, and this seems to supply a serious reason for believing that the proper mass of the photon is not quite rigorously zero.

Finally, let us note that a many-meson field could be considered in the interaction, but only if the sum of all the meson charges η_i is equal to $-\epsilon$. This relation between the charges of a particular particle could be of importance in the theory of nuclear fields.[6]

[1] L. de Brogie, *Une nouvelle théorie de la Lumière: la Mécanique ondulatoire du photon* (Hermann and cie, Paris, 1940–42), Vol. 2; *Théorie générale des particules à spin* (Gauthier-Villars, Paris, 1943); *La Mécanique ondulatoire du photon et la théorie quantiche des champs* (Gauthier-Villars, Paris, 1949).
[2] L. de Brogie, Comptes Rendus **200**, 361 (1935).
[3] R. P. Feynman, Phys. Rev. **74**, 939 (1948). A complete bibliography of the question is found in this paper.
[4] L. de Broglie, *Mécanique ondulatoire du photon*, see reference 1, p. 38.
[5] See reference 4, p. 172.
[6] If the relation is valid for a neutral particle, the sum of all its meson charges must be zero.

Atmospheric Ozone Temperatures As Determined by Spectroscopic Observations from Below

WILLIAM M. BENESCH
Physics Department, Johns Hopkins University, Baltimore, Maryland
July 21, 1949

THE moon at dichotomy provides a light source with a continuously variable surface temperature suitable for measuring the effective temperature of atmospheric ozone in the manner of the line reversal method for flame temperatures. If a relatively cold area of the lunar light source is focused on a spectrometer slit, the 9.6μ ozone band will appear as an emission band when that region of the spectrum is scanned. On the other hand, if a relatively hot strip of the moon is used, the ozone band will appear as an absorption band. That lunar strip which fails to reveal the ozone band has the same temperature, radiatively speaking, as the ozone. I am indebted to Professor Strong for suggesting the use of this method.

To facilitate observations, a hot area on the moon was used at all times and adjusted to cover just that fraction of the slit which would "wash out" the ozone band. This modification makes observations possible using the full moon or even the sun. The ozone temperatures obtained were determined from spectral intensities on the long wave-length side of the 9.6μ band when the slit was so covered that the band was "washed out." These intensities were converted to equivalent temperature by substituting local calibrating black bodies for the moon in front of the moon-follower mirror.

Figure 1 shows three typical spectra. They were taken with (a) excess, (b) matching, and (c) deficient lunar energy.

The following ozone temperatures were obtained in this manner:

April 9, 1949	−47°C
April 11, 1949	−46°C
May 8, 1949	−43°C.

It is to be noted that the precision to which temperatures could be read in these observations was considerably less than is indicated by the consistency of the data above, owing to the inferior sensitivity and resolving power of the dispersing and detecting system. Furthermore, these "effective ozone temperatures," however carefully measured, are restricted in meaning by the effect of pressure broadening on the individual lines of the band. That is, the results obtained here are only representative of the ozone as seen from below, from which aspect the lower layers tend to obscure those at greater altitudes.

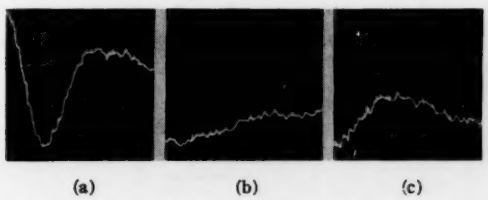

FIG. 1. Three typical spectra with (a) excess, (b) matching, and (c) deficient lunar energy.

I am grateful to Project N5ori-166, Task Order V at Hopkins, for the equipment used and for help in carrying out these observations.

Lambda-Temperatures of He^3—He^4 Mixtures

B. M. Abraham, B. Weinstock, and D. W. Osborne
Argonne National Laboratory, Chicago, Illinois
July 29, 1949

IT has been shown[1] by comparing the isothermal flow of liquid He^3 and of liquid He^4 through a small channel or superleak that no superfluid flow occurs in pure He^3, at least down to 1.05°K. These experiments have been extended to mixtures of He^3 and He^4 in order to study the feasibility of concentrating He^3 by means of a superleak and to determine the effect of composition on the lambda-temperature.

The first experiment was made in an attempt to separate the He^3 from approximately 10 cc of a mixture containing 92.1 percent He^3 and 7.9 percent He^4. Subsequently, experiments were made with 2.4 percent He^3 and with mixtures prepared by diluting a portion of the 92.1 percent He^3 with He^4.

The He^3—He^4 mixture was condensed in the capillary tube leading to the platinum-glass superleak used previously,[1] which was immersed in a bath of ordinary liquid helium whose temperature was regulated by pumping. The rate of isothermal flow through the superleak was then determined at successively lower temperatures by observing the rate of pressure rise in a large volume on the exit side of the leak. The starting material, the portion which flowed through the leak during the course of the measurements, and the residuum were analyzed by means of a mass spectrograph.

With the 92.1 percent He^3 it was found that the rate of flow decreases monotonically as the temperature is lowered to 1.05°K, and it is therefore concluded that the lambda-temperature of this mixture is lower than 1.05°K. With pure He^4, as well as with the other mixtures tested, the curve of flow rate *versus* temperature rises sharply below a temperature which is characteristic of the liquid. With pure He^4 this rise begins at the lambda-point, 2.19°K, and hence the point at which the sharp rise begins is considered to be the lambda-point of the mixture. The breaks in the curves for the mixtures were located with an estimated uncertainty of 0.05°K.

The lambda-temperatures determined in this way and the mass spectrographic analyses are given in Table I. It is believed that there was little change in composition until the temperature was reduced below the lambda-point of the mixture, so that the lambda-temperatures tabulated correspond to the composition of the starting material.

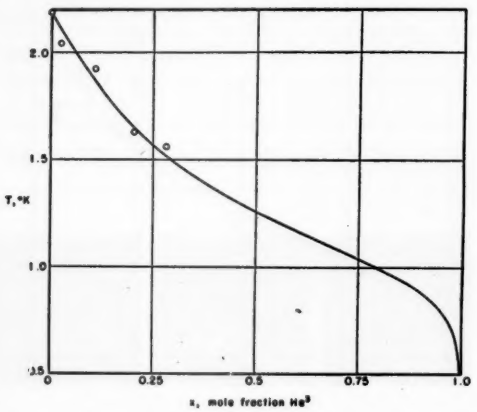

FIG. 1. Lambda-temperatures of He^3—He^4 mixtures. Points determined with a superleak. Curve calculated (see text).

TABLE I. Lambda-temperatures and composition changes of He^3—He^4 mixtures, as observed in superleak experiments.

Starting material	Mole percent He^3 Effluent	Residuum	λ-point (°K)
2.4	0.32	8.2	2.04
10.7	2.7	13.8	1.92
20.3	—	—	1.63
28.2	10.9	43.7	1.56
92.1	91.0	93.6	<1.05

In Fig. 1 the experimental lambda-temperatures are plotted against composition, along with a curve calculated by J. W. Stout as described in the following letter.[2] The agreement is within the estimated experimental error.

It is seen from Table I that large changes in He^3 concentration can be effected by isothermal flow through a superleak at temperatures below the lambda-point of the mixture. A slight change in concentration will occur above the lambda-point if the amount of gas above the liquid on the entrance side of the leak is appreciable. Since the concentration of He^3 is higher in the vapor phase than in the liquid,[3] the liquid flowing through the leak, even without fractionation by superfluid flow of He^4, has a slightly lower He^3 concentration than the starting material. This effect is sufficient to account for the concentration change observed with the 92.1 percent He^3 but is far too small to account for the changes observed with the other mixtures.

The limit of He^3 concentration attainable by any of the various methods of separation[4,5] which depend on the superfluid flow of liquid He^4 and the lack of superfluid flow of He^3 can be predicted approximately from Fig. 1. Thus, the concentration limit at a temperature of 1.8°K is about 14 percent He^3, and the limit at 1.5°K is about 30 percent He^3.

It is planned to extend these measurements to lower temperatures obtained by adiabatic demagnetization, and to measure the He^3/He^4 ratio of the material as it issues from the superleak by means of a mass spectrograph directly connected to the apparatus.

[1] Osborne, Weinstock, and Abraham, Phys. Rev. **75**, 988 (1949).
[2] J. W. Stout, Phys. Rev. **76**, 864 (1949).
[3] Taconis, Beenakker, Nier, and Aldrich, Phys. Rev. **75**, 1966 (1949).
[4] Daunt, Probst, and Smith, Phys. Rev. **74**, 495 (1948).
[5] Reynolds, Fairbank, Lane, McInteer, and Nier, Phys. Rev. **76**, 64 (1949).

Solutions of He^3 in He^4

J. W. Stout
Institute for the Study of Metals, University of Chicago, Chicago, Illinois
July 29, 1949

IN order to represent their measurements of the liquid-vapor equilibrium in dilute solutions of He^3 in He^4, Taconis, Beenakker, Nier, and Aldrich[1] suggested that below the lambda-point the fugacity of He^3 in the solutions is given by Raoult's law counting only that fraction of the He^4 atoms which on the two-fluid model of liquid helium are in the normal state. From this picture one can calculate thermodynamically the change of the lambda-temperature of He^3—He^4 solutions to compare with the observations of Abraham, Weinstock, and Osborne,[2] reported in the preceding letter.

The number of normal atoms of He^4 may be approximately represented[3] by $n=n_4(T/T_\lambda)^6$. n_4 is the total number of atoms of He^4 and T_λ is the temperature of the lambda-transition. Then the fugacity of He^3 is given by

$$f_3=(f_3^0 n_3)/[n_3+n_4(T/T_\lambda)^6]=(f_3^0 x)/[x+(1-x)(T/T_\lambda)^6]. \quad (1)$$

f_3^0 is the fugacity of pure He^3 at the same temperature and x is the mole fraction of He^3. We shall assume that above the lambda-point the solutions are ideal.

The necessary thermodynamic equations have been given previously;[4] the same notation is used here. If the transition remains

second order then the mole fractions, x, will be the same for the two phases in equilibrium at the transition temperature and it is further necessary that the T_λ in Eq. (1) be the transition temperature of the solution rather than that of pure He^4. By differentiating Eq. (1) one obtains, along the transition curve,

$$\Delta\bar{S}_4-\Delta\bar{S}_3=6R$$

and

$$\Delta\bar{C}_{P3}=-6R(1-x)(1+6x).$$

We shall assume that $\Delta\bar{C}_{P4}$ remains equal to its value in pure He^4 which is given by Keesom[5] as -7.6 cal. mole^{-1} deg.$^{-1}$. From Eq. (11) of the previous paper[4]

$$dT_\lambda/dx=T_\lambda(\Delta\bar{S}_4-\Delta\bar{S}_3)/\Delta C_P$$
$$=-T_\lambda/[x(1-x)(1+6x)+(1-x)7.6/6R]. \quad (2)$$

The curve of T_λ against x as calculated from Eq. (2) is shown and compared with the experimental points in Fig. 1 of the preceding letter by Abraham, Weinstock, and Osborne.[2] The curve asymptotically approaches $T=0$ as x approaches 1.

If one assumes that the parameter T_λ in Eq. (1) is not a function of x but is always equal to its value in He^4 then the transition must change to first order upon addition of He^3. The initial slope of the change in transition temperature with x is the same in both phases[6] and is -6.8 deg. per mole fraction. This is just twice the initial slope given by Eq. (2). Although the experimental data at present do not permit a clear decision as to whether the transition remains second order or changes to first order upon the addition of He^3 it seems probable that the former is true.

[1] Taconis, Beenakker, Nier, and Aldrich, Phys. Rev. **75**, 1966 (1949).
[2] Abraham, Weinstock, and Osborne, Phys. Rev. **76**, 864 (1949).
[3] W. Band and L. Meyer, Phys. Rev. **74**, 386 (1948).
[4] J. W. Stout, Phys. Rev. **74**, 605 (1948).
[5] W. H. Keesom, *Helium* (Elsevier Publishing Company, Inc., Amsterdam and London, 1942), Chapter V.
[6] See reference 4, Eq. (12).

Proton-Proton Scattering at 5.11 Mev*

R. O. Bondelid, P. G. Bohlman, and K. B. Mather
Physics Department, Washington University, St. Louis, Missouri
August 8, 1949

A COINCIDENCE type of scattering chamber, to be described in a later paper, was used to examine the scattering of 5.11-Mev protons produced by the Washington University cyclotron. The protons were scattered by a foil of polyethelene terephthalate. Only the scattering that occurred from the protons in the foil was observed as recording was accomplished by two proportional counters connected in coincidence and set at 90° relative to one another.

The number of hydrogen atoms per cm² of foil was determined in the following way: A section of the foil whose area was accurately determined was weighed on a microbalance. The percentage of hydrogen in the specimen was then determined by chemical analysis. Finally, a comparison of the analysis with the manufacturer's composition formula was made. The resulting figures were:

$$(1.46\pm0.01)\times10^{19}\text{ H atoms/cm}^2\text{ in foil }A,$$

and

$$(1.75\pm0.01)\times10^{19}\text{ H atoms/cm}^2\text{ in foil }B.$$

The number of incident protons was determined by collecting the beam, after it had crossed the scattering chamber, in a Faraday cage connected to a standard mica condenser, and reading the voltage with a Compton electrometer. After corrections for leakage, and calibration, the charge collected was estimated to be known to within a probable error of ±0.75 percent. The proportional counters collecting the scattered and recoil protons were set at the desired angles to within 0.05 degree. For each angle setting, a minimum of 5000 coincidence counts was obtained on each of the two foils. In some cases the number exceeded 20,000 counts. Because of the excellent performance of the Washington University cyclotron in producing a beam of 60 to 70 microamperes of protons, the large number of counts could be obtained in a relatively short time. It may be of interest to add that the cyclotron produced these intense proton beams by acceleration of molecular hydrogen without change from its normal deuteron adjustments.

TABLE I. Cross sections for proton-proton scattering.

θ	β	$\sigma_{cm}\times10^{24}$	$\sigma_{obs}/\sigma_{Mott}$
29.9	59.8	0.0998	39.9
34.9	69.8	0.104	75.4
39.9	79.8	0.106	115.2
44.9	89.8	0.108	136.7
49.9	99.8	0.107	117.6
54.9	109.8	0.102	75.0
59.9	119.8	0.102	41.8

The results obtained are shown in Table I. In the table, θ is the angle between the incident proton beam and the line from the scattering foil to the slit defining the solid angle. The column headed β contains the same angle when transformed to center-of-mass coordinates. The third column contains observed cross sections in the center-of-mass system, and the fourth column contains the ratio of observed to Mott cross sections. These ratios are believed to have a probable error of approximately ±2.5 percent.

Details of equipment and procedure will be described in forthcoming papers as well as a more extensive analysis of results.

The assistance of Dr. R. N. Varney is gratefully acknowledged. The highly successful performance of the cyclotron is attributed to Mr. A. A. Schulke, cyclotron engineer, whose assistance has been indispensable.

* Assisted by the joint program of the ONR and the AEC.

Decay of a Heavy τ-Meson into Three Lighter Mesons

S. Power*
Institute for Advanced Study, Princeton, New Jersey
July 29, 1949

EVIDENCE for the existence of a heavy τ-meson, with mass about 900 m, where m is the electron mass, is very meager, consisting almost wholly of three photographs,[1] each representing a different event. It is regarded with some scepticism, since no further evidence has been forthcoming. Yet the three pieces of existing evidence seem quite convincing. In particular, the very beautiful picture of Powell and his co-workers, of the disintegration of a τ-meson into three lighter mesons seems hardly to admit of an alternative interpretation.

The τ-meson, assuming it exists, must be created by the primary protons of cosmic rays, which suggests that it is coupled to nucleons at least fairly strongly; π-mesons we also know to be strongly coupled to nucleons. Therefore, it has seemed worth while to consider the disintegration process $\tau\rightarrow3\pi$, assuming the virtual creation and annihilation of intermediate nucleon pairs.

We consider both the τ- and π-mesons to be pseudoscalar particles, each being coupled to nucleons with pseudoscalar coupling. The method of computation is that of the Feynman diagrams, which is equivalent to the older perturbation method. As is usual in such calculations, the matrix elements contain an integral, with an infinite upper limit, over the momenta of the intermediate nucleons, which for this process, leads to a logarithmic divergence. This divergence is dealt with here by means of the introduction of a Pauli "regulator" function. The use of Pauli's regulators, or subtraction fields in meson decay problems has been dealt with in detail in a recent paper by J. Steinberger.[2] Of the six conditions for the masses of the subsidiary fields, which he enumerates as being necessary to make finite the infinite integrals occuring in such calculations, two are necessary here, *viz.*:

(a) $\Sigma C_i=0.$

(b) $\Sigma C_i \log M_i=0.$

Apart from this, it will be sufficient here to give results only. Taking the mass of the τ-meson to be 900 m, and that of the π-meson as 285 m, the process $\tau^+\to\pi^-+\pi^+\pi^+$ is found to have a reciprocal lifetime

$$\tau^{-1}=\frac{g_\pi^6}{(\hbar c)^3}\cdot\frac{g_\tau^2}{\hbar c}\cdot 5,\ 10^{11}\cdot\text{sec.}^{-1}. \tag{1}$$

Nothing is known of the value of $g_\tau^2/\hbar c$, except that it cannot be very small compared to unity; $g_\pi^2/\hbar c$ we now know to be of the order of unity:[3] therefore, Eq. (1) seems a fairly reasonable result, in keeping with experimental lower-limit for the lifetime, $\tau\geqslant 10^{-11}$ sec. suggested by an analysis of Powell's photograph. Nakamura has calculated the lifetime for this process, by the former perturbation method. Assuming both τ and π to be spin -1 particles, his preliminary results suggest a somewhat shorter lifetime for the decay.

The alternative process of disintegration suggested by Powell, *viz.* $\tau\to\pi+\mu+\mu$, has also been considered by the same methods. Here τ and π are considered to be spin -0, pseudoscalar particles, as in the previous case; the μ-mesons, which it is now known are very weakly coupled to nucleons, are considered as spin $-\frac{1}{2}$ particles, which are coupled to nucleon pairs by a Fermi-like interaction of the form:

$$g\bar{\psi}_{(1)}\psi_{(2)}\bar{\varphi}_{(1)}\varphi_{(2)}, \tag{2}$$

ψ being the nucleon wave-function, and φ the μ-meson wave-function, and $\psi=\psi^*\beta$ where ψ^* is the usual complex conjugate transpose, and β is the usual Dirac operator. We assume, following Tiomno and Wheeler,[3] as coupling constant, the Fermi $g\sim 2.2$, 10^{-49} ergs cm^3. This process again leads to a logarithmic divergence in its matrix elements. When dealt with as before, by the introduction of a "regulator," and with the same conditions (a) and (b), it gives a reciprocal lifetime for the process $\tau^-\to\pi^-+\mu^+\mu^-$

$$\tau^{-1}=\frac{g_\pi^2}{\hbar c}\cdot\frac{g_\tau^2}{\hbar c}2,\ 10^2\ \text{sec.}^{-1}$$

which seems rather too long. There is also a rather severe criticism against this second viewpoint, which is that the form of the interaction (2) fixes the relative sign of the charges of the τ- and π-meson, in fact here they must be of the same charge. From the photograph, however, they appear to be oppositely charged. The τ-meson appears to be positively charged, since, if negative, it would almost certainly have been absorbed by a nucleon during its passage through the plate, and have given rise to a star, as in Leprince-Ringnet's photograph, rather than to this spontaneous disintegration. The π-meson, which subsequently gives rise to a star, is certainly negative. Thus the most likely process would appear to be $\tau^+\to\pi^-+\mu^+\mu^+$. This cannot be dealt with by a simple interaction of type (2); it is a higher order process: therefore, interaction (2) seems to impose too severe a restriction on the process considered.

Finally, it is interesting, though rather puzzling to compare the lifetime for $\tau\to 3\pi$-decay with those of the competing processes:

(i) $\tau^+\to\pi^+\pi^0$.
(ii) $\tau^+\to\pi^+\gamma$,
(iii) $\tau^+\to\pi^+2\gamma$.

If we consider only pseudoscalar mesons, with pseudoscalar coupling, process (i) is forbidden. If, on the other hand, we consider the π^0-meson as a scalar particle, this process would be permissible; it would again give rise to a logarithmic divergence, which would be regulated as in previous cases. Its lifetime would, of course, depend on what mass we assume for the π^0-meson; there is no experimental evidence for this, but if we take it as being almost the same as that of π^+, this process would have a reciprocal lifetime of the order

$$\tau^{-1}\sim\frac{g_\tau^2 g_\pi^2 g_{\pi^0}^2}{(\hbar c)^3}10^{17}\ \text{sec.}^{-1}.$$

Process (ii) is forbidden. Process (iii) gives a reciprocal lifetime

$$\tau^{-1}\sim\frac{g_\tau^2}{\hbar c}\frac{g_\pi^2}{\hbar c}\,10^{12}\ \text{sec}^{-1},$$

if one takes the τ-meson as scalar, with scalar coupling, and the π as pseudoscalar, with pseudoscalar coupling. This process is convergent in this case. Taking both mesons pseudoscalar, again leads to a logarithmic divergence. When regulated in the usual manner, it gives a slightly larger probability for this process, by about a factor 10^2 or so. In any case, this process and the $\tau\to 3\pi$-decay seem to have roughly the same order of probability, process (iii) being a little more frequent; and yet this process has not yet been observed experimentally.

I wish to acknowledge my indebtedness to Professor J. R. Oppenheimer and the Institute for Advanced Study for their kind hospitality; and to Doctors A. Pais, J. Steinberger, and Professor H. Yukawa for their very generous help.

* On leave from University College, Dublin, Ireland.

[1] Brown, Camerini, Fowler, Muirhead, and Powell, Nature **163**, No. 4133 (1949); L. Leprince-Ringuet, and M. Lhénitien, Comptes Rendus **219**, 618 (1944); L. Leprince-Ringuet, Rev. Mod. Phys. **21**, 42 (1949). Rochester and Butler, Nature **20**, 855 (1947).
[2] J. Steinberger, Phys. Rev. (to be published).
[3] J. Tiomno and J. A. Wheeler, Rev. Mod. Phys. **21**, 144 (1949).

A New Formulation of the Variational Principle for Scattering Problems

SU-SHU HUANG
Yerkes Observatory, University of Chicago, Williams Bay, Wisconsin
July 27, 1949

SINCE the stationary property of the phase shifts for a two particle collision was first established by Hulthén,[1] various authors[2] have derived variational principles for determining the wave functions belonging to the continuous spectrum. In recent communications the present author[3] has generalized these formulations to the case of electron scattering where more than two particles are involved in each encounter. Moreover attention has also been called to the relative merit of the different formulations of the variational method. The very general nature of Hulthén's method suffers from the defect of being very cumbersome in practical applications, since it involves a process of successive numerical approximation in which at each stage of the approximation we have to solve a set of simultaneous equations. On the other hand, in spite of its relative simplicity, Tamm's method is restricted by the use of a trial wave function of a very special type. However it appears that a formulation of the variational principle can be given which combines the merits of the methods of Hulthén and Tamm without their disadvantages.

Considering the head-on collision of two particles, we have the wave equation

$$(d^2\psi/dr^2)+[k^2-V(r)]\psi(r)=0. \tag{1}$$

Substituting

$$\psi(r)=f(r)\sin kr+g(r)\cos kr \tag{2}$$

in Eq. (1), we obtain the pair of equations:

$$(d^2f/dr^2)-2k(dg/dr)-Vf=0 \tag{3}$$

and

$$(d^2g/dr^2)+2k(df/dr)-Vg=0. \tag{4}$$

The boundary conditions for $f(r)$ and $g(r)$ are that $\lim_{r\to\infty}f(r)$ and $\lim_{r\to\infty}g(r)$ exist; also $f(0)$ should be finite, and $g(0)=0$.

It can now be shown that Eqs. (3) and (4) are the Euler equations of the following variational problem:

$$\delta\int_0^\infty F(f_1, g_1, f, g; r)dr=0, \tag{5}$$

where

$$F\equiv f_1^2+g_1^2+2k(fg_1-gf_1)+V(f^2+g^2), \tag{6}$$

and subscripts denote differentiation with respect to r.

Once the variational problem has been solved, the phase shift η_0 can be obtained from the relation

$$\tan\eta_0=\lim_{r\to\infty}[g(r)/f(r)]. \tag{7}$$

The foregoing method is not limited to head-on collisions only. For collisions with higher angular momenta, we assume the wave function to be of the form:

$$\psi_l(r)=f(r)(\pi kr/2)^{\frac{1}{2}}J_{l+\frac{1}{2}}(kr)+g(r)(\pi kr/2)^{\frac{1}{2}}J_{-l-\frac{1}{2}}(kr), \quad (8)$$

where $J_{\pm(l+\frac{1}{2})}(kr)$ denotes the Bessel function of order $\pm(l+\frac{1}{2})$.

Substituting Eq. (8) into the wave equation, we can derive after suitable transformations a variational integral of the type given by Eq. (5). Thus for $l=1$, we find

$$F\equiv[1+(1/k^2r^2)](f_1^2+g_1^2)+2k(gf_1-fg_1) +[1+(1/k^2r^2)]V(f^2+g^2). \quad (9)$$

From this we infer that the functions $f(r)$ and $g(r)$ for the case $l=1$ must be of order at least r^2 for $r\to 0$.

The foregoing method can also be generalized for the S scattering of electrons by a neutral hydrogen atom. We now assume

$$\psi=(e^{-r_1}/r_2)[f(r_1, r_2, r_{12})\sin kr_2+g(r_1, r_2, r_{12})\cos kr_2]. \quad (10)$$

Substituting this form for ψ in the appropriate wave equation in the variables r_1, r_2 and r_{12}, we find that the resulting pair of differential equations obtained by putting the coefficients of $\sin kr_2$ and $\cos kr_2$ equal to zero, are the Euler equations of the variational problem

$$\delta\int_0^\infty dr_1\int_0^\infty dr_2\int_{|r_1-r_2|}^{r_1+r_2} dr_{12}\cdot F(f_1, f_2, f_{12}, g_1, g_2, g_{12}, f, g; r_1, r_2, r_{12})=0, \quad (11)$$

where

$$\begin{aligned}F\equiv{}&(e^{-2r_1}/r_2^2)[r_1r_2r_{12}(f_1^2+f_2^2+2f_{12}^2+g_1^2+g_2^2+2g_{12}^2)\\&+r_2(r_1^2-r_2^2+r_{12}^2)(g_1g_{12}+f_1f_{12})+r_1(r_2^2-r_1^2+r_{12}^2)\\&\times(f_2f_{12}+g_2g_{12})+2kr_1r_2r_{12}(g_2f-f_2g)\\&+kr_1(r_2^2-r_1^2+r_{12}^2)(g_{12}f-gf_{12})-2r_1(r_{12}-r_2)(f^2+g^2)],\end{aligned} \quad (12)$$

and f_1, f_2 and f_{12} are derivatives of f with respect to r_1, r_2 and r_{12}, respectively.

The advantage of the variational principle in the form derived here is its simplicity for practical applications. Examples of the application of this formulation will be given in a later paper.

Finally I should like to express my sincere thanks to Professor S. Chandrasekhar for valuable discussions.

[1] L. Hulthén, K. Fysiogr. Sällsk. Lund Förhandl. **14**, No. 21 (1944); Arkiv. f. Mat. Ast. o. Fys. **35A**, No. 25 (1948); W. Kohn, Phys. Rev. **74**, 1763 (1948).
[2] J. Schwinger, Phys. Rev. **72**, 742 (1947); I. E. Tamm, J. Exper. Theor. Phys. (Russian) **18**, No. 4 (1948); J. M. Blatt and J. D. Jackson, Phys. Rev. **76**, 18 (1949).
[3] S. S. Huang, Phys. Rev. **75**, 980 (1949); **76**, 477 (1949).

Finite Relativistic Charge-Current Distributions

D. Bohm, M. Weinstein, and H. Kouts
Palmer Physical Laboratory, Princeton University, Princeton, New Jersey
August 1, 1949

HITHERTO, it has been supposed that Lorentz's theory of the non-point electron could not be made covariant without either: (a) making electrodynamics non-linear, or (b) taking into account the effects of non-electromagnetic forces which are assumed to hold the charge together. We wish to report here preliminary results concerning a method of making Lorentz's theory covariant, without resorting to either of these alternatives.

The principal difficulty is that one must describe the change of shape of the electron as it accelerates and simultaneously preserve conservation of charge-current without which Maxwell's equations become inconsistent. Let the world line of the center of the electron be parametrically described by the 4 vector $\xi_\mu(s)$, and let the shape be described by another 4 vector, $v_\mu(s)$, which may be, but is not necessarily the same as $d\xi_\mu/ds$. (A criterion for correct equations of motion is that the two should tend to be the same for steady motion.) The following charge-current distribution is found to be conserved identically.

$$j^\mu(x)=\int ds F(r_\alpha r^\alpha)g\left(\frac{r_\alpha v^\alpha}{(v_\sigma v^\sigma)^{\frac{1}{2}}}\right)\left\{\frac{d\xi^\mu}{ds}-r_\gamma\frac{v^\gamma\dot{v}^\mu-v^\mu\dot{v}^\gamma}{v_\alpha v^\alpha}\right\}, \quad (1)$$

where $r_\alpha=x_\alpha-\xi_\alpha$, F and g are arbitrary functions and the integral is over the whole world line. This expression contrasts in two ways with the ordinary expression[1]

$$j_\mu'(x)=\int ds\frac{d\xi_\mu}{ds}\,\Pi_\alpha\,\delta(x_\alpha-\xi_\alpha). \quad (2)$$

First, the δ-function kernel is replaced by $F(r_\alpha r^\alpha)g(r_\alpha v^\alpha/(v_\sigma v^\sigma)^{\frac{1}{2}})$ so that the charge distribution is spread out. Secondly, there is added to the current a spin-like term involving the anti-symmetric tensor, $v^\mu\dot{v}^\nu-\dot{v}^\nu v^\mu\equiv S^{\mu\nu}$. This latter turns out to be essential for conservation of charge. The present theory differs from that of MacManus and Peierls[2] in that now the charge associated with a given center can be localized in time as well as in space. The theory of MacManus and Peierls results in convergence factors which are functions of ω^2-k^2, where ω is the angular frequency of the electromagnetic wave and k is its wave number. Thus, for a light wave, it leads essentially to a point electron. It is able to yield finite self-energies in classical theory, but the effects of quantum field fluctuations would not in general be affected. The localization of the charge in time, as well as space, would remove all infinities.

To obtain the equations of motion, one adds to the usual free particle Lagrangian the term

$$\int j_\mu(x)A^\mu(x)d^4x, \quad (3)$$

where j_μ is evaluated from (1). Variation of this Lagrangian leads to covariant and finite classical equations of motion. We have not investigated these equations in detail nor have we succeeded as yet in quantizing them. We believe, however, that quantization will inolve methods closely related to those proposed by Yukawa.[3]

The "shape variables," v^μ, can be described in an alternative way which suggests a close relation to Dirac's equation. In three dimensions, a rigid body is described by three rotations, which may, for example, be specified by the three Euler parameters. In four dimensions, one needs three more complex rotations, representing the Lorentz transformations needed to transform the electron to the shape it has when at rest. These six rotations are conveniently represented in terms of the eight quantities corresponding to real and imaginary parts of a 4 component Dirac spinor, among which there are two covariant relations, leaving six independent quantities. Representing such a classical spinor by $\psi(s)$ one then obtains

$$v^\mu=\psi^+\gamma^\mu\psi \quad (4)$$

with $\psi^+\psi=\pm 1$, $\psi^+\gamma^5\psi=0$. The ψ's are now the basic coordinates replacing the v's. We are now investigating the possibility that the Dirac equation wave equation is an approximation to the lowest quantum state of this system. If this were so, then the "Zitterbewegung" could be related to quantum fluctuations in the shape of the electron.

[1] P. A. M. Dirac, Proc. Roy. Soc. **167**, 148 (1938).
[2] H. MacManus, Proc. Roy. Soc. **195**, 323 (1948).
[3] H. Yukawa, Phys. Rev. **76**, 300 (1949).

Note on the Variational Method for Finding Extrapolated Endpoints*

H. Hurwitz, Jr.
General Electric Knolls Atomic Power Laboratory, Schenectady, New York
July 25, 1949

A VARIATIONAL method which can be used to treat integral equations of the form

$$f(x)=\int_0^\infty f(x')G(|x-x'|)dx'\int_{-\infty}^{+\infty}G(|x|)dx=1 \quad (1)$$

has recently been described by R. E. Marshak.[1]

TABLE I. Comparison of the values of x_0 from Eq. (3) with the actual values

$H(r)$	x_0(actual)	x_0 from Eq. (3)
$\frac{e^{-r}}{4\pi r^2}$	0.7104*	0.7083
$\frac{e^{-r}}{4-r}$	1	1**
$\frac{e^{-r^2/4}}{(4\pi)^{3/2}}$	0.8239***	0.8192

* To make this value of x_0 comparable with those for the other two kernels, one should change the scale so that $\langle r^2\rangle_{Av}$ is the same. Thus, 0.7104 should be multiplied by $\sqrt{3}$, giving 1.230.
** In this case the constant trial function is the exact solution of Eq. (1).
*** This value is due to G. M. Volkoff. An equivalent result has been obtained independently by S. Frankel and E. Nelson.

He has observed that in the case of the Milne kernel a good value for the extrapolated endpoint can be obtained by using a constant trial function. This procedure, when applied to a general kernel, leads to a simple formula for the extrapolated endpoint which is of some value in physical problems where the kernel is not known analytically. The formula also indicates those properties of the kernel which are most important in determining the extrapolated endpoint. If the asymptotic solution of Eq. (1) is written in the form

$$f(x)=a(x+x_0),$$

where x_0 is the extrapolated endpoint, we find

$$x_0\geqq\frac{1}{6}\frac{\langle|x|^3\rangle_{Av}}{\langle|x|^2\rangle_{Av}}+\frac{1}{4}\frac{\langle|x|^2\rangle_{Av}}{\langle|x|\rangle_{Av}},\quad \langle|x|^n\rangle_{Av}=\int_{-\infty}^{+\infty}G(|x|)\,|x|^n dx. \quad (2)$$

The kernel $G(|x|)$ is sometimes given in terms of a "spherical geometry" kernel, $H(r)$, by the relation

$$G(|x|)=2\pi\int_{|x|}^{\infty}H(r)r dr.$$

Then

$$\langle|x|^n\rangle_{Av}=\frac{\langle r^n\rangle_{Av}}{(n+1)}=\frac{4\pi}{(n+1)}\int_0^{\infty}H(r)r^n r^2 dr$$

so that Eq. (2) becomes

$$x_0\geqq\frac{1}{8}\frac{\langle r^3\rangle_{Av}}{\langle r^2\rangle_{Av}}+\frac{1}{6}\frac{\langle r^2\rangle_{Av}}{\hat{r}}. \quad (3)$$

The accuracy of Eqs. (2) and (3) is indicated by Table I.

For kernels obtained by the convolution of a "Yukawa" and "Gaussian" kernel, the values of x_0, and the errors in (3) are intermediate between those indicated in the table for the two simple kernels.

* Based on Knolls Atomic Power Laboratory Report A-4249 dated September 5, 1947.
[1] R. E. Marshak, Phys. Rev. 71, 688 (1947).

Microwave Magnetic Resonance Absorption in Nitric Oxide

ROBERT BERINGER AND J. G. CASTLE, JR.
Sloane Physics Laboratory, Yale University, New Haven, Connecticut*
August 5, 1949

WE have studied the magnetic absorption spectrum arising from transitions between the Zeeman components of a single rotational state of NO. The apparatus and technique have been briefly described in connection with a similar spectrum[1] observed in O_2.

As is well known, the NO molecule has a $^2\Pi$-ground state, and the molecular paramagnetism arises from the upper or $^2\Pi_{3/2}$ doublet component which is appreciably populated at room temperature. The spin-orbit coupling and doublet splitting are quite large in NO so that this coupling is not broken down by laboratory magnetic fields. Thus, in distinction to O_2, the main features of the magnetic absorption in NO are as predicted by the ordinary Zeeman theory. This theory[2] gives four magnetic levels separated by a constant energy interval $(4/5)\mu_0 H$ erg, for the lowest, $J=3/2$, rotational state of the upper doublet component. H and μ_0 are, respectively, the external magnetic field and the Bohr magneton. Magnetic dipole transitions, $\Delta m_J=\pm 1$, would give rise to a single absorption line at about 8360 gauss for the experimental frequency of 9360 mc/sec. Similar transitions for the $J=5/2$ state lie above the available field strengths for this frequency.

The observed spectrum consists of nine lines of about equal intensity arranged in a trio of triplets with an approximately constant spacing of 27 gauss between members of a triplet and an approximately constant spacing of 100 gauss between the triplet centers. The center of the pattern is at about 8660 gauss. The lines have equal half-widths of 4 to 5 mc/sec. at a pressure of 0.6 mm Hg. The measured absolute intensity of a single line is roughly 10^{-10} when expressed as the imaginary part of the magnetic susceptibility. This is in agreement with theory.

The nature of the nine-line spectrum has been tentatively explained as arising from a combination of molecular perturbations and nuclear spin effects. Hill[3] has calculated the effect of spin uncoupling by a magnetic field for molecules in doublet states. This effect produces a general shift of the pattern by about the observed amount but does not cause differences in level separations as large as those observed. Hill has also indicated the effects of magnetic perturbations by nearby rotational states. This may be the largest source of the observed level separation differences. As for the nuclear perturbations, several kinds should be present since N^{14} has a spin of unity and both magnetic dipole and electric quadrupole moments. There will be a total of twelve hyperfine levels for the $J=3/2$ rotational state. The IJ coupling with N^{14} might be expected to be fairly large because of the resultant molecular moment but still quite small as compared with the JH coupling. IH and electric quadrupole coupling are quite small. A combination of the molecular perturbations and IJ coupling gives a nine-line spectrum similar to that observed. There is some suggestion of non-interval spacing due to quadrupole coupling, but our present magnetic field stability must be improved to determine this quantitatively.

* Assisted by the ONR.
[1] R. Beringer and J. G. Castle, Jr., Phys. Rev. 75, 1963 (1949).
[2] F. H. Crawford, Rev. Mod. Phys. 6, 90 (1934).
[3] E. L. Hill, Phys. Rev. 34, 1507 (1929).

A Particular Case in Einstein's Generalized Theory of Gravitation

V. V. NARLIKAR AND RAMJI TIWARI
Benares Hindu University, U. P., India
March 22, 1949

FOLLOWING Einstein's generalized theory of gravitation,[1] we have set up a total field of Hermitian quantities which reduced to the isotropic field of a point mass in classical relativity when the electromagnetic field is switched off, and which reduces to the uniform field of monochromatic radiation ($E_y=H_z=-\phi$, $E_x=E_z=H_x=H_y=0$, $\phi=A\cos 2\pi(x-t)/\lambda$) when the gravitational field is removed. For the Hermitian tensor $g_{ij}=a_{ij}+(-1)^{\frac{1}{2}}b_{ij}$ we have

$$a_{ii}=-\left(1+\frac{2m}{r}+\frac{3}{2}\frac{m^2}{r^2}+\frac{m^3}{2r^3}-h_{ii}\right),\quad i=1,2,3$$

$$a_{44}=1-\frac{2m}{r}+\frac{2m^2}{r^2}-\frac{3}{2}\frac{m^3}{r^3}+h_{44},\quad a_{ij}=h_{ij},\quad i\neq j \quad (1)$$

$$b_{12}=\alpha,\quad b_{13}=\phi+\beta,\quad b_{14}=\gamma,$$
$$b_{23}=\delta,\quad b_{24}=\epsilon,\quad b_{34}=\phi+\chi.$$

The electromagnetic potentials appear through

$$\alpha=-\Phi_{,3}-H_{,4},\quad \beta+\phi-2m\phi/r=G_{,4}+\Phi_{,2},$$
$$-\gamma=H_{,2}-G_{,3},\quad \delta=-\Phi_{,1}-F_{,4}, \quad (2)$$
$$-\epsilon=F_{,3}-H_{,1},\quad -\chi-\phi-2m\phi/r=G_{,1}-F_{,2},$$

where the normal notation is used. m and ϕ are of the first order of magnitude, α, β, γ, δ, χ and ϵ are of the second order, and the ten h_{ij} are of the third order. To the second order of approximation the field equations satisfied by the electromagnetic potentials are found to be

$$\begin{aligned}
&\Box^2 F+\Box(4m\Phi/r)_{,14}=8(m/r)_{,12}\phi_{,1},\\
&\Box^2 G+\Box(4m\Phi/r)_{,24}=8(m/r)_{,22}\phi_{,1}-8(m/r)_{,1}\phi_{,11},\\
&\Box^2 H+\Box(4m\Phi/r)_{,34}=8(m/r)_{,32}\phi_{,1},\\
&\Box^2\Phi-\Box(4m\Phi/r)_{,44}=0,
\end{aligned} \tag{3}$$

where $\Box^2$ is $\Box\Box$ and $\Box\equiv(\partial^2/\partial x^2)+(\partial^2/\partial y^2)+(\partial^2/\partial z^2)-(\partial^2/\partial t^2)$, the equation of continuity to the second order of approximation being

$$F_{,1}+G_{,2}+H_{,3}+\Phi_{,4}(1+4m/r)=0. \tag{4}$$

The ten h_{ij}, which are of the third order, are given by

$$\begin{aligned}
&R_{11}+L_{,11}+\phi\Box\beta+2\phi_{,1}\gamma_{,3}-(4m/r)\phi\phi_{,11}-8(m/r)_{,1}\phi\phi_{,1}=0,\\
&R_{12}+L_{,12}+\tfrac{1}{2}\phi\Box\delta-\phi_{,1}(\alpha-\epsilon)_{,3}-(2m/r)_{,2}\phi\phi_{,1}=0,\\
&R_{13}+L_{,13}-\tfrac{1}{2}\Box(\phi\gamma)-\phi_{,1}(\beta-\chi)_{,3}-(2m/r)_{,3}\phi\phi_{,1}=0,\\
&R_{14}+L_{,14}-\tfrac{1}{2}\phi\Box(\beta+\chi)-2\phi_{,1}\gamma_{3}+(4m/r)\phi\phi_{,11}+6(m/r)_{,1}\phi\phi_{,1}=0,\\
&R_{22}+L_{,22}=0,\\
&R_{23}+L_{,23}+\tfrac{1}{2}\Box\{\phi(\alpha-\epsilon)\}=0,\\
&R_{24}+L_{,24}-\tfrac{1}{2}\phi\Box\delta+\phi_{,1}(\alpha-\epsilon)_{,3}+2\phi\phi_{,1}(m/r)_{,2}=0,\\
&R_{33}+L_{,33}+\Box L=0,\\
&R_{34}+L_{,34}+\tfrac{1}{2}\Box(\phi\gamma)+\phi_{,1}(\beta-\chi)_{,3}+(2m/r)_{,3}\phi\phi_{,1}=0,\\
&R_{44}+L_{,44}+\phi\Box\chi+2\phi_{,1}\gamma_{,3}-4\phi\phi_{,1}(m/r)_{,1}+(4m/r)\phi\phi_{,14}=0,
\end{aligned} \tag{5}$$

where

$$R_{kl}=-\tfrac{1}{2}\delta^{\sigma\rho}\left(\frac{\partial^2 h_{kl}}{\partial x^\sigma\partial x^\rho}+\frac{\partial^2 h_{\sigma\rho}}{\partial x^k\partial x^l}-\frac{\partial^2 h_{k\sigma}}{\partial x^l\partial x^\rho}-\frac{\partial^2 h_{l\rho}}{\partial x^k\partial x^\sigma}\right) \tag{6}$$

and

$$L=\phi(\beta-\chi)-(2m/r)\phi^2,\qquad \delta^{11}=\delta^{22}=\delta^{33}=-\delta^{44}=-1,\quad \delta^{ij}=0,\quad i\neq j. \tag{7}$$

It can be verified that the ten field equations of gravitation are subject to the four identities of the type,

$$(\partial R_{11}/\partial x)+(\partial R_{12}/\partial y)+(\partial R_{13}/\partial z)-(\partial R_{14}/\partial t)=-\tfrac{1}{2}(\partial R/\partial x). \tag{8}$$

It is believed that the derivation of Eqs. (3) and (5) in this particular case of the unified field marks an advance in the understanding of Einstein's generalized theory of gravitation. A preliminary paper in this connection is in the press for the Proceedings of the National Institute of Sciences of India.

[1] A. Einstein, Rev. Mod. Phys. **20**, 35 (1948). References to the earlier papers on this theory will be found in the paper.

Second Sound Velocity in Paramagnetically Cooled Liquid Helium II†

JOHN R. PELLAM AND RUSSELL B. SCOTT
National Bureau of Standards, Washington, D. C.
August 8, 1949

THE qualitative behavior of the velocity of second sound in the temperature range below 1°K has been experimentally observed. Although the present measurements are strictly of a preliminary nature, sufficient information is provided for a decision between certain aspects of the theories of Tisza[1] and Landau.[2]

Cooling of the helium II to temperatures well below 1°K was attained by conventional demagnetization methods. Crystals of hydrated iron-ammonium-alum immersed in the liquid were subjected to magnetic fields of up to 12 kilogauss under isothermal conditions (about 1°K starting temperature). Upon removal of the field the redistribution of entropy between the salt and the liquid provided the necessary cooling of the latter.

The portion of the helium II bath not occupied by the salt contained apparatus for generating and detecting second sound by the pulse method.[3] The velocity was determined by observing the transit time of the second sound with an oscilloscope. Since the distance between the transmitter and receiver was fixed, the position of the second sound signal on the oscilloscope screen provided a direct visual indication of velocity. The velocity was thus continuously observed as the temperature of the helium II decreased following demagnetization.

TABLE I. Typical set of velocity values obtained during the warm-up process.

Temperature (°K)	Second sound velocity (m/sec.) (±1 percent)
——	33.9
——	20.2
——	19.8
——	18.9
——	18.7
——	18.6
——	18.5
——	18.5
——	18.6
——	18.5
——	18.8
——	18.8
1.23°K	18.9
1.25°K	19.0
1.29°K	19.4
1.69°K	20.1

Because of the significance to theory of immediate qualitative results, the precise determination of temperature has thus far been set aside in favor of learning trends.

The three essential facts to be drawn from the present experiments are:

(1) *The velocity increases markedly with decrease of temperature below 1°K.* This is in line with the predictions of Landau.

(2) At the lowest temperatures reached (where the velocity was nearly double the value at 1°K) the received d.c. pulse widths increased by a factor of from 3 to 5. This suggests either a possible frequency dispersion* or a gradual partial return to the classical diffusive type of heat flow. No observable decrease in signal strength occurred.

(3) The velocity minimum of about 18.4 m/sec. previously reported by Peshkov[4] just above 1°K was verified** as the helium II bath was warming up from the lowest temperatures.

Of these observations the velocity behavior is of primary interest. A typical set of velocity values observed during the warming up process is given in Table I, where velocities are listed in chronological order as the temperature rose. A maximum value of 33.9 m/sec. was observed for the lowest temperature reached This velocity represents a rise of 83 percent above the minimum near 1°K and greatly exceeds the previously known maximum[3,4a] of 20.3 m/sec. occurring at about 1.65°K.

Although the second sound velocity data are obviously incomplete without accurate determinations of the corresponding temperature, at present we can offer only a rough guess as to the minimum temperatures reached. It was believed prior to the experiments that the low temperature reached following each demagnetization could be deduced from knowledge of the initial magnetic field strength, the geometry, and the known properties of iron-ammonium-alum.[5] For instance for true isentropic conditions we should have obtained temperatures as low as 0.06°K. However, because of excessive heat inflow, only a fraction of the expected temperature drop was realized and its accurate estimation was precluded by the resultant non-equilibrium conditions following demagnetization. The helium reached its lowest temperature within 3 seconds after demagnetization, whereupon

TABLE II. Maximum velocity following each demagnetization.

Initial magnetic field (kilogauss)	Velocity at lowest temperature (m/sec.)
11.8	33.9
11.9	30.4
11.6	22.0
11.4	21.8
10.8	21.8

further cooling by the salt was more than offset by heat influx. Taking this into account, it is likely that the temperature corresponding to the highest observed velocity of 33.9 m/sec. was above 0.3 or 0.4°K

Due to this heat influx (and the relatively small dependence of velocity on temperature near 1°K) the marked velocity increases were observed only for initial fields approaching 12 kilogauss. This is illustrated in Table II where the maximum velocity following each demagnetization is given for the corresponding initial field strength.

As the result of the fundamentally opposite nature of Tisza's[1] and Landau's[2] expectations for second sound behavior in the extreme low temperature range, a choice on the basis of this present evidence is not difficult. Tisza predicted a systematic decrease in velocity with decreased temperature, setting in near 1.5°K and presumably continuing toward zero velocity at absolute zero. Landau conversely predicted a strong increase in velocity as temperature is lowered below 1°K. This latter prediction appears thus far to be substantiated.

This should not necessarily be taken as evidence against London's[6] original hypothesis of helium II as a condensed Bosé-Einstein gas. In fact the recent experiments of D. Osborne *et al.*[7] showing non-superfluidity in He^3 are exceedingly strong evidence for the condensation theory. Rather one would expect that a reformulation of Tisza's second sound picture would be desirable, based on the Bosé-Einstein hypothesis, but with the assumption of no phonon entropy carried by the superfluid. Fundamentally Tisza's and Landau's formulations accrue from essentially the same thermodynamic relationship, the distinction lying in the manner of its interpretation. In the upper temperature range Tisza's analysis appears completely adequate.

In a recent paper Pomeranchuk[8] predicted that impurities in helium II (in the form of He^3) might preclude Landau's predicted sharp rise in velocity with decrease in temperature below 1°K. For the He^3 concentration in our helium II (gas-well helium) this does not appear to be the case.

By reducing the heat leak it is hoped that future measurements can be made at lower temperatures and under conditions which permit reliable temperature determinations.

* Tisza[1] in fact has suggested that relaxation type dispersion should appear at temperatures well below 1°K.

** This substantiates the doubts expressed by one of the authors[3] over the reliability of his own low temperature data in earlier second sound measurements.

† Supported by the ONR, Contract Na-onr-12-48.

[1] L. Tisza, Phys. Rev. **72**, 838 (1947); also Phys. Rev. **75**, 885 (1949).
[2] L. Landau, J. Phys. U.S.S.R. **5**, 71 (1941); also **8**, 1 (1944); also Phys. Rev. **75**, 884 (1949).
[3] J. Pellam, Phys. Rev. **75**, 1183 (1949).
[4] V. Peshkov, J. Exp. Theor. Phys. U.S.S.R. **18**, 951 (1948).
[4a] V. Peshkov, J. Phys. U.S.S.R. **10**, 389 (1946).
[5] N. Kurti and F. Simon, Proc. Roy. Soc. London **149**, 152 (1935).
[6] F. London, Nature **141**, 643 (1938); Phys. Rev. **54**, 947 (1938).
[7] Osborne, Weinstock, and Abraham, Phys. Rev. **75**, 988 (1949).
[8] I. Pomeranchuk, J. Exp. Theor. Phys. U.S.S.R. **19**, 42 (1949).

On the Tripartition and Quadripartition of Uranium Nuclei

R. Chastel and L. Vigneron
Laboratoire de Chimie Nucléaire du Collège de France, Paris, France
June 20, 1949

We have been surprised that several recent publications about tripartitions of uranium nuclei make no reference to the French results on this subject,[1] or make reference only to the preliminary results,[2] omitting the detailed report[3] published by Mr. Tsien San Tsiang, Mrs. Ho Zah Wei[4] and the writers.

Therefore, we wish to point out that our work had been undertaken after the presentation at the Meeting on Fundamental Particles held in Cambridge (England) on July, 1946, by Green and Livesy of uranium fission tracks photograph showing the emission of long range light particles. We think we were the first to publish a correct interpretation of this new fission process in our publication "Sur la tripartition de l'uranium provoquée par capture d'un neutron."[5] We were also the first to publish a mass determination of the light fragment.[6] We published the first experimental evidence of quadripartition of uranium nuclei.[7] A preliminary report of our work was given in English in a letter to the editor of the Physical Review[8] as well as in Nature;[9] in these two communications we announced that a more detailed report was to be published in the Journal de Physique et le Radium.[3] Mr. Tsien San Tsiang published a detailed theoretical interpretation of these phenomena in that same journal.[10]

The first photograph of nearly symmetrical tripartition (with fragment of masses: 127, 77 and 32 mass unit) was published in our paper in Nature on June, 1947.[9]

[1] J. T. Dewan and K. W. Allen, Phys. Rev. **76**, 181 (1949).
[2] L. Marshall, Phys. Rev. **75**, 1339 (1949).
[3] Tsiang, Wei, Chastel and Vigneron, J. de phys. et rad. **8**, 165 (1947); **8**, 200 (1947).
[4] Both now at the National Tsinghua University of Peiping, China.
[5] Tsiang, Chastel, Wei, and Vigneron, Comptes Rendus **223**, 986 (1946).
[6] Tsiang, Wei, Chastel, and Vigneron, Comptes Rendus **224**, 272 (1947).
[7] Wei, Tsiang, Vigneron, and Chastel, Comptes Rendus **223**, 1119 (1946).
[8] Tsiang, Wei, Chastel, and Vigneron, Phys. Rev. **71**, 382 (1947).
[9] Tsiang, Wei, Vigneron, and Chastel, Nature **159**, 773 (1947).
[10] Tsien San Tsiang, J. de phys. et rad. **9**, 6 (1948).

The Future Nuclear Interaction

Alex E. S. Green
Department of Physics, University of Cincinnati, Cincinnati, Ohio
July 7, 1949

In the future theory the energy of interaction of nucleons may be expressible in the form $V=OJ$ where O is an operator containing the isotopic, Dirac matrix, and positional coordinates of the nucleons and J is the Green's function of the field. Recently promising forms of J have been derived from a generalized linear field theory.[1] It remains, however, to fix O on a theoretical basis.

In conformity with the second form of a proposed principle of generalization[1] we might seek an appropriate operator among the various developments of one-meson theory. To determine the suitability of the final result of such developments and to detect inadmissible assumptions we propose three tests to augment those previously formulated.[2]

I. The interaction must be well-behaved in the limit of zero-meson mass, reducing to a reasonable Newtonian or Coulombian interaction.

II. Dipole terms must have as co-factors a natural length which is characteristic of the nucleons, rather than the field, in correspondence with the classical case.

III. The infinite self-energies and inadmissible interaction singularities among static and relativistic terms must vanish when Yukawa's potential is replaced by our generalized meson potential.

In applying these tests to the four interactions derived by Kemmer[3] (Eq. (67a–d)) we find that the eight terms with factors κ^{-2} fail with respect to all three tests. Most of these defects may be removed, however, by a trivial modification of Kemmer's development. We first assign the role of the classical potentials to the ϕ's in the scalar and vector cases and the χ's in the pseudovector and pseudoscalar cases and the role of the classical field strengths to the χ's and the ϕ's in the corresponding cases. With this identification we see that four of the interaction Lagrangians ((39a), (39b), (40c), and (40d)) correspond to the classical interaction of a pole with the field whereas the other four correspond to a dipole interacting with the field. In conformity with the corresponding principle in the latter cases we must associate with the coupling constants (f_a, f_b, g_c and g_d) a length a, presumably $\hbar/Mc$,[4] which is characteristic of the nucleon. We may do this simply by multiplying these four of Kemmer's coupling constants by $a\kappa$, a step which does not disturb the subsequent development. The final explicit interactions are improved considerably by this modification and we are left with only two defective terms, one

each in V_0[b] and V_f[c]. These terms have their origins in the more difficult and subtle questions connected with auxiliary conditions. In one development of these interactions by the writer they do not appear at all. In another they are replaced by innocuous terms. It must be noted that the uniform introduction of the factor $a\kappa$ in all coupling constants or the equivalent device commonly employed,[5] while giving interactions which satisfy tests II and III, is not permissible according to test I. In particular the Newtonian and Coulombian static fields then are lost in the limit of zero-meson mass.

Assuming tentatively that the pi-meson is the principal nuclear force meson then $(a\kappa)^2=(m/M)^2\sim 1/40$. We come then to the important physical conclusion that only if the fine structure constants (α_p for pole coupling and α_d for dipole coupling) are related by $\alpha_d\sim 40\alpha_p$ will the static interactions arising from dipole coupling be of the same order of magnitude as the static pole interaction. Since α_d is then greater than one we are forced to strong coupling for this part of the interaction. On the other hand if we assume $\alpha_d\sim\alpha_p$ we find that the effects of dipole coupling are small compared to the static pole interactions and, in fact, are of the same order of magnitude as the relativistic pole interactions. Thus the assumption of simultaneous pole and dipole coupling is an undesirable complication. Indeed, the complication is even greater than indicated by Kemmer's treatment which does not bring out the pole-dipole interference terms and which discards contact interactions.[6] We can, nevertheless, utilize the Kemmerian interactions, with the suggested modifications, by regarding them as eight distinct interactions four of which, the pole cases, have a more elementary nature. Three of these cases, the scalar-scalar, the vector-vector and the pseudovector-pseudovector[7] have large static terms, but they are not promising nuclear interactions. The pseudoscalar-pseudoscalar, a synthesis of the first two,[8] and the four dipole cases give rise to more interesting interactions which, however, are too small in the case of a one-meson field for $\alpha<1$. In a later communication we shall discuss the possibility that these latter interactions, in conjunction with a generalized multiple-meson field, may contain the correct nuclear interaction.

[1] A. Green, Phys. Rev. **75**, 1926 (1949).
[2] E. Wigner, Phys. Rev. **51**, 106 (1937).
[3] N. Kemmer, Proc. Roy. Soc. **A166**, 145 (1938). As usual the factor $c\kappa/4\pi$ has been removed and we consider for convenience the neutral theory.
[4] Admittedly a factor 2π would nullify some of the ensuing arguments.
[5] G. Wentzel, Rev. Mod. Phys. **19**, 3 (1947), Eqs. (1) and (2).
[6] L. Van Hove, Phys. Rev. **75**, 1519 (1949).
[7] For some treatments of the auxiliary conditions.
[8] A. Green, Phys. Rev. **76**, 460 (1949).

Mass Assignment of Xenon Activities Produced in Fission

SIGVARD THULIN, INGMAR BERGSTRÖM AND ARNE HEDGRAN
Nobel Institute for Physics, Stockholm, Sweden
July 25, 1949

THE electromagnetic isotope separator[1] of this Institute has been used in order to ascertain the mass-numbers of the Xe isotopes produced in fission. The gaseous fission products from neutron irradiated uranium oxide were fed to the ion source and the active isotopes collected on a thin aluminium plate. This method has recently been used by J. Koch, Copenhagen, in an investigation of the Kr isotopes produced in fission (private communication). The method of determining the mass numbers, corresponding to the different activities, was the same as used for the mass assignment of 43^m Hg^{199}[2] and 53^d Hg^{203}.[1]

TABLE I. Summary of results.

Element	Mass number	Half-life	Parent isotope (according to Seaborg's tables and our measurements)
Xe	133	~5.4 d	
Xe	135	9.1 hr.	
Xe	137	3.5 min.	I^{137} 22.0 sec.
Xe+Cs	138	30.0 min.	I^{138} 5.9 sec.

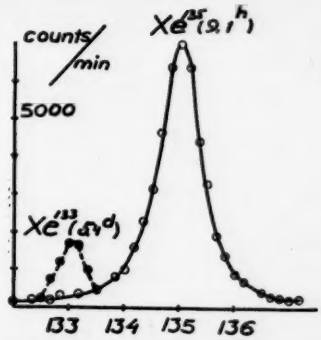

FIG. 1a. The activity of the 5.4 d and 9.1 hr. xenon isotopes. Dotted curve is the 5.4 d activity, measured 3 days after the 9.4 hr. activity and drawn to a 5 times larger scale.

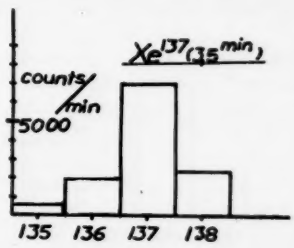

FIG. 1b. The activity of the 3.5 min. Xe isotope measured immediately after separation and 8 minutes after stopping the cyclotron.

Figures 1a, b, and c show the measured activity as a function of the position on the collector plate and the results are summarized in Table I. This confirms that the assignments of these isotopes in Seaborg's tables[3] are correct (the mass numbers 137 and 138 were classified as *B* and *D*).

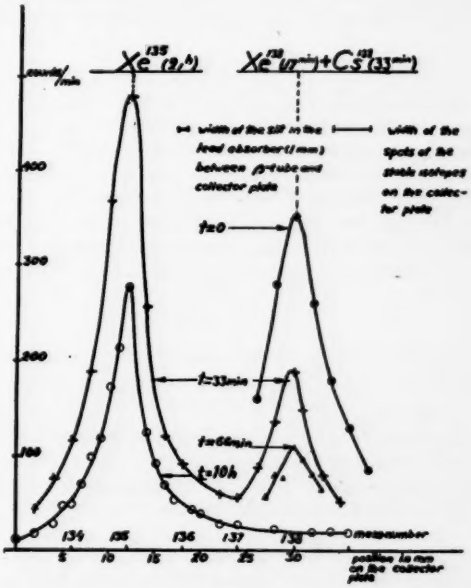

FIG. 1c. The activity of the 17 min. Xe and 33 min. Cs isotopes.

TABLE II. Summary of β-spectrometer investigations.

Isotope	β-max. kev	β-lines	$h\nu$
Xe^{133}	315	25.6 (Auger, medium)	
		30.9 (Auger, weak)	
		46.5 (K 1, very strong)	82.4
		59.3 (K 2? weak)	95.2 (?)
		77.9 (L 1, medium)	83.6
		200 (K 3 weak)	236
Xe^{135}	930	214 (K)	250
		242 (L)	
Xe^{138}	2680		

The activities of Xe^{133}, Xe^{135}, and Cs^{138} on the collector plate, were sufficient for β-spectrometer investigations. The β-spectrometer data are summarized in Table II.

[1] Bergström, Thulin, Svartholm, and Siegbahn, Ark. för Fysik **1**, No. 11 (1949).
[2] I. Bergström and S. Thulin, Phys. Rev. **76**, 313 (1949).
[3] Koch, Kofoed-Hansen, Kristensen, and Drost-Hansen, Phys. Rev. **76**, 279 (1949).

Second Sound and Classical Heat Flow[a,*]

JOHN R. PELLAM
National Bureau of Standards, Washington, D. C.
August 1, 1949

THE reversibility of the thermomechanical effect in liquid helium II and the inertial characteristics of the associated heat flow result in the true wave characteristics of second sound. In the portion of a second sound cycle where heat flows toward cooler regions, mechanical energy is stored as energy of internal convection. During the opposite half of the cycle heat flows toward warmer regions at the expense of this stored energy. The resulting average mechanical energy content of the wave provides a net mechanical energy flow or *intensity* in the direction of propagation.

Considerations of second sound are simplified by assuming square wave pulses, logical justification lying in the known absence of frequency dispersion. This obviates the distinction between instantaneous and average values. If heat flow density $\dot{H}$ (cal./sec. cm^2) is sustained by liquid helium II during the generation of a one-dimensional square wave heat pulse, the temperature is raised by τ within a heated region which is progressing at the rate of second sound velocity v_2. This requires[1-4] that

$$\dot{H}=\rho c_v \tau v_2, \tag{1}$$

where ρ is the density and c_v the specific heat capacity per gram for helium II. The generation of this second sound actually requires slightly greater heat input than the heating rate $\dot{H}$, to provide the kinetic energy of internal convection stored in the pulse. At the abrupt front of the temperature pulse heat flows continuously out toward the ambient temperature region, cooler by amount τ. According to the second law of thermodynamics** the rate of mechanical energy generation, or intensity γ, is related to temperature by

$$\gamma/\dot{H}=\tau/T_0, \tag{2}$$

where T_0 is the ambient absolute temperature (°K). The intensity becomes[3,5]

$$\gamma=\tau\dot{H}/T_0=\rho c_v v_2 \tau^2/T_0. \tag{3}$$

This expression*** is equally significant with respect to classical heat flow within ordinary materials.

Finally, combining (1) and (2) the expression for total energy flow (thermal plus mechanical) becomes

$$\text{energy flow}=\rho c_v v_2 \tau[1+\tau/T_0] \tag{4}$$

indicating the flow of mechanical energy within a second sound packet to be but the fraction τ/T_0 of the associated heat flow.

Second sound possesses a wave momentum and a radiation pressure. At a chosen position and instant, whichever fluid component happens to be moving in the direction of propagation possesses greater than ambient density, whereas the other component is necessarily retrogressing at less. Accordingly therefore, in the identical manner as for classical sound, the wave momentum flow J for the pulses equals the mechanical energy density divided by wave velocity, equal in turn to radiation pressure P_{rad}.

$$P_{\text{rad}}=J=\rho c_v \tau^2/T_0 \tag{5}$$

or twice (5) for reflection from a thermally non-conducting barrier.**** Although of second-order magnitude, this is the sole existent pressure for second sound! This should not be confused with the small amount of first sound coupled[6] to second sound by the thermal coefficient of expansion of helium II. (It should be noted that the method of deriving the expression automatically includes both kinetic and potential energy density; for continuous waves a factor $\frac{1}{2}$ would appear). Thus under appropriate experimental conditions there would be a "sound current" associated with second sound (as with ordinary sound) of velocity $c_v\tau^2/v_2T_0$.

Thermal boundary conditions early employed by the author (for setting up "thermal impedances") in design of second sound systems were the continuity of temperature and heat flow density between liquid helium II and adjacent classical solids. Thus for second sound normally incident upon a classical barrier

$$\tau_i+\tau_r=\tau_{tr}, \quad \dot{H}_i-\dot{H}_r=\dot{H}_{tr}, \tag{6}$$

where the subscripts (i) and (r) refer, respectively, to incident and reflected second sound, (tr) to transmitted classical thermal waves.

Employing (1) we obtain from (6)

$$\frac{\tau_i\dot{H}_i}{T_0}-\frac{\tau_r\dot{H}_r}{T_0}=\frac{\tau_{tr}\dot{H}_{tr}}{T_0}, \tag{7}$$

where complex conjugates are not used since instantaneous values are desired. Equations (1) and (6) can also be employed to show that for most cases not all of the incident second sound energy is reflected; thermal impedance[4] $\tau/\dot{H}$ equals $[\rho c_v v_2]^{-1}$ for helium II [see (1)] and is entirely real, and may for solid boundaries possess a real component as large as the imaginary component. The essence of (7) is therefore that the temperature wave† entering the solid possesses an *intensity* $\tau\dot{H}/T_0$ in the same manner as does second sound. (This is likewise required for the converse case of second sound waves in helium II being set up by thermal waves emerging from an adjacent solid.) But the well-known *expression for classical thermal waves involves rapid damping, so that the associated energy thereby lost reappears in other forms.*

Certain speculations may be made in this regard. The "kinetic energy" density of the thermal pulse may tentatively be regarded as associated with the mass flow inherent to thermal conduction. Correspondingly "potential energy" density should be related to pressure alterations accompanying thermal flow. The second law of thermodynamics as given by (2) thus holds for thermal conduction across a layer of classical material of thickness less than the thermal wave-length. Analysis based on the thermal impedance concept[4] reveals that second sound pulses should be transmitted without distortion†† or appreciable loss through layers of classical material of such thinness immersed in liquid helium II, thus conforming to conditions of complete reversibility. Arguments similar to those employed by Rayleigh[7] for a classical sound pulse indicate that the mechanical energy flow $\tau\dot{H}/T_0$ involved is shared equally between kinetic and potential forms, not only for second sound but also for classical thermal waves.

When penetration of thermal waves into classical materials exceeds several mean-free-path lengths, the reversibility between heat flow and mechanical energy stated by (2) is necessarily affected by the natural collisions occurring between particles or between phonons. Accordingly the well-known damping sets in and converts the "mechanical energy" content of the thermal wave to acoustical or thermal forms, depending upon the geometry and the substances (thermal coefficient of expansion) involved.

For propagation along the x axis the "source strength" of such converted energy is just $Re(\partial/\partial x)(\tau\dot{H}/T_0)$.

Thus, whereas liquid helium II provides the only example of complete thermal and mechanical interdependence, the more limited thermomechanical properties of ordinary substances are evident from general thermodynamic considerations. Further implications are being investigated.

The author expresses his sincere gratitude to Professor Philip M. Morse for helpful and stimulating discussions.

* Supported by the ONR, Contract Na-onr-12-48.
* Since this study was undertaken, related work by several other investigators has appeared. Where overlap does now occur, the independently obtained results of the author are believed to present fresh viewpoints.
** A particularly clear derivation of the velocity of second sound has been given by Peshkov (see reference 3) based on the use of the second law.
*** In reference 5 the author gave the equivalent expression in mechanical terms. The thermodynamic properties of liquid helium II lead to a direct conversion between the two forms.
**** We are indebted to H. W. Woolley for an independent derivation of a form equivalent to (5).
† Peshkov mentions in reference 3 that the expression applies to materials other than helium II but without interpretation or consideration of the inherent decay.
†† The thermal impedance of a classical layer of thickness l backed by helium II is $(i\omega\rho_0 c_0\kappa_0)^{-\frac{1}{2}}\coth[(i\omega\rho_0 c_0/\kappa_0)^{\frac{1}{2}}l]+\coth^{-1}(i\omega\rho_0 c_0/\kappa_0)^{\frac{1}{2}}/\rho_0 c_0 v_2]$, where ρ_0, c_0, and κ_0 are, respectively, the density, heat capacity, and heat conductivity of the material. For a thin layer this approaches $(\rho_0 c_0 v_2)^{-1}+a/\kappa_0$ independent of frequency and nearly equal to the thermal impedance of helium II.

[1] D. Osborne, Nature **162**, 213 (1948).
[2] R. Dingle, Proc. Phys. Soc. London **61**, 9 (1948).
[3] V. Peshkov, J. Exp. Theor. Phys., U.S.S.R. **18**, 857 (1948).
[4] J. Pellam, Phys. Rev. **75**, 1183 (1949).
[5] J. Pellam, Phys. Rev. **73**, 608 (1948).
[6] L. Tisza, Phys. Rev. **72**, 838 (1947).
[7] J. Rayleigh, *The Theory of Sound* (Dover Publications, New York, 1945).

Nuclear Spin 5/2 for $_{40}Zr^{91}$

O. H. Arroe and J. E. Mack
University of Wisconsin, Madison, Wisconsin*
July 29, 1949

In interference spectrograms** of a Zr^{91}-enriched sample of zirconium*** in a hollow cathode source,[1] the $4d^2 5s^2\ {}^3P_0-4d^2 5s(^2P)5p\ {}^3S_1$ line[2] at ν_{17777} presents the following structure, showing that the spin, I, of the interesting[3] nucleus $_{40}Zr^{91}$ is undoubtedly 5/2 units:

$(I+1)$		-0.0701 ± 0.0010 cm^{-1},[4]
even isotopes	(arbitrary)	0.0000 ± 0.0012 cm^{-1},
(I)		$+0.0273\pm0.0010$ cm^{-1},
$(I-1)$		$+0.0983\pm0.0010$ cm^{-1},

I, from the Landé interval rule $2.69^{+0.58}_{-0.41}$.

Details, including the structure of other lines, will be submitted later.

* Work done on Navy contract N7 onr-285TO #1, NR 019 107.
** With auxiliary dispersion produced by a special Hilger spectrograph bought with funds granted by the University research committee.
*** Produced by the Y-12 plant, Carbide and Carbon Chemicals Corporation, and obtained by allocation from the AEC.
[1] O. H. Arroe and J. E. Mack, Phys. Rev. **76**, 173 (1949).
[2] W. F. Meggers and C. C. Kiess, J. Research Nat. Bur. Stand. **9**, 309 (1932).
[3] E. Feenberg and K. C. Hammack, Phys. Rev. **75**, 1877 (1949), especially pp. 1882 and 1893.
[4] The quantities preceded by the symbol ± have been made larger than the spread of the data by amounts judged to be enough to make it highly improbable that the true values lie outside the ranges indicated.

The Binding Energy of the Triton

R. E. Clapp*
Lyman Laboratory of Physics, Harvard University, Cambridge, Massachusetts
August 8, 1949

A VARIATIONAL calculation of the binding energy of the H^3 nucleus has been performed using the Rarita-Schwinger[1] interaction (square well with tensor force), as modified to include a charge-exchange factor $(-\frac{1}{2}\tau_i\cdot\tau_j)$. Except for the charge-exchange factor, which has very small effect on the triton binding energy, this is the same problem as that studied by Gerjuoy and Schwinger[2] and by Feshbach and Rarita.[3] The same variational method was used here, but a much more elaborate trial function was inserted. The calculations are still in progress, but the results so far obtained (and reported in Table I) show that other D-states not included in the previous calculations[2,3] make a substantial contribution to the binding energy.

TABLE I. Computed triton binding energy.

Trial functions (see text)		Triton binding energy	
S-state	D-states	In Mev	In percent of 8.3 Mev
(Finite power series)			
I	—	1.80	21.7
I	II	3.74	45.1
I	II, III, IV	5.60	67.5
(Extrapolated)			
I	—	1.80	21.7
I	II	3.88	46.7
I	II, III, IV	5.80	69.9
(Gerjuoy and Schwinger; S-state and D-state			39
(Feshbach and Rarita)			
S-state alone			21
S-state and D-state (estimated maximum)			40–50

The basis for the present method is the construction of a denumerable series of orthogonal functions which form a complete set for the nuclear three-body problem. With the type of potential that was assumed, the triton ground state can include only a selected group of these functions, characterized by even parity, by $J=\frac{1}{2}$ for the total angular momentum, by $T=\frac{1}{2}$ for the total isotopic spin, and by $T_3=-\frac{1}{2}$ for the third component of isotopic spin (to denote two neutrons and one proton). This sub-set of functions may then be arranged in order of increasing kinetic energy (which is roughly equivalent to the order of decreasing importance) and introduced systematically into the variational principle.

In setting up the system of orthogonal functions the usual relative coordinates, $\mathbf{r}:(r,\theta,\varphi)$ and $\boldsymbol{\varrho}:(\rho,\eta,\psi)$, have been transformed to a six-dimensional spherical coordinate system, with a single radial variable,

$$R=(\tfrac{2}{3}r^2+\tfrac{1}{2}\rho^2)^{\frac{1}{2}} \tag{1}$$

and five angular variables. The angular parts of the orthogonal functions are hyperspherical harmonics $Y_{K,L}$ which satisfy the defining equation:

$$\nabla^2(R^K\cdot Y_{K,L})=0 \tag{2}$$

with

$$\nabla^2\equiv\tfrac{2}{3}\nabla_r^2+2\nabla_\rho^2. \tag{3}$$

These harmonics can be classified by their value of L into S, P, D, etc., states, and combined with suitable spin and isotopic spin functions to give the admissible set of $^2S_{\frac{1}{2}}$, $^2P_{\frac{1}{2}}$, $^4P_{\frac{1}{2}}$, and $^4D_{\frac{1}{2}}$ triton functions. With each harmonic $Y_{K,L}$ there will also be a radial factor $R^K\cdot f(R)$, where the function $f(R)$ need be defined only for $R>0$ and may therefore be written as a function of R^2. The form chosen was a Gaussian multiplied by a power series:

$$f(R)=\epsilon^{-\mu R^2}(a+bR^2+cR^4+\cdots). \tag{4}$$

In Table I are listed the binding energies resulting from the successive inclusion of one ^2S-state function (I) and three ^4D-state functions (II, III, IV). The S-state is essentially the same as that used by Gerjuoy and Schwinger and by Feshbach and Rarita, and function II corresponds to their D-state, but functions III and IV contain D-states which they omitted. The binding energy is given in Mev and in percent of the experimental value which they used, 8.3 Mev.**

In the present calculations, the same Gaussian parameter μ was used for all of the four functions. This does no harm if each power series is sufficiently long. The power series for functions I,

II, III, and IV contained 7, 5, 3, and 3 terms, respectively.*** There were thus 18 adjustable coefficients and one Gaussian parameter, or a total of 19 independent variational parameters. In order that the rate and degree of convergence might be estimated, most of the 18 terms in the variational function were added one at a time. From the regularities which appeared it was possible to extrapolate with some assurance to the binding energy which would have been computed from the same four angular functions if it had been possible to use infinite rather than finite power series in the radial factors. The extrapolated results are also given in Table I. The effects of other ^3S and ^4D functions are being investigated, as well as the (very small) contributions of P-state functions. A detailed report will be submitted later. Although only the Rarita-Schwinger potential has been used so far, the method of analysis is designed to handle any proposed potential and to test its ability to account for the properties of the triton.

This letter reports the results of research for a Ph.D. thesis written at Harvard under Professor Julian Schwinger. The writer is very grateful for discussions with Professor Schwinger, and with Professors Feshbach of M.I.T. and Rarita of Brooklyn College.

* Coffin Fellow (General Electric Educational Fund), 1947–48; AEC Predoctoral Fellow, 1948–49. (The work reported on here extended over both years.) The writer is now at the Massachusetts Institute of Technology.

** The experimental triton binding energy given by L. Rosenfeld (*Nuclear Forces II* (Interscience Publishers, Inc., New York, 1949), p. 501) is 8.39 Mev. A still more recent value, 8.50 Mev, is based on the redetermination by Bell and Elliott of 2.235 Mev for the deuteron binding energy (Phys. Rev. **74**, 1552 (1948)). The old value, 8.3 Mev, was used in Table I for comparison with the previous calculations. It should be noted also that the Rarita-Schwinger constants are based on the value of 2.17 Mev for the deuteron binding energy

*** To simplify the large secular equations, each power series was written as the sum of an equivalent series of orthogonal polynomials.

[1] W. Rarita and J. Schwinger, Phys. Rev. **59**, 436 (1941).
[2] E. Gerjuoy and J. Schwinger, Phys. Rev. **61**, 138 (1942).
[3] H. Feshbach and W. Rarita, Phys. Rev. **75**, 1384 (1949).

Proceedings of The American Physical Society

MINUTES OF THE MEETING OF THE DIVISION OF FLUID DYNAMICS AT WHITE OAK, MARYLAND JUNE 30, JULY 1, 1949

THE third meeting of the Division of Fluid Dynamics of the American Physical Society and the first meeting of the Division without its parent Society took place at the Naval Ordnance Laboratory at White Oak, Maryland on June 30 and July 1, 1949. The meeting was held in conjunction with the dedication ceremonies and symposia of the Laboratories which took place in the preceding three days. The Naval Ordnance Laboratory proved to be an excellent host largely through the efforts of R. J. Seeger and his many assistants who organized the program and provided all the necessary arrangements.

The program consisted of three symposia, (1) Aerothermodynamics, (2) Shock-Wave Phenomena, and (3) Turbulence, and five sessions totaling fifty-six contributed papers. The high quality of the papers delivered at this meeting was universally acclaimed, but the secretary was distressed by the many poor abstracts and vague titles which were submitted on the contributed program.

The program follows.

WALKER BLEAKNEY, *Secretary*
American Physical Society
Division of Fluid Dynamics
Princeton University,
Princeton, New Jersey

Symposium on Aerothermodynamics

Chairman: P. S. EPSTEIN, *California Institute of Technology.*

Transport Properties of Gases. J. O. HIRSCHFELDER, *University of Wisconsin.*

Transport Phenomena In Dilute Gases. G. E. UHLENBECK, *University of Michigan.*

The Effect of Relaxation on Shock Waves in Gasses. K. F. HERZFELD, *The Catholic University of America.*

Study of Condensation of Components of Air at High Mach Numbers. L. LEES AND S. M. BOGDONOFF, *Princeton University.*

The Aerothermodynamics of Sound Waves. P. S. EPSTEIN, *California Institute of Technology.*

Symposium on Shock-Wave Phenomena

Chairman: K. O. FRIEDRICHS, *New York University.*

Shock Wave Phenomena In Astronomy. Z. KOPAL, *Massachusetts Institute of Technology.*

The Flow Behind Stationary Shocks of Varying Strength. C. C. LIN, *Massachusetts Institute of Technology.*

An Experimental Study of the Interaction of Shock Waves. W. BLEAKNEY, *Princeton University.*

Shock Wave Phenomena: Water-Like Substances. R. J. SEEGER AND H. POLACHEK, *Naval Ordnance Laboratory.*

Impact Shock Waves in Water. J. HOWARD MCMILLEN AND R. L. KRAMER, *Naval Ordnance Laboratory.*

Symposium on Turbulence

Chairman: J. M. BURGERS, *Technische Hoogeschool, Delft, Holland.*

Spectral Tensor of a Homogeneous Turbulence. J. KAMPÉ DE FÉRIET, *University of Lille, France.*

The Nature of Turbulent Motion at Large Wave-Numbers. G. K. BATCHELOR, *University of Cambridge, England.*

Development of Heisenberg's Theory of the Decay of Isotropic Turbulence. S. CHANDRASEKHAR, *University of Chicago.*

Investigation of the Turbulence Characteristics of an Experimental Low-Turbulence Wind Tunnel. H. B. SQUIRE, *Royal Aircraft Establishment, South Farnborough, England.*

Some Remarks on Turbulent Diffusion. F. N. FRENKIEL, *Naval Ordnance Laboratory.*

Contributed Papers

A. Plasticity, Mathematics, Theory of Mixed Flows

A1. Two-Dimensional Problems of the Ideal Plastic Body. HILDA GEIRINGER, *Wheaton College.* (Introduced by R. J. Seeger.)—For an ideal plastic body, that is, a body without stress hardening, there exists a limit surface, $F(\sigma_1,\sigma_2,\sigma_3)=0$ (with σ_i denoting the principal stresses) such that the plastic stresses vary only on this surface. In Saint Venant's theory this surface is a hexagonal prism with the line $\sigma_1=\sigma_2=\sigma_3$ as axis; in v. Mises' theory it is the circular cylinder circumscribed about this prism. In the *plane problem*, $\sigma_3=0$, the prism and cylinder intersect the x–y-plane in a hexagon and a circumscribed ellipse, respectively. v. Mises has also proposed a "parabolic limit" consisting of parts of parabolas circumscribed about the hexagon. Any such limit condition,

together with the well-known equations of equilibrium constitutes a *quadratic* problem. These equations can, however, be replaced by two linear differential equations by an appropriate choice of the dependent and independent variables (v. Mises). The equations exhibit a close mathematical analogy to the compressible fluid theory equations obtained by the hodograph transformation. The problem is hyperbolic for the parabolic limit, but "mixed" for the other limits. In various ways the two equations may be replaced by *one linear equation of second order*. This equation may then be reduced to a *standard form* to which Bergman's *operator method* may be applied. In addition, useful *particular solutions* are obtained for the elliptic and for the parabolic limit. The *characteristics* for both problems are investigated, the fixed characteristics in the "stress plane" as well as those in the "physical plane;" the solution of the "initial value problem" is also discussed. The theory of *simple waves* is worked out including various examples. Since the parabolic limit seems to offer an efficient mathematical simplification in the two-dimensional case, the *corresponding three-dimensional limit surface* has been derived and studied.

A2. Plastic Behavior of Stiffened Panels Subjected to Underwater Explosive Load. WOLFE MOSTOW, *Naval Ordnance Laboratory.* (Introduced by R. J. Seeger.)—This paper contains an analysis of experiments conducted by the Bureau of Ships on stiffened rectangular plates subjected to side-on non-contact underwater explosive load. Sufficient instrumentation was available from which to determine the deflection-time histories of a number of points on the stiffeners, strain distribution over the panel, and shock wave energy (from pressure-time records) delivered to the structure. Hydrodynamically, it was found that the energy in the primary shock wave was sufficient to account for the energy absorbed by the structure in plastic deformation. Structurally, it was found that the stiffeners behaved, to a first approximation, like simply supported uniformly loaded beams deformed statically into the elasto-plastic range. The theory for the latter was developed on the basis of the variational principle for the complementary energy which is known to apply to deformations outside the elastic range. Theoretical expressions derived for energy absorption, curvature distribution, and deflection contour are in good agreement with the observed data.

A3. Non-Linear Transformations of Divergent and Slowly Convergent Sequences and an Example from Hydrodynamics. DANIEL SHANKS, *Naval Ordnance Laboratory.*—Some non-linear transforms of mathematical sequences are derived from an analogy between sequences and transients. Given a sequence, A_n, one may pass a curve through every $2K+1$ points (n,A_n) of the sequence, $(N-K \leqslant n \leqslant N+K)$, of the form $A_N = B_{KN} + \sum_{i=1}^{K} a_i e^{\alpha_i n}$ with the $2K+1$ unknowns B_{KN}, a_i, and α_i; and solve for the constant term B_{KN}. This constant is given as the ratio of two $K+1$ order determinants whose elements are unity, the A_n and their differences. Two non-linear transforms are $A_N \rightarrow B_{NN}$ and $A_N \rightarrow B_{KN}$ (with K fixed). As an example, the second-order transform, $K=2$, is applied to a divergent series of Goldstein for the drag of a sphere in a viscous fluid. One obtains a rational approximation for the drag in terms of the Reynolds' number.

A4. On Conformal Mapping of Multiply-Connected Domains.* GEORGE SPRINGER, *Massachusetts Institute of Technology.* (Introduced by R. J. Seeger.)—The author gives a new method of determining the function $w=w(z)$ which maps a given domain B of connectivity $p(p>2)$ in the z-plane onto a domain D in the w-plane when such a mapping is possible. Let $K_B(z,\bar{\zeta}) = \sum_{\nu=1}^{\infty} \varphi_\nu(z)\overline{(\varphi_\nu(\zeta))}_{AV}$ be the Bergman kernel function of the domain B[1], the φ_ν representing a complete set of orthonormal functions found by orthogonalizing z^ν and $(z-\gamma_s)^{-\nu}$, $\nu=1,2,\cdots$, for suitably chosen points γ_s, $s=1,2,\cdots, p-1$, using the scalar product $\iint_B \varphi_\nu(z)\overline{(\varphi_\mu(z))}_{AV}dxdy$. If B is bounded by closed curves b_ν, $\nu=1,2,3,\cdots p$, the function $\int_{b_\nu} K(z,\bar{\zeta})d\bar{\zeta}$, (the derivative of the harmonic measure) can be used to determine a critical point in B and in D which must correspond to each other under conformal mapping. Under translation, we may assume that these critical points are at the origin. Substituting in the relation $K_B(z,\bar{z}) = |dw/dz|^2 K_D(w,\bar{w})$ the function element $w = \sum_{n=1}^{\infty} \alpha_n z^n$, one can successively express the coefficients α_ν in terms of the derivatives $d^n K_B(z,\bar{z})/dz^n]_{z=0}$ and $d^n K_D(w,\bar{w})/dw^n]_{w=0}$, $n=1,2,\cdots\nu$. From these coefficients, one obtains an expression for w in terms of orthogonal functions which converges in the entire domain, giving the mapping function in the large. Using the above solutions as a first approximation, subsonic flow patterns can be determined.

* Work done under Contract NOrd 10-449, Task 3.
[1] See Memorial des Sciences Math. **106**, **108**, p. 30, 40, 51.

A5. On Flows of a Compressible Fluid.*,** STEFAN BERGMAN, *Harvard.* (Introduced by R. J. Seeger.)—The equation for the stream function ψ of a compressible fluid is non-linear when considered in the physical plane. If, however, it is considered in the plane with the coordinates $H=\int \rho q^{-1}dq$ and θ, where $qe^{i\theta}$ is the velocity vector and $\rho=\rho(q)$ is the density, the equation assumes the form $l(H)\psi_{\theta\theta}+\psi_{HH}=0$, where $l(H) = (1-M^2)/\rho^2$, M being the Mach number. It is advantageous to consider ψ in the H,θ-plane, since the equation is linear. On the other hand, it implies the complication that the function ψ which represents a regular flow in the physical plane may be multi-valued and possess singularities in the H,θ-plane. In order to investigate functions of this kind, the author (in analogy with the representation of harmonic functions in terms of functions of one complex variable) represents solutions of the compressibility equation in terms of an arbitrary function f of one variable $Z=\lambda(H)+i\theta$, $\lambda(H) = -\int_{\tau=0}^{-H} \times[l(-\tau)]^{\frac{1}{2}}d\tau$ in the form $\psi = Im\{\int_{i=-1}^{1} E(Z,\bar{Z},l)f(Z/2(1-l^2))dl/(1-l^2)^{\frac{1}{2}}\}$. The function E (the generating function of the operator) is a fixed function which can be determined. In the case of a simplified pressure density relation, in which case $l(H) = -CH$, $E = F(\frac{1}{6},\frac{5}{6},\frac{1}{2},l^2Z/2\lambda)$ where F is the hypergeometric function.

* Work done under Contract NOrd 10-449, Task 3.
** The ideas expressed in this paper represent the personal views of the author and are not necessarily those of the Bureau of Ordnance.

A6. A Representation of Transonic Flow Patterns around a Closed Body.* ARTHUR ZEICHNER, *Harvard.* (Introduced by R. J. Seeger.)—$x = \Sigma i b_\nu^{(n)} \tilde{X}^{(\nu)}(\bar{\eta},\theta;\eta_0)$, $y = \Sigma i b_\nu^{(n)} \tilde{Y}^{(\nu)}(\bar{\eta},\theta;\eta_0)$, $\tilde{\psi} = \Sigma i b_\nu^{(n)} \tilde{\psi}^{(\nu)}(\bar{\eta},\theta;\eta_0) = \text{constant}$ where $\tilde{\psi}^{(\nu)}(\bar{\eta},\theta;\eta_0) = Re\{[\bar{\eta}+i\theta-\eta_0]^{\nu-\frac{1}{2}}\}$, $\bar{\eta}=\log q$, where $qe^{i\theta}$ is the velocity vector, q_0 is the speed at infinity, $\Sigma = \lim_{n\to\infty} \sum_{\nu=0}^{n}$; $\tilde{X}^{(\nu)}$ and $\tilde{Y}^{(\nu)}$ are functions depending only on a parameter $\eta_0=\log q_0$ and where the $b_\nu^{(n)}$ are arbitrary constants (subject to certain general conditions) represents a general formula for the stream function of a flow of an incompressible fluid in the x,y plane around a closed profile. Applying the Bergman integral operator (see Am. J. Math. vol 70, 869 (1948)) to the expressions $[\zeta-\eta_0]^{-\frac{1}{2}}$, the author obtains as the representation of a stream function, around a closed body of a compressible fluid, the expressions $\psi = \Sigma i b_\nu^{(n)} \psi^{(\nu)}(\eta,\theta;\eta_0) = \text{constant}$, $x = \Sigma i b_\nu^{(n)} X^{(\nu)}(\eta,\theta;\eta_0)$, $y = \Sigma i b_\nu^{(n)} Y^{(\nu)}(\eta,\theta;\eta_0)$, where $\psi^{(\nu)}(\eta,\theta;\eta_0) = Re\{S_0(-\eta)^{-\frac{1}{2}}F[\frac{1}{6},\frac{5}{6},\nu+\frac{1}{2},$

$(\zeta-\eta_0)/(-2c)(-\eta)^{\frac{1}{2}}](\zeta-\eta_0)^{\nu-\frac{1}{2}}\}$, $\zeta=[-c(-\eta)^{\frac{1}{2}}+i\theta]$, $\eta=\eta(M)$ a known function of the Mach number M. $X^{(\nu)}$ and $Y^{(\nu)}$ are fixed functions depending only on η_0, which may be determined once and for all. $\eta_0=\eta(M_0)$ where M_0 is the Mach number corresponding to the speed at infinity. These formulas hold for the case of the simplified pressure-density relation. (See v. Mises-Schiffer: Advances in Applied Mechanics, 1948, pp. 270). Analogous formulas can be derived for the general adiabatic case, $p=A\rho^k$, k arbitrary. The author discusses the applications of these formulas to the determination of flow patterns.

* Work done under Contract NOrd 10-449, Task 3.

A7. The Calculation and Use of Logarithmic Singularities in the Hodograph Representation of Isentropic Subsonic Compressible Flow. HANS KRAFT, *General Electric Company.* (Introduced by R. J. Seeger.)—Weinig has shown that the incompressible flow through profile lattices such as used in turbines and compressors can be represented by the addition of comparatively few logarithmic singularities. This composition can be carried through in the hodograph plane as well as in physical coordinates. The linear differential equation of compressible flow permits the same procedure. Bergman has shown that solutions of this equation for a logarithmic singularity can be obtained. An effort is under way to obtain a large number of these fields. The computational difficulties are very large but can be overcome by the modern electronic computer. The result of this computation will be flux and potential function of source and vortex type singularities located at a large number of Mach numbers in the range between 0.2 and 0.95. The simple addition of these fields in various constellations and scale will result in pictures of desired flow patterns. The equivalent procedure for the case of incompressible flow is also being developed and has already yielded important information.

A8. On the Non-Existence of Limiting Lines and Their Relation to Shock in Viscous Gases. PROFESSOR M. Z. KRZYWOBLOCKI, *University of Illinois and Naval Ordnance Laboratory.* (Introduced by R. J. Seeger.)—The extension of Tollmien's method to the case of viscous gases shows that, mathematically, the limiting lines exist also in viscous gases. The condition for the appearance of the limiting lines is the same as in the case of an irrotational, inviscid fluid: the vanishing Jacobian of the transformation. The extension of Friedrichs' theorems on limiting lines to the case of viscous gases shows that limiting lines do not exist in an actual flow. The remaining possibility is that the shock is due to viscous forces and the corresponding hypothesis is presented by the author at the closure of the paper.

A9. Inconsistencies in the Prandtl-Glauert Transformation. H. W. SIBERT, *University of Colorado.* (Introduced by R. J. Seeger.)—It is proved that the Prandtl-Glauert transformation for changing the linear differential equations for a compressible flow into differential equations for an incompressible flow is not a conformal transformation. From this fact it is demonstrated that the flow resulting from this transformation is not a true incompressible flow but one with the impossible characteristic of having two distinct streamlines through each point in space. Hence, the Prandtl-Glauert formulas, whose derivation is unwittingly based on this impossible incompressible flow, cannot have any valid theoretical basis.

A10. Approximate Method for Predicting the Form and Location of Detached Shock Waves. W. E. MOECKEL, N.A.C.A.—A simple form of the continuity equation is applied to the air that crosses the sonic line between a body and its detached shock wave. The assumptions are made that the sonic line is straight and that the portion of the detached wave between its sonic points is adequately represented by an hyperbola asymptotic to the free-stream Mach lines. With these assumptions no limitations need be imposed on the magnitude or rotationality of the velocity components and the location of the detached wave relative to the body sonic point is determinable for plane or axially-symmetric bodies of arbitrary shape. Results of the procedure show good agreement with available experimental data. The method is also applied to the problem of predicting the relationship between shock location and the spillage around the cowling of supersonic inlets.

A11. Shock Waves in Inhomogeneous Flow. MAC C. ADAMS, *Cornell University.* (Introduced by R. J. Seeger.)—It is of interest to determine the perturbed "normal" shock that would result from small disturbances initiated in the supersonic flow field. By considering Mach numbers large enough to justify the linearized theory, a method is devised to treat the above problem to a first approximation in the case of two-dimensional disturbances. It is clear that a curved shock will generally result from any such inhomogeneity of the supersonic field, and thus the flow in the subsonic region will be rotational. It is easily determined that the vorticity is of the same order of magnitude as the velocity perturbations. The velocity components on either side of the shock wave are related by the Rankine-Hugoniot shock-wave equations; to the first order, this relation can be satisfied at the undeflected shock-wave location. The perturbation velocity components in the supersonic region are governed by the customary linearized potential equation; those in the subsonic region by a linear equation appropriate for rotational flow. Simultaneous solution of these equations leads finally to the slope of the shock wave and, by integration, its displacement. Two particular upstream disturbance profiles are considered: (1) a sinusoidal disturbance, such as might be produced by an infinite wavy wall far upstream, and (2) a linear roof-top profile, such as would be produced by a parabolic bump of finite extent. In case (1), the shock wave assumes a sinusoidal shape, whose amplitude (for given amplitude of the wavy wall) diminishes with increasing Mach number. For very great Mach numbers the ratio of amplitudes approaches the value $(\gamma+1/2\gamma)^{\frac{1}{2}}$ (approximately 0.925 for air). For any continuous disturbance, the shape of the disturbed shock wave becomes similar to that of the generating wall at a Mach number of $(\gamma+3/2)^{\frac{1}{2}}$ (approximately 1.48), and at this Mach number the flow immediately downstream of the shock is rendered parallel but non-uniform. In case (1) the amplitude ratio for this Mach number is $(\gamma+3)\div[2(\gamma+1)]^{\frac{1}{2}}$ (approximately 2).

B. Theory of Supersonic Flow; Turbulence

B1. Plane, Rotational, Prandtl-Meyer Flows. M. H. MARTIN, *University of Maryland and Naval Ordnance Laboratory.* (Introduced by R. J. Seeger.)—The theory of Prandtl-Meyer flows, originally discovered among the irrotational flows of polytropic gases, is extended to rotational flows of a wide class of gases which includes polytropic gases as special cases.

B2. Differential Relations of Rotationally Symmetric and Plane Supersonic Flows. P. ZETTLER-SEIDEL, *Naval Ordnance Laboratory.* (Introduced by R. J. Seeger.)—In order to evaluate the pattern of the above kinds of supersonic flow, one usually follows a network of characteristics. This procedure is simple in the case of a graphical method; for mere numerical evaluation (especially by high speed computing machines), however, it becomes rather complicated, and it is then desirable to follow a preassigned network suitable to the ge-

ometry of the problem. This is possible under certain restrictions. Differential relations are derived from the characteristic equations which permit such procedure. Only ordinary points of the flow and boundary points with continuous slope are considered, shock waves not. Vorticity is included.

B3. Numerical Computation of Three-Dimensional Supersonic Flows with Vorticity. R. F. CLIPPINGER AND J. H. GIESE, *Ballistic Research Laboratory.* (Introduced by R. H. Kent.)—Thornhill[1] and Moeckel[2] have developed numerical methods to calculate non-linearized three-dimensional irrotational supersonic flows. This paper contains a method, intended for high speed computing machines with large memories, to calculate non-linearized three-dimensional supersonic flows with vorticity, but no viscosity or heat conduction, about bodies with general conical noses and with attached shock wave. Such flows have two types of characteristic surfaces: stream and Mach surfaces. The equations for velocity components and stagnation pressure can be transformed to characteristic variables with Mach coordinate surfaces, so that the body's surface and the unknown shock wave have known plane maps, especially convenient for systematic computation. From initial data on a Mach surface extending from the body to the shock wave, the flow can be calculated step-by-step by solving the corresponding difference equations with initial data on a (1) non-characteristic surface; (2) Mach surface intersecting the body; or (3) Mach surface intersecting the undetermined shock wave. Moeckel's method is used to compute the flow about the conical nose with attached conical shock wave to obtain the required initial data. The convergence of the numerical processes has not been established.

[1] Armament Research Establishment Rep. No. 29/48.
[2] N.A.C.A. TN 1849.

B4. Supersonic Flow with Vorticity about a Slightly Yawing Body of Revolution. W. C. CARTER, *Ballistic Research Laboratory.* (Introduced by R. H. Kent.)—The method of numerical computation of three-dimensional supersonic flows with vorticity developed by Clippinger and Giese is adapted to compute the flow about slightly yawing bodies of revolution which may have edges. Two new variables, whose constant surfaces are Mach characteristic surfaces, are introduced to transform the system of equations. The perturbational method of A. H. Stone[1] is applied, and as in his paper a system of only six linear partial differential equations for the perturbations of the three velocity components, the cylindrical coordinates in each meridianal plane, and the vorticity term is obtained, except in scattered exceptional cases. Another equation for the calculation of the displacement of the shock wave is derived, and the shock wave conditions and the conditions that the body be a stream surface are found. A numerical method for the solution of these equations with the appropriate boundary conditions has been developed. To this order of approximation the solutions depend linearly upon the angle of yaw. No discontinuities in the solution are introduced if the slope of the body profile is discontinuous.

[1] J. Math. Phys. **27**, 67–81 (1948).

B5. Supersonic Aerodynamic Characteristics of Triangular Planform Wings. H. C. SANDERSON, JR. AND BERG PARAGHAMIAN, *Glenn L. Martin Company.* (Introduced by R. J. Seeger.)—The report presents the results of IBM calculations of the zero lift drag of triangular planform wings of double wedge airfoil section at supersonic speeds. The linearized, conical flow theory of Puckett and Stewart is extended to include the entire range of variables, and a simple reversal theorem derived to permit application to sweptforward wings. It is shown that for constant thickness in the stream direction the effects of sweepback are detrimental so long as the leading edge and maximum thickness line are supersonic but that large benefits in minimum drag and maximum (L/D) ratio are possible with the use of highly swept wings. It is also shown that minimum drag and maximum (L/D) ratio is obtained when the maximum thickness is placed at about 50 percent chord for supersonic leading edges and at about 20 percent chord for subsonic leading edges.

B6. Results of a Theory of the Blade Shapes of Compressors. H. J. REISSNER, *Polytechnic Institute of Brooklyn.* (Introduced by R. J. Seeger.)—A design theory of compressor, turbine, and deflector blades, such that the data of required pressure and velocity change are satisfied, has originally been started by H. Lorenz in 1912 for incompressible, non-viscous flow. It was extended and generalized in a course given at the Polytechnic Institute of Brooklyn in 1945–46 and in a paper of mine in the Courant Anniversary Volume in 1948. The extension furnishes compressible and viscous flow and the transition from infinitesimal blade spacing to finite blade spacing.

B7. Ship Forms of Least Wave Resistance. J. V. WEHAUSEN, *David Taylor Model Basin.* (Introduced by R. J. Seeger.)—The minimization of Michell's integral for the wave resistance of a ship of given displacement leads to an integral equation of the first kind with positive definite kernel for the ordinates perpendicular to the vertical plane of symmetry of the ship. In the particular case of a two-dimensional ship of infinite draft the integral equation reduces to the following: $\int_{-1}^{1} f(x)\, Y_0(|x-y|/F^2)dx = -\lambda$ for $|y| \leqq 1$, where Y_0 is a Weber function [Watson, *Theory of Bessel Functions*, p. 64], λ is some constant, F is the Froude number $v/(gL)^{\frac{1}{2}}$, and $\int_{-1}^{1} f(x)dx = 1$ must hold. The question as to whether a solution exists is of considerable interest in evaluating the significance of numerical computations. L. N. Sretenskii [C. R. Acad. Sci. URSS **3**, 247–248 (1935)] has given a proof that there can be no solution. However, this proof contains an error in that it tacitly assumes that the kernel function is periodic with period 2. If, in the case of very large Froude number, one replaces $Y_0(|t|/F)^2$ by $(2/\pi)\log(|t|\,C/2F^2)$ where $\log C$ is Euler's constant, the equation may be solved and, with proper choice of λ, the solution is $f(x) = 1/\pi(1-x^2)^{\frac{1}{2}}$. Such a solution is, of course, of no practical interest and, in fact, the conditions for the valid use of Michell's integral are no longer present. However, a tendency toward such behavior for large Froude numbers is found in numerical computations by G. P. Weinblum [3rd Int. Congr. Appl. Mech., Stockholm, 1930], who minimized Michell's integral for certain classes of polynomials, and by G. E. Pavlenko [Trans. Sci. Techn. Soc. Shipbuilding and Mar. Engng. **2**, No. 3, 28–62] who replaced the integral equation by a system of linear equations. The question of existence of a solution for Froude numbers of practical interest remains open.

B8. Some Features of Boundary-Layer Turbulence.* G. B. SCHUBAER, *National Bureau of Standards.*—Using hot-wire apparatus and narrow band-pass filters, the spectrum of the turbulence has been measured in the turbulent boundary layer along a flat plate with zero pressure gradient. The spectrum is used to determine whether the characteristics of turbulence depend on the origin of the turbulent boundary layer, i.e., depend on how and where transition from laminar to turbulent flow occurs. The question involved here is whether the turbulence has characteristics determined entirely by local conditions or whether it retains some features of the disturbances that were originally responsible for transition. The answer to this question appears to be required before undertaking a detailed study of boundary-layer turbulence, first to be certain that there does exist a turbulence of universal character, and second to know what liberties may be taken in setting up a turbulent boundary layer of convenient thickness.

* Project sponsored by the N.A.C.A.

B9. On the Stability of the Laminar Boundary Layer between Parallel Streams.*,** MARTIN LESSEN, *National Advisory Committee for Aeronautics.* (Introduced by R. J. Seeger.)—The analysis and calculations on the stability of the laminar boundary layer between parallel streams were made for an incompressible fluid using the Tollmien-Schlichting theory of small disturbances. Because the boundary conditions are at infinity, two solutions of the Orr-Sommerfeld stability equation need not be considered and the remaining two solutions are exponential in character at said boundaries. The solution of the stability equation was obtained in powers of $-i/\alpha R$ where R=Reynolds number and α=disturbance wave number. With an asymptotic solution as a start, the stability equation was integrated numerically. The eigenvalue problem between α, R, and the disturbance phase velocity c was thus explored by a trial and error process. The calculations show that the flow is unstable except for very low Reynolds numbers. The regions of stability and instability in the α, R plane were checked by obtaining damped and amplified solutions on opposite sides of the neutrally stable solution.

* Work performed at M.I.T. as part of a doctorate thesis.
** Computations performed gratuitously by IBM Corporation on the Selective Sequence Electronic Computer.

B10. Shear Stress in a Turbulent Boundary Layer.* DONALD ROSS AND J. M. ROBERTSON, *Ordnance Research Laboratory, The Pennsylvania State College.*—Although the ultimate solution of the problem of turbulent boundary layer flow in adverse pressure gradients may involve a statistical theory of turbulence, a reasonable solution can be obtained by analyses based on the mean motion. As the velocity variation in a boundary layer results from turbulent shearing motions, evaluation of the shear stress distribution is important. Fediaevsky[1] expressed the shear stress as a power series and evaluated the constants in terms of boundary conditions. The present analysis uses a more suitable polynomial and boundary conditions which include the concept that the shear at any point is the result of turbulence generated at the surface upstream from its present location. This "history" theory predicts that the transverse shear gradient in the outer portion of the boundary layer remains constant as the boundary layer develops. Comparison with shear distributions measured at the National Bureau of Standards[2] along a simulated airfoil shows good qualitative agreement and appreciable improvement over Fediaevsky's theory.

* Work done under U. S. Navy Contract NOrd 7958.
[1] J. Fediaevsky, Aero. Sci. 4, 491 (1937).
[2] Dryden, N.A.C.A. TN 1168 (1947).

B11. The Non-Linear Cooling of the Hot-Wire Anemometer. R. BETCHOV, *Technische Hogeschool, Delft.* (Introduced by R. J. Seeger.)—The paper is concerned with the influence of the term BT^2 in the expression $AT+BT^2$ for the heat carried away from the wire with a given velocity of the air (T=difference between wire-temperature and air-temperature). Attention is also given to the non-linear term in the formula connecting the electric resistance and T. It is shown that then non-linear effects, together with the cooling effect due to conduction of heat towards the supports of the wire, have an important influence on the thermal inertia of the wire, account of which must be taken in the calibrations.

C. Experimental Supersonic Flow; Instrumentation

C1. A Method for Calculating the Drag Coefficient from Data Obtained in a Precision Aeroballistics Range. G. L. SHUE, *Naval Ordnance Laboratory.* (Introduced by R. J. Seeger.)—Consider a model in free flight in a precision range in which the data are recorded as shadowgraph pictures and in which the time intervals between the sparks at successive stations are accurately measured. This paper suggests an engineering method for the determination of the basic parameters of speed and drag coefficient. In the integrations of the equations the identity of all parameters considered is retained and the final equation is solved for the speed and the drag coefficient by theory of least squares.

C2. Pressurized Range for Small Caliber Projectiles in Free Flight. V. E. BERGDOLT, A. J. GREENWALD, AND D. B. SLEATOR, *Ballistic Research Laboratory.* (Introduced by F. D. Bennett.)—A pressurized firing range has been built for the purpose of studying the air flow around projectiles in free flight. The range permits the firing of projectiles up to caliber 0.30 in size at air pressures of several atmospheres. The range is constructed in three sections, namely, the gun section, the working section, and the stopping section, all of which are pressurized. A Mach-Zehnder interferometer of the type used by previous investigators is located externally about a set of windows in the working section of the range. Interferograms of the projectiles and the surrounding air flow patterns are taken with the interferometer by means of a short duration light source. A rotating-mirror camera-lens combination is used to reduce the effective light source duration by stopping the motion of the image on the film. Interferograms will be shown of standard projectiles and cone-cylinders with 15, 20, and 25 degree half-angles taken at one atmosphere pressure. In addition, interferograms of the 20-degree cone-cylinder taken at 4, 5, and 6 atmospheres will be presented.

C3. Measurement of Temperature Recovery Factors and Heat Transfer Coefficients on Cones at Supersonic Speeds in the 40 by 40 cm² White Oak Wind Tunnel. G. R. EBER, *Naval Ordnance Laboratory.* (Introduced by R. J. Seeger.)—New measurements, which are the first part of an extensive measurement program of recovery factors and heat transfer coefficients, have been made in the White Oak wind tunnel installation to check previous similar measurements made in the same tunnel at Peenemuende and to extend the Peenemuende measurements to higher Mach numbers. Greater measurement accuracy is obtained in the White Oak installation because the tunnel blowing time has been about doubled (from 20 up to about 40 seconds) and also because of the improved air drying installation, which gives a more nearly constant supply temperature of the tunnel blast air. Measurements of heat transfer coefficients and recovery factors have been made on cones of 10, 20, and 60 degree total angle at Mach numbers 1.56 and 2.48. Results of these measurements are given and compared with previous measurements.

C4. An Electrical Analog for Heat Flow with Varying Parameters. J. M. KENDALL, *Naval Ordnance Laboratory.*—Throughout its trajectory, the aerodynamic friction heating of a missile varies with the velocity of the missile, as well as with the density and temperature of the ambient atmosphere. In considering the temperature distribution $T(x,t)$ in the wall of a missile, temperatures attained are frequently high enough to require taking into consideration radiation, the variation of thermal conductivity, and the variation of specific heat of the wall material. On account of the number of these variables, which are functions of time and temperature, computation of the temperature distribution as a function of trajectory variables becomes too involved for "hand" computational methods. An electrical analog has been worked out which takes into account all of the above (variable) parameters, and provides the possibility of obtaining wall temperature distributions of sufficient accuracy for engineering purposes.

C5. Electrically Exploded Wires as a Light Source for Hydrodynamical Studies. THOMAS P. LIDDIARD AND RALPH D. DROSD, *Naval Ordnance Laboratory.* (Introduced by R. J. Seeger.)—Electrically exploded wires are used as a source of

high intensity light. The confinement of the wires in capillary tubes increases the light output. The useful duration of the light may be adjusted from about 20 microseconds to almost a millisecond independently of the capacity and voltage. With the proper choice of wire and capillary the intensity is great enough to overexpose film in a rotating mirror camera with its aperture set at *f*:45 and exposure time of 0.2 microsecond. Some examples of the use of these light sources in studies of shock waves and detonations will be described.

C6. Vacuum Thermocouple Microsecond Timer. RICHARD H. F. STRESAU, *Naval Ordnance Laboratory.* (Introduced by R. J. Seeger.)—An instrument for the measurement of times of the order of one microsecond has been constructed. Its operation depends upon the delivery of a square electrical pulse to the heater of a vacuum thermocouple. If the current is constant, the energy delivered to the heater, and hence its temperature change, is proportional to the duration of the pulse. The peak temperature is measured by means of a fluxmeter, attached to the thermocouple element, which integrates the voltage over the cooling time of the element. The square pulse is generated by two hydrogen thyratrons, one of which is in series with the thermocouple heater and the other of which is in shunt with both the thermocouple and the first tube. Thus the duration of the pulse is the time between conduction of the first tube and conduction of the second. The range of the instrument can be readily varied by changing resistance elements. Times of the order of one microsecond can be measured with an error of one or two percent and times of the order of one hundredth of a microsecond can be measured with about ten percent error.

C7. Interferometric Analysis of Flow around Small Caliber Projectiles. F. D. BENNETT AND W. C. CARTER, *Ballistic Research Laboratory.*—Using the techniques described in the previous paper by Bergdolt, Greenwald, and Sleator, an interferogram has been obtained of a 15° semi-angle, cone-cylinder projectile in free flight. In the absence of yaw the disturbance around such a projectile may be assumed axially symmetric. Under this condition the integral equation relating air density within the disturbance to fringe shift on the interferogram may be solved by the Abel operator method. The resulting integral is then replaced by a sum of finite differences and a numerical approximation to the density function obtained. Methods of obtaining the fringe shift data are discussed and certain aspects of the coding of the problem for the Eniac are described. Whereas previous investigators using IBM or hand computation methods have found tables of coefficients prepared in advance to be of use, the Eniac because of its great speed but small memory capacity is better adapted to calculating the coefficients as needed at each stage. This feature allows considerable flexibility in the assignment of zone widths within the disturbed region. Comparison is made between the calculated densities of the flow and those expected from theoretical considerations, and a discussion is given of the validity of the axial symmetry hypothesis for this example.

C8. The Light-Intensity Distribution in the Mach-Zehnder Interferometer.* E. H. WINKLER, *Naval Ordnance Laboratory.* (Introduced by R. J. Seeger.)—The interference phenomena which results from an incident plane wave in the Mach-Zehnder interferometer has been investigated. An expression is derived which gives the light intensity distribution as function of (a) the arrangement of the mirrors, (b) the angles through which the mirrors are rotated, (c) fringe direction, (d) the wave-length of the light, (e) the directional coordinates of the incident wave, (f) the space coordinates, and (g) the orientation of the screen. For an extended light source the light intensity distribution is obtained by integration over the light source area. The expression derived furnishes information about (a) the fringe spacing, (b) the position of the most distinct interference plane, (c) the visibility of the fringes, (d) the intensity profile of the fringes, and (e) the departure from straight fringes. From this information the most favorable operating conditions of the Mach-Zehnder interferometer can be determined.

* Sponsored by the ONR.

C9. Boundary Layer Optics in Two-Dimensional Gas Flow Interferometry.* D. BERSHADER AND G. P. WACHTELL, *Princeton University.*—The interferometric analysis of flow through a rectangular channel such as the working section of a supersonic wind tunnel, is subject to special considerations arising from at least three types of boundary layer phenomena, each of which affects the assumption of glass-to-glass homogeneity used in the evaluation. They are (a) boundary layer on the glass windows, (b) the "corner effect," (c) refraction. A previous study** has described the action of these effects and established quantitative criteria for the fringe-shift corrections in each case. In recent work, a more refined estimate of the evaluation error caused by refraction has taken into further account the optical system between boundary layer and photographic plate, leading to the result that this error depends upon the choice of focal plane for the photography. If h be the distance of the focal plane from the window through which the light leaves, the fringe shift correction is linear in h, reducing to the previously found value when $h=D$, the channel depth (plane of focus located where light enters channel) and becomes zero when $h=D/3$.

* Performed under a contract with the ONR.
** D. Bershader, Rev. Sci. Inst. **20**, 260 (1949).

C10. Free Flight Aerodynamics. L. G. POOLER, *Bureau of Ordnance.* (Introduced by R. J. Seeger.)—To supplement wind tunnel data free flight tests are necessary to check the validity of the assumptions required to correlate the scale model with the actual body. To interpret the results of free flight tests in terms of the aerodynamic coefficients requires a knowledge of the instantaneous displacement, velocity, and acceleration of the center of mass and of the angular quantities measured with respect to the center of mass. Various methods using photography and electromagnetic waves are described for obtaining the required quantities and the precision of the measurements are considered.

C11. Flow Characteristics During the Starting and Stopping of a Supersonic Wind Tunnel. G. E. BURKHEIMER, *Ordnance Aerophysics Laboratory, Consolidated Vultee Aircraft Corporation.* (Introduced by R. J. Seeger.)—A study of the flow configuration existing in supersonic nozzles in the range of Mach numbers from 1.25 to 2.50 during the transient conditions of starting and stopping was made. The techniques employed include shadowgraph and schlieren movies taken at speeds up to 3000 frames per second, and recording the variation of the differential pressure existing on a cone placed in the test section, using a high frequency response pressure pick-up. Sample movies of the shock wave configurations during the transient conditions show as many as ten distinct shock waves passing through the test section. These movies also show very plainly the effect of boundary layer shock wave interaction and the resulting lambda shocks. From measurements of the transient pressures at two points one hundred eighty degrees apart on a cone, pressure differentials equivalent to over five degrees angle of attack at stabilized supersonic conditions were observed. These pressure differentials may reverse in sign very rapidly several times during one start or stop.

D. Shockwaves, Explosions, Non-Steady Supersonic Flow

D1. A Ratio Delay Device for Simplifying the Photography of Shocks in a Tube. P. E. SHAFER AND J. F. MOULTON, JR., *Naval Ordnance Laboratory.*—The photography of transient air shock waves by schlieren or shadowgraph techniques involves the problem of accurately timing a flash of light so that the shock wave will be at a desired position when the photograph is taken. A new electronic device has been designed and constructed to eliminate the necessity for computing the shock velocity and for presetting a conventional time delay mechanism prior to photographing shocks produced under various temperature and pressure conditions. The shock velocity is measured over a fixed distance as the shock interrupts two separated light screens and detectors. These time-separated pulses are put into the device which emits a pulse after a delay which is proportional to the time lapse between the two input pulses. The constant of proportionality may be selected within a wide range to suit experimental conditions. A description of the unit and its internal operation, together with results obtained will be presented.

D2. The Shock Tube as a Tool for the Investigation of Flow Phenomena.* F. W. GEIGER,** *University of Michigan.*—In the shock tube used by Mautz,*** the nature of the flow and the formation of substantially steady transonic and supersonic flows were investigated further. Photographs of such formation are expected to yield information about partially understood phenomena of aerodynamics. Photographic investigation of the flow just ahead of the diaphragm indicated that irregularities in the tube flow were primarily due to its non-ideal removal. Shadowgraphs showed that substantially steady flows past various two-dimensional models were produced. Studies included transonic and supersonic flows past double wedges and the choking of a duct. The choking of the tube is apparently not as serious as that of the wind tunnel because of a thin tube boundary layer. It is shown that the shock wave usually associated with overexpansion at a corner is attributable to viscous effects. It is concluded that the shock tube is a highly useful tool for the investigation of flow phenomena.

* Supported by ONR.
** Now at Cornell Aeronautical Laboratory, Buffalo, New York.
*** C. W. Mautz, Dissertation, University of Michigan, 1949.

D3. A New High Speed Frame Camera. S. J. JACOBS AND A. A. KLEBBA, *Naval Ordnance Laboratory and Woods Hole Oceanographic Institution.*—The camera described is a modification of the Bowen camera, and is designed to operate in the range of 10,000–30,000 pictures a second at an aperture of *f*:8. An image is formed on a mirror which rotates at 100–300 r.p.s. Around the mirror 100 equally spaced framing lenses are arranged in a circle, the axis of which coincides with the axis of rotation. Each lens in turn focuses the image from the mirror to the segment of the film immediately behind it. Considerations governing the choice of optical systems will be discussed.

D4. High Speed Photography of Explosion Bubbles at Depths of One and Two Miles. PAUL M. FYE AND ROBERT S. PRICE, *Naval Ordnance Laboratory,* AND D. F. BARNES, *Woods Hole Oceanographic Institution.*—High speed photographs of 1 lb. explosive charges detonated at depths of one and two miles in the ocean show several oscillations of the explosion gas bubble. Examples of these photographs which were taken at camera speeds of 10,000 and 20,000 frames per second will be shown. The variation of bubble size with time will be presented. At these great depths the bubble is much smoother that at shallow depths and appears to remain spherical throughout the first oscillations. Hence, estimates of its minimum size can be obtained. Maximum radii will be compared with those predicted by explosions at depths less than 1000 ft.

D5. Determination of Adiabatic Parameters of Explosion Bubbles From Charges Fired at Great Depths. H. G. SNAY AND E. SWIFT, JR., *Naval Ordnance Laboratory.* (Introduced by R. J. Seeger.)—Study of bubble period and maximum radius indicates that these two experimentally determined properties cannot be determined with sufficient accuracy to yield significant values of the adiabatic parameters. It is shown how measurements of bubble minima allow calculations of the parameters γ and K. Some conclusions as to these values are drawn from recently obtained photographs of bubble minima at great depths.

D6. Explosion Bubble Period at Great Depths. JOHN P. SLIFKO AND E. SWIFT, JR., *Naval Ordnance Laboratory* AND W. S. SHULTZ, *Woods Hole Oceanographic Institution.* (Introduced by R. J. Seeger.)—One-pound TNT charges were fired at depths of one and two miles and eight-pound charges at three and four miles in the Atlantic Ocean. Period measurements were made at the surface, using tourmaline piezoelectric gauges of about two-inch diameter, and recording oscillographic traces at film speeds of 0.8 in. per millisecond. Depths of detonation were found by a siesmic ranging apparatus which measured times of arrival of pressure waves reflected from the surface and bottom of the ocean. The preliminary results will be compared to those predicted by the equation $T=4.36W^{1/3}/Z_0^{5/6}$, where T is time in seconds, W is weight of charge in lb., and Z_0 is depth in feet $+33$.

D7. The Interaction of a Plane Shock Wave with a Contact Surface of General Type. G. N. PATTERSON, I. I. GLASS, D. BITONDO, *University of Toronto and Naval Ordnance Laboratory.* (Introduced by R. J. Seeger.)—The problem of the interaction of a plane shock wave with a contact surface in one dimension is considered in detail. The contact surfact is of the most general type which can be produced in a shock tube, i.e., a discontinuity of internal energy. When the ratio of the internal energies separated by the contact surface is greater than a certain minimum value, the resulting wave system after the interaction is a transmitted shock wave and a reflected rarefaction wave. The transmitted shock wave is of lower strength than the original incident shock wave. This effect is defined as absorption. The calculations show that large absorption occurs when the incident shock wave is strong and the discontinuity of internal energy is large. Absorption can also be increased by an appropriate combination of gases.

D8. The Reflection of a Weak Plane Shock at Nearly Glancing Incidence.* C. H. FLETCHER AND W. BLEAKNEY, *Princeton University.*—In 1945, Bargmann[1] treated the nearly glancing reflection of a weak plane shock by solving the hydrodynamical flow equations in an approximation suited to this case. The solution was developed in terms of powers of the tangent of the angle between the normal to the incident shock and the wall. This treatment permits calculation of the length and shape of the Mach shock, the distribution of the isopycnals behind the reflected shock and several other details. An attempt has been made to compare the predictions of this theoretical treatment with experiment using the shock tube and interferometer at Princeton. A shock strength $P_0/P=0.8$ and an angle of incidence 10° from glancing were used. With a 4-inch light path, a variation of about 2 fringes was observed in the field behind the reflected shock when $P_0=1$ atmos. Bargmann's treatment indicates that the reflected shock should have a maximum strength some distance behind the incident shock and zero strength at the triple point. This

maximum is observed. No angular phenomenon at the triple point is predicted or observed.

* This work is being supported by the Navy Department through Contract N6ori-105, Task II.

[1] V. Bargmann, *On Nearly Glancing Reflection of Shocks*, AMP Report No. 108.2R, Nat. Def. Res. Comm., March 1945.

D9. Refraction of Shock Waves at a Gas Interface. R. G. STONER AND M. H. GLAUBERMAN, *The Pennsylvania State College.*—Assuming a simple configuration consisting of single transmitted and reflected shocks, and using the appropriate boundary conditions, Taub has obtained solutions of the hydrodynamic equations for the interaction of a plane shock wave with the interface between two different gases.[1] To investigate the possibility of using a soap film to produce such an interface experimentally, a preliminary investigation has been undertaken, using spherical soap bubbles containing CO_2, argon, helium, and air. Spark shadowgraphs of shock waves produced by a semiconfined spark discharge have been taken, showing reflected and transmitted shock waves. The reflection at an air/air boundary, caused solely by the soap film itself, is weak, and shows that the incident wave is not appreciably disturbed by passage through the soap film. Since neither the incident shock nor the gas interface is plane, the results are qualitative only, but the method is considered promising. A shock tube is being constructed with which quantitative results may be obtained.

[1] A. H. Taub, Phys. Rev. 72, 51 (1947).

D10. A Method for Solving Certain Time-Dependent Problems for Wings in Supersonic Flow, with an Application to the Calculation of Stability Derivatives. CLIFFORD GARDNER, *New York University.* (Introduced by R. J. Seeger.)—The problem of calculating the pressure distribution on an airplane wing caused by a constant time rate of change in angle of attack is of interest in connection with dynamic stability. If it is assumed that the flow is a small disturbance away from a constant flow, so that the linearized theory can be applied, it is shown that this time-dependent problem is equivalent to two steady-flow problems. More generally it is indicated how a time-dependent problem of linearized supersonic flow, in which the boundary data are a polynomial of the nth degree in the time, can be reduced to n steady-flow problems. Also a method is indicated for solving the problem of the supersonic flow past a flat wing having one straight subsonic edge, with boundary data depending on the time in an arbitrary manner.

D11. A Note on Non-Stationary Supersonic Wing Theory. H. J. STEWART, *California Institute of Technology.* (Introduced by R. J. Seeger.)—Most problems in non-stationary supersonic wing theory are associated with small irrotational disturbances in a uniform air stream. The velocity potential equation for a disturbance is then (A) $(1/a^2)\varphi_{tt}+(2M/a)\varphi_{xt}+(M^2-1)\varphi_{xx}=\varphi_{yy}+\varphi_{zz}$, where the undisturbed flow of Mach number M is in the x direction and a is the speed of sound in the undisturbed flow. Many finite wing problems have been solved by planar superpositions of the steady-state supersonic source solution, $\varphi=1/r$, where $r=[x^2-\beta^2(y^2+z^2)]^{\frac{1}{2}}$ is the hyperbolic radius. The corresponding non-steady oscillating source is (B) $\varphi=1/r\exp[i\nu(t-Mx/\beta^2a)]\cos(\nu r/\beta^2a)$, where $\beta=(M^2-1)^{\frac{1}{2}}$. These source solutions are Green's functions for the half-plane, and make it possible to write down solutions for any problem where the normal velocity is defined for the entire plane (x,z) or (x,y), i.e., for wings with supersonic edges. The source concept can be generalized so as to form suitable singularities for more restricted regions such as those encountered in wings with subsonic leading edges. A consideration of the harmonic solutions of (A) shows that (B) can be generalized to (C) $\varphi=1/r\exp\{i\nu[t-(Mx/\beta^2a)]\}\cos(\nu r/\beta^2a)F(\epsilon)$, where $F(\epsilon)$ is either the real or imaginary part of an analytic function of the complex variable $\epsilon=se^{i\theta}$ where $\theta=\tan^{-1}(y/z)$; $2s/1+s^2=\beta/x(y^2+z^2)^{\frac{1}{2}}$. This complex variable is the same one found to be important in the linearized theory of steady-state conical flows. It appears to be possible to choose the function $F(\epsilon)$ so that more complex boundary value problems such as those associated with the delta-wing with subsonic leading edges can be solved.

E. Hypersonic Flow, Kinetic Theory, Heat Addition

E1. On the Kinetic Theory of Rarefied Gases. HAROLD GRAD, *New York University.* (Introduced by R. J. Seeger.)—The starting point of this paper is the Boltzmann equation for point molecules undergoing only binary collisions. Enskog's "solution" of this equation has been generally accepted. Uhlenbeck has given this solution in terms of quantum mechanics. Tsien has proposed that the slip-flow regime be described by the third approximation of Enskog's scheme (the Burnett equations). Mathematically, the presentation of Enskog is highly unsatisfactory; although a more rigorous presentation based on the work of Hilbert can be given, convergence of the Enskog procedure is unlikely; even if it can be proved to converge, this solution can at best represent only certain special solutions of the Boltzmann equation (the so-called "normal" solutions). A symptom of this defect is the difficulty of finding appropriate boundary conditions for the Enskog approximations. In this paper a method is proposed which seems capable of arbitrary approximations to general solutions of the Boltzmann equation. Appropriate boundary conditions are easily formulated. Specific problems which already have been solved are the dispersion of sound and the determination of the profile of a stationary shock front.

E2. Investigation of the Excitation of Molecular Vibrations by High Speed Missiles.* Z. I. SLAWSKY, *Naval Ordnance Laboratory.*—When projectiles move through air with speeds around 3 km/sec., one can expect considerable excitation of the vibrational frequencies of O_2 and N_2. This paper reports the theoretical and experimental investigation now underway to determine the degree of excitation and the space distribution of excited molecules around a missile. Gases consisting of molecules with bending energies much smaller than O_2 or N_2 are being investigated to determine the feasibility of simulating high velocities with actual speeds less than 3 km/sec. The principle used is to maintain the ratio of the kinetic energy per particle ($\frac{1}{2}mv^2$) to the bending energy $h\nu$.

* Sponsored by the ONR.

E3. Some Studies in Gas Dynamics, Conducted at the Polytechnic Institute of Brooklyn. PAUL LIEBER, *Polytechnic Institute of Brooklyn.* (Introduced by R. J. Seeger.)—A brief summary of results obtained in some investigations in gas dynamics at the Polytechnic Institute of Brooklyn will be given.

E4. Flow of a Gas Characterized by the Beattie-Bridgman Equation of State and Variable Specific Heats: Part I. Isentropic Flows. J. C. CROWN, *Naval Ordnance Laboratory.* (Introduced by R. J. Seeger.)—The usual aerothermodynamic relations for flow in a quasi-unidimensional channel have been rederived using the Beattie-Bridgman equation of state in place of the perfect gas law and allowing for the component of specific heat due to the vibrational mode of freedom (for polyatomic gases). Graphs permitting rapid numerical evaluation of resulting formulae are presented. Part II of this investigation will deal with shock waves.

E5. Wind Tunnel Investigation of Condensation Phenomena. R. HEAD, *California Institute of Technology.* (Intro-

duced by R. J. Seeger.)—The results of a systematic wind tunnel investigation into the attainment and ultimate collapse of the supersaturated state of water vapor are presented. These results together with those of other recent investigations, are collected and compared with the theory. It is found that the deviations from the quasi-stationary conditions upon which the theory is based are very pronounced in the supersonic wind tunnel. A much higher degree of supersaturation can, therefore, be attained before condensation occurs than is predicted theoretically. Measurements at low temperatures indicate that if the water vapor reaches a temperature of about 153°K without the occurrence of condensation, the vapor will not condense upon further expansion, regardless of how highly supersaturated it becomes. This observation is in agreement with some recent Wilson cloud-chamber investigations. The shock relations for flow involving condensation are discussed. It is shown that two types of discontinuities can occur; the condensation shock and the shock with condensation (or vaporization). The latter solution has been disregarded in the past, but it is shown that the shock with vaporization is of importance and can result in appreciable errors in Mach number determination when droplets are present in the flow. Various techniques of measurement of the condensation processes in supersonic flow are considered.

E6. Experiments on the Influence of Temperature Gradient and Humidity on Condensation Shocks in Supersonic Wind Tunnels. P. P. WEGENER, *Naval Ordnance Laboratory.* (Introduced by R. J. Seeger.)—Possible condensation phenomena of gases in hypersonic wind tunnels are of increasing interest. The most accessible experimental case is the isentropic expansion of moist air which leads to condensation shocks. These shocks occur only after the moist air has been supercooled by about 40 to 80°C. The molecular theory of these phenomena has been given by K. Oswatitsch. A comparison with experimental data led him and others to the assumption of constant supercooling regardless of initial humidity. However, a new evaluation of tests by G. Eber and K. H. Grunewald in the Kochel tunnel revealed that the supercooling varies considerably with humidity. In order to investigate this discrepancy more thoroughly, a series of experiments has been carried out in a small wind tunnel. From these results it appears that the possible supercooling is a function of the temperature gradient in the nozzle, the humidity and other parameters, most of which could be varied in a wide range. Some conclusions can be drawn with regard to the scale factor entering these phenomena and a qualitative understanding of the problem can be derived from molecular considerations.

E7. Some Aspects of Air Flow at Mach No. 7 as Observed in the University of Minnesota Aeronautical Laboratory. J. W. BRAITHWAITE AND J. L. FRAME, *University of Minnesota.* (Introduced by R. J. Seeger.)—Basically, the flow at Mach number 7 evidenced no unusual observable effects. Expansion to this velocity occurred in a simple one-dimensional wedge nozzle with throat dimensions of 0.050 inch by 6 inches and test section of 6 inches by 9 inches. Attainment of Mach 7 was checked by conical flow theory (112° cone), one-dimensional shock theory (86.5° wedge), and pitot pressure measurements. A shadowgraph optical system was employed in conjunction with a mercury manometer for all shock and pressure observations. Quality (inclination, distribution, turbulence) of the flow was impossible to determine since only the strongest of shocks become visible on shadowgraph. No sign of a normal shock was apparent in the channel. The compression ratio at start of a run was 236, the flow was stable for about 10 seconds and broke down at a pressure ratio of approximately 130. More accurate measurements are being taken to determine something more of the flow quality and the limiting pressure ratio. An anomalous effect due to temperature hampered early tests. At stagnation temperatures in the range of atmospheric and below, no difficulty was encountered in establishing stable Mach 7 flow. When the stagnation temperature rose above approximately 120°F, strong oblique shocks appeared, originating at about the Mach 6 position in the nozzle. Under this condition the flow never completely stabilized, and Mach 7 was never reached. This phenomenon is as yet unexplained, but further testing under controlled conditions should provide some instructive data. These tests were conducted in the supersonic blowdown tunnel which is a part of the research facilities of the Department of Aeronautical Engineering at the University of Minnesota, Rosemount Research Center, and as a part of a Master's thesis.

E8. Investigation of the Possible Utilization of an Electrical Glow Discharge as a Means for Measuring Air Flow Characteristics. F. D. WERNER, *Aeronautical Laboratories, University of Minnesota.*—An instrument for measuring such air flow characteristics as very rapid variations in pressure and velocity, should be of small size for high resolving power and for some purposes, should respond to variations as rapid as several hundred thousand cycles per second or higher. Considerable work on corona discharge has been done by many investigators, but this investigation is concentrated on glow discharges from very sharp points. The glow (corona) discharge at atmospheric pressure from a point of fine platinum wire has been experimentally investigated in its sensitivity to variations of pressure, velocity, temperature, and humidity, as well as such variables of the instrument as needle point characteristics, location and shape of the other electrode (to be referred to as the "plate"), and magnitude of the discharge current. It has been concluded that the glow current is markedly pressure sensitive, is velocity sensitive, is only slightly humidity sensitive, and is negligibly sensitive to ordinary temperature variations. The device offers a significant improvement over conventional instruments by the small size of its sensitive portion (0.001-inch wire and 0.002-inch glow diameter) and in its response to high frequency variations. The use of this instrument as a microphone for very high frequencies will be described in a separate paper very soon, but at present it can be stated that successful pick-up of one megacycle per second has been made. The sensitivity to variations is not greatly altered by the location, shape, or material of the "plate" within rather wide limits. The device has rather high background noise, but it is still useful for measurement of turbulence in airflow, and as a microphone for loud sounds, if used with a fairly narrow band filter.

E9. The Thermodynamics of Flow Systems.* CHARLES F. CURTISS AND JOSEPH O. HIRSCHFELDER, *University of Wisconsin.*—The rate of change of entropy in a flow system is evaluated explicitly taking into account heat conductivity, viscosity, diffusion, and chemical reactions. The equations are developed rigorously from the kinetic theory of gases.

* This work was carried out under Contract NOrd 9938 with the United States Navy Bureau of Ordnance.

E10. Heat Delivery in a Two-Dimensional Compressible Flow at Subsonic and Supersonic Speeds. CHAN-MOU TCHEN, *National Bureau of Standards.* (Introduced by R. J. Seeger.)—In a two-dimensional space Ox, Oy, a gas has a steady main velocity U. At the origin O of the coordinates, heat is introduced to the fluid by means of a fine metallic body which has the form of a very thin ribbon. Given the heating temperature ϑ_w of the body, and the free stream velocity U, the heat delivery Q is calculated. If the heat delivery is expressed by the Nusselt number N, the free stream velocity by the Peclet number P_∞ (a dimensionless quantity equal to the product of the Reynolds number by the Prantl number), and the heating temperature by ϑ_w/T_0, where T_0 is the stagnation tem-

perature, the following formulas for the heat delivery are obtained: (a) for a subsonic speed: $N=(P_\infty/\pi)^{\frac{1}{2}}C'(1+\frac{1}{2}s_1C')+C''(1+\frac{1}{2}s_1C')$; (b) for a supersonic speed: $N=(P_\infty/\pi)^{\frac{1}{2}}\times C'(1-\frac{1}{2}s_2C')-C''(1-\frac{1}{2}s_2C')$ where the C's are dimensionless functions decreasing with the free stream Mach number, s_1 and s_2 are dimensionless functions increasing with ϑ_w/T_0. It is seen that the heat delivery in a fluid at supersonic speed is less efficient than at subsonic speed. It can be remarked that even at moderate speeds, the first formula does not reduce to the well-known formula of L. V. King.

E11. The Effects of Heat Addition on the Aerodynamic Design of Ramjet Diffusers. M. ROGERS AND S. FAGIN, *Naval Ordnance Laboratory.* (Introduced by R. J. Seeger.)—In the aerodynamic design of ramjet diffusers, previous work has been confined primarily to the design of an "ideal, cold" diffuser, i.e., a diffuser configuration that would give maximum pressure recovery without fuel. This paper attempts to broaden the theoretical concepts by indicating a possible solution for the effects of heat addition on the ramjet diffuser performance and design. It is shown that to have maximum pressure recovery in the "hot" or burning condition it is necessary to design the cold diffuser such that the normal shock is well downstream of the maximum pressure recovery in the "cold" condition.

E12. Performance of Multiple Shock Diffusers. NEWMAN A. HALL, *University of Minnesota and Naval Ordnance Laboratory.* (Introduced by R. J. Seeger.)—A general procedure for obtaining the performance of supersonic ramjets of arbitrary configuration is developed. The analytical development emphasizes the aerodynamic aspects of the propulsive action. This is developed in a manner such that thrust and mass flow can be specifically obtained without any reference to the type of fuel to be used or the efficiency of the combustion process. In this manner, problems of internal aerodynamic design are separated from those of combustion and fuel selection.